UNIVERSIDAD DE GRANADA

Departamento de Microbiología

Facultad de Ciencias

ESTRUCTURA Y DIVERSIDAD DE LAS COMUNIDADES MICROBIANAS DE BENTONITAS Y SUS INTERACCIONES CON RADIONUCLEIDOS

STRUCTURE AND DIVERSITY OF BENTONITE MICROBIAL COMMUNITIES AND THEIR INTERACTIONS WITH RADIONUCLIDES

Programa Oficial de Doctorado en Biología Fundamental y de Sistemas

Margarita López Fernández

TESIS DOCTORAL

Granada, 2014

Editor: Universidad de Granada. Tesis Doctorales
Autor: Margarita López Fernández
ISBN: 978-84-9083-291-2
URI: http://hdl.handle.net/10481/50863

UNIVERSIDAD DE GRANADA

Departamento de Microbiología

Facultad de Ciencias

Estructura y diversidad de las comunidades microbianas de bentonitas y sus interacciones con radionucleidos

Structure and diversity of bentonite microbial communities and their interactions with radionuclides

Margarita López Fernández

Memoria presentada por la licenciada en Farmacia Dña. Margarita López Fernández para aspirar al grado de doctor con mención internacional

Vº Bº del Director del Trabajo

Mohamed Larbi Merroun
Profesor Titular de Microbiología
Universidad de Granada

La doctoranda

Margarita López Fernández

Esta Tesis Doctoral ha sido realizada en el Departamento de Microbiología (Facultad de Ciencias) de la Universidad de Granada durante los años 2010-2014 dentro del grupo de investigación Mixobacterias (BIO-103).

Para realizar este trabajo la doctoranda disfrutó de una beca F.P.I a cargo del proyecto CGL2009-09760 del Ministerio de Ciencia e Innovación, cuyo investigador principal era el Dr. Mohamed L. Merroun, Profesor Titular del Departamento de Microbiología de la Universidad de Granada.

La realización de esta Tesis Doctoral también ha sido financiada a través del proyecto CGL-2012-36505 y de tres Estancias Breves FPI en centros extranjeros (BES-2010-032098, EEBB-I-12-05830 y EEBB-I-14-08420) del Ministerio de Ciencia e Innovación.

Durante el transcurso de esta Tesis Doctoral se han mantenido colaboraciones con otros grupos de investigación, entre ellos con el Institute of Resource Ecology, HZDR (Dresde, Alemania), la Universidad de Sheffield (Reino Unido) y la Universidad de Gante (Bélgica). Estas colaboraciones se han consolidado durante las estancias breves realizadas y como resultado se han publicado o se están elaborando los siguientes artículos científicos:

Artículos científicos publicados o en elaboración con los resultados obtenidos de esta Tesis Doctoral:

- **López-Fernández, M.**, Fernández-Sanfrancisco, O., Moreno-García, A., Martin-Sanchez, I., Sánchez-Castro, I., Merroun, M.L. Microbial communities in bentonite formations and their interactions with uranium. Applied Geochemistry (2014), 49: 77-86.
- **López-Fernández, M.,** Sánchez-Castro, I., Sandoval, R., Dietmar Pieper, D., Boon, N., Vílchez-Vargas, R., Cherkouk, A., Merroun, M.L. Bacterial diversity in bentonites, engineered barrier for deep geological disposal of radioactive wastes. En preparación.
- **López- Fernández, M.,** Sánchez-Castro, I., Sandoval, R., Dietmar Pieper, D., Boon, N., Vílchez-Vargas, R., Merroun, M.L. Bacterial community changes induced by uranyl nitrate treatment under aerobic conditions. En preparación.
- **López- Fernández, M.,** Sánchez-Castro, I., Guenther, A., Solari, P.L., Moll, H., Merroun, M.L. *Rhodotorula mucilaginosa* interactions with actinides and lanthanides. En preparación.

Otras publicaciones con los resultados obtenidos de esta Tesis Doctoral:

- **López-Fernández, M.**, Sanchez-Castro, I., Amador-García, A., Romero-Gonzalez, M., Merroun, M.L. Molecular scale speciation of U(VI) association with clay bacterial isolates. Mineralogical Magazine (2013), 77(5): 1638.
- **López-Fernández, M.**, Moreno-García, A., Lazuen-Alcon, J., Geissler, A., Merroun, M.L. Bacterial Interactions with radionuclides in bentonite samples from Spanish clays. Mineralogical Magazine (2012), 76(6): 2032.
- **López-Fernández, M.,** Merroun, M. L., Geissler, A. Bacterial diversity in Spanish Clays. Annual Report HZDR, 2012. HZDR-013 2012.

- **López-Fernández, M.**, Fernández-Sanfrancisco, O., Martinéz-García, M., Ranea-Robles, P., Galera-Monge, T., Moreno-García, A., Merroun, M. Microbial populations of clay formations and their interactions with uranium. Mineralogical Magazine, (2011), 75(3): 1356.

Artículos científicos publicados o en elaboración en temas afines aunque no objeto de la presente Tesis Doctoral:

- Sánchez-Castro, I., Amador-García, A., **López-Fernández, M.**, Phrommavanh, V., Nos, J., Descostes, M., Merroun, M.L. Bacterial diversity in porewaters from uranium mill tailings revealed by culture-dependent approaches and U biomineralization potential of isolated strains. Enviado a Journal of Applied Microbiology, 2014.
- Sánchez-Castro, I., **López-Fernández, M.**, Amador-García, A., Phrommavanh, V., Nos, J., Descostes, M., Merroun, M.L. Changes in bacterial diversity and community structure within a geochemically variable uranium mine water treatment plant. Mineralogical Magazine (2013), 77(5): 2123.
- Merroun, M.L., Nedelkova, M., Ojeda, J.J., Reitz, T., **López-Fernández, M.**, Arias, J.M., Romero-Gonzalez, M., Selenska-Pobell, S. Bio-precipitation of uranium by two bacterial isolates recovered from extreme environments as estimated by potentiometric titration, TEM and X-ray absorption spectroscopic analyses. Journal of Hazardous Materials (2011), 197: 1-10.

Parte de los resultados de esta Tesis Doctoral han sido presentados en congresos nacionales e internacionales:

- Merroun, M.L., **López-Fernández, M.,** Sánchez-Castro, I., Guenther, A., Solari, P.L., Moll, H. Póster: Interactions of U(VI) and Cm(III) with microbes isolated from clay geological formations. Geodisposal 2014, Manchester, Reino Unido, 2014.
- **López-Fernández, M.** Ponencia invitada: Towards the Taxonomic and Catabolic landscape of clay-microcosms under long-term Uranium stress. University of Ghent, Bélgica, 2014.
- Merroun, M.L., **López-Fernández, M.,** Sánchez-Castro, I. Comunicación oral: Application of microscopic and synchrotron-based techniques in microbe/radionuclide interaction studies. 9th Soleil User's Meeting. Francia, 2014.
- **López-Fernández, M**., Sánchez-Castro, I., Merroun, M.L. Póster: Caracterización molecular de la asociación de U(VI) con aislados microbianos de arcillas españolas. I Workshop Jovenes Biotecnólogos, Universidad de Granada. Granada, España, 2013.
- **López-Fernández, M**., Sánchez-Castro, I., Merroun, M.L. Póster: Molecular Characterization of U(VI) association with bacteria isolated from Spanish clay. 14th International Conference on the Chemistry and Migration Behaviour of Actinides and Fission Products in the Geosphere. Brighton, Reino Unido, 2013.
- **López-Fernández, M**., Sánchez-Castro, I., Merroun, M.L. Comunicación oral: Molecular scale speciation of U(VI) association with clay bacterial isolates. Florencia, Italia, 2013.
- **López Fernández, M.** Ponencia invitada: Study of an isolated strain of *Stenotrophomas* sp. from Spanish clay formations. Kroto Research Institute, University of Sheffield, Reino Unido, 2012.
- **López Fernández, M.** Ponencia invitada: Objectives for the chemichal study of an isolated strain from Spanish clay formations. Kroto Research Institute, University of Sheffield, Reino Unido, 2012.

- **López-Fernández, M**., Moreno-Garcia, Lazuen-alcon, J., Geissler, A., Merroun, M.L. Comunicación oral: Bacterial interactions with radionuclides in bentonite samples from Spanish clays. The 22nd V.M. Goldschmidt Conference. Montreal, Canadá, 2012.
- **López-Fernández, M**., Fernandez-Sanfrancisco, O., Moreno-Garcia, A., Geissler, A., Merroun, M.L. Comunicación oral: Bacterial populations from Spanish clay formations and their effects in the transport and mobility of uranium in the environment. Geomicrobiology and its significance for biosphere processes. Manchester, Reino Unido, 2012.
- Merroun, M.L. Fernandez-sanfrancisco, O., Moreno-garcia, A., **López-Fernández, M.,** Fernández-Vivas, M.A. Comunicación oral: High U(VI) tolerance levels of an environmental *Stenotrophomonas* sp. isolate. Uranium biogeochemistry: transformations and applications conference. Ascona, Suiza, 2012.
- **López-Fernández, M**. Ponencia invitada: Comunidades bacterianas en formaciones arcillosas y sus interacciones. II Jornadas Doctorales de investigadores Interculturalidad y Ciencia, 2011. Universidad de Granada Granada, España, 2011.
- **López-Fernández, M**., Fernández-Sanfrancisco, O., Martínez-García, M., Merroun, M.L. Comunicación oral: Bacterial communities in clay formations and their interactions with radionuclides and heavy metals. 15th International Biodeterioration and Biodegradation Symposium. Vienna, Austria, 2011.
- **López-Fernández, M**., Fernández-Sanfrancisco, O., Martínez-García, M., Ranea-Robles, P., Galera-Monge, T., Moreno-García, A., Merroun, M.L. Comunicación oral: Microbial populations of clay formations and their interactions with uranium. Goldschmidt 2011, Earth, Life and Fire. Praga, Republica Checa, 2011.
- **López-Fernández, M.**, Fernández-Sanfrancisco, O., Moreno-García, A., Geissler, A., Merroun, M.L. Póster: Interacciones bacterianas con radionucleidos y metales pesados en formaciones arcillosas. XXIII Congreso Nacional de Microbiología, Sociedad Española de Microbiología. Salamanca, España, 2011.

Estancias realizadas en centros extranjeros durante el desarrollo de esta Tesis Doctoral:

- **Institute of Resource Ecology, Helmholtz-Zentrum Dresden-Rossendorf, Dresde, Alemania**. Tema: Análisis de biodiversidad bacteriana de muestras de bentonita recogidas de formaciones arcillosas de Cabo de Gata, Almería. Duración: 119 días (14/03/2011-10/07/2011). Financiación: Ayudas para la realización de estancias breves en otros centros de I+D 2010 (FPI), Ministerio de Ciencia e Innovación.
- **Institute of Resource Ecology, Helmholtz-Zentrum Dresden-Rossendorf, Dresde, Alemania.** Tema: Análisis de biodiversidad bacteriana de muestras de bentonita recogidas de formaciones arcillosas de Cabo de Gata, Almería. Duración: 62 días (06/10/2011-06/12/2011). Financiación: Grupo de Investigación BIO-103, Universidad de Granada.
- **Kroto Research Institute, University of Sheffield, Sheffield, Reino Unido.** Tema: Análisis químico de la pared celular de una cepa bacteriana aislada de bentonitas de formaciones arcillosas de Cabo de Gata, Almería y sus interacciones con radionúclidos. Duración: 123 días (15/08/2012-15/12/2012). Financiación: Ayudas para la realización de estancias breves en otros centros de I+D 2011 (FPI), Ministerio de Ciencia e Innovación.
- **Synchrotron Soleil, Saint–Aubin, Paris, Francia.** Tema: XAS characterization of the U(VI) coordination to clay bacterial isolates. Duración: 5 días (06/10/2013-10/06/2013). Financiación: Synchrotron Soleil, Saint–Aubin, Paris, Francia.
- **Laboratory of Microbial Ecology, Ghent University, Gante, Bélgica.** Tema: Estudio de la diversidad microbiana de microcosmos de arcillas tratados con nitrato de uranilo. Duración: 121 días (01/03/2014-29/16/2014). Financiación: Ayudas para la realización de estancias breves en otros centros de I+D 2013 (FPI), Ministerio de Ciencia e Innovación.

A mis padres, Francisco y Lola

A Fran

AGRADECIMIENTOS

En primer lugar, me gustaría agradecerle a mi director de tesis, el Dr. Mohamed Merroun, la oportunidad que me ofreció de trabajar con él, pero sobre todo, el apoyo y la confianza que depositó en mi. Muchas gracias Mohamed, por todo lo que me has enseñado, por las oportunidades que me has dado y por ayudarme a lo largo de toda la tesis, sin ti no lo habría conseguido.

Por supuesto, a todos mis compañeros y amigos del departamento: Fadwa, Iván, Sonia, Rubén, Platero, Fernando, Teresa, Carmen, Arantxa, Mª del Mar, Marta, Omar, Alberto, Ahinara, Elena, Cisco…por todos los buenos y malos momentos compartidos, por las risas y los cafés con churros. En especial a Fadwa, por estar siempre ahí, por ayudarme durante todo el camino y por la preciosa portada (me encanta); a Sonia, por apoyarme siempre, por ser mi compañera de juegos y por nuestras "conversaciones" secretas en las escaleras; a Iván, por sus consejos, su ayuda inestimable y por su sentido del humor; y a Carmen que, aún desde el exilio, también me ha ayudado en esta última etapa.

No puedo dejar de mencionar a los profesores: Eva, Mercedes, Inés, Enrique, Kika, Aurelio, José, Juani y José Mª, gracias por estar siempre dispuestos a ayudar. Mi más sincero agradecimiento a Mª Teresa, por su valioso ejemplo y por todas sus recomendaciones; a Pirri y a Conchi por su apoyo y ánimo, especialmente durante este último año, y por las conversaciones tanto científicas como filosóficas que hemos compartido. Gracias también a Javier, por guiarme desde la recogida de muestras hasta los últimos coletazos geológicos de la tesis.

A nuestra fantástica secretaria, Mª Carmen, gracias por toda su ayuda y por las charlas matinales; y por supuesto a Conchi M. por los buenos ratos en el laboratorio de prácticas, por las meriendas compartidas entre grupo y grupo, y por estar siempre dispuesta a echarme una mano. En general, gracias a todo el departamento de Microbiología de la Facultad de Ciencias.

Sin embargo, también me gustaría destacar a los "halófilos" de la Facultad de Farmacia, donde inicié mis pasos en esta disciplina. Gracias a Emilia, Victoria, Inma y Fernando, por permitirme empezar a conocer el mundo de la Microbiología, y por enseñarme con paciencia e ilusión a trabajar en un laboratorio de investigación; así como a mis ex-compañeros Alí, Nahid y Hakima. Y de forma muy especial a Rocío, mi mentora, gracias por dedicarme tu tiempo y por confiar en mí.

I would also like to acknowledge my external supervisors during my short stays abroad: Andrea, Sonja, Maria and Ramiro. My first stay was in Germany, where I met Andrea and Sonja. It was an amazing experience and I learnt a lot. Thanks to both of you for sharing your knowledge with me, but specially for making me feel as part of your family. Maria, with you it was easier, just because it was the second time! I arrived

to the UK and you, with your smile and your cheerful personality made me even forget the British weather, thanks for that. You taught me to work independently in a chemical lab and you showed me that there are different ways to enjoy being a researcher. In my last stay I met a brilliant and an optimistic person. Ramiro, I really enjoyed my time in Belgium, and you know it was mainly because of you, thanks. I learnt many things with you, not only about work; you gave me a new perspective of life.

A mis farmacéuticas Fátima, Mª José y Mariem, por todos los buenos ratos que hemos pasado juntas durante y después de la carrera, por esas comidas en comedores y por vuestro apoyo constante, gracias chicas. A Aurelio, gracias por ser mi amigo, por escucharme, por animarme, por creer en mí y por estar siempre.

Al resto de mis amigos, a los incondicionales, a los de toda la vida: Adri, Cristina, Manolo, Pedro, Noelia, José, Encarni….gracias, gracias y gracias, por ser como sois, pero sobre todo, por aguantarme estos últimos meses (¿cuántos burritos os debía?).

Y por supuesto, a mi familia, que me han hecho ser como soy. A mis padres, por educarme como todavía lo hacen, por ofrecerme la libertad de elegir y aprender equivocándome, por enseñarme a luchar en la vida y por demostrarme cada día su amor incondicional. A mis hermanas Silvia y Sonia, por ayudarme a crecer, por jugar conmigo, por enseñarme a valorar las cosas y por estar siempre a mi lado, a pesar de todo. Sois muy importantes en mi vida. A mi Cuñaillo, que ya sabe todo lo que podría decirle; aún así, gracias Fernando. A José Luis, por formar parte de nuestras vidas y por esas cervecitas en la terraza. Finalmente, no podía faltar la última adquisición en la familia, Iván, que desde que nació me ha alegrado la existencia, gracias "cuqui muki" por tu inocente sonrisa. Sin todos y cada uno de vosotros no habría llegado hasta aquí, gracias de corazón.

Por último, muchas gracias Fran, porque una parte de esta tesis es tuya. Gracias por hacerme reír, por cuidarme, por apoyarme en cada nueva locura y por demostrarme que esta sensación duraría más de ocho meses. Gracias por compartir tu vida conmigo. Cada día me haces ser mejor persona.

“Hay que hacer de la vida un sueño y de un sueño una realidad”

Pierre Curie

ÍNDICE

RELACIÓN DE ACRÓNIMOS/ACRONYMS

AGP: Almacenamiento Geológico Profundo

ATP: Adenosine Triphosphate

BLAST: Basic Local Alignment Tool

BSR: Bacteria Sulfato Reductoras

CFU: Colony Forming Unit

CMI: Concentración Mínima Inhibitoria

DGR: Deep Geological Repository

DNA: Deoxyribonucleic Acid

dNTP: Deoxyribonucleotide Tri-Phosphate

EBS: Engineered Barrier System

EDX: Energía de Dispersión de Rayos X/Energy Dispersive X-ray

Eh: Potencial Redox/Redox Potential

EMBL: European Molecular Biology Laboratory

EPS: Extracellular polymeric substances

EXAFS: Extended X-ray Absorption Fine Structure

FDA: Fluorescein Diacetate

FMN: Flavina Mononucleótido

FT: Fourier Transform

ICP-MS: Inductively Coupled Plasma-Mass Spectrometry

ITS: Internal Transcribed Spacer

LOI: Loss On Ignition

LPM: Low Phosphate Medium

LPS: Lipopolisacárido/Lipopolysaccharide

LSI: Laboratorio Subterráneo de Investigación

MIC: Minimal Inhibitory Concentration

MTC: Maximum Tolerated Concentration

NCBI: National Centre for Biotechnology Information

NGS: Next Generation Sequencing

nt: nucleotide

OTU: Operational Taxonomic Unit

PBS: Phosphate Buffered Saline

PCA: Principal Component Analysis

PCR: Polymerase Chain Reaction

pH: Potencial de Hidrógeno/Hydrogen potential

PI: Propidium Iodide

RAA: Residuos de Alta Actividad

RBMA: Residuos de Baja y Media Actividad

RFLP: Restriction Fragment Length Polimorphism

RISA: Ribosomal Intergenic Spacer Analysis

rRNA: ribosomal Ribonucleic Acid

STEM-HADFF: Microscopía Electrónica de Barrido y de Transmisión de Campo Oscuro Anular de Alto Ángulo/Scanning Transmission Electron Microscopy-High-Angle Annular Dark-Field

TBE: Tris-Borate-EDTA

TEM: Transmission Electron Microscopy

TOC: Total Organic Carbon

TRLFS: Espectroscopía de Fluorescencia Inducida por Láser en Tiempo Resuelto/Time-Resolved Laser-Induced Fluorescence Spectroscopy

TSAP: Thermosensitive Alkaline Phosphatase

XAS: Espectroscopía de Absorción de Rayos X/X-ray Absorption Spectroscopy

XRD: X-ray Diffraction

XRF: X-ray Fluorescence Spectroscopy

RESUMEN

Los residuos radiactivos, principalmente generados por la industria de la energía nuclear, constituyen una seria preocupación debido a sus implicaciones medioambientales. Estos materiales peligrosos deben ser almacenados de forma segura durante muchos años para que la radio-toxicidad decaiga a niveles insignificantes. Por ese motivo, el denominado almacenamiento geológico profundo de residuos radiactivos, encapsulados en contenedores metálicos resistentes a la corrosión, es considerado, a nivel internacional, como la forma más segura para este tipo de almacenaje. Diversos tipos de rocas hospedantes, potencialmente adecuadas para este uso, como rocas graníticas, formaciones arcillosas y depósitos de sales, han sido consideradas aptas por diferentes países. Los ambientes de roca granítica han sido ampliamente estudiados en Finlandia, Suecia y Canadá. Estados Unidos ha propuesto los depósitos salinos para este tipo de almacenaje. En otros países europeos como Francia, Bélgica y Suiza, las formaciones arcillosas son las candidatas seleccionadas como depósito geológico para el almacenamiento de residuos nucleares de alta actividad. Centrándonos en el caso de España, las formaciones geológicas consideradas como candidatas son los granitos, las arcillas y las sales. En este sentido, numerosos estudios han llevado a la selección y caracterización de arcillas para el relleno y sellado de los almacenes de desechos radiactivos. Las formaciones de bentonitas de los depósitos de arcillas de El Cortijo de Archidona, en el Parque Natural de Cabo de Gata (Almería), han sido elegidas para este propósito como las mejor caracterizadas a nivel físico-químico desde distintos puntos de vista. Sin embargo, la seguridad de los almacenamientos geológicos profundos a largo plazo puede verse comprometida no solo por factores físicos y químicos, sino también por la actividad biogeoquímica, tanto de los microorganismos de la roca hospedante como de los microorganismos introducidos durante la construcción del almacén.

Los procesos microbianos pueden afectar a la seguridad del almacenamiento geológico profundo a través de tres mecanismos diferentes: la transformación de los minerales de la arcilla, la degradación de los contenedores metálicos y la movilización de los radionucleidos. Por este motivo, es de gran importancia estudiar la presencia microbiana en estas formaciones de bentonitas españolas y los mecanismos de interacción de sus poblaciones microbianas con los radionucleidos.

Los principales objetivos de esta tesis doctoral son estudiar la diversidad microbiana de las formaciones de bentonita seleccionadas como material de referencia para su uso como barreras artificiales de seguridad en el almacenamiento geológico profundo y elucidar los mecanismos de interacción de las cepas microbianas aisladas, altamente tolerantes a los radionucleidos, con el uranio(VI) y el curio(III) como representantes de los actínidos hexavalentes y trivalentes, respectivamente.

Para la realización de este trabajo, y con los objetivos mencionados más arriba, se tomaron muestras de tres formaciones de bentonitas diferentes en el Parque Natural de Cabo de Gata: El Cortijo de Archidona (muestra BI-2, tomada de la superficie y muestra BI-3, recogida a 20 cm de profundidad), El Toril (BII-2, superficial) y Los Trancos (BIV-2, superficial y BIV-3, a 20 cm de profundidad). La mineralogía de las bentonitas estudiadas está dominada por la presencia de montmorillonita, con cuarzo y feldespatos como fases minoritarias. La diferencia más importante entre estas muestras es la presencia en la muestra BII de jarosita, un mineral de sulfato de hierro.

El primer paso fue el estudio de la diversidad bacteriana de las cinco muestras recogidas, para conocer mejor cómo estos microorganismos pueden influir, potencialmente, en la seguridad de los almacenes de residuos radiactivos. Para ello se utilizaron dos métodos independientes de cultivo basados en el análisis del gen del ARN ribosomal 16S (secuenciación con la plataforma Illumina y librerías de clones tradicionales). Se obtuvieron secuencias correspodientes a doce *phyla* bacterianos (*Acidobacteria*, *Actinobacteria*, *Armatimonadetes*, *Bacteroidetes*, *Choloroflexi*, *Cyanobacteria*, *Firmicutes*, *Gemmatimonadetes*, *Planctomycetes*, *Proteobacteria*, *Nitrospirae* y *Verrucomicrobia*) mediante la técnica de secuenciación de nueva generación Illumina. *Proteobacteria* (mayoritariamente *Alpha-* y *Betaproteobacteria*), *Bacteroidetes*, *Actinobacteria* y *Acidobacteria* fueron los principales *phyla* bacterianos detectados en las muestras de bentonita. Se identificaron varios clones relativos a *Alphaproteobacteria*, como *Sphingomonas*, *Porphyrobacter*, *Brevundimonas*, *Rhodobacter*, *Blastomonas*, *Tabrizicola* y *Mesorhizobium* entre otros. Algunos de los clones afiliados a las betaproteobacterias han sido descritos por: (i) su alta tolerancia a los metales pesados (como por ejemplo *Ralstonia* y *Variovorax)*, (ii) por solubilizar el hierro de los minerales de las arcillas (p.ej. *Herbaspirillium*, *Janthinobacterium* y *Massilia*), (iii) así como por la reducción de U(VI) (p. ej. *Acidovorax).* Relativos al *phylum Bacteroidetes* se identificaron los siguientes géneros: *Pontibacter*,

Hymenobacter y *Pedobacter*. Y perteneciente a *Actinobacteria*, se identificó el género *Arthrobacter*. La alta diversidad bacteriana detectada en las muestras de bentonita podría ser capaz de interactuar de forma eficiente con el hierro de las bentonitas y los radionucleidos, afectando a la seguridad del almacenamiento geológico profundo de residuos radiactivos.

La diversidad microbiana de las muestras BI y BII también fue analizada mediante técnicas dependientes de cultivo, usando una combinación de medios de cultivo complejos y oligotróficos. En este caso no se incluyó la muestra BIV, debido a la diversidad bacteriana encontrada en esta muestra, que fue similar a la de las muestras BI y BII. Se encontró una alta diversidad bacteriana cultivable en las muestras estudiadas. *Proteobacteria* fue el *phylum* dominante en la muestra BI (50% de los aislados). Pertenecientes a la clase *Alphaproteobacteria* se identificaron *Paracoccus* (3 aislados) y *Sphingomonas* (1 aislado). Dos *Betaproteobacteria* aisladas fueron identificadas como *Janthinobacterium* y *Herbaspirillium* y otros dos aislados (*Pseudomonas* y *Pantoea*) se identificaron como pertenecientes a *Gammaproteobacteria*. El segundo *phylum* dominante en la muestra BI fue *Actinobacteria* (44%), representado únicamente por *Arthrobacter* (7 aislados). Finalmente, sólo se aisló un *Firmicutes*, identificado como *Staphylococcus*. El *phylum* más abundante en la muestra BII fue *Actinobacteria*, al que pertenecían el 75% del total de los aislados presentando entre ellos una distribución heterogénea: *Micrococcus* (4 aislados), *Modestobacter* (2 aislados), *Amycolatopsis*, *Arthrobacter*, *Dermacoccus*, *Kocuria*, *Janibacter* e *Isoptericola*. El *phylum Proteobacteria* (19% de los aislados en BII) estaba representado por *Massilia*, *Herbaspirillium* y *Stenotrophomonas*. Solo se aisló una cepa de *Bacillus*, perteneciente al *phylum Firmicutes*. También se aisló una levadura de la muestra BII, identificada como *Rhodotorula mucilaginosa*.

En un segundo paso se evaluó la tolerancia al uranio de los aislados microbianos, mediante la determinación de la concentración mínima inhibitoria (CMI) y por citometría de flujo. Más de un 60% de los aislados de la muestra BI y más de un 30% de los aislados de la BII crecieron satisfactoriamente a 2 mM de concentración de uranio, pero al incrementar la concentración a 3 mM, el crecimiento microbiano disminuyó hasta el 31% y el 38%, respectivamente. Sin embargo, en la muestra BII, dos de los aislados demostraron tener una alta tolerancia al uranio, creciendo hasta concentraciones de 6 mM (la cepa bacteriana *Stenotrophomonas* sp. BII-R7) y hasta 8

mM (la levadura *R. mucilaginosa* BII-R8). Mediante la técnica de citometría de flujo se determinó la viabilidad celular de estas dos cepas microbianas altamente tolerantes al uranio. En ausencia de este radionucleido, el 96% de las células de la levadura *R. mucilaginosa* BII-R8 estaban vivas. La viabilidad celular disminuyó ligeramente en función de la concentración creciente de uranio. A la concentración de 3 mM, el 55% de las células presentaban sus membranas celulares intactas. La concentración de uranio 4 mM se determinó como citotóxica, ya que el 99.45% de las células de la levadura no eran viables. La alta tolerancia al uranio demostrada por las células de la levadura es un proceso mediado biológicamente, debido a que en las mismas condiciones experimentales (concentración de uranio, tiempo de contacto, etc.) las células de la levadura y las de la bacteria *Stenotrophomonas* sp. BII-R7 mostraron diferentes niveles de tolerancia al uranio. Por ejemplo, mientras que a la concentración de 2 mM casi el 74% de las células de la levadura eran viables, el 100% de las bacterias no lo eran. Para estudiar la respuesta metabólica frente a concentraciones crecientes de uranio se empleó el fluorocromo $DiOC_6$, que reveló la capacidad de BII-R8 para lidiar con altas concentraciones de este radionucleido, concretamente, la actividad metabólica disminuyó de forma proporcional a la reducción de la viabilidad celular hasta 1 mM U. Como aclaración, hay que hacer constar que la aparente contradicción entre el comportamiento de estas cepas microbianas frente al uranio, se debe a la forma de realizar los cultivos para cada técnica (sólido para CMI y líquido para citometría de flujo).

Para determinar los mecanismos responsables de la alta tolerancia de la levadura *R. mucilaginosa* BII-R8 se usaron técnicas espectroscópicas [Espectroscopía de Absorción de Rayos X (X-ray Absorption Specytyocopy, XAS), Espectroscopía de Fluorescencia Inducida por Láser en Tiempo Resuelto (Time-Resolved Laser-Induced Fluorescence Spectroscopy, TRLFS)] y microscópicas [Microscopía Electrónica de Barrido y de Transmisión de Campo Oscuro Anular de Alto Ángulo (Scanning Transmission Electron Microscopy-High-Angle Annular Dark-Field, STEM-HADDF)]. Los análisis de XAS indicaron que la coordinación local del U(VI) en las células era similar a la de la meta-autunita, una fase mineral de fosfatos de uranio. Sin embargo, los análisis de TRLFS mostraron que los parámetros de fluorescencia de los complejos de uranio formados eran diferentes a los de la meta-autunita, y más parecidos a los de los grupos fosfato orgánicos. Estos resultados demostraron que el uranio es acomplejado

por grupos fosforilos cuatro veces monodentados coordinados en el plano ecuatorial con los dioxo-cationes de uranilo, revelando una gran homología con las fases minerales de uranilo de la meta-autunita. El estudio de las células de la levadura mediante STEM-HAADF reveló la presencia de acúmulos de metal en las superficies celulares e intracelulares, en concreto, algunos de ellos localizados en las membranas concéntricas de los orgánulos.

La interacción entre el curio(III) y la levadura *R. mucilaginosa* BII-R8 se estudió mediante TRLFS, a concentraciones traza (0.3 μM) de Cm(III). Estos estudios demostraron que la biosorción del Cm(III) es un proceso reversible en el que dos especies de Cm(III) fueron identificadas. La especie 1 de Cm(III)-*R. mucilaginosa* BII-R8 se caracteriza por tener una emisión máxima a 599 ± 1 nm y un tiempo medio de vida de luminicencia de 215 ± 36 μs. La especie 2 de Cm(III)-*R. mucilaginosa* BII-R8 mostró una emisión máxima a 602.0 ± 0.5 nm y un tiempo medio de vida de luminiscencia más corto, de 124 ± 15 μs. Comparando las propiedades de la luminiscencia de las dos especies de Cm(III)-*R. mucilaginosa* BII-R8 con datos seleccionados en la literatura publicada, la especie 1 de Cm(III)-*R. mucilaginosa* BII-R8 se puede asignar a especies de Cm(III) unidas a sitios fosfato y la especie 2 de Cm(III)-*R. mucilaginosa* BII-R8 a especies de Cm(III) unidas a sitios carboxilo. Estos datos de TRLFS indicaron que la cepa microbiana adsorbe este radionucleido haciéndolo más móvil, facilitando así que pueda alcanzar la biosfera. Finalmente, el europio(III) se utilizó en este estudio como análogo inactivo del Cm(III). Mediante la técnica STEM-HAADF se observaron precipitados de Eu(III) y de fosfato, localizados en la superficie celular.

El último paso fue simular el escenario en el que la movilización de uranio desde los almacenes hasta las formaciones arcillosas pudiera ocurrir. Para ello se diseñó un sistema de microcosmos con las muestras de bentonita españolas sin tratar (control) y tratadas con nitrato sódico (control de nitrato) y con nitrato de uranilo, para evaluar la respuesta, a largo plazo, de las comunidades bacterianas de las bentonitas a la adición de este radionúclido y el efecto de estos microorganismos en la especiación del U(VI). Tras cinco meses de incubación en condiciones aerobias, los datos obtenidos mediante secuenciación con Illumina indicaron que *Firmicutes* (75%) y *Alphaproteobacteria* (20%) fueron los principales *phyla* detectados en los microcosmos no tratados (control) de la muestra BI. La diversidad del microcosmo de esa misma muestra, tratado con

nitrato sódico difiere ligeramente del control, ya que *Alphaproteobacteria* (42%), *Betaproteobacteria* (30%) y *Firmicutes* (26%) son los *phyla* dominantes. Se identificaron familias de bacterias aerobias heterotróficas. Así mismo, la adición de nitrato estimuló la actividad de bacterias nitrato-reductoras. Además, se detectaron diferencias significativas en la estructura de la población bacteriana del microcosmo BI tratado con nitrato de uranilo, en comparación con los dos microcosmos controles de esta muestra. Estas diferencias se concretaron en los siguientes resultados: *Proteobacteria* (55%), principalmente representada por *Gammaproteobacteria* (especialmente *Pseudomonas*) y *Firmicutes* (40%). En el caso de la muestra BII, la diversidad bacteriana del microcosmo control (no tratado) estaba completamente dominada por el *phylum Firmicutes* (97%). El tratamiento con nitrato sódico también afectó a la diversidad del microcosmo BII, ya que la presencia de *Firmicutes* disminuyó hasta el 6%, mientras que *Betaproteobacteria* (63%) se convirtió en la clase dominante. El tratamiento con nitrato de uranilo en el microcosmo BII provocó un enriquecimiento en cepas bacterianas, como por ejemplo *Bacillus* o *Pseudomonas*, descritas por su capacidad de precipitar uranio como fases minerales de fosfato, con una estructura similar a la de la meta-autunita, mediada por la actividad fosfatasa.

En este sentido, resultó interesante el incremento de la actividad de la fosfatasa ácida en el microcosmo BII tratado con nitrato de uranilo. Esto motivó la aplicación de un nuevo enfoque para crear una base de datos de los genes catabólicos de la fosfatasa ácida, con el propósito de entender mejor el proceso de bioprecipitación de uranio. Así pues, este nuevo enfoque permite dar un paso más en la posibilidad de usar la información taxonómica de los ecosistemas estudiados para una mejor comprensión de su potencial catabólico. Además, permitirá a la comunidad científica identificar los microorganismos potenciales para llevar a cabo la biomineralización de uranio, diseñando marcadores biológicos que podrán ser usados tanto en muestras medioambientales como en microorganismos aislados de zonas contaminadas con uranio.

SUMMARY

Radioactive wastes, mainly produced by the nuclear energy industry, are of serious environmental concern. These hazardous materials must be safely stored for many years for the radiotoxicity to decrease to non dangerous levels. For this reason, the deep geological disposal of radioactive wastes, encapsulated in corrosion-resistant metal containers, has been internationally considered as the safest option for their disposal. A number of potentially suitable host rock types, such as granitic rocks, clay formations and salt deposits, have been identified and are being studied in different countries. Granitic rock environments have been extensively studied in Finland, Sweden and Canada as potential host rocks for deep geological repository of radioactive wastes. The USA proposed salt deposits for this kind of disposal. In Europe, mainly in France, Belgium and Switzerland, clay formations are the candidate host rock for a high-level nuclear waste repository. In Spain, the geological formations considered are granites, clays and salts. In addition, several studies investigated the selection and characterization of suitable clays for sealing and backfilling of the Spanish radioactive waste repository. The bentonite formations from the clay deposits of El Cortijo de Archidona, in the Cabo de Gata National Park, Almeria, were selected as the best characterized from different physico-chemical points of view, for this purpose. However, the safety of this long-term geological disposal could be compromised not only by physical and chemical factors, but also by the biogeochemical activity of either indigenous microorganisms of the host rock or microorganisms introduced during the construction of the repository.

Microbial processes can affect the security of the deep geological repository through three different mechanisms: transformation of clay minerals, degradation of the metal containers, and mobilization of radionuclides. So far, it is of great importance to study the microbial occurrence in the selected Spanish bentonite formations and the interaction mechanisms of their microbial populations with radionuclides.

The main objectives of this doctoral thesis are to study the microbial diversity in bentonite formations selected as reference material for safety barriers in a deep geological repository, and to elucidate the interaction mechanisms of the highly

radionuclide tolerant isolated microbial strains with uranium(VI) and curium(III) as representatives of hexavalent and trivalent actinides, respectively.

In this study, three different bentonite formations were sampled in Cabo de Gata National Park: El Cortijo de Archidona (sample BI-2, collected from the surface and sample BI-3, taken from 20 cm depth), El Toril (BII-2, surface) and Los Trancos (BIV-2, surface and BIV-3, 20 cm depth). The mineralogy of the studied bentonite samples is dominated by the presence of montmorillonite, with quartz and feldspars as minor phases. The most relevant difference between sample BI, BII and BIV is the presence of jarosite, an iron sulphate mineral, in sample BII.

The first step was to study the bacterial diversity of the five samples collected, to get a better knowledge about how these microorganisms may potentially influence the performance of the nuclear waste repository. For that, two different culture-independent molecular approaches based on the 16S ribosomal RNA gene analysis (Illumina sequencing platform and traditional clone libraries) were applied. Twelve different bacterial phyla (*Acidobacteria*, *Actinobacteria*, *Armatimonadetes*, *Bacteroidetes*, *Choloroflexi*, *Cyanobacteria*, *Firmicutes*, *Gemmatimonadetes*, *Planctomycetes*, *Proteobacteria*, *Nitrospirae* and *Verrucomicrobia*) were identified by next generation Illumina sequencing platform. *Proteobacteria* (mainly *Alpha*- and *Betaproteobacteria*), *Bacteroidetes*, *Actinobacteria* and *Acidobacteria* were the main bacterial phyla present in the bentonite samples. Belonging to *Alphaproteobacteria*, several clones were identified as *Sphingomonas*, *Porphyrobacter*, *Brevundimonas*, *Rhodobacter*, *Blastomonas*, *Tabrizicola* and *Mesorhizobium* among others. Some of betaproteobacterial clones identified were described for: (i) their high tolerance to heavy metals (e.g. *Ralstonia* and *Variovorax)*; (ii) the solubilization of the iron in the clay minerals (e.g. *Herbaspirillium*, *Janthinobacterium* and *Massilia)*; (iii) as well as for the reduction of U(VI) (e.g. *Acidovorax).* Affiliated to phylum *Bacteroidetes*, *Pontibacter*, *Hymenobacter* and *Pedobacter* genus were identified; and *Arthrobacter*, belonging to *Actinobacteria*. The high bacterial diversity found in the bentonite samples might be able to interact efficiently with iron and radionuclides, affecting the safety of the deep geological repository of radioactive wastes.

The microbial diversity was also analyzed by culture dependent methods, by using a combination of complex and oligotrophic culture media. A high microbial

diversity was found in these samples. *Proteobacteria* was the dominant phylum in sample BI (50% of the isolates). *Alphaproteobacteria* was represented by *Paracoccus* (3 isolates) and *Sphingomonas* (1 isolate) genera. Two *Betaproteobacteria* were recovered, related to *Janthinobacterium* and *Herbaspirillium*, and another two isolates belonging to *Gammaproteobacteria*, *Pseudomonas* and *Pantoea*. *Actinobacteria* was another dominant phylum (44%) in sample BI and it was only represented by *Arthrobacter* (7 isolates). Finally, only one *Firmicutes* was isolated, affiliated to *Staphylococcus*. *Actinobacteria* was the most abundant phylum in sample BII with 75% of the total isolates and with a heterogeneous distribution, including *Micrococcus* (4 isolates), *Modestobacter* (2 isolates), *Amycolatopsis*, *Arthrobacter*, *Dermacoccus*, *Kocuria*, *Janibacter* and *Isoptericola*. *Proteobacteria* (19% of BII isolates) was represented by *Massilia*, *Herbaspirillium* and *Stenotrophomonas*. Only one *Bacillus* strain (*Firmicutes* phylum) was isolated. In addition to bacteria, one yeast strain affiliated to *Rhodotorula mucilaginosa* was isolated from sample BII.

The second step was to evaluate the uranium tolerance of the microbial isolates, by the determination of the minimal inhibitory concentration (MIC) and by flow cytometry technique. More than 60% and 30% of the BI and BII isolates, respectively, grew successfully at 2 mM of uranium concentration, but increasing the concentration of uranium at 3 mM the microbial growth decreases to 31% and 38%, respectively for BI and BII isolates. However, in sample BII, two strains revealed a high uranium tolerance, growing up to 6 mM of uranium (bacterial strain *Stenotrophomonas* sp. BII-R7) and up to 8 mM of uranium (the yeast strain *R. mucilaginosa* BII-R8). By flow cytometry technique the cell viability of these two highly uranium tolerant isolated strains, was measured. In the absence of uranium, 96% of the yeast *R. mucilaginosa* BII-R8 cells are alive. The cell viability decreases slightly in function of the increasing uranium concentrations. At 3 mM of uranium, 55% of the cells exhibited intact cell membranes. 4 mM is a cytotoxic concentration since 99.45% of the yeast cells are not viable. The high uranium tolerance exhibited by the yeast cells is a biological mediated process since under the same experimental conditions (uranium concentration, time of contact, etc.), cells of the yeast strain and those of the bacterium *Stenotrophomonas* sp. BII-R7 exhibited different levels of uranium tolerance. For instance, whereas at 2 mM of uranium concentration, almost 74% of the yeast cells are alive, 100% of the *Stenotrophomonas* cells are not viable. The metabolic potential response to increasing

uranium concentrations was studied by $DiOC_6$ staining, revealing the ability of BII-R8 to cope with high concentrations of this radionuclide. The metabolic activity of BII-R8 cells was decreasing proportionally to the decrease of the cell viability up to 1 mM of uranium concentration. It is necessary to clarify that the obvious contradiction in the microbial strains behavior with uranium is due to the culture preparation for each technique (solid medium for MIC and liquid medium for the flow cytometry).

In order to determine the mechanisms responsible for the high uranium tolerance of the cells of the yeast *R. mucilaginosa* BII-R8, spectroscopic [(X-ray Absorption Spectroscopy (XAS), Time Resolved Laser Induced Fluorescence Spectroscopy (TRLFS)] and microscopic [(Scanning Transmission Electron Microscopy-High-Angle Annular Dark-Field (STEM-HAADF)] techniques were used. XAS analysis indicated that the local coordination of U(VI) within the cells is similar to that of meta-autunite, U-phosphate mineral phase. However, TRLFS analysis, showed that fluorescence parameters of the uranium complexes formed are different to those of meta-autunite, and much well to those of organic phosphate complexes. These results demonstrated that uranium is complexed by phosphoryl groups four-fold monodentately coordinated in the equatorial plan of the uranyl dioxo-cation showing great homologies to the uranyl mineral phase meta-autunite. STEM-HAADF analysis of the U-treated yeast cells showed the presence of metal accumulates at the cell surfaces. In addition, intracellular uranium accumulates were localized within and at the membranes of concentric organelles.

The interaction between curium(III) and the yeast strain *R. mucilaginosa* BII-R8 was studied at trace Cm(III) concentrations (0.3 µM) using TRLFS. These results revealed that the biosorption of Cm(III) is a reversible process where two Cm(III) yeast species were identified. Cm(III)-*R. mucilaginosa* BII-R8 specie 1 is characterized by an emission maximum at 599 ± 1 nm and an average luminescence lifetime of 215 ± 36 µs. Whereas Cm(III)-*R. mucilaginosa* BII-R8 specie 2 shows a more red shifted emission maximum at 602.0 ± 0.5 nm and a shorter average luminescence lifetime of 124 ± 15 µs. By comparing the luminescence properties of both Cm(III)-*R. mucilaginosa* BII-R8 species with selected literature data, Cm(III)- *R. mucilaginosa* BII-R8 specie 1 can be asigned to a Cm(III) species bound to phosphoryl sites and Cm(III)-*R. mucilaginosa* BII-R8 specie 2 to a Cm(III) species bound to carboxyl sites of the cell envelope. These TRLFS data indicated that the microbial strains sorb this radionuclide making it more

mobile and more likely to reach the biosphere. Finally, europium(III), used in this study as inactive analogue of Cm(III), was precipitated as Eu(III)-phosphate at the cell surface of BII-R8, as it demonstrated by STEM-HAADF.

The last step was to simulate a scenario where the mobilization of uranium from the planned repository to the clay formations may occur. Therefore, microcosms elaborated with the Spanish bentonite samples, were non-treated (control), and long-term treated with sodium nitrate (nitrate control) and uranyl nitrate to evaluate the response of the subsurface bacterial community of bentonites to addition of this radionuclide and the effect of these microorganisms on the speciation of uranium(VI). After five months of aerobic incubation, by Illumina sequencing, *Firmicutes* (75%) and *Alphaproteobacteria* (20%) were the main phyla detected in the non-treated microcosm of BI. The sodium nitrate-treated microcosm diversity differs slightly to that of the control microcosm since *Alpha*-(42%), *Betaproteobacteria* (30%) and *Firmicutes* (26%) are the dominant phyla. Heterotrophic aerobic families were detected. Furthermore, the nitrate addition stimulates the increase of the activity of nitrate reducing bacteria. Moreover, significant differences were observed in the structure of bacterial population of the uranyl nitrate-treated BI microcosm in comparison to the other two control microcosms of this sample. These differences were represented by *Proteobacteria* (55%) which was mainly represented by *Gammaproteobacteria* (specifically, *Pseudomonas*), and followed by *Firmicutes* (40%). In the case of sample BII, the non-treated microcosm bacterial divesity was completely dominated by phylum *Firmicutes* (97%). The sodium nitrate treatment affects the diversity of the microcosm BII, because the presence of *Firmicutes* decreases to 6%, while *Betaproteobacteria* (63%) becomes the most represented class. The uranyl nitrate treatment result in the enrichment of bacterial strains (e.g. *Bacillus*, *Pseudomonas*) described for their ability to precipitate uraniun as uranium phosphate mineral phases with a structure similar to that of meta-autunite through phosphatase activity.

Interestingly, the acid phosphatase activity was increased in the uranium-treated microcosm of sample BII. Therefore, a novel approach was applied to create a database of acid phosphatase catabolic genes, with the aim of fulfilling the uranium bioprecipitation process. So far, this study takes one step further in the possibility of using the taxonomic information of a studied ecosystem to better understand its catabolic potential. Moreover, it will allow the scientific community to identify the best

qualified microorganisms for the uranium biomineralization, by designing biological labels to be used in environmental samples as well as in microorganisms isolated from uranium contaminated sites.

INTRODUCCIÓN

1. Algunos datos históricos sobre la energía nuclear

El físico francés Antoine-Henri Becquerel es considerado el "padre de la energía nuclear" desde que, en 1896, descubrió la radioactividad al comprobar que determinadas sustancias, como las sales de uranio, producían radiaciones penetrantes de origen desconocido. Posteriormente en 1898, Marie y Pierre Curie descubrieron otras sustancias aún más radiantes, como el polonio y el radio. A finales de 1938, el descubrimiento de la fisión nuclear por la física Lise Meitner y los químicos Otto Hahn y Fritz Strassmann, en su laboratorio de Berlín, representó una auténtica sorpresa. Ninguna teoría física había predicho que un neutrón podía dividir en dos el núcleo de un átomo. La fisión es una reacción que produce la rotura del núcleo de un átomo, liberando energía. El núcleo se divide generando subproductos más pequeños, como neutrones libres, rayos gamma, núcleos de helio (partículas alfa) o electrones y positrones de alta energía (partículas beta). La fisión nuclear es una reacción exotérmica, es decir, que implica la emisión de energía. Este proceso genera mucha más energía que la liberada en las reacciones químicas convencionales. No pasó mucho tiempo hasta que este descubrimiento se empezó a aplicar en la fabricación de bombas atómicas y en la fabricación de energía eléctrica en las centrales nucleares.

Actualmente no se puede definir la energía nuclear sólo como el resultado de una reacción que divide un núcleo atómico, sino como un concepto más amplio que incluye los conocimientos y las técnicas que permiten la utilización de esta energía por parte del ser humano. Estas reacciones se dan en los núcleos atómicos de ciertos elementos químicos, siendo la más conocida la fisión del ^{235}U, con la que funcionan los reactores nucleares, y que es la más habitual en la naturaleza. Los hitos más importantes en la historia de la energía nuclear están representados en la Figura 1.

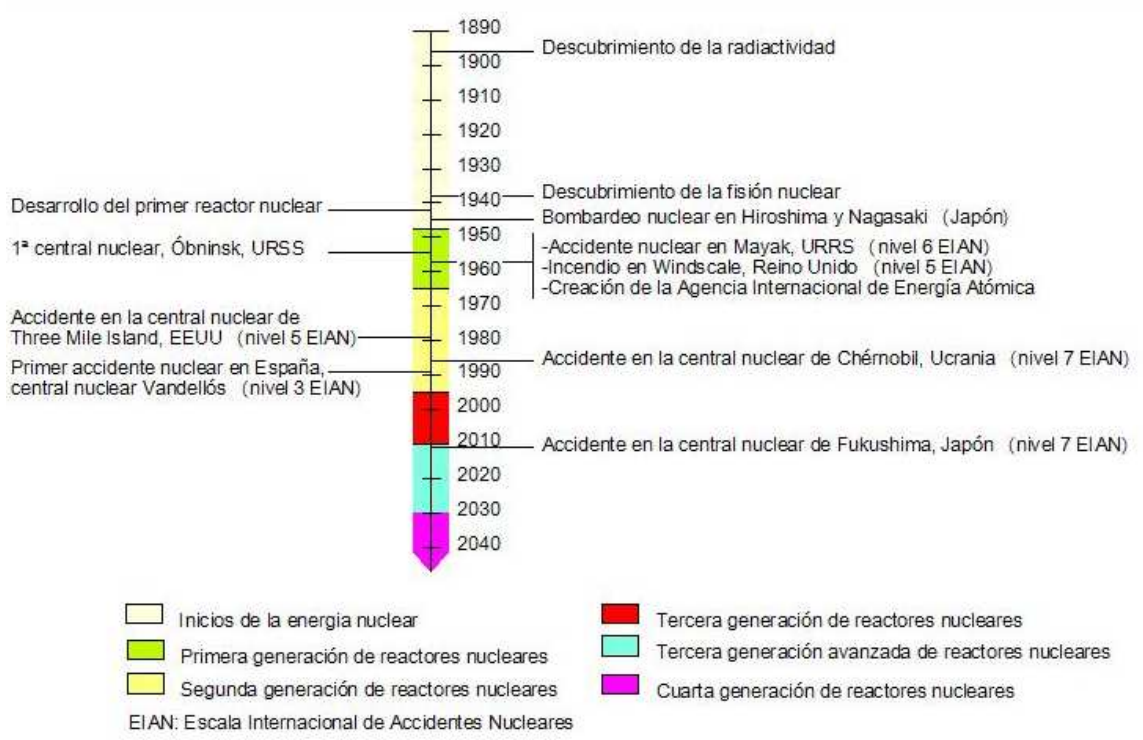

Figura 1. Representación de los eventos más importantes en la historia de la energía nuclear.

En 1951 se comenzó a producir electricidad mediante el uso de energía nuclear, gracias a un pequeño reactor experimental construido en Estados Unidos. A pesar de este éxito tecnológico, fue en Óbninsk (URSS, actualmente Rusia), en 1954, donde se creó la primera central nuclear del mundo. Seguida en 1956 por "Calder Hall" en el Reino Unido, que fue, de hecho, la primera estación nuclear comercial cuyo reactor tenía una capacidad de generación de 196 megavatios y se mantuvo en funcionamiento hasta 2003. Propiciada por el lanzamiento de bombas nucleares en agosto de 1945 sobre Hiroshima y Nagasaki (Japón), en 1957 se creó la Agencia Internacional de Energía Atómica (AIEA) con el apoyo de 81 naciones, para elaborar un estatuto internacional que supervisara la seguridad del uso de la energía atómica en el mundo y evitara sus iniciales usos bélicos.

A partir de 1960 muchos países se unieron a la construcción de centrales nucleares, de hecho, fue en 1969 cuando se abrió la Central nuclear José Cabrera, en Guadalajara, la primera construida en España. Así, la producción de energía nuclear no dejó de crecer a la vez que fue aumentando espectacularmente la capacidad productora de las centrales. De los 17 reactores existentes en sólo 4 países en 1960, generando un

total de 1200 megavatios, se pasó en 1970 a 90 reactores en 15 naciones, capaces de producir 17500 megavatios, y en 1980 a 253 reactores en 22 países productores de 135000 megavatios (Cavero, 2011). Actualmente, según la Sociedad Nuclear Europea, hay un total de 437 reactores distribuidos en 31 países, con una capacidad de producción de 374000 megavatios.

Sin embargo, además de producir una gran cantidad de energía eléctrica, también producen un elevado número de residuos radiactivos de distintos tipos. Los residuos radiactivos son aquellos materiales que contienen isótopos radiactivos por encima de un valor legalmente establecido. Los isótopos radiactivos o radionucleidos son átomos inestables, cuyos núcleos permanecen estables en cuanto a cantidad de neutrones, pero que varían en el número de protones, lo que hace que emitan radiación. La radiación emitida por los radionucleidos puede ser ionizante (partículas alpha, beta, gamma o rayos X) o no ionizante.

2. Tratamiento y gestión de residuos radiactivos

En España, en 1984, se creó la Empresa Nacional de Residuos Radiactivos (ENRESA) para gestionar los residuos radiactivos generados. Estos residuos especiales se pueden clasificar en dos grandes grupos:

- Residuos de Baja y Media Actividad (RBMA) que contienen isótoposradiactivos con períodos de semidesintegración iguales o inferiores a 30 años. Estos residuos emiten radiación beta y gamma en niveles menores a 0,04 GBq/m³ (baja actividad) o inferiores a 4 GBq/m³ (media actividad). En España, estos residuos son generados principalmente por la industria minera (grandes volúmenes de residuos de muy baja actividad), en la fabricación de combustible para las centrales nucleares (residuos sólidos y líquidos), en el funcionamiento de las centrales nucleares (residuos húmedos: resinas de intercambio iónico, concentrados de evaporador y lodos; residuos secos: papel, plásticos, etc.), en la desmantelación de las centrales nucleares (grandes volúmenes de residuos de baja actividad, con una pequeña proporción de media actividad), por el ámbito sanitario (debido al uso de isótopos radiactivos para diagnosis y tratamiento de enfermedades) y en las

actividades industriales (ya que usan fuentes encapsuladas para el control e inspección de procesos).

- Residuos de Alta Actividad (RAA) que contienen radionucleidos con períodos de semidesintegración superiores a 30 años, que además emiten radiación alfa, suelen ser emisores de calor y pueden ser activos durante miles o decenas de miles de años. Los residuos de alta actividad están constituidos básicamente por el combustible gastado en los reactores nucleares y por otros materiales con niveles elevados de radiactividad, como uranio, plutonio, productos de fisión y productos de activación.

La gestión de ambos grupos de residuos requiere, lógicamente, soluciones tecnológicas distintas (Astudillo Pastor, 2001). Para los RBMA, el aislamiento y confinamiento debe asegurarse para períodos establecidos de aproximadamente 300 años, considerando que la actividad habrá desaparecido prácticamente transcurrido 10 veces el período de semi-desintegración. El diseño de instalaciones que aseguren estos períodos de confinamiento y aislamiento es una práctica industrial real y viable con los materiales tecnológicos actuales (hormigones, aceros, etc.). Para estos residuos existen por tanto soluciones industriales probadas. En España se cuenta para su gestión con la instalación de almacenamiento de El Cabril (Córdoba), diseñada y construida por ENRESA, en operación desde 1992. (Fig. 2).

Figura 2: Instalaciones del almacén de residuos de baja y media actividad de El Cabril (www.enresa.es).

Los RAA contienen isótopos radiactivos con períodos de semi-desintegración de cientos o miles de años que requieren otros sistemas de gestión definitiva que aseguren su aislamiento y confinamiento por períodos de decenas o centenas de miles de años. Actualmente, en España, más del 95% del total de los residuos de alta actividad son generados por la industria nuclear (Ojovan and Lee, 2005), constituidos generalmente por el combustible gastado en las centrales nucleares y una pequeña cantidad de materiales procedentes del reproceso (vidrios, residuos tecnológicos, etc.); el resto proviene de la minería, la investigación, los hospitales, etc.

Estos residuos de alto nivel producen calor y radioactividad, por lo que deben ser adecuadamente gestionados de forma segura en instalaciones especiales (Clarke, 1996) durante al menos 100.000 años, para que la radioactividad decaiga a niveles similares a los del uranio natural o sus productos de desintegración (Hedin, 1999). Por ese motivo, muchos países están considerando distintas opciones para el tratamiento a largo plazo de los residuos nucleares de alta actividad. Una de las opciones más analizadas fue el envío al espacio de este tipo de residuos, pero las consecuencias catastróficas de un posible fallo en alguno de los lanzamientos la catalogó finalmente como una insegura (Astudillo Pastor, 2001).

Otra opción considerada fue la colocación de los residuos radiactivos de alta actividad en fosas oceánicas próximas a zonas de subducción de la corteza marina. Pero la lentitud de estos procesos, así como la imposibilidad de controlar y evitar que los organismos vivos subacuáticos fueran afectados por las radiaciones y estas entraran en la cadena trófica de otros seres vivos, desaconsejó también esta opción (Astudillo Pastor, 2001). Además, el Tratado de Londres de prohibición de verter residuos radiactivos al mar corroboró esta opción como inviable.

Otras posibilidades, como la colocación en los casquetes polares donde los residuos fueran hundiéndose progresivamente por efecto de la disolución del hielo debido al calor generado por los propios residuos fue también desechada, al igual que la inyección en sondeos muy profundos por su coste y por la dificultad de analizar su impacto ambiental futuro (Astudillo Pastor, 2001).

El potencial confinante de la geosfera se ha puesto de manifiesto en repetidas ocasiones, como en los yacimientos minerales, por ejemplo, donde acumulaciones explotables de diversas substancias (petróleo, gas, metales, etc.) han sido confinadas

durante millones de años sin contacto con la atmósfera en lugares que reúnen una serie de características geológicas, geoquímicas, estructurales e hidrogeológicas adecuadas. Con estas premisas, el almacenamiento geológico profundo (AGP) es la opción internacionalmente aceptada para la gestión final de este tipo de residuos radiactivos de alta actividad.

3. Almacenamiento Geológico Profundo de residuos nucleares

El concepto de AGP se basa en un sistema de almacenaje, formado por una combinación de barreras, tanto naturales como artificiales, para proporcionar un alto nivel de aislamiento de los desechos radiactivos de alta actividad durante largo tiempo. Se trata de aislar este tipo de residuos radiactivos disponiéndolos encapsulados en contenedores metálicos resistentes a la corrosión rodeados por una serie de materiales de relleno y sellado (considerados como barreras artificiales o de ingeniería) y colocados, a su vez, en un almacén subterráneo excavado normalmente a 500-1000m de profundidad en una formación geológica estable, llamada roca hospedante, que se considera como barrera natural (Stroes-Gascoyne *et al.* 2007a) y que se caracteriza por su alta estabilidad y su bajo flujo de agua subterránea (IAEA, 2003).

Los sistemas multibarrera del AGP están formados por tres tipos de barreras distintos, representados en la Figura 3:

- Barrera artificial o de ingeniería: se trata de todo el conjunto de barreras artificiales dispuestas para contener y aislar los residuos nucleares. Sus funciones principales son aislar los residuos del agua presente en la barrera geológica, aportar protección mecánica frente a eventos disruptivos o sísmicos y retardar la salida de estos materiales al exterior a largo plazo.

- Barrera natural o geológica: es el almacén natural donde se entierran los residuos. Se debe elegir adecuadamente con el fin de conseguir un entorno estable que mantenga a los residuos aislados del resto del medio en caso de que atravesaran las barreras de ingeniería (Savage and Chapman, 1982). La elección de la barrera geológica se hace en base a consideraciones de estabilidad físico-química, hidráulica, mecánica y geoquímica.

- Barrera biosférica: es la que limita con el medio ambiente. Se trata de los ecosistemas situados justo encima de la barrera geológica.

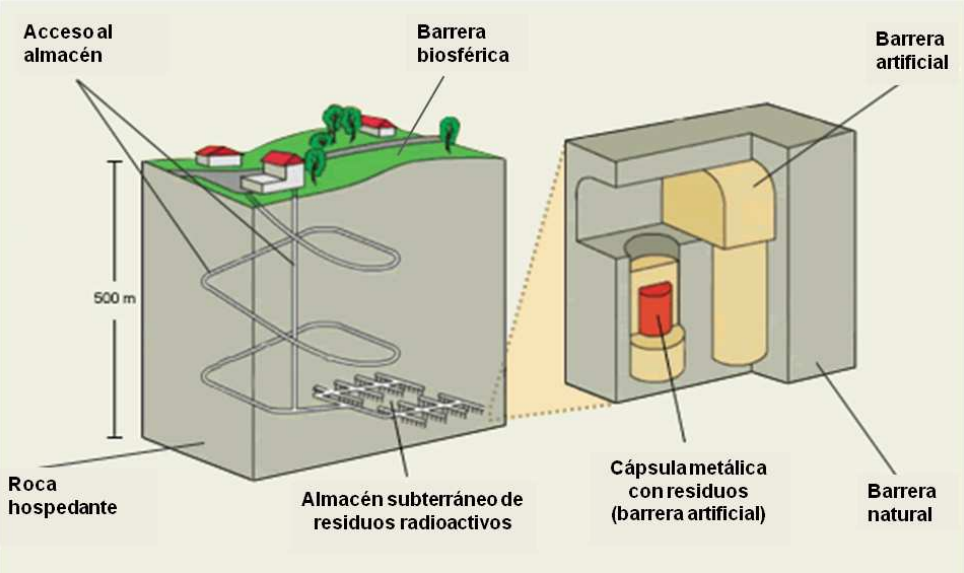

Figura 3. Esquema representativo de las distintas partes de un almacenamiento geológico profundo de residuos nucleares (modificado de Visaginas Nuclear Power Plant project).

Buscando la finalidad del AGP se han identificado distintos tipos de barreras artificiales y de barreras naturales. En el caso de las barreras artificiales se han seleccionado las bentonitas en países como Suecia, Finlandia o Canadá (Landais and Aranyossy, 2011) y el cemento en el caso de Reino Unido (NEA/CE, 2003). Como barrera natural, se han elegido tres posibles formaciones geológicas diferentes: rocas de granito, depósitos de sales y formaciones de arcillas, cuyas características reúnen los requisitos necesarios de seguridad, a largo plazo, para el almacenamiento de este tipo de residuos. Finlandia, Suecia o Canadá han optado por las formaciones de granito como roca hospedante (Stroes-Gascoyne and Sargent, 1998; Pedersen, 1999; Itavaara *et al*., 2011). Estados Unidos ha considerado la posibilidad de usar formaciones de sales (Fredrickson *et al*., 2004). Por otra parte, en otros países de Europa, como Suiza, Francia o Bélgica, la tendencia mayoritaria favorece el uso de depósitos de arcillas como formaciones geológicas estables para el confinamiento de residuos radiactivos (ONDRAF/NIRAS., 2001; Stroes-Gascoyne *et al*., 2007a; Wouters *et al*., 2013).

En el caso concreto de España, durante la década de 1990, se realizaron estudios geológicos sistemáticos por toda la geografía española, para comprobar la viabilidad de estos tres tipos de formaciones: granito, sales y arcilla (Astudillo Pastor, 2001; Zuloaga and Astudillo, 2012). Además, en el caso de las arcillas, se llevaron a cabo diversos estudios para la selección y caracterización de arcillas aptas como material de relleno y sellado (barreras artificiales) para almacenamientos de este tipo de residuos (Villar *et al*., 2006). En particular, se seleccionó el yacimiento arcilloso del Cortijo de Archidona, en el Parque Natural de Cabo de Gata (Almería), y la bentonita procedente de él ha sido objeto de diversas investigaciones, que dieron lugar a que esta bentonita sea una de las más intensamente caracterizadas en sus aspectos mineralógico, térmico, hidráulico, mecánico, geoquímico y de alterabilidad. Además, también se ha estudiado el comportamiento de esta bentonita, en condiciones similares a las de un almacenamiento, tanto a escala de laboratorio como natural, y la posible evolución de su comportamiento a largo plazo como barrera artificial (Villar *et al*., 2006).

Uno de los criterios más importantes a la hora de evaluar la seguridad de los AGPs de residuos radiactivos es determinar la capacidad de aislamiento para los distintos radionucleidos. Los riesgos asociados a este tipo de almacenamiento dependen tanto de la cantidad de elementos radiactivos almacenados, como de la seguridad de su inmovilización. En este sentido, se han llevado a cabo diversos estudios para determinar los efectos que pueden tener los procesos inorgánicos en la alteración de la roca hospedante considerada barrera natural, en la corrosión de las barreras artificiales que contienen los residuos radiactivos de alta actividad y en la movilidad de los radionucleidos desde los AGPs. Desafortunadamente, aún se conoce poco del papel que los microorganismos juegan en estos tres procesos.

4. Microbiología en los sistemas de Almacenamiento Geológico Profundo

El estudio de las comunidades microbianas en los sistemas de AGP de residuos radiactivos comenzó con la comprobación de que los microorganismos podían estar presentes en las formaciones geológicas consideradas para el almacenamiento de este tipo de residuos y de que los efectos de la actividad microbiana podían tener influencia sobre los procesos de contención de los mismos (West *et al*., 1982). Más tarde se presentaron pruebas concluyentes de la presencia de microorganismos vivos en

sedimentos muy antiguos (desde 16 millones hasta 111 millones de años), con una abundancia de más de 10^6 células/cm^3 en profundidades desde 400 m hasta 1.6 km del fondo marino (Schippers *et al*., 2005; Roussel *et al*., 2008). Este estudio tuvo una gran relevancia, ya que, por ejemplo, los ambientes marinos presentan una abundancia microbiana de 10^3-10^6 microorganismos/cm^3 (Whitman *et al*., 1998).

Además, estimaciones basadas en numerosas observaciones experimentales sugieren que más del 20% de los procariotas del planeta tierra se encuentran por debajo de los 200 m de la superficie de sedimentos terrestres y marítimos (Whitman *et al*., 1998). Posteriormente Pedersen (2002a) describió que la presencia de microorganismos podía llegar hasta profundidades de 500-1000 m, similares a las de los repositorios radiactivos planeados, corroborando las estimaciones de Whitman.

De las tres formaciones geológicas que han sido consideradas para el AGP de residuos radiactivos, la presencia de microorganismos y su biodiversidad en rocas de granito y depósitos de sales han sido estudiadas muy ampliamente (Itavaara *et al*., 2011; Pedersen, 2013). Sin embargo, en el caso de las formaciones geológicas de arcillas, su microbiología ha sido poco estudiada hasta ahora.

Debido a que las poblaciones microbianas son diversas y pueden ser únicas para un ambiente concreto, no se pueden aplicar los resultados anteriormente mencionados de los estudios de granitos y sales para los almacenes radiactivos de países como Suiza, Francia, Bélgica, que han optado por las formaciones arcillosas como formación geológica para el AGP de sus residuos de alta actividad. Por lo tanto, es necesario estudiar las comunidades microbianas que habitan en las formaciones arcillosas seleccionadas por cada país, e investigar los mecanismos de interacción de las mismas con los radionucleidos de mayor relevancia para los residuos radiactivos.

Algunos países europeos han llevado a cabo diversos estudios para obtener más información acerca de la viabilidad de la comunidad microbiana presente y de su actividad en ciertas formaciones arcillosas previamente seleccionadas, como la arcilla Opalinus de Suiza, la arcilla Boom de Bélgica y la arcilla Callovo-Oxfordian de Francia.

En el caso de Suiza, se hicieron excavaciones para construir un Laboratorio Subterráneo de Investigación (LSI) en la formación geológica arcillosa Opalinus, el Laboratorio Subterráneo Mont Terri (Fig. 4).

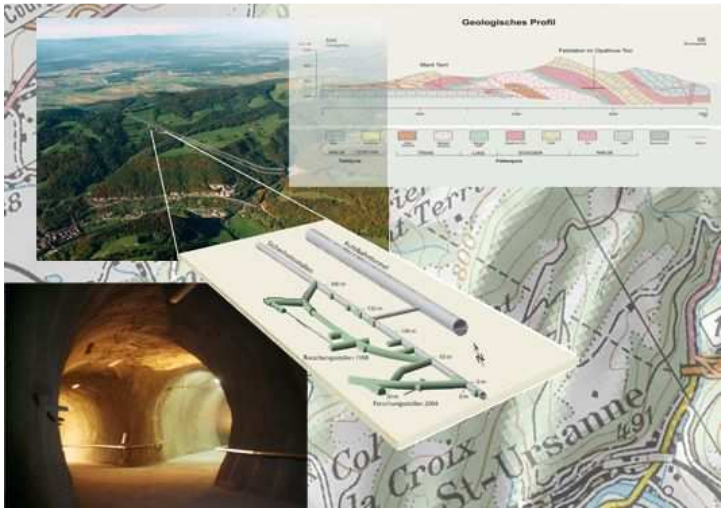

Figura 4. Instalaciones del Laboratorio Subterráneo de Investigación Mont Terri, en la formación geológica arcillosa Opalinus, Suiza (http://www.swisstopo.admin.ch/).

Desde el año 1995 este LSI ha estado en funcionamiento para analizar las propiedades hidrogeológicas, geoquímicas y mecánicas de esta formación. La arcilla Opalinus es una formación de esquisto del Mesozoico formada hace 180 millones de años, donde se ha detectado la presencia de microorganismos viables, aproximadamente de 10^5-10^6 células viables por gramo de arcilla, aunque metabólicamente casi inactivos o en estado de latencia (Stroes-Gascoyne *et al*., 2007b). La población microbiana está formada mayoritariamente por microorganismos, tanto bacterias como arqueas, sulfato reductores, nitrato reductores y metanógenos (Stroes-Gascoyne *et al*., 2011). Además, se han aislado e identificado, entre otros microorganismos, *Pseudomonas stutzeri*, *Bacillus licheniformis*, especies de *Desulfosporosinus*, *Hyphomonas*, *Sphingomonas* y *Alicyclobacillus*, entre otros (Poulain *et al*., 2008; Stroes-Gascoyne *et al*., 2011; Wersin *et al*., 2011).

Los depósitos de arcilla Boom, en Bélgica, son el resultado de un proceso de sedimentación marina que ocurrió hace 35 millones de años. A 224 metros de profundidad, en esta formación arcillosa belga, hay una galería de una antigua mina, que está siendo utilizada para estudiar la diversidad microbiana de esa formación geológica

seleccionada como barrera natural para el AGP de residuos radiactivos. La porosidad de la arcilla Boom es menor que el tamaño estimado de las bacterias, lo que dificulta el análisis de las muestras que contienen una pequeña proporción de bacterias activas metabólicamente. El mayor número de células viables se ha encontrado en condiciones aerobias, poniendo de manifiesto que hay una disminución de la densidad bacteriana cuanto mayor es la distancia hasta la galería minera (Boivin-Jahns *et al*., 1996). Recientemente se ha estudiado la diversidad y actividad microbiana en aguas de poro de las arcillas Boom, encontrando una comunidad bacteriana representada por siete filos, *Proteobacteria*, *Actinobacteria*, *Chlorobi*, *Firmicutes*, *Bacteroidetes*, *Chloroflexi* y *Spirochaetes*, incluyendo géneros bacterianos tanto aerobios como anaerobios (Wouters *et al*., 2013). Además, una amplia fracción de esta comunidad era activa y cultivable, a pesar de que en unas condiciones tan austeras como las de la arcilla Boom, lo predecible sería encontrar una gran cantidad de microorganismos no cultivables (Breuker *et al*., 2011).

En el LSI de Meuse/Haute-Marne, situado en Bure, a 300 km al este de Paris, en Francia, se está evaluando el uso de la formación de argilita Callovo-Oxfordian (Cox) como roca hospedante para el AGP de residuos de alta actividad. La formación arcillosa Callovo-Oxfordian se encuentra a una profundidad de entre 420 y 550 m rodeada por la parte superior y posterior por formaciones de carbonatos de baja permeabilidad. Una de las mayores preocupaciones en la construcción del almacén es la aparición de fracturas provocadas por la excavación y que pueden crear caminos para el agua subterránea, facilitando la migración de los radionucleidos (Armand *et al*., 2014). Análisis microbiológicos revelaron que la diversidad en las arcillas Callovo-Oxfordian es mayor de lo que se esperaba, con respecto a previos estudios realizados en formaciones arcillosas, como los anteriormente descritos (Urios *et al*., 2012). La diversidad microbiana en la arcilla francesa varía en función del contenido en oxígeno y en humedad, aunque probablemente también se vea afectada por la disponibilidad de espacio. En el estudio microbiológico llevado a cabo por Urios *et al*. (2012) se identificaron bacterias aerobias y anaerobias heterótrofas en todas las zonas de la formación arcillosa, como bacterias Gram-positivas pertenecientes a los filos *Firmicutes* (*Bacillus* y *Staphylococcus*) y *Actinobacteria* (*Propionibacterium acnes*, *Leucobacter*, *Microbacterium* y *Citricoccus*). Y algunos generos Gram-negativos, incluyendo bacterias de los filos *Proteobacteria* y *Bacteroidetes*. Sin embargo, solamente en las

zonas más húmedas de la falla se aislaron Bacterias Sulfato Reductoras (BSR) como *Desulfotomaculum* y *Clostridium*.

Además, en trabajos como los de Deniau *et al*. (2008) se han comparado geoquímicamente las arcillas Callovo-Oxfordian y Boom, de Francia y Bélgica respectivamente. También se han realizado estudios sobre la estabilidad y la longevidad de bentonitas en distintos ambientes (Cuevas *et al*., 1997; Cama *et al*., 2000; Ramírez *et al*., 2002). Debido a que la difusión es el principal mecanismo de transporte de los radionucleidos en los materiales arcillosos, la determinación de los coeficientes de difusión en condiciones lo más similares posibles a las del AGP están siendo estudiadas en algunas arcillas, como la Opalinus y la Callovo-Oxfordian (Cormenzana *et al*., 2008).

5. Efecto de la actividad microbiana en las condiciones del AGP

El estudio de la diversidad microbiana en los AGP de residuos radiactivos de alta actividad en formaciones arcillosas es de gran relevancia para identificar las propiedades de seguridad que se pueden ver afectadas por la influencia de la actividad microbiana. En general, los microorganismos pueden afectar las condiciones de estabilidad del almacén mediante tres procesos principales:

1) Transformación de los minerales de las arcillas:

Pueden verse afectadas 8 propiedades esenciales de la arcilla para mantener las funciones de contención del sistema de almacenaje, que son: el aumento de la presión, la superficie específica total, la capacidad de intercambio catiónico, la capacidad de sorción de aniones, la porosidad, la permeabilidad, la presión de los fluidos y la plasticidad (De Craen *et al*., 2008; SKAB, 2011).

2) Degradación de los contenedores metálicos:

Los contenedores metálicos que albergan los residuos radiactivos pueden ser de metal fundido, como aleaciones de titanio o níquel, de acero al carbón o de acero inoxidable (Astudillo Pastor, 2001; Smart, 2009) y pueden verse gravemente afectados por la actividad microbiana en las arcillas (Smart, 2009; Stroes-Gascoyne *et al*., 2011).

3) Movilización de radionucleidos.

Debido a los diferentes procesos que pueden ocurrir entre los microorganismos y los radionucleidos, como la alteración de la química del agua de poro (particularmente el pH y el Eh), la producción de agentes complejantes orgánicos o la acumulación de estos elementos en la superficie o/y citoplasma celular, los microorganismos juegan un papel importante en la movilidad y transporte de los radionucleidos desde los depósitos de residuos radiactivos al medio ambiente (West *et al*., 2002).

5.1 Transformación microbiana de minerales de las arcillas

Hace ya casi 30 años que se observó la primera interacción redox entre bacterias y minerales de arcilla. Fueron Stucki y Getty en 1986, los primeros en demostrar la influencia de los microorganismos en el estado de oxidación del hierro (Fe) estructural en las esmectitas.

Hoy en día se sabe que el metabolismo microbiano está principalmente controlado por las reacciones químicas de oxidación-reducción del Fe en la mayoría de los ambientes naturales (Weber *et al*., 2006). Además, el suelo contiene una gran variedad de microorganismos endémicos capaces de mantener su metabolismo reduciendo el Fe(III) estructural de los minerales de arcilla (como la montmorillonita, la nontronita, la ilita, la clorita o la biotita), lo que repercute en las propiedades físicas y químicas del suelo, que pueden ser alteradas (Dong *et al*., 2009; Pentrakova *et al*., 2013).

Es importante remarcar que la habilidad de reducir el Fe(III) de los minerales no está limitado a los microorganismos que usan exclusivamente Fe(III), como aceptor final de electrones, sino también a los microorganismos sulfato-reductores o a los productores de metano. En cualquier caso, estas condiciones pueden influenciar negativamente la seguridad del AGP, si se usan arcillas como barrera natural o artificial, ya que alteran las propiedades de la superficie de los minerales de arcilla, aumentando la presión, afectando a la energía de hidratación y al área de su superficie específica (Lear and Stucki, 1989; Stucki and Lear, 1989; Stucki *et al*., 2002), además de que al incrementar tanto la capacidad de intercambio de cationes se favorece la fijación de estos, poniendo en peligro la seguridad de la instalación (Meleshyn, 2011).

Los procesos microbianos de disolución y reducción de minerales de las arcillas están estrechamente relacionados entre ellos, ya que los dos están motivados por la demanda de Fe(III) como aceptor final de electrones (Meleshyn, 2011). La reducción microbiana de Fe(III) ha sido descrita por Jaisi *et al*. (2008) como un posible mecanismo para liberar Fe(II) de la estructura del mineral, como por ejemplo de la esmectita. Sin embargo, el aumento en la liberación de Fe(II) y su biosorción en los minerales de la arcilla, disminuye la reducción del hierro estructural de los minerales y por lo tanto su disolución, ya que el Fe(II) sorbido puede bloquear la cadena de electrones desde el microorganismo hasta la superficie del mineral (Jaisi *et al*., 2007), así pues, la transferencia de electrones entre el Fe(II) sorbido y el Fe(III) estructural, permite la reducción microbiana directa de los óxidos secundarios de Fe(III) en lugar del mineral de la arcilla (Schaefer *et al*., 2011).

La ilita formada como consecuencia de la disolución de Fe(II) estructural, como por ejemplo de esmectita, de caolinita, de mica o feldespato potásico de las bentonitas, precipita de forma directa de la solución en el espacio entre poros (Nadeau *et al*., 2002). Además, la reducción microbiana y la extracción de Fe estructural de los minerales de arcillas permiten, simultáneamente, la liberación y precipitación de sílice en los espacios entre poros (Vorhies *et al*., 2009). Por lo tanto, la disolución microbiana de minerales de arcilla puede afectar negativamente la seguridad del AGP al disminuir tanto la porosidad como la permeabilidad de la arcilla (Meleshyn, 2011).

Se han propuesto tres mecanismos primarios para explicar la transferencia de electrones al Fe(III) incorporado en la estructura del mineral arcilloso: a) el contacto directo entre el microorganismo y el mineral; b) la producción endógena o el uso exógeno de transportadores de electrones solubles; y c) la producción de ligandos quelantes (sideróforos) para facilitar la disolución del mineral al aportar Fe(III) soluble, o el uso de compuestos quelantes exógenos (Meleshyn, 2011):

a) Hay dos modos de contacto directo microorganismo-mineral:

- el primero requiere una aproximación muy cercana del microorganismo a la superficie del mineral, de forma que la transferencia de electrones ocurre via metaloproteínas asociadas a la membrana celular

- el segundo requiere la formación de apéndices extracelulares por parte del microorganismo en respuesta a la limitación de aceptores de electrones (O_2) (El-Naggar *et al*., 2010).

b) Producción endógena o uso exógeno de transportadores de electrones solubles:

Los microorganismos son capaces de reducir los transportadores de electrones exógenos solubles, que difunden hasta la superficie del mineral, donando los electrones al Fe(III) estructural. La ausencia de transportadores de electrones exógenos es superada por los microorganismos a través de la producción de transportadores de electrones endógenos, como la flavina mononucleótido (FMN) y la riboflavina (Von Canstein *et al*., 2008).

c) Uso de compuestos quelantes (sideróforos) exógenos o producción de ligandos quelantes para facilitar la solubilización del Fe(III):

El uso de compuestos orgánicos exógenos como oxalato, citrato o malato, facilita la disolución microbiana del Fe(III). Sólo en presencia de microorganismos estos ácidos orgánicos de bajo peso molecular, agentes quelantes débiles del Fe(III), son capaces de solubilizar el Fe(III) de la esmectita (Meleshyn, 2011).

5.2 Degradación microbiana de los contenedores metálicos

Los microorganismos son capaces de degradar compuestos orgánicos que pueden formar parte del material del contenedor metálico de los residuos nucleares o de los propios desechos, afectando a la duración del metal en el almacén subterráneo (Said *et al*., 1991; Stroes-Gascoyne *et al*., 2011). El comportamiento corrosivo depende de la combinación de las propiedades de corrosión del metal utilizado en el AGP y de la corrosividad del medio ambiente que lo rodea (Landolt *et al*., 2009).

La corrosión del contenedor metálico influenciada por los microorganismos a nivel anaerobio es llevada a cabo, principalmente por bacterias sulfato-reductoras (BSR), mediante los siguientes mecanismos: mediante un ataque indirecto del ácido sulfhídrico (SH_2); por adsorción de polímeros microbianos extracelulares entre el metal y la interfase del agua; mediante el uso de átomos de hidrógeno acumulados en la

superficie del metal como resultado de la corrosión; y la absorción de electrones metálicos por parte de la célula microbiana (Meleshyn, 2011).

La reducción microbiana de Fe(III) o de sulfato, descrita en los apartados anteriores, conlleva el posible consumo o producción de gases por parte de los microorganismos, que son capaces de utilizar compuestos orgánicos para obtener la energía suficiente para llevar a cabo estos dos procesos, produciendo CO_2. En ausencia o limitación de compuestos orgánicos, los microorganismos pueden usar también el H_2 como donador de electrones, para la reducción del Fe(III) o de sulfato. Actualmente se ha reconocido que el H_2 producido como resultado de la corrosión de Fe es el gas más importante a la hora de evaluar la integridad técnica de las barreras y de la roca en el AGP de residuos nucleares en arcillas (Meleshyn, 2011).

La reducción microbiana de Fe(III) o de sulfatos provoca la producción de gases (H_2, CH_4, CO_2, SH_2) o su consumo (H_2, CH_4, CO_2). Hay tres procesos microbianos de gran importancia en la producción/consumo de gases: a) la fermentación, b) la producción anaeróbica de metano y c) la oxidación anaeróbica de metano en un AGP de residuos radiactivos (Meleshyn, 2011).

a) <u>Fermentación</u>

La fermentación es un proceso metabólico que no utiliza aceptores de electrones externos para la oxidación de compuestos orgánicos, dando como resultado compuestos reducidos como el acetato, formiato e H_2 y oxidados, como el CO_2 (McMahon *et al*., 1992).

Ejemplo de fermentación de la glucosa (Thauer *et al*., 1977):

$$C_6H_{12}O_6 + 2\mathbf{H_2O} \longrightarrow 2CH_3COOH + 2CO_2 + 4H_2$$

b) <u>Producción anaeróbica de metano</u>

La metanogénesis o producción de metano por microorganismos estrictamente anaerobios se produce principalmente a través de:

i) la reducción de CO_2, obteniendo los electrones de la oxidación del H_2, del formiato o del CO:

$$4H_2 + \mathbf{CO_2} \longrightarrow CH_4 + 2H_2O$$
$$4\mathbf{HCO_2H} \longrightarrow CH_4 + 3CO_2 + 2H_2O$$
$$4\mathbf{CO} + 2H_2O \longrightarrow CH_4 + 3CO_2$$

ii) la fermentación de acetato, oxidando el grupo carboxilo hasta CO_2 para aportar los electrones necesarios para la reducción del grupo metilo hasta metano:

$$\mathbf{CH_3COO^-} + H^+ \longrightarrow CH_4 + CO_2$$

iii) y la fermentación de metanol o metilaminas, mediante los electrones obtenidos de la oxidación de grupos metilo o H_2:

$$4\mathbf{CH_3OH} \longrightarrow 3CH_4 + CO_2 + 2H_2O$$

c) Oxidación anaeróbica de metano

Los organismos anaeróbicos metanotróficos obtienen la energía de utilizar metano como donadores de electrones y sulfato, nitrato, nitrito, Mn (IV) o Fe(III) como aceptor de electrones para convertir metano en CO_2.

Ejemplos para el caso del hierro y el sulfato:

$CH_4 + 8\mathbf{Fe}(OH)_3 + 15H^+ \longrightarrow HCO_3^- + 8Fe^{2+} + 21H_2O$ (Beal *et al*., 2009)

$CH_4 + \mathbf{SO_4^{2-}} \longrightarrow HCO_3^- + HS^- + H_2O$ (Knittel and Boetius, 2009)

El aumento o disminución de estos gases en el AGP de residuos radiactivos de alta actividad genera una sobrepresión de gas, provocada por la desigualdad entre la difusión y la producción de gases, que puede inducir la formación de fracturas en la roca de arcilla (Nagra, 2002; Ortiz et el., 2002; Glass and Orthan, 2012).

La corrosión del acero en las condiciones anaerobias de la arcilla Opalinus, por ejemplo, permite la liberación de H_2 desde la superficie del contenedor metálico hacia la arcilla. El transporte de H_2 a lo largo de la barrera geológica debe ocurrir sin causar daños irreversibles en la arcilla, que puedan crear nuevas rutas de escape de los

productos radiactivos desde el depósito (Landolt *et al*., 2009). Los mecanismos de transporte de gases más importantes para el caso del AGP de residuos nucleares en la formación de arcilla Opalinus son tres (Johnson *et al*., 2004):

a) Difusión y advención de gases disueltos en el agua de poro
b) Flujo de gases basado en la visco-capilaridad
c) Dilatación, controlada por el flujo del gas

5.3 Movilización microbiana de radionucleidos

Actualmente, se está considerando la gran importancia del efecto de los procesos microbianos en el transporte de los contaminantes inorgánicos radiactivos, ya que los microorganismos viven tanto en condiciones aerobias como anaerobias. Las interacciones metal-microorganismo, representadas en la Figura 5, pueden clasificarse en cinco grandes grupos: mecanismos de biosorción, bioacumulación, biomineralización, biotransformación (por oxidación o reducción) y quelación (Gadd, 2000).

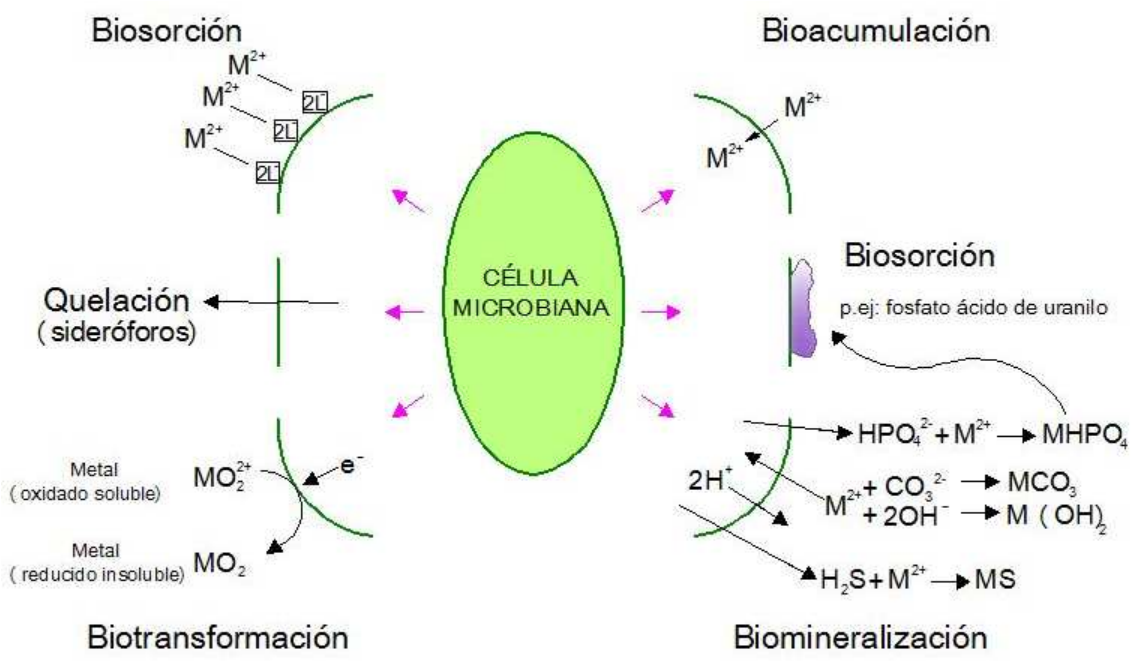

Figura 5. Mecanismos de interacción entre radionucleidos y microorganismos (modificado de Lloyd and Macaskie, 2002).

A. Biosorción

El término biosorción hace referencia a los fenómenos de adsorción y absorción de radionucleidos a biomasa, independientemente del metabolismo. (Lloyd and Macaskie, 2002). La adsorción es la acumulación en la superficie celular del radionucleido mediante procesos electrostáticos; mientras que la absorción es el paso uniforme de átomos o moléculas del radionucleido en solución, a la célula microbiana (Merroun and Selenska-Pobell, 2008).

Tanto la biomasa viva como la inerte, son capaces de adsorber y absorber radionucleidos debido a la presencia de diferentes grupos funcionales con cierta afinidad por estos elementos. Los grupos funcionales que participan en los fenómenos de biosorción son carboxilo, amino, hidroxilo, fosfato y sulfhidrilo (Lloyd and Macaskie, 2002). En el caso de las bacterias Gram negativas, estos grupos, principalmente fosfatos, se encuentran localizados a nivel Lipopolisacárido (LPS), en la membrana externa de la célula (Barkleit *et al*., 2008).

Un ejemplo de sorción de U(VI) lo encontramos en un aislado natural de una zona de residuos de una mina de uranio en Alemania. Las células de *Bacillus sphaericus* JG-A12 están envueltas en una capa proteica, la capa S, que tiene la habilidad de fijar uranio y otros metales pesados, mediante grupos carboxilo y fosfato, formando depósitos a nivel de la superficie celular (Merroun *et al*., 2005). Otros ejemplos son los que se muestran en la Figura 6.

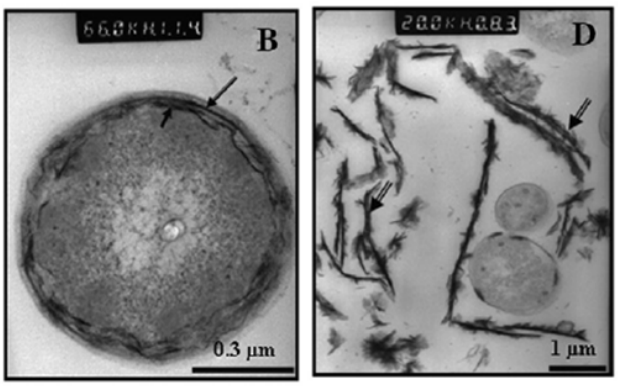

Figura 6. Ejemplo de biosorción de uranio en las células de (B) *Bacillus sphaericus* JG-7B and (D) *Pseudomonas stutzeri* DSMZ 5190 (Merroun and Selenska-Pobell, 2008).

Recientemente se ha descrito el proceso de biosorción de U(VI) por parte de *Paenibacillus* sp. MT-2.2, un aislado de la arcilla suiza Opalinus, capaz de fijar uranio con grupos fosfato o carboxílicos en función del pH (Lütke *et al*., 2013).

Sin embargo, el proceso de biosorción de metales pesados no se da exclusivamente en células bacterianas, sino también en hongos y levaduras (Wang and Chen, 2009). Por ejemplo, diversas especies de la levadura *Rhodotorula* han sido descritas por su tolerancia al uranio, como *R. mucilaginosa* (de Silóniz *et al*., 2002) o por su capacidad de biosorción en el caso de *R. glutinis* (Bai *et al*., 2012). Además, uno de los últimos casos descritos en la bibliografía corresponde al hongo *Schizophyllum commune*, capaz de formar fosfatos de uranilo orgánicos e inorgánicos (Fig. 7), en función de la concentración inicial de uranio y en algunos casos del pH, tanto a nivel intracelular como extracelular (Günther *et al*., 2014).

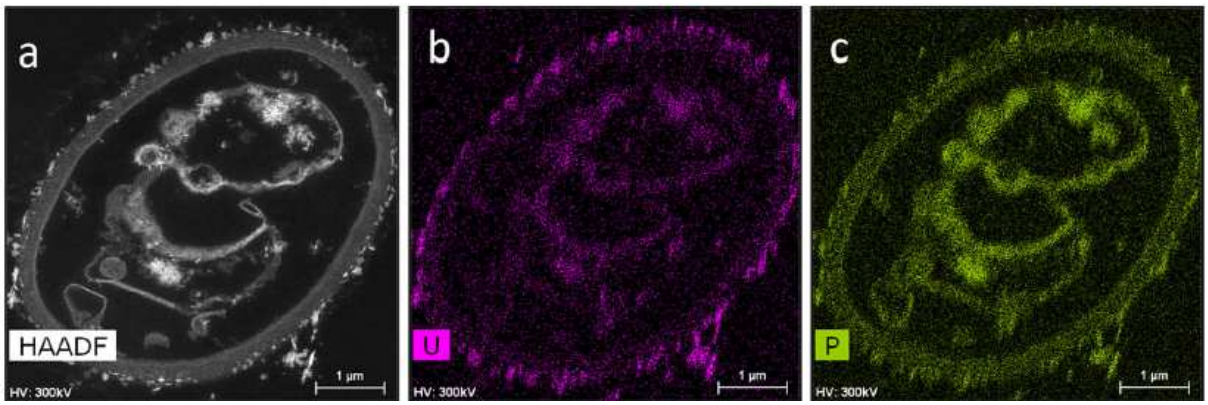

Figura 7. Ejemplo de biosorción de U(VI), como fosfatos de uranilo, por células fúngicas de *Schizophyllum commune* (Günther *et al*., 2014).

Sin embargo, a pesar de la gran cantidad de estudios realizados sobre la biosorción, no hay apenas aplicaciones industriales que utilicen esta herramienta de bio-remediación para ambientes contaminados (Gadd, 2009).

B. Bioacumulación: acumulación intracelular

La bioacumulación es el proceso de incorporación e inmovilización de metales por células vivas, en el interior celular (Vijayaraghavan, 2009). Los metales penetran en la célula a través de transportadores de membrana y, una vez en el interior celular, son secuestrados por diferentes componentes o incluso incluidos en vacuolas (Lloyd and Macaskie, 2002).

En el caso del uranio, se ha descrito esporádicamente su acumulación intracelular, pero aún se desconocen los mecanismos por los cuales se produce el paso al interior celular. Este fenómeno podría estar asociado a un incremento en la permeabilidad de la membrana, llevado a cabo mediante un proceso independiente del metabolismo (Merroun *et al*. 2002), o debido a daños en la integridad de la membrana celular provocados por la toxicidad del uranio (Merroun and Selenska-Pobell, 2008), como se muestra en la Figura 8.

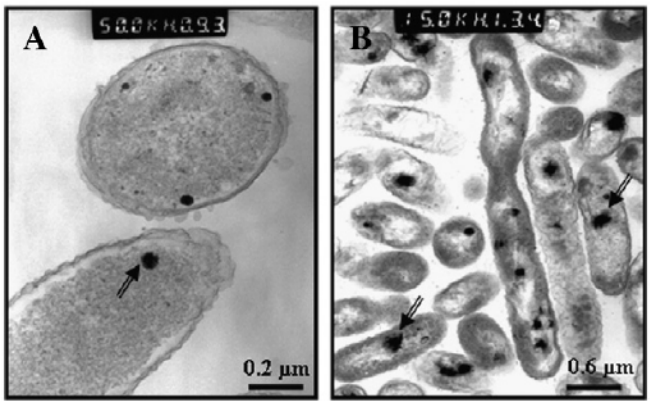

Figura 8. Ejemplo de acumulación intracelular de U(VI) por células de (A) *Pseudomonas migulae* y (B) *Stenotrophomonas maltophilia* JG-2 (Merroun and Selenska- Pobell, 2008).

Se han propuesto varios mecanismos para explicar la acumulación intracelular del uranio. Uno de los procesos mejor estudiados es la quelación del metal en forma de gránulos de polifosfato inorgánicos, que son polímeros lineales con residuos de fosfato inorgánico (Merroun *et al*, 2002). Este proceso ha sido observado en diferentes tipos de bacterias, aisladas de lugares contaminados por metales pesados (Keasling and Hupf, 1996) y se trataría de un fenómeno de tolerancia pasiva ante la toxicidad de los metales pesados presentes en el medio (Merroun *et al*., 2003a, b; Merroun *et al*., 2006).

C. Biomineralización (precipitación)

La biomineralización es un proceso a través del cual los microorganismos precipitan metales pesados mediante la producción de ligandos generados enzimáticamente, tales como fosfatos, sulfatos, carbonatos, oxalatos, etc. (Lloyd and Macaskie, 2002), o bien mediante la alcalinización localizada en la superficie celular, generando carbonatos e hidróxidos (Merroun and Selenska-Pobell, 2008). Este proceso de biomineralización se inicia con una interacción estequiométrica entre el ión metálico y los ligandos reactivos en la superficie de la pared de la célula, lo que reduce la barrera energética para la formación de complejos de metal adicionales y favorece, a su vez, la precipitación del metal. Los iones metálicos disponibles en solución dictan la composición química del precipitado (Kalin *et al*. 2004). En condiciones aerobias, la precipitación de uranio se produce principalmente en forma de fosfatos de uranio, como meta-autunita. Este proceso está mediado por la actividad enzimática de fosfatasas ácidas o alcalinas (Nilgiriwala *et al*., 2008; Merroun *et al*., 2011; Reitz *et al*., 2014) y se considera un mecanismo de detoxificación microbiana ante este metal pesado. Aunque Benzerara *et al*. (2011) ponen de manifiesto la contradicción entre algunos estudios como los referidos anteriormente y otros, en los que se asume el proceso de biomineralización de metales como perjudicial para las células.

Recientemente se ha descrito la biomineralización en forma de fosfatos de uranio como la mejor estrategia de biorremediación en ambientes contaminados con este radionucleido (Newsome *et al*., 2014). Y se ha observado que las células microbianas de un suelo con alto contenido en uranio (Fig. 9) estaban completamente cubiertas de minerales de fosfatos de uranio, sugiriendo el proceso de precipitación bacteriana como un mecanismo natural en este sistema (Mondani *et al*., 2011).

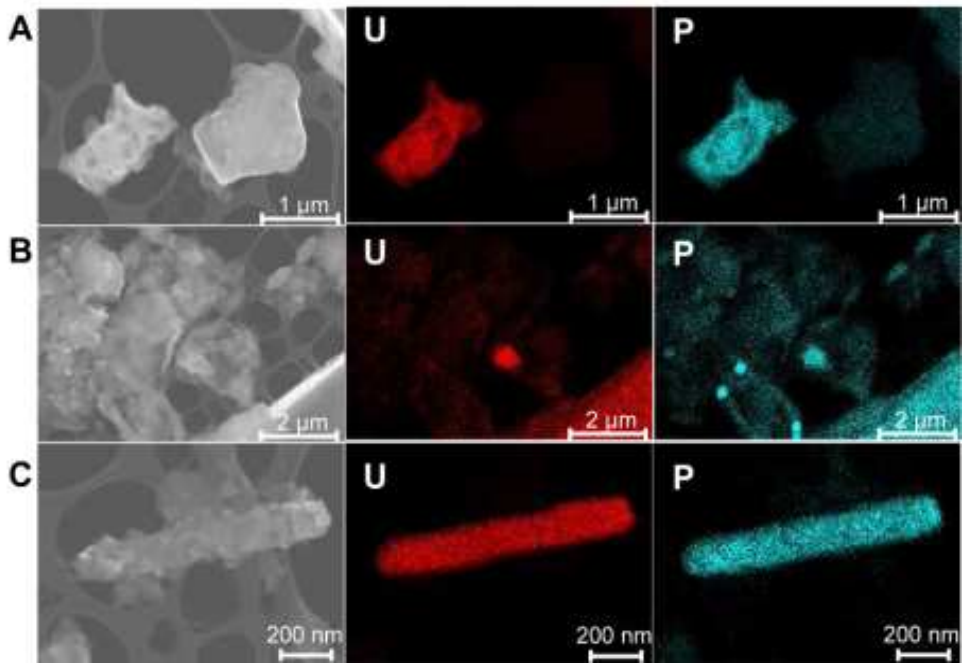

Figura 9. Ejemplo de precipitación de uranio por las células bacterianas de suelo (Mondani *et al*., 2011).

También se ha descrito la bioprecipitación de U(VI) en el caso de levaduras, como *Saccharomyces cerevisia*e, cuyas células vivas (Ohnuki *et al*., 2005a) y muertas (Lu *et al*., 2013) son capaces de precipitar fosfatos de uranio en la pared celular (Fig. 10). Además, previamente Liu *et al*. (2010) describieron que el crecimiento de *S. cerevisia*e no se veía especialmente afectado a concentraciones de uranio inferiores a 300 mg/l, poniendo así de manifiesto su alta tolerancia a este radionucleido.

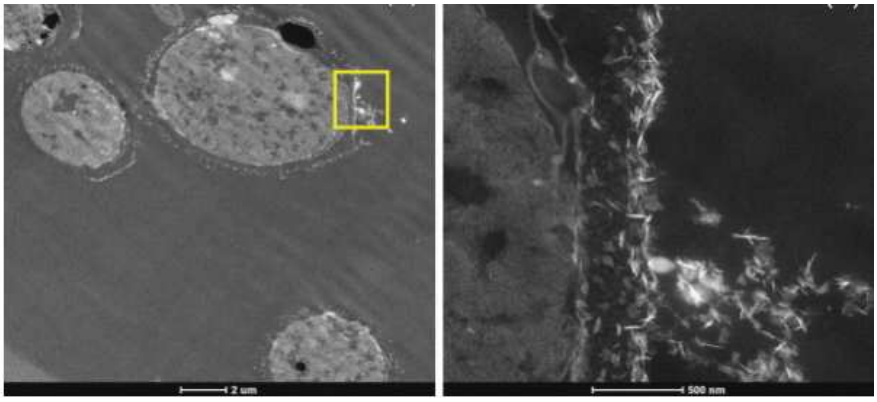

Figura 10. Ejemplo del proceso de biomineralización de U(VI) en células muertas de la levadura *Saccharomyces cerevisia*e (Lu *et al*., 2013).

D. Biotransformación

Los procesos de biotransformación son aquellos en los que el metal se reduce o se oxida como consecuencia de la actividad microbiana de tipo enzimático. Los fenómenos de oxidación-reducción llevan consigo un cambio en la especiación del metal, que suele ir asociada con un cambio en la solubilidad del mismo.

D.1 Biotransformación por oxidación

En el caso del uranio, la movilización se produce por oxidación de U(IV) a U(VI) lo que provoca un aumento en la solubilidad de este radionucleido, aumentando así su toxicidad. La oxidación de U(IV) mediada por microorganismos se ha descrito en diversas ocasiones (Finneran *et al*., 2002; Beller, 2005). La oxidación de U(IV), que suele encontrarse en forma de uraninita (UO_2), hace al uranio más soluble (Lovley and Phillips, 1992; Suzuki *et al*., 2002).

D.2 Biotransformación por reducción

El proceso de reducción de radionucleidos se traduce en su inmovilización, debido a una reducción de su solubilidad. Esta reducción se debe a que los propios radionucleidos actúan como aceptores finales de electrones en procesos de respiración bacteriana (Lloyd and Macaskie, 2002).

En el caso del uranio, la reducción de U(VI), generalmente forma de ión uranilo, (UO_2^{2+}), a U(IV) la realizan BSR (por ejemplo especies del género *Desulfovibrio*), fermentadoras (especies del género *Clostridium*) y reductoras de Fe(III) (*Geobacter metallireducens* y *Shewanella putrefaciens*) (Shelobolina *et al*., 2008; Merroun and Selenska-Pobell, 2008) (Fig. 11). Este mecanismo de reducción de U(VI) a U(IV) ha sido propuesto como una estrategia para prevenir la migración de este elemento tóxico en aguas subterráneas (Joeng *et al*., 1997).

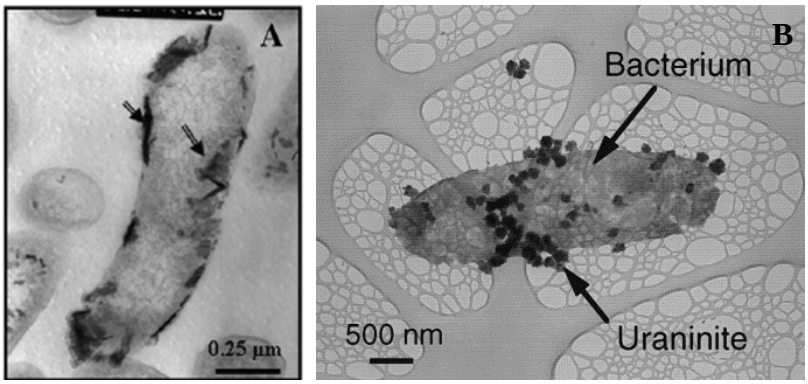

Figura 11. Ejemplos de reducción de uranio a uraninita a nivel intracelular por células de (A) *Desulfovibrio äspönensis* (Merroun and Selenska-Pobell, 2008) and (B) a bacterium (Abdelouas *et al*., 1998)

La biorreducción de uranio es ampliamente utilizada como herramienta de bioremediación en ambientes contaminados, pero el uranio que se bioreduce puede volver a ser movilizado en determinadas condiciones geoquímicas de pH, e incluso reoxidarse a U(VI) en presencia de oxígeno, nitrato, Fe(II) y ácidos húmicos, revirtiendo los efectos beneficiosos de este proceso (Wang *et al*. 2013; Singh *et al*. 2014). Así pues, este mecanismo de inmovilización de uranio presenta ciertas desventajas en comparación con la bioprecipitación, descrita anteriormente, principalmente debido a la versatilidad de este último proceso, que puede ocurrir tanto en condiciones aerobias como anaerobias y por la estabilidad química y física a largo plazo de las especies de uranio formadas (Martinez *et al*., 2014).

E. Quelación

Los microorganismos también pueden influir en la movilización de radionucleidos mediante la liberación de sideróforos (Kalinowski *et al*., 2006), ácidos orgánicos como citrato u oxalato (Brandl *et al*., 1999) y la formación de complejos estables que hacen más soluble a dichos elementos, generalmente mediante el proceso de lixiviación.

En Moll *et al*. (2008), se describió la interacción entre curio, Cm(III), y una especie de desferrioxamina B, que es un sideróforo del tipo de los hidroxamatos que se encuentra de forma ubicua en la naturaleza. Este agente quelante, producido por la

bacteria *Pseudomonas*, mostró su capacidad de movilizar el Cm(III) formando complejos solubles en este estudio.

5.4 Resumen

Según lo descrito hasta ahora, los microorganismos reductores de Fe(III), sulfato reductores, fermentadores, productores de metano y oxidadores de metano están presentes en cualquiera de las formaciones de arcilla que se utilizarán, tanto como barrera natural como artificial, en el AGP de residuos radiactivos de alta actividad (Meleshyn, 2011).

Por lo tanto, se puede concluir que las arcillas estudiadas para su uso en el AGP contienen donadores y aceptores de electrones en cantidad suficiente para que los microorganismos se mantengan activos, aunque sea en un estado metabólico muy bajo, durante largos periodos de tiempo (Pentrakova *et al*., 2013). Otras fuentes adicionales de donadores y aceptores de electrones serán añadidos de forma inevitable al sistema de almacenamiento durante la excavación del AGP (Meleshyn, 2011).

En la Figura 12 se muestra un esquema de las posibles fuentes donadoras y aceptoras de electrones en el caso del AGP en arcillas y de los productos del metabolismo microbiano más importantes para su uso a largo plazo.

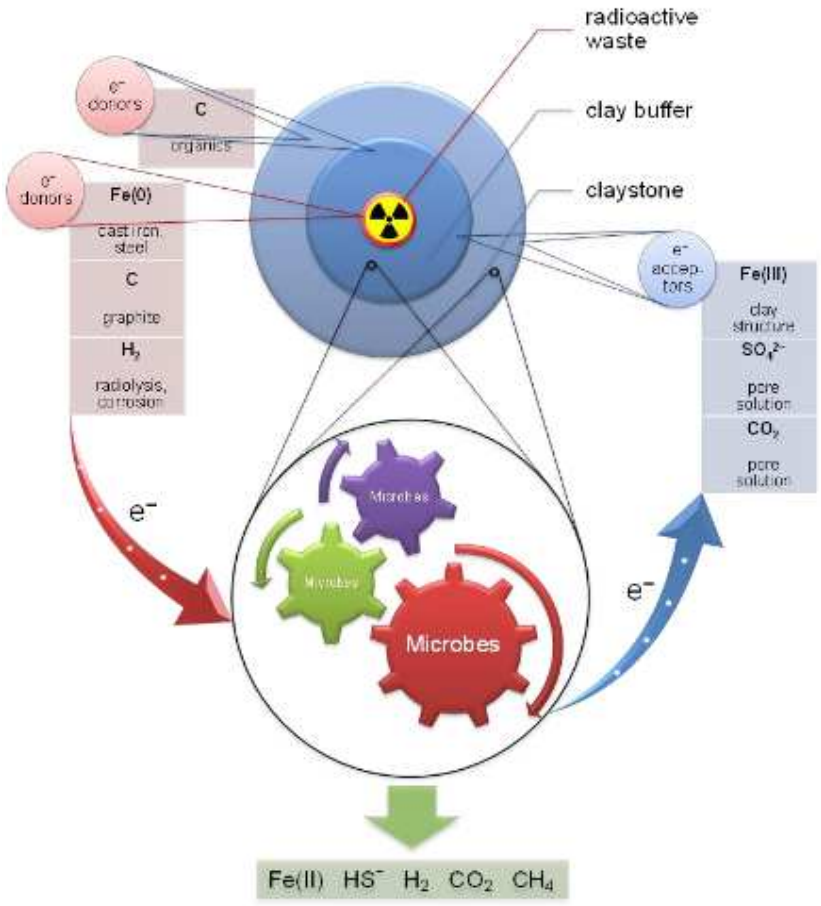

Figura 12. Representación esquemática de las fuentes de donadores y aceptores de electrones para la actividad microbiana en AGP en arcillas y de los productos del metabolismo microbiano más importantes para su uso a largo plazo (modificado de Meleshyn, 2011).

6. Bentonitas de Cabo de Gata, Almería

Los afloramientos volcánicos de la región de Cabo de Gata son parte de un área volcánica muy extensa y mayoritariamente sumergida bajo el Mar de Alborán. La mayor parte de los afloramientos no sumergidos se encuentran al sureste de las provincias de Almería y Murcia, en la Isla de Alborán y en el norte de África. El origen de estas rocas volcánicas está asociado con la dinámica geotectónica de la parte oeste del Mar Mediterráneo durante el Neógeno (Caballero *et al*., 2005), formadas en dos etapas de actividad volcánica, una hace aproximadamente 14 a 10 millones de años y otra hace 9 a 7,5 millones de años, es decir, Mioceno Medio y Superior. En la Figura 13

se muestra el complejo volcánico de Cabo de Gata en el contexto del Mar de Alborán (Fernández Soler, 2007).

Figura 13. Complejo volcánico de Cabo de Gata en el contexto del Mar de Alborán (Fernández Soler, 2007).

La especial composición del complejo volcánico de Cabo de Gata hace que en su interior se desarrolle la mayor concentración de yacimientos de bentonitas de España. La bentonita es una roca compuesta por minerales del grupo de las arcillas. Su principal característica se debe a que su estructura interna está formada por láminas superpuestas de diferente composición química, que favorecen que sean capaces de absorber líquidos en un volumen varias veces superior al suyo propio. Esta característica se produce al almacenar el fluido en los huecos existentes entre las diferentes láminas.

Las bentonitas de Cabo de Gata tienen su origen en la alteración de rocas volcánicas, por procesos hidrotermales, que consisten en el ascenso de soluciones calientes a favor de fracturas; o por fenómenos de alteración supergénica, debido a la acción de aguas meteóricas (Caballero *et al*., 2005). En Reyes *et al*. (1987) se afirma que el sistema geotérmico que actuó en la región de Cabo de Gata debió de ser muy simple. Probablemente, las aguas meteóricas se infiltraron en profundidad aprovechando la gran fracturación de la región (fracturas alineadas principalmente en dirección noreste y suroeste). Estos acuíferos debieron seguir una dirección norte-sur en dirección al mar. Una vez calientes penetraron en los distintos niveles cineríticos

porosos alterándolos a bentonitas. Estos yacimientos están mayoritariamente compuestos por filosilicatos, con minerales acompañantes como plagioclasa, cuarzo y calcita. El resto de los minerales que pueden aparecer lo hacen en porcentajes muy bajos. Las fracciones finas están formadas casi exclusivamente por esmectita con pequeñas cantidades de illita e interestratificados illita/montmorillonita (Reyes *et al*., 1987).

Las bentonitas han sido explotadas a la largo de toda la región, desde Níjar a San José, pasando por la Serrata de Níjar. En la actualidad constituyen la única explotación de minerales industriales que existe dentro del Parque Natural de Cabo de Gata (Feixas Rodríguez, 2007). Se han descrito más de 30 afloramientos de bentonitas, muchos de ellos se han estado explotando desde los años 50. Se trata de canteras a cielo abierto de bentonitas de excelente calidad, con porcentajes de esmectita superiores al 90 %. Además, estos afloramientos bentoníticos han sido objeto de numerosos estudios sobre sus características mecánicas, mineralógicas y químicas, así como sobre los procesos involucrados en su génesis (Caballero *et al*., 2005).

En función de las características mineralógicas y químicas de esta bentonita determinadas por Caballero *et al.* (1985a, b) y Reyes *et al*. (1987), se han clasificado los yacimientos en tres grandes grupos (Fig. 14):

a) Serrata de Níjar. Donde aparecen numerosas zonas bentonitizadas: Cerro Colorado, Collado del Aire, Cortijo de Archidona, Pecho de los Cristos, Palma del Muerto.

b) Zona Norte de la Sierra de Cabo de Gata. En ella aparecen los yacimientos de: Mata Lobera, Rambla Vieja, Rincón de Agua Amarga, Rincón de las Caleras, Los Trancos, Jayón, Pozo Usero, La Valentina, Majada de las Vacas, Plomo, Cala Montoya, Bornos, Horicuelas.

c) Zona Sur de la Sierra de Cabo de Gata. Formada por los yacimientos de: Cortijo de la Loma, Cerro Amatista, Los Escullos, Cortijo del Gitano, La Isleta del Moro, Morrón de Mateo, La Capitana, El Toril y Las Hermanicas.

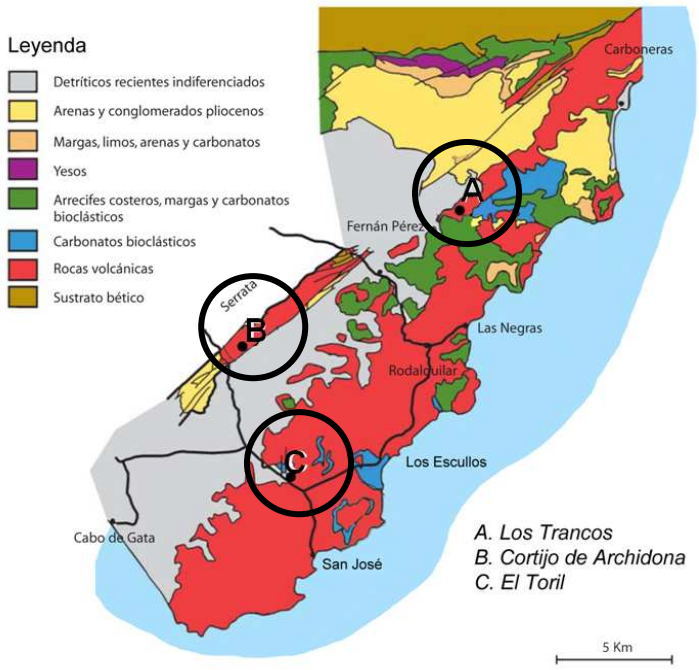

Figura 14. Localización de los afloramientos de bentonitas de Cabo de Gata clasificados en función de sus características mineralógicas y químicas. A: El Cortijo de Archidona, Serrata de Níjar; B: Los Trancos, Zona Norte de la Sierra de Cabo de Gata y C: El Toril, Zona Sur de la Sierra de Cabo de Gata (modificado de Feixas Rodriguez, 2007).

Las bentonitas de cada una de estas tres zonas presentan diferentes coloraciones, blanco y gris en la zona norte de Cabo de Gata, en contraste con los colores ocre y verdoso en la zona sur. En la Serrata de Níjar los depósitos de bentonitas muestran una variedad de colores, desde distintas tonalidades de rojo, morado, verde y blanco, entre otros. Esta coloración diferente se debe a los elementos traza que contiene cada yacimiento, como hierro ferroso, cobre, níquel y cobalto (Linares *et al*., 1973, 1987).

Se han realizado diversas estimaciones sobre la temperatura de los fluidos hidrotermales que originaron las bentonitas. Parece ser que en el caso de las bentonitas de la Sierra de Gata la temperatura debió encontrarse en torno a 70 ºC, mientras que en las de la Serrata de Níjar debieron de estar alrededor de unos 40 ºC (Leone *et al*. 1983; Linares, 1985).

Por otro lado, según Caballero *et al*. (2005), desde un punto de vista geomorfológico, estos afloramientos de bentonitas se clasifican en dos grupos diferentes:

a) los formados cerca de la zona de la falla de Carboneras: estos afloramientos están más extendidos porque la propia falla favorece la movilidad de los fluidos y la subsecuente alteración. En este grupo se encuentran los yacimientos de El Cortijo de Archidona y Los Trancos.

b) los que no están relacionados geológicamente con la falla de Carboneras: en este tipo de afloramientos las soluciones hidrotermales fluyen a través de los numerosos poros de las tobas volcánicas (rocas muy porosas) y de las discontinuidades formadas por el contacto entre las tobas volcánicas y las rocas volcánicas del entorno. Los afloramientos de El Toril o el Morrón de Mateo pertenecen a este segundo grupo.

6.1 Bentonitas de El Cortijo de Archidona

Este yacimiento se localiza en el extremo sureste de la Serrata de Níjar en la Hoja 1046 del MAGNA E. 1:50.000 (Carboneras). La mineralización se produjo en dos direcciones preferentes, noroeste-sureste y noreste-sureste, que coinciden con dos zonas de fracturación sobre ignimbritas de colores claros. Los materiales originales eran riodacitas vesiculares de color obscuro, vidrios e ignimbritas débilmente coloreadas. Los procesos de alteración sufridos en El Cortijo de Archidona estuvieron favorecidos por la intensa brechificación que presentaban las rocas (Delgado, 1993). Son bentonitas de gran pureza (92%), de composición motmorillonítica y una superficie específica total de 615 m^2/g (Caballero *et al*., 2005). Tienen un aspecto jabonoso y su coloración va desde el gris al rosa pasando por verde y blanco (Fig. 15).

Figura 15. Fotografía de El Cortijo de Archidona, Febrero 2010.

6.2 Bentonitas de El Toril

El yacimiento de bentonitas de El Toril (Fig. 16) se localiza a unos 50 metros al norte del Cerro del Toril (Hoja 1060 del IGME (1981) escala 1:50000 correspondiente al Pozo de los Frailes).

La mineralogía de este yacimiento ha sido estudiada en diversos trabajos (Caballero *et al*., 1985b; Linares *et al*., 1996). La zona superior del yacimiento presenta bentonita con jarosita, un mineral de sulfato de hierro por lo que tiene una coloración ocre amarillenta intensa. La zona inferior está formada por bentonita blanca o beige claro, muy pura.

Figura 16. Fotografía de El Toril, Febrero 2010.

6.3 Bentonitas de Los Trancos

El yacimiento de Los Trancos (Fig. 17) es el mayor de la Sierra de Gata. Se sitúa al noreste de la Sierra de Cabo de Gata, aproximadamente a 8 Km de Fernán Pérez (Hoja 1046 del MAGNA E. 1:50.000 (Carboneras)).

Este yacimiento se desarrolló a favor de dos grandes fracturas de orientación noreste que afectaron a materiales tobáceos y aglomerados de composición dacítica

(Reyes *et al*., 1979) o riodacita (Martín Vivaldi and Linares, 1968). Se trata de bentonitas de extrema pureza (97%), muy homogéneas, de composición tanto beidellítica como montmorillonítica, con una superficie específica total de 795 m^2/g (Reyes *et al*., 1979).

Figura 17. Fotografía de Los Trancos, Febrero 2010.

OBJETIVOS

Los siguientes objetivos han sido fijados con una doble finalidad: en primer lugar, estudiar la diversidad microbiana en formaciones de bentonitas españolas del Parque Natural de Cabo de Gata, Almería, debido a que estas bentonitas han sido seleccionadas como material de referencia en el caso de las barreras de ingeniería en el almacenamiento geológico profundo de residuos radiactivos. En segundo lugar, se pretende dilucidar el posible papel desarrollado por los microorganismos de estas formaciones en la movilidad y migración de los radionucleidos desde un almacenamiento arcilloso de residuos radiactivos hasta el medio ambiente.

Los objetivos específicos de esta tesis doctoral son:

1. Estudiar la estructura de las poblaciones microbianas dominantes en las formaciones de bentonitas mediante el uso de:

a) métodos moleculares basados en el estudio del gen ARN ribosomal 16S: secuenciación con Illumina y librería tradicional de clones

b) técnicas dependientes de cultivo

2. Evaluar los mecanismos de toxicidad de uranio sobre microorganismos aislados de las bentonitas usando técnicas de citometría de flujo

3. Elucidar el mecanismo de interacción microbiana con uranio y curio como representantes de actínidos hexavalentes y trivalentes, respectivamente, mediante:

a) Caracterización espectroscópica de los complejos metálicos
b) Estudio de la localización celular de los complejos metálicos

4. Determinar el efecto de la adición de uranio en la diversidad microbiana de las bentonitas en condiciones similares a las del almacenamiento geológico profundo, mediante la elaboración de microcosmos

5. Elaborar bases de datos de los genes involucrados en la biomineralización de uranio en condiciones aerobias

CHAPTER I

Chapter I: Bacterial diversity in bentonites, engineered barrier for deep geological disposal of radioactive wastes

Capítulo I: Diversidad bacteriana en bentonitas, barreras de ingeniería en el almacenamiento geológico profundo de residuos nucleares

Margarita Lopez-Fernandez[1], Iván Sánchez-Castro[1], Ruy Sandoval[2], Dietmar Pieper[2], Nico Boon[3], Ramiro Vílchez-Vargas[3], Andrea Cherkouk[4], Mohamed L. Merroun[1]

[1]Departamento de Microbiología, Universidad de Granada, Granada, Spain

[2]Helmholtz Centre for Infection Research, Braunschweig, Germany

[3]Laboratory of Microbial Ecology and Technology, Ghent University, Ghent, Belgium

[4]Institute of Resource Ecology, Helmholtz Zentrum Dresden Rossendorf, Dresden, Germany

1. Resumen

El almacenamiento geológico profundo de residuos radiactivos a largo plazo es la solución internacionalmente aceptada para el tratamiento de estos desechos especiales, principalmente producidos por la industria de la energía nuclear. La comunidad microbiana de las rocas hospedantes seleccionadas para este tipo de almacenamiento geológico profundo (granitos, sales y arcillas) puede afectar tanto a la integridad de los contenedores metálicos, como a la transformación de los minerales de la formación geológica y a la movilización de radionucleidos desde el almacén hasta el medio ambiente. Por ese motivo es importante analizar el tipo de microorganismos que están presentes en estas formaciones geológicas y cómo pueden estos afectar la seguridad del almacén de residuos radiactivos.

En este capítulo se estudia la comunidad bacteriana presente en las formaciones de bentonitas españolas del Parque Natural de Cabo de Gata, Almería, seleccionadas como material de referencia para las barreras artificiales en este tipo de almacenamiento geológico profundo de residuos radiactivos.

Para ello, se utilizaron técnicas basadas en el estudio del gen del ARN ribosomal 16S, mediante librerías de clones y secuenciación con Illumina. Estos resultados mostraron una alta diversidad bacteriana, detectándose filotipos relacionados con trece *phyla* bacterianos diferentes: *Acidobacteria*, *Actinobacteria*, *Armatimonadetes*, *Bacteroidetes*, *Choloroflexi*, *Cyanobacteria*, *Deinococcus-Thermus*, *Firmicutes*, *Gemmatimonadetes*, *Planctomycetes*, *Proteobacteria*, *Nitrospirae* y *Verrucomicrobia*. Los grupos predominantes de la comunidad estaban principalmente representados por *Proteobacteria* (en cuatro muestras) y *Bacteroidetes* en una muestra. Algunos de los géneros identificados en este estudio han sido descritos por su capacidad para interactuar con hierro y con diferentes metales pesados y radionucleidos, como por ejemplo *Acidovorax, Ralstonia, Variovorax* y *Sphingomonas*.

Los resultados obtenidos en este capítulo demostraron la alta diversidad bacteriana natural de las formaciones de bentonitas de Cabo de Gata, así como sus posibles interacciones con diferentes radionucleidos, lo que afectaría a la seguridad del almacenamiento geológico profundo de residuos radiactivos.

2. Abstract

The long-term disposal of radioactive wastes in a deep geological repository is the accepted international solution for the treatment and management of these special residues, mainly produced by the nuclear energy industry. The microbial community of the selected host rocks for the deep geological repository may affect the metal corrosion of the containers, the transformation of clay minerals, and the migration of radionuclides from the deposit to the environment. For this reason is important to analyze what kinds of microorganisms are present and how the bacterial community might affect the safety of the radioactive waste repository.

In this work the bacterial community in the Spanish bentonite formations of Cabo de Gata Natural Park, Almeria, selected as reference material for bentonite engineered barriers in the disposal of radioactive wastes, was studied.

16S rRNA gene-based approaches were considered to study the bacterial community of the bentonite samples by traditional clone libraries and Illumina-sequencing. A high bacterial diversity was found with phylotypes belonging to 13 different bacterial phyla: *Acidobacteria*, *Actinobacteria*, *Armatimonadetes*, *Bacteroidetes*, *Choloroflexi*, *Cyanobacteria*, *Deinococcus-Thermus*, *Firmicutes*, *Gemmatimonadetes*, *Planctomycetes*, *Proteobacteria*, *Nitrospirae* and *Verrucomicrobia*.

The dominant groups of the community were mainly represented by *Proteobacteria* (in four of the samples) and *Bacteroidetes* in one sample. Some of the identified genera were previously described for their capacity to interact with iron and different heavy metals and radionuclides, as for example, *Acidovorax*, *Ralstonia*, *Variovorax* and *Sphingomonas*.

The results obtained in this chapter demonstrate the high bacterial diversity of the Cabo de Gata bentonite formations, and their possible interactions with different radionuclides, which may affect the safety of the deep geological repository of radioactive wastes.

3. Introduction

Many countries are considering long-term deep geological disposal of nuclear waste, encapsulated in metal container, surrounded by an bentonite-engineered barrier, and emplaced in the host rock (e.g. clay, granite or salt deposits) (Thury and Bossart, 1999; Stroes-Gascoyne *et al*., 2007a; Alonso *et al*., 2008). In Spain, bentonite formations located in Almeria region have been intensely studied due to their possible use as natural analogue of the bentonite-engineered barrier in the deep geological repository for radioactive waste. In addition, these bentonite formations were selected as Spanish reference material because they are well characterized from mineralogical, geochemical and technological pointers view (Villar *et al*., 2006). Clay (e.g. bentonite) is not only a candidate as backfill or sealing material but also a suitable host rock for a high-level radioactive waste repository in other European countries as for example Opalinus clay in Switzerland, Boom clay in Belgium, and Bure clay in France.

In some of these clay formations, microbiological studies were performed to get information about what kind of microorganisms are present, about their viability and activity. Occurrence of viable indigenous microbes, including sulphate-reducing bacteria and also some isolated strains belonging to genus *Sphingomonas*, was evidenced in Opalinus Clay at the Mont Terri Underground Research Laboratory by culture-based methods (Stroes-Gascoyne *et al*., 2007b; Poulain *et al*., 2008). A multidisciplinary approach was performed to study the microbial diversity in Boom clay formation, a deep-subsurface clay deposit in Mol, Belgium (Wouters *et al*., 2013). In the Meuse/Haute-Marne Underground Research Laboratory located at Bure (300 km east of Paris) the Callovo-Oxfordian argillite formation was evaluated for its use as a potential host rock for a high-level radioactive waste repository in France (Cormenzana *et al*., 2008), and its microbial diversity was studied by culturing methods in Urios *et al*. (2012). The bacterial diversity found at the French formations was dominated by *Firmicutes, Actinobacteria* and *Proteobacteria* (Urios el al., 2012).

It is of great importance to know the microbial occurrence in the selected Spanish clay formation because microbial presence could impact the rate of processes

implicated in the, 1) metal corrosion, 2) transformation of clay minerals, and 3) radionuclide migration and transport (Meleshyn, 2011). All of these processes may impact the safety case by compromising a repository's isolation and containment functions.

Microorganisms can potentially affect radionuclide migration by various processes including biosorption, biomineralization, intracellular accumulation, biotransformations, etc. (Macaskie *et al*., 2000; Pedersen, 2002b; Merroun *et al*., 2005; Lloyd and Renshaw, 2005; Merroun *et al*., 2011; Lütke *et al*., 2013; Moll, *et al*., 2014). In addition, microbial occurrence can influence the release of radionuclides by changing geochemical conditions (especially pH and Eh), by producing organic complexantes (West *et al*., 1982). Moreover, microorganisms can also affect the conditions in the repository by microbial reduction or dissolution of the clay minerals (Pentrakova *et al*., 2013), by microbial production or consumption of gases, which can generate an overpressure and form fractures (Glass and Orphan, 2012) as well as by microbial degradation of organics, which can be parts of the radioactive waste or container material, affecting the longevity of the metal waste container in the repository (Stroes-Gascoyne *et al*., 2011). However, in the case of Spanish clay formations, so far only few investigations on the presence of microorganisms were performed. Culture-dependent analysis of microbial diversity from Cabo de Gata clay formations were presented in Lopez-Fernandez *et al*. (2014a). Bacteria from different phyla were isolated, whereas representatives from *Proteobacteria*, *Firmicutes* and *Actinobacteria* were dominant. In addition, a pigmented yeast strain namely *Rhodotorula mucilaginosa* BII-R8 was also recovered (Lopez-Fernandez *et al*., 2014a). Nevertheless, this approach is limited as only a few natural microbial populations can be cultured and studied in the laboratory due to the limited knowledge about their nutrient requirements and other life-necessities (Pace, 1997; Service, 1997). Different methods based on 16S ribosomal gene sequences have been used to characterize the microbial diversity since beginning of the 80´s and they have revealed a tremendous prokaryotic diversity which was overlooked by traditional culture enrichment techniques (Pace, 1997).

Next Generation Sequencing (NGS) is a good method to study the richness and evenness of a prokaryotic community. Illumina-sequencing platform allows a full characterization of the bacterial community, with the major advantage of obtaining thousands of gene sequences (Cardenas and Tiedje, 2008). However, this new

technology is limited by the short length of the reads. Therefore, to improve the taxonomical affiliation of the system studied, analysis of 16S rRNA gene clone libraries might be applied. The latter method provides longer reads, analyzing almost the full 16S rRNA gene, which makes allowance to go deeper into the taxonomy, up to genera and species. However, it is necessary to analyze a high amount of clones per sample to reach sufficient reads to completely characterize the most abundant represents of the community (Degnan and Ochman, 2012).

The work presented in this study is focused on the bacterial diversity analysis of the already mentioned Spanish bentonites, by two different culture- independent molecular approaches based on the 16S ribosomal RNA gene analysis via (i) Illumina sequencing platform and (ii) cloning and sequencing, to get a better knowledge about how these microorganisms can potentially influence the performance of the nuclear waste repository.

4. Materials and methods

4.1 Description of bentonite samples

Five bentonite samples were collected from clay formations from three different sites in Cabo de Gata, Almeria, in the south-east of Spain during March 2011 (Fig. 1). Bentonites from these clay formations are best described as a natural analogue of the bentonite-engineered barrier in the context of deep geological disposal of radioactive waste for their best compaction properties (Villar *et al*., 2006). Two samples called BI-2 and BI-3 were collected from El Cortijo de Archidona. Bentonites from this site are mainly made up of ash and pumice fragments, with a predominance of green and blue colours (Fig. 1B). They are very plastic materials that shown extrusion signals from the reactivation of the fault after the bentonite formation process (Caballero *et al*., 2005). Another sample called BII-2 was collected from the acid area of El Toril, which is 50 meters to the north of El Cerro del Toril. This area results from an acid alteration of the original deposits caused by physical, chemical and mineralogical changes in the bentonite material (Martinez *et al*., 2007). The superficial area of the fault contains jarosite, an iron sulfate mineral responsible for its ocher coloration, as it is shown in Figure 1C. The last two samples called BIV-2 and BIV-3 were collected from Los Trancos, over the Carboneras fault, at the south-east of Carboneras. This is the site with

the highest presence of bentonites in the region of Cabo de Gata (Fig. 1D). Samples called BI-2, BII-2 and BIV-2 were taken from the surface; whereas samples BI-3 and BIV-3 were taken from a depth of twenty centimeters and considered as less exposed to oxygen levels. All samples were collected under sterile conditions and stored frozen at −80 ºC until used for further analysis.

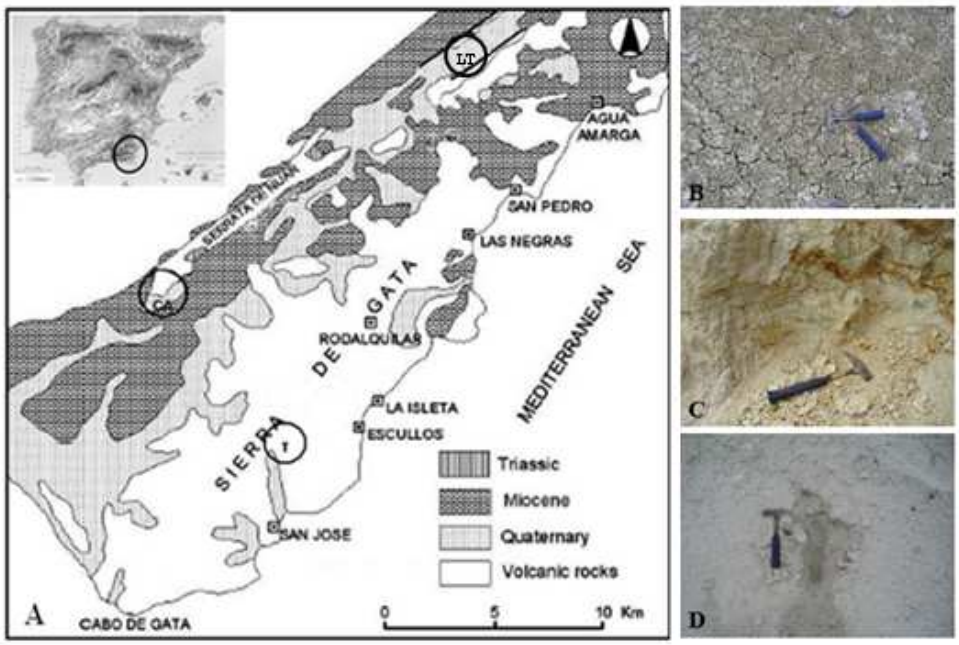

Figure 1. Geographical position of the clay sampling site: A: Location map of the bentonite sampling site in Cabo de Gata region, Almeria, South-East of Spain. B: El Cortijo de Archidona sampling site, C: El Toril sampling site. And D: Los Trancos sampling site. CA: El Cortijo de Archidona deposits (samples BI-2 and BI-3), T: El Toril deposits (sample BII-2), LT: Los Trancos deposits (samples BIV-2 and BIV-3).

4.2 Geochemical and Mineralogical Analyses

X-ray diffraction (XRD) characterization of the bentonite samples was done as described in Lopez-Fernandez *et al*. (2014a).

Composition of the major elements was determined by X-ray fluorescence spectroscopy (XRF), on pressed pellets made of 1:10 lithium tetraborate dilution. A portion of this pellet was burned at 1000 ºC for 1 hour to calculate the Loss On Ignition

(LOI). The instrument used for the XRF measurements was Philips-Magix Pro (PW-2440), Netherland. De Jongh model (de Jongh, 1973) was used to convert the X-Ray intensities into concentrations (Philips software).

Trace elements content of the samples was determined in triplicate by Inductively Coupled Plasma-Mass Spectrometry (ICP-MS) using NexION 300d spectrometer (Perkin Elmer) with a precision of ±5% for an analyte concentration of 10 ppm. Thus, 0.1 g of sample powder was digested with a mixture of HNO_3 and HF digestion of in a Teflon-lined vessel, evaporated to dryness, and subsequently disolved in 100 ml of 4 vol. % HNO_3.

4.3 Organic carbon content and pH measurements

Total organic carbon of the bentonite samples was determined by wet oxidation according to the optimized Walkley and Black's method described by Mingorance *et al*. (2007). Walkley and Black's method (1934) is a standard method to measure organic carbon in agricultural soils.

The pH was measured on a 1:5 (w/v) soil:water suspension. One part of clay was combined with five parts of distillated water. Suspensions were shaken for 10 minutes and after decantation, the pH of the supernatant was measured three times using a Crison pH-meter (MicropH 2002). The instrument was previously standardized against pH 4.00, 7.02 and 9.18 commercial reference solutions. The reported accuracy was of ± 0.02 pH units.

4.4 DNA Extraction and Ribosomal Intergenic Spacer Analysis (RISA)

Total DNA was recovered from 10 g of bentonite soil sample by a method devoloped by Selenska-Pobell and co-workers (Selenska-Pobell *et al*., 2001) which combines a very effective direct lysis of microorganisms in environmental samples and the precipitation of the extracted DNA with polyethyleneglycol, with the final purification steps based on the use of AXG-100 cartridges (Macherey-Nagel, Düren, Germany). The resulting DNA pellet was dissolved in 35 µl of sterile Milli-Q water. For screening the bacterial communities, Ribosomal Intergenic Spacer Analysis (RISA) with the primers $16S_{969f}$ and $23S_{130r}$ was performed. The amplification mixture had a

final volume of 20 µl and contained 1 µl of DNA template, 2.5 mM of $MgCl_2$, 125 µM of each of the four deoxynucleoside triphosphates, 350 nM each of the forward and reverse primers and 1 unit Go Taq® DNA Polymerase with the corresponding Go Taq® Flexi Buffer (Promega, Mannheim, Germany). The PCR amplification was performed in T3000 thermocycler from Biometra using the following cycling conditions: initial denaturation at 95 °C for 6 min, followed by 5 cycles of 95 °C for 60 s, 57 ºC for 40s, 72 ºC for 90 s, followed by 30 cycles of 95 °C for 60 s, 55 °C for 60 s, and 72 °C for 2 min, with a final extension at 72 °C for 10 min.

4.5 Illumina sequencing

Total DNA extracted was also sequenced by Illumina following the procedure of Camarinha-Silva *et al*. (2014). Hypervariable region V5-V6 of the 16S rRNA gene was amplified by using universal primers based on $16S_{807f}$ and $16S_{1050r}$ (Bohorquez *et al*., 2012). Resulting PCR products were amplified using sequencing primers for V5-V6 region, the forward primer contains a 6-nt barcode (Meyer and Kircher, 2010) and a 2-nt CA linker (Hamady *et al*., 2008). Forward and reverse primers comprised sequences complementary to the Illumina specific adaptors to the 5′-ends. Amplification was performed in a total volume of 50 µl with 5x PrimeSTAR TM buffer (Clontech Laboratories, Mountain View, CA, USA), containing each deoxynucleoside triphosphate at a concentration of 2.5 mM, each primer at a concentration of 0.2 µM, 1 µl of template DNA and 0.5 µl PrimeSTAR TM HS DNA polymerase (2.5 units, Clontech Laboratories, Mountain View, CA, USA). An initial denaturation step of 95 °C for 3 min was followed by 15 cycles of denaturation at 98 °C for 10 s, annealing at 55 °C for 10 s and extension at 72 °C for 45 s. One microlitre of this reaction mixture served as template in a second PCR performed under the same conditions as described above, but for 10 cycles using PCR primers designed to integrate the sequence of the specific Illumina multiplexing sequencing primers and index primers. Non-template controls (using water as template) were performed and were free of any amplification products after both rounds of PCR. PCR amplicons were verified by agarose gel electrophoresis, purified using Macherey-Nagel 96-well plate purification kits (Macherey- Nagel, Düren, Germany) following the manufacturer's instructions and quantified with the Quant-iT PicoGreen dsDNA reagent and kit (Invitrogen, Darmstadt, Germany).

Libraries were prepared by pooling equimolar ratios of amplicons (200 ng of each sample), all having been tagged with a unique barcode. In total, five libraries were prepared. To remove any contaminants or PCR artefacts, each library was precipitated on ice for 30 min after addition of 20 µl of NaCl (3M) and three volumes of ice-cold 100% ethanol. The precipitated DNA was centrifuged at 16000 rpm for 30 min at 4 °C. The supernatant was removed, the pellet air dried, resuspended in 30 µl of double distilled water and separated on a 2% agarose gel. PCR products of the correct size were extracted and recovered using the QIAquick gel extraction kit (Qiagen, Hilden, Germany). Libraries were sent for paired-end sequencing on a MiSeq System Sequencer (Illumina, California, USA), obtaining 92832 sequences of 280 nt length. R-program (with vegan y phyloseq packages) was used to normalize to the minimum the pool of sequences, for plotting the rarefaction curves and for calculating the diversity indexes. The sequences were annotated to the least common ancestor using SILVA Incremental Aligner (SINA) (Pruesse *et al*., 2012).

4.6 Clone library analysis

16S rRNA gene fragments were amplified PCR in a reaction mixture of 60 µl, containing 3 µl of (≈100ng/µl) DNA template, 2.5 mM of $MgCl_2$ Solution, 125 µM of each of the four deoxynucleoside triphosphates 350 nM each of the forward and reverse primers and 1 unit Go Taq® DNA Polymerase with the corresponding Go Taq® Flexi Buffer (Promega, Mannheim, Germany)**.** The primers used for this reaction were the bacterial universal primers $16S_{8F}$ (5'-AGAGTTTGATCCTGGCTCAG-3') (Turner *et al*., 1999), and $16S_{1492R}$ (5'-TACGGYTACCTTGTTACGACTT-3') (Lane, 1991).

The PCR amplifications were performed in a T3000 thermocycler of Biometra (Göttingen, Germany). After an initial denaturation at 95 °C for 3 min, and the annealing temperature was decreased from 59 to 55 °C over five cycles and then another 25 cycles followed with 94 °C for 1 min, 55 °C for 40 s, and 72 °C for 1.5 min, and completed with an extension period of 20 min at 72 °C. The right size of the reaction products was checked by electrophoresis in a 1% agarose gel. The three parallel replicates were combined and 2 µl of the reaction mixture was used for cloning in *Escherichia coli* using a TOPO-TA cloning® system (Invitrogen, Gröningen, Netherlands) following the manufacturer's instructions. A total of 100 single white

colonies were randomly selected. The inserted 16S rRNA gene fragments were amplified by PCR directly from the host cells with vector-specific M13(-40)f (5'-GTTTTCCCAGTCACGAC-3') and M13rev (5'-CAGGAAACAGCTATGACC-3') primers (each 350 pmol) by using *Taq*® *DNA Polymerase* (Promega, Mannheim, Germany) in the same conditions as described before.

By electrophoresis, the efficiency of the amplification was checked in 1% agarose gel. The clones with correct inserts were stored as glycerol cultures at −80 °C. The amplified rRNA gene PCR products were further analyzed by restriction fragment length polymorphism (RFLP) analysis and digested in parallel with each of the four-base-specific restriction endonucleases *Msp*I and *Hae*III, in the corresponding buffer (Promega, Germany) overnight at 37 °C. The digestion products were separated in 3% agarose gels in a 0.5x TBE buffer and visualized by staining with ethidium bromide and UV illumination. The resulting RFLP patterns of 100 clones per library were compared and grouped in RFLP-types. One representative of the predominant RFLP types, consisting of two or more clones, was selected for sequencing.

The PCR products of the selected clones were purified using Exo-SAP purification protocol, which uses two hydrolytic enzymes, Exonuclease I (New Englands Biolabs, U.K.) and Thermosensitive Alkaline Phosphatase (TSAP) (Promega, Germany), in a specially formulated buffer for the removal of unwanted primers and dNTPs. After adding the enzymes to the PCR product a 30 min incubation at 37 °C is following and then an enzyme inactivation at 85 °C for a further 15 min. Purified 16S rRNA gene PCR products were sequenced using an ABI Prism® Big Dye® Terminator Cycle Sequencing Kit (Applied Biosystems) according to the instructions of the manufacturer in combination with an automated sequencer (Model 310 ABI PRISM®, Applied Biosystems). The rest of the clones, not grouped in any predominant type, were classified as individual representatives of the community.

The PCR products of these clones were sent to GATC Biotech (Germany) to be purified and sequenced. Phylogenetic and molecular evolutionary analyses were conducted using MEGA version 5 (Tamura *et al*., 2007). The sequences were aligned using software MEGA 5 (ClustalW) and compared to those from GenBank using the Basic Local Alignment Tool (BLAST) server at the National Centre for Biotechnology Information (NCBI) (http://www.ncbi.nlm.nih.gov). Phylogenetic trees were generated

also with MEGA5 using the neighbour-joining algorithm and bootstrapped (500 trial replicates). The possibility of chimera formation by 16S rRNA gene sequences was checked by submitting sequences and their closest phylogenetic relative to the pintail program, version 1.1 (http://www.mybiosoftware.com). Possible chimeras were excluded from the phylogenetic analyses. 16S rRNA gene sequences of the bacterial clones were submitted to the European Nucleotide Archive, under accession numbers HG970666- HG970729 and LK023520- LK023709.

5. Results

5.1 Sampling and characterization of the bentonites

The mineralogy of the bentonites samples from Cabo de Gata region is dominated by smectites, combined with minor quantities of feldspars, quartz, and so on (Caballero *et al*., 2005). The bentonites show different colours: white, green, red, blue, brown, and so forth, depending on the trace elements contents of the first transition series (Linares *et al*., 1973). In this work we focused on three different sampling areas, in Cabo de Gata Natural Park, which were characterized from a mechanical, mineralogical and chemical point of view, as well as by the processes involved in their genesis (Delgado, 1993). In each sampled area, the bentonites exhibit different characteristics, due to the type of rock undergoing alteration, or chemical composition for example (Caballero, 1985).

The XRD semi-quantitative estimation of the mineralogical composition of the samples studied revealed that smectites (montmorillonites) are the dominant mineral phase, 84%, 71% and 96% in sample BI, BII (Lopez-Fernandez *et al*., 2014a) and BIV, respectively (Table 1). Moreover, feldspars were detected: K-feldspar (sanidine) in sample BII and plagioclase (albite) in sample BI and BIV. The presence of jarosite, an iron sulphate mineral phase, was detected in sample BII. XRD diffractograms are shown in Figure 2.

Table 1. DRX semi-quantitative estimation of the mineralogy of the samples studied.

Sample	Mineral	Chemical Formula	SemiQuant (%)
BI	Montmorillonite	$Ca_{0.2}(Al, Mg)_2Si_4O_{10}(OH)_2 \cdot 4H_2O$	84
	Plagioclase (Albite)	$(Na_{0.75}Ca_{0.25})(Al_{1.26}Si_{2.74}O_8)$	12
	Quartz	SiO_2	3
BII	Montmorillonite	$(Na, Ca)_{0.3}(Al, Mg)_2Si_4O_{10}(OH)_2 \cdot nH_2O$	71
	K-feldspar (sanidine)	$K(AlSi_3O_8)$	18
	Quartz	SiO_2	10
	Jarosite	$K(Fe_3(SO_4)_2(OH)_6)$	1
BIV	Montmorillonite	$Ca_{0.2}(Al, Mg)_2Si_4O_{10}(OH)_2 \cdot 4H_2O$	96
	Plagioclase (Albite)	$Na(AlSi_3O_8)$	3
	Quartz	SiO_2	1

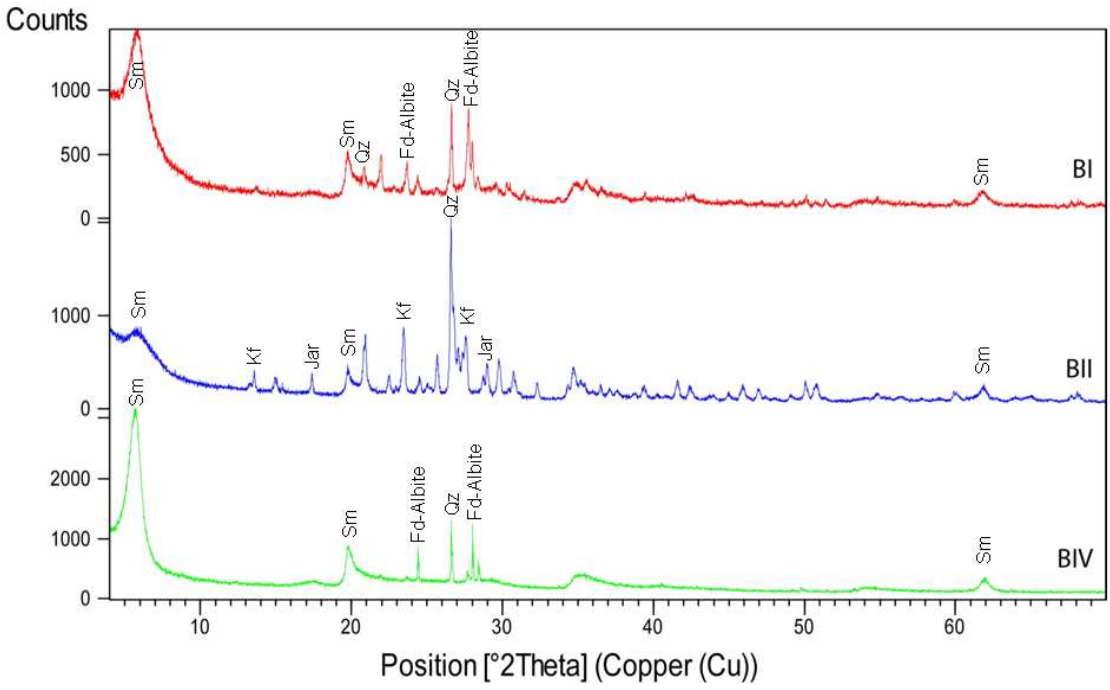

Figure 2. XRD-patterns of powder samples from the bentonite samples (BI, BII and BIV). Sm: smectite; Qz: quartz; Fd-Albite: plagioclase-feldspar albite; Kf-Sanidine: potassium-feldspar sanidine and Jar: jarosite.

Elemental analysis of the bentonite samples revealed that an increased concentration of iron oxides (Fe_2O_3) and sodium oxide (Na_2O) is present in samples BI-2 and BI-3, respectively. However, sample BII-2 showed the biggest differences compared to the rest of the samples (Table 2).

Table 2. Chemical composition, determined by XRF, of the samples studied.

Element (ppm)	SiO_2	Al_2O_3	TiO_2	Fe_2O_3	MnO	MgO	CaO	Na_2O	K_2O	P_2O_5	LOI	TOTAL
BI-2	61.07	17.20	0.24	5.22	0.03	4.15	2.43	1.22	1.55	0.07	6.48	99.65
BI-3	69.81	15.43	0.20	2.36	0.02	2.54	2.06	2.08	1.24	0.04	3.91	99.69
BII-2	54.64	14.50	0.55	11.26	0.01	1.58	0.59	0.48	6.59	0.36	8.91	99.47
BIV-2	61.90	17.79	0.25	2.33	0.11	4.90	2.13	0.88	0.75	0.05	8.49	99.57
BIV-3	58.85	20.55	0.24	2.69	0.14	5.41	1.67	0.34	0.24	0.05	9.18	99.36

For example, this sample has high concentrations of potassium oxides (K_2O), iron oxides (Fe_2O_3) and phosphorus pentoxides (P_2O_5) compared with previous data published for Cabo de Gata region (Marcos, 2004; Garcia-Romero, 2012). The high content of Fe_2O_3 confirms the characteristic composition because of the presence of jarosite in sample BII. Comparing samples BIV-2 and BIV-3 with the rest of the samples, a ten times higher concentration of manganese oxide (MnO) was detected, although it was similar to MnO average published (Reyes *et al*., 1987). In addition, minor elements were detected by ICP-MS. Samples BI-2 and BI-3 showed a high concentration of elements like lithium (Li) and zirconium (Zr) compared to the values for samples BII and BIV. Sample BII-2 presented a high concentration of minor elements such as rubidium (Rb), strontium (Sr), vanadium (V) and cerium (Ce). Finally, in sample BIV-2 barium (Ba) concentration and in sample BIV-3, lanthanium (La) and europium (Eu) concentrations were much higher than in the other samples (Table S1).

5.2 Organic carbon content and pH measurements

The organic carbon content measured, on a dry weight basis, for the bentonite samples was very low in the range of 0.03-0.06% (Table 3), with the exception of sample BI-2, which contains 0.12%.

Table 3. Determination of the percentage of total organic carbon (TOC) and pH of the samples studied.

Sample	% OC	pH
BI-2	0.12 ± 0.02	9.03
BI-3	0.03 ± 0.01	
BII-2	0.04 ± 0.00	7.82
BIV-2	0.04 ± 0.00	8.03
BIV-3	0.06 ± 0.00	

Standard deviation is included as ±SD

These values are much lower than those described for other clays. Clays contain, generally, organic carbon in the range of 0.1 – 5.0% (e.g. 0.6 ± 0.3% in Opalinus Clay (Nagra, 2002), and 1 – 5% in Boom Clay (Van Geet *et al*., 2003). The pH measured was 9.03, 7.82 (Lopez-Fernandez *et al*., 2014a) and 8.03, for sample BI, BII and BIV, respectively (Table 3).

5.3 Bacterial diversity analysis

Due to the differences observed in the RISA profiles (Fig. S1), the five bentonite samples were further analysed to study the bacterial community. Therefore, two complementary techniques were applied to get a deep characterization, by semi-quantification of bacterial diversity using Illumina-sequencing and to get a precise taxonomical affiliation of the bacterial community by classical clone libraries analysis.

NGS platform offers a high-throughput culture-independent analysis. After normalization, a total of 13179 sequences, 280 nucleotides length, of each sample were annotated. A number of 174 Operational Taxonomic Units (OTUs) were discretely separated and classified into class (98% of phylotypes), order (96% of phylotypes),

family (83% of phylotypes) and genus (51% of phylotypes) levels (Table S2). In total, 173 phylotypes belonging to 12 different bacterial phyla (*Acidobacteria*, *Actinobacteria*, *Armatimonadetes*, *Bacteroidetes*, *Choloroflexi*, *Cyanobacteria*, *Firmicutes*, *Gemmatimonadetes*, *Planctomycetes*, *Proteobacteria*, *Nitrospirae* and *Verrucomicrobia*) were identified. The remaining phylotype was classified as belonging to an unknown bacterial phylum. Rarefaction curves were plotted to evaluate the quality of the sampling (Fig. S2). As the curves reached a plateau, the sequencing for each sample was deep enough to detect all phylotypes. Richness, evenness and phylotype diversity were measured using conventional diversity indices, such as Species Richness, Shannon index, Simpson index, Inverse Simpson index, Unbias Simpson index, Fisher alpha index and Pielou evenness index (Table S3). These indices are based on species richness/evenness data from each sample.

The resulting RFLP-predominant groups and RFLP-individuals of 100 clones per library were sequenced as follow: 18 predominant groups and 40 individual clones in sample BI-2; 8 predominant groups and 71 individual clones in sample BI-3; in the case of sample BII-2 and BIV-2, 14 and 57 individuals clones, respectively, and 13 dominant groups for each of both samples; finally, 12 predominant groups and 8 individual clones in sample BIV-3. After the sequencing, 13 bacterial phyla were taxonomically affiliated to *Acidobacteria*, *Actinobacteria*, *Armatimonadetes*, *Bacteroidetes*, *Choloroflexi*, *Cyanobacteria*, *Deinococcus-Thermus*, *Firmicutes*, *Gemmatimonadetes*, *Planctomycetes*, *Proteobacteria*, *Nitrospirae* and *Verrucomicrobia*, as well as to one unkown phylum.

The predominant phylum in sample BI-2 was *Bacteroidetes* (Fig. 3), represented by 48.9% of all sequences. The principal families semi-quantified were *Cytophagaceae* and *Chitinophagaceae*, as well as *Flaviobacteriaceae* (Table S2).

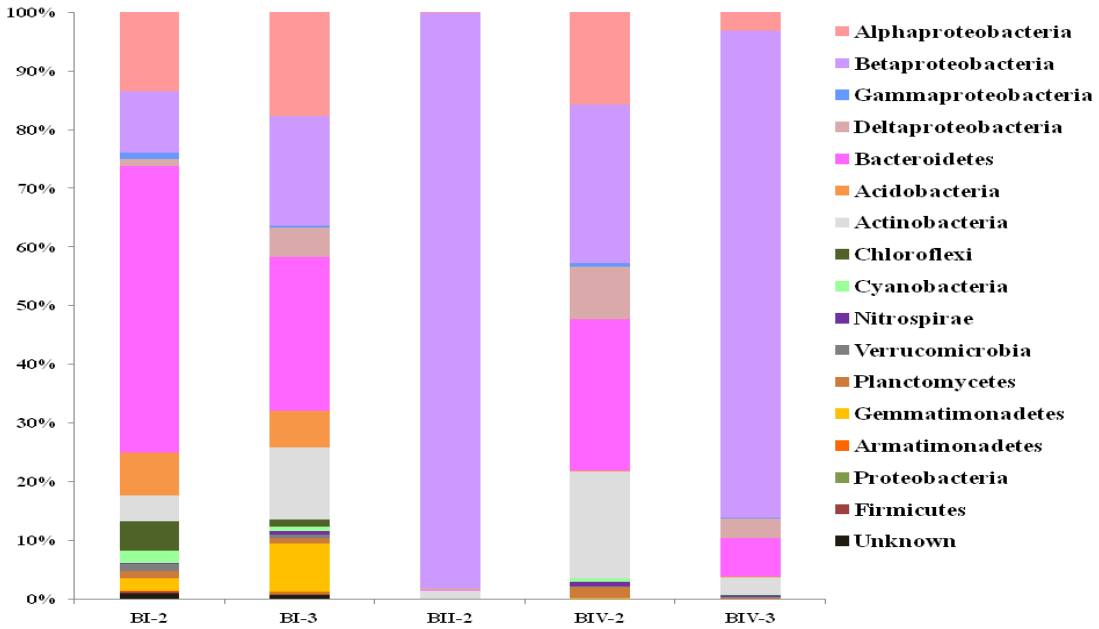

Figure 3. Community structure of the five samples studied by Illumina sequencing.

Belonging to family *Cytophagaceae* some clones were taxonomically identified up to genus, as for example, BI-2-62 affiliated to *Pontibacter* sp. MDT2-9. Clones belonging to family *Chitinophagaceae* were also identified: BI-2-2 affiliated to *Flavisolibacter ginsengisoli* strain Gsoil 643, and BI-2-64 affiliated to *Flavisolibacter* sp. MDT2-37 (Table S4). One of the dominant genera was *Flavobacterium*, OTU-77 (Table S2), also detected as the individual clone BI-2-113, which affiliated to the uncultured *Flavobacterium* sp. clone bsc41. However, most of the *Bacteroidetes* clone sequences in sample BI-2 were affiliated to uncultured *Bacteroidetes* bacteria (Table S4). The second dominant phylum in sample BI-2 was *Proteobacteria* (26.2%) with affiliations to *Alpha-*, *Beta-*, *Delta-* and *Gammaproteobacteria* (Fig. 3 and 4).

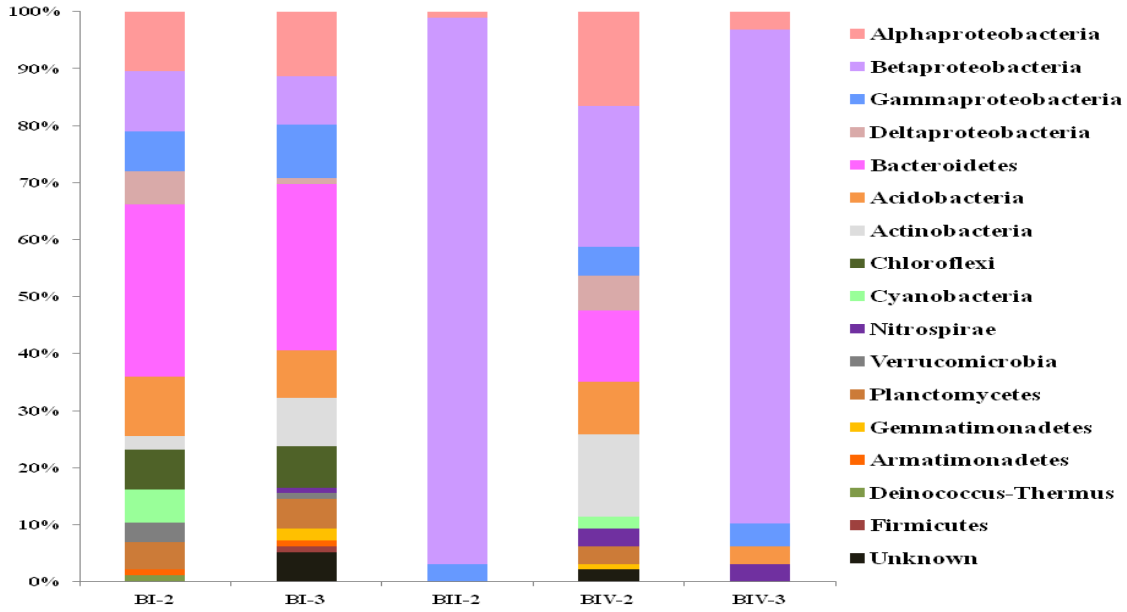

Figure 4. Microbial diversity of the 16S rRNA gene sequences of the samples studied.

Alphaproteobacteria class was represented by 13% of the proteobacterial phylotypes, mainly by genus *Sphingomonas* (15 OTUs). This genus was not one of the most abundant, since alphaproteobacterial clone sequences were taxonomically affiliated to other genera, such as *Porphyrobacter*, *Brevundimonas* and *Rhodobacter* (Table S4). *Betaproteobacteria* class was mainly dominated by families *Comamonadaceae* and *Oxalobacteraceae*. BI-2 clone sequences were mainly represented by family *Oxalobacteraceae* (*Herbaspirillum* spp. and *Massilia* sp.). Interestingly, one clone sequence belonged to phylum *Deinococcus-Thermus*, which was only found in sample BI-2. This represents a minor abundant phylum that could not be detected by Illumina sequencing. Slight differences were observed between the samples BI-2 (surface) and BI-3 (20 cm deep).

Analysing the bacterial community of sample BI-3, *Proteobacteria* and *Bacteroidetes* and *Actinobacteria* where the main phyla identified, represented by the 42%, 26% and 12% of all the sequences, respectively (Fig. 3). *Beta-* and *Alphaproteobacteria* were the predominant *Proteobacteria* classes. In this sample, *Comamonadaceae* was the most significant betaproteobacterial family (Table S2), represented by two identified clones affiliated to uncultured *Comamonadaceae* bacterium clone Ppss Ma80 (clone BI-3-27) and *Comamonadaceae* bacterium b4M (clone BI-3-102). Moreover, several clones belonging to family *Oxalobacteraceae* were

detected, as *Herbaspirillum* spp. (clones BI-3-24 and BI-3-46) and clone BI-3-100, which sequence affiliated with uncultured *Janthinobacterium* sp. clone cEIII43 (Table S5). *Sphingomonas* (85%) was the predominant alphaproteobacterial genus (Table S3), as in the sample BI-2. In addition, the majority of the alphaproteobacterial clones belonged to genera *Blastomonas*, *Tabrizicola* and *Mesorhizobium* (Table S5). Belonging to *Bacteroidetes*, *Cytophagaceae* was detected as the principal family (Table S2), delimited by the via clone library analysis identified genera *Pontibacter* (clones BI-3-55, BI-3-56 and BI-3-98 and *Rufibacter* (clone BI-3-51). Different *Flavisolibacter* species (BI-3-5, -43, -68 and -69) and uncultured *Bacteroidetes* bacteria (BI-3-1, -2, -29, -9, -59, -71, -72) were also affiliated to some clones of this sample (Table S5). In the case of *Actinobacteria* phylum two different genera were dominant, *Arthrobacter* and *Gaiella* (Table S2). Moreover, some of the actinobacterial clones sequences were affiliated with *Arthrobacter* spp. (Table S5).

In sample BIV-2, the overbearing phylum was *Proteobacteria* (52% of all sequences) with affiliations mainly to *Betaproteobacteria* (27%), followed by *Alpha-* (16%), *Delta-* (9%) and *Gammaproteobacteria* in very low proportion (Fig. 3). The prevailing betaproteobacterial order was *Burkholderiales*, the major families were *Comamonadaceae* (genus *Variovorax*: clones BIV-2-30, -31 and -66) and *Oxalobacteraceae* (genus *Herbaspirillum*: clones BIV-2-5, -23, -35 and -104) (Table S8). Belonging to *Alpha-* and *Gammaproteobacteria*, genus *Sphingomonas* and *Xanthomonadaceae* family were dominant, respectively. Other abundant phylum in sample BIV-2 was *Bacteroidetes*. The principal families of this pylum were *Sphingobacteriaceae, Chitinophagaceae* and *Cytophagaceae* (Table S2). On the genus level could be only *Hymenobacter* identified, which was also detected in the clone library (clone BIV-2-103. The majority of the *Bacteroidetes* clone sequences in sample BIV-2 were affiliated, as in the case of BI-2 and BI-3 samples, to uncultured *Bacteroidetes* bacteria (two predominant group and one individual clone), but also, belonged to *Sphingobacteriaceae* family: genus *Pedobacter* and uncultured *Sphingobacteria* bacterium (Table S8), which were not detected in BI-samples Tables S5 and S6). Additionally, clones representatives of the phyla *Actinobacteria*, *Planctomyces*, *Cyanobacteria*, and *Gemmatimonadetes* were found in the sample BIV-2, which were also detected in both or just one of the BI samples. Taxonomical affiliation to *Actinobacteria* (one predominant group and twelve individual clones) was

more abundant than to *Bacteroidetes* (two predominant groups and six individual clones) in sample BIV-2 (Table S8).

Finally, bacterial distribution in sample BII-2 was significantly different to that of the samples BI-2, BI3, and BIV-2, but similar to BIV-3. Although samples BII-2 and BIV-3 were taken from different bentonite formations, they present a similar bacterial community composition (Fig. 3 and 4). Indeed, the same predominant phylotypes of sample BII-2 were also prevalent in sample BIV-3 (Table S2). The main class was *Betaproteobacteria* (98% and 83% of all the sequences, for BII-2 and BIV-3, respectively, as shown in Fig. 3). The betaproteobacterial clone sequences were affiliated with different genera, as shown in Fig. 5.

In correlation with Fig. 6, where it is observed that *Ralstonia* spp. and *Burkholderia* spp. were the most detected ones in both samples, the dominant phylotypes were genus *Ralstonia*, *Comamonadaceae* family and genus *Burkholderia*, in decreasing order (Table S2). The genera *Pelomonas* and *Curvibacter* were, in contrast to the rest of the samples, only identified in samples BII-2 and BIV-3. Clone sequences belonging to genera, *Hydrogenophaga* and *Acidovorax* were only detected in sample BII-2 (Table S6) and clone sequences belonging to *Ramlibacter* only in sample BIV-3 (Table S7). *Variovorax* spp. were detected by cloning in sample BII-2, but not in sample BIV-3 (Fig. 6). Taxonomical affiliation to *Acidobacteria* was more abundant, in sample BIV-3, than to *Bacteroidetes* which was not affiliated to any clone (Table S7) but was detected via Ilumina sequencing.

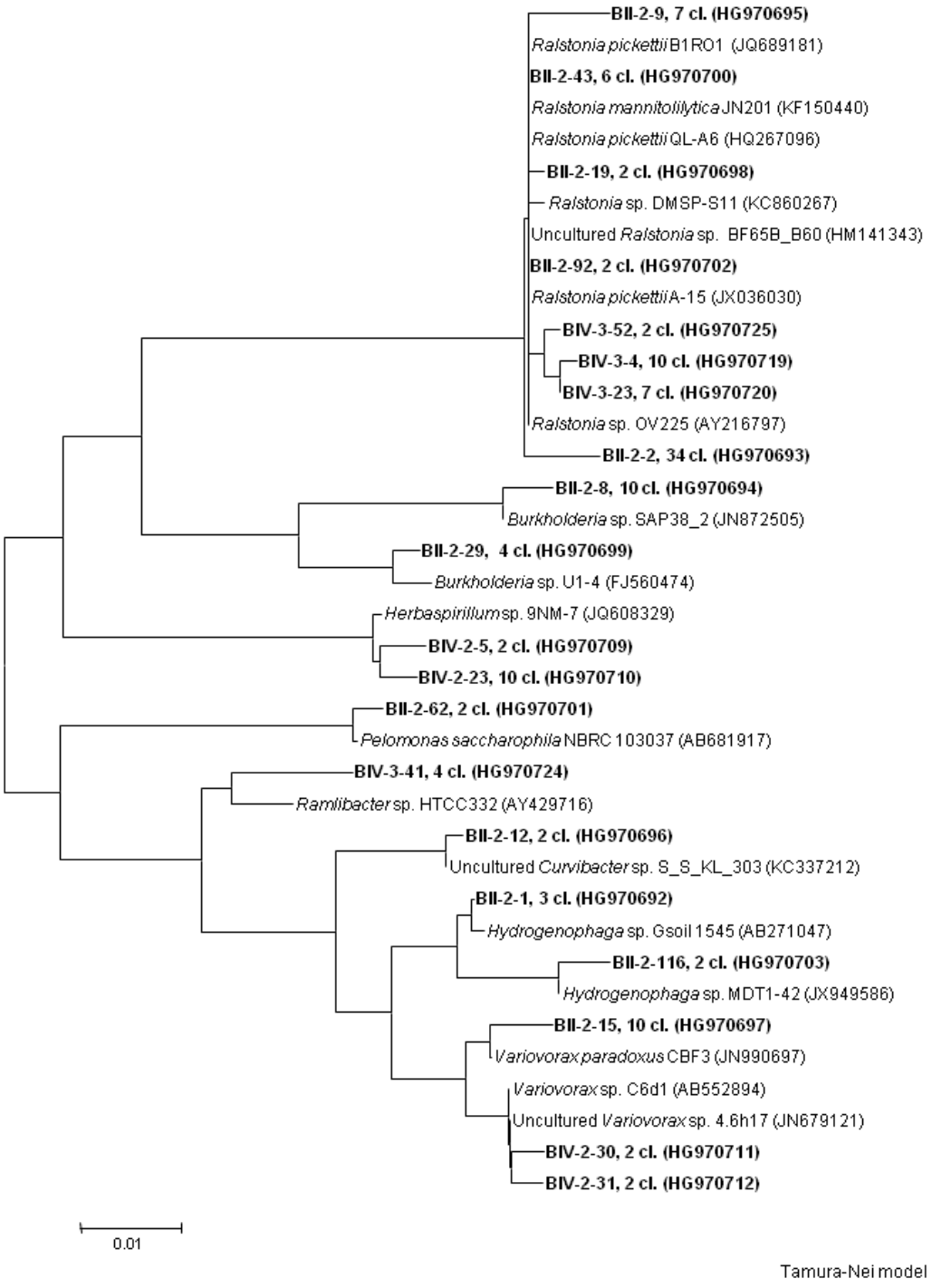

Figure 5. 16S rRNA gene based phylogenetic tree showing the β-proteobacterial diversity of some of the identified clones in the bentonite samples BII-2, BIV-2 and BIV-3, obtained by the neighbor joining algorithm (Maximum Composite Likelihood corrections).

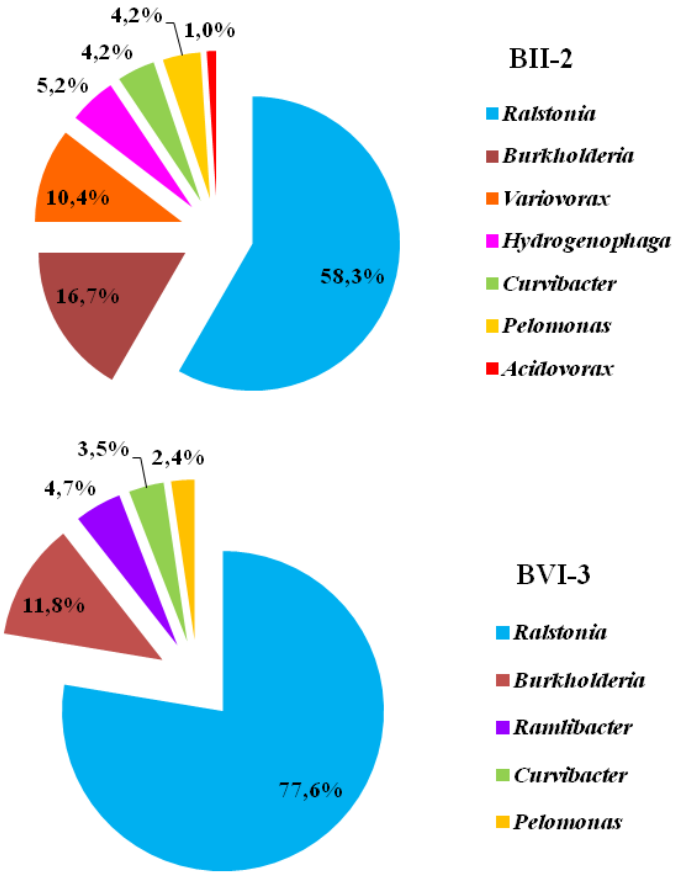

Figure 6. Diversity of the 16S rRNA gene sequences of the betaproteobacterial clones identified in samples BII-2 and BIV-3.

There were also some predominant OTUs in each of the five samples analyzed (Table S2). In sample BI-2, OTU-22, -24 and -30, annotated as *Chitinophagaceae*, *Cytophagaceae* and *Flexibacter*, respectively, were highly enriched compared to the rest. In the case of sample BI-3, the most enriched OTUs were OTU-22, -26 and 42, affiliated, respectively, to *Chitinophagaceae*, *Comamonadaceae* and *Gemmatimonadaceae* families. *Ralstonia* (OTU-6), *Comamonadaceae* (OTU-13) and *Burkholderia* (OTU-14) were the highest enriched OTUs in both samples BII-2 and BIV-3. For sample BIV-2, the predominant OTUs were OTU-18 and -27, annotated as *Sphingobacteriaceae* and *Sphingomonas*, respectively.

6. Discussion

Studies on the bacterial diversity in natural oligotrophic environments including safety barriers (e.g. natural and artificial barriers) for future nuclear waste repositories are needed to know what microorganisms are present, if they are viable, and to predict their effect in the safety of this kind of disposal system.

In this study, the structure and composition of bacterial populations in bentonite formations, considered as safety barriers (i.e., clay buffer and stone) within a future Spanish Deep Geological Repository (DGR) was analyzed by a combination of two different culture-independent assessments of 16S ribosomal RNA genes: classical clone libraries analysis and analysis of the V5–V6 hypervariable region through Illumina platform.

Wouters and coworkers (2013) suggested that the clear correlation between microbial diversity and TOC content in water samples collected from the underground Boom Clay Facility in Belgium, is due to the bioavailability of the carbon source. In our case, there is no clear correlation between the bacterial diversity and the total organic carbon content determined in the studied samples. Sample BI-2 and BI-3 are the samples with the highest and the lowest carbon content, respectively. However, both samples present very similar species richness (Table S3). In the case of sample BII-2, the one with the smaller species richness (46) has a low TOC content (0.04%), but still, it does not confirm the correlation. On the other side there is no information about the bioavailability of the carbon sources available.

Proteobacteria (mainly *Alpha-* and *Betaproteobacteria*), *Bacteroidetes*, *Actinobacteria* and *Acidobacteria* were the main bacterial phyla present in the bentonite samples. The structure and composition of bacterial population in clays considered as host rock for deep geological disposal of radioactive wastes are poorly studied (Stroes-Gascoyne *et al*., 2011; Urios el al., 2012). The prevalence and abundance of particular phylotypes differed between the 3 bentonite surface samples (BI-2, BII-2 and BIV-2). For example, while *Betaproteobacteria* was the most abundant class (98% of the total of phylotypes) in sample BII-2, in comparison to the other bentonite surface samples BI-2 and BIV-2, which contain only 10% and 27%, respectively of the total of the sequences, *Bacteroidetes* dominates the bacterial populations of sample BI-2. The variations in bacterial diversity observed between clay samples could likely be derived

from differences in their mineralogical and geochemical properties (pH, iron oxides content, etc.).

The sample BII-2 differs in the chemical content (Table 1, 2 and S1) in many aspects. For example, this sample is characterized by the presence of sanidine, jarosite and a high amount of Fe_2O_3 (10% of the total oxides content) in comparison to the samples where the Fe oxides content range is between 5 and 2%, respectively (Table 2). Betaproteobacterial clones identified in the sample BII-2 belonged mainly to *Burkolderiales* specially *Ralstonia* spp., *Burkholderia* spp., *Variovorax* spp. as well as *Curvibacter* spp. and *Acidovorax* spp. (Table S2 and S7). *Ralstonia* spp. are implicated in the biogeochemical cycle of Fe through oxidation of Fe(II) (Swanner *et al*., 2011) including solubilization by siderophore production. The high tolerance to heavy metals and organic compounds of *Ralstonia* spp. was previously described (Utturkar *et al*., 2013; Mijnendonckx *et al*., 2013). For example, *Ralstonia metallidurans* (renamed as *Cupriavidus metallireducens*) is a model microorganism for studies of metal resistance and metal tolerance (Borremans *et al*., 2001; Janssen *et al*., 2010). It was also demonstrated that *Variovorax* species are resistant to several metals: Cu, Cd, Pb and Zn (Piotrowska-Seget *et al*., 2005), moreover, arsenite-oxidising *Variovorax* strains were identified in Majumder *et al*. (2013). Similar betaproteobacterial sequences were also detected in sample BIV-3, which is also dominated by *Betaproteobacteria*. But in addition to these, betaproteobacterial sequences belonging to the family *Comamonadaceae* and *Oxalobacteraceae* (e.g. *Massilia* spp.) were detected which were typically found in the samples BI-2, BI-3 and BIV-2 (Table S2). For instance, *Betaproteobacteria* represented also a major part of the bacterial community in deep subsurface clay borehole water (Wouters *et al*., 2013).

However, in the case of *Bacteroidetes*, this phylum only dominates the bacterial community of sample BI-2, probably due to its high content of organic matter. This sample contains 3 orders of magnitude of TOC more than the two other samples (as shown in Table 3). It is interesting, that in the two BI samples different *Bacteroidetes* genera were identified in contrast to sample BIV-2 and BIV-3. In the BI samples were typically the genera *Cytophaga* (OTU-62) and *Flexibacter* (OTU-30, OTU-142) as well as *Pontibacter* identified. *Cytophaga* spp. are aerobic chemoorganotroph bacteria able to degrade cellulose (Xie *et al*., 2007). This could be an explanation why these kinds of bacteria were found in the samples with a higher organic matter content. In the BIV

samples were instead a higher portion of *Hymenobacter* spp. (OTU-30, OTU-142, OTU-158) found. *Alphaproteobacteria* were observed in almost all studied samples (just not in BII-2), but represented different species belonging to the order *Rhizobiales*, *Rhodobacterales* and *Sphingomonadales*. Representatives of this phylum were also found in other clay samples (Poulain *et al*., 2008) and in deep subsurface clay borehole water (Wouters *et al*., 2013).

The samples BI-2, BI-3 and BIV-2 showed overall a higher bacterial diversity, where *Gammaproteobacteria, Actinobacteria* and *Firmicutes* were detected in small quantities similar to bacterial phyla found in deep subsurface clay borehole water (Wouters *et al*., 2013). These results of sample BI-2 and BI-3 (Table S2, S5 and S6) demonstrate that even if the sample BI-3 is taken 20 cm deeper than the sample BI-2, the predominant population in both samples, is dominated by representatives of two phyla, *Bacteroidetes* and *Proteobacteria.* Surprisingly, the bacterial diversity was very similar at phylum level in these two samples, with small variations (Fig. 3 and 4). Although, sample BI-3 contains a lower amount of organic carbon and was collected from a higher depth. In addition, *Chloroflexi*, *Armatimonadetes*, *Firmicutes* and unknown phyla were only detected in samples BI-2 and BI-3. In the case of *Firmicutes*, only the clone BI-3-106 was identified as *Anoxybacillus* sp. SCSIO 15096 in sample BI-3 (Table S5).

Microbial diversity at iron-clay interfaces inside a deep argillite geological formation in France was dominated by *Firmicutes, Actinobacteria* and *Proteobacteria* (Urios *et al*., 2013). Bacteria related to *Firmicutes* could be isolated from Opalinus clay in Mont Terri, Switzerland (Lütke *et al*., 2013; Moll *et al*., 2014), but did not dominated the bacterial community by using culture-independent approaches. Sporulation is a common ability within the *Firmicutes* (Onyenwoke *et al*., 2004), which could make them more resistant against extraction of DNA by the method used in this study.
During the excavation operations of a repository, microbes will be introduced to this disposal system. The biogeochemical processes of microorganisms, either indigenous to the repository´s host rock or introduced during the construction of a repository (Stroes-Gascoyne and West, 1997; Meleshyn, 2011), may affect the safety of this long-term deep geological disposal system. Microbial processes can affect the geochemistry of clays and also the mobility and transport of radionuclides from the repository to the geosphere.

Three different clay-microbe interaction mechanisms were described: (i) structural Fe-clay mineral transformation (oxidation/reduction), (ii) alteration of mineral surfaces by the production of siderophores and small-organic acids, (iii) formation of biofilm in the clay mineral surface (Meleshyn, 2011). The largest portion of the bacterial populations found in the clay samples BII-2 (98%), BIV-3 (83%), BIV-2 (27%) and BI-3 (19%) belongs to *Betapropteobacteria* class, whose members are able to affect the structure of the Fe-containing clay minerals through different processes. For example, through redox based transformation of Fe, in the case of *Ralstonia* spp. or *Acidovorax* spp. (Hedrich *et al*., 2011; Swanner *et al*., 2013), production of siderophores by *Raltstonia* (Münzinger *et al*., 1999) and formation of biofilm on the surfaces of minerals (e.g. *Acidovorax*). *Ralstonia* was the main genus identified (almost 50% of the total clones) in BII-2 and BIV-3 samples. For example, in sample BII-2, the biggest group of clones identified belonged to *Ralstonia pickettii* strain QL-A6, which is a congener strain of *Ralstonia solanacearum*, a soil-isolated strain, described for their capacity to oxidize Fe (II) in smectite soil (Shelobolina *et al*., 2012). Another clone identified in sample BII-2 was affiliated to *Ralstonia mannitolilytica* strain JN201, isolated from potassic trachyte soils and interacting with silicate minerals.

In sample BII-2 a predominant group of clones was closely related to *Acidovorax* and *Variovorax* genera, described for their ability to oxidize iron (Sun *et al*., 2014). *Acidovorax* plays important roles in iron corrosion, by biofilm formations in flowing environment (Li *et al*., 2010). Other betaproteobacterial clones identified in these clay samples were affiliated to genera including *Herbaspirillium*, *Janthinobacterium, Massilia*, which were reported, as in the case of *Ralstonia*, to produce siderophores for the solubilization of Fe present in the clay minerals (Münzinger *et al*., 1999). Some of these bacteria as for example different species of *Sphingomonas, Herbaspirillum* and *Massilia* have been also isolated from sample BI and BII using culture dependent approaches (Lopez-Fernandez *et al*., 2014a). Additionally, some isolates were affiliated to *Micrococcus* spp., *Arthrobacter* spp. and *Kocuria* spp., belonging to phylum Actinobacteria;, *Pseudomonas*, and *Stenotrophomonas* , belonging to *Proteobacteria* phylum; *Bacillus simplex* strain Qtx-12, belonging to *Firmicutes* and in addition, a pigmented yeast strain related to *Rhodotorula mucilaginosa* was also recovered from these formations (Lopez-Fernandez *et al*., 2014a). All these microbe-clay interactions processes may affect negatively the

structure of clay minerals, affecting the function of the clay as a barrier by losing swelling capacity, and enhance the risk of radionuclide mobilization.

In addition, the bacterial populations of the bentonite samples were represented by bacterial strains described for their ability to interact efficiently with radionuclides including U, Cm, Np, Pu, etc. For instance, species of the genus *Sphingomonas* has been described for their high tolerance to heavy metals (Kavamura *et al*., 2010), for their biosorption of radionuclides like U(VI), Am(III) and Sr(II) (Nazina *et al*., 2010) and for changing the speciation of uranium through the transformation of mobile and soluble species of uranium to insoluble uranium phosphate compounds by biomineralization processes (Merroun *et al*., 2011). This process is mediated by the activity of acid phosphatase which cleaves organic phosphate substrate liberating inorganic phosphates needed for the precipitation of uranium (Mondani *et al*., 2011). A well-known example of U(VI) reduction are different species of *Acidovorax* described in Nyman *et al*. (2006) .

7. Conclusions

The current work describes the bacterial diversity of Spanish bentonite formations, by 16S rRNA gene-based analysis via Illumina sequencing and traditional clone libraries. Results revealed a high microbial diversity in the bentonite samples, dominated by bacterial phyla *Proteobacteria*, *Bacteroidetes* and *Actinobacteria*. The majority of the bacterial OTUs and clones identified are strict or facultative aerobic microorganisms. Some of them are affiliated to bacterial strains described for their ability to affect the biogeochemical cycle of Fe by different processes or to interact efficiently with radionuclides. Hence, the effect of this bacterial community might play a role in the safety concept of the deep geological repository of radioactive wastes. Further analyses are required to get a deeper knowledge about the bacterial activity at the planned depth of the repository and about the interaction mechanisms of the microorganisms with the radionuclides.

8. Acknowledgments

This work was funded by Grants CGL2009-09760, BES-2010-032098 and EEBB-2011-43985 (Ministerio de Ciencia e Innovación, España). We acknowledge the assistance of F. Javier Huertas-Puerta (Instituto Andaluz de Ciencias de la Tierra, CSIC – University of Granada, Spain), for his assistance in XRD analyses; of José Antonio Rodríguez-Liébana (Instituto Andaluz de Ciencias de la Tierra, CSIC), for his assistance with the TOC content determination; of Monika Dudek and Katrin Fleming with the clone libraries sequencing (HZDR, Germany) and Iris Plumeier with the Illumina sequencing (HZI, Germany).

9. Supplementary material

Table S1. Chemical composition of the studied bentonite samples, determined by ICP-MS

Element (ppm)	BI-2	BI-3	BII-2	BIV-2	BIV-3
Li	**48.92**	**48.24**	17.11	20.11	23.32
Be	3.31	3.32	1.61	6.27	7.84
Sc	18.44	10.12	19.90	3.00	4.12
V	26.90	11.01	**154.05**	6.07	10.74
Cr	10.44	6.81	21.80	5.48	7.50
Co	4.18	1.72	0.76	0.82	1.36
Ni	11.55	7.91	1.58	3.39	2.44
Cu	21.10	7.85	7.15	1.67	2.36
Zn	73.35	46.64	38.03	42.56	56.60
Ga	20.19	18.40	18.87	18.30	23.53
Rb	64.72	34.10	**220.49**	36.03	18.23
Sr	175.03	171.11	**983.71**	103.67	87.77
Y	24.75	32.06	5.71	19.75	34.92
Zr	**146.40**	**137.18**	66.32	81.24	99.66
Nb	8.77	7.15	3.83	8.69	11.38
Mo	0.27	0.20	2.11	0.26	0.32
Sn	8.83	8.69	4.44	7.31	8.68
Cs	7.67	3.74	5.73	7.47	2.51
Ba	132.70	231.82	384.75	**684.34**	196.78
La	28.82	28.69	53.75	29.93	**88.29**
Ce	63.73	55.88	**172.21**	55.73	97.96
Pr	7.08	6.64	24.24	6.48	18.52
Nd	26.92	24.96	59.46	22.52	63.35
Sm	5.81	5.37	2.54	4.09	11.04
Eu	0.82	0.87	0.35	0.70	**2.01**
Gd	5.14	5.01	1.64	3.20	7.80
Tb	0.83	0.91	0.26	0.51	1.09
Dy	4.74	5.25	0.92	2.97	5.96
Ho	0.93	1.15	0.22	0.63	1.14
Er	2.33	3.21	0.64	1.81	3.11
Tm	0.37	0.52	0.11	0.31	0.51
Yb	2.28	3.21	0.74	1.98	3.12
Lu	0.33	0.52	0.13	0.35	0.49
Hf	4.80	4.53	2.18	2.91	3.50
Ta	1.05	1.04	0.41	0.93	1.14
Tl	0.16	0.10	14.00	1.10	1.38
Pb	33.98	20.39	54.74	49.43	62.33
Th	14.97	16.16	7.52	13.26	20.21
U	2.31	2.05	2.79	0.78	0.27

Table S2. Phylogenetic assignment. Description of all 174 phylotypes determined using Illumina-based amplicon deep-sequencing.

Phylotipe	BI-2	BI-3	BII-2	BIV-2	BIV-3	Domain	Phylum	Class	Order	Family	Genus
OTU60	129	443	0	7	7	Bacteria	*Acidobacteria*	*Acidobacteria*	Subgroup 4	Family *Incertae Sedis*	*Blastocatella*
OTU84	304	156	0	0	0	Bacteria	*Acidobacteria*	*Acidobacteria*	Subgroup 4	Family *Incertae Sedis*	*Blastocatella*
OTU94	186	77	0	16	4	Bacteria	*Acidobacteria*	*Acidobacteria*	Subgroup 4	Family *Incertae Sedis*	*Blastocatella*
OTU105	164	69	0	0	0	Bacteria	*Acidobacteria*	*Acidobacteria*	Subgroup 4	Family *Incertae Sedis*	*Blastocatella*
OTU104	168	72	0	0	0	Bacteria	*Acidobacteria*	*Acidobacteria*	Subgroup 4	-	-
OTU109	126	95	0	2	0	Bacteria	*Actinobacteria*	*Acidimicrobiia*	*Acidimicrobiales*	*Acidimicrobiaceae*	-
OTU229	0	0	19	0	0	Bacteria	*Actinobacteria*	*Acidimicrobiia*	*Acidimicrobiales*	-	-
OTU57	0	0	0	349	45	Bacteria	*Actinobacteria*	*Acidimicrobiia*	*Acidimicrobiales*	-	-
OTU156	0	26	0	36	13	Bacteria	*Actinobacteria*	*Acidimicrobiia*	*Acidimicrobiales*	-	-
OTU163	8	5	0	43	10	Bacteria	*Actinobacteria*	*Acidimicrobiia*	*Acidimicrobiales*	-	-
OTU167	8	22	22	17	8	Bacteria	*Actinobacteria*	*Acidimicrobiia*	*Acidimicrobiales*	-	-
OTU205	0	40	0	0	0	Bacteria	*Actinobacteria*	*Acidimicrobiia*	*Acidimicrobiales*	-	-
OTU35	0	9	0	675	105	Bacteria	*Actinobacteria*	*Actinobacteria*	*Frankiales*	-	-
OTU40	29	20	35	421	63	Bacteria	*Actinobacteria*	*Actinobacteria*	*Frankiales*	-	-
OTU48	7	15	0	401	65	Bacteria	*Actinobacteria*	*Actinobacteria*	*Frankiales*	-	-
OTU174	0	0	0	36	4	Bacteria	*Actinobacteria*	*Actinobacteria*	*Frankiales*	-	-
OTU161	24	27	0	24	10	Bacteria	*Actinobacteria*	*Actinobacteria*	*Micrococcales*	*Microbacteriaceae*	-
OTU47	102	608	0	66	19	Bacteria	*Actinobacteria*	*Actinobacteria*	*Micrococcales*	*Micrococcaceae*	*Arthrobacter*

OTU90	26	22	76	4	0	Bacteria	*Actinobacteria*	*Actinobacteria*	*Micrococcales*	*Micrococcaceae*	*Arthrobacter*
OTU177	35	83	0	0	0	Bacteria	*Actinobacteria*	*Actinobacteria*	*Micrococcales*	*Micrococcaceae*	*Arthrobacter*
OTU210	30	13	0	0	0	Bacteria	*Actinobacteria*	*Actinobacteria*	*Micrococcales*	-	-
OTU73	132	54	0	125	18	Bacteria	*Actinobacteria*	*Actinobacteria*	*Propionibacteriales*	*Nocardioidaceae*	*Nocardioides*
OTU201	0	43	19	0	0	Bacteria	*Actinobacteria*	*Actinobacteria*	*Propionibacteriales*	*Nocardioidaceae*	*Nocardioides*
OTU200	0	0	3	5	5	Bacteria	*Actinobacteria*	*Actinobacteria*	*Propionibacteriales*	*Propionibacteriaceae*	*Propionibacterium*
OTU78	56	512	0	22	6	Bacteria	*Actinobacteria*	*Thermoleophilia*	*Gaiellales*	*Gaiellaceae*	*Gaiella*
OTU141	0	26	1	154	17	Bacteria	*Actinobacteria*	*Thermoleophilia*	*Solirubrobacterales*	-	-
OTU179	25	25	0	0	0	Bacteria	*Armatimonadetes*	-	-	-	-
OTU112	0	0	0	75	57	Bacteria	*Bacteroidetes*	*Cytophagia*	*Cytophagales*	*Cyclobacteriaceae*	-
OTU117	37	38	0	122	12	Bacteria	*Bacteroidetes*	*Cytophagia*	*Cytophagales*	*Cytophagaceae*	*Adhaeribacter*
OTU196	12	20	0	5	0	Bacteria	*Bacteroidetes*	*Cytophagia*	*Cytophagales*	*Cytophagaceae*	*Adhaeribacter*
OTU62	259	209	0	0	0	Bacteria	*Bacteroidetes*	*Cytophagia*	*Cytophagales*	*Cytophagaceae*	*Cytophaga*
OTU30	909	107	0	0	0	Bacteria	*Bacteroidetes*	*Cytophagia*	*Cytophagales*	*Cytophagaceae*	*Flexibacter*
OTU142	75	129	0	0	0	Bacteria	*Bacteroidetes*	*Cytophagia*	*Cytophagales*	*Cytophagaceae*	*Flexibacter*
OTU158	15	89	1	16	33	Bacteria	*Bacteroidetes*	*Cytophagia*	*Cytophagales*	*Cytophagaceae*	*Flexibacter*
OTU54	0	0	0	359	108	Bacteria	*Bacteroidetes*	*Cytophagia*	*Cytophagales*	*Cytophagaceae*	*Hymenobacter*
OTU81	0	0	0	165	51	Bacteria	*Bacteroidetes*	*Cytophagia*	*Cytophagales*	*Cytophagaceae*	*Hymenobacter*
OTU107	0	0	0	217	31	Bacteria	*Bacteroidetes*	*Cytophagia*	*Cytophagales*	*Cytophagaceae*	*Hymenobacter*
OTU192	28	0	3	9	0	Bacteria	*Bacteroidetes*	*Cytophagia*	*Cytophagales*	*Cytophagaceae*	*Hymenobacter*

OTU221	2	0	0	0	0	Bacteria	*Bacteroidetes*	*Cytophagia*	*Cytophagales*	*Cytophagaceae*	*Hymenobacter*
OTU115	194	142	0	0	0	Bacteria	*Bacteroidetes*	*Cytophagia*	*Cytophagales*	*Cytophagaceae*	*Pontibacter*
OTU24	1516	450	0	96	17	Bacteria	*Bacteroidetes*	*Cytophagia*	*Cytophagales*	*Cytophagaceae*	-
OTU59	388	97	0	0	0	Bacteria	*Bacteroidetes*	*Cytophagia*	*Cytophagales*	*Cytophagaceae*	-
OTU79	181	152	0	0	0	Bacteria	*Bacteroidetes*	*Cytophagia*	*Cytophagales*	*Cytophagaceae*	-
OTU92	164	100	0	0	0	Bacteria	*Bacteroidetes*	*Cytophagia*	*Cytophagales*	*Cytophagaceae*	-
OTU123	94	88	0	0	0	Bacteria	*Bacteroidetes*	*Cytophagia*	*Cytophagales*	*Cytophagaceae*	-
OTU139	109	46	0	0	0	Bacteria	*Bacteroidetes*	*Cytophagia*	*Cytophagales*	*Cytophagaceae*	-
OTU144	170	38	0	0	11	Bacteria	*Bacteroidetes*	*Cytophagia*	*Cytophagales*	*Cytophagaceae*	-
OTU187	22	21	0	0	0	Bacteria	*Bacteroidetes*	*Cytophagia*	*Cytophagales*	*Cytophagaceae*	-
OTU77	489	217	0	0	5	Bacteria	*Bacteroidetes*	*Flavobacteria*	*Flavobacteriales*	*Flavobacteriaceae*	*Flavobacterium*
OTU121	131	90	0	0	0	Bacteria	*Bacteroidetes*	*Sphingobacteriia*	*Sphingobacteriales*	*Chitinophagaceae*	*Flavisolibacter*
OTU213	8	5	0	39	4	Bacteria	*Bacteroidetes*	*Sphingobacteriia*	*Sphingobacteriales*	*Chitinophagaceae*	*Flavisolibacter*
OTU227	0	9	0	3	3	Bacteria	*Bacteroidetes*	*Sphingobacteriia*	*Sphingobacteriales*	*Chitinophagaceae*	*Flavisolibacter*
OTU236	3	16	0	0	0	Bacteria	*Bacteroidetes*	*Sphingobacteriia*	*Sphingobacteriales*	*Chitinophagaceae*	*Flavisolibacter*
OTU22	1032	964	24	2	26	Bacteria	*Bacteroidetes*	*Sphingobacteriia*	*Sphingobacteriales*	*Chitinophagaceae*	-
OTU28	0	0	0	740	121	Bacteria	*Bacteroidetes*	*Sphingobacteriia*	*Sphingobacteriales*	*Chitinophagaceae*	-
OTU64	377	208	0	0	0	Bacteria	*Bacteroidetes*	*Sphingobacteriia*	*Sphingobacteriales*	*Chitinophagaceae*	-
OTU89	25	30	0	255	57	Bacteria	*Bacteroidetes*	*Sphingobacteriia*	*Sphingobacteriales*	*Chitinophagaceae*	-
OTU128	72	76	0	19	7	Bacteria	*Bacteroidetes*	*Sphingobacteriia*	*Sphingobacteriales*	*Chitinophagaceae*	-

OTU140	23	9	0	79	6	Bacteria	*Bacteroidetes*	*Sphingobacteriia*	*Sphingobacteriales*	*Chitinophagaceae*	-
OTU151	104	93	0	4	1	Bacteria	*Bacteroidetes*	*Sphingobacteriia*	*Sphingobacteriales*	*Chitinophagaceae*	-
OTU18	0	0	0	1191	320	Bacteria	*Bacteroidetes*	*Sphingobacteriia*	*Sphingobacteriales*	*Sphingobacteriaceae*	-
OTU118	77	152	0	0	0	Bacteria	*Chloroflexi*	*Caldilineae*	*Caldilineales*	*Caldilineaceae*	-
OTU51	594	8	0	0	0	Bacteria	*Chloroflexi*	*Chloroflexia*	*Chloroflexales*	*Chloroflexaceae*	*Chloronema*
OTU86	165	84	0	0	0	Bacteria	*Cyanobacteria*	*Cyanobacteria*	-	-	-
OTU127	37	0	0	76	10	Bacteria	*Cyanobacteria*	*Cyanobacteria*	SubsectionIII	Family I	-
OTU166	64	12	0	3	0	Bacteria	*Cyanobacteria*	*Chloroplast*	-	-	-
OTU208	0	4	3	9	10	Bacteria	*Cyanobacteria*	*ML635J-21*	-	-	-
OTU21	17	15	0	0	0	Bacteria	*Firmicutes*	*Clostridia*	*Clostridiales*	Family XVIII *Incertae Sedis*	-
OTU87	6	12	0	0	0	Bacteria	*Firmicutes*	*Clostridia*	*Clostridiales*	Family XVIII *Incertae Sedis*	-
OTU102	0	3	0	0	0	Bacteria	*Firmicutes*	*Clostridia*	*Clostridiales*	Family XVIII *Incertae Sedis*	-
OTU5	12	0	0	0	0	Bacteria	*Firmicutes*	*Clostridia*	*Clostridiales*	Family XVIII *Incertae Sedis*	-
OTU241	9	12	0	3	0	Bacteria	*Gemmatimonadetes*	*Gemmatimonadetes*	AT425-EubC11 terrestrial group	-	-
OTU216	0	20	6	0	0	Bacteria	*Gemmatimonadetes*	*Gemmatimonadetes*	AT425-EubC11 terrestrial group	-	-
OTU97	95	100	0	22	11	Bacteria	*Gemmatimonadetes*	*Gemmatimonadetes*	*Gemmatimonadales*	*Gemmatimonadaceae*	*Gemmatimonas*
OTU149	124	36	0	0	0	Bacteria	*Gemmatimonadetes*	*Gemmatimonadetes*	*Gemmatimonadales*	*Gemmatimonadaceae*	*Gemmatimonas*
OTU42	5	794	0	0	0	Bacteria	*Gemmatimonadetes*	*Gemmatimonadetes*	*Gemmatimonadales*	*Gemmatimonadaceae*	-
OTU150	47	124	0	2	0	Bacteria	*Gemmatimonadetes*	*Gemmatimonadetes*	S0134 terrestrial group	-	-
OTU122	20	81	0	108	38	Bacteria	*Nitrospirae*	*Nitrospira*	*Nitrospirales*	*Nitrospiraceae*	*Nitrospira*

OTU88	144	0	0	191	4	Bacteria	*Planctomycetes*	vadinHA49	-	-	-
OTU98	13	128	0	55	16	Bacteria	*Planctomycetes*	*Planctomycetacia*	*Planctomycetales*	*Planctomycetaceae*	*Pirellula*
OTU153	63	57	0	20	0	Bacteria	*Proteobacteria*	*Alphaproteobacteria*	*Caulobacterales*	*Caulobacteraceae*	*Phenylobacterium*
OTU188	0	7	0	20	6	Bacteria	*Proteobacteria*	*Alphaproteobacteria*	*Rhizobiales*	*Bradyrhizobiaceae*	*Bradyrhizobium*
OTU185	0	2	0	60	6	Bacteria	*Proteobacteria*	*Alphaproteobacteria*	*Rhizobiales*	*Methylobacteriaceae*	*Methylobacterium*
OTU220	0	0	0	13	3	Bacteria	*Proteobacteria*	*Alphaproteobacteria*	*Rhizobiales*	*Phyllobacteriaceae*	-
OTU111	100	80	0	5	0	Bacteria	*Proteobacteria*	*Alphaproteobacteria*	*Rhizobiales*	-	-
OTU223	6	19	0	0	0	Bacteria	*Proteobacteria*	*Alphaproteobacteria*	*Rhizobiales*	-	-
OTU120	62	64	0	49	6	Bacteria	*Proteobacteria*	*Alphaproteobacteria*	*Rhodobacterales*	*Rhodobacteraceae*	*Rubellimicrobium*
OTU96	142	82	0	6	6	Bacteria	*Proteobacteria*	*Alphaproteobacteria*	*Rhodobacterales*	*Rhodobacteraceae*	-
OTU211	7	4	0	0	0	Bacteria	*Proteobacteria*	*Alphaproteobacteria*	*Rhodobacterales*	*Rhodobacteraceae*	-
OTU164	32	19	0	12	4	Bacteria	*Proteobacteria*	*Alphaproteobacteria*	*Rhodospirillales*	*Acetobacteraceae*	-
OTU224	3	7	0	4	8	Bacteria	*Proteobacteria*	*Alphaproteobacteria*	*Rhodospirillales*	*Acetobacteraceae*	-
OTU27	57	84	0	1012	159	Bacteria	*Proteobacteria*	*Alphaproteobacteria*	*Sphingomonadales*	*Sphingomonadaceae*	*Sphingomonas*
OTU32	95	119	0	572	123	Bacteria	*Proteobacteria*	*Alphaproteobacteria*	*Sphingomonadales*	*Sphingomonadaceae*	*Sphingomonas*
OTU56	148	400	0	12	10	Bacteria	*Proteobacteria*	*Alphaproteobacteria*	*Sphingomonadales*	*Sphingomonadaceae*	*Sphingomonas*
OTU61	232	302	0	92	41	Bacteria	*Proteobacteria*	*Alphaproteobacteria*	*Sphingomonadales*	*Sphingomonadaceae*	*Sphingomonas*
OTU69	263	141	0	0	0	Bacteria	*Proteobacteria*	*Alphaproteobacteria*	*Sphingomonadales*	*Sphingomonadaceae*	*Sphingomonas*
OTU82	186	352	0	7	2	Bacteria	*Proteobacteria*	*Alphaproteobacteria*	*Sphingomonadales*	*Sphingomonadaceae*	*Sphingomonas*
OTU83	13	9	0	168	38	Bacteria	*Proteobacteria*	*Alphaproteobacteria*	*Sphingomonadales*	*Sphingomonadaceae*	*Sphingomonas*

OTU124	55	127	9	6	5	Bacteria	*Proteobacteria*	*Alphaproteobacteria*	*Sphingomonadales*	*Sphingomonadaceae*	*Sphingomonas*
OTU132	116	77	0	9	0	Bacteria	*Proteobacteria*	*Alphaproteobacteria*	*Sphingomonadales*	*Sphingomonadaceae*	*Sphingomonas*
OTU137	37	180	0	2	0	Bacteria	*Proteobacteria*	*Alphaproteobacteria*	*Sphingomonadales*	*Sphingomonadaceae*	*Sphingomonas*
OTU145	97	82	0	0	0	Bacteria	*Proteobacteria*	*Alphaproteobacteria*	*Sphingomonadales*	*Sphingomonadaceae*	*Sphingomonas*
OTU186	14	36	0	0	0	Bacteria	*Proteobacteria*	*Alphaproteobacteria*	*Sphingomonadales*	*Sphingomonadaceae*	*Sphingomonas*
OTU189	13	27	0	10	1	Bacteria	*Proteobacteria*	*Alphaproteobacteria*	*Sphingomonadales*	*Sphingomonadaceae*	*Sphingomonas*
OTU204	17	41	0	0	0	Bacteria	*Proteobacteria*	*Alphaproteobacteria*	*Sphingomonadales*	*Sphingomonadaceae*	*Sphingomonas*
OTU247	11	14	0	5	6	Bacteria	*Proteobacteria*	*Alphaproteobacteria*	*Sphingomonadales*	*Sphingomonadaceae*	*Sphingomonas*
OTU14	0	0	1978	3	1616	Bacteria	*Proteobacteria*	*Betaproteobacteria*	*Burkholderiales*	*Burkholderiaceae*	*Burkholderia*
OTU38	0	0	356	0	234	Bacteria	*Proteobacteria*	*Betaproteobacteria*	*Burkholderiales*	*Burkholderiaceae*	*Burkholderia*
OTU72	0	0	121	0	106	Bacteria	*Proteobacteria*	*Betaproteobacteria*	*Burkholderiales*	*Burkholderiaceae*	*Burkholderia*
OTU168	5	0	4	0	0	Bacteria	*Proteobacteria*	*Betaproteobacteria*	*Burkholderiales*	*Burkholderiaceae*	*Burkholderia*
OTU225	0	0	8	0	3	Bacteria	*Proteobacteria*	*Betaproteobacteria*	*Burkholderiales*	*Burkholderiaceae*	*Burkholderia*
OTU180	37	0	0	4	6	Bacteria	*Proteobacteria*	*Betaproteobacteria*	*Burkholderiales*	*Burkholderiaceae*	*Limnobacter*
OTU6	0	2	6163	9	4805	Bacteria	*Proteobacteria*	*Betaproteobacteria*	*Burkholderiales*	*Burkholderiaceae*	*Ralstonia*
OTU136	0	0	449	0	331	Bacteria	*Proteobacteria*	*Betaproteobacteria*	*Burkholderiales*	*Burkholderiaceae*	*Ralstonia*
OTU183	0	0	300	0	190	Bacteria	*Proteobacteria*	*Betaproteobacteria*	*Burkholderiales*	*Burkholderiaceae*	*Ralstonia*
OTU199	0	0	58	0	63	Bacteria	*Proteobacteria*	*Betaproteobacteria*	*Burkholderiales*	*Burkholderiaceae*	*Ralstonia*
OTU218	0	0	100	0	91	Bacteria	*Proteobacteria*	*Betaproteobacteria*	*Burkholderiales*	*Burkholderiaceae*	*Ralstonia*
OTU231	0	0	43	0	50	Bacteria	*Proteobacteria*	*Betaproteobacteria*	*Burkholderiales*	*Burkholderiaceae*	*Ralstonia*

OTU238	0	0	41	0	40	Bacteria	*Proteobacteria*	*Betaproteobacteria*	*Burkholderiales*	*Burkholderiaceae*	*Ralstonia*
OTU240	0	0	62	0	43	Bacteria	*Proteobacteria*	*Betaproteobacteria*	*Burkholderiales*	*Burkholderiaceae*	*Ralstonia*
OTU243	0	0	61	0	57	Bacteria	*Proteobacteria*	*Betaproteobacteria*	*Burkholderiales*	*Burkholderiaceae*	*Ralstonia*
OTU245	0	0	25	0	11	Bacteria	*Proteobacteria*	*Betaproteobacteria*	*Burkholderiales*	*Burkholderiaceae*	*Ralstonia*
OTU250	0	0	21	0	12	Bacteria	*Proteobacteria*	*Betaproteobacteria*	*Burkholderiales*	*Burkholderiaceae*	*Ralstonia*
OTU253	0	0	11	0	10	Bacteria	*Proteobacteria*	*Betaproteobacteria*	*Burkholderiales*	*Burkholderiaceae*	*Ralstonia*
OTU254	0	0	1	0	6	Bacteria	*Proteobacteria*	*Betaproteobacteria*	*Burkholderiales*	*Burkholderiaceae*	*Ralstonia*
OTU255	0	0	5	0	5	Bacteria	*Proteobacteria*	*Betaproteobacteria*	*Burkholderiales*	*Burkholderiaceae*	*Ralstonia*
OTU58	0	8	283	3	237	Bacteria	*Proteobacteria*	*Betaproteobacteria*	*Burkholderiales*	*Comamonadaceae*	*Acidovorax*
OTU116	5	3	56	1	89	Bacteria	*Proteobacteria*	*Betaproteobacteria*	*Burkholderiales*	*Comamonadaceae*	*Hydrogenophaga*
OTU63	10	9	0	172	123	Bacteria	*Proteobacteria*	*Betaproteobacteria*	*Burkholderiales*	*Comamonadaceae*	*Polaromonas*
OTU113	11	2	0	36	52	Bacteria	*Proteobacteria*	*Betaproteobacteria*	*Burkholderiales*	*Comamonadaceae*	*Polaromonas*
OTU2	82	53	386	528	471	Bacteria	*Proteobacteria*	*Betaproteobacteria*	*Burkholderiales*	*Comamonadaceae*	-
OTU13	0	0	1515	0	1066	Bacteria	*Proteobacteria*	*Betaproteobacteria*	*Burkholderiales*	*Comamonadaceae*	-
OTU15	62	11	210	105	200	Bacteria	*Proteobacteria*	*Betaproteobacteria*	*Burkholderiales*	*Comamonadaceae*	-
OTU26	193	1315	0	25	22	Bacteria	*Proteobacteria*	*Betaproteobacteria*	*Burkholderiales*	*Comamonadaceae*	-
OTU29	8	0	614	0	404	Bacteria	*Proteobacteria*	*Betaproteobacteria*	*Burkholderiales*	*Comamonadaceae*	-
OTU36	165	360	0	303	87	Bacteria	*Proteobacteria*	*Betaproteobacteria*	*Burkholderiales*	*Comamonadaceae*	-
OTU65	177	71	0	272	23	Bacteria	*Proteobacteria*	*Betaproteobacteria*	*Burkholderiales*	*Comamonadaceae*	-
OTU125	46	83	0	91	9	Bacteria	*Proteobacteria*	*Betaproteobacteria*	*Burkholderiales*	*Comamonadaceae*	-

OTU181	8	22	0	12	5	Bacteria	*Proteobacteria*	*Betaproteobacteria*	*Burkholderiales*	*Comamonadaceae*	-
OTU182	38	3	0	0	0	Bacteria	*Proteobacteria*	*Betaproteobacteria*	*Burkholderiales*	*Comamonadaceae*	-
OTU212	11	30	0	2	0	Bacteria	*Proteobacteria*	*Betaproteobacteria*	*Burkholderiales*	*Comamonadaceae*	-
OTU232	0	0	9	7	5	Bacteria	*Proteobacteria*	*Betaproteobacteria*	*Burkholderiales*	*Comamonadaceae*	-
OTU239	0	0	37	4	26	Bacteria	*Proteobacteria*	*Betaproteobacteria*	*Burkholderiales*	*Comamonadaceae*	-
OTU110	13	16	0	232	40	Bacteria	*Proteobacteria*	*Betaproteobacteria*	*Burkholderiales*	*Oxalobacteraceae*	*Massilia*
OTU131	170	35	0	131	31	Bacteria	*Proteobacteria*	*Betaproteobacteria*	*Burkholderiales*	*Oxalobacteraceae*	*Massilia*
OTU135	23	0	0	6	8	Bacteria	*Proteobacteria*	*Betaproteobacteria*	*Burkholderiales*	*Oxalobacteraceae*	*Massilia*
OTU154	0	0	0	13	9	Bacteria	*Proteobacteria*	*Betaproteobacteria*	*Burkholderiales*	*Oxalobacteraceae*	*Massilia*
OTU242	0	4	0	16	0	Bacteria	*Proteobacteria*	*Betaproteobacteria*	*Burkholderiales*	*Oxalobacteraceae*	*Massilia*
OTU44	15	21	0	595	126	Bacteria	*Proteobacteria*	*Betaproteobacteria*	*Burkholderiales*	*Oxalobacteraceae*	-
OTU67	64	6	0	0	0	Bacteria	*Proteobacteria*	*Betaproteobacteria*	*Burkholderiales*	*Oxalobacteraceae*	-
OTU126	34	49	0	75	19	Bacteria	*Proteobacteria*	*Betaproteobacteria*	*Burkholderiales*	*Oxalobacteraceae*	-
OTU195	0	0	0	33	8	Bacteria	*Proteobacteria*	*Betaproteobacteria*	*Burkholderiales*	*Oxalobacteraceae*	-
OTU222	0	0	0	15	8	Bacteria	*Proteobacteria*	*Betaproteobacteria*	*Burkholderiales*	*Oxalobacteraceae*	-
OTU25	161	182	5	848	175	Bacteria	*Proteobacteria*	*Betaproteobacteria*	*Burkholderiales*	-	-
OTU138	57	176	0	0	0	Bacteria	*Proteobacteria*	*Betaproteobacteria*	*Burkholderiales*	-	-
OTU99	121	39	0	83	18	Bacteria	*Proteobacteria*	*Deltaproteobacteria*	*Myxococcales*	*Polyangiaceae*	-
OTU175	14	12	12	1	7	Bacteria	*Proteobacteria*	*Gammaproteobacteria*	*Oceanospirillales*	*Halomonadaceae*	*Halomonas*
OTU226	0	0	8	9	8	Bacteria	*Proteobacteria*	*Gammaproteobacteria*	*Oceanospirillales*	*Halomonadaceae*	*Halomonas*

OTU209	0	0	0	7	0	Bacteria	*Proteobacteria*	*Gammaproteobacteria*	*Pseudomonadales*	*Moraxellaceae*	*Acinetobacter*
OTU234	0	0	0	4	0	Bacteria	*Proteobacteria*	*Gammaproteobacteria*	*Pseudomonadales*	*Moraxellaceae*	*Enhydrobacter*
OTU130	17	10	0	52	33	Bacteria	*Proteobacteria*	*Gammaproteobacteria*	*Pseudomonadales*	*Pseudomonadaceae*	*Cellvibrio*
OTU4	0	0	0	6	0	Bacteria	*Proteobacteria*	*Gammaproteobacteria*	*Pseudomonadales*	*Pseudomonadaceae*	*Pseudomonas*
OTU152	26	47	14	0	0	Bacteria	*Proteobacteria*	*Gammaproteobacteria*	*Pseudomonadales*	*Pseudomonadaceae*	*Pseudomonas*
OTU228	4	0	0	1	8	Bacteria	*Proteobacteria*	*Gammaproteobacteria*	*Pseudomonadales*	*Pseudomonadaceae*	*Pseudomonas*
OTU39	4	0	0	382	168	Bacteria	*Proteobacteria*	*Gammaproteobacteria*	*Xanthomonadales*	*Xanthomonadaceae*	-
OTU41	10	0	0	499	105	Bacteria	*Proteobacteria*	*Gammaproteobacteria*	*Xanthomonadales*	*Xanthomonadaceae*	-
OTU52	0	516	0	55	2	Bacteria	*Proteobacteria*	*Gammaproteobacteria*	*Xanthomonadales*	*Xanthomonadaceae*	-
OTU71	0	0	0	88	101	Bacteria	*Proteobacteria*	*Gammaproteobacteria*	*Xanthomonadales*	*Xanthomonadaceae*	-
OTU93	88	85	0	74	6	Bacteria	*Proteobacteria*	*Gammaproteobacteria*	*Xanthomonadales*	*Xanthomonadaceae*	-
OTU219	0	0	0	10	0	Bacteria	*Proteobacteria*	*Gammaproteobacteria*	*Xanthomonadales*	*Xanthomonadaceae*	-
OTU11	4	22	2	0	13	Bacteria	*Proteobacteria*	-	-	-	-
OTU162	115	62	0	11	6	Bacteria	*Verrucomicrobia*	*Spartobacteria*	*Chthoniobacterales*	-	-
OTU176	46	13	0	4	0	Bacteria	*Verrucomicrobia*	*Spartobacteria*	*Chthoniobacterales*	-	-
OTU100	139	90	0	0	0	Bacteria	-	-	-	-	-

Table S3: Ecological biodiversity indices of bentonite samples communities. The indices presented are: Species richness (S), Shannon index (H'), Simpson index (λ), Inverse Simpson index (1/λ), Unbias Simpson index (Unbias Simp), Fisher Alpha index (α) and Pielou's evenness (J').

Sample	**S**	**H'**	**λ**	**1/λ**	**Unbias Simp**	**α**	**J'**
BI-2	119	3.96	0.96	28.24	0.96	17.74	0.83
BI-3	122	3.96	0.97	30.44	0.97	18.60	0.82
BII-2	46	2.00	0.74	3.86	0.74	5.64	0.52
BIV-2	108	3.66	0.96	25.90	0.96	15.00	0.78
BIV-3	111	2.87	0.84	6.29	0.84	14.92	0.60

Table S4. Affiliation of the 16S rRNA gene sequences of BI-2 bacterial clones.

Clone	Accession no. EMBL	no. of clones	Closest phylogenetic relative/accession no.	Similarity (%)	Isolation source
			Alphaproteobacteria		
BI-2-12	HG970671	2	*Brevundimonas* sp. FWC04 (AJ227793)	99	-
BI-2-33	HG970672	2	*Rhodobacter* sp. J8 (KC174860)	97	wastewater treatment system
BI-2-35	HG970673	3	*Porphyrobacter donghaensis* SW-158 (AY559429)	99	sea water
BI-2-95	HG970674	2	Unc. *Rhodobacteraceae* bact. TDNP_Bbc97_260_1_68 (FJ516785)	96	biofilm
			Betaproteobacteria		
BI-2-38	HG970675	2	Uncultured *Herbaspirillum* sp. OTUst26 (KF385227)	99	stems
BI-2-4	LK023522	1	Uncultured beta proteobacterium D9 (JF833754)	98	potassium mine soil
BI-2-15	LK023524	1	*Massilia* sp. RHLT3-10 (JX949432)	99	glacier
BI-2-19	LK023525	1	*Ralstonia* sp. A52 (KF788027)	99	red soil
BI-2-23	LK023527	1	*Herbaspirillum* sp. SCL-124 (KC455427)	94	rhizosphere of sugarcane
BI-2-36	LK023532	1	*Herbaspirillum* sp. THG-e31 (KF314195)	96	soil
BI-2-86	LK023551	1	*Herbaspirillum* sp. H6558 (KF212501)	99	sugarcane plant
BI-2-112	LK023558	1	Uncultured beta proteobacterium B-AB39 (AY622250)	94	subsurface soil
			Deltaproteobacteria		
BI-2-11	HG970676	2	Uncultured *Byssovorax* sp. T282H11 (HM438448)	93	soil with anthracene
BI-2-51	HG970677	2	Uncultured delta proteobacterium A183 (JF833494)	92	potassium mine soil
BI-2-111	LK023557	1	Uncultured *Myxococcales* bacterium Plot18-E11 (FJ889280)	98	agricultural soil
			Gammaproteobacteria		
BI-2-24	HG970678	2	Uncultured *Rhizobacter* sp. H16 (KF003203)	99	grass carp gut mucus
BI-2-61	HG970679	2	Uncultured bacterium AN0C1CH07 (JQ426285)	99	soil
BI-2-72	LK023544	1	*Lysobacter* sp. RCML-52 (EU833988)	99	abandoned gold mine in desert

BI-2-85	LK023550	1	*Xanthomonas* sp. 35/23 (AY571841)	100	soil with hydrocarbon
			Bacteroidetes		
BI-2-2	HG970666	7	*Flavisolibacter ginsengisoli* Gsoil 643 (NR_041500)	97	soil of the ginseng field
BI-2-5	HG970667	4	Uncultured *Bacteroidetes* bacterium HG-J02178 (JN409061)	95	rhizosphere soil
BI-2-67	HG970668	2	Uncultured *Flavisolibacter* sp. SGR217 (JQ793553)	98	rhizospheric soil
BI-2-26	LK023528	1	Uncultured *Flexibacteraceae* bacterium 9 (EU362138)	96	dune sand
BI-2-30	LK023529	1	Uncultured *Flexibacteraceae* bacterium 9 (EU362138)	96	dune sand
BI-2-52	LK023534	1	Uncultured *Bacteroidetes* bacterium QZ-J40 (JF776933)	99	rhizosphere soil
BI-2-55	LK023536	1	Uncultured *Bacteroidetes* bacterium HG-J02178 (JN409061)	98	rhizosphere soil of cucumber
BI-2-62	LK023538	1	*Pontibacter* sp. MDT2-9 (JX949545)	99	glacier
BI-2-64	LK023539	1	*Flavisolibacter* sp. MDT2-37 (JX949543)	99	glacier
BI-2-68	LK023540	1	Uncultured *Bacteroidetes* bacterium G1-16 (JF703303)	95	root and rhizophere soil
BI-2-69	LK023541	1	Uncultured *Bacteroidetes* bacterium HG-J02178 (JN409061)	98	rhizosphere soil of cucumber
BI-2-71	LK023543	1	Uncultured *Bacteroidetes* bacteriumHG-J01202 (JN408956)	99	rhizosphere soil of cucumber
BI-2-74	LK023546	1	Uncultured *Bacteroidetes* bacterium HG-J02178 (JN409061)	98	rhizosphere soil of cucumber
BI-2-80	LK023548	1	Uncultured *Pontibacter* sp. T102 (GQ202647)	98	soil from transgenic cotton field
BI-2-91	LK023552	1	Uncultured *Bacteroidetes* bacterium 2H9 (KC442517)	99	soil
BI-2-113	LK023559	1	Uncultured *Flavobacterium* sp. bsc41 (KC011140)	98	soil
			Acidobacteria		
BI-2-7	HG970669	2	Uncultured *Acidobacteria* bacterium Sliv-103 (FM877669)	98	vicinity of a uranium mine
BI-2-10	HG970670	3	Uncultured *Acidobacteria* bacterium HEG_08_216 (HQ597545)	95	grassland soil
BI-2-1	LK023520	1	Uncultured *Acidobacteria* bacterium SEG_08_419 (HQ597955)	96	grassland soil
BI-2-3	LK023521	1	Uncultured *Acidobacteria* bacterium UMAB-cl-76 (FN811260)	98	soil
BI-2-32	LK023530	1	Uncultured *Acidobacterium* sp. sw-xj59 (GQ302569)	99	cold spring sediment
BI-2-79	LK023547	1	Uncultured *Acidobacteria* bacterium HEG_08_046 (HQ597431)	99	grassland soil

			Chloroflexi		
BI-2-6	HG970683	2	Uncultured *Caldilineaceae* bacterium T9222f9 (HM447656)	86	agricultural soil
BI-2-54	LK023535	2	Uncultured *Chloroflexi* bacterium IAFpp7227 (GU214149)	92	slime sample
BI-2-22	LK023526	1	Uncultured *Chloroflexus* sp. Dolo_23 (AB257647)	99	dolomite rock
BI-2-39	LK023533	1	Uncultured *Chloroflexi* bacterium AKYH948 (AY921747)	96	soil adjacent to a silage storage
			Cyanobacteria		
BI-2-103	HG970680	2	*Phormidium* sp. SAG 61.90 (EU624415)	97	-
BI-2-109	HG970681	2	*Leptolyngbya* sp. LLi18 (DQ786166)	93	hot stream cyanobacterial mat
BI-2-34	LK023531	1	*Trichocoleus sociatus* SAG 26.92 (EF654080)	96	marine water
			Verrucomicrobia		
BI-2-8	LK023523	1	Uncultured *Verrucomicrobia* bacterium g3 (EU979012)	99	soil
BI-2-70	LK023542	1	Unc. *Verrucomicrobia* bact. Cl. Alchichica (JN825628)	94	alkaline lake microbialites
BI-2-73	LK023545	1	Uncultured *Verrucomicrobia* bacterium bsc6 (KC011105)	99	soil
			Actinobacteria		
BI-2-84	LK023549	1	Uncultured actinobacterium PET-054 (JF344178)	99	petroleum spot on marine sediments
BI-2-101	LK023555	1	Uncultured *Actinomycetales* bacterium T501F11 (HM438032)	99	soil with anthracene
			Planctomycetes		
BI-2-66	HG970682	3	Uncultured *Gemmata* sp. A370 (EU283557)	98	Anderson Lake
BI-2-98	LK023553	1	*Gemmata* sp. Ha1-6 (GQ889433)	93	lawn soil
			Armatimonadetes		
BI-2-60	LK023537	1	Uncultured *Armatimonadetes* bacterium CO1/3c (HF566128)	97	marine deep subsurface sediments
			Deinococcus-Thermus		
BI-2-99	LK023554	1	Unc. *Thermus/Deinococcus* group bact. R18-435 (AY905381)	98	fallow agricultural soil

Table S5. Affiliation of the 16S rRNA gene sequences of BI-3 bacterial clones.

Clone	Accession no. EMBL	no. of clones	Closest phylogenetic relative/accession no.	% similarity	Isolation source
			Alphaproteobacteria		
BI-3-18	LK023567	1	*Blastomonas* sp. 16-28 (HM124371)	98	Taihu Lake sediment
BI-3-47	LK023586	1	Unc. *Sphingomonadaceae* bacterium T312H11 (HM438364)	98	soil with anthracene
BI-3-58	LK023595	1	Uncultured *Rubellimicrobium* sp. CH1-34 (JX079390)	96	contaminated soil CH-1
BI-3-60	LK023597	1	*Blastomonas* sp. 16-28 (HM124371)	98	Taihu Lake sediment
BI-3-81	LK023608	1	*Tabrizicola aquatica* RCRI19 (HQ392507)	95	Qurugol Lake water samples
BI-3-83	LK023609	1	Uncultured *Sphingomonadaceae* bacterium T921c4 (HM447692)	99	agricultural soil
BI-3-88	LK023612	1	*Mesorhizobium* sp. CCNWQLS7 (JX840388)	99	-
BI-3-94	LK023617	1	*Mesorhizobium alhagi* strain UrPL08 (KC618482)	99	rhizospheric soil
BI-3-101	LK023621	1	Uncultured *Rhizobiales* bacterium PRTBB8484 (HM798923)	92	deep ocean water
BI-3-109	LK023626	1	*Tabrizicola aquatica* RCRI19 (HQ392507)	99	
BI-3-111	LK023628	1	*Blastomonas* sp. 16-28 (HM124371)	99	Taihu Lake sediment
			Betaproteobacteria		
BI-3-24	LK023571	1	*Herbaspirillum* sp. THG-e31 (KF314195)	99	soil
BI-3-27	LK023573	1	Uncultured *Comamonadaceae* bacterium Ppss_Ma80 (JF421144)	99	petroleum-contaminated soil
BI-3-39	LK023580	1	Uncultured beta proteobacterium YZ23 (JQ861421)	99	peanut rhizosphere soil
BI-3-46	LK023585	1	*Herbaspirillum* sp. Sco-A35 (FN386722)	99	volcanic ash
BI-3-76	LK023605	1	Uncultured *Burkholderiales* bacterium CTRL50 (EU404008)	99	infiltrative surface clean water
BI-3-100	LK023620	1	Uncultured *Janthinobacterium* sp. cEIII43 (AY359837)	95	flowering plants of Ni accumulator
BI-3-102	LK023622	1	*Comamonadaceae* bacterium b4M (EF540485)	98	semi-coke
BI-3-110	LK023627	1	Uncultured beta proteobacterium R109 (FR820574)	99	rhizosphere

			Gammaproteobacteria		
BI-3-8	LK023562	1	Uncultured *Pseudomonas* sp. 404 (EU097342)	91	soil of radish-rich area
BI-3-30	LK023575	1	Uncultured *Lysobacter* sp. HKTUI113 (GU012072)	99	arid sand
BI-3-32	HG970691	5	Uncultured bacterium AC14C1CF08 (JQ427104)	99	soil
BI-3-97	LK023618	1	Uncultured *Lysobacter* sp. Y38 (KF003206)	99	grass carp gut mucus
BI-3-104	LK023624	1	Unc. *Gammaproteobacteria* bacterium MP-R11(JN038687)	95	Chongxi wetland soil
			Deltaproteobacteria		
BI-3-77	LK023606	1	Uncultured *Myxococcales* bacterium Plot18-E11 (FJ889280)	96	agricultural soil
			Bacteroidetes		
BI-3-1	HG970684	4	Uncultured *Bacteroidetes* bacterium A3_3_3B_142 (JQ627486)	96	biofilm on mineral substrate
BI-3-2	HG970685	2	Uncultured *Bacteroidetes* bacterium g31 (EU979040)	99	soil
BI-3-5	HG970686	3	*Flavisolibacter ginsengiterrae* Gsoil 492(NR_041499)	97	soil of the ginseng field
BI-3-21	HG970687	4	Uncultured *Bacteroidetes* bacterium MLS188 (JX240867)	96	coastal soil
BI-3-23	HG970688	2	Uncultured *Sphingobacteriales* bacterium 7 (EU362136)	95	dune sand
BI-3-9	LK023563	1	Uncultured *Bacteroidetes* bacterium LV60-5 (AY642574)	95	microbialithe
BI-3-43	LK023583	1	*Flavisolibacter* sp. MDT2-37 (JX949543)	97	glacier
BI-3-50	LK023589	1	Unc. *Chitinophagaceae* bacterium SNNP_2012-93 (JX114426)	97	Sierra Nevada National Park soil
BI-3-51	LK023590	1	*Rufibacter* sp. DG31D (KF303587)	99	soil
BI-3-55	LK023592	1	*Pontibacter* sp. HMD3030 (HM135525)	98	saltern
BI-3-56	LK023593	1	*Pontibacter* sp. ZLD-7 (KC894746)	99	soil
BI-3-59	LK023596	1	Uncultured *Bacteroidetes* bacterium HG-J01246 (JN408981)	98	soil of cucumber in Dalian
BI-3-68	LK023599	1	*Flavisolibacter ginsengiterrae* Gsoil 492 (NR_041499)	99	soil of the ginseng field
BI-3-69	LK023600	1	*Flavisolibacter* sp. MDT2-37 (JX949543)	99	glacier
BI-3-71	LK023602	1	Uncultured *Bacteroidetes* bacterium De3151 (HQ183947)	96	leachate sediment
BI-3-72	LK023603	1	Uncultured *Bacteroidetes* bacterium HG-J02178 (JN409061)	98	soil of cucumber in Dalian
BI-3-92	LK023615	1	Unc. *Sphingobacteriales* bacterium SNNP_2012-66 (JX114399)	99	Sierra Nevada National Park soil

BI-3-98	LK023619	1	*Pontibacter* sp. HMD3125 (GU339183)	99	solar saltern
			Actinobacteria		
BI-3-17	LK023566	1	Unc. *Acidimicrobineae* bacterium1_20_H11_b (JQ087121)	96	contaminated aquifer sediment
BI-3-19	LK023568	1	Uncultured *Actinomycetales* bacterium N-35 (HM565047)	99	concrete
BI-3-22	LK023570	1	Uncultured *Iamiaceae* bacterium C.la-137 (JX505021)	99	soil
BI-3-29	LK023574	1	Uncultured *Actinomycetales* bacterium Plot18-2C11 (FJ889256)	95	agricultural soil
BI-3-42	LK023582	1	*Arthrobacter* sp. NBMS25 (KC447330)	99	mangrove sediment
BI-3-57	LK023594	1	*Actinotalea ferrariae* CF5-4 (HQ730135)	99	iron mine
BI-3-70	LK023601	1	Uncultured *Arthrobacter* sp. H55(HG917256)	99	soil from wall painting
BI-3-114	LK023629	1	*Arthrobacter phenanthrenivorans* BGR18 (KC789777)	99	soil
			Chloroflexi		
BI-3-7	LK023561	1	Uncultured *Chloroflexi* bacterium A03L-1 (HE614815)	96	arsenic and gold mine
BI-3-12	LK023564	1	Uncultured *Chloroflexi* bacterium HG-J0279 (JN409011)	99	rhizosphere soil of cucumber
BI-3-37	LK023578	1	Uncultured *Chloroflexi* bacteriumAKYG1903 (AY922003)	93	farm soil
BI-3-38	LK023579	1	Uncultured *Caldilinea* sp. T9222B8 (HM447654)	97	agricultural soil
BI-3-45	LK023584	1	Uncultured *Sphaerobacter* sp.De182 (HQ183885)	97	leachate sediment
BI-3-103	LK023623	1	Unc. *Chloroflexi* bact. Alchichica_AL52_2_1B_94 (JN825474)	96	microbialites from alkaline lake
BI-3-115	LK023630	1	Uncultured *Chloroflexi* bacterium AKYG1903 (AY922003)	92	farm soil
			Acidobacteria		
BI-3-6	HG970689	3	Uncultured *Acidobacteria* bacterium SEG_08_583 (HQ729816)	99	grassland soil
BI-3-41	LK023581	1	Uncultured *Acidobacteria* bacterium SEG_08_583 (HQ597771)	96	grassland soil
BI-3-48	LK023587	1	Uncultured *Acidobacteria* bacterium 2G1 (KC442706)	98	soil
BI-3-49	LK023588	1	Uncultured *Acidobacteria* bacterium 2G1 (KC442706)	98	soil
BI-3-54	LK023591	1	Uncultured *Acidobacteria* bacterium 2G1 (KC442706)	99	soil
BI-3-85	LK023610	1	Uncultured *Acidobacteria* bacterium 3F2 (KC442541)	97	soil

			Planctomycetes		
BI-3-15	HG970690	2	Uncultured planctomycete AKYH691 (AY922147)	96	farm soil
BI-3-33	LK023576	1	Uncultured *Gemmata* sp. AV_7R-N-B01 (EU341265)	95	commercial aircraft cabin air
BI-3-78	LK023607	1	Uncultured *Planctomycetales* bacterium ROM_34 (HE575397)	99	reverse osmosis membrane
BI-3-90	LK023613	1	Uncultured *Gemmata* sp. A370 (EU283557)	99	Anderson Lake
			Gemmatimonadetes		
BI-3-3	LK023560	1	Uncultured *Gemmatimonas* sp. T9233B2 (HM447783)	99	agricultural soil
BI-3-36	LK023577	1	*Gemmatimonas* sp. AOCRB-EC-6 (GU557153)	94	anaerobically sewage sludge
			Verrucomicrobia		
BI-3-26	LK023572	1	Uncultured *Verrucomicrobia* bacterium 38 (AY942964)	97	rhizoplane of peashrub
			Nitrospirae		
BI-3-20	LK023569	1	Uncultured *Nitrospira* sp. fjc-17 (JQ278765)	99	groundwater
			Armatimonadetes		
BI-3-93	LK023616	1	Uncultured candidate division OP10 bacterium (EU403982)	98	infiltrative surface clean water
			Firmicutes		
BI-3-106	LK023625	1	*Anoxybacillus* sp. SCSIO 15096 (JX555982)	97	marine sediment
			unknown		
BI-3-13	LK023565	1	Uncultured bacterium F3_166X (GQ263200)	99	simulated low level waste site
BI-3-66	LK023598	1	Uncultured bacterium P-11_B14 (HQ910268)	98	desert soil
BI-3-75	LK023604	1	Uncultured bacterium Elev_16S_1861 (EF020305)	89	rhizosphere
BI-3-86	LK023611	1	Uncultured bacterium HglApr130 (JX015617)	96	marine bulk water
BI-3-91	LK023614	1	Uncultured bacterium MLS45 (JX240836)	97	coastal soil

Table S6. Affiliation of the 16S rRNA gene sequences of BII-2 bacterial clones.

Clone	Accession no. EMBL	no. of clones	Closest phylogenetic relative/accession no.	% similarity	Isolation source
			Betaproteobacteria		
BII-2-1	HG970692	3	*Hydrogenophaga* sp. Gsoil 1545 (AB271047)	99	soil of ginseng field
BII-2-2	HG970693	34	*Ralstonia pickettii* QL-A6 (HQ267096)	98	rhizosphere
BII-2-8	HG970694	10	*Burkholderia* sp. SAP38_2 (JN872505)	99	floral nectar
BII-2-9	HG970695	7	*Ralstonia mannitolilytica* JN201 (KF150440)	99	potassic trachyte
BII-2-12	HG970696	2	Uncultured *Curvibacter* sp. S_S_KL_303 (KC337212)	99	drinking water treatment plant membrane
BII-2-15	HG970697	10	*Variovorax paradoxus* CBF3 (JN990697)	99	soil
BII-2-19	HG970698	2	Uncultured *Ralstonia* sp. BF65B_B60 (HM141343)	98	supraglacial spring outflow
BII-2-29	HG970699	4	*Burkholderia* sp. U1-4 (FJ560474)	99	rhizospheric soil of rape
BII-2-43	HG970700	6	*Ralstonia* sp. DMSP-S11 (KC860267)	99	seawater and sediment
BII-2-62	HG970701	2	*Pelomonas saccharophila* NBRC 103037 (AB681917)	99	-
BII-2-92	HG970702	2	*Ralstonia pickettii* B1RO1 (JQ689181)	99	mineral water
BII-2-116	HG970703	2	*Hydrogenophaga* sp. MDT1-42 (JX949586)	99	glacier
BII-2-4	LK023631	1	*Burkholderia* sp. SAP38_2 (JN872505)	99	wild plant communities
BII-2-7	LK023632	1	*Burkholderia* sp. SAP38_2 (JN872505)	99	wild plant communities
BII-2-13	LK023633	1	*Ralstonia* sp. D23 (KF788130)	99	red soil
BII-2-18	LK023634	1	*Ralstonia* sp. SR4-06 (KF891410)	98	root
BII-2-20	LK023635	1	*Pelomonas puraquae* AR-174 (KF817777)	99	*Populus euphratica* in forest
BII-2-21	LK023636	1	Uncultured *Ralstonia* sp. BF65B_B105 (HM141278)	98	supraglacial spring outflow
BII-2-24	LK023637	1	Uncultured *Pelomonas* sp. spr019 (KC886831)	99	Lake Zurich epilimnion 5m depth
BII-2-32	LK023638	1	Uncultured *Ralstonia* sp. F3Bjun3 (GQ417751)	98	biological degreasing systems
BII-2-34	LK023639	1	*Ralstonia* sp. SR4-06 (KF891410)	99	root

BII-2-57	LK023641	1	Uncultured *Curvibacter* sp. S_S_KL (KC337212)	99	gut
BII-2-73	LK023642	1	*Acidovorax* sp. B18 (KF826887)	97	solid-phase denitrification biofilm
BII-2-105	LK023644	1	*Curvibacter gracilis* OFB-5 (HM439457)	96	fermented onion
			Gammaproteobacteria		
BII-2-85	LK023643	1	Unc. γ-proteobacterium ADK-MOe02-41 (EF520575)	94	acid-impacted lake
BII-2-27	HG970704	2	*Pseudomonas* sp. BBCT8 (DQ337559)	97	soil
			Alphaproteobacteria		
BII-2-40	LK023640	1	*Afipia* sp. sc_12 (EU878929)	99	soil

Table S7. Affiliation of the 16S rRNA gene sequences of BIV-3 bacterial clones.

Clone	Accession no. EMBL	no. of clones	Closest phylogenetic relative/accession no.	% similarity	Isolation source
			Alphaproteobacteria		
BIV-3-35	LK023703	1	*Mesorhizobium* sp. CCANP27 (HF931046)	100	host root nodule
BIV-3-37	LK023704	1	*Afipia* sp. sc_12 (EU878929)	99	soil
BIV-3-65	LK023707	1	*Agrobacterium* sp. FB1406 (JX943864)	99	root nodule
			Betaproteobacteria		
BIV-3-1	HG970718	33	*Ralstonia pickettii* VIT-SRM1 (KJ716446)	99	west Indian cherry fruit
BIV-3-4	HG970719	10	*Ralstonia pickettii* A-15 (JX036030)	99	activated sludge
BIV-3-10	HG970721	2	*Burkholderia* sp. SAP38_2 (JN872505)	99	floral nectar
BIV-3-23	HG970720	7	*Ralstonia* sp. DMSP-S11 (KC860267)	99	seawater and sediment
BIV-3-25	HG970722	13	Unc. *Ralstonia* sp. IODP_305_1309D_273_13 (HQ379137)	95	gabbroic central dome
BIV-3-34	HG970723	7	Uncultured *Burkholderia sp.*OTU35 (KF956504)	95	contaminated groundwater
BIV-3-41	HG970724	4	*Ramlibacter* sp. HTCC332 (AY429716)	98	contaminated groundwater
BIV-3-52	HG970725	2	*Ralstonia* sp. OV225 (AY216797)	99	potato field site soil
BIV-3-66	HG970726	3	*Curvibacter* sp. W2.09-301r (JX458451)	97	deep mineral water aquifer
BIV-3-12	LK023702	1	*Pelomonas puraquae* AT-91 (KF817703)	99	*Populus euphratica* in forest
BIV-3-54	LK023705	1	*Ralstonia* sp. D18_10 (KF819691)	99	well water in dry season
BIV-3-63	LK023706	1	*Burkholderia* sp. WR-50a (AB839881)	99	ginseng rhizosphere soil
BIV-3-87	LK023708	1	*Pelomonas saccharophila* NBRC 103037 (AB681917)	99	-
			Gammaproteobacteria		
BIV-3-2	HG970727	4	Uncultured *Thermomonas* sp. Plot18-A02 (FJ889350)	97	agricultural soil

			Acidobacteria		
BIV-3-104	HG970728	2	Uncultured *Acidobacteria* bacterium SeqSEEZ173 (JN367194)	99	soil
BIV-3-101	LK023709	1	Uncultured *Acidobacteria* bacterium SeqSEEZ173 (JN367194)	100	soil
			Nitrospirae		
BIV-3-6	HG970729	3	Uncultured *Nitrospirae* bacterium DM2-139 (KC172193)	99	ginger cropping soil

Table S8. Affiliation of the 16S rRNA gene sequences of BIV-2 bacterial clones.

Clone	Accession no. EMBL	no. of clones	Closest phylogenetic relative/accession no.	% similarity	Isolation source
			Alphaproteobacteria		
BIV-2-56	HG970707	2	*Erythrobacter aquimaris* g3 (JQ661145)	96	soil
BIV-2-64	HG970708	3	Uncultured *Sphingomonadales* bacterium CTRL51 (EU404009)	98	surface clean water
BIV-2-15	LK023654	1	Uncultured *Sphingomonadaceae* bacterium t281c10 (HM438325)	99	soil with anthracene
BIV-2-22	LK023655	1	Uncultured *Brevundimonas* sp. S110 (KF003174)	96	grass carp gut mucus
BIV-2-34	LK023659	1	Uncultured *Hyphomicrobiaceae* bacterium (FR681863)	98	geothermal microbial mats
BIV-2-41	LK023663	1	Uncultured *Caulobacterales* bacterium (FN689613)	97	rhizosphere of tomato plants
BIV-2-58	LK023670	1	*Devosia* sp. R-36756 (FR691413)	99	Forlidas Pond, Antarctica
BIV-2-59	LK023671	1	*Rubellimicrobium aerolatum* (AB682444)	97	-
BIV-2-71	LK023679	1	*Sphingomonas* sp. LRR22 (JX138997)	99	soil of a red pool
BIV-2-78	LK023683	1	*Brevundimonas* sp. W24 (KF560390)	99	soil from military site
BIV-2-81	LK023685	1	Uncultured *Mesorhizobium* sp. OUT12 (EU372810)	99	agriculture waste compost
BIV-2-86	LK023687	1	*Altererythrobacter* sp. CC-VAM-21 (KC169804)	98	marine sediment
BIV-2-102	LK023697	1	Uncultured *Sphingomonas* sp. Wbfc21 (KC138682)	99	saffron bulk soil
			Betaproteobacteria		
BIV-2-5	HG970709	2	*Herbaspirillum* sp. 9NM-7 (JQ608329)	98	lead-zinc ore tailings
BIV-2-23	HG970710	10	*Herbaspirillum* sp. 9NM-7 (JQ608329)	99	lead-zinc ore tailings
BIV-2-30	HG970711	2	*Variovorax* sp. C6d1 (AB552894)	99	Algal-bacterial consortia
BIV-2-31	HG970712	2	Uncultured *Variovorax* sp. 4.6h17 (JN679121)	98	membrane bioreactor
BIV-2-35	LK023660	1	*Herbaspirillum* sp. THG-e31 (KF314195)	99	soil
BIV-2-49	LK023667	1	Uncultured *Burkholderiales* bacterium 49-1_5 (FJ517712)	95	epithelium
BIV-2-52	LK023668	1	*Methylibium* sp. T2-YC6780 (GQ369048)	99	rhizosphere of a rice field

BIV-2-66	LK023676	1	*Variovorax* sp. Van34 (HQ222271)	99	enrichment culture with nitrate
BIV-2-74	LK023680	1	Uncultured *Methylophilus* sp. Acro220 (KC110974)	99	soil microcosm
BIV-2-90	LK023689	1	Uncultured *Polaromonas* sp. R77 (JQ861817)	94	groundwater with diesel
BIV-2-104	LK023699	1	*Herbaspirillum* sp. THG-e31 (KF314195)	99	soil
BIV-2-108	LK023701	1	Uncultured beta proteobacterium P-R68 (JN038855)	98	Chongxi wetland soil
			Deltaproteobacteria		
BIV-2-25	HG970713	5	Uncultured delta proteobacterium SNNP_2012-102 (JX114435)	99	Sierra Nevada NP soil
BIV-2-61	LK023673	1	Uncultured delta proteobacterium KCM-C-14 (AJ581623)	97	Soil sample
			Gammaproteobacteria		
BIV-2-65	HG970714	2	Uncultured *Thermomonas* sp. EHFS1_S15a (EU071527)	99	ESTEC HYDRA facility
BIV-2-37	LK023661	1	Uncultured gamma proteobacterium 33F (JN178912)	99	Kartchner Caverns, AZ
BIV-2-55	LK023669	1	Uncultured Xanthomonadaceae bacterium L1-20 (JF703511)	98	root and rhizophere soil
BIV-2-63	LK023675	1	Uncultured *Rhizobacter* sp. SNNP_2012-9 (JX114342)	99	Sierra Nevada NP soil
			Actinobacteria		
BIV-2-16	HG970717	2	Uncultured actinobacterium 1E1 (KC442672)	99	soil
BIV-2-2	LK023645	1	*Nocardioides* sp. M79 (KC464843)	99	forest rhizophere
BIV-2-8	LK023649	1	Uncultured *Aciditerrimonas* sp. D.an-164 (JX505231)	97	soil
BIV-2-9	LK023650	1	Uncultured *Micrococcineae* bacterium MLS194 (JX240871)	99	coastal soil
BIV-2-12	LK023653	1	Uncultured actinobacterium HG-B01170 (JN409119)	98	rhizosphere soil of cucumber
BIV-2-27	LK023657	1	Uncultured actinobacterium BPS_L377(HQ857735)	98	Soils with hydrocarbon
BIV-2-60	LK023672	1	Uncultured actinobacterium HG-B01170 (JN409119)	99	rhizosphere soil of cucumber
BIV-2-76	LK023681	1	Uncultured actinobacterium g43 (EU979052)	95	soil
BIV-2-77	LK023682	1	Uncultured actinobacterium E1B-A4-114 (EF016798)	99	soil
BIV-2-94	LK023692	1	Uncultured actinobacterium 500M2_B5 (DQ514194)	99	newly deglaciated soil
BIV-2-97	LK023695	1	Uncultured actinobacterium HG-B01170 (JN409119)	99	rhizosphere soil of cucumber
BIV-2-99	LK023696	1	Uncultured actinobacterium E1B-A4-114 (EF016798)	98	soil

BIV-2-105	LK023700	1	Uncultured *Sporichthyaceae* bacterium C.la-103 (JX504987)	97	soil
			Acidobacteria		
BIV-2-6	LK023647	1	Uncultured *Acidobacteria* bacterium HG-B0245 (JN409164)	99	rhizosphere soil of cucumber
BIV-2-42	LK023664	1	Uncultured *Acidobacteria* bacterium SeqSEEZ177 (JN367197)	100	soil
BIV-2-62	LK023674	1	Uncultured *Acidobacteria* bacterium SEG_08_567 (HQ729801)	99	grassland soil
BIV-2-67	LK023677	1	Uncultured *Acidobacteria* bacterium SEG_08_326 (HQ597906)	97	grassland soil
BIV-2-70	LK023678	1	Uncultured *Acidobacteria* bacterium AEG_08_306 (HQ597242)	99	grassland soil
BIV-2-89	LK023688	1	Uncultured *Acidobacteriales* bacterium Plot4-2C07 (EU449659)	100	agricultural soil
BIV-2-92	LK023690	1	Uncultured *Acidobacteria* bacterium AEW_08_616 (HQ598388)	99	woodland soil
BIV-2-95	LK023693	1	Uncultured *Acidobacteria* bacterium 3F5 (HQ003630)	100	Carrizo shallow lake
BIV-2-96	LK023694	1	Uncultured *Acidobacterium* sp. sw-xj145 (GQ302579)	98	cold spring
			Bacteroidetes		
BIV-2-1	HG970705	2	Uncultured *Bacteroidetes* bacterium LJ-B48 (JF319169)	95	rhizosphere soil
BIV-2-18	HG970706	4	Uncultured *Bacteroidetes* bacterium HG-J01116 (JN408920)	98	rhizosphere soil
BIV-2-7	LK023648	1	*Pedobacter* sp. M1-27 (KC569794)	99	soil
BIV-2-11	LK023652	1	Uncultured *Bacteroidetes* bacterium UHAS5.26 (JN037900)	99	saline-alkaline soil
BIV-2-26	LK023656	1	*Pedobacter* sp. M1-27 (KC569794)	96	soil
BIV-2-32	LK023658	1	Uncultured *Sphingobacteria* bacterium SeqSEEZ223 (JN367243)	99	soil
BIV-2-38	LK023662	1	Uncultured *Sphingobacteria* bacterium SeqSEEZ223 (JN367243)	99	soil
BIV-2-103	LK023698	1	Uncultured *Hymenobacter* sp. SeqSEEZ193 (JN367213)	99	soil
			Nitrospirae		
BIV-2-80	HG970715	2	Uncultured *Nitrospirae* bacterium DM2-139 (KC172193)	99	ginger cropping soil
BIV-2-48	LK023666	1	Uncultured *Nitrospira* sp. fjc-17 (JQ278765)	99	groundwater
			Planctomycetes		
BIV-2-98	HG970716	2	Uncultured *Planctomyces* sp. N-111 (HM565043)	96	concrete
BIV-2-10	LK023651	1	Uncultured Planctomycetales bacterium LIM15 (HM241109)	98	limestone rock

			Cyanobacteria		
BIV-2-3	LK023646	1	*Leptolyngbya scottii* EcFYyyy_00 (KC463191)	99	Soil Crust
BIV-2-93	LK023691	1	*Leptolyngbya frigida* ANT.L52B.3 (AY493612)	99	Antarctica
			Gemmatimonadetes		
BIV-2-85	LK023686	1	Unc. *Gemmatimonadetes* bacterium HG-B02245 (JN409277)	99	rhizosphere soil of cucumber
			unknown		
BIV-2-79	LK023684	1	Uncultured bacterium AC14C1CF08 (JQ427104)	99	soil
BIV-2-44	LK023665	1	Uncultured bacterium AN1C2AF10 (JQ428809)	100	soil

Figure S1. RISA analysis of the samples: (1) BI-2; (2) BI-3; (3) BIV-2; (4) BIV-3; (5) BII-2; (M) 1kb DNA Ladder.

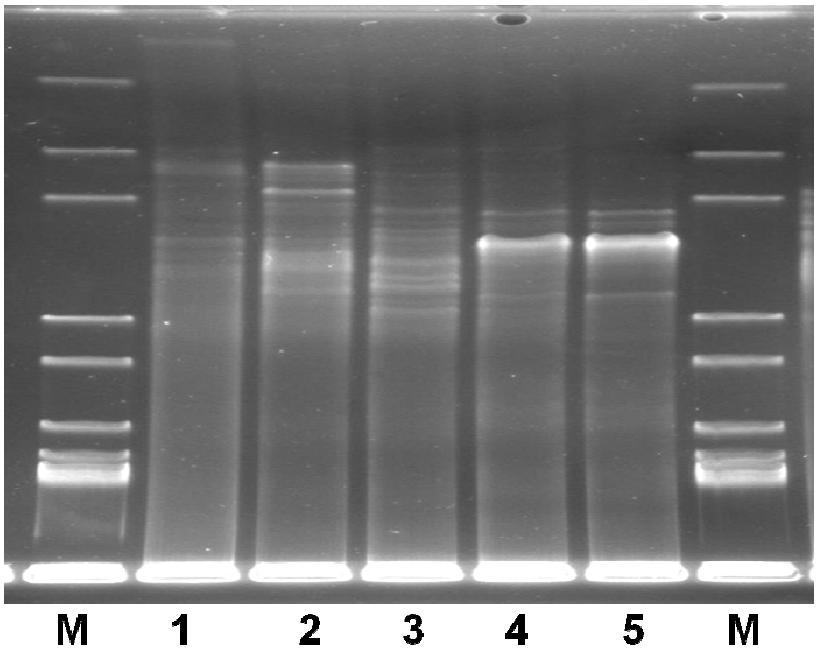

Figure S2. Rarefaction curves portraying the number of species against sampling depth of each sample.

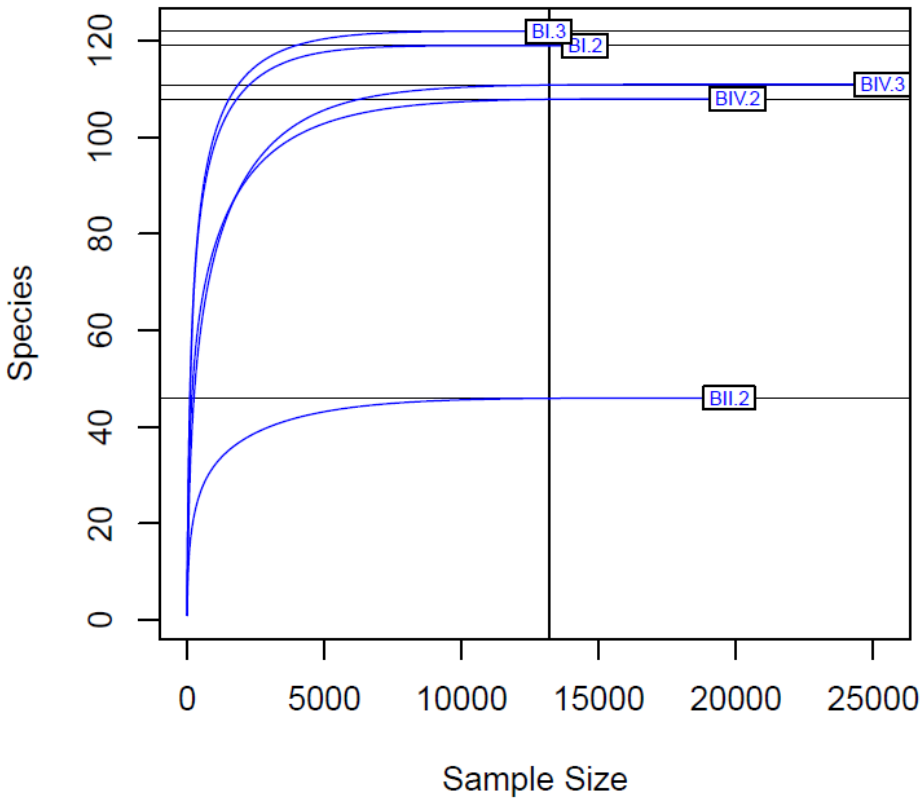

CHAPTER II

Chapter II: Microbial communities in bentonite formations and their interactions with uranium

Capítulo II: Comunidades microbianas en formaciones bentoníticas y sus interacciones con uranio

Margarita López-Fernández, Omar Fernández-Sanfrancisco, Alberto Moreno-García, Inés Martín-Sánchez, Iván Sánchez-Castro, Mohamed Larbi Merroun

Departamento de Microbiología, Universidad de Granada, Campus Fuentenueva, 18071 Granada, Spain

This chapter contains the following published paper/Este capítulo contiene el siguiente artículo publicado:

López-Fernández, M., *et al*. (2014). Microbial communities in bentonite formations and their interactions with uranium.

Applied Geochemistry, http://dx.doi.org/10.1016/j.apgeochem.2014.06.022

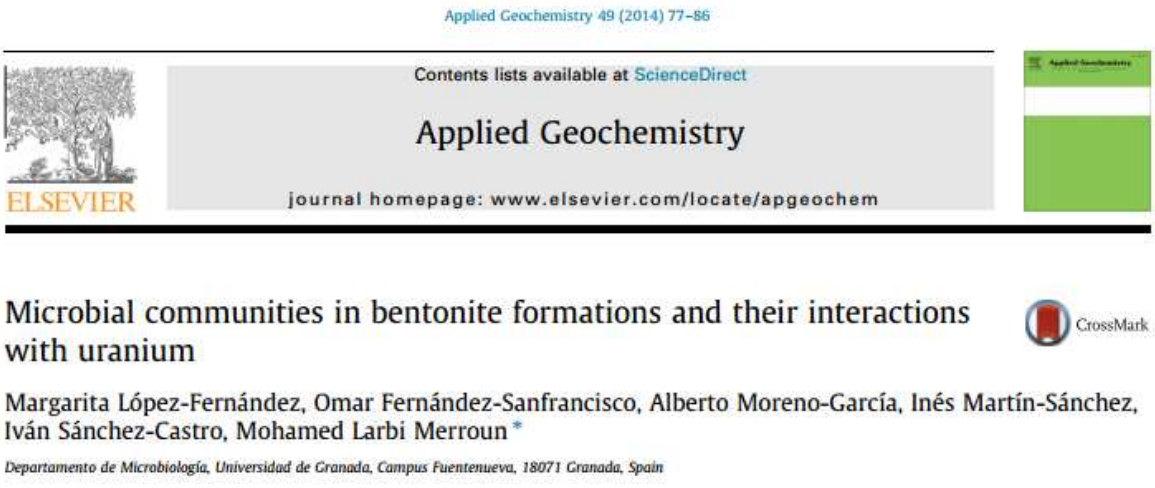

Applied Geochemistry 49 (2014) 77–86

Contents lists available at ScienceDirect

Applied Geochemistry

journal homepage: www.elsevier.com/locate/apgeochem

Microbial communities in bentonite formations and their interactions with uranium

Margarita López-Fernández, Omar Fernández-Sanfrancisco, Alberto Moreno-García, Inés Martín-Sánchez, Iván Sánchez-Castro, Mohamed Larbi Merroun *

Departamento de Microbiología, Universidad de Granada, Campus Fuentenueva, 18071 Granada, Spain

1. Resumen

Para garantizar la seguridad en un almacenamiento geológico profundo de residuos radiactivos es muy importante ampliar el conocimiento sobre las interacciones de los radionucleidos con los microorganismos presentes de forma natural en las formaciones geológicas (rocas de granito, formaciones arcillosas y depósitos de sales) que alojarán este tipo de sistemas de almacenaje. En España, los depósitos arcillosos de la región de Cabo de Gata, en Almería, han sido investigados para este propósito.

En el presente capítulo se caracteriza la diversidad microbiana mediante métodos dependientes de cultivo de dos muestras de bentonita (BI y BII) recogidas de depósitos de arcillas españoles, como material de referencia para su uso en el almacenamiento geológico profundo de residuos radiactivos. La evaluación de la población microbiana aerobia y anaerobia facultativa reveló la presencia de un alto número de bacterias cultivables (como por ejemplo: *Stenotrophomonas*, *Micrococcus*, *Arthrobacter*, *Kocuria*, *Sphingomonas*, *Bacillus*, *Pseudomona*s, etc.) pertenecientes a los *phyla Proteobacteria*, *Actinobacteria* y *Firmicutes*. Además, se aisló una cepa de una levadura pigmentada, BII-R8, asociada a *Rhodotorula mucilaginosa*.

Para estudiar la tolerancia al uranio de los microorganismos aislados se determinó su Concentración Mínima Inhibitoria (CMI) en un rango de 4 a 10 mM. Los resultados pusieron de manifiesto que, por ejemplo, la cepa *R. mucilaginosa* BII-R8 presenta una tolerancia de hasta 8 mM de concentración de uranio. Los estudios realizados mediante citometría de flujo, analizando la viabilidad celular y el potencial metabólico, indicaron que la alta tolerancia al uranio de esta levadura es un proceso mediado biológicamente.

Finalmente, gracias al análisis de Microscopía Electrónica de Barrido y Transmisión en Campo Oscuro de Alto Ángulo Anular (STEM-HAADF), se observaron precipitados intracelulares y a nivel de la pared celular. Asimismo, se elaboró un mapa mediante Energía de dispersión de Rayos X (EDX) mostrando la distribución de los distintos elementos, que reveló la presencia de uranio y fósforo en el interior de los precipitados observados. Estos resultados demostraron la habilidad de estas células para precipitar uranio como minerales de fosfato de uranio(VI).

Sin embargo, es necesario un profundo conocimiento de la diversidad microbiana en las formaciones arcillosas y especialmente de las interacciones microbianas con radionucleidos para poder predecir el impacto microbiológico en el almacenamiento de residuos nucleares nucleares, así como en el desarrollo de estrategias de biorremediación para zonas contaminadas con uranio.

2. Abstract

A reliable performance assessment of deep geological disposal of nuclear waste depends on better knowledge of radionuclide interactions with natural microbes of geological formations (granitic rock, clay, salts) used to host these disposal systems. In Spain, clay deposits from Cabo de Gata region, Almeria, are investigated for this purpose.

The present work characterizes the culture-dependent microbial diversity of two bentonite samples (BI and BII) recovered from Spanish clay deposits, studied as references material for the deep geological repository of radioactive wastes. The evaluation of aerobe and facultative anaerobe microbial populations shows the presence of a high number of cultivable bacteria (e.g. *Stenotrophomonas*, *Micrococcus*, *Arthrobacter*, *Kocuria*, *Sphingomonas*, *Bacillus*, *Pseudomona*s, etc.) affiliated to three phyla Proteobacteria, Actinobacteria, and Firmicutes. In addition, a pigmented yeast strain BII-R8 related to *Rhodotorula mucilaginosa* was also recovered from these formations.

To study the uranium tolerance of the natural isolated microorganisms, their minimal inhibitory concentration was determined, in a range from 4 to 10.0 mM. Results revealed that, for instance, strain *R. mucilaginosa* BII-R8 tolerated up to 8 mM of uranium. In addition, flow cytometry studies were performed to analyze the cell viability and the metabolic potential, indicating that the high uranium tolerance of this yeast isolate is a biologically mediated process.

Finally, intracellular and cell wall-bound precipitates were observed by Scanning Transmission Electron Microscopy-High-Angle Annular Dark-Field (STEM-HAADF). Energy Dispersive X-ray (EDX) element-distribution maps showed the presence of uranium and phosphorus within these accumulates. Thess EDX results demonstrate the ability of the yeast cells to precipitate uraniium as U(VI) phosphate minerals.

However, fundamental understanding of the microbial diversity of clays and microbial interaction with radionuclides is necessary. And it will be useful for predicting the microbial impacts on the performance of the waste repositories, as well as in the development of bioremediation strategies for uranium contaminated sites.

3. Introduction

Nuclear wastes generated at all steps in the nuclear fuel cycle (e.g. uranium ores milling and mining, fuel fabrication, etc.) must be safely stored for at least 100,000 years for the radiotoxicity to decrease to levels similar to those of natural uranium and its daughter products (Hedin, 1999). Deep geological disposal of wastes encapsulated in corrosion-resistant metal containers has been considered as the safest option for the disposal of these hazardous materials (IAEA, 2003). A number of potentially suitable host rock types, such as granite, clay stone and salt deposits, have been identified. Granitic rock environments have been extensively studied in Finland, Sweden and Canada as potential host rocks for a repository (Stroes- Gascoyne and Sargent, 1998; Pedersen, 1999; Itavaara *et al*., 2011).

The USA has proposed salt deposits (Fredrickson *et al*., 2004). In Europe, mainly in Germany, France, Belgium and Switzerland, clay formation is a candidate host rock for a high-level nuclear waste repository (ONDRAF/NIRAS, 2001; Stroes-Gascoyne *et al*., 2007a; Wouters *et al*., 2013). In Spain, the geological formations considered are granite, clay and salt (Villar *et al*., 2006). In addition, several studies have investigated the selection and characterization of suitable clays for the sealing and backfilling of Spanish radioactive waste repositories. These studies indicated that bentonite, taken from clay deposits of El Cortijo de Archidona (Cabo de Gata region, Almeria, Spain), was one of the best characterized from the mineralogical, thermal, hydraulic, mechanical, geochemical and alterability points of view (Villar *et al*., 2006).

The safety of this long-term geological disposal could be compromised by physical and chemical factors, and also by the biogeochemical activity of either indigenous to the repository´ s host rock or introduced during the construction of a repository (Meleshyn, 2011; Stroes-Gascoyne and West, 1997). Microbial processes can affect the geochemistry of clays through three different mechanisms: (i) reduction of structural Fe(III) of clay minerals, (ii) alteration of mineral surfaces by the production of siderophores and small-organic acids, (iii) formation of biofilm in the clay mineral

surface (Meleshyn, 2011). In addition, microbes are able to control the speciation and mobility of radionuclides (Newsome *et al*., 2014) through processes such as biosorption to the cell surface (Lloyd and Macaskie, 2000; Merroun *et al*., 2005), intracellular accumulation (Brookshaw *et al*., 2012; Merroun *et al*., 2002; Suzuki and Banfield, 2004), biomineralization (Macaskie *et al*., 2000; Merroun *et al*., 2011), or biotransformations (Brookshaw *et al*., 2012; Lovely *et al*., 1999). Several studies characterized the structure and composition of indigenous microbial populations in deep-subsurface clay environments (Mauclaire *et al*., 2007; Poulain *et al*., 2008; Stroes-Gascoyne *et al*., 2011, 2007b), and in bentonite engineered barriers surrounding waste containers (Motamedi *et al*., 1996). For instance, the numbers of aerobic and anaerobic heterotrophs (e.g. sulphate reducing bacteria) detected by Stroes-Gascoyne (2010) in commercial Wyoming MX-80 bentonite were 105 CFU/g and 102 CFU/g, respectively. Fukunaga *et al*. (2005) studied the microbiology of bentonite deposits in Japan as a natural analogue of bentonite based buffer material using culture-based methods and microscopic counting of viable cells.

However, no microbial diversity studies were conducted on subsurface bentonite as sink of aerobe and facultative anaerobe microbes which could be introduced during the construction operations of a repository. In addition, studies aimed to elucidate the mechanisms of interactions between these microbial populations and radionuclides (e.g. uranium) are needed. However, whilst there is considerable data on effect of prokaryotic microorganisms (e.g. bacteria and archaea) in the speciation of uranium (Suzuki and Banfield, 2004; Merroun and Selenska-Pobell, 2008; Reitz *et al*., 2011), the effects of eukaryotic microbes (e.g. yeasts) are not yet fully understood.

The objective of the present work is twofold: (i) to extend the knowledge of prokaryotic and eukaryotic life in bentonite of the safety barriers (host rock and engineered barriers) using culture dependent techniques, and (ii) to characterize the interaction mechanisms of highly uranium tolerant yeast strain *Rhodotorula mucilaginosa* BII-R8 with this radionuclide using a multidisciplinary approach combining Scanning Transmission Electron Microscopy-High- Angle Annular Dark-Field (STEM-HAADF) and flow cytometry techniques.

4. Materials and methods

4.1. Geographical description of the clay sample recovery sites

The two clay samples used in this work were recovered from the surface of the bentonite of El Cortijo de Archidona (sample BI) and that of outcrop of El Toril (sample BII) (Cabo de Gata, Almeria, Spain) (Fig. 1) in April 2009 and stored at -20 °C until use. The El Toril bentonite deposits result from acid alteration of the original deposits caused by physical, chemical and mineralogical changes in the bentonite material (Martínez *et al*., 2007).

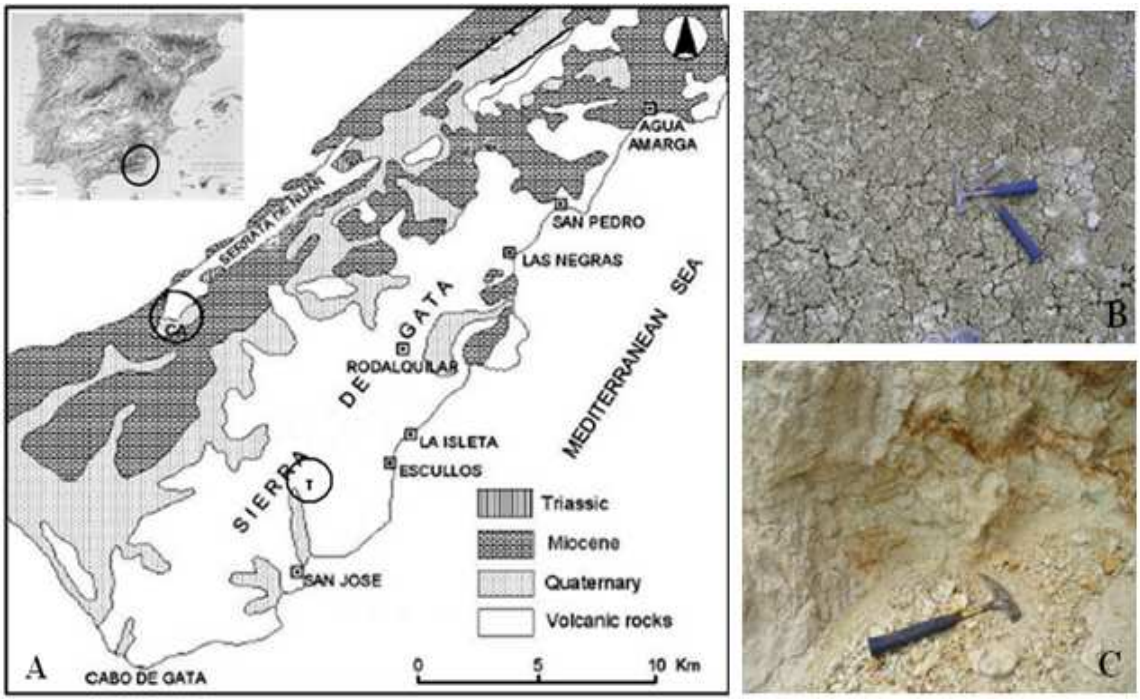

Fig. 1. Geographical position of the clay sampling site: A: Location map of the bentonite sampling site in Cabo de Gata region, Almeria, South-East of Spain. B: El Cortijo de Archidona sampling site, and C: El Toril sampling site. CA: El Cortijo de Archidona deposits (sample BI), T: El Toril deposits (sample BII).

4.2. XRD characterization and pH measurements of the clay samples

Solid clay samples were examined by X-ray diffraction (XRD) using a PANalytical X'Pert Pro diffractometer equipped with an X'Celerator solid-state detector and a sample spinning (Instituto Andaluz de Ciencias de la Tierra, CSIC-University of Granada, Granada, Spain). X-ray powder diffraction patterns of the bulk samples were recorded using random oriented mounts with CuK a-radiation, at 45 kV,

40 mA, in the range of 3 to 70 °2θ. Semi-quantitative estimation of the solid composition in crystalline phases was obtained by X'Pert High Score Plus (PANalytical, 2008), on basis of the Reference Intensity Ratio (RIR) values (Chung, 1975, 1974a,b). The pH of the clay samples was measured using a Crison pH-meter (MicropH, 2002) standardized against pH 4.00, 7.02 and 9.18 commercial reference solutions. The reported accuracy was of ± 0.02 pH units.

4.3. Chemical analysis of the clay samples pore water

Trace element composition of clay samples pore water was performed at the Institute of Resource Ecology, Helmholtz-Zentrum Dresden-Rossendorf (HZDR) using Inductively Coupled Plasma-Mass Spectrometry ICP-MS (Table S1). ICP-MS is a powerful analytical technique with application in the determination of trace-elements composition of different environmental samples.

4.4. Microbial isolation media and culture conditions

The microbial diversity of the two clay samples was studied using a culture-dependent approach. For the bacterial isolation different culture media were used, including oligotrophic R2A medium (Reasoner and Geldreich, 1985), Luria–Bertani (LB) medium (Miller, 1972) and Nutrient Broth (NB). Samples of 1 g of aseptically recovered material were transferred into 100 ml sterile, distilled water and incubated at 28 °C for 24 h. After agitation, dilutions of the supernatants were spread on agar plates with different culture media. Plates were incubated at 28 °C.

4.5. Molecular characterization of the microbial isolates

DNA extraction was performed from 1 ml bacterial cultures collected at the mid-exponential growth phase using the protocol described in Martín-Platero *et al*. (2007). The 16S rRNA gene fragments were amplified using the primer pair $16S_{7\text{-}27:F}$ (5'-AAGAGTTTGATYMTGGCTCAG-3') and $_{16S1492\text{-}1513:R}$ (5'-TACGGYTACCTTGTTACGACTT-3'), *E. coli* numbering. Before sequencing, the PCR products were purified using the MBL-PCR QuickClean kit (Dominion-MBL SL, Spain) according to the instructions of the manufacturer. The purified 16S rRNA gene products were bi-directionally sequenced using the same primers used during the amplification step, BigDye Terminator v3.1 Cycle Sequencing kits (Applied

Biosystems) and a 3130 DNA Analyzer (Applied Biosystems). The sequences were compared with those available in the GenBank by BLAST (Basic Local Alignment Search Tool) analysis. The multiple sequence alignment program BioEdit (Hall, 1999) was used for sequence alignment. Phylogenetic trees were generated by using MEGA software (Tamura *et al*., 2007) based on the results of the neighbor-joining algorithm with distance analysis (Kimura corrections). In the case of the yeast strain BII-R8, we performed DNA extraction and sequencing of the rDNA ITS fragment, which is the DNA-barcode established for fungi (Schoch *et al*., 2012). Comparison of assembled rDNA ITS sequence was performed with GenBank and MycoID databases. The nucleotide sequences reported here were submitted to the EMBL Nucleotide Sequence Database under accession numbers HG800026–HG800061.

4.6. Uranium solution preparation

1 M stock solution of $UO_2(NO_3)_2 \cdot 6HO$ was prepared by dissolving the appropriate quantity of metal salt in 0.1 M $NaClO_4$. The stock solution was sterilized by filtration through 0.22 µm nitrocellulose filters and stored at 4 °C until use. Working solutions were prepared by dilution of the stock solution. The pH was adjusted by addition of small volumes of acid (HCl) or base (NaOH).

4.7. Determination of Minimal Inhibitory Concentrations of uranium for the microbial growth

The MIC of uranium for the growth of the microbial strains was determined in triplicate. Cells were grown to the mid-exponential phase in low phosphate medium (LPM) (Rossbach *et al*., 2000), washed twice with 0.9% NaCl, and then 10 µl of the cell suspension was inoculated in LPM agar, containing increasing concentrations of uranium from 0.5 to 16 mM. After spreading, the plates were incubated at room temperature for one week. The MIC was defined as the lowest concentration at which complete inhibition of colony formation was observed (Rossbach *et al*., 2000). The preparation of the LPM medium includes two steps: the first one consists in the preparation of a saline solution (10X) which contains in (g/l): NaCl, 46.8; KCl, 14.9; NH_4Cl, 10.7; $(NH_4)_2SO_4$, 4.3; $MgCl_2$, 0.95; $ZnSO_4$, 0.0027; Tris base, 143.3. In the second step, 100 ml of the previously prepared saline solution (10%) is mixed with the following components: glycerol (5 ml), thiamine (50 mg/ml, 0.4 ml), peptone (10%, 100

ml), $CaCl_2$ (100 mM, 1 ml). For the preparation of solid media Bacto agar (15 g/l) was added.

4.8. Effect of uranium on cellular viability using flow cytometry studies: live/dead staining

Cells were harvested from LPM medium (loaded during 48 h with different uranium concentrations) by centrifugation (11000 rpm, 15 min, 4 °C), suspended and diluted in Phosphate Buffered Saline (PBS) to approx. 106 cells/ml. Solutions of Fluorescein diacetate (FDA) (20 µl, 0.1 mg/ml) and Iodide Propidium (IP) (2 µl, 1 mg/ml) were mixed with cell suspensions for staining for 15 min in the dark, at room temperature. Microbial suspensions incubated in the presence of both stains simultaneously were analyzed by flow cytometry for green (i.e. viable) and red (i.e. dead). Measurements were taken in triplicate using a FACS CantoII cytometer Becton Dickinson (San Jose Palo Alto, California), equipped with three lasers: 488 nm blue, 620 nm red and 405 nm UV. Samples were measured in FL1 (FITC) and FL2 (PE-IP), in logarithmic scale channels, at medium speed. Filters used were 530 nm and 580 nm Band Pass. Samples were analysed using BD Diva 6.1.

4.9. Sample preparation for STEM-HAADF/EDX analyses

Uranium treated microbial cells were harvested by centrifugation at 11000 rpm for 15 min at 4 °C and washed twice with 0.9% NaCl to remove the interfering ingredients of the growth medium. TEM samples were prepared as described in Merroun *et al*. (2005). Samples were examined under high-angle annular dark field scanning transmission electron microscope (STEM-HAADF), FEI TITAN G2 80-300. TEM specimen holders were cleaned by plasma prior to STEM analysis to minimize contamination. The high resolution STEM is equipped with HAADF detector and EDAX energy dispersive X-ray.

5. Results

5.1. Mineralogical characterization of the clay samples

The mineralogy of the studied clay samples is dominated by the presence of montmorillonite, with quartz and feldspars as minor phases (Table 1). XRD patterns of the samples and peaks belonging to the identified phases are shown in Fig. 2. No peaks remain unidentified.

Table 1: Semi-quantitative estimation of mineralogy of samples BI and BII by DRX.

Sample	Mineral	SemiQuant (%)
BI	Montmorillonite	84
	Albite	12
	Quartz	3
BII	Montmorillonite	71
	K-feldspar	18
	Quartz	10
	Jarosite	1

Other minerals of interest for mineralogical characterization of clay samples (e.g., pyrite, calcite, siderite, dolomite) were not detected. However, the presence of accessory minerals has been reported for some bentonites recovered from Cabo de Gata area (Huertas *et al*., 2000; Caballero *et al*., 2005; Villar *et al*., 2006). The most relevant difference between BI and BII is the presence of jarosite in sample BII.

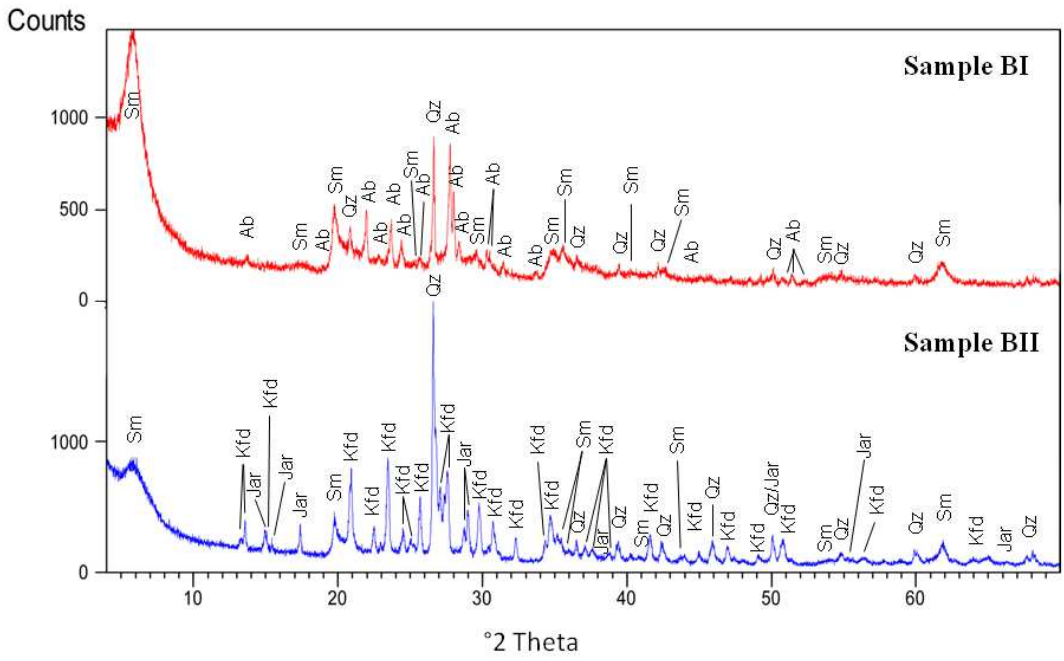

Fig. 2. XRD-patterns of powder samples from the two bentonite samples (BI and BII). Sm: smectite; Qz: quartz; Fd-Albite: plagioclase-feldspar albite; Kf-Sanidine: potassium-feldspar sanidine and Jar: jarosite.

The mineralogy of the Boom Clay at Mol (Belgium), used as host rock reference for the disposal of Belgian radioactive waste, is dominated by clay minerals including illite (20–30%), kaolinite (20–30%), smectite (10%) (Lima *et al*., 2012). The non-clay fraction is dominated by quartz (25%) and feldspar (Lima *et al*., 2012). The pH of sample BI and BII was 9.03 ± 0.02 and 7.82 ± 0.02, respectively.

5.2. Culture dependent microbial diversity of Spanish clay formations

In this study, a combination of complex culture media, containing peptides, sugar and minerals (LB, NB), and oligotrophic culture medium such as R2A were used to isolate microbial strains from the two clay samples. R2A medium was developed for its use in heterotrophic plate count analyses and for subculture of bacteria isolated from potable water samples. This medium was successfully used for the isolation and numeration of a high and diverse number of microbial strains isolated from oligotrophic environments including soil, clays and heavy metal/radionuclide contaminated sites (Nedelkova *et al*., 2007; Merroun *et al*., 2011). The phylogenetic affiliation of the microbial strains isolated from the two clay samples based on 16S/ITS rRNA gene analysis is shown in Fig. 3, Table 2 and 3.

Table 2. Affiliation of the 16S rDNA of BI microbial isolates

Phylum	Isolate	Accession no EMBL	Closest phylogenetic relative/ Accession no/similarity (%)	Origin of closed related sequence
Actinobacteria	BI-2	HG800026	*Arthrobacter pascens* L-14 (HQ202831, 99)	soil
	BI-4	HG800028	*Arthrobacter* sp. K4-10C (EF612294, 100)	semiarid Pb-Zn mine
	BI-5	HG800029	*Arthrobacter oryzae* H34 (KC934820, 98)	purple siltstone
	BI-7	HG800030	*Arthrobacter oryzae* H34 (KC934820, 99)	purple siltstone
	BI-11	HG800032	*Arthrobacter* sp. TF11 (KC294102, 99)	iron mine
	BI-36	HG800044	*Arthrobacter* sp. 210_2 (FJ938113, 99)	soil
	BI-31	HG800041	*Arthrobacter* sp. A105-06 (KC422660, 99)	As-groundwater sediment
Proteobacteria	BI-15	HG800035	*Paracoccus homiensis* SB1252 (JF260871, 97)	mussel
	BI-21	HG800038	*Paracoccus homiensis* SB1252 (JF260871, 98)	mussel
	BI-33	HG800042	*Paracoccus homiensis* SB1252 (JF260871, 96)	mussel
	BI-34	HG800043	*Sphingomonas* sp. BAC318 (EU131002, 99)	water treatment filters
	BI-13	HG800033	*Herbaspirillum* sp. Sco-D19 (FN386763, 99)	volcanic ash
	BI-26	HG800040	*Janthinobacterium* sp. TP-Snow-C16 (HQ327125, 99)	snow
	BI-3	HG800027	*Pseudomonas* sp. TF9 (KC294100, 99)	iron mine
	BI-14	HG800034	*Pantoea agglomerans* Z01 (JX257179, 98)	soil
Firmicutes	BI-9	HG800031	*Staphylococcus equorum* +Y111 (JX077102, 99)	tobacco leaf

Using LB, NB and R2A culture media, 16 bacterial strains were isolated from each sample (BI and BII). These isolates belonged to the phyla *Actinobacteria*, *Proteobacteria* and *Firmicutes*. *Proteobacteria* was the dominant phylum in sample BI, representing 50% of the isolates and just 18.75% of BII isolates. *Alphaproteobacteria* were distributed only in sample BI, represented by *Paracoccus* (3 isolates) and *Sphingomonas* (1 isolate) genera. Three *Betaproteobacteria* were recovered from the clay samples and were related to *Massilia*, *Herbaspirillium*, and *Janthinobacterium*. *Actinobacteria* was the most abundant phylum in sample BII with 75% of the total isolates. In the case of sample BI, this group was represented by 43.75% and it was dominated by *Arthrobacter* (7 isolates; 100%). However, the distribution of *Actinobacteria* in sample BII was heterogeneous and represented by different genera including *Micrococcus* (4 isolates), *Modestobacter* (2 isolates), *Amycolatopsis*, *Arthrobacter*, *Dermacoccus*, *Kocuria*, *Janibacter* and *Isoptericola*. Firmicutes members were represented only by two isolates, *Bacillus* and *Staphylococcus*. The strain BII-S2

was affiliated with 99% of 16S rRNA gene identity to the sporulating *Bacillus simplex*. Sporulation is described as a strategy used by bacteria to survive in oligotrophic environments such as Cabo de Gata clays.

Table 3. Affiliation of the 16S/18S rDNA of BII microbial isolates.

Phylum	Isolate	Accession no. EMBL	Closest phylogenetic relative/ Accession no./similarity (%)	Origin of closed related sequence
Actinobacteria	BII-L1	HG800045	*Arthrobacter* sp. S44 (HE662658, 99)	*Rumex acetosa*
	BII-L2	HG800046	*Dermacoccus* sp. Ellin185 (AF409027, 99)	soil
	BII-L3	HG800047	*Kocuria rhizophila* R-42745 (FR682683, 99)	soil
	BII-L5	HG800048	*Modestobacter* sp. R-36506 (FR682686, 98)	soil
	BII-R1	HG800049	*Modestobacter* sp. R-36506 (FR682686, 98)	soil
	BII-R2	HG800050	*Janibacter* sp. N2M (GU086450, 99)	rape leaves
	BII-R3	HG800051	*Amycolatopsis* sp. 05-St-016 (GU574104, 98)	water
	BII-R6	HG800054	*Micrococcus* sp. X2Bc2 (KF465977, 99)	schist soil
	BII-S1	HG800056	*Micrococcus* sp. PA-E028 (FJ233852, 99)	Kizhanelli root
	BII-S3	HG800058	*Isoptericola dokdonensis* DS-3 (NR_043779, 99)	soil
	BII-S4	HG800059	*Micrococcus luteus* SSN2 (HF562858, 99)	textile effluent
	BII-S5	HG800060	*Micrococcus* sp. PA-E028 (FJ233852, 99)	Kizhanelli root
Proteobacteria	BII-R4	HG800052	*Massilia* sp. P-105 (AM412138, 99)	soil
	BII-R5	HG800053	*Herbaspirillum* sp. 5410S-62 (JX275858, 99)	air
	BII-R7	HG800055	*Stenotrophomonas* sp. bB2 (JF772547, 99)	rhizosphere
Firmicutes	BII-S2	HG800057	*Bacillus simplex* Qtx-12 (GU201859, 99)	soil
Basidiomycota	BII-R8	HG800061	*Rhodotorula mucilaginosa* CBS 316 (AF444541, 99)	soil

In addition to bacteria, one yeast strain affiliated to *R. mucilaginosa* was isolated from sample BII. The yeast specie *R. mucilaginosa* is considered to be ubiquitous due to its global distribution in terrestrial, freshwater and marine habitats, and its ability to colonise a large variety of substrates. It has been found in extreme environments, such as chemical wastewater evaporation ponds (Libkind *et al*., 2008) and the leachate of a uranium mineral heap (de Silóniz *et al*., 2002), among others.

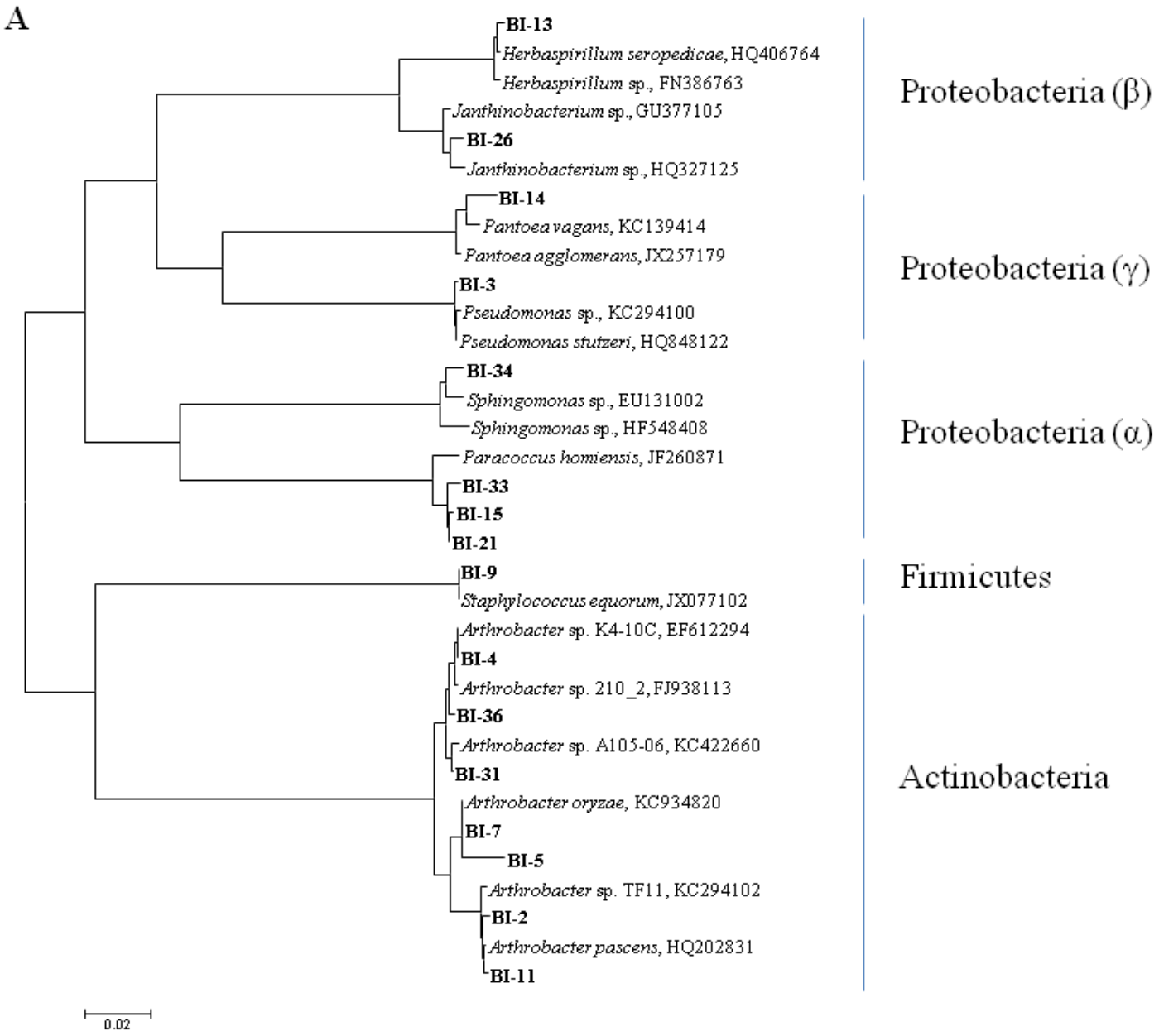

Fig. 3A. 16S rRNA gene based phylogenetic trees showing the diversity of the isolates from the bentonite samples, obtained by the neighbor joining algorithm (Kimura corrections). A. BI-phylogenetic tree.

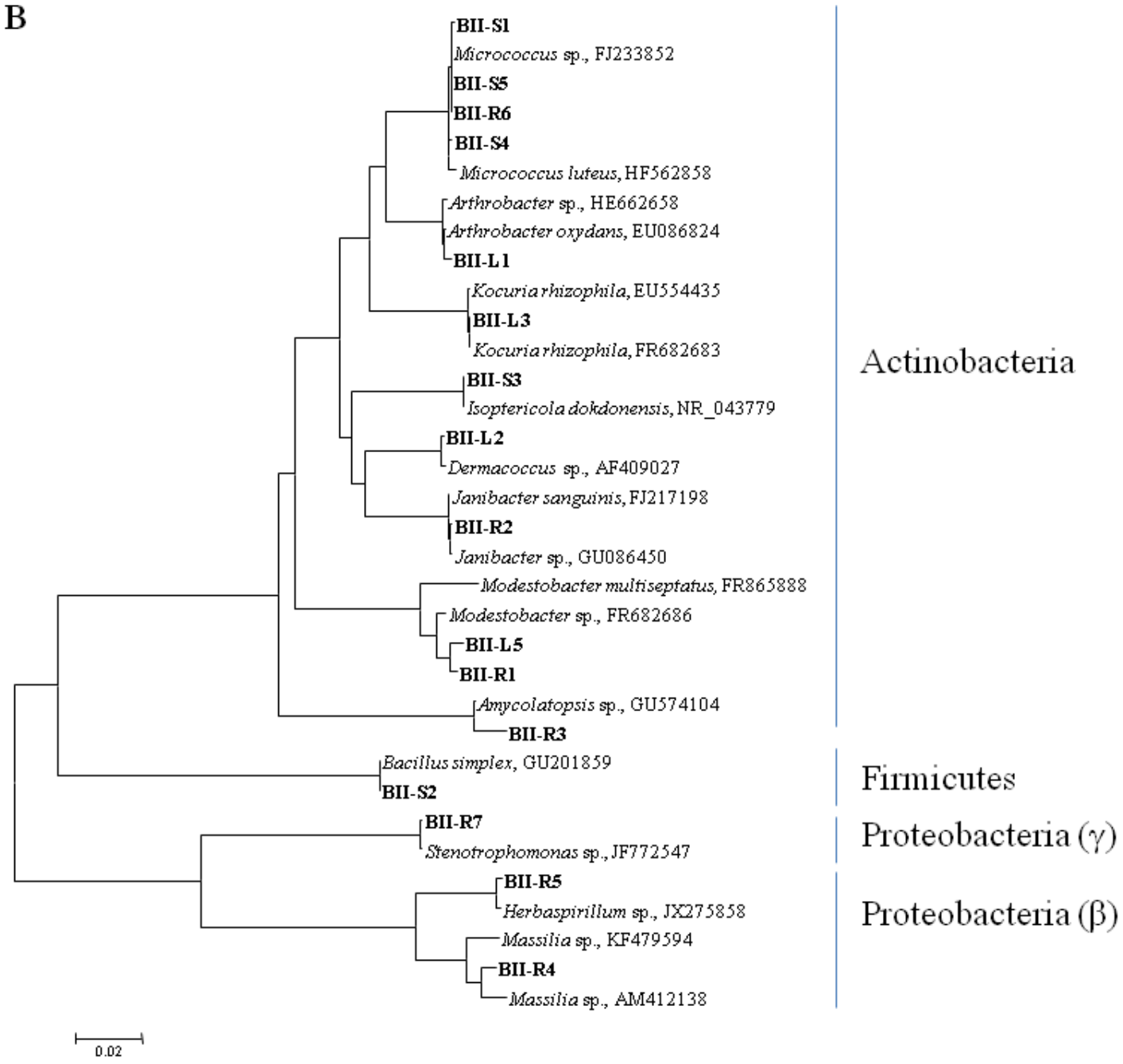

Fig. 3B. 16S rRNA gene based phylogenetic trees showing the diversity of the isolates from the bentonite samples, obtained by the neighbor joining algorithm (Kimura corrections). B. BII- phylogenetic tree.

5.3. Uranium tolerance of microbial isolates

5.3.1. Determination of Minimal Inhibitory Concentrations of uranium in solid media

Minimal inhibitory concentrations of uranium for the growth of more than 25 microbial strains isolated from the two clay samples are represented in Fig. S1 and Table 4. Results indicated that: (a) 61.5% and 13.3% of the microbial isolates recovered from sample BI and BII, respectively, grew successfully on LPM medium containing 3 mM uranium. 38.5% of BI and 40.0% of BII clay isolates tolerated up to 4 mM of U; (b) the bacterial strain *Stenotrophomonas* sp. BII-R7 and the yeast strain *R. mucilaginosa* BII-R8 showed high uranium tolerance, being able to grow up to 6 and 8 mM U, respectively.

Table 4. Minimal inhibitory concentration (MIC) of uranium for the growth of clay microbial isolates.

BI	MIC/MTC[a] U (mM)	BII	MIC/MTC U (mM)	BII	MIC/MTC U (mM)
BI-2	3/2	BII-L1	4/3	BII-S3	2/1
BI-3	3/2	BII-L2	4/3	BII-S4	2/1
BI-4	4/3	BII-L3	4/3	BII-S5	2/1
BI-5	3/2	BII-L5	4/2		
BI-7	3/2	BII-R1	nd/2		
BI-9	3/2	BII-R2	4/2		
BI-11	4/3	BII-R3	4/3		
BI-14	4/3	BII-R5	3/2		
BI-15	4/3	BII-R6	3/2		
BI-21	3/2	BII-R7	8/6		
BI-31	3/2	BII-R8	10/8		
BI-34	3/2	BII-S1	2/1		
BI-36	4/3	BII-S2	2/1		

[a]MTC: maximum tolerated concentration; nd: not determined data

5.3.2. Flow cytometry characterization of the effect of uranium on cell viability

The high uranium tolerance of the yeast *R. mucilaginosa* BII-R8 was also studied by flow cytometry using the live/dead staining approach. This approach is based on the use of a kit consisting of two stains, FDA and PI, both stain nucleic acids. FDA, which stains viable cells in green, is able to enter all cells and is used for assessing total cell counts, whereas red fluorescing PI enters only cells with damaged cytoplasmic membranes, i.e. dead cells. The percentages of viable and dead cells of yeast population treated with uranium concentration ranging from 0.5 to 4 mM during 48 h are presented in Table 5.

In the absence of U, 96% of the cells are alive. The cell viability decreases slightly in function of the increasing uranium concentrations from 0.5 mM to 3 mM. At 3 mM of uranium, 55% of the cells exhibited intact cell membranes. 4 mM is a cytotoxic concentration since 99.45% of the cells are not viable. The high uranium tolerance exhibited by cells of the yeast strain is a biological mediated process since under the same experimental conditions (uranium concentration, time of contact, etc.), cells of the yeast strain and those of the bacterium *Stenotrophomonas* sp. BII-R7 exhibited different levels of uranium tolerance. For instance, whereas at 2 mM U, almost 74% of yeast cells are alive, 100% of the *Stenotrophomonas* sp. BII-R7 cells are not viable.

Table 5. Effect of uranium concentration on the cell viability of the isolated strains BII-R7 and BII-R8.

Isolate	U concentration (mM)					
	0	0.5	1	2	3	4
	Viable cells (%)					
BII-R7	99.50 ± 1.30	100.00 ± 0.00	99.90 ± 0.10	0.00 ± 0.00	-	-
BII-R8	96.05 ± 1.05	92.40 ± 5.80	85.35 ± 3.35	73.95 ± 1.15	55.00 ± 5.40	0.55 ± 0.05

Standard deviation is included as ±SD

5.4. STEM-HAADF imaging of cellular localization of the accumulated uranium

A combination of STEM-HAADF and HRTEM were applied to determine the cellular localization of uranium accumulated by strain *R. mucilaginosa* BII-R8 and to elucidate the key mechanisms by which cells of this yeast strain cope with radionuclide toxicity. This is the first study reporting the molecular scale characterization of uranium interactions with *R. mucilaginosa* BII-R8. STEM micrographs of thin sections of *R. mucilaginosa* BII-R8 cells loaded with 1 mM U are presented in Fig. 4a and b. In these micrographs, electron-dense precipitates were observed at the cell surfaces. In addition, intracellular uranium accumulates are localized within and at the membranes of concentric organelles. EDX element-distribution maps derived from these uranium precipitates showed that they are mainly composed of U and P (Fig. 4c and d). The copper (Cu) peak resulted from the copper grid used to support the specimen. The presence of the silicon (Si) peak can be attributed to impurities in the culture medium and/or from the glass material of the flasks in which the cells were grown.

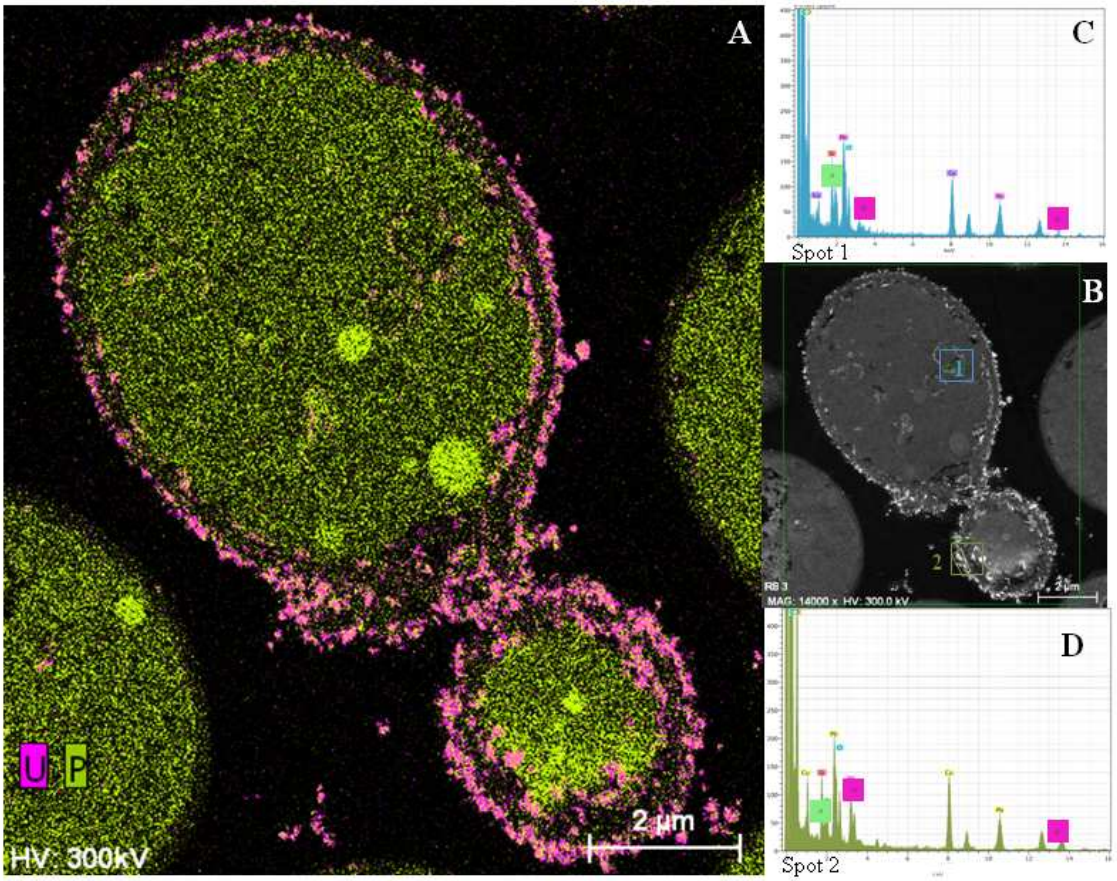

Fig. 4. Scanning Transmission Electron Microscopy -High-Angle Annular Dark-Field (STEM-HAADF) micrographs of thin sections of 1 mM U-treated cells of BII-R8 (A and B). EDX spectra of U-precipitates located in the interior of the U-treated cells (C), and at the cell walls (D).

6. Discussion

6.1. Impact of bentonite microbial diversity in the long-term performance of a Deep Geological Repository

Excavation operations of a DGR for radioactive wastes will most probably introduce microorganisms in the undisturbed properties of the host rock formation (Meleshyn, 2011). Therefore, the main aim of this work is to gain insights into the structure and composition of aerobic and facultative anaerobe microbes of the two bentonite formations considered as safety barriers, i.e., clay buffer and clay stone within a DGR. The microbial strains isolated were affiliated phylogenetically to bacteria described for their ability to interact efficiently with different elements of clay minerals, e.g. Fe(III), and also to control the speciation of radionuclides.

6.1.1. Effect of introduced microbial populations in the biogeochemical cycle of Iron

Microbial reduction of Fe(III): Bentonite studied in this work appears to contain many aerobe and facultative anaerobe bacterial strains belonging to Gammaproteobacteria (e.g. *Pseudomonas*, *Pantoea*, etc.) and to *Firmicutes* (e.g. *Bacillus*), described in literature for their ability to reduce structural Fe(III) in the clay minerals which in turn alter the chemical and physical properties of the clay formations for future DGR. Stroes-Gascoyne *et al*. (2011) has demonstrated through an in situ experiment in the Opalinus Clay formation that Fe(III)-reducing microbes would be most probably introduced by human activity during DGR construction and operation. Stucki and Getty (1986) observed that stimulation of microbial growth of 4 Bacillus species in the clay mineral (smectites) converted structural Fe(III) to Fe(II). In another study, a consortium of 5 Pseudomonas species was able to reduce ferruginous smectites (Gates *et al*., 1993). Further evidence showed that bacterial strains isolated from bentonite may play a role in the Fe reduction in clay minerals was reported by Maurice *et al*. (2001). These authors found that an aerobic strain of *Pseudomonas mendocina* enhanced kaolinite dissolution under aerobic environments with limited Fe availability. The bacteria solubilizes Fe(III) used as a terminal electron acceptor for oxidative phosphorylation and, thereby, acting as a bleaching agent for the kaolinite.

Biofilm formation in the surface of clay minerals: Several bacterial strains isolated from Spanish bentonite and affiliated to *Sphingomonas*, *Pseudomonas*, *Stenotrophomonas*, etc. are reported to produce extracellular polymers (mainly polysaccharides but also proteins and nucleic acids), which facilitate the cells to adhere to mineral surface and to solubilize Fe(III) needed for the cell growth. Mixtures of hectorite clay and *Pseudomonas syringae* in a minimal media suspension evolve into a polysaccharide-rich biofilm aggregate (Alimova *et al*., 2009). Representatives of *Sphingomonas* have also been identified as major populations in biofilms formed in naturally nickel-polluted river water (Lawrence *et al*., 2004). The extracellular polymer matrix and the biofilm boundary allow microbes to control the level of metal ions, to which they are exposed due to the contact with the overlying aqueous solution and the underlying mineral surface (Brown *et al*., 1994). For instance, EPS of *Pseudomonas stutzeri* was involved in the biomineralization of U(VI) as U-phosphate mineral phases with a structure similar to that of meta-autunite (Merroun and Selenska-Pobell, 2008).

Microbial dissolution of clay minerals: In this study, we could isolate microbial strains with siderophore production capacity including species of the genus *Modestobacter*, *Massilia*, *Herbaspirillum*, *Paracoccus*, *Kocuria*, etc. Microbial production of low molecular-weight compounds (e.g. siderophores and small organic acid such as citrate, malate, oxalate, etc.) with high affinity to Fe(III) facilitate the mobilization of Fe(III) from clay minerals, aiding the cells in acquiring this essential nutrient, which frequently is available in the external environment only as highly insoluble iron oxide.

6.1.2. Effect of bentonite microbial populations in the speciation of radionuclides

In addition to their effect in the biogeochemical cycle of Fe in clay minerals, the bacterial strains isolated in this work (e.g. *Stenotrophomonas*, *Pseudomonas*, *Bacillus*, *Arthrobacter*, etc.) might be able to change the speciation of radionuclides (e.g. uranium) in a future DGR. For instance, cells of the strains *Arthrobacter* sp. X34 and *Bacillus sphaericus*, isolated from radionuclide contaminated sites, have the potential to undertake aerobic U(VI) precipitation to insoluble U-phosphate phases due to the activity of acidic phosphatase (Martinez *et al*., 2006; Merroun *et al*., 2011). Fe(II) generated by the activity of Fe(III) reducing bacteria in clays may act as reducing agent

for the reduction of different radionuclides including U(VI) (Zhang *et al*., 2009), Tc(VII) (Bishop *et al*., 2011), leading to the immobilization of these radionuclides.

6.2. Interactions of the eukaryotic microorganism, *R. mucilaginosa* BII-R8, with U(VI)

In the present study, we could screen for some highly uranium tolerant microbial strains including the yeast strain *R. mucilaginosa* BII-R8, which was selected for U(VI) interaction and tolerance detailed study. Yeasts from the genus *Rhodotorula* were isolated from groundwater below the surface of the Baltic Sea (201–444 m) at the Aspö Hard Rock Laboratory in Sweden (Ekendal *et al*., 2003), and have been described for their high tolerance to copper due to presence of carotenoid pigments (Villegas *et al*., 2005). In this work, microscopic analysis indicated that the cells of the strain BII-R8 precipitate U(VI) at the cell surface and intracellularly. Uranium accumulation at the cell surface by yeasts has been reported previously for *Saccharomyces cerevisiae* (Suzuki and Banfield, 1999; Wang and Chen, 2006). In addition, Ohnuki *et al*. (2005b), identified the cell surface U-precipitates as uranyl-phosphate mineral with a structure similar to that of meta-autunite. Intracellular uranium uptake has been described in fungi, including the lichen *Piltigera membranacea* where uranium was localized mainly within cellular organelles termed ‘‘concentric bodies’’ (Griffiths and Greenwood, 1972; Banfield *et al*., 1999). Phosphate groups are important functional groups for the complexation of U(VI) on the cell surface and in our case also inside the fungal cells.

The ability of the BII-R8 bentonite isolate to biomineralize U(VI) phosphates indicates that indigenous microbes may play an important role in retarding the migration and transport of uranium in repositories. The biomineralization of U(VI) under anaerobic conditions was undertaken by a strain of *Rhanella* sp., which precipitates U(VI) as chernikovite mineral phase in the absence of oxygen (Beazley *et al*., 2009). The high uranium tolerance of the bentonite natural isolates such as *R. mucilaginosa* BII-R8 could be helpful for in situ bioremediation of uranium contaminated environments. For instance, the yeast cells enriched from bentonite could be used as a biofilter to eliminate heavy metals from contaminated waters. Similar applications were described for bacterial biofilm formed in the surface of bentonite during the bioremediation of Phenanthrene contaminated sites. The bacterial strains

responsible for the degradation of this organic contaminant were belonging to *Sphingomonadaceae* and *Rhodobacteraceae* (Huang *et al*., 2013).

7. Conclusions

The present study describes the culture-dependent microbial diversity of Spanish bentonite formations. In addition, the mechanisms by which some highly uranium tolerant microorganisms overcome the toxicity of this radionuclide are elucidated. Results showed a high microbial diversity in these samples, dominated by bacterial phyla *Proteobacteria*, *Firmicutes* and *Actinobacteria*. In addition, a pigmented yeast strain *R. mucilaginosa* BII-R8 was also recovered. Some of the microbial isolates are able to tolerate high uranium concentrations and to precipitate this radionuclide as uranium phosphate mineral phases. Thus, the role of these microbial communities in the biogeochemical cycle of Fe(III) clay minerals and of uranium (U-biominrealization) could be taken in consideration for the selection of this kind of geological formation for bioremediation purposes. Further studies on the effect of indigenous host rock microbes on the speciation of actinides are needed to predict the safety of a planned nuclear waste repository. Moreover, screening for microbes with high heavy metal tolerance and the study of their characteristic resistance is advisable to define cost-effective remediation strategies.

8. Acknowledgments

This work was funded by Grants CGL2009-09760 and CGL2012- 36505 (Ministerio de Ciencia e Innovación). We acknowledge the assistance of Maria del Mar Abad Ortega, and Concepcion Hernandez Castillo (Centro de Instrumentación Científica, University of Granada, Spain) for their help with STEM-HAADF measurement; of Jaime Lazuen-Alcon (Flow Cytometry Service, Centro de Instrumentación Científica University of Granada, Spain) for his help with flow cytometry measurements; of F. Javier Huertas-Puerta (Instituto Andaluz de Ciencias de la Tierra, CSIC – University of Granada, Spain), for his assistance in XRD analyses; and of HZDR, Germany, for the ICP-MS analysis.

9. Supplementary material

Table 1S. Elemental composition (µg/l) of the interstitial water of the bentonite samples (BI and BII).

Element	Content (µg/l)	
	BI	BII
Na	191000	152000
Mg	2090	4930
Al	413	211
Si	18700	12900
K	15300	8390
Ca	4140	14400
Cr	12.5	9.67
Fe	< 10	< 10
Mn	4.56	4.57
Co	0.117	0.263
Ni	10.8	9.95
Cu	9.54	10.3
Zn	16.5	26.2
Sr	60.2	85.3
Ag	< 0.01	< 0.01
Cd	< 0.01	< 0.01
Sn	< 0.01	< 0.01
Cs	0.0681	0.297
Pb	0.388	0.802
Th	< 0.1	< 0.1
U	6.16	1.29

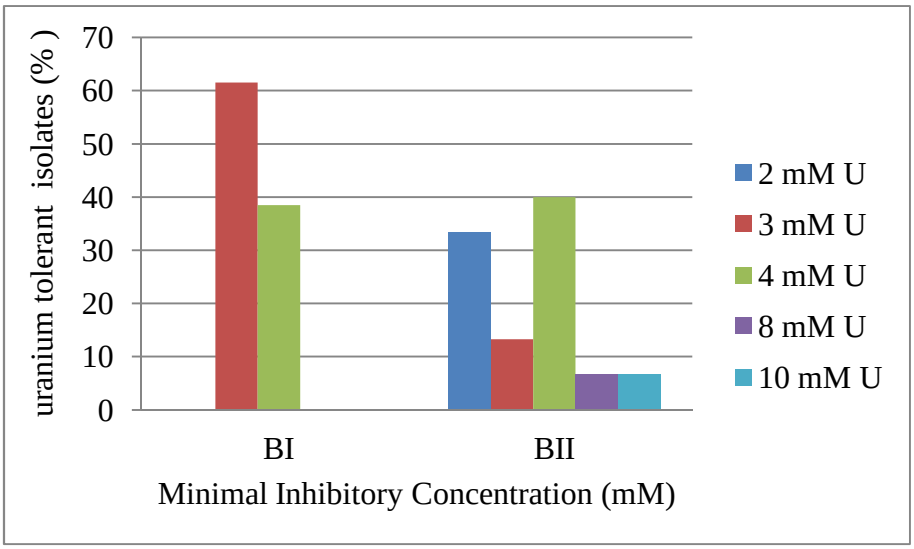

Fig. 1S. Minimal inhibitory concentration (MIC) of uranium for the growth of clay microbial isolates.

CHAPTER III

Chapter III: Interactions of the actinides U(VI) and Cm(III) with R*hodotorula mucilaginosa* BII-R8

Capítulo III: Interacciones de los actínidos U(VI) y Cm(III) con R*hodotorula mucilaginosa* BII-R8

Margarita López Fernández[1], Iván Sánchez Castro[1], Alix Guenther[2], Pier L. Solari[3], Henry Moll[2], Mohamed L. Merroun[1]

[1]Departamento de Microbiología, Universidad de Granada, Granada, Spain

[2]Institute of Resource Ecology, Helmholtz-Zentrum, Dresden Rossendorf, Dresden, Germany

[3]Synchrotron SOLEIL, L'Orme des Merisiers, Saint-Aubin - BP 48, F-91192 Gif-sur-Yvette Cedex, France

1. Resumen

Este trabajo describe los mecanismos de interacción a nivel molecular de *Rhodotorula mucilaginosa* BII-R8, un microorganismo aislado de bentonitas, con uranio(VI) y curio(III), como representantes de los actínidos hexavalentes y trivalentes, respectivamente. Para este estudio se utilizó una metodología multidisciplinar, combinando Espectroscopía de Fluorescencia Inducida por Láser en Tiempo Resuelto (TRLFS), Espectroscopía de Absorción de Rayos X (XAS), Microscopía Electrónica de Barrido y de Transmisión de Campo Oscuro Anular de Alto Ángulo (STEM-HAADF) y citometría de flujo.

Para el estudio de las interacciones de U(VI) con la levadura BII-R8 en *Low Phosphate Medium* (LPM) a pH 7, se utilizaron dos fluorocromos (yoduro de propidio y diacetato de fluoresceína) que permiten diferenciar entre las células vivas y las muertas. Los resultados de este análisis mediante la técnica de citometría de flujo, demostraron que la viabilidad celular de la levadura BII-R8 se ve afectada por la concentración de uranio y por el tiempo de contacto. El U(VI) genera una pausa temporal del crecimiento de *R. mucilaginosa*, de más de 24 h. Para estudiar la actividad metabólica frente a concentraciones crecientes de uranio se empleó el fluorocromo $DiOC_6$, que reveló la actividad de BII-R8 a altas concentraciones de este radionucleido.

Los análisis de interacciones de la levadura con uranio mediante XAS y TRLFS indicaron que el U(VI) es acomplejado por grupos fosfato orgánicos cuatro veces monodentados, coordinados en el plano ecuatorial del dioxo-catión uranilo. Esta estructura presenta una gran homología con la meta-autunita, un mineral de fosfato de uranio. Mediante STEM-HAADF se observaron acúmulos de uranio, localizados en la pared celular, así como en las membranas de los orgánulos, a nivel intracelular.

En el caso del Cm(III) los análisis realizados mediante TRLFS demostraron que para las células de la levadura *R. mucilaginosa* BII-R8 la bioadsorción del Cm(III) es un proceso reversible en el que dos especies fueron identificadas. La especie 1 de Cm(III)-*R. mucilaginosa* BII-R8 se caracteriza por tener una emisión máxima a 599 ± 1 nm y un tiempo medio de vida de luminiscencia de 215 ± 36 µs. La especie 2 de Cm(III)-*R. mucilaginosa* BII-R8 mostró una emisión máxima a 602.0 ± 0.5 nm y un tiempo medio de vida de luminiscencia mas corto, de 124 ± 15 µs. Comparando las propiedades de luminiscencia de las dos especies de Cm(III)-*R. mucilaginosa* BII-R8 con datos

recogidos en la literatura publicada, la especie 1 de Cm(III)-*R. mucilaginosa* BII-R8 se puede asignar a especies de Cm(III) unidas a grupos fosfato y la especie 2 de Cm(III)-*R. mucilaginosa* BII-R8 a especies de Cm(III) unidas a grupo carboxilo. Por lo tanto, los grupos carboxilo y fosfato están involucrados en la bioadsorción de este radionucleido, haciéndolo más móvil, facilitando así que pueda alcanzar la biosfera. Finalmente, el europio(III) se utilizó en este estudio como análogo inactivo del Cm(III). Mediante la técnica STEM-HAADF se observaron precipitados de Eu(III) y de fosfato, localizados en la superficie celular.

Los resultados obtenidos en este trabajo demuestran que los mecanismos de interacción de U(VI) y Cm(III) con las células de la levadura *R. mucilaginosa* BII-R8 transforman a estos dos radionucleidos en formas más móviles, lo que supondría un efecto negativo en la seguridad de los almacenamientos geológicos profundos de residuos nucleares.

2. Abstract

This work describes the molecular characterization of the interaction mechanisms of a bentonite natural isolate, *Rhodotorula mucigilanosa* BII-R8, with uranium(VI) and curium(III), as representative of hexavalent and trivalent actinides, respectively. A multidisciplinary approach combining Scanning Transmission Electron Microscopy-High Angle Annular Dark-Field (STEM-HAADF), X-ray Absorption Spectroscopy (XAS), Time-Resolved Laser-Induced Fluorescence Spectroscopy (TRLFS) and flow cytometry technique was applied.

For the study of the U(VI) interactions under growing conditions (Low Phosphate culture Medium (LPM) and pH 7), live/dead staining approach was used. Results of this analysis by flow cytometry technique showed that, the cell viability of the BII-R8 yeast strain is affected by uranium concentration and time contact. U(VI) caused a temporary growth arrest in *R. mucilaginosa* and the duration of the growth arrest was larger than 24 h. The metabolic potential response to increasing uranium concentrations was studied by $DiOC_6$ staining, revealing the ability of BII-R8 to cope with high concentrations of this radionuclide.

Uranium XAS and TRLFS analyses indicated, that U(VI) is complexed by organic phosphoryl groups four-fold monodentately coordinated in the equatorial plan of the uranyl dioxo-cation showing great homologies with the uranyl mineral phase meta-autunite. By STEM-HAADF uranium accumulates were observed, located at the cell wall and intracellulary, at the membranes of concentric organelles.

In the case of Cm(III), TRLFS analysis demonstrated that for the yeast cells of *R. mucilaginosa* BII-R8, the biosorption of Cm(III) is a reversible and pH dependent process, where two Cm(III) yeast species were detected. Cm(III)-*R. mucilaginosa* BII-R8 specie 1 is characterized by an emission maximum at 599 ± 1 nm and an average luminescence lifetime of 215 ± 36 µs. Whereas Cm(III)-*R. mucilaginosa* BII-R8 specie 2 shows a more red shifted emission maximum at 602.0 ± 0.5 nm and a shorter average luminescence lifetime of 124 ± 15 µs. By comparing the luminescence properties of both Cm(III)-*R. mucilaginosa* BII-R8 species with selected literature data, Cm(III)-*R. mucilaginosa* BII-R8 specie 1 can be asigned to a Cm(III) species bound to phosphoryl sites and Cm(III)-*R. mucilaginosa* BII-R8 specie 2 to a Cm(III) species bound to carboxyl sites of the cell envelope. So far, both carboxyl and phosphates were involved

in the sorption of this actinide, making it more mobile and more likely to reach the biosphere. Finally, europium(III), used in this study as inactive analogue of Cm(III), was accumulated as Eu(III)-phosphates at the cell surface as it was demonstrated by STEM-HAADF.

The results obtained in this work showed that the interaction mechanisms of U(VI) and Cm(III) with the cells of the yeast *R. mucilaginosa* BII-R8 makes both radionuclide more mobile, having a negative effect in the safety case of deep geological disposal of radioactive wastes.

3. Introduction

Large amounts of radioactive wastes generated by human activities (e.g. uranium mining processes, nuclear energy industry, etc.) should be safely disposed in future deep geological repository (Hedin, 1999; IAEA, 2003). These wastes will be encapsulated into iron or copper canisters. The canisters will be surrounded by an engineered barrier consisting of bentonite, and embedded in the host rock (e,g. granite, salts, clay) (Alonso *et al*., 2008). The metal and the clay barriers are commonly denoted engineered barrier systems (EBS) and are susceptible to deterioration processes of microbial origin. A high microbial diversity and activity were detected in clay engineered and natural barriers (Poulain *et al*., 2008; Lopez-Fernandez *et al*., 2014a, b). Microbial activity could impact the rate of each of these barrier systems through different processes 1) corrosion of metal canisters, 2) transformation of clay minerals, and 3) radionuclide migration from the repository. These activities affect the safety case by compromising a repository's isolation and containment functions.

Microbe interact with radionuclides through different mechanisms including biosorption at the cell surface (Merroun and Selenska-Pobell, 2008; Morcillo *et al*., 2014), intracellular accumulation (Brookshaw *et al*., 2012), biomineralization (Merroun *et al*., 2011; Mondani *et al*., 2011), biotransformations (Martinez *et al*., 2014), etc. The effect of these radionuclide-microbial interactions in the fate and transport of radionuclide depend in several parameters including the microbial species, physical state of the microbe (planktonic or within biofilm), environmental conditions, etc. (Pedersen, 2002b). Understanding the interaction mechanisms of microbe with radionuclide will be helpful in getting insights into the impact of microbial processes in the mobilization of radionuclides from repositories and also on processes by which microbes cope with the toxicity of these inorganic contaminants in near- and far field of thesis repository system.

Several works investigated the interaction mechanisms of actinides with bacterial strains isolated from clay considered as host rock for deep geological disposal of radioactive wastes. For instance, Moll *et al*. (2013a) reported the effect of the gram negative bacterium, *Pseudomonas fluorescens*, and Lütke *at al*. (2013) the gram positive strain *Paenibacillus*, in the speciation of uranium and curium. These strains were isolated from Mont Terri Opalinus clay formations (Switzerland) which are currently investigated as a potential host rock for future nuclear waste storage. In the case of the yeast, most actinide interactions studies were focused in representative of *Ascomycota*, *Saccharomyces cerevisiae* (Ohnuki *et al*., 2005a; Lu *et al*., 2013). Although the wide distribution of yeasts from the *Basidiomycota* phylum in the environment including clays considered playing a role in DGR, rare studies were conducted to get insight into the influence of these eukaryotes in the fate and behavior of actinides. For instance Bai *et al*. (2012, 2014) reported the uranium binding capacity of Ca-alginate mobilized cells of *R. glutinis* using macroscopic approaches (effect of metal concentration, pH, temperature, etc. on uranium bisorption). No molecular scale studies were conducted to investigate how these yeasts interact with uranium, and in turn how they cope with the toxicity of this radionuclide.

The objectives of this work are threefold: 1) to determine how the cells of *Rhodotorula mucilaginosa* BII-R8 cope with the toxicity of uranium using flow cytometry and STEM-HAADF techniques, 2) to investigate the local coordination of uranium within the cells of the strain BII-R8 by means of X-ray Absorption spectroscopy (XAS) and Time-Resolved Laser Induced Fluorescence Spectroscopy (TRLFS), 3) to study the speciation of curium associated with the strain BII-R8 using TRLFS. *Rhodotorula mucilaginosa* BII-R8 has been isolated from Clay deposits of Cabo de Gata, (Spain). These geological formations have been studied as analogue of engineered for deep geological disposal of radioactive wastes. Yeast species belonging to the genus *Rhodotorula* have been documented for their high heavy metal (Pb, Cd, Ag, etc.) binding capacity (Li *et al*., 2008; Cho *et al*. 2011). *Rhodoturala mucilaginosa* is pigmented yeast with high Cu tolerance potential due to the presence of carotenoid pigments.

4. Material and Methods

4.1 Microbial strains, media, and growth conditions

The microbial strains used in this work were isolated from bentonite samples recovered form Cabo de Gata region (Lopez-Fernandez *et al*., 2014a). These strains include the yeast *R. mucilaginosa* BII-R8 and the gram-negative bacterium *Stenotrophomonas* sp. BII-R7. The pH of the medium was adjusted to 7 with 1M NaOH and 1M HCl. The microbial cells were grown in LB medium consisting 1.0 g/l tryptone, 0.5 g/l yeast extract, and 0.5 g/l NaCl at 28 ºC on agitation (120 rpm).

4.2 Uranium(VI) and europium(III) solution preparation

1 M stock solution of $UO_2(NO_3)_2 \cdot 6H_2O$ was prepared by dissolving the appropriate quantity of metal salt in 0.1 M $NaClO_4$. The stock solution was sterilized by filtration through 0.22 µm nitrocellulose filters and stored at 4 ºC until use. Working solutions were prepared by dilution of the stock solution. The pH was adjusted by addition of small volumes of acid (HCl) or base (NaOH).

The europium stock solution was prepared by dissolving $EuCl_3 \cdot 6H_2O$ (Sigma–Aldrich, trace elements basis, 99.99% in UHQ water.

4.3 Calculation of the chemical speciation of uranium

The speciation of U(VI) in LPM and in 0.1 M $NaClO_4$, at pH 7 and temperature of 25 ºC was determined by using Visual Minteq 3.0 software (Gustafsson *et al*., 2009).

4.4 Flow cytometry studies: sample preparation and experimental setup

BII-R8 cells, loaded for 24/48 h with different uranium concentrations, were harvested from LPM medium (Table 1), by centrifugation (11000 rpm, 15 min, 4 ºC), suspended and diluted in Phosphate Buffered Saline (PBS) to approx. 10^6 cell/ml. The same experimental conditions were applied to BII-R7 cells, as comparison with the yeast cells.

Table 1. Low Phosphate Medium composition.

***Saline solution10x, pH 7.2**	**100 ml/l**
	*Saline solution10X, pH 7.2, composition
	NaCl 46,8 g/l
	KCl 14,9 g/l
	NH4Cl 10,7 g/l
	$(NH_4)_2SO_4$ 4,3 g/l
	$MgCl_2$ 10 ml/l
	$ZnSO_4$ 2,7 mg/l
	Tris-base 143,3 g/l
Glycerol	**5 ml/l**
Tiamine (50 mg/ml)	**0,4 ml/l**
Peptone 10%	**100 ml/l**
CaCl2 (100 mM)	**1 ml/l**
Destillated water	**793,6 ml/l**

For live dead/staining, solutions of Fluorescein Diacetate (FDA) (Acros Organics) (20 µl, 0.1 mg/ml) and Propidium Iodide (PI) (2 µl, at 1 mg/ml) (Invitrogen) were mixed with cell suspensions for staining for 15 min in the dark, at room temperature. Cell suspensions incubated in the presence of both stains simultaneously were analyzed by flow cytometry for green (i.e. viable) and red (i.e. dead).

To study the effect of U(VI) on the metabolic activity of the cells, 10^6 cells were incubated with 20 µl, 10 µM $DiOC_6$ (Invitrogen) in PBS in dark for 15 min at room temperature.

Measurements were taken in triplicate using a FACSCantoII cytometer Becton Dickinson (San Jose Palo Alto, California), equipped with three lasers: 488 nm blue, 620 nm red and 405 nm UV. Samples were measured in FL1 (FITC) and FL2 (PE-IP), in logarithmic scale channels, at medium speed. Filters used were 530 nm and 580 nm Band Pass. Samples were analysed using BD Diva 6.1.

4.5 Sample Preparation for STEM-HAADF and EDX Analyses

Uranium and europium treated microbial cells were harvested by centrifugation at 11000 rpm for 15 min at 4 °C and washed twice with 0.9% NaCl to remove the interfering ingredients of the growth medium. TEM sample were prepared as described in Lopez-Fernandez *et al*. (2014a). Samples were examined by using a STEM -HAADF FEI TITAN G2 80-300. TEM specimen holders were cleaned by plasma prior to STEM analysis to minimize contamination. The high resolution STEM is equipped with HAADF detector and EDAX energy dispersive X-ray.

4.6 Time-Resolved Laser Induced Fluorescence Spectroscopy analysis

4.6.1 TRLFS U(VI)/yeast suspension preparation and experimental setup

For TRLFS measurements, cells of *R. mucilaginosa* BII-R8 were incubated for 48 h in LPM and 0.1 M $NaClO_4$ at pH 7, each in the presence of 1 mM U(VI). After incubation, the cells were washed and suspended in 0.1 M $NaClO_4$, at pH 7. The cells were harvested by centrifugation, dried under vacuum and subsequently powdered. Samples were placed in a quartz micro cuvette.

U(VI) luminescence was excited using a Nd YAG laser system (Spectra Physics, Santa Clara, CA, USA) (Geipel *et al*., 1996) with an excitation wavelength of 410 nm and a low intensity of 300 µJ to avoid sample damage. All measurements were performed at room temperature at the Institute of Resource Ecology, Helmholtz Centre Dresden-Rossendorf, Dresden, Germany. Luminescence spectra were recorded between 454 and 589 nm. The central wavelength of the spectrograph was set to 520 nm and the gate width of the ICCD camera was 5 µs (complete detection system: HORIBA Jobin Yvon GmbH, Darmstadt, Germany). For time-resolved measurements a digital delay generator (DG535, Stanford Research Systems, Sunnyvale, CA, USA) was used. Before each series of measurements the background signal was recorded 2 µs after the laser pulse and afterwards automatically subtracted from each spectrum.

The spectrograph was calibrated using a mercury lamp with known emission lines. Luminescence was excited by 50 to 80 laser pulses, depending on the amount of uranium in the sample. Subsequently, 101 U(VI) luminescence spectra (each calculated by averaging three single measurements) were recorded after defined delay times. The

obtained luminescence data were processed by using Origin 7.5 software (OriginLab Corporation, Northampton, MA, USA) including the PeakFit module 4.0.

4.6.2 TRLFS Cm(III)/yeast suspension preparation and experimental setup

A stock solution of the long-lived curium isotope ^{248}Cm (half-life: 3.4 x 10^5 years) was used. This solution had the following composition: 97.3% ^{248}Cm, 2.6% ^{246}Cm, 0.04% ^{245}Cm, 0.02% ^{247}Cm, and 0.009% ^{244}Cm in 1.0 M $HClO_4$. The experiments were performed in a glove box under an N_2 atmosphere at 25º C. As a background electrolyte, analytical grade 0.1 M $NaClO_4$ (Merck, Darmstadt, Germany) was used. To prevent the carbonate complexation of Cm(III), carbonate-free water and NaOH solution were used. The pH was measured using an InLab Solids combination pH puncture electrode (Mettler-Toledo, Giessen, Germany) calibrated with standard buffers. The pH was changed by adding analytical grade NaOH (Merck) or $HClO_4$ (Merck) with an accuracy of ± 0.02 units. Two series of experiments were performed at 0.3 µM Cm^{3+} to explore its interaction behavior with *R. mucilaginosa* BII-R8. The biomass concentration was kept constant at 0.2 and 0.45 $g_{dry\ weight}/L$, while varying pH between 8.0–2.0.

The time-resolved luminescence spectra were recorded using a unique pulsed flash lamp pumped Nd:YAG-OPO laser system (Powerlite Precision II 9020 laser equipped with a Green PANTHER EX OPO from Continuum, Santa Clara, CA, USA). The laser pulse energy, which was between 1.5 and 2.5 mJ depending on the excitation wavelength used, was monitored using a photodiode. The luminescence spectra were detected using an optical multi-channel analyzer-system, consisting of an Oriel MS 257 monochromator and spectrograph with a 300 or 1200 line mm^{-1} grating and an Andor iStar ICCD camera (Lot-Oriel Group, Darmstadt, Germany). The Cm(III) single luminescence emission spectra were recorded in the 570–650 nm (1200 line mm^{-1} grating with 0.2 nm resolution) range. The time-dependent luminescence spectra were detected in the 500–700 nm (300 line mm^{-1} grating: high intensity with a lower resolution >0.6 nm) range. A constant time window of 1 ms length was applied. Due to the high absorption of the F-band usually observed in Cm^{3+} excitation spectra and an excitation wavelength of 396 nm was used. More details concerning the TRLFS setup and data evaluation are summarized in Moll *et al*. (2014).

4.7 X-ray Absorption Spectroscopy Analysis

Samples for XAS studies were prepared as previously described in Merroun *et al*. (2005). After contact with the uranium solution, cells were harvested and washed with 0.1 M $NaClO_4$. The pellets were dried in an oven at 30 ºC for 24 h and subsequently powdered.

Uranium L_{III}–edge X-ray absorption spectra were collected at the MARS beamline at the SOLEIL synchrotron facility (ring operated at 2.75 GeV with 400 mA), which is the new French bending magnet beamline dedicated to the study of radioactive materials (Sitaud *et al.*, 2012) using a Si(220) double-crystal monochromator with horizontal dynamical focusing, and Pt-coated mirrors for vertical focusing and rejection of higher harmonics (Solari *et al*., 2009). Data were collected in fluorescence mode using a 13-element Ge detector (EG & G ORTEC, USA).

The data were processed by using the ATHENA code (Ravel and Newville, 2005). Background removal was performed by means of a pre-edge linear function. Atomic absorption was simulated with a square-spline function. The theoretical phase and amplitude functions used in data analysis were calculated with FEFF8 (Ankudinov *et al*., 1998) using the crystal structure of meta-autunite, $Ca(UO_2)_2(PO_4)_2.6H_2O$ (Makarov and Ivanov, 1960) as a model. FEFF is an automated program for ab initio multiple scattering calculations of EXAFS, X-ray Absorption Near-Edge Structure (XANES) and various other spectra for clusters of atoms.

All fits included the four-legged multiple scattering (MS) path of the uranyl group, U-Oax-U-Oax. The coordination number (N) of this MS path was linked to N of the single-scattering (SS) path U-Oax. The radial distance (R) and Debye-Waller factor (σ^2) of the MS path were linked at twice the R and σ^2 of the SS path U-Oax, respectively (Hudson *et al*., 1996). During the fitting procedure, N of the U-Oax SS path was held constant at two. The amplitude reduction factor ($S0^2$) was held constant at 1.0 for the FEFF8 calculation and EXAFS fits. The shift in threshold energy, $\Delta E0$, was varied as a global parameter in the fits.

5. Results

5.1 Interactions of U(VI) with the cells of *R. mucilaginosa* BII-R8

5.1.1 Chemical speciation of uranium in LPM and $NaClO_4$

The chemical speciation of U(VI) in the presence of 0.1M $NaClO_4$ and LPM at different metal concentrations (in the absence of microbial cells) is shown in Table 2. In the 0.1 M $NaClO_4$ system, at 0.5 and 1 mM concentration (pH 7), the uranium speciation is dominated by hydroxo-uranyl complexes. In both cases, the uranium speciation is controlled by $(UO_2)_3(OH)_5^+$ (56% and 50%) and $(UO_2)_4(OH)_7^+$ (44.5% and 50%), at 0.5 and 1 mM, respectively.

In contrast, in LPM at uranium concentrations ranging from 0.5 mM to 4 mM, the speciation of U(VI) is dominated by uranyl hydroxo-carbonate ($(UO)_2CO_3(OH)_3^-$). The minor uranium species are $(UO_2)_3(OH)_5^+$, represented by 9% to16% at the ranging uranium concentrations 0.5 mM to 4 mM, respectively, and $(UO_2)_4(OH)_7^+$ with values going from 4% to 19%, ranging at the mentioned above uranium concentrations.

Table 2. Aqueous speciation of uranium in LPM and $NaClO_4$ 0.1M, before adding cells.

Uranium species	U(VI) concentration (mM)						
	0.5		1		2	3	4
	LPM	$NaClO_4$	LPM	$NaClO_4$	LPM	LPM	LPM
$(UO_2)_2CO_3(OH)_3^-$	85.7%	-	80.0%	-	73.0%	68.0%	64.0%
$(UO_2)_3(OH)_5^+$	9.1%	54.9%	11.7%	50.0%	14.0%	16.0%	16,50%
$(UO_2)_4(OH)_7^+$	4.5%	44.5%	7.8%	49.6%	13.0%	16.0%	19.5%

5.1.2 Effect of U(VI) on cell viability and metabolic activity: flow cytometry studies

In order to study the effect of U(VI) in the cell viability and metabolic activity of the yeast *R. mucilaginosa* BII-R8 flow cytometry technique was used. For the cell viability studies live/dead staining approach based on two different stains, propidium iodide (PI), which stains dead cells in red and Fluoresceine Diactetate (FDA), staining alive cells in green, was applied. The cell viability depends on the U concentration and incubation time assayed. After 24 h of incubation at 1 mM of U, 99% of the yeast cells are alive. However, the cells treated with 2 mM U are 100% not viable (Table 3 and Fig.1).

Table 3. Cell viability of BII-R8 after 24 h at different uranium concentrations.

U concentration	Cell viability	
(mM)	Alive (%)	Dead (%)
0	99.8 ± 0.00	0.2 ± 0.00
0,5	99.2 ± 0.10	0.8 ± 0.10
1	99.3 ± 0.25	0.6 ± 0.25
2	0 ± 0.00	100 ± 0.00
3	0 ± 0.00	100 ± 0.00
4	0 ± 0.00	100 ± 0.00

Standard deviation is included as ± SD

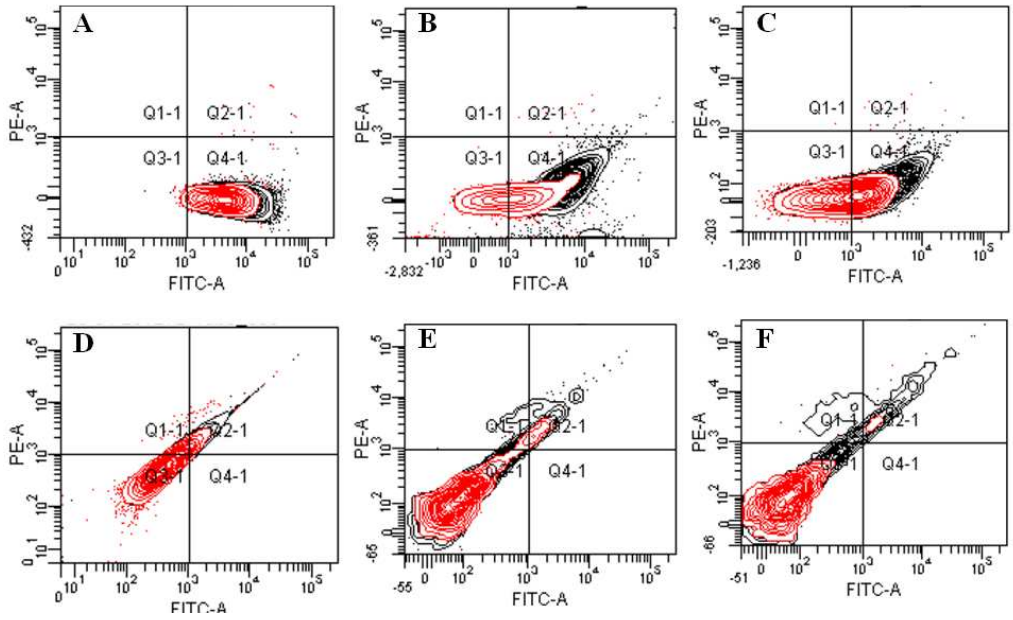

Figure 1. Flow cytometry scatterplots of BII-R8 cell viability after 24 h, at different uranium concentrations. A. 0 mM, B. 0.5 mM, C. 1 mM, D. 2 mM, E. 3 mM, F. 4 mM. Q1-1: dead cells (IP+, FDA-), Q2-1: damaged cells, considered as dead cells (IP+, FDA+), Q3-1: cellular rest, not considered in this study (IP-, FDA-), Q4-1: alive cells (IP-, FDA+).

In the case of incubation time of 48 h, the uranium cell viability of BII-R8 was slightly reduced when increasing the metal concentration (Fig. 2). The yeast cells revealed a high uranium tolerance since at 2 mM, 74% of the cells were alive. Even, 55% of the population was alive at 3 mM U concentration (Table 4).

Table 4. Cell viability and membrane potential of BII-R8 after 48 h at different uranium concentrations.

U concentration	Cell viability		Membrane potential	
(mM)	Alive (%)	Dead (%)	Active (%)	Non active (%)
0	96.05 ± 1.05	3.99 ± 1.05	97.40 ± 0.00	2.60 ± 0.00
0.5	92.40 ± 5.80	7.60 ± 5.80	94.65 ± 2.45	6.35 ± 2.45
1	85.35 ± 3.35	14.65 ± 3.35	74.30 ± 2.40	25.70 ± 2.40
2	73.95 ± 1.15	26.05 ± 1.15	34.60 ± 1.90	65.40 ± 1.90
3	55.00 ± 5.40	45.00 ± 5.40	7.25 ± 0.35	92.75 ±0.35
4	0.55 ± 0.05	99.45 ± 0.05	0.00 ± 0.00	100.00 ± 0.00

Standard deviation is included as ± SD

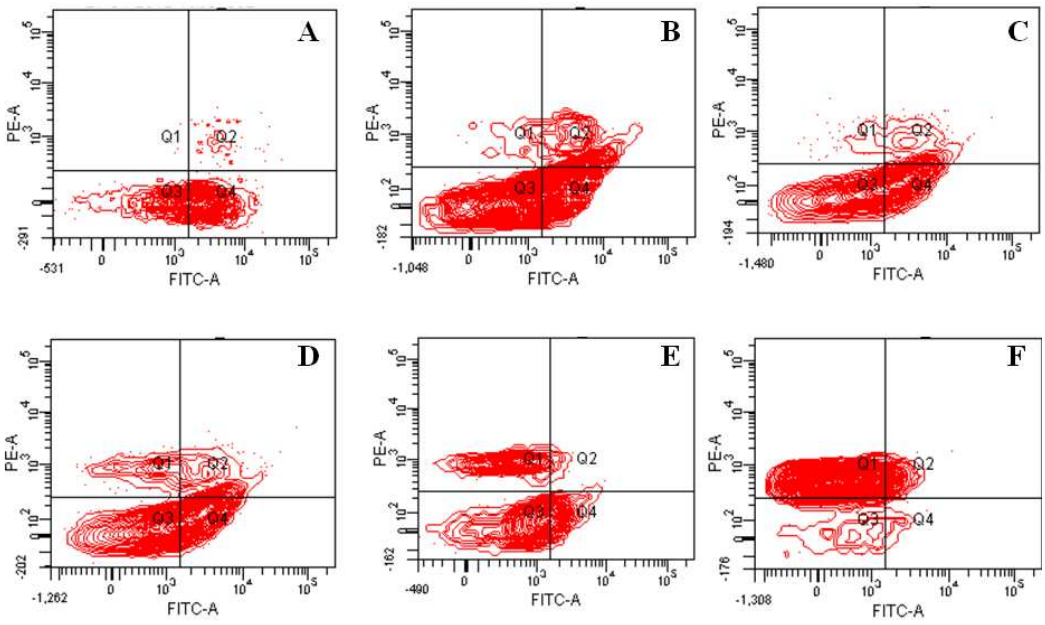

Figure 2. Flow cytometry scatterplots of BII-R8 cell viability after 48 h, at different uranium concentrations. A. 0 mM, B. 0.5 mM, C. 1 mM, D. 2 mM, E. 3 mM, F. 4 mM. Q1: dead cells (IP+, FDA-), Q2: damaged cells, considered as dead cells (IP+, FDA+), Q3: cellular rest, not considered in this study (IP-, FDA-), Q4: alive cells (IP-, FDA+).

The metabolic activity of BII-R8 cells after 48 h of incubation was decreasing proportionally to the decrease of the cell viability up to 1 mM of U concentration (Table 4). At higher concentrations, the metabolic activity of the yeast cells was more affected than the cell viability (Fig. 2 and 3). The cell viability at 3 mM of U concentration was

55%, while the metabolic activity was reduced to 7% (Table 4). At 4 mM of uranium all the cells were dead and, consequently, non metabollicaly active.

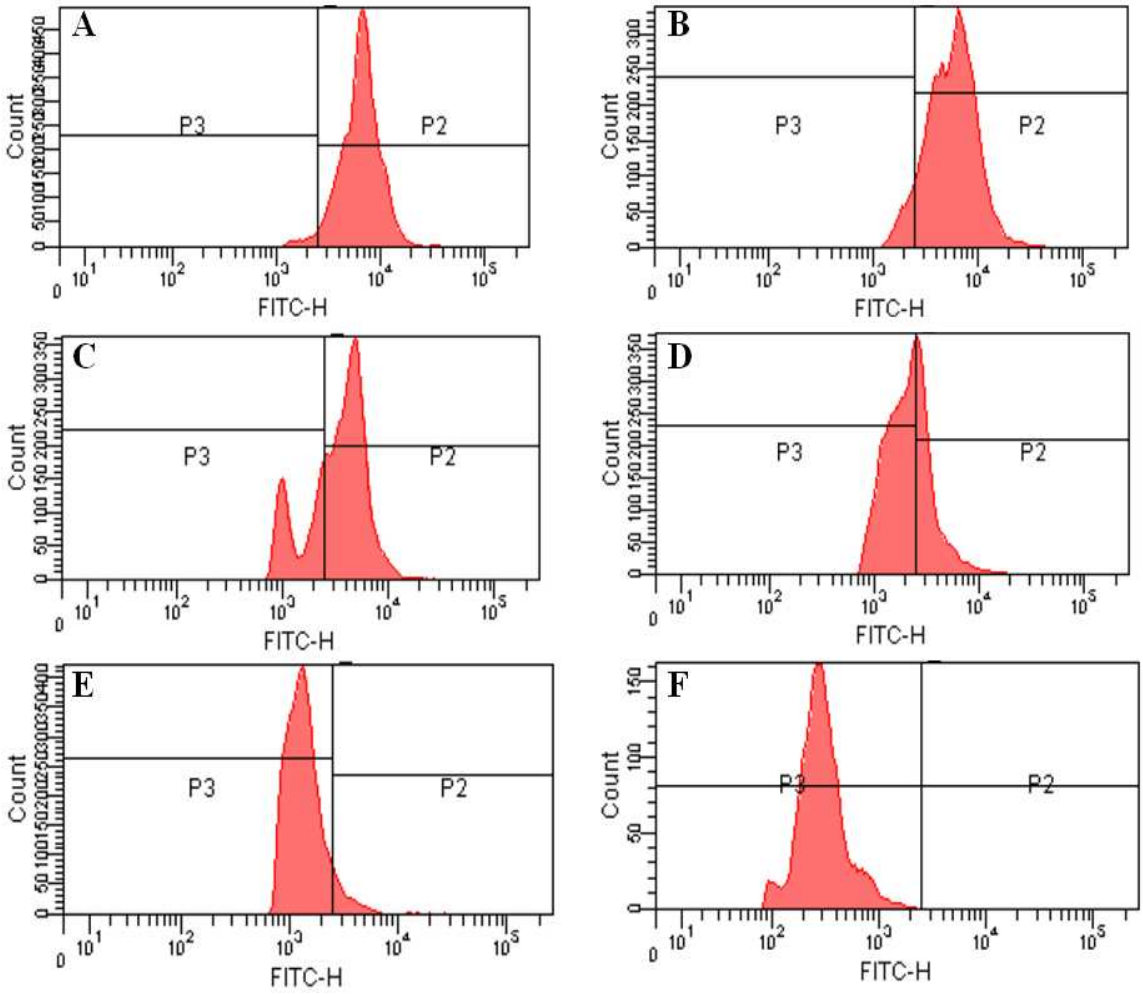

Figure 3. Flow cytometry scatterplots of BII-R8 membrane potential after 48 h, at different uranium concentrations. A. 0 mM, B. 0.5 mM, C. 1 mM, D. 2 mM, E. 3 mM, F. 4 mM. P2: metabolically active cells, P3: metabolically inactive cells.

To study whether the high uranium tolerance of the yeast strain *R. mucilaginosa* BII-R8 was a biological mediated process, it was compared to that of the isolated bacterial cells of *Stenotrophomonas* sp. BII-R7. The flow cytometry analysis of the bacterial cells treated with uranium for 24 h revealed a different behavior of that of the yeast strain BII-R8, since up to 0.5 mM the cell viability was not significantly affected 98% of alive cells (Table 5). The viability decreased at 1 mM of uranium concentration, since 12% of the cells are still alive (Fig. 4).

Table 5. Cell viability of BII-R7 after 24 h, at different uranium concentrations.

U concentration	Cell viability	
(mM)	Alive (%)	Dead (%)
0	96.2 ± 0.10	3.8 ± 0.10
0.5	98.5 ± 1.05	1.5 ± 1.05
1	11.7 ± 4.55	88.3 ± 4.55
2	0 ± 0.00	100 ± 0.00

Standard deviation is included as ± SD

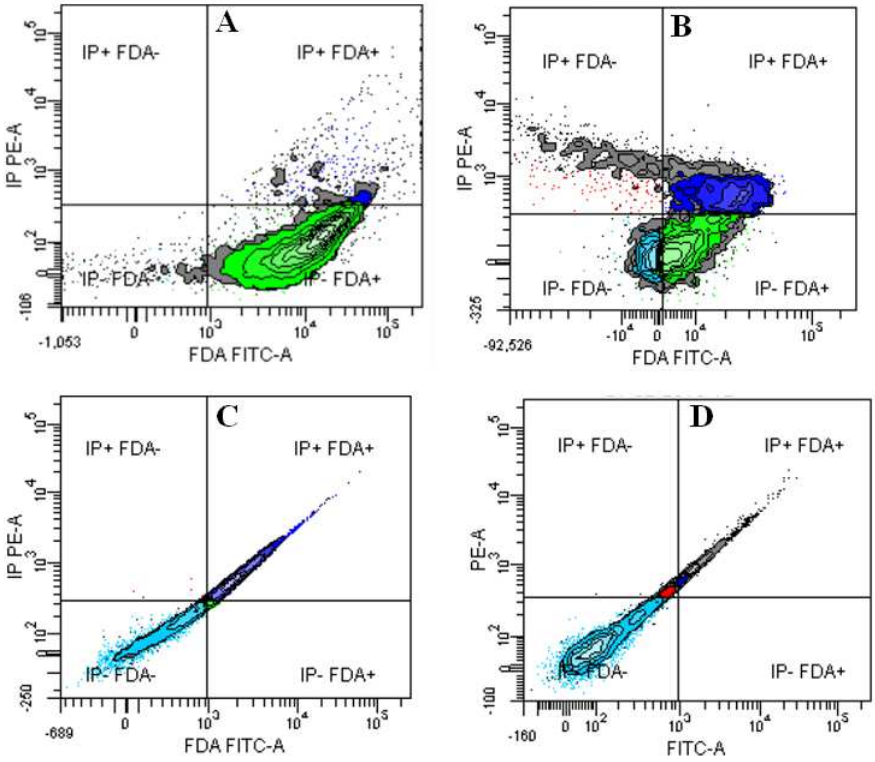

Figure 4. Flow cytometry scatterplots of BII-R7 cell viability after 24 h, at different uranium concentrations. A. 0 mM, B. 0.5 mM, C. 1 mM, D. 2 mM. IP+, FDA-: dead cells, IP+, FDA+: damaged cells, considered as dead cells, IP-, FDA-: cellular rest, not considered in this study, IP-, FDA+: alive cells.

The results of the flow cytometry analysis of the uranium tolerance of BII-R7 after 48 h are shown in Table 6. The cell viability was negatively affected at higher concentrations than 1 mM (Fig. 5). However, the membrane potential study revealed

that although at 1 mM of U concentration almost 100% of the BII-R7 cells were alive (Fig. 5), only 68% of them were metabolically active (Fig. 6).

Table 6. Cell viability and membrane potential of BII-R7 after 48 h, at different uranium concentrations.

U concentration (mM)	Cell viability		Membrane potential	
	Alive (%)	Dead (%)	Active (%)	Non active (%)
0	99.5 ± 0.65	0.5 ± 0.65	100 ± 0.00	0 ± 0.00
0.5	100 ± 0.00	0 ± 0.00	100 ± 0.00	0 ± 0.00
1	99.9 ± 0.14	0.1 ± 0.14	67.8 ± 0.65	32.2 ± 0.65
2	0 ± 0.00	100 ± 0.00	0 ± 0.00	0 ± 0.00

Standard deviation is included as ± SD

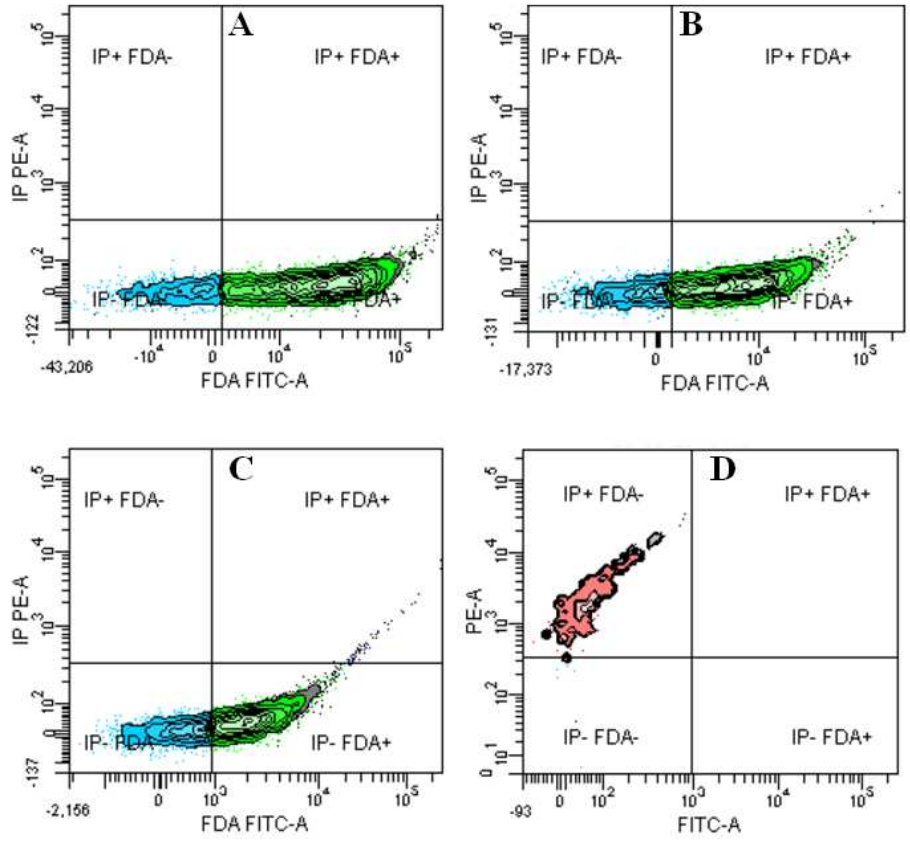

Figure 5. Flow cytometry scatterplots of BII-R7 cell viability after 48 h, at different uranium concentrations. A. 0 mM, B. 0.5 mM, C. 1 mM, D. 2 mM. IP+, FDA-: dead cells, IP+, FDA+: damaged cells, considered as dead cells, IP-, FDA-: cellular rest, not considered in this study, IP-, FDA+: alive cells.

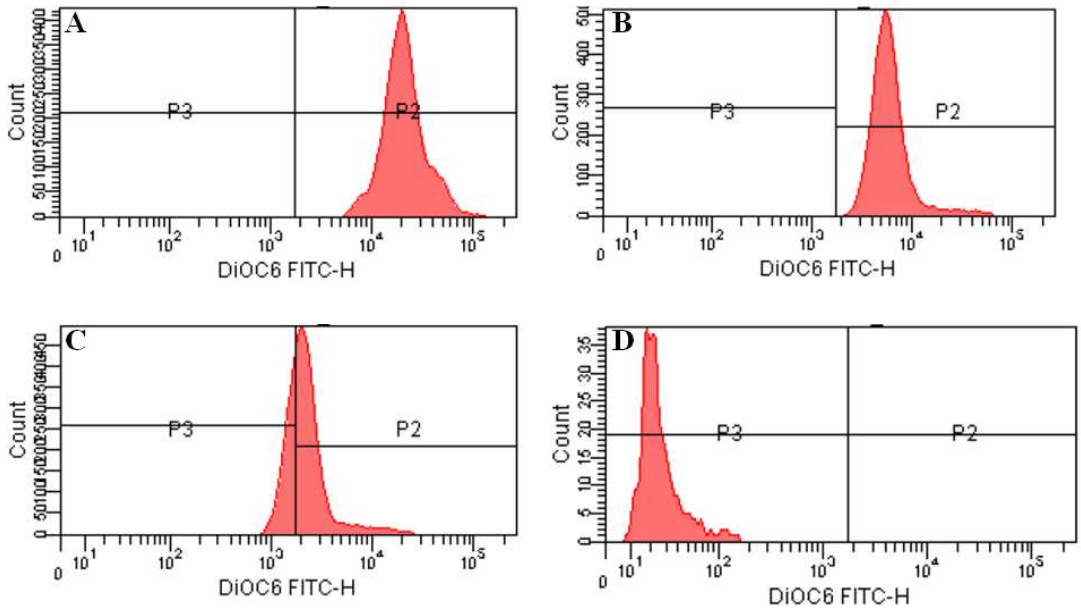

Figure 6. Flow cytometry scatterplots of BII-R7 membrane potential after 48 h, at different uranium concentrations. A. 0 mM, B. 0.5 mM, C. 1 mM, D. 2 mM. P2: metabolically active cells, P3: metabolically inactive cells.

5.1.3 TRLFS analysis of uranium complexes formed by the cells of the yeast *R. mucilaginosa* BII-R8

TRLFS was used to determine the fluorescence parameters (fluorescence emission bands and lifetime) of the U(VI) complexes formed by the cells of the strain BII-R8 in LPM and $NaclO_4$ at U concentration of 1 mM. The parameters determined are compared to those of reference compounds providing insight into the speciation of metal associated with the functional groups of the yeast cells.

The luminescence spectra recorded from *R. mucilaginosa* BII-R8 cells, incubated with 1 mM U(VI) at pH 7 in 0.1 M $NaClO_4$ and LPM solution, are shown in Figure 7 and the corresponding luminescence emission maxima are summarized in Table 7.

Table 7. Luminescence emission maxima of the U(VI) complexes formed by *R. mucilaginosa* BII-R8 cells in LPM and $NaClO_4$ at 1 mM U and selected uranyl model complexes.

	Main fluorescence emissions bands (nm)			Luminiscence lifetime (µs)		Reference
Samples						
R. mucilaginosa-$NaClO_4$	498.4	517.7	540	1.8 ± 0.1	11.1 ± 0.3	This work
R. mucilaginosa-LPM	497.9	518.1	538.9	2.2 ± 0.1	11.3 ± 0.4	This work
Reference samples						
Organic uranyl phosphate complexes						
UO_2-fructose(6)phosphate	497.1	519.0	543.3	0.13 ± 0.05		Koban *et al*., 2004
UO_2-AMP	497.0	519.0	542.0	n.d.		Merroun *et al*., 2003a
R-O-PO_3-UO_2	498.1	519.6	542.9	1.2 ± 0.4		Barkleit *et al*., 2008
Inorganic uranyl phosphate complexes						
$UO_2PO_4^-$	502.2	524	548	n.d.		Bonhoure *et al*., 2007
$(UO_2)_x(PO_4)_y$	503	523.7	546.9	n.d.		Brendler *et al*., 1996
Organic uranyl carboxylate complexes						
$(R\text{-}COO)_2$-UO_2 466.0	498.1	518	539	0.7 ± 0.1		Barkleit *et al*., 2009
UO_2^{2+} and hydrolytic species						
UO_2^{2+} (pH 1.5)	489.5	511	534.3	1.92 ± 0.12		
UO_2OH^+	497.3	518.4	541.3	32.8 ± 2.0		Eliet *et al*., 1995
$(UO_2)_3(OH)_5^+$	496	514	535	23 ± 3		Moulin *et al*., 1998
$(UO_2)_2(OH)_2^{2+}$	498.3	519.7	543.4	9.5 ± 0.3		Eliet *et al*., 1995
Uranyl carbonate minerals						
$Ca_2[UO_2(CO_3)_3]\cdot 10\ H_2O$ 465.4	502.7	524.5	545.5	145 ± 5		Amayri *et al*., 2005
$Ca_2(UO_2)(CO_3)_3 \cdot 11\ H_2O$ 466.9	502.7	524.1	545.9	313 ± 10		Amayri *et al*., 2005
$Ca_2[UO_2(CO_3)_3]$ in solute 465	504	524		0.04 ± 0.01		Bernhard *et al*., 2001
Uranyl phosphates minerals						
Autunite	504	524.2	548	5.15 ± 0.28		Geipel *et al*., 2000
Meta-autunite	501.8	522.9	546.9	0.74 ± 0.1		Geipel *et al*., 2000
$Mg[UO_2PO_4]_2 \cdot 10\ H_2O$	501.1	522.1	545.7	2.25 ± 0.2		Geipel *et al*., 2000

Error of emission bands is ± 0.5 nm.

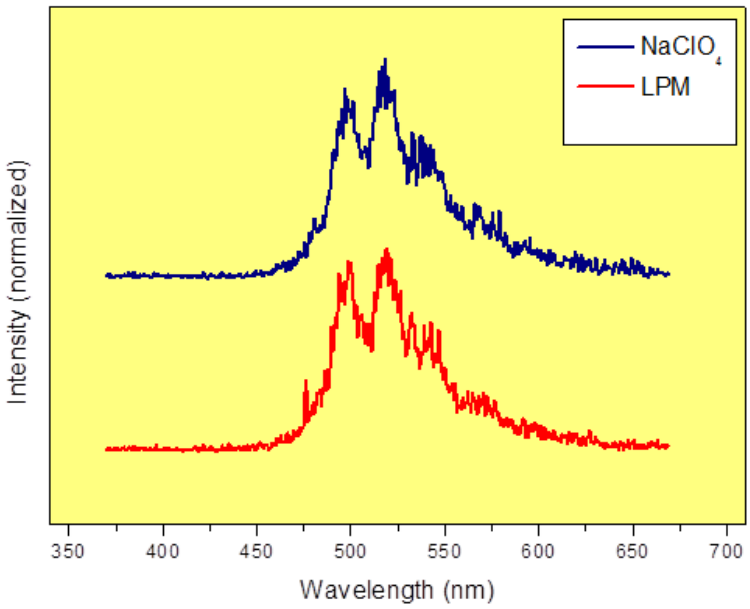

Figure 7. Luminescence spectra of the U(VI) complexes formed by the yeast cells *R. mucilaginosa* BII-R8 at neutral pH, in 0.1 M $NaClO_4$ and in LPM.

The luminescence properties of the cell sample incubated at pH 7 are characteristic of U(VI) complexes formed at phosphate groups of organic molecules such as sugar phosphates including fructose phosphates (Koban *et al.*, 2004), phosphorylated nucleosides (e.g. ATP) (Merroun *et al.*, 2003a), or lipopolysaccharides of the gram-negative bacterium *E. coli* (Barkleit *et al.*, 2008). These results indicate that organic phosphate residues of the yeast cells are implicated in the complexation of U(VI). The two luminescence lifetimes of the two studied samples (pH 7) are highly comparable to each other with average values of about 2 µs and 11 µs (Table 7). Fitting procedures at different delay times showed no shift of the luminescence emission maxima, indicating a high structural similarity of the formed complexes.

5.1.4 Uranium XAS Analysis

Extended X-ray absorption fine structure (EXAFS) analysis was conducted to investigate the local coordination of uranium associated to the cells of the yeast *R. mucilaginosa* BII-R8 by providing information about the coordination number and identity of neighboring atoms (Merroun *et al.*, 2005). Uranium L_{III}-edge EXAFS spectra of the uranium species formed at metal concentration of 1 mM in two different

background electrolytes (LPM and 0.1 M $NaClO_4$,) by the cells of the yeast strain BII-R8 and their corresponding Fourier transforms (FT) are presented in Figure 8.

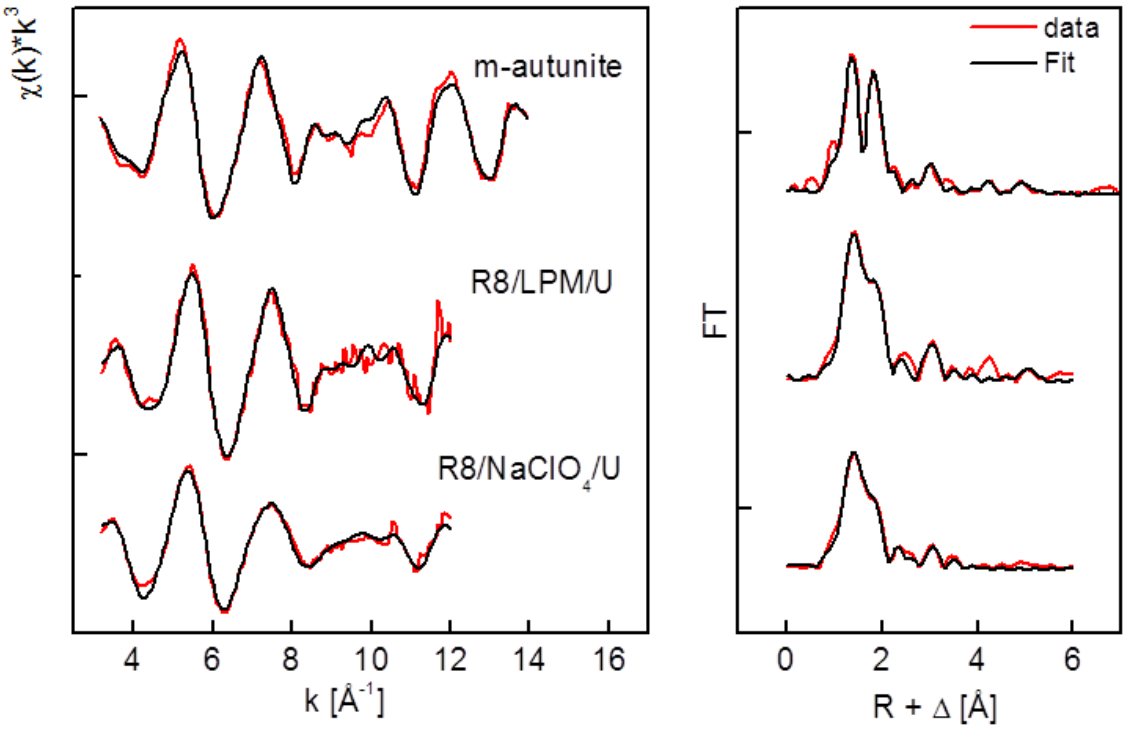

Figure 8. Uranium L_{III}-edge k^3–weighted EXAFS spectra (left) and the corresponding Fourier transforms (FT) (right) of the uranium complexes formed by *R. mucilaginosa* BII-R8 cells at U concentrations of 1 mM in LPM and $NaClO_4$, and reference compound (m-autunite).

The FT represents a pseudo-radial distribution function of the uranium near-neighbor environment. The FT peaks appeared at lower *R*-values (R+Δ) relative to the true near-neighbor distances R as a result of the EXAFS phase shift. This shift depends on the scattering phase function ϕ of the electron wave and originate a shift in the interatomic distance of Δk = 0.2-0.5 Å.

The uranyl unit consists of a uranium center with a formal charge of +6 coordinated to two double-bonded oxygen atoms to form a trans- dioxo cation, UO_2^{2+}. This “axial” unit is highly stable and binds to other ligands via the formation of U-O bonds in a plane perpendicular to the axis of the uranyl ion. The “equatorial” oxygen (O_{eq}) coordination number varies from 4 to 6 depending on the chemical environment, and these equatorial bonds are the sole means of complexation available for uranyl units

under normal conditions. Standard compounds used for comparison where inorganic uranyl phosphate (m-autunite). A representation of the molecular structure of the uranyl complexes obtained in this study is shown in Figure 9a. The structure represented in Figure 9b is that of m-autunite. The chemical structure of the uranyl complexes formed with phosphate groups of LPS of *E.coli*, with a structure similar to that of meta-autunite, where the organic phosphate groups are the main uranium binding sites (Barkleit *et al*., 2011) is shown in Figure 9c.

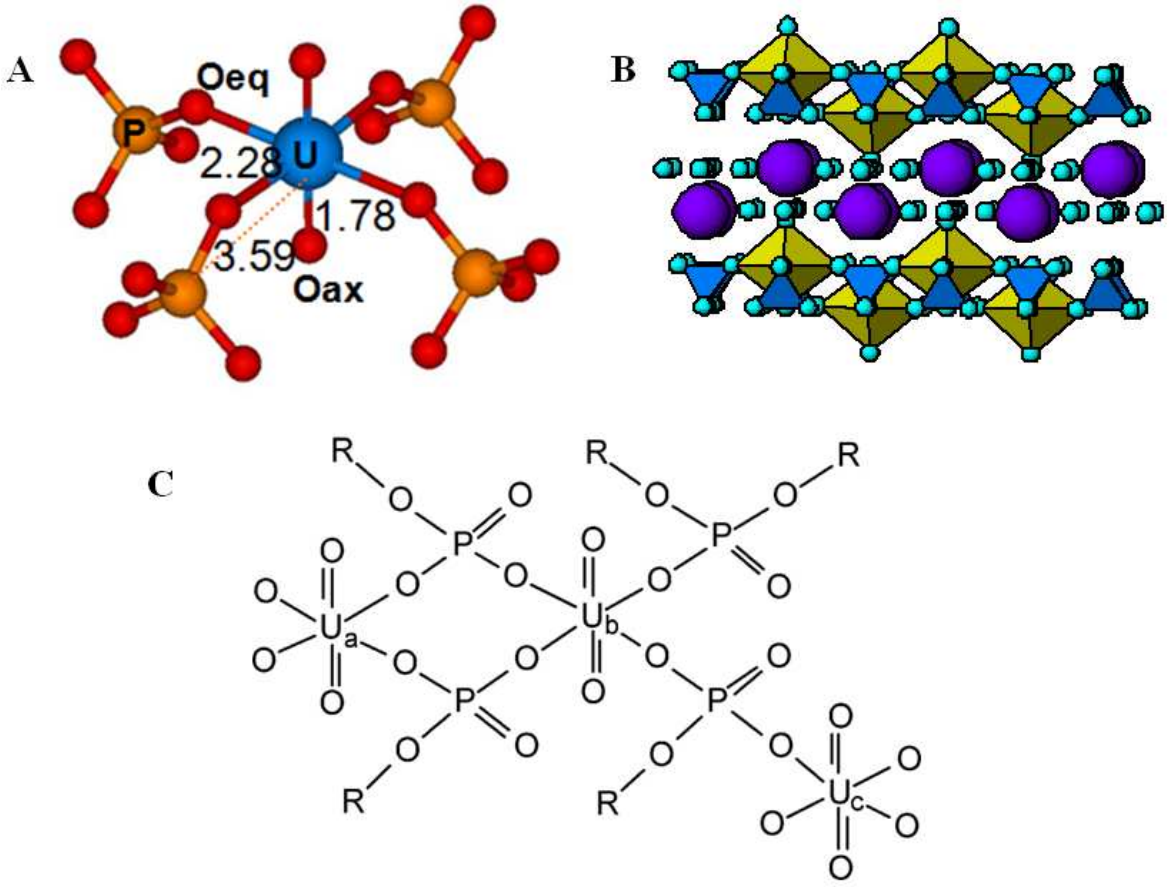

Figure 9. Representation of the molecular structure of three uranyl complexes. A. U-*R. mucilaginosa* BII-R8 complex at 1 mM U, in LPM. B. Meta-autunite reference compound. C. U-*E.coli* complex (Barkleit *et al*., 2011).

The FT of the EXAFS spectra of two samples, in LPM and in 0.1 M $NaClO_4$ show five to six significant peaks (Fig. 8). The EXAFS spectra of the two samples presented high similarity indicating that the local coordination of U(VI) within the two samples is similar.

Quantitative fit results (Table 8) (distances are phase shift corrected) indicated that the adsorbed U(VI) has the common linear trans-dioxo structure: two axial oxygen atoms at about 1.77 - 1.78± 0.02 Å, and an equatorial shell of 4 oxygen atoms at 2.28 ± 0.02 Å. As evident from the results presented in the Table 9, the Debye-Waller factors of the U-O_{eq1} shell is affected by the background electrolyte (LPM and $NaClO_4$). In the EXAFS spectra of the LPM, we observed a fourth-fold coordination of uranium to ligands of the bacterial cells (N ~ 4 and R= 2.28 ± 0.02 Å). The lower Debye-Waller factors (0.0063 $Å^2$) implying the absence of a disorder in U-O_{eq1} distances contributing to the EXAFS. However, the higher Debye-Waller factor of the EXAFS spectrum of $NaClO_4$ (0.011 $Å^2$) indicated that there is probably a wide spread of U-O_{eq1} distances with a averaged value of 2.28 ± 0.02 Å. The U-Oeq1 bond distance in the two samples is within the range of previously reported values for the oxygen atom of the phosphate bound to uranyl (Merroun *et al*., 2003, 2011; Nedelkova *et al*., 2007).

In all samples, the addition of a shell of one oxygen scatter at distance of R = 2.86-2.88 ± 0.02 Å improve significantly the fit. Such a distance between uranium and oxygen atoms is not related to direct bonding but they are interpreted in several systems as scattering contributions from neighboring ligand shells known as “short contacts” in crystallography (Merroun *et al*., 2003; Jroundi *et al*., 2007; Nedelkova *et al*., 2007).

The fifth FT peak, which appears at R+Δ ~ 3 Å (radial distance R = 3.58 Å) is a result of the back-scattering from phosphorus atoms. This distance is typical for a monodentate coordination of U(VI) by phosphate.

The EXAFS spectra of the U-treated yeast cell samples in LPM and $NaClO_4$ are similar to that of m-autunite with regard to the U-Oeq, U-P distances, suggesting that an inorganic m-autunite-like uranyl phosphate phase was precipitated by the yeast cells at in these two samples.

Table 8. Structural parameters of the uranium complexes formed by the cells of the strain *R. mucilaginosa* BII-R8 in 1 mM using $NaClO_4$ and LPM as background electrolyte.

Sample	Shell	N[a]	R(Å)[b]	σ^2 (Å^2)[c]	ΔE (eV)
LPM	U-O_{ax}	2[d]	1.78	0.0039	0.56
	U-O_{eq1}	4.2(4)	2.28	0.0063	
	U- O_{eq2}	0.8(2)	2.86	0.0038[d]	
	U-P	3.3(4)	3.58	0.004	
	U- O_{eq1}-P (MS)	6.6	3.68	0.004	
	U-U	2.2	5.22	0.008[d]	
$NaClO_4$	U-O_{ax}	2[d]	1.79	0.0069	-0.2
	U-O_{eq1}	4.5(3)	2.27	0.011	
	U- O_{eq2}	1.0(2)	2.87	0.0038[d]	
	U-P	3.2(5)	3.58	0.0040	
	U- O_{eq1}-P (MS)	5	3.69	0.0040	
m-autunite	U-O_{ax}	2[d]	1.77	0.0025	-13.40
	U-O_{eq1}	4.8(5)	2.34	0.0105	
	U- O_{eq2}	0.8(2)	2.86	0.0038[d]	
	U-P	1.5(3)	3.60	0.0010	
	U- O_{eq1}-P (MS)	3.0	3.73	0.0010	

[a]Errors in coordination numbers are ±25%, and standard deviations, as estimated by EXAFSPAK, are given in parentheses.
[b]Errors in distance are ±0.02 Å.
[c]Debye-Waller factor.
[d]Value fixed for calculation.

5.1.5 STEM-HAADF and EDX Analyses

STEM-HAADF micrographs of thin sections of *R. mucilaginosa* BII-R8 cells exposed to 1 mM U(VI) are shown in Figure 10a and b. In these micrographs, electron-dense precipitates were observed at the cell surface. In addition, intracellular U accumulates are localized within and at the membranes of concentric organelles. The EDX spectra of the accumulated uranium displayed X ray emission peaks corresponding to U and P (Figure 10c). The copper (Cu) peak resulted from the copper grid used to support the specimen and the presence of the silicon (Si) peak can be attributed to culture impurities.

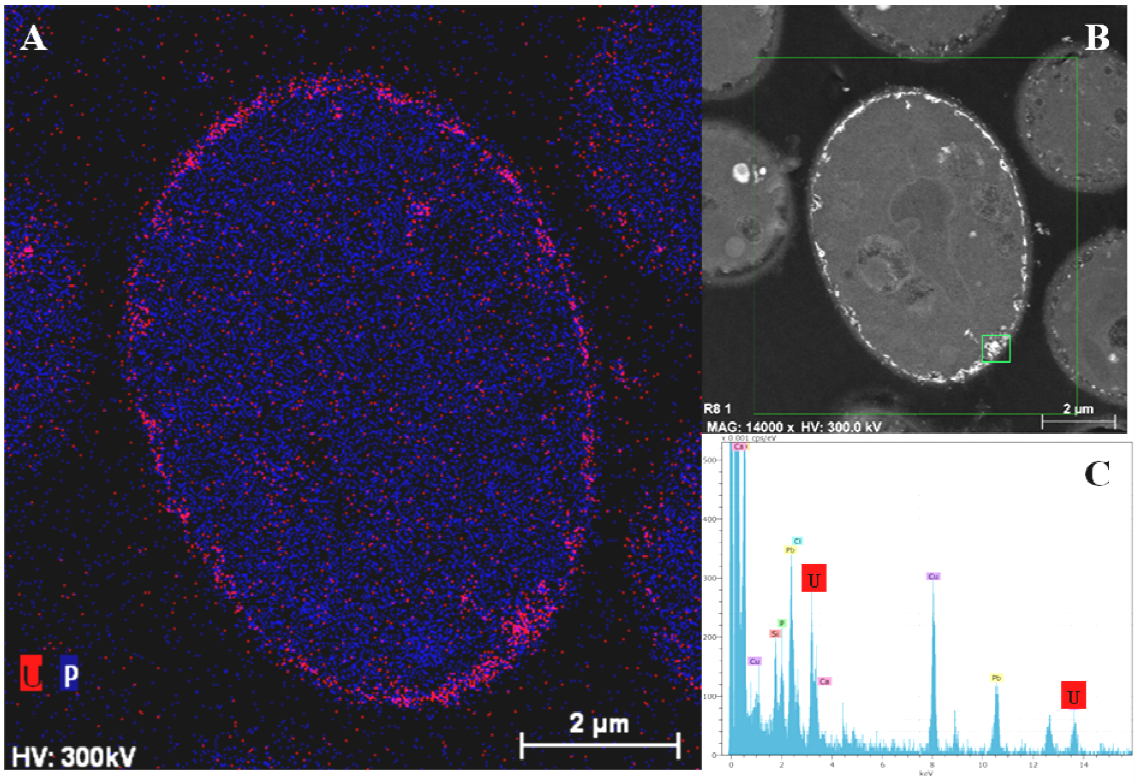

Figure 10. Scanning Transmission Electron Microscopy-High-Angle Annular Dark-Field (STEM-HAADF) micrographs of thin sections of *R. mucilaginosa* BII-R8 treated with 1 mM U (A and B). Energy Dispersive X-ray spectrum of U precipitates at the cell walls (C).

5.2 Interactions of Cm(III)/Eu(III) with the cells of *R. mucilaginosa* BII-R8

5.2.1 TRLFS analysis of Cm(III) complexes formed by the cells of the yeast *R. mucilaginosa* BII-R8

The interaction between Cm(III) and the the yeast strain *R. Mucilaginosa* BII-R8 was studied at trace Cm(III) concentrations (0.3 µM) using TRLFS. The pH dependent spectroscopic Cm(III) speciation at the cell envelope is depicted in Figure 11. From the dependencies found in the TRLFS spectra it can be concluded that there are two coordination environments of Cm(III) due to interactions with functional groups of the cell envelope. Also the Parafac analysis (Andersson and Bro, 2000) of both the single emission spectra and the time dependent measurements revealed two Cm(III) yeast species. Cm(III)-*R. mucilaginosa* BII-R8 specie 1 is characterized by an emission maximum at 599 ± 1 nm and an average luminescence lifetime of 215 ± 36 µs. Whereas Cm(III)-*R. mucilaginosa* BII-R8 specie 2 shows a more red shifted emission maximum at 602.0 ± 0.5 nm and a shorter average luminescence lifetime of 124 ± 15 µs.

TRLFS of the supernatants and the Cm(III) loaded biomass after washing with 0.1 M $NaClO_4$ showed that 30 % of the total Cm(III) luminescence intensity remained in solution at pH 6.2. At pH 8.1 even 82 % of the total Cm(III) luminescence intensity remained in solution. Hence, between pH 6 and 8 approximately 70 % to only 18 % of the Cm(III) was associated with the biomass. This points to a pH-dependent release of complexing agents possibly phosphates by the cells.

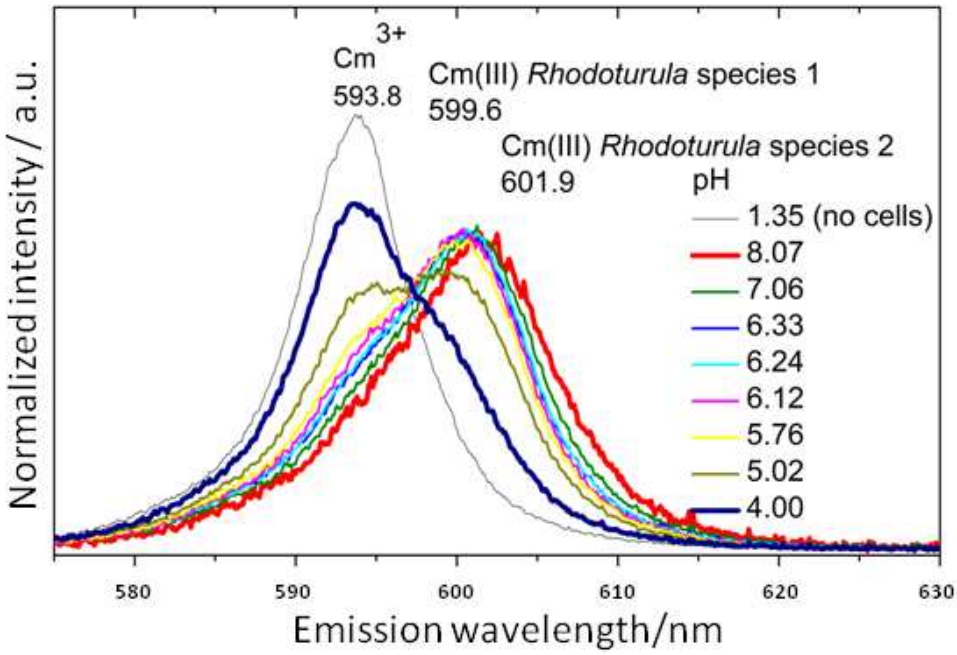

Figure 11. Luminiscence emission spectra of 0.3 µM Cm(III) in 0.1M $NaClO_4$ measured as a function of pH at a fixed biomass concentration of 0.45 $g_{dry\ weight}/l$.

By comparing the luminescence properties of both Cm(III)-*R. mucilaginosa* BII-R8 species with selected literature data (Table 9), Cm(III)-*R. mucilaginosa* BII-R8 specie 1 can be assigned to a Cm(III) species bound to phosphoryl sites and Cm(III)-*R. mucilaginosa* BII-R8 specie 2 to a Cm(III) species bound to carboxyl sites of the cell envelope, respectively.

Table 9. Luminiscence emission data of the Cm^{3+}—*Rhodotorula mucilaginosa* BII-R8 system including those of relevant model systems for comparison.

Species	Emission peak maxima/nm	Lifetime/ µs	Reference
Cm^{3+} (aq)	593.9	67 ± 2	This work
Cm^{3+}—*Rhodotorula* species 1	597.8	215 ± 36	This work
Cm^{3+}—*Rhodotorula* species 2	602.6	124 ± 15	This work
Cm^{3+}—*Sporomusa* sp. MT-2.99 complexes			Moll *et al*., 2014
R—COO—Cm^{2+}	601.6	108 ± 15	
R—O—PO_3H— Cm^{2+}	599.8	252 ± 46	
Cm^{3+}—*Pseudomonas fluorescens* complexes			Moll *et al*., 2013a
R—COO—Cm^{2+}	601.9	121 ± 10	
R—O—PO_3H— Cm^{2+}	599.6	390 ± 78	
Cm^{3+}—*Paenibacillus* sp. complex			Lütke, 2013
R—O—PO_3H— Cm^{2+}	598.8	477 ± 73	

5.2.2 STEM-HAADF Analysis

R. mucilaginosa BII-R8 cells were also exposed to 1 mM Eu(III). In the STEM-HAADF micrographs of thin sections of BII-R8 shown in Figure 12. Electron-dense precipitates located at the cell surface were observed. Element-distribution mapping showed that these Eu precipitates were mainly composed of Eu and P (Figure 12a, c).

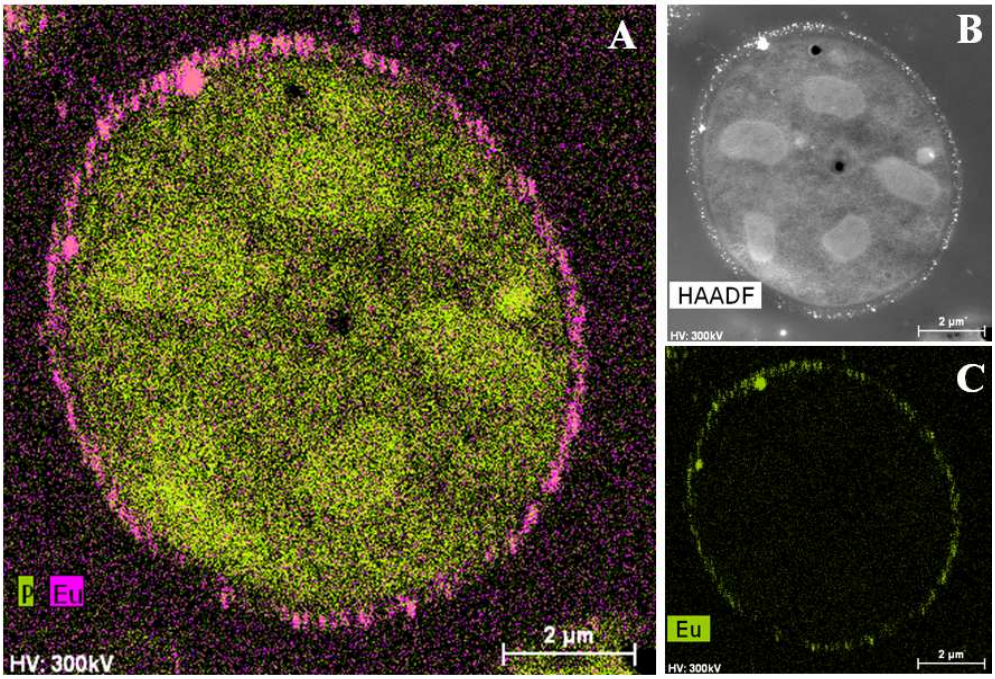

Figure 12. Scanning Transmission Electron Microscopy-High-Angle Annular Dark-Field (STEM-HAADF) micrographs of thin sections of *R. mucilaginosa* BII-R8 treated with 1 mM Eu (A and B).

6. Discussion

The present work describes the interaction mechanisms of bentonite yeast isolate *R. mucilaginosa* BII-R8, with U(VI) and Cm(III) as representatives of hexavalent and trivalent actinides. In addition, interactions studies were also complemented with Eu(III) as inactive analogue of Cm(III). For this study, a multidisciplinary approach combining microscopy, spectroscopy, radiochemistry and flow cytometry technique was applied. It is of great importance to investigate the effect of microbial processes on the fate and behavior of U(VI) and Cm(III) since they will be included in the inventory of high radioactive wastes to be disposed safely within future respository.

The toxicity of uranium towards microbes depend in its speciation, which in turn is intimately related to physico-chemical parameters including pH, presence of cations/anions, metal concentration, etc (Park and Jiao, 2014; Zhang *et al.*, 2013). Under oxic conditions, uranium occur as uranyl U(VI) ion, which is more toxic and more soluble than the U(IV), which dominate the U speciation at reducing conditions. At neutral pH, U(VI) form stable complexes with carbonate, phosphate, sulfate, silicates and organic substances which affect considerably the mobility and toxicity of U(VI) (Markish *et al*., 2002; Burns, 1999). These reactions lead to the formation of mobile aqueous species or precipitation of U-bearing minerals (Finch and Murakami, 1999).

In this work, the U(VI) speciation, at uranium concentrations ranging from 0.5-3 mM, is dominated by U-carbonate and U-hydroxy species which tend to form insoluble U species, reducing the U bioavailability, and consequently, its toxicity towards the cells of *R. mucilaginosa* BII-R8. Previous studies indicated that the strain BII-R8 tolerate up to 8 mM in solid medium (Lopez-Fernandez *et al.*, 2014a). These results are confirmed in the present work, through the use of flow cytometry techniques. The toxic effect of uranium on the cell viability of the yeast strain, studied by live/dead staining approach, is a time-incubation dependent process. For instance, after 24 h of incubation with uranium, the cells tolerate up to 1 mM U, however, at 2 mM there is no evidence of cell viability (100% dead cells). Interestingly, the yeast cells become viable at 2 mM of uranium concentration after 48 h of incubation. At this concentration, 74% of the cells were alive. These results indicated that U(VI) caused a temporary growth arrest in *R. mucilaginosa* and the duration of the growth arrest was larger than 24 h. This phenomenon was described for the case of *Caulobacter crescentus*, which did not grow

with U(VI) concentrations at or above 0.5 mM, after 2 weeks. During the majority of the growth arrest period, cell morphology was unaltered and DNA replication initiation was inhibited (Park and Jiao, 2014). However, in the case of *R. mucigilanosa* BII-R8 the mechanisms behind the growth arrest is unknown.

The results obtained in the present work indicated that the high U tolerance of BII-R8 cells is a biologically mediated process, due to the differences in the level of U tolerance within several microbial strains isolated from the same bentonite samples under the same experimental conditions (Fernandez-Sanfrancisco, 2011; Moreno-Garcia, 2012).

In addition, the effect of U on the cell metabolic activity was also investigated using $DiOC_6$, a fluorescent lipophilic dye used for staining mitochondria in living yeast cells (Koning *et al*., 1993). These results revealed that after 48 h of incubation at 1 mM of uranium concentration, a high percentage of the cell metabolism (74%) was still active. Even at 2 mM, 35% of the cells were metabolically active, showing their ability to cope with the toxicity of this radionuclide.

The oxidative stress induced by the yeast cells at high uranium concentrations may result in the formation of reactive oxygen species (ROS) including oxygen ions, free radicals and peroxides which highly damage cellular components, like DNA, lipids and proteins (Imlay, 2003). To cope with the toxicity of these ROS, microorganisms have developed different strategies including reduction or precipitation of the dangerous component causing the ROS, ion exchange and reverse osmosis (Cheung and Gu, 2007). In the case of the yeast, the ROS are eliminated via superoxide dismutases, which dismutate the superoxide in two steps to O_2 and H_2O_2. Subsequently, the H_2O_2 is detoxified by catalases. Both enzymes create the first and the most important line of antioxidant defense (Lushchak and Gospodaryov, 2005). An example of yeast detoxification mechanisms against different heavy metals was described for *Schizosaccharomyces pombe* in Preveral *et al*. (2008). Moreover, *Rhodotorula mucilaginosa* is a pigmented yeast strain known for their high resistance to different heavy metals, as for example Zn and Cd (Jian *et al*., 2013) or Cu and Cr (Villegas *et al*., 2011). In the case of cupper, the response of *Rhodotorula mucilaginosa* to the induced oxidative stress have been well investigated, revealing over expression of proteins such as chaperones, superoxide dismutase or catalase at high copper concentrations (Villegas

et al., 2009; Irazusta *el al*., 2012), or increased of carotenoid biosynthesis (Irazusta *et al*., 2013).

In order to determine the mechanisms responsible for the high U tolerance of the cells, under growing conditions (LPM), spectroscopic (XAS, TRLFS) and microscopic (STEM-HAADF) techniques were used. The molecular speciation of U(VI)-yeast cells was also studied under non-growing conditions (in $NaClO_4$).

Under growing and non-growing conditions, XAS analysis indicated that the local coordination of U(VI) within the cells is similar to that of meta-autunite, a U-phosphate mineral phase. However, TRLFS analysis, showed that fluorescence parameters of the U complexes formed are different to those of meta-autunite, and much well those of organic phosphate groups. These results demonstrated that U is complexed by phosphoryl groups four-fould monodentately coordinated in the equatorial plan of the uranyl dioxo-cation showing great homologies to the uranyl mineral phase meta-autunite. These results are in agreement with those of Barkleit, *et al*. (2011) where although XAS showed that the structural parameters of U(VI) complexes formed by purified LPS of *E. coli* are similar to that of meta-autunite, their fluorescence parameters are comparable to those of U-phosphate group complexes and different to those of m-autunite. In the case of Cu, carboxyl groups are the main binding sites of this transition metal.

Uranyl organic phosphate groups seem to play a major role in detoxification of U(VI) since STEM analysis showed that uranium is accumulated mainly at the cell wall. Three main components form the yeast cell wall: glucan (up to 56 %), mannoprotein, previously called mannan (up to 50%) and chitin (6%), whereas only small and variable amounts of lipid have been reported (Aguilar-Uscanga and François, 2003; Villegas *et al.*, 2009). The functional groups involved in the binding of U(VI) by the yeast are probably the carboxyl sites within the polysaccharides of the cell as well as the phosphoryl groups of the phospholipid bilayer of the cytoplasmic membrane.

The speciation of Cm(III) with the cells of the yeast BII-R8 under environmental relevant conditions (3 µM concentration) was studied by using TRLFS spectroscopy. TRLFS is a useful technique for the determination of the fluorescence parameters and lifetime of actinides (e.g. U(VI), Cm(III), etc.) complexes formed by different biological samples (Lütke *el at.*, 2013; Moll *et al*., 2014). TRLFS analysis indicated that the

biosorption of Cm(III) by *R. mucilaginosa* BII-R8 is a reversible and pH dependent process, where two different species were identified, $(R{-}O{-}PO_3){-}Cm^{2+}{-}(NH_2\text{-}R)$ and $R{-}COO{-}Cm^{2+}$. These yeast TRLFS results indicated that the phosphate groups might be originated by the phospholipids of the yeast cells, and carboxylic groups from the cell wall of the yeast, as described above. This the first study reporting the molecular scale coordination of Cm(III) to yeast cells. The speciation of Cm(III) with gram positive and gram negative bacteria have been well studied, as in the case of Cm^{3+}-*Bacillus subtililis* complexes (Moll *et al*., 2009), or Cm^{3+}-*Desulfovibrio äspöensis* complex (Moll *et al.,* 2004). Moreover, in the case of *Paenibacillus* sp. the $R\text{-}O\text{-}PO_3\text{-}H\text{-}Cm^{2+}$ complex dominates the speciation up to pH 8 in the same conditions than in our study (Moll *et al.,* 2013b). The interaction mechanisms of Cm(III) with *Sporomusa* sp. cells is dominated by a major process of reversible biosorption reaction and the speciation is dominated by $R\text{-}O\text{-}PO_3H\text{-}Cm^{2+}$ complex (Moll *et al*., 2013b).

The biosorption of Cm(III) by the yeast strain BII-R8 will lead to the mobilization of this actinide within the deep geological repository affecting negatively the safety of the radioactive waste disposal system. Therefore, in order to guarantee the security of the repository, it will be necessary to modify the physical properties of the bentonites to inhibit the microbial mobilization of Cm(III) from the deposit to the environment.

7. Conclusions

This study showed that the interaction mechanisms of U(VI) and Cm(III) with the cells of the yeast *R. mucilaginosa* BII-R8 is a biosorption mediated process. Organic phosphate groups are the main binding sites for U(VI) with local coordination similar to that of meta-autunite. In the case of Cm(III), both carboxyl and phosphates were involved in the sorption of this actinide. These data indicated that the Cm(III)/U(VI)-yeast interaction makes those radionuclides more mobile, having a negative effect in the concept of radioactive waste disposal.

8. Acknowledgments

This work was funded by Grants CGL2009-09760 and CGL-2012-36505 (Ministerio de Ciencia e Innovación, España). We acknowledge the assistance of María del Mar Abad Ortega, and Concepción Hernández Castillo (Centro de Instrumentación Científica, University of Granada, Spain) for their help with STEM/HAADF measurement; of Jaime Lazuen-Alcon (Flow Cytometry Service, Centro de Instrumentación Científica University of Granada, Spain) for his help with flow cytometry measurements; of Björn Drobot for the Parafac calculations and Monika Dudek for microbiology support (HZDR, Germany); and of Ahinara Amador García (Department of Microbiology, University of Granada) for her appreciated help with the EXAFS measurements. The authors are indebted to the U.S. Department of Energy, Office of Basic Energy Sciences, for the use of ^{248}Cm via the transplutonium element production facilities at Oak Ridge National Laboratory; ^{248}Cm was made available as part of collaboration between HZDR and the Lawrence Berkeley National Laboratory (LBNL).

CHAPTER IV

Chapter IV: Bacterial community changes induced by uranyl nitrate treatment in aerobic bentonite microcosms

Capítulo IV: Cambios inducidos por el tratamiento con nitrato de uranilo en las comunidades bacterianas, en microcosmos de bentonitas en condiciones aerobias

Margarita Lopez-Fernandez[1], Iván Sánchez-Castro[1], Ruy Sandoval[2], Dietmar Pieper[2], Nico Boon[3], Ramiro Vílchez-Vargas[3], Mohamed L. Merroun[1].

[1]Departamento de Microbiología, Universidad de Granada, Granada, Spain

[2]Helmholtz Centre for Infection Research, Braunschweig, Germany

[3]Laboratory of Microbial Ecology and Technology, Ghent University, Ghent, Belgium

1. Resumen

El almacenamiento geológico profundo de residuos radiactivos, encapsulados en contenedores metálicos resistentes a la corrosión, es considerada, a nivel internacional, la forma más segura para almacenar este tipo de residuos peligrosos. En el caso concreto de España, las formaciones de arcillas del Parque Natural de Cabo de Gata (Almería) fueron seleccionadas para ser usadas como material de referencia en las barreras artificiales del almacenamiento geológico profundo, debido a su amplia caracterización desde distintos puntos de vista. Sin embargo, la seguridad de los almacenamientos geológicos profundos puede verse comprometida no solo por factores físicos y químicos, sino también por la actividad biogeoquímica, tanto de los microorganismos de la roca hospedante como de los microorganismos introducidos durante la construcción del almacén. Para simular el escenario en el que la movilización de uranio desde los almacenes previstos hasta las formaciones arcillosas pudiera ocurrir, se elaboraron microcosmos con las bentonita españolas.

En este capítulo se han estudiado los cambios en la comunidad bacteriana de los microcosmos de bentonitas elaborados, en función de los distintos tratamientos aplicados a los mismos. Los microcosmos se trataron con nitrato de sodio y nitrato de uranilo durante 5 meses para evaluar la respuesta de las comunidades bacterianas de las bentonitas a la adición de este radionúclido. Mediante secuenciación con Illumina, se demostró que la estructura de la comunidad bacteriana de las muestras BI y BII difería de la de los controles (no tratado y tratado con nitrato de sodio). El análisis de los resultados obtenidos reveló que dos filotipos, anotados como *Pseudomonas* y *Bacillus*, estaban altamente representados en los microcosmos de la muestra BI y BII, respectivamente, tratados con nitrato de uranilo. Estos géneros bacterianos han sido previamente descritos por su capacidad de precipitar uranio como fases minerales de fosfato, con estructuras similares a la de la meta-autunita, mediante la actividad enzimática fosfatasa.

Por ese motivo, en este estudio se aplicó un nuevo enfoque, creando en primer lugar, una base de datos de los genes catabólicos de la fosfatasa ácida. Esta base de datos ofrece la posibilidad de relacionar la información taxonómica obtenida del estudio de un ecosistema con su potencial catabólico, además de ser una herramienta para el futuro, que permitirá conocer mejor el proceso de bioprecipitación de uranio mediado

por la actividad de la fosfatasa ácida. Sin embargo, esta actividad enzimática no es la única descrita en la bibliografía implicada en la biomineralización de uranio, por lo que sería necesaria la elaboración de nuevas bases de datos para otros genes involucrados en este proceso, como la fosfatasa alcalina y el citocromo C.

2. Abstract

The deep geological repository of radioactive wastes, encapsulated in corrosion-resistant metal containers, is the safest internationally accepted option for the disposal of these hazardous materials. For the planned Spanish deep geological repository, Cabo de Gata National Park clay formations, Almeria, were selected as the best characterized from different physicochemical points of view, to be used as reference material of the artificial barriers. However, the safety of this long-term geological disposal could be compromised not only by physical and chemical factors, but also by the biogeochemical activity of either indigenous microorganisms of the host rock or microorganisms introduced during the construction of the repository. To simulate a scenario where the mobilization of uranium from the planned repository to the clay formations may occur, long-term microcosms were elaborated with these Spanish bentonite samples.

This chapter is focused on the study of the bacterial community changes of the bentonite microcosms, based on the different treatment applied. The microcosms were non-treated (control) and treated with sodium nitrate (nitrate control) and uranyl nitrate for 5 months to evaluate the response of the subsurface bacterial community of the bentonites, to the addition of this radionuclide.

By using Illumina sequencing, it was demonstrated that the structure of the bacterial community of the uranyl nitrate-treated BI and BII microcosms differs to that of the controls microcosms (non-treated and sodium nitrate-treated). *Pseudomonas* and *Bacillus*, already described for their ability to precipitate uranium as U-phosphate mineral phases with a structure similar to that of meta-autunite through phosphatase activity, were highly enriched due to the uranyl treatment.

Therefore, a novel approach was applied to create a database of the acid phosphatase catabolic genes, with the aim of fulfilling the uranium bioprecipitation process. So far, this study takes one step further in the possibility of using the taxonomic information of a studied ecosystem to better understand its catabolic potential. Moreover, it will be a useful tool in the uranium bioprecipitation mediated by acid phosphatase activity. However, this enzymatic activity is not the only one involved in the biomineralization of uranium described in literature. Therefore, it will be necessary to elaborate new databases for others genes involved in this process, such as alkaline phosphatase or cytochrome C.

3. Introduction

Deep geological repositories (DGR) must provide a safe disposal way for waste containing radioactive hazardous materials (IAEA, 2003). Granitic rocks, salt deposits and clay formations are the three suitable host rocks proposed for this kind of repository. Some European countries selected clay formations as candidate host rock. For example, Callovo-Oxfordian Clay (COx) in the case of France, and Opalinus Clay in Switzerland, were both considered for DGR (Johnson *et al*., 2002). Boom clay was selected as host rock in Belgium (ONDRAF/NIRAS, 2011) and El Cortijo de Archidona Bentonite Clay as engineering barrier in Spain (Villar *et al*., 2006).

Occurrence of viable microorganisms has been extensively studied at the Mont Terri Underground Research Laboratory (Mauclaire *et al*., 2007; Stroes-Gascoyne *et al*., 2007b; Poulain *et al*., 2008). Microbial diversity studies were also performed in Boom clay formation (Boivin-Jahns *et al*., 1996). As well as in the case of the bentonite clay deposits from Spain, where the indigenous microbial population was characterized by using culture dependent and independent methods (Lopez-Fernandez *et al*., 2014a, b). Moreover, microbial processes occurring in these clay formations might play an important role in the mobilization and speciation of radionuclides in these environments. There are several studies describing that microorganisms can influence the speciation of radionuclides to be stored within a DGR, such as uranium, (Merroun *et al.*, 2011; Lütke *et al*., 2012, 2013; Lopez-Fernandez *et al*., 2014a) through a biomineralization process resulting in U(VI) phosphate mineral phases probably due to the activity of acid or alkaline phosphatases.

However, these studies were conducted using bacterial pure cultures that did not simulate natural conditions, as they can be pretended under microcosm conditions. Nevertheless, there are some works studying soil microcosms (Geissler *et al.*, 2009), dune sand microcosms (Handley-Sidhu *et al*., 2009) and sediment microcosms (Salome *et al.*, 2013) treated with uranium. For example, Geissler *et al*. (2009) described the

bacterial community changes in a uranium mining waste pile treated with uranyl nitrate by 16S rRNA gene analysis, but it did not consider any kind of phosphatase enzymatic activity study. On the other hand, the mentioned works were not focused on clays considered as safety barriers for a future DGR. Although the structure and composition of bacterial communities of the bentonite formations were previously studied in Lopez-Fernandez *et al*. (2014b), it is important to consider the specific scenarios where uranium may be mobilized from DGR bentonite-engineered barriers.

Therefore, in this work microcosms elaborated with Spanish bentonite samples, were treated with sodium nitrate and uranyl nitrate and studied in term of bacterial diversity and U biomineralization potential. Evidences of uranium precipitation through phosphatase enzymatic activity have been described by pure culture of natural isolates (e.g. *Rhanella*, *Bacillus*, *Panteoa*, *Pseudomonas*, etc.) from metal and radionuclide contaminated sites (Martinez *et al*., 2007; Beazley *et al*., 2011). In addition, microbial phosphatase expressed by abundant microbial populations within uranium contaminated sites is considered as a strategy to improve microbial phosphate acquisition phenotypes to support *in situ* biomineralization of uranium as U-phosphate mineral phases (Martinez *et al*., 2014). For this reason, catabolic key genes involved in the immobilization of U are of great importance and must be deeply studied. Hence, the second objective of this work was firstly, to measure the microbial phosphatase activity participating in the uranium immobilization process of the elaborated microcosms. And secondly, a novel approach was applied to create databases of the described catabolic key genes involved in the immobilization of uranium, such as acid- and alkaline-phosphatases (Macaskie *et al*., 1992; Thomas and Macaskie, 1996; Mondani *et al*., 2011), because uranium immobilization may be a useful tool for bioremediation processes in radionuclide contaminated places (Kumar *et al*., 2013).

4. Materials and methods

4.1 Sample description

Clay soil samples were collected from two different locations of Cabo de Gata, Almería Spain. Sample called BI was collected from El Cortijo de Archidona and sample BII was taken from El Toril. Geochemical and mineralogical characterization of these two different clay samples was described in Lopez-Fernandez *et al*. (2014a).

4.2 Preparation of clay microcosms

Three microcosms were prepared using 20 g of sterile ground clay soil from El Cortijo de Archidona (BI-A, BI-B and BI-C) and other three using the same amount of clay soil, but from El Toril (BII-A, BII-B and BII-C). Microcosms called BI-A and BII-A were treated with distillated water (water controls). BI-B and BII-B microcosms were nitrate-controls, in this case, treated with 151 mg/kg of $NaNO_3$. And microcosms BI-C and BII-C were the studied samples, treated with 300 mg/kg of $UO_2(NO_3)_2$. In total, six microcosms were prepared under the same conditions (Fig. 1). Sodium nitrate and uranyl nitrate solutions were sterilized by filtration (0.45µm) and added to the different clay soils (Table 1).

Table 1. Conditions of the different treatments of the six microcosms.

Sample	Treatment	mg/kg	Incubation time
BI-A	Control	-	5 months
BI-B	$NaNO_3$	151	5 months
BI-C	$UO_2(NO_3)_2$	300	5 months
BII-A	Control	-	5 months
BII-B	$NaNO_3$	151	5 months
BII-C	$UO_2(NO_3)_2$	300	5 months

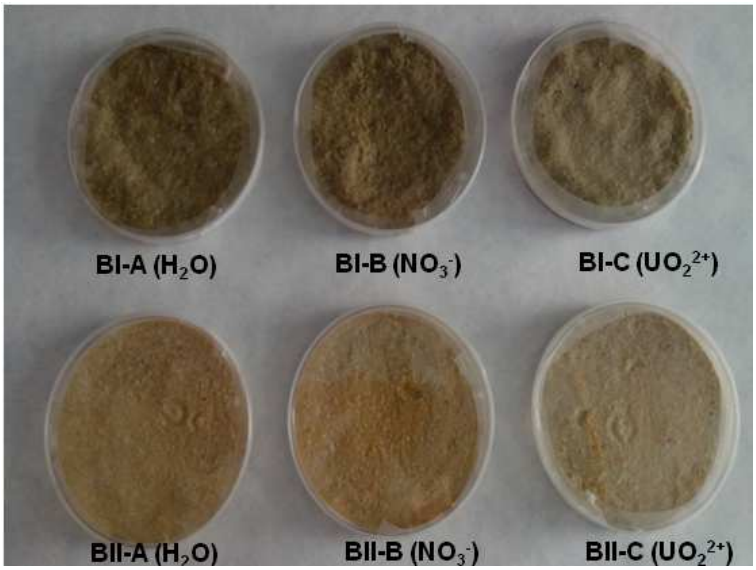

Figure 1. Picture showing the different microcosms prepared for the study.

Water-controls (A) were included in this study to check the effect of the long term incubation under the same experimental conditions. Nitrate-controls (B) were studied to investigate if the nitrate was affecting the bacterial diversity of the microcosms in C-microcosms, since uranyl ion was added as uranyl nitrate. The pH of the water-controls microcosms was measured as described in López-Fernández *et al*. (2014b). The pH of the rest of the microcosms (B- and C- microcosms) was measured in the same conditions but on a 1:5 (w/v) soil:sodium nitrate-solution suspension, or soil:uranyl nitrate-solution suspension, respectively. The pool of microcosms was incubated at room temperature under aerobic conditions, for five months, in darkness.

4.3 DNA extraction and Illumina sequencing

To study the microbial diversity of the six microcosms total DNA was extracted using the FastPrep modified DNA extraction protocol described in Vilchez-Vargas *et al.* (2013). Microcosm samples (1 g) were mixed with 200 mg of glass beads and 1000 µl of lysis buffer. Cells were lysed in a Fast Prep instrument (1800 rpm for 40 s, two times). Samples were centrifuged at 11000 rpm for 5 min. Supernatants were collected in new tubes and pellets were dissolved into 1000 µl of MilliQ water and disrupt another two times at 1800 rpm, 40s. This extra step was included to avoid cells to keep attached to clay particles. Samples were centrifuged at 11000 rpm for 5 min and supernatants were washed with one volume of phenol/chloroform/isoamilic alcohol (1:1:1), pH 7.

Afterwards, samples were centrifuged for 1 min and the aqueous phase was washed with one volume of chloroform. After centrifugation, nucleic acids present in the aqueous phase were precipitated with one volume of ice-cold isopropanol and 1:10 volume of 3 M sodium acetate. After centrifugation, total DNA was dissolved into 100 µl of MilliQ water and purified with Wizard® DNA Clean-Up System (Promega). The quality and quantity of the extracted DNA was analysed on 1% agarose gels and sequenced by Illumina following the procedure of Camarinha-Silva *et al*. (2014). Hipervariable region V5-V6 of the 16S rRNA gene was amplified by using universal primers based on 16S-$_{807f}$ and 16S-$_{1050r}$ (Bohorquez *et al*., 2012). Resulting PCR products were amplified using sequencing primers for V5-6 region, the forward primer contains a 6-nt barcode (Meyer and Kircher, 2010) and a 2-nt CA linker (Hamady *et al.*,

2008). Forward and reverse primers comprised sequences complementary to the Illumina specific adaptors to the 5′-ends. Illumina indices were included in the last step of the amplification. Libraries were sent for paired-end sequencing on a MiSeq System Sequencer (Illumina, California, USA), obtaining sequences of 280 nt length. R-program (with vegan y phyloseq packages) was used to normalize to the minimum the pool of sequences, for plotting the rarefaction curves and for calculating the diversity indices. The sequences were annotated to the least common ancestor using SILVA Incremental Aligner (SINA) (Pruesse *et al*., 2012).

4.4 Phosphatase activity of the microcosm samples

To study the microbial processes involved in the precipitation of uranium, different enzymatic activities were measured. It is already described that acid and alkaline phosphatase are key enzymes involved in this process (Macaskie *et al*., 2000; Bencheikh-Latmani *et al*., 2005; Nilgiriwala *et al*., 2008; Beazley *et al*., 2011). In this study, total acid and alkaline phosphatase activities were measured according to the modified method of Berman, (1970), as described in Vilchez *et al*. (2007), using 1g of bentonite microcosm suspended in 10 ml of sterile distillated water.

Acid phosphatase activity

Two milliliters of acetic/acetate buffer (0.2 M, pH 4.8) and 1 ml of p-nitrophenyl phosphate solution (1% w/v) were added to 1 ml of the bentonite suspension to determine the total acid phosphatase activity of the microcosm samples. After 30 min of incubation at 37 ºC in darkness, the reactions were stopped by adding 2 ml of NaOH (0.2 M). Samples were centrifuged for 10 min at 2500 rpm to eliminate the suspension particles and absorbance was measured at 410 nm. Samples were measured in triplicate.

Alkaline phosphatase activity

To determine the total alkaline phosphatase activity of the microcosm sample, one milliliter of the bentonite suspension was added to a mixture of 2 ml of carbonate/bicarbonate buffer (0.2 M, pH 9.6) and 1 ml of a p-nitrophenyl phosphate solution (1% w/v). After 30 min of incubation at 37 ºC in darkness, reactions were stopped by addition of 2 ml NaOH (0.2M). Samples were centrifuged for 10 min at

2500 rpm to eliminate the suspension particles and absorbance was measured at 410 nm. Samples were measured in triplicate.

4.5 Database of the involved genes in uranium immobilization

In the uranium immobilization process might be more key genes involved than the two genes previously described. Therefore, a novel approach was applied and a database of the key gene acid phosphatase was created based on the published protein sequences. It is important to mention that some of the published sequences are missannotated, thus it is required to curate them manually.

5. Results

5.1 Microbial diversity phylotypes

By Illumina-sequencing a total of 184766 sequences were obtained for the six samples. After normalization, 22068 sequences per sample, with 280-nucleotide length, were annotated. A number of 121 phylotypes were separated and classified into order (97.5% of phylotypes), family (93.4% of phylotypes) and genus (67% of phylotypes) levels (Table S1and S2). In total, 121 phylotypes belonging to phyla *Thaumarchaeota*, *Actinobacteria*, *Armatimonadetes*, *Bacteroidetes*, *Deinococcus-Thermus*, *Firmicutes*, *Nitrospirae* and *Proteobacteria*. *Proteobacteria*, *Bacteroidetes* and *Actinobacteria* were previously described as the most abundant bacterial phyla in bentonite clay formations (Lopez-Fernandez *et al*., 2014b).

To evaluate if the sampling depth was adequate, six rarefaction curves were plotted into Fig. S1. The curves of the six microcosms studied reached a plateau, meaning that the sequencing per sample was deep enough to detect all the present species and hence the complete microbial diversity of each microcosms. Richness, evenness and phylotype diversity were measured using conventional diversity indices, such as Shannon diversity (H'), Simpson index (λ), Inverse Simpson index (λ), Fisher alpha index (α) and Pielou evenness index (J') (Table S2). These indices are based on species richness/evenness data from each sample. Principal component analysis (PCA) was used to extract the important information from the dataset of the six microcosms,

by displaying the pattern of similarity of the different samples as points in maps (Fig. 2).

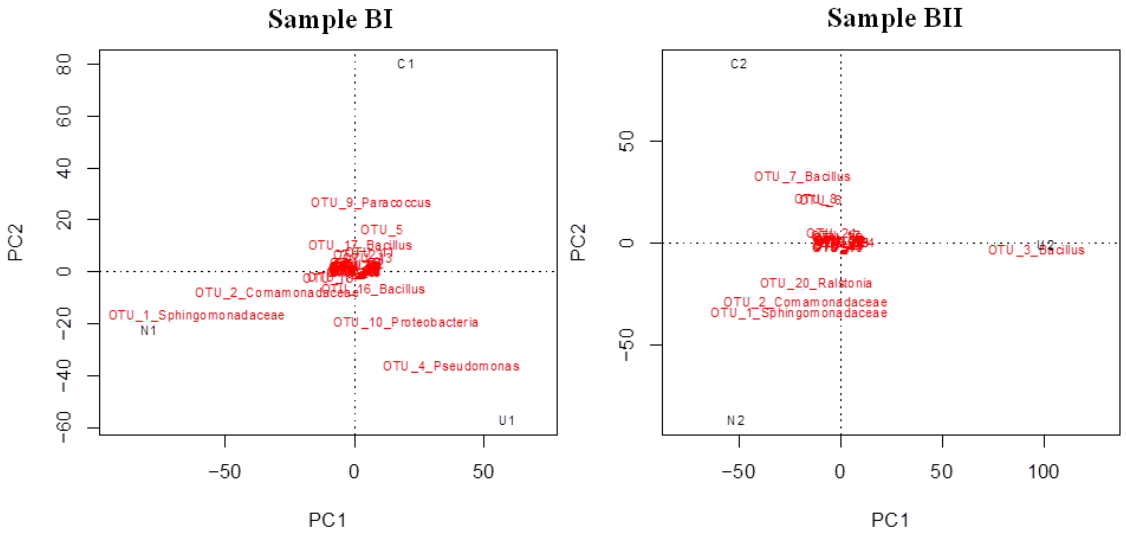

Figure 2. Principal component analysis (PCA) plot comparing the microbial community structure of the six microcosms. C1: BI-A microcosm, N1: BI-B microcosm, U1: BI-C microcosm, C2: BII-A microcosm, N2: BII-B microcosm and U2: BII-C microcosm.

5.2 Diversity of the microcosm communities

The effect of the uranyl treatment in the structure and composition of the microbial communities of the six different microcosms was studied. It revealed that *Firmicutes* and *Proteobacteria* are the main phyla detected. In the case of sample BI, microcosm BI-A, the non-treated control, was mainly dominated by *Firmicutes* (75%). *Alphaproteobacteria* made up of 20% of the community (Fig. 3). The bacterial diversity in BI-B microcosm, the nitrate-control, differs slightly to that of the sample BI-A. *Alpha-*, *Betaproteobacteria* and *Firmicutes* dominate the community, in decreasing order. Moreover, significant differences, compared to both control samples (BI-A and BI-B), were observed in the structure of bacterial population of sample BI-C, probably due to the uranium treatment. The dominant phylum in sample BI-C was *Proteobacteria* (55%), mainly represented by *Gammaproteobacteria*, followed by *Firmicutes* (40%) (Fig.3).

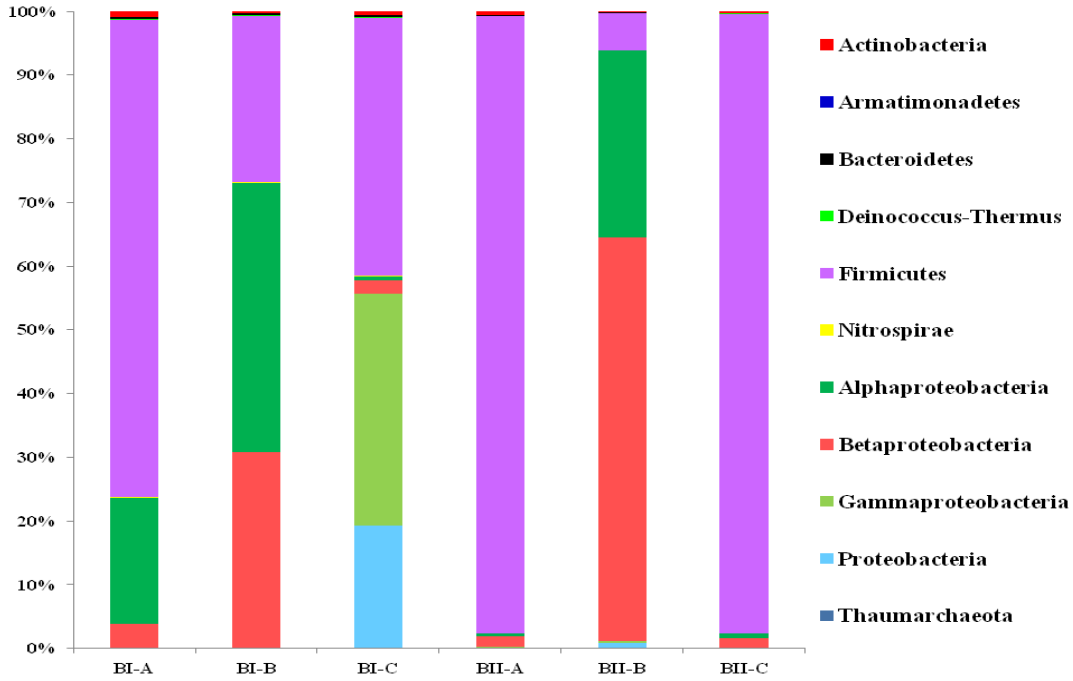

Figure 3. Taxonomic composition of the microbial communities of the six microcosms, represented at phylum/class level.

In the case of sample BII, control microcosm called BII-A was completely dominated by phylum *Firmicutes* (97%), as shown in Figure 3. The sodium nitrate treatment affects the diversity of the microcosm BII-B, because the presence of *Firmicutes* decreases to a 6%, while *Betaproteobacteria* (63%) becomes the most represented class. The phyla diversity of microcosm BII-C is similar to that of BI-A, thus the main phylum is *Firmicutes* (97%).

Taking into consideration the Operational Taxonomic Units (OTUs) annotated, the bacterial diversity in the control microcosms BI-A and BII-A was the highest, since both samples, as water controls, were not treated (Fig. 4). In the microcosms elaborated with bentonite BI, some changes in the microbial distribution of the population were clearly observed in the sodium nitrate and uranyl nitrate treated microcosms. For example, it was detected that in microcosm BI-A, OTU-10, annotated as *Paracoccus* was one of the dominant, in comparison with the rest of the OTUs, representing 19% of the population (Fig. 4). In addition, another two OTUs were highly represented, like OTU-5 (17%) and OTU-12 (11%), annotated as *Clostridiales* Family XVIII *Incertae Sedis* and *Symbiobacterium*, respectively. Moreover, OTU-17 and OTU-20, annotated as *Bacillus*, were also predominant (Table S1).

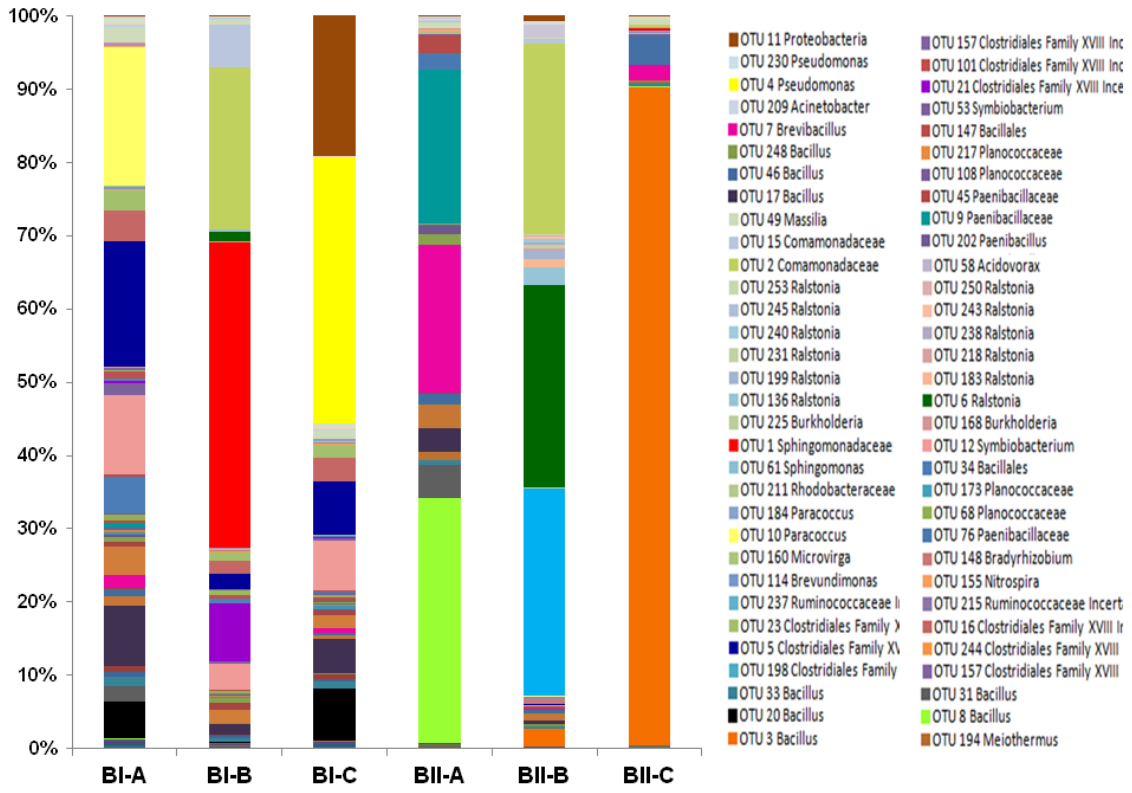

Figure 4. Structure of the microbial community of the six microcosms by OTUs annotated to the least common ancestor. Represented only by the dominant OTUs.

In microcosm BI-B, these majority OTUs of sample BI-A were decreased in number. However, OTU-1, annotated as *Sphingomonadaceae*, and OTU-2, annotated as *Comamonadaceae*, were highly enriched (42% and 22%, respectively) (Fig.4). Moreover, other OTUs as OTU-21 and -6, annotated as *Clostridiales* Family XVIII *Incertae Sedis* and *Ralstonia*, respectively, were also enriched, but in less proportion (Table S1). These differences might be due to the sodium nitrate added to the microcosms, which has a negative or positive effect in the diversity of BI sample population.

In the uranyl nitrate treated microcosm BI-C, OTU-5, -12 and -17 were slightly decreased in comparison with BI-A, where they were dominant OTUs (Table S1). Although those OTUs were surprisingly enriched compared to that of sample BI-B, which can be understood as the combined uranyl nitrate treatment is affecting less the population than only the sodium nitrate treatment. On the other hand, OTU-4 (Fig. 4),

annotated as *Pseudomonas*, was highly enriched (36%), as well as OTU-11, annotated as *Proteobacteria*, enriched in a lower percentage (19%). The OTU-20, annotated as *Bacillus*, was slightly enriched (7%) in comparison to its presence in sample BI-A (5%), but highly enriched compared to that of sample BI-B (0.1%) (Table S1). These might be due to a positive effect of the uranyl nitrate treatment in this specific OTU.

The bacterial diversity of BII microcosm differs of that of the BI microcosm, as it was expected due to the distinct geochemical and mineralogical characteristics of these two bentonites (Lopez-Fernandez *et al*., 2014a). In the case of sample BII-A, *Bacillales,* the dominant *Firmicutes* class compared to the treated microcosms BII-B and BII-C (Figure 3), was mainly represented by OTU-8 (33%), annotated as *Bacillus*, as well as by OTU-9, -7 and OTU-31, annotated as *Paenibacillaceae*, *Brevibacillus* and *Bacillus*, respectively (Table S1).

In the sodium nitrate-treated microcosm BII-B, OTU-1 and OTU-2, annotated as *Sphingomonadaceae*, (*Alphaproteobacteria*) and *Comamonadaceae* (*Betaproteobacteria*), respectively, were highly enriched in comparison with the control microcosm BI-A. Moreover, *Ralstonia*, annotated for OTU-6, -136, -183, -199, -218-, -231, -238, -240, -243, -245, -250 and OTU-253, were only enriched in microcosm BII-B (Fig. 4 and Table S1), revealing an interesting influence of the sodium nitrate treatment for this genus (Dalsing and Allen, 2014). Therefore, in the case of the uranyl nitrate-treated microcosm BII-C, there was a remarkable case for the OTU-3, annotated as *Bacillus*, which was highly enriched (90%) compared to microcosms BII-A and BII-B where it was not even detected (Fig. 4).

5.3 Acid and alkaline phosphatase enzymatic activity

To study the microbial activity involved in the uranium biomineralization as U-phosphates, acid and alkaline phosphatase enzymatic activitiy was measured in the bentonite microcosm samples. The measured activity of the acid phosphatase was increased only in microcosm BII-C, compared to both controls (BII-A and BII-B) as it is shown in Fig. 5. In sample BI there was no evidence of any change in the acid phosphatase activity measured. No significant differences were observed for the alkaline phosphatase activity, in the six microcosm samples, as is evident in Figure 5.

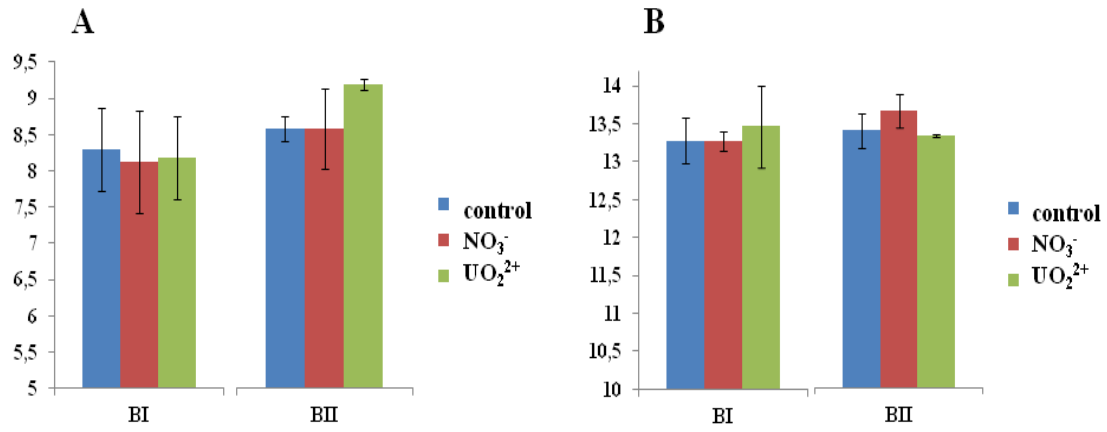

Figure 5. Enzymatic activity measured in bentonite suspensions of the microcosms. A: Acid phosphatase activity. B: alkaline phosphatase activity.

5.4 Novel approach: database of the acid phosphatase catabolic genes

A database was created based on the published protein sequences for acid phosphatase catabolic genes, a key gene described for been involved in the uranium biomineralization. After a manual curation of thousands of protein sequences, the acid phosphatase database contains more than 6000 sequences. The interesting finding is that the catabolic genes included in the database are taxonomically related, as shown in Figure 6. The thousands of protein sequences were phylogenetically classified in 16 different clusters to build the phylogenetic trees (Fig. S2-S17). Each cluster was represented by one or two sequences depending on its phylogeny.

This taxonomical relationship means that it is feasible to design specific primers for a particular branch of the acid phosphatase database phylogenetic tree, to quantify the catabolic acid phosphatase gene expression of the selected branch applying RT-PCR approaches. This novel approach will allow the scientific community to identify the best qualified microorganisms for the uranium biomineralization, by designing biological labels to be used in environmental samples as well as in microorganisms isolated from uranium contaminated sites.

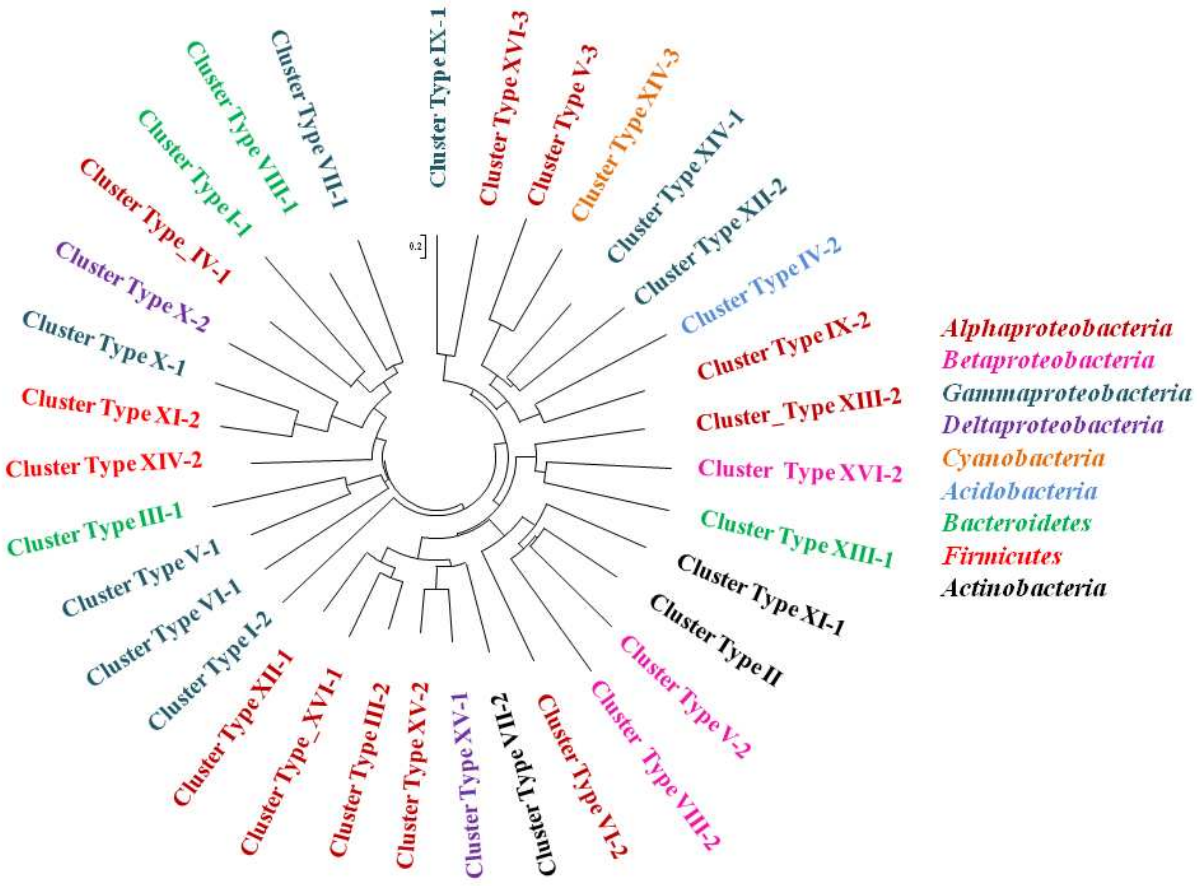

Figure 6. Phylogenetic tree of the 16 representative clusters of the acid phosphatase sequences included in the database.

6. Discussion

Since bentonite formations were selected as backfilling material for the planned Spanish DGR, a deep knowledge of microbial diversity and the influence of radionuclides is required. This work studied the changes induced by the addition of sodium nitrate and uranyl nitrate on the bacterial community of bentonite microcosms using Illumina sequencing platform. In addition, the microbial enzymatic phosphatase activity was measured to determine if it is involved in the U(VI) bioprecipitation and a data base of acid phosphatase genes was elaborated. Several studies have examined the influence of sodium nitrate in the microbial population. For instance, Huang *et al.* (2012) demonstrated that the accumulation of nitrate in soil decreased the microbial diversity. However, Bougon *et al.* (2012) described that if the nitrate concentration is stable along the time, the nitrate reducing bacteria community, don't vary.

A total of 121 phylotypes were detected by Illumina sequencing, semiquantifying the microbial community of the six different microcosms studied. Changes induced by sodium nitrate- or uranyl nitrate treatment were different depending on the bentonite sample (BI or BII) studied. For example, in the BI-A control microcosm the dominant OTUs, annotated as *Paracoccus*, *Bacillus*, *Symbiobacterium* and *Clostridiales* Family XVIII *Incertae Sedis*, have an interesting relationship. *Paracoccus* is a heterotrophic aerobic *Alphaproteobacteria* identified also in natural bentonites (Lopez-Fernandez *et al.,* 2014b). *Bacillus* is described for including both, aerobic or facultative anaerobic bacterial species. So far, facultative anaerobic microorganisms are well adapted to cyclic changes in their oxygen tension, by switching their metabolism according to the presence or absence of oxygen (Reitz *et al.,* 2014). In addition, *Symbiobacterium* is a Gram-negative bacterium whose growth is dependent on co-culture with an associating thermophilic *Bacillus* strain (Ohno *et al*., 2000). This combination of microorganisms may use the available oxygen, creating anaerobic conditions that allow the presence of the *Clostridiales* family (obligate anaerobe).

In the sodium nitrate-treated sample BI-B, heterotrophic aerobic families *Sphingomonadaceae* and *Comamonadaceae* where highly enriched. Its dominance might reduce the oxygen level, leading to the enrichment of another *Clostridiales* Family XVIII *Incertae Sedis* and *Ralstonia*. The increased of *Ralstonia* in sample BI-B may be due to the ability of this genus to use nitrate as terminal electron acceptor, as it was described for the case of *Ralstonia eutropha* (Tiemeyer *et al.,* 2007). Furthermore, the nitrate addition stimulates the increase of the activity of nitrate reducing bacteria, as for example *Paracoccus denitrificans* (Villahermosa *et al*., 2013). However, the opposite behavior of OTU-10 in response to the sodium nitrate treatment (BI-B) could be because the *Paracoccus* detected was not belonging to a nitrate reducing specie of this genus. In sample BI-C, the presence of uranyl nitrate might be strengthening the enrichment of OTU-4, annotated as *Pseudomonas*. *Pseudomonas aeruginosa* has been described for their ability to bioprecipitate uranium (Renninger *et al*., 2004). A metal-resistant *Pseudomonas aeruginosa* strain isolated from uranium mine waste was characterized for its potential of U biomineralization (Choudhary and Sar, 2011). Macaskie *et al*. (2000) identified LPS at the exocellular membrane of *P. aeruginosa* used to transport alkaline phosphatase. Moreover, U uptake was demonstrated in live

and dead cells of *Pseudomonas* sp., showing a higher absorbance in dead cells (Prasath *et al.*, 2010). In the case of U(VI) influences in the microbial population, Geissler *et al*. (2009) define a decrease in the predominant bacterial groups for short-term incubation with uranyl nitrate, although the situation changes completely after longer incubations, when the bacterial diversity is increased. The latter change may be understood as a fact of uranium immobilization by the bacterial community.

The bacterial community of sample BII-A was dominated by phylum Firmicutes, mainly represented by *Bacillus*, *Paenibacillaceae* family and *Brevibacillus*. In correlation with these results, BII-S2 strain, belonging to *Bacillus simplex*, was isolated from bentonites (Lopez-Fernandez *et al*., 2014a). Moreover, some other *Firmicutes* bacteria were found in similar oligotrophic environments as the Spanish bentonite formations, for example, a facultative anaerobic *Paenibacillus* sp. was isolated from a uranium mining waste pile in Germany (Reitz *et al*., 2014), as well as a facultative iron-reducing *Paenibacillus* sp. was isolated from subsurface sediment biofilms (Ahmed *et al.*, 2012). A *Brevibacillus brevis* isolated from cadmium contaminated soil, was described for the Cd immobilization and its use for bioremediation (Vivas *et al*., 2005). The influence of the sodium nitrate treatment affects the bacterial population of sample BII-B in a similar way than in sample BI-B. In the microcosm BII-C, belonging to *Firmicutes*, the specific case of OTU-3, annotated as *Bacillus*, was highly enriched in the presence uranium. Different strains of aerobic *Bacillus* spp. have been described for their U(VI) biosorption capacity (Li *et al.*, 2014) and U(VI) biomineralization mediated by bacterial acid phosphatase activity (Martinez *et al*., 2007; Merroun *et al*., 2011). This characteristic can be of interest for the DGR, as well as for bioremediation of U contaminated sites and might be the reason why OTUs annotated as *Bacillus* in this study were so enriched after U(VI)-long-term incubation. Moreover, the capacity of the genus *Bacillus* to deal with uranium might be a survival mechanism of the cells to tolerate high concentrations of this radionuclide, as described for the case of *B. subtilis*, showing almost linear growth at uranium concentration under 450 mg/l (Liao *et al*., 2013).

The bioremediation of uranium contaminated environments could be achieved via enzimatically phosphatase activity mediated by U(VI) biomineralization process, in bacteria (Beazley *et al*., 2011; Merroun *et al*., 2011), as well as in fungi (Fomina *et al*., 2008). For this reason is important to get a deeper knowledge of the catabolic potential

of the microbial community in complex ecosystems. In this study, a novel approach was applied creating a database of acid phosphatase catabolic genes, with the aim of fulfilling the U bioprecipitation process. So far, this study takes one step further in the possibility of using the taxonomic information of a studied ecosystem to better understand its catabolic potential.

7. Conclusions

This work describes the bacterial community changes, of bentonite microcosms, induced by the uranyl nitrate treatment under aerobic condition. The structure of the bacterial community of the uranyl nitrate-treated microcosms (BI-C and BII-C) differs to that of the controls microcosms (water- and sodium nitrate treatment). *Pseudomonas* and *Bacillus*, microorganisms described for their ability to precipitate uranium as U-phosphate mineral phases with a similar structure to that of meta-autunite through phosphatase activity, are highly enriched due to the uranyl nitrate treatment. Moreover, a database of acid phosphatase catabolic genes was created. This study describes a novel approach to provide more information about the uranium bioprecipitation process, by using the taxonomic information of an ecosystem. Further analyses are required to continue this novel approach, fulfilling the knowledge about the catabolic potential of the microorganisms involved in the uranium bioprecipitation, and to use this information in the deep geological repository of radioactive wastes, as well as in the bioremediation of uranium contaminated sites.

8. Acknowledgments

This work was funded by Grants CGL2009-09760, CGL-2012-36505**,** BES-2010-032098 and EEBB-I-14-08420 (Ministerio de Ciencia e Innovación, España). We acknowledge the assistance of Tim Lacoere with the lab work (LabMET, Belgium) and Iris Plumeier with the Illumina sequencing (HZI, Germany).

9. Supplementary material

Table S1. Phylogenetic assignment. Description of all 121 phylotypes determined using Illumina-based amplicon deep-sequencing.

Phylotype	BI-A	BI-B	BI-C	BII-A	BII-B	BII-C	Domain	Phylum	Class	Order	Family	Genus
OTU235	0	0	9	0	0	0	Archaea	*Thaumarchaeota*	Soil *Crenarchaeotic* Group(SCG)	-	-	-
OTU172	11	4	16	8	0	16	Bacteria	*Actinobacteria*	*Acidimicrobiia*	*Acidimicrobiales*	*Incertae Sedis*	*Candidatus Microthrix*
OTU229	0	0	0	5	0	0	Bacteria	*Actinobacteria*	*Acidimicrobiia*	*Acidimicrobiales*	-	-
OTU40	0	0	0	4	0	0	Bacteria	*Actinobacteria*	*Actinobacteria*	*Frankiales*	-	-
OTU91	74	33	26	58	11	16	Bacteria	*Actinobacteria*	*Actinobacteria*	*Micrococcales*	*Microbacteriaceae*	*Microbacterium*
OTU90	0	0	0	31	22	30	Bacteria	*Actinobacteria*	*Actinobacteria*	*Micrococcales*	*Micrococcaceae*	*Arthrobacter*
OTU129	102	13	84	0	0	0	Bacteria	*Actinobacteria*	*Actinobacteria*	*Micromonosporales*	*Micromonosporaceae*	
OTU201	0	0	0	11	0	8	Bacteria	*Actinobacteria*	*Actinobacteria*	*Propionibacteriales*	*Nocardioidaceae*	*Nocardioides*
OTU200	0	0	0	27	0	0	Bacteria	*Actinobacteria*	*Actinobacteria*	*Propionibacteriales*	*Propionibacteriaceae*	*Propionibacterium*
OTU190	5	21	0	0	9	3	Bacteria	*Armatimonadetes*	-	-	-	-
OTU179	0	4	0	0	0	0	Bacteria	*Armatimonadetes*	-	-	-	-
OTU191	23	10	12	3	0	0	Bacteria	*Bacteroidetes*	*Cytophagia*	*Cytophagales*	*Cytophagaceae*	*Hymenobacter*
OTU203	22	7	9	0	0	3	Bacteria	*Bacteroidetes*	*Cytophagia*	*Cytophagales*	*Cytophagaceae*	*Hymenobacter*
OTU221	0	4	6	0	0	0	Bacteria	*Bacteroidetes*	*Cytophagia*	*Cytophagales*	*Cytophagaceae*	*Hymenobacter*
OTU24	0	11	0	0	0	0	Bacteria	*Bacteroidetes*	*Cytophagia*	*Cytophagales*	*Cytophagaceae*	-

OTU133	36	33	30	21	8	3	Bacteria	*Bacteroidetes*	*Flavobacteria*	*Flavobacteriales*	*Flavobacteriaceae*	*Chryseobacterium*
OTU170	5	21	30	0	0	5	Bacteria	*Deinococcus-Thermus*	*Deinococci*	*Thermales*	*Thermaceae*	*Meiothermus*
OTU194	0	8	6	0	16	0	Bacteria	*Deinococcus-Thermus*	*Deinococci*	*Thermales*	*Thermaceae*	*Meiothermus*
OTU3	0	0	0	0	516	19825	Bacteria	*Firmicutes*	*Bacilli*	*Bacillales*	*Bacillaceae*	*Bacillus*
OTU8	41	13	11	7361	12	32	Bacteria	*Firmicutes*	*Bacilli*	*Bacillales*	*Bacillaceae*	*Bacillus*
OTU20	1117	30	1586	0	7	0	Bacteria	*Firmicutes*	*Bacilli*	*Bacillales*	*Bacillaceae*	*Bacillus*
OTU31	451	3	0	1017	0	0	Bacteria	*Firmicutes*	*Bacilli*	*Bacillales*	*Bacillaceae*	*Bacillus*
OTU33	277	95	196	127	53	101	Bacteria	*Firmicutes*	*Bacilli*	*Bacillales*	*Bacillaceae*	*Bacillus*
OTU75	7	4	0	264	19	80	Bacteria	*Firmicutes*	*Bacilli*	*Bacillales*	*Bacillaceae*	*Bacillus*
OTU103	142	62	58	0	0	0	Bacteria	*Firmicutes*	*Bacilli*	*Bacillales*	*Bacillaceae*	*Bacillus*
OTU106	157	38	168	0	0	0	Bacteria	*Firmicutes*	*Bacilli*	*Bacillales*	*Bacillaceae*	*Bacillus*
OTU159	12	3	19	5	62	0	Bacteria	*Firmicutes*	*Bacilli*	*Bacillales*	*Bacillaceae*	*Bacillus*
OTU197	19	12	16	4	0	0	Bacteria	*Firmicutes*	*Bacilli*	*Bacillales*	*Bacillaceae*	*Bacillus*
OTU17	1817	300	1038	690	104	8	Bacteria	*Firmicutes*	*Bacilli*	*Bacillales*	*Bacillaceae*	*Bacillus*
OTU43	278	37	86	729	226	0	Bacteria	*Firmicutes*	*Bacilli*	*Bacillales*	*Bacillaceae*	*Bacillus*
OTU46	219	14	70	322	95	0	Bacteria	*Firmicutes*	*Bacilli*	*Bacillales*	*Bacillaceae*	*Bacillus*
OTU246	10	0	3	21	2	0	Bacteria	*Firmicutes*	*Bacilli*	*Bacillales*	*Bacillaceae*	*Bacillus*
OTU248	6	0	0	6	0	0	Bacteria	*Firmicutes*	*Bacilli*	*Bacillales*	*Bacillaceae*	*Bacillus*
OTU249	19	8	18	0	0	0	Bacteria	*Firmicutes*	*Bacilli*	*Bacillales*	*Bacillaceae*	*Bacillus*

OTU7	380	4	117	4464	55	441	Bacteria	*Firmicutes*	*Bacilli*	*Bacillales*	*Paenibacillaceae*	*Brevibacillus*
OTU19	848	392	402	0	0	0	Bacteria	*Firmicutes*	*Bacilli*	*Bacillales*	*Paenibacillaceae*	*Paenibacillus*
OTU37	7	1	8	0	0	885	Bacteria	*Firmicutes*	*Bacilli*	*Bacillales*	*Paenibacillaceae*	*Paenibacillus*
OTU50	137	197	123	0	0	0	Bacteria	*Firmicutes*	*Bacilli*	*Bacillales*	*Paenibacillaceae*	*Paenibacillus*
OTU66	161	127	26	305	0	0	Bacteria	*Firmicutes*	*Bacilli*	*Bacillales*	*Paenibacillaceae*	*Paenibacillus*
OTU74	42	9	20	262	0	0	Bacteria	*Firmicutes*	*Bacilli*	*Bacillales*	*Paenibacillaceae*	*Paenibacillus*
OTU95	80	43	128	0	0	0	Bacteria	*Firmicutes*	*Bacilli*	*Bacillales*	*Paenibacillaceae*	*Paenibacillus*
OTU119	73	46	14	0	0	0	Bacteria	*Firmicutes*	*Bacilli*	*Bacillales*	*Paenibacillaceae*	*Paenibacillus*
OTU143	25	7	33	23	0	7	Bacteria	*Firmicutes*	*Bacilli*	*Bacillales*	*Paenibacillaceae*	*Paenibacillus*
OTU165	25	6	20	17	59	8	Bacteria	*Firmicutes*	*Bacilli*	*Bacillales*	*Paenibacillaceae*	*Paenibacillus*
OTU193	7	6	8	10	0	0	Bacteria	*Firmicutes*	*Bacilli*	*Bacillales*	*Paenibacillaceae*	*Paenibacillus*
OTU202	13	14	10	12	0	12	Bacteria	*Firmicutes*	*Bacilli*	*Bacillales*	*Paenibacillaceae*	*Paenibacillus*
OTU233	11	11	0	0	0	6	Bacteria	*Firmicutes*	*Bacilli*	*Bacillales*	*Paenibacillaceae*	*Paenibacillus*
OTU9	134	0	48	4644	0	0	Bacteria	*Firmicutes*	*Bacilli*	*Bacillales*	*Paenibacillaceae*	-
OTU76	0	0	1	500	0	0	Bacteria	*Firmicutes*	*Bacilli*	*Bacillales*	*Paenibacillaceae*	-
OTU45	75	0	96	522	0	0	Bacteria	*Firmicutes*	*Bacilli*	*Bacillales*	*Paenibacillaceae*	-
OTU68	162	71	83	0	0	0	Bacteria	*Firmicutes*	*Bacilli*	*Bacillales*	*Planococcaceae*	-
OTU108	40	14	54	26	4	18	Bacteria	*Firmicutes*	*Bacilli*	*Bacillales*	*Planococcaceae*	-
OTU173	10	5	14	24	0	2	Bacteria	*Firmicutes*	*Bacilli*	*Bacillales*	*Planococcaceae*	-

OTU217	2	1	6	3	5	8	Bacteria	*Firmicutes*	*Bacilli*	*Bacillales*	*Planococcaceae*	-
OTU34	1089	0	23	0	2	0	Bacteria	*Firmicutes*	*Bacilli*	*Bacillales*	-	-
OTU147	94	24	27	0	0	0	Bacteria	*Firmicutes*	*Bacilli*	*Bacillales*	-	-
OTU12	2380	792	1489	10	15	10	Bacteria	*Firmicutes*	*Clostridia*	*Clostridiales*	F. XVIII *Incertae Sedis*	*Symbiobacterium*
OTU53	348	82	86	0	0	0	Bacteria	*Firmicutes*	*Clostridia*	*Clostridiales*	F. XVIII *Incertae Sedis*	*Symbiobacterium*
OTU252	9	0	3	0	0	0	Bacteria	*Firmicutes*	*Clostridia*	*Clostridiales*	F. XVIII *Incertae Sedis*	*Symbiobacterium*
OTU21	77	1734	19	0	0	20	Bacteria	*Firmicutes*	*Clostridia*	*Clostridiales*	F. XVIII *Incertae Sedis*	-
OTU87	49	132	42	0	0	0	Bacteria	*Firmicutes*	*Clostridia*	*Clostridiales*	F. XVIII *Incertae Sedis*	-
OTU101	245	124	17	0	0	0	Bacteria	*Firmicutes*	*Clostridia*	*Clostridiales*	F. XVIII *Incertae Sedis*	-
OTU102	22	140	21	0	0	0	Bacteria	*Firmicutes*	*Clostridia*	*Clostridiales*	F. XVIII *Incertae Sedis*	-
OTU157	51	39	0	0	0	0	Bacteria	*Firmicutes*	*Clostridia*	*Clostridiales*	F. XVIII *Incertae Sedis*	-
OTU198	30	0	9	0	0	0	Bacteria	*Firmicutes*	*Clostridia*	*Clostridiales*	F. XVIII *Incertae Sedis*	-
OTU244	10	4	0	0	0	0	Bacteria	*Firmicutes*	*Clostridia*	*Clostridiales*	F. XVIII *Incertae Sedis*	-
OTU5	3800	449	1606	0	31	0	Bacteria	*Firmicutes*	*Clostridia*	*Clostridiales*	F. XVIII *Incertae Sedis*	-
OTU16	920	388	694	8	7	3	Bacteria	*Firmicutes*	*Clostridia*	*Clostridiales*	F. XVIII *Incertae Sedis*	-
OTU23	592	240	400	2	0	3	Bacteria	*Firmicutes*	*Clostridia*	*Clostridiales*	F. XVIII *Incertae Sedis*	-
OTU215	6	4	20	0	0	0	Bacteria	*Firmicutes*	*Clostridia*	*Clostridiales*	*Ruminococcaceae*	*Incertae Sedis*
OTU237	7	7	0	0	0	0	Bacteria	*Firmicutes*	*Clostridia*	*Clostridiales*	*Ruminococcaceae*	*Incertae Sedis*
OTU155	29	34	22	0	3	9	Bacteria	*Nitrospirae*	*Nitrospira*	*Nitrospirales*	*Nitrospiraceae*	*Nitrospira*

OTU114	68	19	39	13	0	18	Bacteria	*Proteobacteria*	*Alphaproteobacteria*	*Caulobacterales*	*Caulobacteraceae*	*Brevundimonas*
OTU148	0	14	0	0	143	0	Bacteria	*Proteobacteria*	*Alphaproteobacteria*	*Rhizobiales*	*Bradyrhizobiaceae*	*Bradyrhizobium*
OTU160	37	10	9	22	0	5	Bacteria	*Proteobacteria*	*Alphaproteobacteria*	*Rhizobiales*	*Methylobacteriaceae*	*Microvirga*
OTU169	5	9	0	0	73	0	Bacteria	*Proteobacteria*	*Alphaproteobacteria*	*Rhizobiales*	*Rhizobiaceae*	*Rhizobium*
OTU10	4152	3	0	12	34	0	Bacteria	*Proteobacteria*	*Alphaproteobacteria*	*Rhodobacterales*	*Rhodobacteraceae*	*Paracoccus*
OTU134	36	20	35	46	7	10	Bacteria	*Proteobacteria*	*Alphaproteobacteria*	*Rhodobacterales*	*Rhodobacteraceae*	*Paracoccus*
OTU184	20	3	14	0	0	6	Bacteria	*Proteobacteria*	*Alphaproteobacteria*	*Rhodobacterales*	*Rhodobacteraceae*	*Paracoccus*
OTU171	16	12	5	6	0	10	Bacteria	*Proteobacteria*	*Alphaproteobacteria*	*Rhodobacterales*	*Rhodobacteraceae*	-
OTU211	0	6	0	0	0	0	Bacteria	*Proteobacteria*	*Alphaproteobacteria*	*Rhodobacterales*	*Rhodobacteraceae*	-
OTU146	46	14	36	12	2	9	Bacteria	*Proteobacteria*	*Alphaproteobacteria*	*Sphingomonadales*	*Sphingomonadaceae*	*Sphingobium*
OTU61	0	0	5	0	0	0	Bacteria	*Proteobacteria*	*Alphaproteobacteria*	*Sphingomonadales*	*Sphingomonadaceae*	*Sphingomonas*
OTU69	0	3	0	0	0	0	Bacteria	*Proteobacteria*	*Alphaproteobacteria*	*Sphingomonadales*	*Sphingomonadaceae*	*Sphingomonas*
OTU1	0	9209	0	0	6242	80	Bacteria	*Proteobacteria*	*Alphaproteobacteria*	*Sphingomonadales*	*Sphingomonadaceae*	-
OTU168	23	4	4	37	3	5	Bacteria	*Proteobacteria*	*Betaproteobacteria*	*Burkholderiales*	*Burkholderiaceae*	*Burkholderia*
OTU225	0	9	0	0	11	0	Bacteria	*Proteobacteria*	*Betaproteobacteria*	*Burkholderiales*	*Burkholderiaceae*	*Burkholderia*
OTU6	0	300	0	8	6100	8	Bacteria	*Proteobacteria*	*Betaproteobacteria*	*Burkholderiales*	*Burkholderiaceae*	*Ralstonia*
OTU136	0	25	0	0	547	0	Bacteria	*Proteobacteria*	*Betaproteobacteria*	*Burkholderiales*	*Burkholderiaceae*	*Ralstonia*
OTU183	0	12	0	0	220	0	Bacteria	*Proteobacteria*	*Betaproteobacteria*	*Burkholderiales*	*Burkholderiaceae*	*Ralstonia*
OTU199	0	11	0	0	273	0	Bacteria	*Proteobacteria*	*Betaproteobacteria*	*Burkholderiales*	*Burkholderiaceae*	*Ralstonia*

OTU218	0	0	0	0	63	0	Bacteria	*Proteobacteria*	*Betaproteobacteria*	*Burkholderiales*	*Burkholderiaceae*	*Ralstonia*
OTU231	0	2	0	0	111	0	Bacteria	*Proteobacteria*	*Betaproteobacteria*	*Burkholderiales*	*Burkholderiaceae*	*Ralstonia*
OTU238	0	0	0	0	50	0	Bacteria	*Proteobacteria*	*Betaproteobacteria*	*Burkholderiales*	*Burkholderiaceae*	*Ralstonia*
OTU240	0	2	0	0	135	0	Bacteria	*Proteobacteria*	*Betaproteobacteria*	*Burkholderiales*	*Burkholderiaceae*	*Ralstonia*
OTU243	0	0	0	0	46	0	Bacteria	*Proteobacteria*	*Betaproteobacteria*	*Burkholderiales*	*Burkholderiaceae*	*Ralstonia*
OTU245	0	0	0	0	28	0	Bacteria	*Proteobacteria*	*Betaproteobacteria*	*Burkholderiales*	*Burkholderiaceae*	*Ralstonia*
OTU250	0	0	0	0	31	0	Bacteria	*Proteobacteria*	*Betaproteobacteria*	*Burkholderiales*	*Burkholderiaceae*	*Ralstonia*
OTU253	0	0	0	0	26	0	Bacteria	*Proteobacteria*	*Betaproteobacteria*	*Burkholderiales*	*Burkholderiaceae*	*Ralstonia*
OTU58	0	0	2	0	0	0	Bacteria	*Proteobacteria*	*Betaproteobacteria*	*Burkholderiales*	*Comamonadaceae*	*Acidovorax*
OTU2	2	4899	0	0	5735	71	Bacteria	*Proteobacteria*	*Betaproteobacteria*	*Burkholderiales*	*Comamonadaceae*	-
OTU13	0	0	0	0	6	0	Bacteria	*Proteobacteria*	*Betaproteobacteria*	*Burkholderiales*	*Comamonadaceae*	-
OTU15	5	1267	0	0	145	9	Bacteria	*Proteobacteria*	*Betaproteobacteria*	*Burkholderiales*	*Comamonadaceae*	-
OTU232	0	10	0	0	0	0	Bacteria	*Proteobacteria*	*Betaproteobacteria*	*Burkholderiales*	*Comamonadaceae*	-
OTU49	467	148	225	178	26	136	Bacteria	*Proteobacteria*	*Betaproteobacteria*	*Burkholderiales*	*Oxalobacteraceae*	*Massilia*
OTU110	3	5	10	5	0	4	Bacteria	*Proteobacteria*	*Betaproteobacteria*	*Burkholderiales*	*Oxalobacteraceae*	*Massilia*
OTU135	78	23	52	35	0	21	Bacteria	*Proteobacteria*	*Betaproteobacteria*	*Burkholderiales*	*Oxalobacteraceae*	*Massilia*
OTU154	26	12	14	7	0	12	Bacteria	*Proteobacteria*	*Betaproteobacteria*	*Burkholderiales*	*Oxalobacteraceae*	*Massilia*
OTU251	9	6	4	6	0	0	Bacteria	*Proteobacteria*	*Betaproteobacteria*	*Burkholderiales*	*Oxalobacteraceae*	*Massilia*
OTU44	6	0	4	0	0	0	Bacteria	*Proteobacteria*	*Betaproteobacteria*	*Burkholderiales*	*Oxalobacteraceae*	-

OTU67	185	57	128	55	13	64	Bacteria	*Proteobacteria*	*Betaproteobacteria*	*Burkholderiales*	*Oxalobacteraceae*	-
OTU85	3	0	0	24	393	1	Bacteria	*Proteobacteria*	*Betaproteobacteria*	*Burkholderiales*	*Oxalobacteraceae*	-
OTU214	17	6	9	0	0	0	Bacteria	*Proteobacteria*	*Betaproteobacteria*	*Burkholderiales*	*Oxalobacteraceae*	-
OTU207	0	0	0	4	0	6	Bacteria	*Proteobacteria*	*Gammaproteobacteria*	*Enterobacteriales*	*Enterobacteriaceae*	-
OTU209	0	0	0	12	0	0	Bacteria	*Proteobacteria*	*Gammaproteobacteria*	*Pseudomonadales*	*Moraxellaceae*	*Acinetobacter*
OTU234	7	1	0	3	0	0	Bacteria	*Proteobacteria*	*Gammaproteobacteria*	*Pseudomonadales*	*Moraxellaceae*	*Enhydrobacter*
OTU4	0	0	8039	0	0	5	Bacteria	*Proteobacteria*	*Gammaproteobacteria*	*Pseudomonadales*	*Pseudomonadaceae*	*Pseudomonas*
OTU152	6	0	0	0	0	0	Bacteria	*Proteobacteria*	*Gammaproteobacteria*	*Pseudomonadales*	*Pseudomonadaceae*	*Pseudomonas*
OTU230	0	0	1	6	59	4	Bacteria	*Proteobacteria*	*Gammaproteobacteria*	*Pseudomonadales*	*Pseudomonadaceae*	*Pseudomonas*
OTU206	0	0	13	0	26	0	Bacteria	*Proteobacteria*	*Gammaproteobacteria*	*Xanthomonadales*	*Xanthomonadaceae*	-
OTU11	11	12	4234	31	177	22	Bacteria	*Proteobacteria*	-	-	-	-

Table S2. Ecological biodiversity indices of the six microcosm communities. The indices presented are: Species richness (S), Shannon index (H'), Simpson index (λ), Inverse Simpson index (1/λ), Unbias Simpson index (Unbias Simp), Fisher Alpha index (α) and Pielou's evenness (J').

Sample	S	H'	λ	1/λ	Unbias Simp	α	J'
BI-A	84	2.92	0.90	10.55	0.90	10.43	0.66
BI-B	89	2.14	0.76	4.21	0.76	10.64	0.48
BI-C	77	2.30	0.81	5.29	0.81	9.57	0.53
BII-A	56	2.06	0.80	4.93	0.80	6.78	0.51
BII-B	53	1.93	0.77	4.42	0.77	6.52	0.49
BII-C	49	0.57	0.19	1.24	0.19	5.77	0.15

Figure S1. Rarefaction curves portraying the number of species against sampling depth of each microcosms.

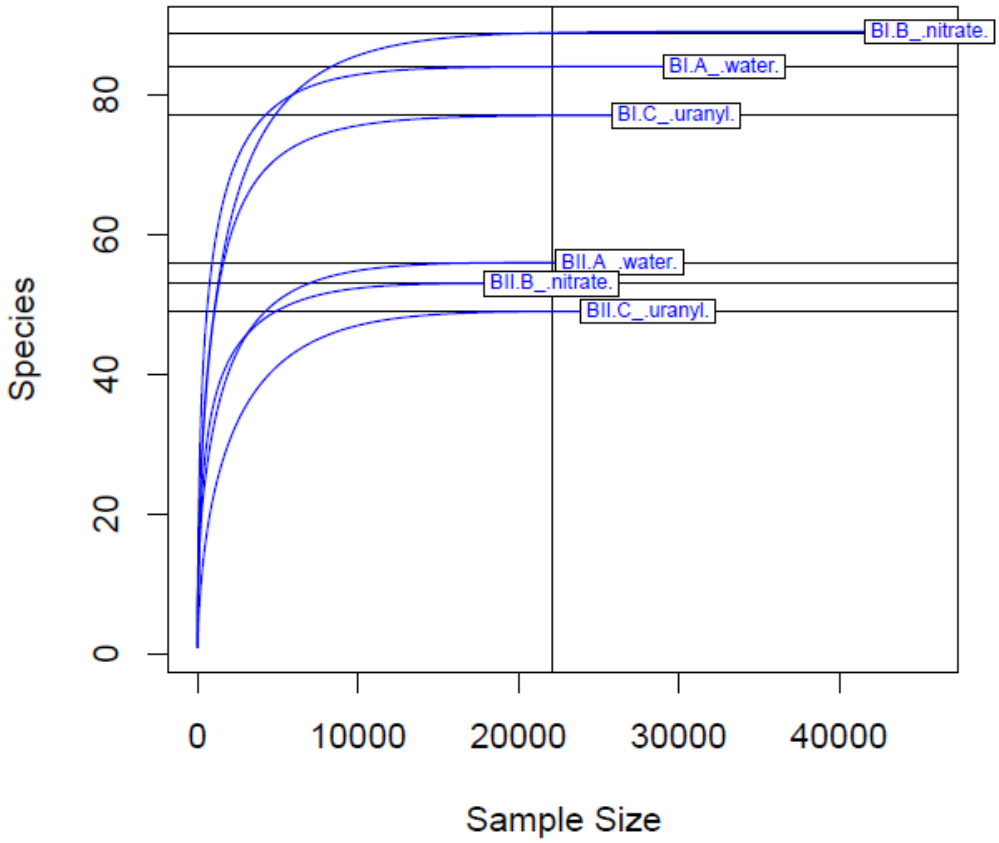

Figure S2. Phylogenetic tree of cluster I of the acid phosphatase sequences included in the database.

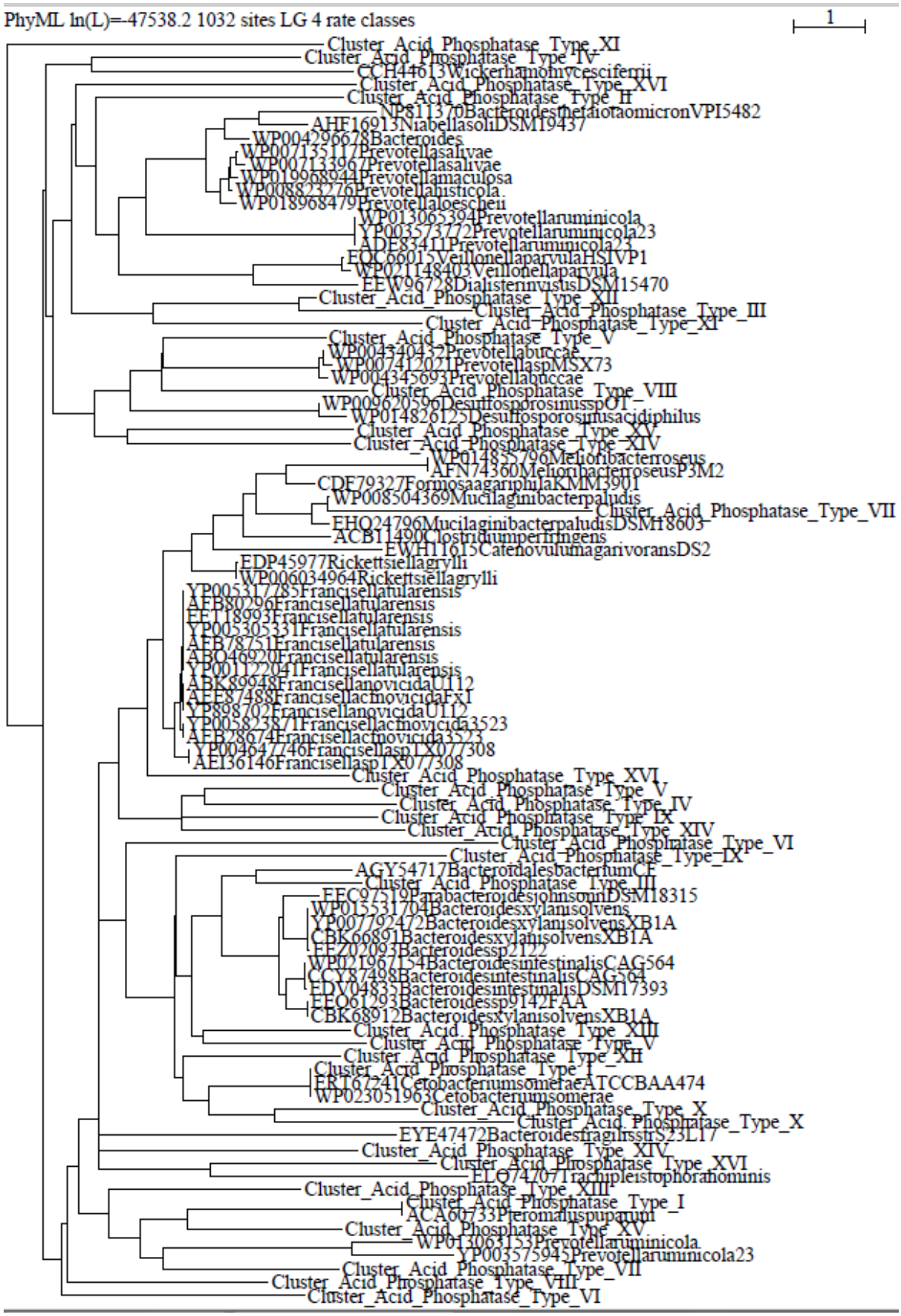

Figure S3. Phylogenetic tree of cluster II of the acid phosphatase sequences included in the database.

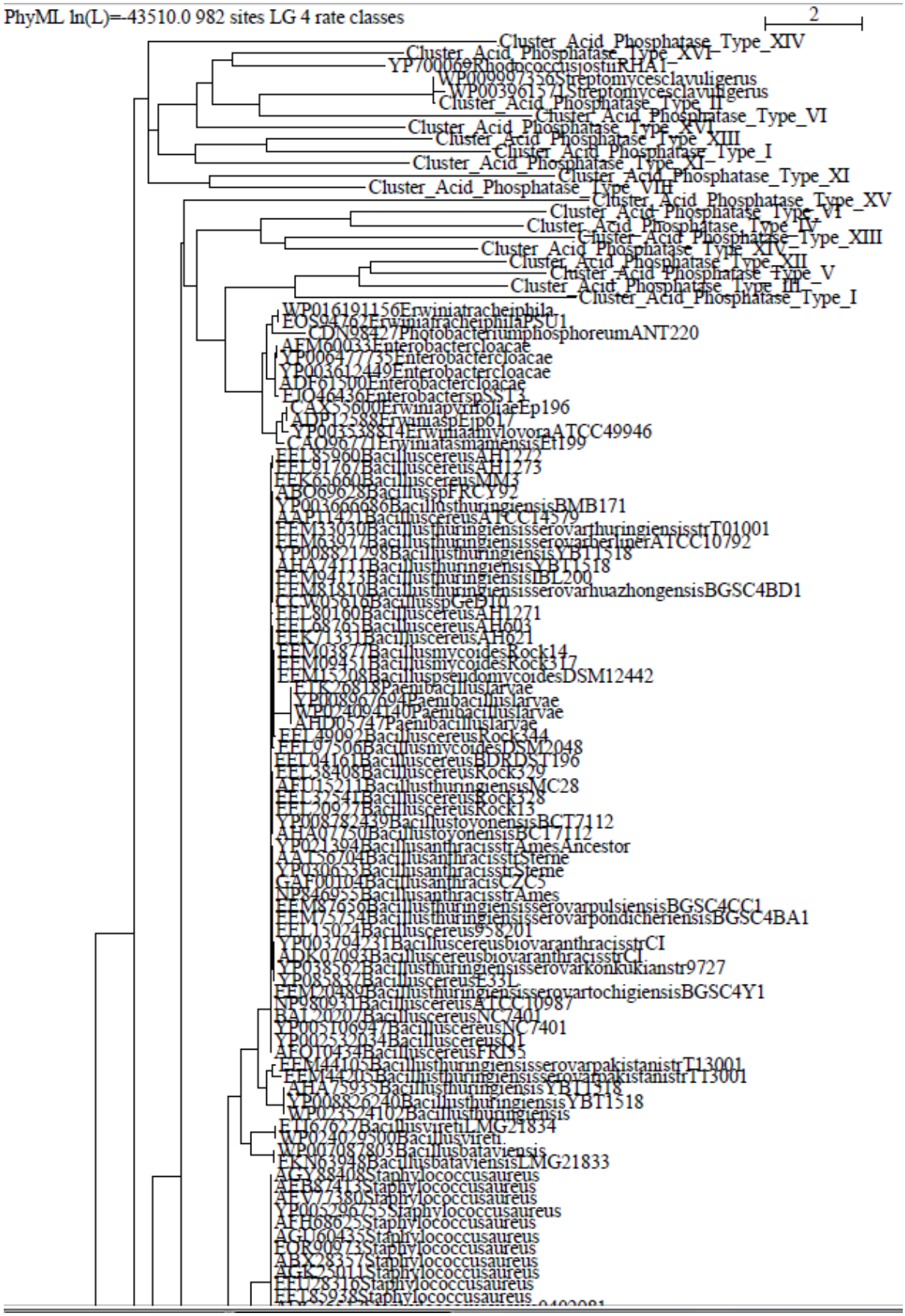


Cluster_Acid_Phosphatase_Type_IX
Cluster_Acid_Phosphatase_Type_V
Cluster_Acid_Phosphatase_Type_I
Cluster_Acid_Phosphatase_Type_VIII
Cluster_Acid_Phosphatase_Type_IX
Cluster_Acid_Phosphatase_Type_XVI
Cluster_Acid_Phosphatase_Type_X
Cluster_Acid_Phosphatase_Type_X
Cluster_Acid_Phosphatase_Type_XIV
Cluster_Acid_Phosphatase_Type_VII
Cluster_Acid_Phosphatase_Type_XII
Cluster_Acid_Phosphatase_Type_III
Cluster_Acid_Phosphatase_Type_IV
Cluster_Acid_Phosphatase_Type_VII
Cluster_Acid_Phosphatase_Type_XV

Figure S4. Phylogenetic tree of cluster III of the acid phosphatase sequences included in the database.

Figure S5. Phylogenetic tree of cluster IV of the acid phosphatase sequences included in the database.

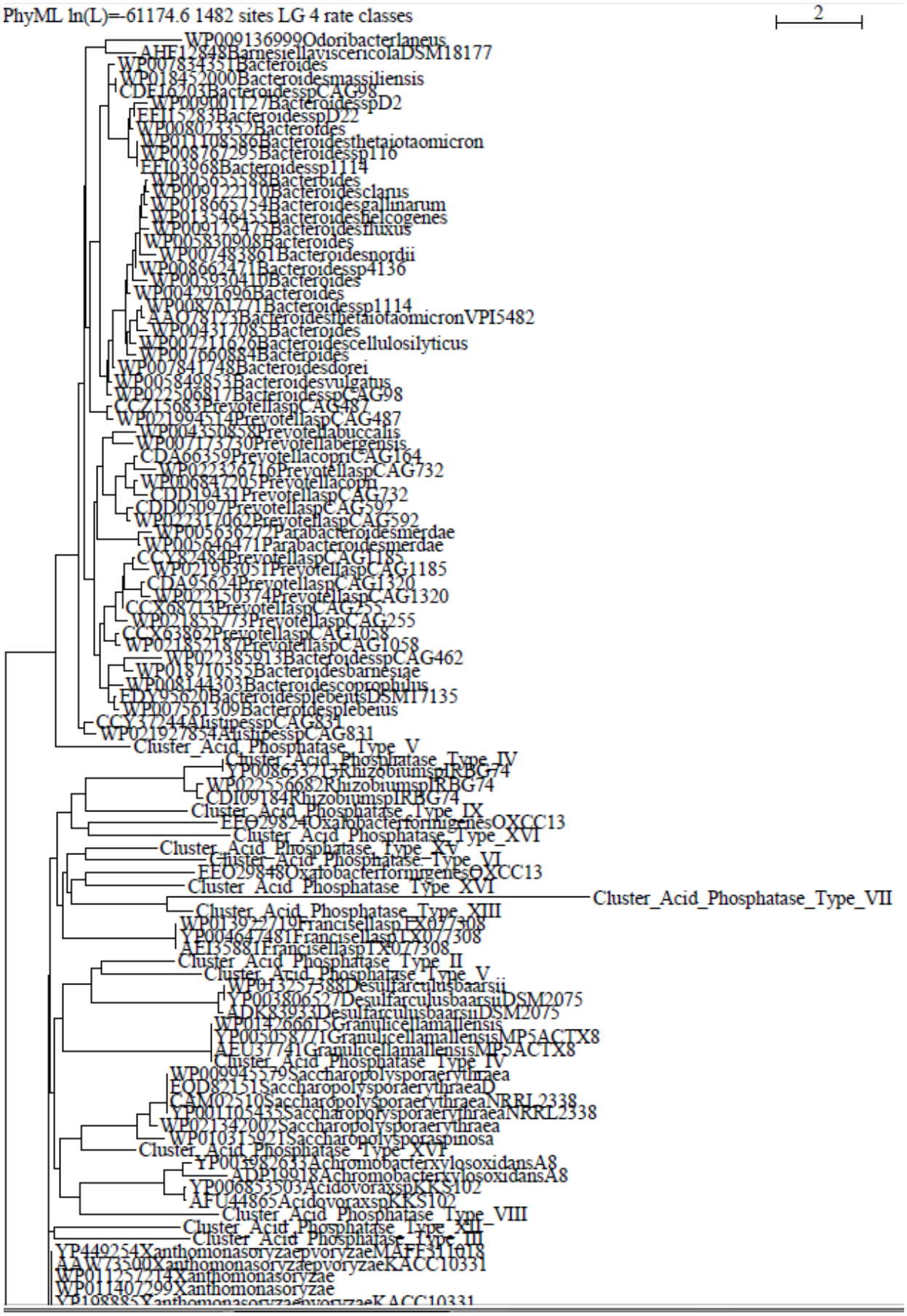

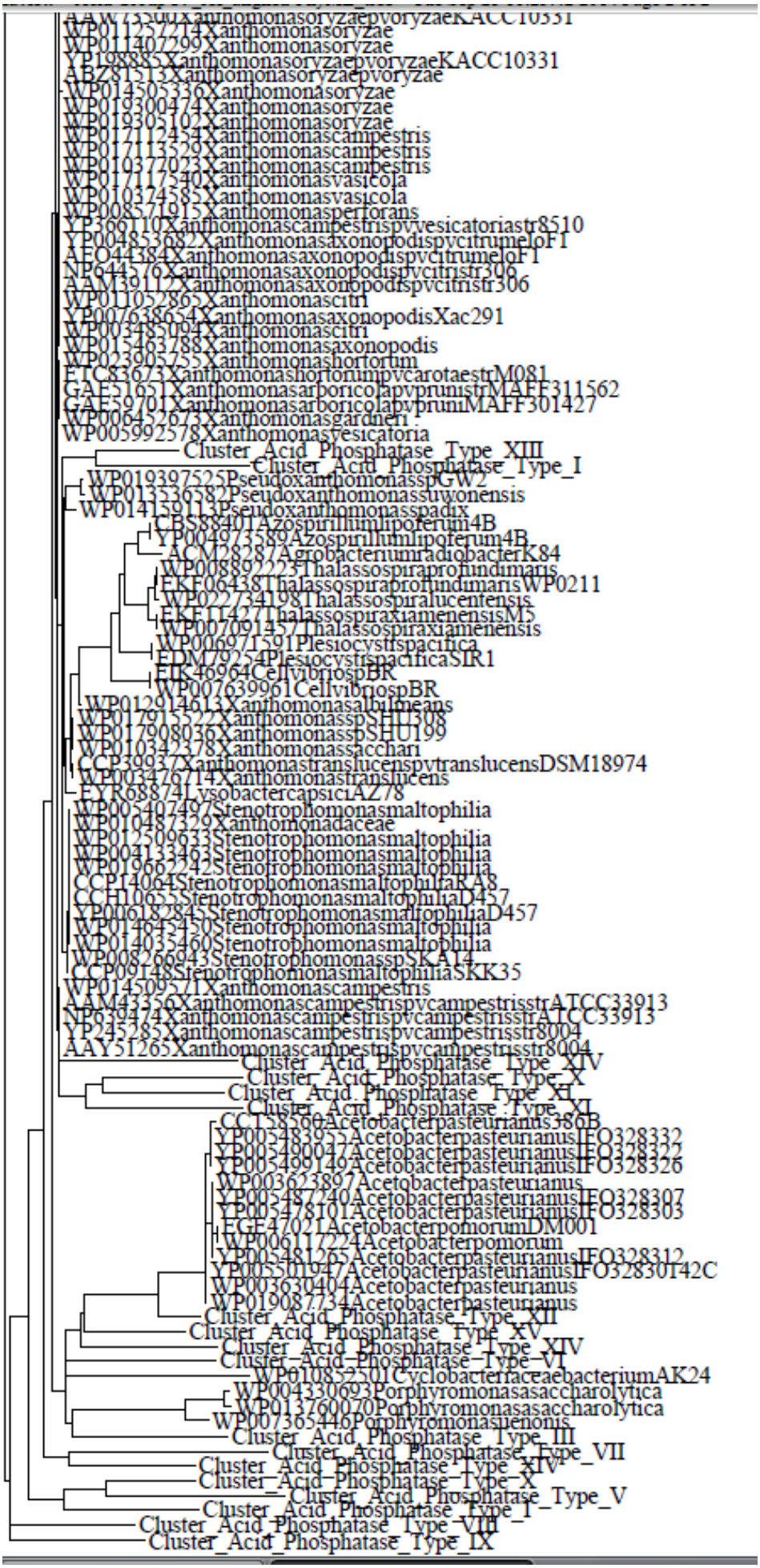
AAW73300XanthomonasoryzaepvoryzaeKACC10331
WP011257214Xanthomonasoryzae
WP011402299Xanthomonasoryzae
YP198885XanthomonasoryzaepvoryzaeKACC10331
ABZ81513Xanthomonasoryzaepvoryzae
WP014505336Xanthomonasoryzae
WP019300474Xanthomonasoryzae
WP019305102Xanthomonasoryzae
WP017112454Xanthomonascampestris
WP017113529Xanthomonascampestris
WP010377023Xanthomonascampestris
WP017117540Xanthomonasvasicola
WP010374585Xanthomonasvasicola
WP008577915Xanthomonasperforans
YP366110Xanthomonascampestrispvvesicatoriastr8510
YP004853682XanthomonasaxonopodispvcitrumeloF1
AEQ44384XanthomonasaxonopodispvcitrumeloF1
NP644576Xanthomonasaxonopodispvcitristr306
AAM39112Xanthomonasaxonopodispvcitristr306
WP011052865Xanthomonascitri
YP007638654XanthomonasaxonopodisXac291
WP003485094Xanthomonascitri
WP015463788Xanthomonasaxonopodis
WP023905755Xanthomonashortorum
ETC83673XanthomonashortorumpvcarotaestrM081
GAE51651XanthomonasarboricolapvprunistrMAFF311562
GAE59701XanthomonasarboricolapvpruniMAFF301427
WP006452673Xanthomonasgardneri
WP005992578Xanthomonasvesicatoria
Cluster_Acid_Phosphatase_Type_XIII
Cluster_Acid_Phosphatase_Type_I
WP019397525PseudoxanthomonasspGW2
WP013536582Pseudoxanthomonassuwonensis
WP014159113Pseudoxanthomonasspadix
CBS88401AzospirillumlipoferumA4B
YP004973589AzospirillumlipoferumA4B
ACM28287AgrobacteriumradiobacterK84
WP008892225ThalassospiraprofundimarisWP0211
EKF06438ThalassospiraprofundimarisWP0211
WP022734198Thalassospiralucentensis
EKF11427ThalassospiraxiamenensisM5
WP007091457Thalassospiraxiamenensis
WP006971591Plesiocystispacifica
EDM79254PlesiocystispacificaSIR1
EIK46964CellvibriosppBR
WP007639961CellvibriosppBR
WP012914613Xanthomonasalbilineans
WP017915522XanthomonasspSHU308
WP017908036XanthomonasspSHU199
WP010342378Xanthomonassacchari
CCP39937XanthomonastranslucenspvtranslucensDSM18974
WP003476714Xanthomonastranslucens
EYR68874LysobactercapsiciAZ78
WP005407497Stenotrophomonasmaltophilia
WP010487329Xanthomonadaceae
WP012509633Stenotrophomonasmaltophilia
WP004133463Stenotrophomonasmaltophilia
WP019662242Stenotrophomonasmaltophilia
CCP14064StenotrophomonasmaltophiliaK279a
CCH10655StenotrophomonasmaltophiliaD457
YP006182845StenotrophomonasmaltophiliaD457
WP014645450Stenotrophomonasmaltophilia
WP014035460Stenotrophomonasmaltophilia
WP008266943StenotrophomonasspSKA14
CCP09148StenotrophomonasmaltophiliaSKK35
WP014509521Xanthomonascampestris
AAM43356XanthomonascampestrispvcampestrisstrATCC33913
NP639474XanthomonascampestrispvcampestrisstrATCC33913
YP245285Xanthomonascampestrispvcampestrisstr8004
AAY51265Xanthomonascampestrispvcampestrisstr8004
Cluster_Acid_Phosphatase_Type_XIV
Cluster_Acid_Phosphatase_Type_X
Cluster_Acid_Phosphatase_Type_XI
Cluster_Acid_Phosphatase_Type_XI
CCG15856AcetobacterpasteurianusIFO3283B
YP005483955AcetobacterpasteurianusIFO3283B2
YP005480047AcetobacterpasteurianusIFO3283B2
YP005499149AcetobacterpasteurianusIFO3283B6
WP003623897Acetobacterpasteurianus
YP005487740AcetobacterpasteurianusIFO3283B7
YP005478101AcetobacterpasteurianusIFO3283B3
EGE47021AcetobacterpomorumDM001
WP006117224Acetobacterpomorum
YP005481265AcetobacterpasteurianusIFO3283B2
YP005501947AcetobacterpasteurianusIFO32830142C
WP003630404Acetobacterpasteurianus
WP019087734Acetobacterpasteurianus
Cluster_Acid_Phosphatase_Type_XII
Cluster_Acid_Phosphatase_Type_XV
Cluster_Acid_Phosphatase_Type_XIV
Cluster_Acid_Phosphatase_Type_VI
WP010852501CyclobacteriaceaebacteriumAK24
WP004330693Porphyromonasasaccharolytica
WP013760070Porphyromonasasaccharolytica
WP007365446Porphyromonasgingivalis
Cluster_Acid_Phosphatase_Type_III
Cluster_Acid_Phosphatase_Type_VII
Cluster_Acid_Phosphatase_Type_XIV
Cluster_Acid_Phosphatase_Type_X
Cluster_Acid_Phosphatase_Type_V
Cluster_Acid_Phosphatase_Type_I
Cluster_Acid_Phosphatase_Type_VIII
Cluster_Acid_Phosphatase_Type_IX

Figure S6. Phylogenetic tree of cluster V of the acid phosphatase sequences included in the database.

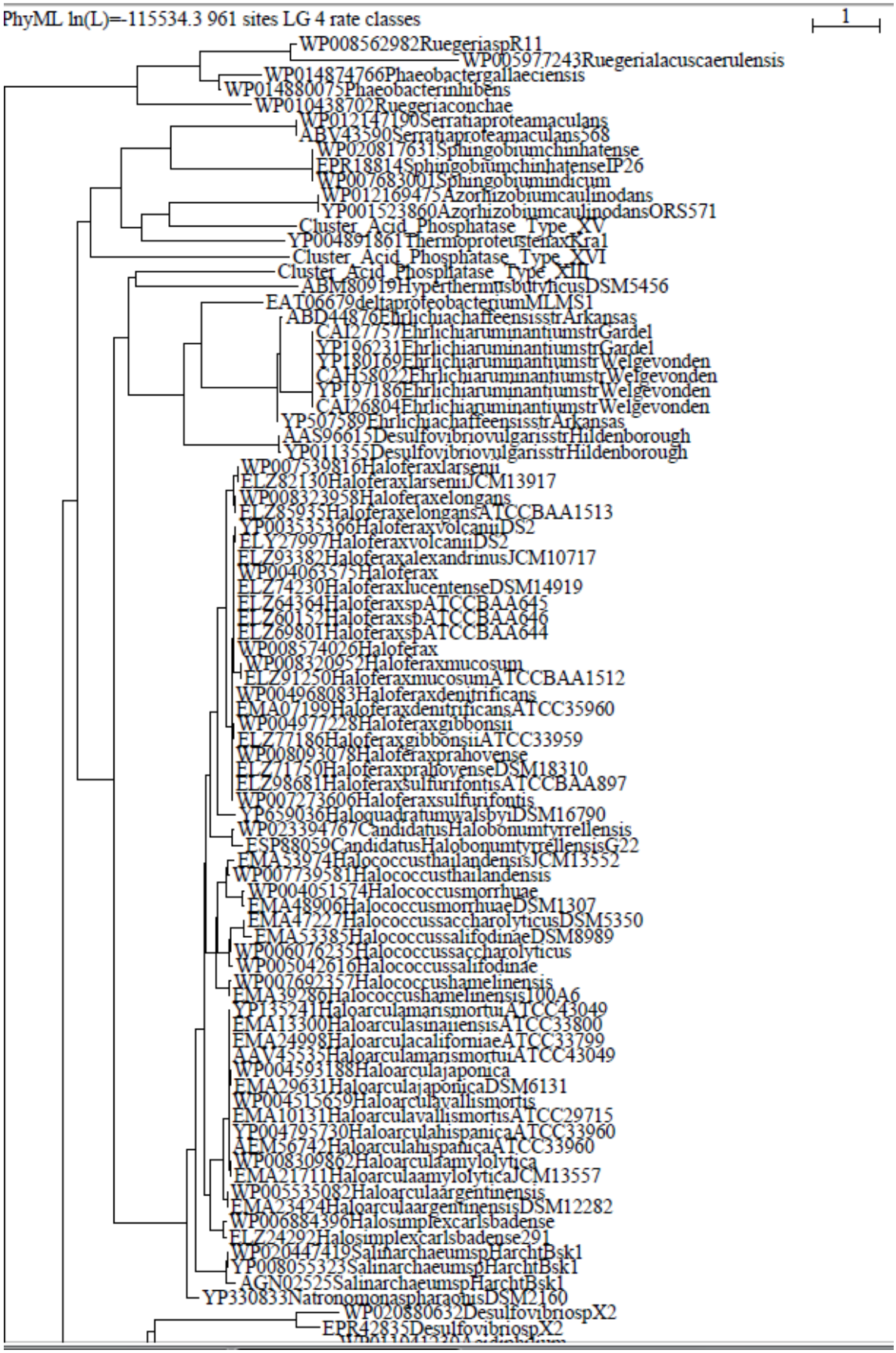

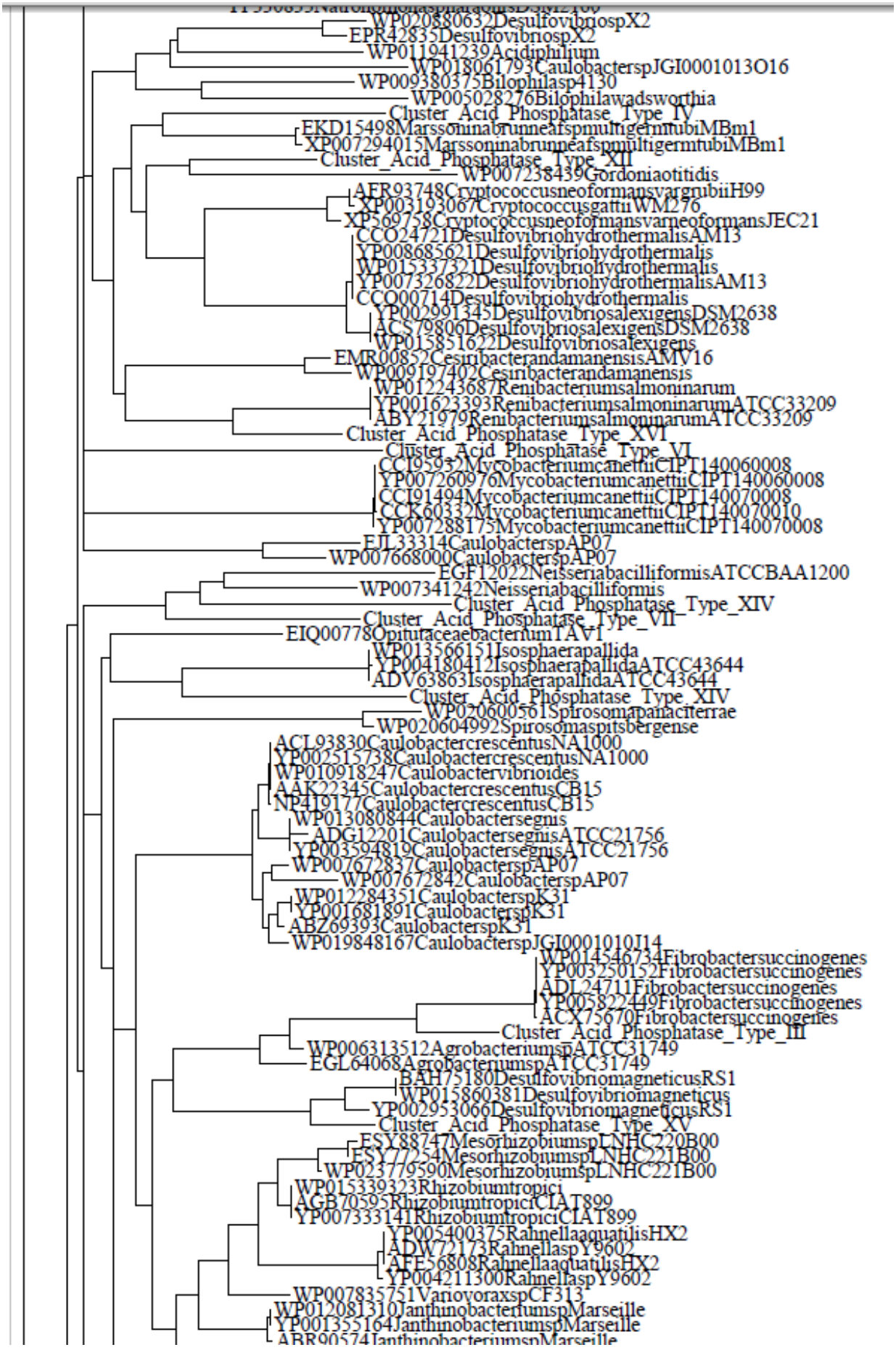
WP020880632DesulfovibriospX2
EPR42835DesulfovibriospX2
WP011941239Acidiphilium
WP018061793CaulobacterspJGI0001013O16
WP009380375Bilophilasp4130
WP005028276Bilophilawadsworthia
Cluster_Acid_Phosphatase_Type_IV
EKD15498MarssoninabrunneafspmultigermtubiMBm1
XP007294015MarssoninabrunneafspmultigermtubiMBm1
Cluster_Acid_Phosphatase_Type_XII
WP007238439Gordoniaotitidis
AFR93748CryptococcusneoformansvargrubiiH99
XP003193067CryptococcusgattiiWM276
XP569758CryptococcusneoformansvarneoformansJEC21
CCO24721DesulfovibriohydrothermalisAM13
YP008685621Desulfovibriohydrothermalis
WP015337321Desulfovibriohydrothermalis
YP007326822DesulfovibriohydrothermalisAM13
CCQ00714Desulfovibriohydrothermalis
YP002991345DesulfovibriosalexigensDSM2638
ACS79806DesulfovibriosalexigensDSM2638
WP015851622Desulfovibriosalexigens
EMR00852CesiribacterandamanensisAMV16
WP009197402Cesiribacterandamanensis
WP012243687Renibacteriumsalmoninarum
YP001623393RenibacteriumsalmoninarumATCC33209
ABY21979RenibacteriumsalmoninarumATCC33209
Cluster_Acid_Phosphatase_Type_XVI
Cluster_Acid_Phosphatase_Type_VI
CCI85932MycobacteriumcanettiiCIPT140060008
YP007260976MycobacteriumcanettiiCIPT140060008
CCI91494MycobacteriumcanettiiCIPT140070008
CCK60332MycobacteriumcanettiiCIPT140070010
YP007288175MycobacteriumcanettiiCIPT140070008
EJL33314CaulobacterspAP07
WP007668000CaulobacterspAP07
EGF12022NeisseriabacilliformisATCCBAA1200
WP007341242Neisseriabacilliformis
Cluster_Acid_Phosphatase_Type_XIV
Cluster_Acid_Phosphatase_Type_VII
EIQ00778OpituraceaebacteriumTAV1
WP013566151Isosphaerapallida
YP004180412IsosphaerapallidaATCC43644
ADV63863IsosphaerapallidaATCC43644
Cluster_Acid_Phosphatase_Type_XIV
WP020600561Spirosomapanaciterrae
WP020604992Spirosomaspitsbergense
ACL93830CaulobactercrescentusNA1000
YP002515738CaulobactercrescentusNA1000
WP010918247Caulobactervibrioides
AAK22345CaulobactercrescentusCB15
NP419177CaulobactercrescentusCB15
WP013080844Caulobactersegnis
ADG12201CaulobactersegnisATCC21756
YP003594819CaulobactersegnisATCC21756
WP007672837CaulobacterspAP07
WP007672842CaulobacterspAP07
WP012284351CaulobacterspK31
YP001681891CaulobacterspK31
ABZ69393CaulobacterspK31
WP019848167CaulobacterspJGI0001010J14
WP014546734Fibrobactersuccinogenes
YP003250152Fibrobactersuccinogenes
ADL24711Fibrobactersuccinogenes
YP005822449Fibrobactersuccinogenes
ACX75670Fibrobactersuccinogenes
Cluster_Acid_Phosphatase_Type_III
WP006313512AgrobacteriumspATCC31749
EGL64068AgrobacteriumspATCC31749
BAH75180DesulfovibriomagneticusRS1
WP015860381Desulfovibriomagneticus
YP002953066DesulfovibriomagneticusRS1
Cluster_Acid_Phosphatase_Type_XV
ESY88747MesorhizobiumspLNHC220B00
ESY77254MesorhizobiumspLNHC221B00
WP023779590MesorhizobiumspLNHC221B00
WP015339323Rhizobiumtropici
AGB70595RhizobiumtropiciCIAT899
YP007333141RhizobiumtropiciCIAT899
YP005400375RahnellaaquatilisHX2
ADW72173RahnellaspY9602
AFE56808RahnellaaquatilisHX2
YP004211300RahnellaspY9602
WP007835751VarioyoraxspCF313
WP012081310JanthinobacteriumspMarseille
YP001355164JanthinobacteriumspMarseille
ABR90574JanthinobacteriumspMarseille

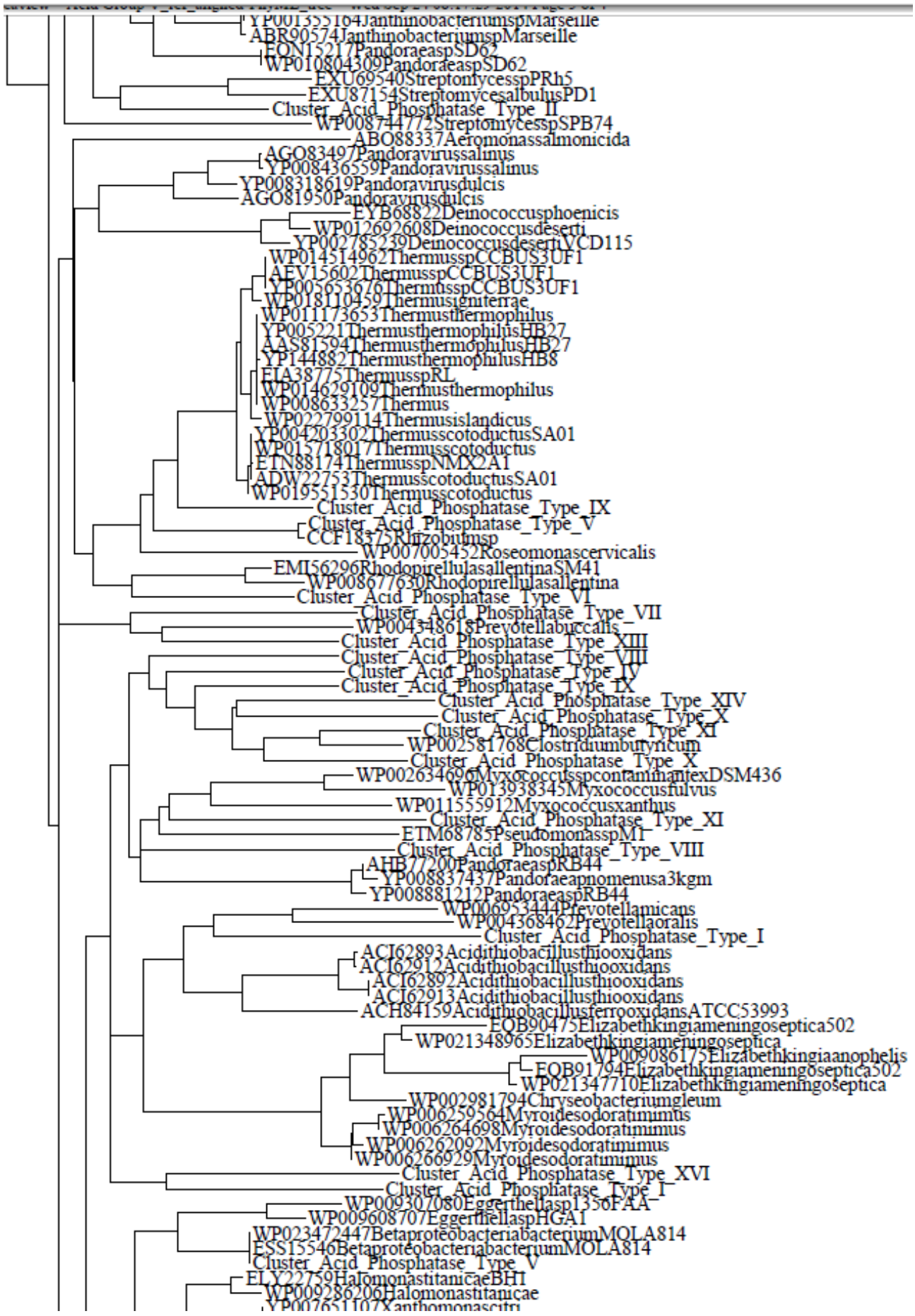
YP001355164JanthinobacteriumspMarseille
ABR90574JanthinobacteriumspMarseille
EQN15217PandoraeaspSD62
WP010804309PandoraeaspSD62
EXU69540StreptomycesspPRh5
EXU87154StreptomycesalbulusPD1
Cluster_Acid_Phosphatase_Type_II
WP008744772StreptomycesspSPB74
ABO88337Aeromonassalmonicida
AGO83497Pandoravirussalinus
YP008436559Pandoravirussalinus
YP008318619Pandoravirusdulcis
AGO81950Pandoravirusdulcis
EYB68822Deinococcusphoenicis
WP012692608Deinococcusdeserti
YP002785239DeinococcusdesertiVCD115
WP014514962ThermusspCCBUS3UF1
AEV15602ThermusspCCBUS3UF1
YP005653676ThermusspCCBUS3UF1
WP018110459Thermusigniterrae
WP011173653Thermusthermophilus
YP005221ThermusthermophilusHB27
AAS81594ThermusthermophilusHB27
YP1448821ThermusthermophilusHB8
EIA38775ThermusspRL
WP014629109Thermusthermophilus
WP008633257Thermus
WP022799114Thermusislandicus
YP004203302ThermusscotoductusSA01
WP015718017Thermusscotoductus
ETN88174ThermusspNMX2A1
ADW22753ThermusscotoductusSA01
WP019551530Thermusscotoductus
Cluster_Acid_Phosphatase_Type_IX
Cluster_Acid_Phosphatase_Type_V
CCF18375Rhizobiumsp
WP007005452Roseomonascervicalis
EMI56296RhodopirellulasallentinaSM41
WP008677630Rhodopirellulasallentina
Cluster_Acid_Phosphatase_Type_VI
Cluster_Acid_Phosphatase_Type_VII
WP004348618Prevotellabuccalis
Cluster_Acid_Phosphatase_Type_XIII
Cluster_Acid_Phosphatase_Type_VIII
Cluster_Acid_Phosphatase_Type_IV
Cluster_Acid_Phosphatase_Type_IX
Cluster_Acid_Phosphatase_Type_XIV
Cluster_Acid_Phosphatase_Type_X
Cluster_Acid_Phosphatase_Type_XI
WP002581768Clostridiumbutyricum
Cluster_Acid_Phosphatase_Type_X
WP002634696MyxococcusspcontaminantexDSM436
WP013938345Myxococcusfulvus
WP011555912Myxococcusxanthus
Cluster_Acid_Phosphatase_Type_XI
ETM68785PseudomonasspM1
Cluster_Acid_Phosphatase_Type_VIII
AHB77200PandoraeaspRB44
YP008837437Pandoraeapnomenusa3kgm
YP008881212PandoraeaspRB44
WP006953444Prevotellamicans
WP004368462Prevotellaoralis
Cluster_Acid_Phosphatase_Type_I
ACI62893Acidithiobacillusthiooxidans
ACI62912Acidithiobacillusthiooxidans
ACI62892Acidithiobacillusthiooxidans
ACI62913Acidithiobacillusthiooxidans
ACH84159AcidithiobacillusferrooxidansATCC53993
EQB90475Elizabethkingiameningoseptica502
WP021348965Elizabethkingiameningoseptica
WP009086175Elizabethkingiaanophelis
EQB91794Elizabethkingiameningoseptica502
WP021347710Elizabethkingiameningoseptica
WP002981794Chryseobacteriumgleum
WP006259564Myroidesodoratimimus
WP006264698Myroidesodoratimimus
WP006262092Myroidesodoratimimus
WP006266929Myroidesodoratimimus
Cluster_Acid_Phosphatase_Type_XVI
Cluster_Acid_Phosphatase_Type_I
WP009307080Eggerthellasp1356FAA
WP009608707EggerthellaspHGA1
WP023472447BetaproteobacteriabacteriumMOLA814
ESS15546BetaproteobacteriabacteriumMOLA814
Cluster_Acid_Phosphatase_Type_V
ELY22759HalomonastitanicaeBH1
WP009286206Halomonastitanicae

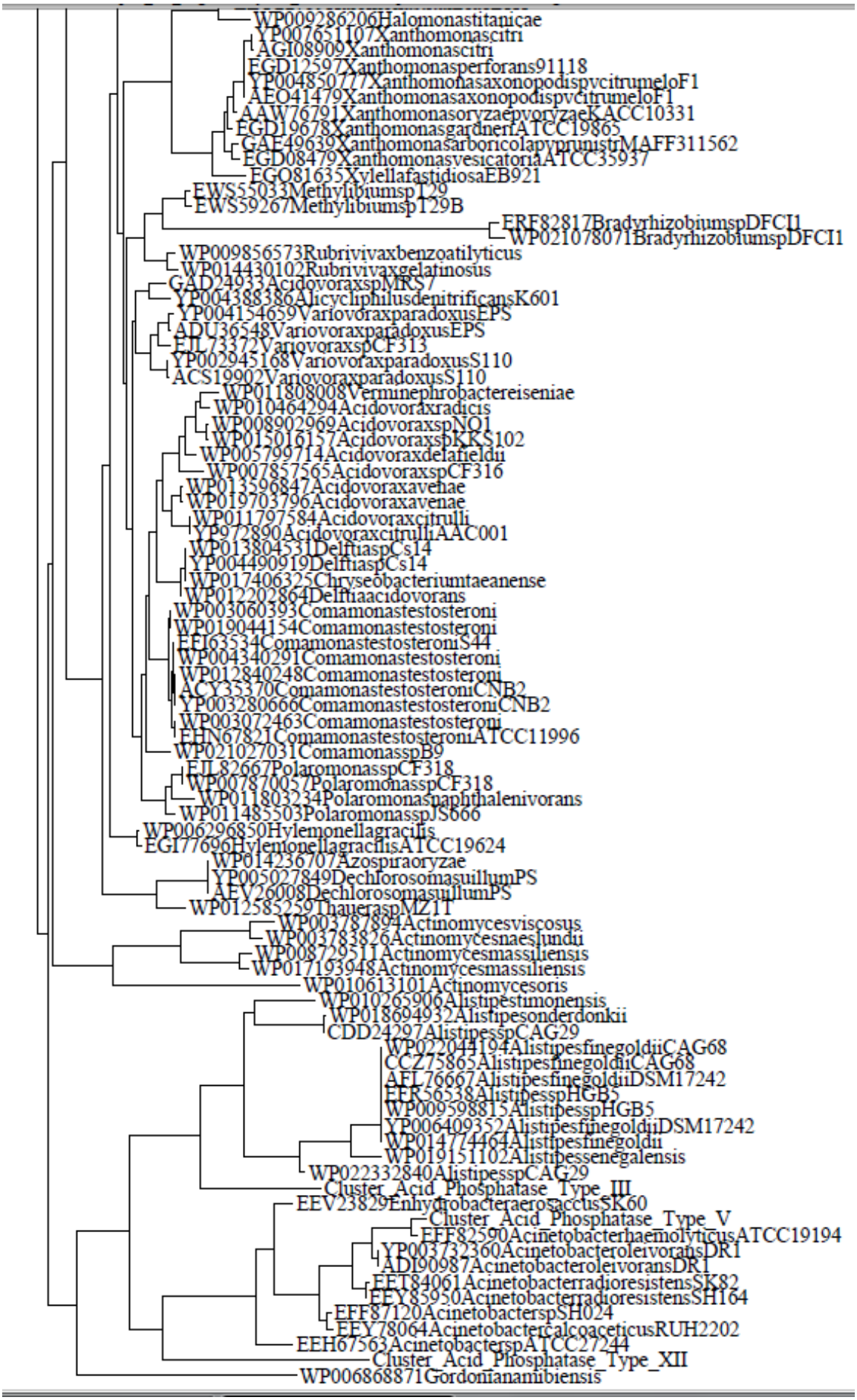
WP009286206Halomonastitanicae
YP007651107Xanthomonascitri
AGI08909Xanthomonascitri
EGD12597Xanthomonasperforans91118
YP004850777XanthomonasaxonopodispvcitrumeloF1
AEO41479XanthomonasaxonopodispvcitrumeloF1
AAW76791XanthomonasoryzaepvoryzaeKACC10331
EGD19678XanthomonasgardneriATCC19865
GAE49639XanthomonasarboricolapvprunistrMAFF311562
EGD08479XanthomonasvesicatoriaATCC35937
EGQ81635XylellafastidiosaEB921
EWS55033Methylibiumsp129
EWS59267Methylibiumsp129B
ERF82817BradyrhizobiumspDFCI1
WP021078071BradyrhizobiumspDFCI1
WP009856573Rubrivivaxbenzoatilyticus
WP014430102Rubrivivaxgelatinosus
GAD24933AcidovoraxspMRS7
YP004388386AlicycliphilusdenitrificansK601
YP004154659VariovoraxparadoxusEPS
ADU36548VariovoraxparadoxusEPS
EJL73372VariovoraxspCF313
YP002945168VariovoraxparadoxusS110
ACS19902VariovoraxparadoxusS110
WP011808008Verminephrobactereiseniae
WP010464294Acidovoraxradicis
WP008902969AcidovoraxspNO1
WP015016157AcidovoraxspKKS102
WP005799714Acidovoraxdelafieldii
WP007857565AcidovoraxspCF316
WP013596847Acidovoraxavenae
WP019703796Acidovoraxavenae
WP011797584Acidovoraxcitrulli
YP972890AcidovoraxcitrulliAAC001
WP013804531DelftiaspCs14
YP004490919DelftiaspCs14
WP017406325Chryseobacteriumtaeanense
WP012202864Delftiaacidovorans
WP003060393Comamonastestosteroni
WP019044154Comamonastestosteroni
EEI63534ComamonastestosteroniS44
WP004340291Comamonastestosteroni
WP012840248Comamonastestosteroni
ACY35370ComamonastestosteroniCNB2
YP003280666ComamonastestosteroniCNB2
WP003072463Comamonastestosteroni
EHN67821ComamonastestosteroniATCC11996
WP021027031ComamonasspB9
EJL82667PolaromonasspCF318
WP007870057PolaromonasspCF318
WP011803234Polaromonasnaphthalenivorans
WP011485503PolaromonasspJS666
WP006296850Hylemonellagracilis
EGI77696HylemonellagracilisATCC19624
WP014236707Azospiraoryzae
YP005027849DechlorosomasuillumPS
AEV26008DechlorosomasuillumPS
WP012585259ThaueraspMZ1T
WP003787894Actinomycesviscosus
WP003783826Actinomycesnaeslundii
WP008729511Actinomycesmassiliensis
WP017193948Actinomycesmassiliensis
WP010613101Actinomycesoris
WP010265906Alistipestimonensis
WP018694932Alistipesonderdonkii
CDD24297AlistipesspCAG29
WP022044194AlistipesfinegoldiiCAG68
CCZ75865AlistipesfinegoldiiCAG68
AFL76667AlistipesfinegoldiiDSM17242
EFR56538AlistipesspHGB5
WP009598815AlistipesspHGB5
YP006409352AlistipesfinegoldiiDSM17242
WP014774464Alistipesfinegoldii
WP019151102Alistipessenegalensis
WP022332840AlistipesspCAG29
Cluster_Acid_Phosphatase_Type_III
EEV23829EnhydrobacteraerosaccusSK60
Cluster_Acid_Phosphatase_Type_V
EFF82590AcinetobacterhaemolyticusATCC19194
YP003732360AcinetobacteroleivoransDR1
ADL90987AcinetobacteroleivoransDR1
EET84061AcinetobacterradioresistensSK82
EEY85950AcinetobacterradioresistensSH164
EFF87120AcinetobacterspSH024
EEY78064AcinetobactercalcoaceticusRUH2202
EEH67563AcinetobacterspATCC27244
Cluster_Acid_Phosphatase_Type_XII
WP006868871Gordoniananubiensis

Figure S7. Phylogenetic tree of cluster VI of the acid phosphatase sequences included in the database.

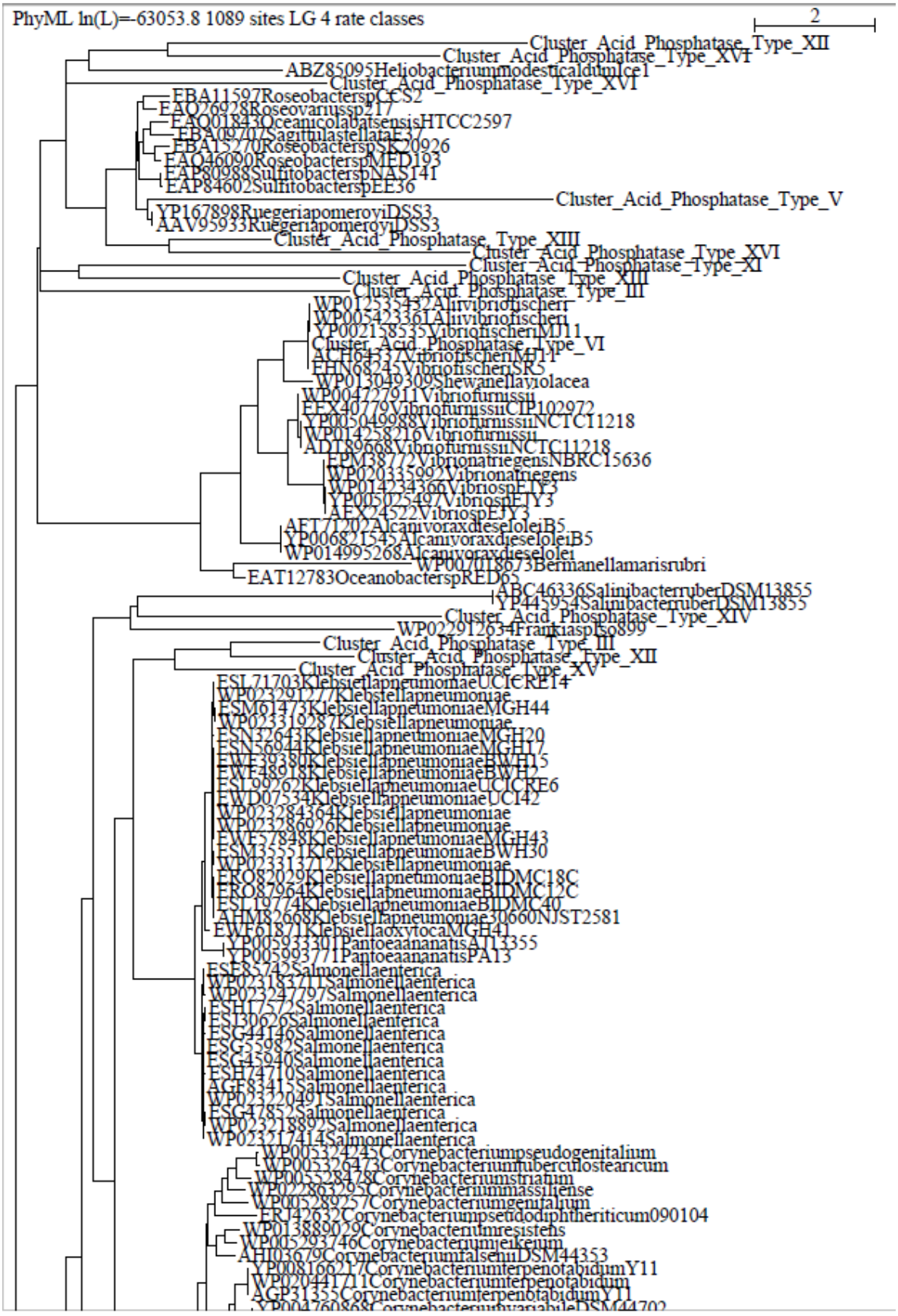

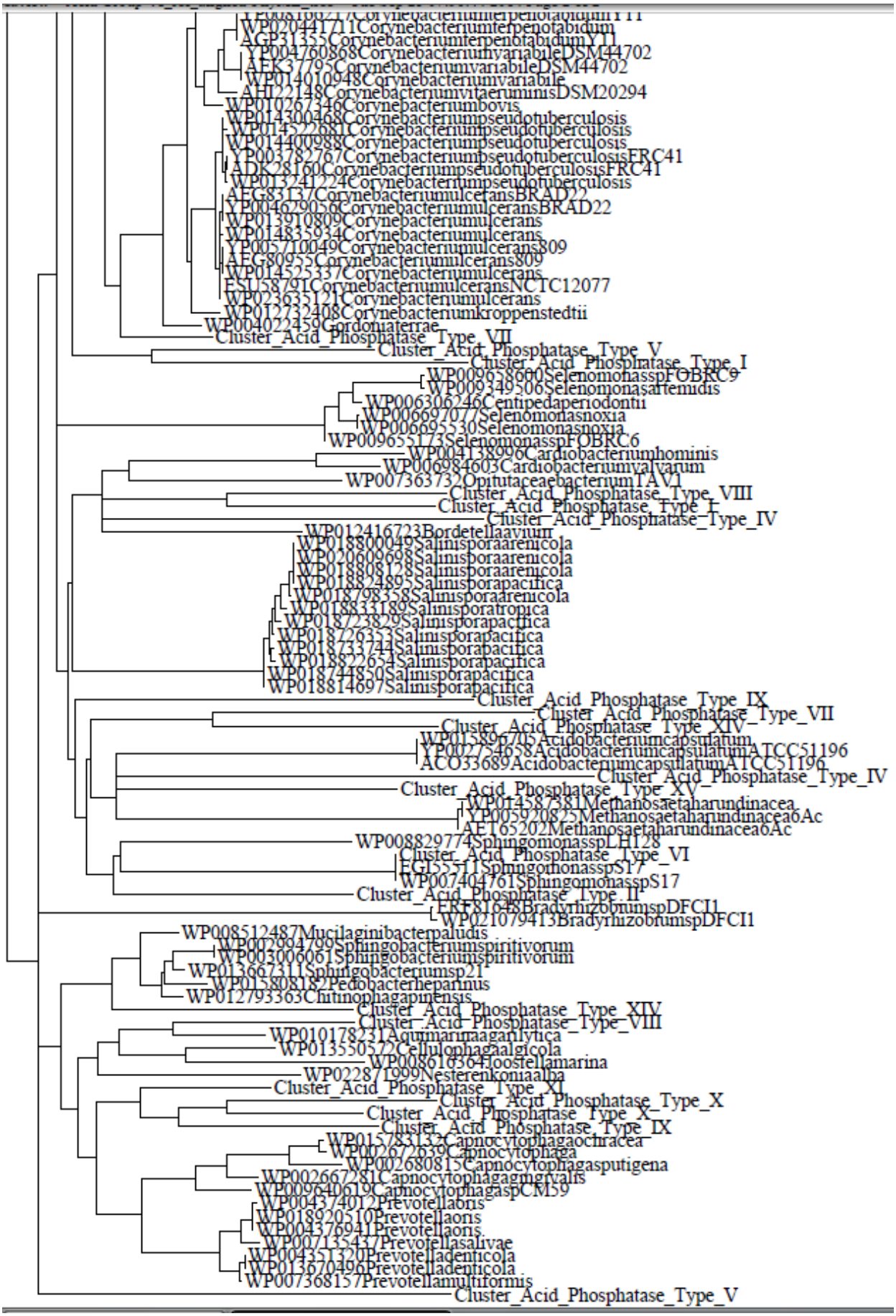
WP020441711Corynebacteriumterpenotabidum
AGP31335Corynebacteriumterpenotabidum
YP004760868Corynebacteriumvariabile
AEK37795Corynebacteriumvariabile
WP014010948Corynebacteriumvariabile
AHI22148Corynebacteriumvitaeruminis
WP010267346Corynebacteriumbovis
WP014300468Corynebacteriumpseudotuberculosis
WP014522681Corynebacteriumpseudotuberculosis
WP014400988Corynebacteriumpseudotuberculosis
YP003782767Corynebacteriumpseudotuberculosis
ADK28160Corynebacteriumpseudotuberculosis
WP013241224Corynebacteriumpseudotuberculosis
AEG83137Corynebacteriumulcerans
YP004629056Corynebacteriumulcerans
WP013910809Corynebacteriumulcerans
WP014835934Corynebacteriumulcerans
YP005710049Corynebacteriumulcerans
AEG80955Corynebacteriumulcerans
WP014525337Corynebacteriumulcerans
ESU58791Corynebacteriumulcerans
WP023635121Corynebacteriumulcerans
WP012732408Corynebacteriumkroppenstedtii
WP004022459Gordoniaterrae
Cluster_Acid_Phosphatase_Type_VII
Cluster_Acid_Phosphatase_Type_V
Cluster_Acid_Phosphatase_Type_I
WP009658600Selenomonassp
WP009349506Selenomonasartemidis
WP006306246Centipedaperiodontii
WP006697077Selenomonasnoxia
WP006695530Selenomonasnoxia
WP009655173Selenomonassp
WP004138996Cardiobacteriumhominis
WP006984603Cardiobacteriumvalvarum
WP007363732OpitutaceaebacteriumTAV1
Cluster_Acid_Phosphatase_Type_VIII
Cluster_Acid_Phosphatase_Type_I
Cluster_Acid_Phosphatase_Type_IV
WP012416723Bordetellaavium
WP018800049Salinisporaarenicola
WP020609698Salinisporaarenicola
WP018808128Salinisporaarenicola
WP018824893Salinisporapacifica
WP018798358Salinisporaarenicola
WP018833189Salinisporatropica
WP018723829Salinisporapacifica
WP018726353Salinisporapacifica
WP018733744Salinisporapacifica
WP018822654Salinisporapacifica
WP018744830Salinisporapacifica
WP018814697Salinisporapacifica
Cluster_Acid_Phosphatase_Type_IX
Cluster_Acid_Phosphatase_Type_VII
Cluster_Acid_Phosphatase_Type_XIV
WP015896705Acidobacteriumcapsulatum
YP002754658Acidobacteriumcapsulatum
ACO33689AcidobacteriumcapsulatumATCC51196
Cluster_Acid_Phosphatase_Type_IV
Cluster_Acid_Phosphatase_Type_XV
WP014587381Methanosaetaharundinacea
YP005920825Methanosaetaharundinacea6Ac
AET65202Methanosaetaharundinacea6Ac
WP008829774SphingomonassplH128
Cluster_Acid_Phosphatase_Type_VI
EGI55511SphingomonasspS17
WP007404761SphingomonasspS17
Cluster_Acid_Phosphatase_Type_II
ERF81648BradyrhizobiumspDFCI1
WP021079413BradyrhizobiumspDFCI1
WP008512487Mucilaginibacterpaludis
WP002994799Sphingobacteriumspiritivorum
WP003006061Sphingobacteriumspiritivorum
WP013667311Sphingobacteriumsp21
WP015808182Pedobacterheparinus
WP012793363Chitinophagapinensis
Cluster_Acid_Phosphatase_Type_XIV
Cluster_Acid_Phosphatase_Type_VIII
WP010178231Aquimarinaagariphytica
WP013550572Cellulophagaalgicola
WP008616364Hoosteilamarina
WP022871999Nesterenkoniaalba
Cluster_Acid_Phosphatase_Type_XI
Cluster_Acid_Phosphatase_Type_X
Cluster_Acid_Phosphatase_Type_X
Cluster_Acid_Phosphatase_Type_IX
WP015783132Capnocytophagaochracea
WP002672639Capnocytophaga
WP002680815Capnocytophagasputigena
WP002667281Capnocytophagagingivalis
WP009640619CapnocytophagaspCM59
WP004374012Prevotellaoris
WP018920510Prevotellaoris
WP004376941Prevotellaoris
WP007135437Prevotellasalivae
WP004351320Prevotelladenticola
WP013670496Prevotelladenticola
WP007368157Prevotellamultiformis
Cluster_Acid_Phosphatase_Type_V

Figure S8a. Phylogenetic tree of cluster VIIa of the acid phosphatase sequences included in the database.

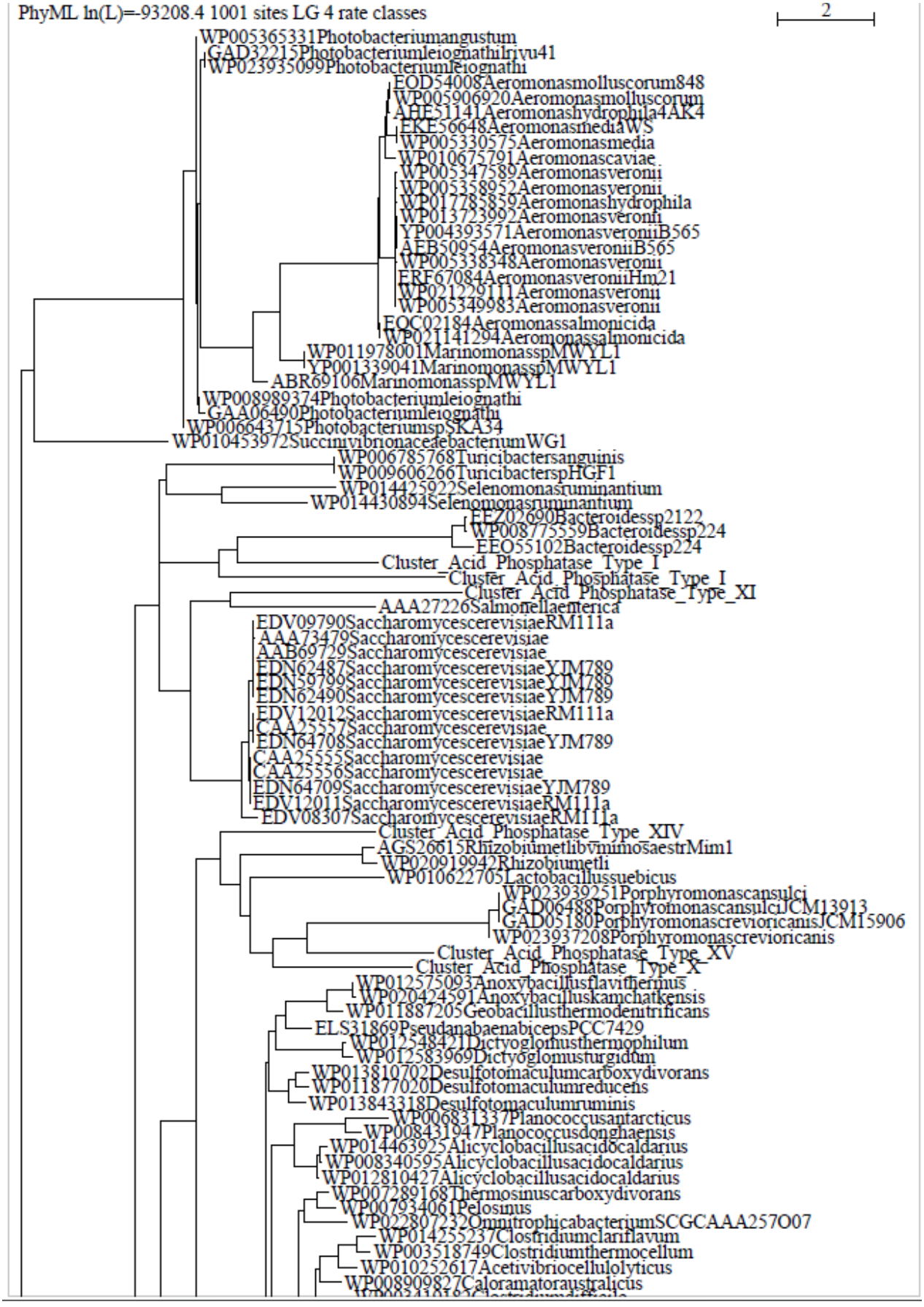

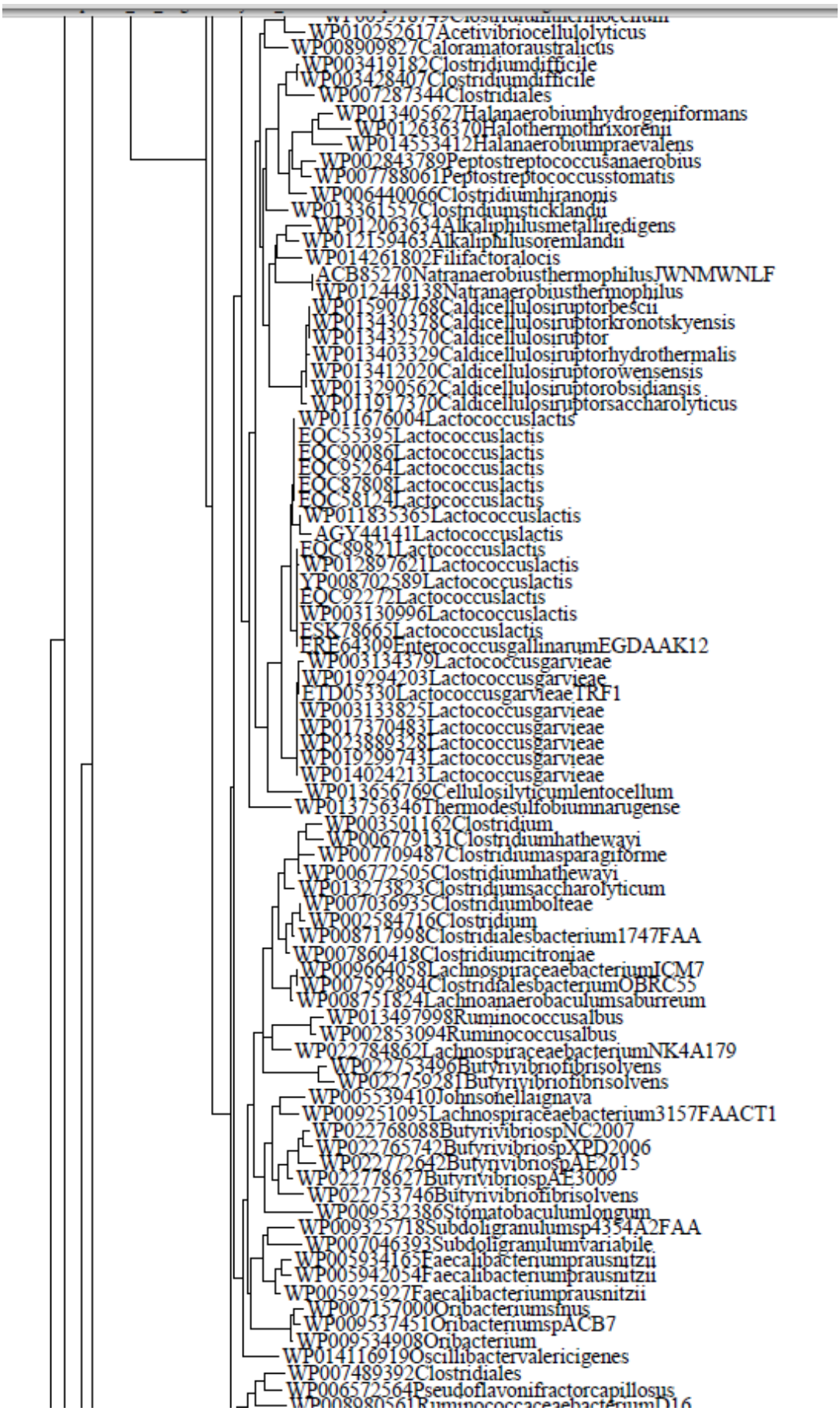
WP010252617Acetivibriocellulolyticus
WP008909827Caloramatoraustralictus
WP003419182Clostridiumdifficile
WP003428407Clostridiumdifficile
WP007287344Clostridiales
WP013405627Halanaerobiumhydrogeniformans
WP012636370Halothermothrixorenii
WP014553412Halanaerobiumpraevalens
WP002843789Peptostreptococcusanaerobius
WP007788061Peptostreptococcusstomatis
WP006440066Clostridiumhiranonis
WP013361557Clostridiumsticklandii
WP012063634Alkaliphilusmetalliredigens
WP012159463Alkaliphilusoremlandii
WP014261802Filifactoralocis
ACB85270NatranaerobiusthermophilusJWNMWNLF
WP012448138Natranaerobiusthermophilus
WP015907768Caldicellulosiruptorbescii
WP013430378Caldicellulosiruptorkronotskyensis
WP013432570Caldicellulosiruptor
WP013403329Caldicellulosiruptorhydrothermalis
WP013412020Caldicellulosiruptorowensensis
WP013290562Caldicellulosiruptorobsidiansis
WP011917370Caldicellulosiruptorsaccharolyticus
WP011676004Lactococcuslactis
EQC55395Lactococcuslactis
EQC90086Lactococcuslactis
EQC95264Lactococcuslactis
EQC87808Lactococcuslactis
EQC58124Lactococcuslactis
WP011835365Lactococcuslactis
AGY44141Lactococcuslactis
EQC89821Lactococcuslactis
WP012897621Lactococcuslactis
YP008702589Lactococcuslactis
EQC92272Lactococcuslactis
WP003130996Lactococcuslactis
ESK78665Lactococcuslactis
ERE64309EnterococcusgallinarumEGDAAK12
WP003134379Lactococcusgarvieae
WP019294203Lactococcusgarvieae
ETD05330LactococcusgarvieaeTRF1
WP003133825Lactococcusgarvieae
WP017370483Lactococcusgarvieae
WP023889328Lactococcusgarvieae
WP019299743Lactococcusgarvieae
WP014024213Lactococcusgarvieae
WP013656769Cellulosilyticumlentocellum
WP013756346Thermodesulfobiumnarugense
WP003501162Clostridium
WP006779131Clostridiumhathewayi
WP007709487Clostridiumasparagiforme
WP006772505Clostridiumhathewayi
WP013273823Clostridiumsaccharolyticum
WP007036935Clostridiumbolteae
WP002584716Clostridium
WP008717998Clostridialesbacterium1747FAA
WP007860418Clostridiumcitroniae
WP009664058LachnospiraceaebacteriumICM7
WP007592894ClostridialesbacteriumOBRC55
WP008751824Lachnoanaerobaculumsaburreum
WP013497998Ruminococcusalbus
WP002853094Ruminococcusalbus
WP022784862LachnospiraceaebacteriumNK4A179
WP022753496Butyrivibriofibrisolvens
WP022759281Butyrivibriofibrisolvens
WP005539410Johnsonellaignava
WP009251095Lachnospiraceaebacterium3157FAACT1
WP022768088ButyrivibriospNC2007
WP022765742ButyrivibriospXPD2006
WP022772642ButyrivibriospAE2015
WP022778627ButyrivibriospAE3009
WP022753746Butyrivibriofibrisolvens
WP009532386Stomatobaculumlongum
WP009325718Subdoligranulumsp4354A2FAA
WP007046393Subdoligranulumvariabile
WP005934165Faecalibacteriumprausnitzii
WP005942054Faecalibacteriumprausnitzii
WP005925927Faecalibacteriumprausnitzii
WP007157000Oribacteriumsinus
WP009537451OribacteriumspACB7
WP009534908Oribacterium
WP014116919Oscillibactervalericigenes
WP007489392Clostridiales
WP006572564Pseudoflavonifractorcapillosus

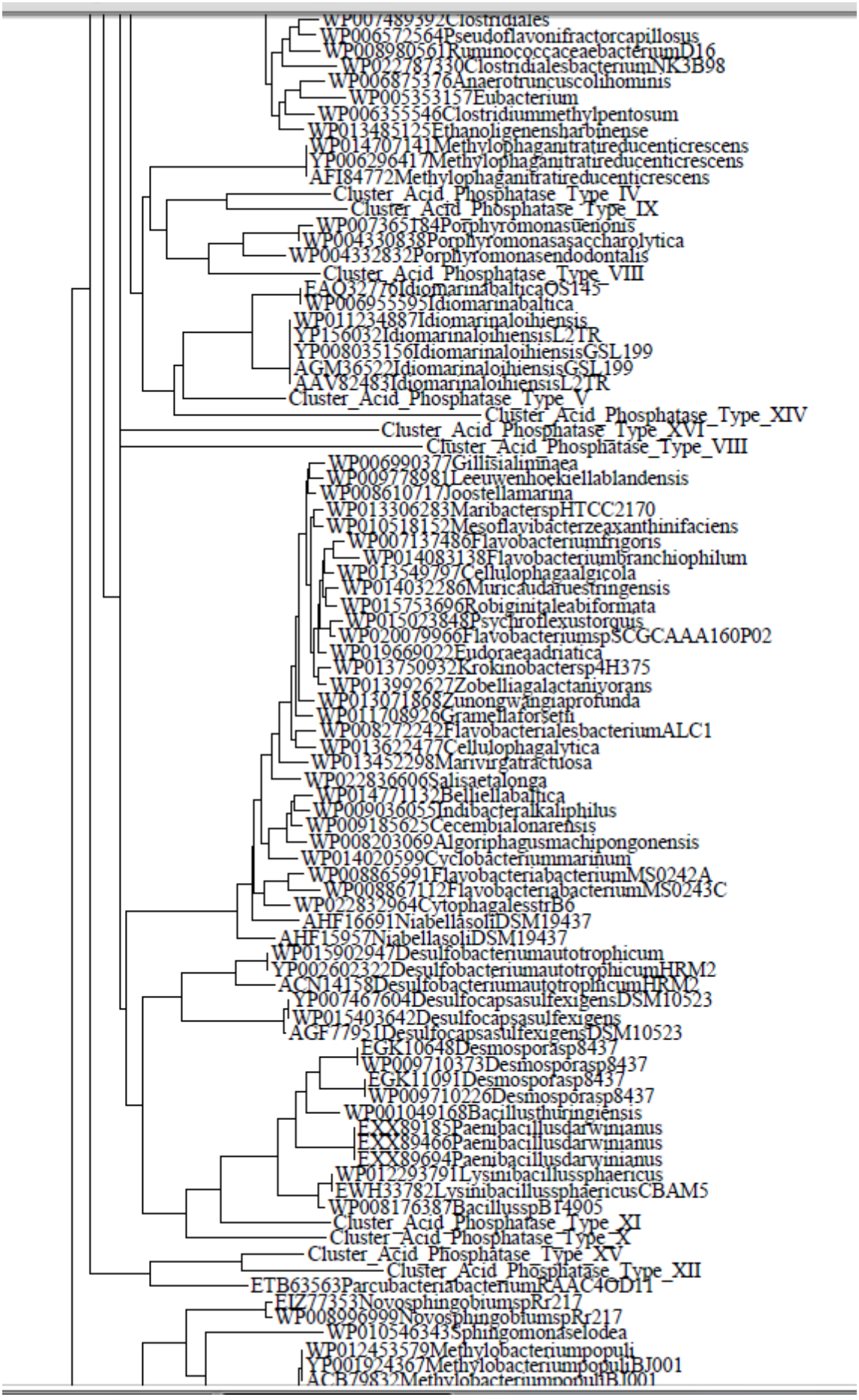
WP007489392Clostridiales
WP006572564Pseudoflavonifractorcapillosus
WP008980561RuminococcaceaebacteriumD16
WP022787330ClostridialesbacteriumNK3B98
WP006875376Anaerotruncuscolihominis
WP005353157Eubacterium
WP006355546Clostridiummethylpentosum
WP013485125Ethanoligenensharbinense
WP014707141Methylophaganatratireducenticrescens
YP006296417Methylophaganatratireducenticrescens
AFI84772Methylophaganatratireducenticrescens
Cluster_Acid_Phosphatase_Type_IV
Cluster_Acid_Phosphatase_Type_IX
WP007365184Porphyromonasuenionis
WP004330838Porphyromonasasaccharolytica
WP004332832Porphyromonasendodontalis
Cluster_Acid_Phosphatase_Type_VIII
EAQ32776IdiomarinabalticaOS145
WP006955595Idiomarinabaltica
WP011234887Idiomarinaloihiensis
YP156032IdiomarinaloihiensisL2TR
YP008035156IdiomarinaloihiensisGSL199
AGM36522IdiomarinaloihiensisGSL199
AAV82483IdiomarinaloihiensisL2TR
Cluster_Acid_Phosphatase_Type_V
Cluster_Acid_Phosphatase_Type_XIV
Cluster_Acid_Phosphatase_Type_XVI
Cluster_Acid_Phosphatase_Type_VIII
WP006990377Gillisialimnaea
WP009778981Leeuwenhoekiellablandensis
WP008610717Joostellamarina
WP013306283MaribacterspHTCC2170
WP010518152Mesoflavibacterzeaxanthinifaciens
WP007137486Flavobacteriumfrigoris
WP014083138Flavobacteriumbranchiophilum
WP013549797Cellulophagaalgicola
WP014032286Muricauda ruestringensis
WP015753696Robiginitaleabiformata
WP015023848Psychroflexustorquis
WP020079966FlavobacteriumspSCGCAAA160P02
WP019669022Eudoraeaadriatica
WP013750932Krokinobactersp4H375
WP013992627Zobelliagalactanivorans
WP013071868Zunongwangiaprofunda
WP011708926Gramellaforsetii
WP008272242FlavobacterialesbacteriumALC1
WP013622477Cellulophagalytica
WP013452298Marivirgatractuosa
WP022836606Salisaetalonga
WP014771132Belliellabalfica
WP009036055Indibacteralkaliphilus
WP009185625Cecembialonarensis
WP008203069Algoriphagusmachipongonensis
WP014020599Cyclobacteriummarinum
WP008865991FlavobacteriabacteriumMS0242A
WP008867112FlavobacteriabacteriumMS0243C
WP022832964CytophagalesstrB6
AHF16691NiabellasoliDSM19437
AHF15957NiabellasoliDSM19437
WP015902947Desulfobacteriumautotrophicum
YP002602322DesulfobacteriumautotrophicumHRM2
ACN14158DesulfobacteriumautotrophicumHRM2
YP007467604DesulfocapsasulfexigensDSM10523
WP015403642Desulfocapsasulfexigens
AGF77951DesulfocapsasulfexigensDSM10523
EGK10648Desmosporasp8437
WP009710373Desmosporasp8437
EGK11091Desmosporasp8437
WP009710226Desmosporasp8437
WP001049168Bacillusthuringiensis
EXX89185Paenibacillusdarwinianus
EXX89466Paenibacillusdarwinianus
EXX89694Paenibacillusdarwinianus
WP012293791Lysinibacillussphaericus
EWH33782LysinibacillussphaericusCBAM5
WP008176387BacillusspB14905
Cluster_Acid_Phosphatase_Type_XI
Cluster_Acid_Phosphatase_Type_X
Cluster_Acid_Phosphatase_Type_XV
Cluster_Acid_Phosphatase_Type_XII
ETB63563ParcubacteriabacteriumRAAC4OD11
EIZ77353NovosphingobiumspRr217
WP008996999NovosphingobiumspRr217
WP010546343Sphingomonaselodea
WP012453579Methylobacteriumpopuli
YP001924367MethylobacteriumpopuliBJ001
ACB79832MethylobacteriumpopuliBJ001

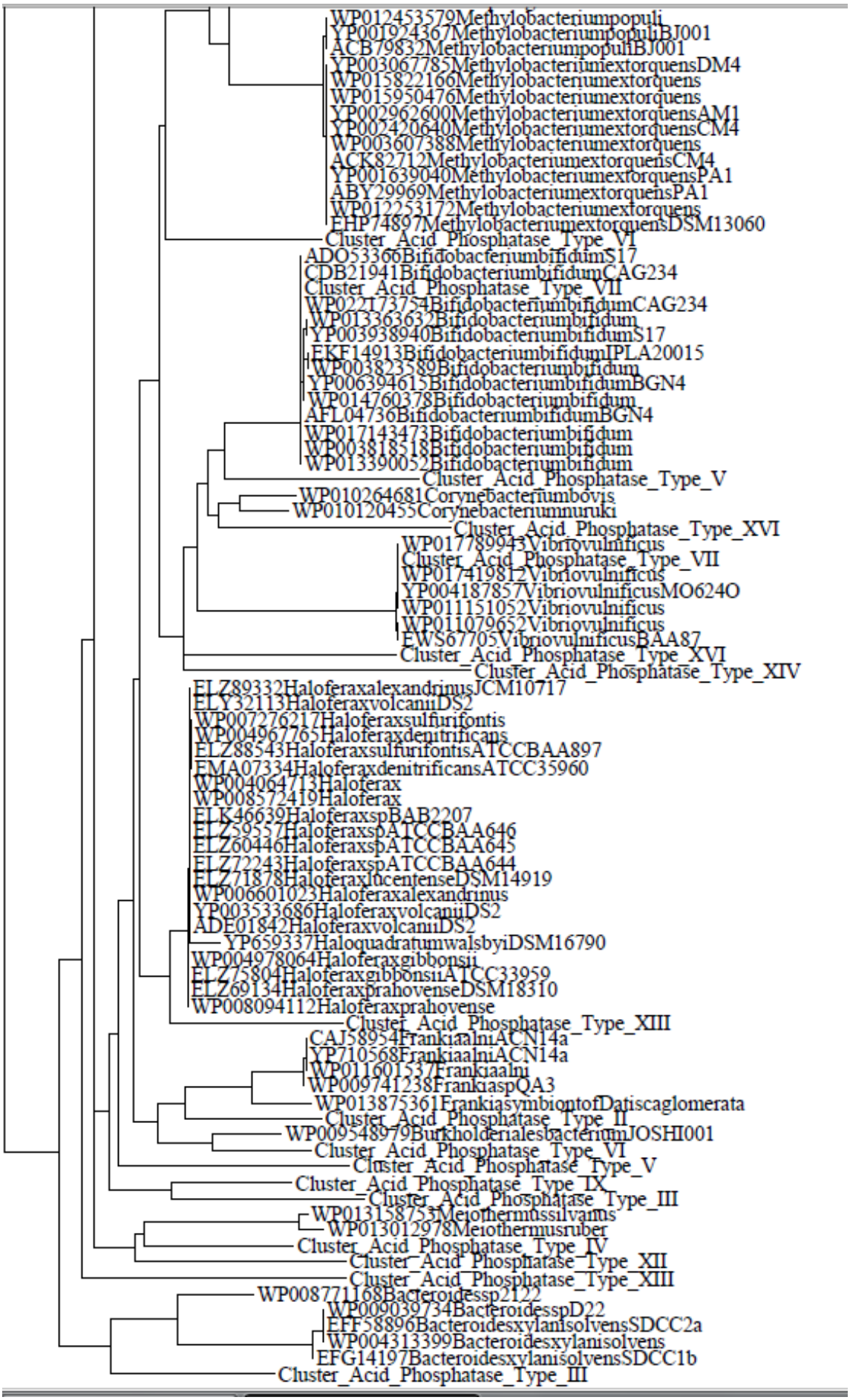
WP012453579Methylobacteriumpopuli
YP001924367MethylobacteriumpopuliBJ001
ACB79832MethylobacteriumpopuliBJ001
YP003067785MethylobacteriumextorquensDM4
WP015822166Methylobacteriumextorquens
WP015950476Methylobacteriumextorquens
YP002962600MethylobacteriumextorquensAM1
YP002420640MethylobacteriumextorquensCM4
WP003607388Methylobacteriumextorquens
ACK82712MethylobacteriumextorquensCM4
YP001639040MethylobacteriumextorquensPA1
ABY29969MethylobacteriumextorquensPA1
WP012253172Methylobacteriumextorquens
EHP74897MethylobacteriumextorquensDSM13060
Cluster_Acid_Phosphatase_Type_VI
ADO53366BifidobacteriumbifidumS17
CDB21941BifidobacteriumbifidumCAG234
Cluster_Acid_Phosphatase_Type_VII
WP022173754BifidobacteriumbifidumCAG234
WP013363632Bifidobacteriumbifidum
YP003938940BifidobacteriumbifidumS17
EKF14913BifidobacteriumbifidumIPLA20015
WP003823589Bifidobacteriumbifidum
YP006394615BifidobacteriumbifidumBGN4
WP014760378Bifidobacteriumbifidum
AFL04736BifidobacteriumbifidumBGN4
WP017143473Bifidobacteriumbifidum
WP003818518Bifidobacteriumbifidum
WP013390052Bifidobacteriumbifidum
Cluster_Acid_Phosphatase_Type_V
WP010264681Corynebacteriumbovis
WP010120455Corynebacteriumnuruki
Cluster_Acid_Phosphatase_Type_XVI
WP017789943Vibriovulnificus
Cluster_Acid_Phosphatase_Type_VII
WP017419812Vibriovulnificus
YP004187857VibriovulnificusMO624O
WP011151052Vibriovulnificus
WP011079652Vibriovulnificus
EWS67705VibriovulnificusBAA87
Cluster_Acid_Phosphatase_Type_XVI
Cluster_Acid_Phosphatase_Type_XIV
ELZ89332HaloferaxalexandrinusJCM10717
ELY32113HaloferaxvolcaniiDS2
WP007276217Haloferaxsulfurifontis
WP004967765Haloferaxdenitrificans
ELZ88543HaloferaxsulfurifontisATCCBAA897
EMA07334HaloferaxdenitrificansATCC35960
WP004064713Haloferax
WP008572419Haloferax
ELK46639HaloferaxspBAB2207
ELZ59557HaloferaxspATCCBAA646
ELZ60446HaloferaxspATCCBAA645
ELZ72243HaloferaxspATCCBAA644
ELZ71878HaloferaxlucentenseDSM14919
WP006601023Haloferaxalexandrinus
YP003533686HaloferaxvolcaniiDS2
ADE01842HaloferaxvolcaniiDS2
YP659337Haloquadratumwalsbyi DSM16790
WP004978064HaloferaxgibbonsiiATCC33959
ELZ75804HaloferaxgibbonsiiATCC33959
ELZ69134HaloferaxprahovenseDSM18310
WP008094112Haloferaxprahovense
Cluster_Acid_Phosphatase_Type_XIII
CAJ58954FrankiaalniiACN14a
YP710568FrankiaalniiACN14a
WP011601537Frankiaalni
WP009741238FrankiaspQA3
WP013875361FrankiasymbiontofDatiscaglomerata
Cluster_Acid_Phosphatase_Type_II
WP009548979BurkholderialesbacteriumJOSHI001
Cluster_Acid_Phosphatase_Type_VI
Cluster_Acid_Phosphatase_Type_V
Cluster_Acid_Phosphatase_Type_IX
Cluster_Acid_Phosphatase_Type_III
WP013158753Meiothermussilvanus
WP013012978Meiothermusruber
Cluster_Acid_Phosphatase_Type_IV
Cluster_Acid_Phosphatase_Type_XII
Cluster_Acid_Phosphatase_Type_XIII
WP008771168Bacteroidessp2122
WP009039734BacteroidesspD22
EFF58896BacteroidesxylanisolvensSDCC2a
WP004313399Bacteroidesxylanisolvens
EFG14197BacteroidesxylanisolvensSDCC1b
Cluster_Acid_Phosphatase_Type_III

Figure S8b. Phylogenetic tree of cluster VIIb of the acid phosphatase sequences included in the database.

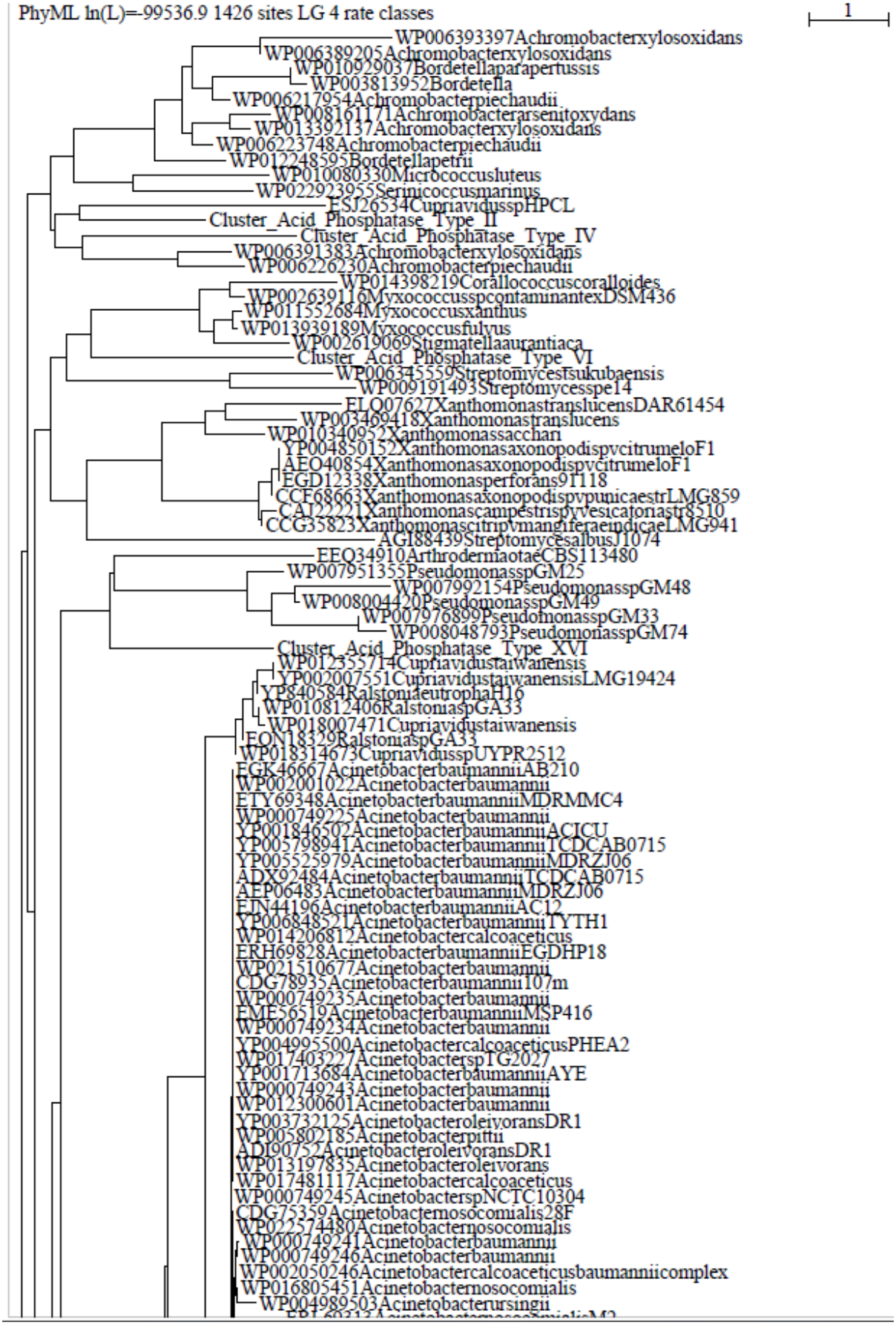

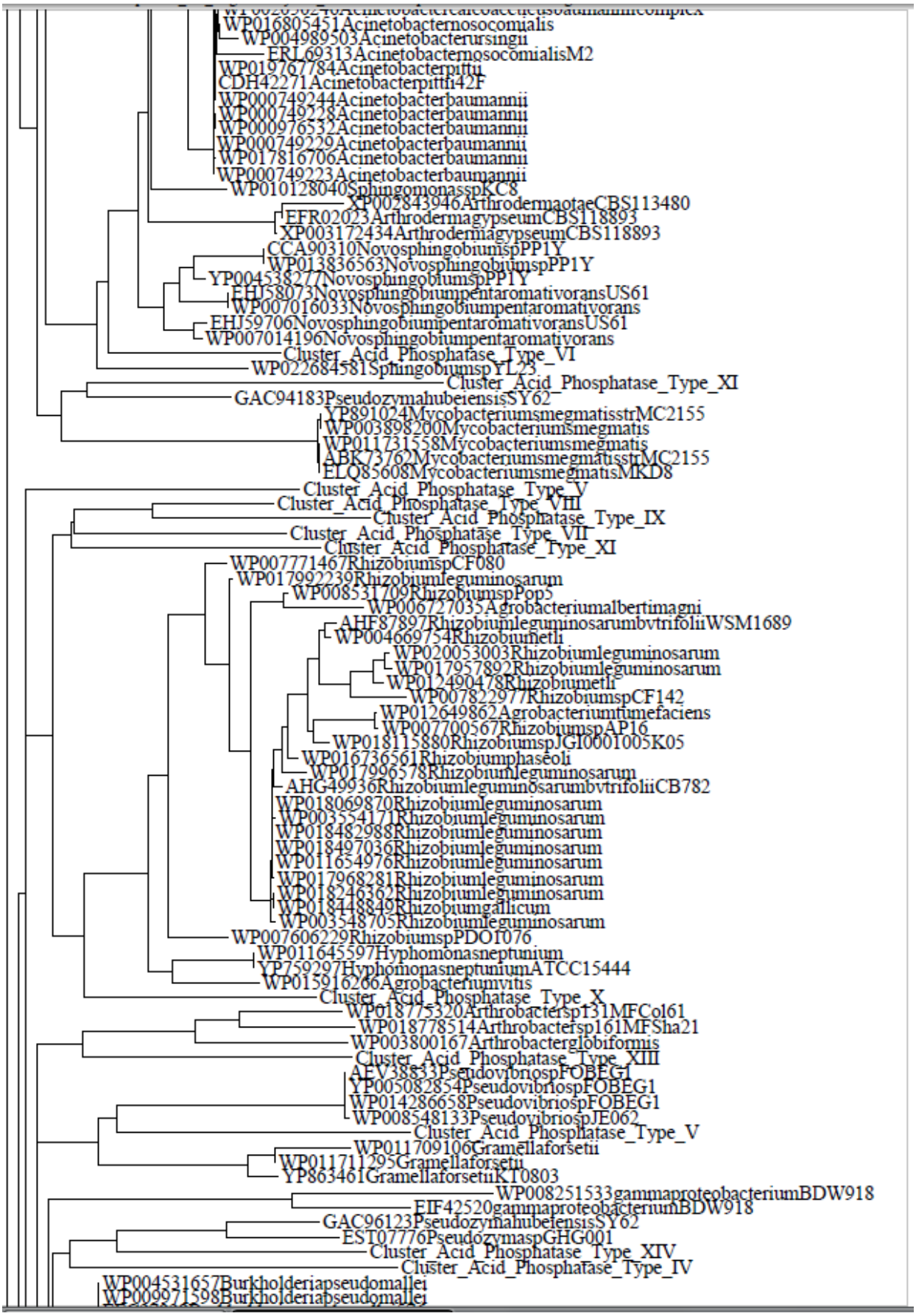
WP016805451Acinetobacternosocomialis
WP004989503Acinetobacterursingii
ERL69313AcinetobacternosocomialisM2
WP019767784Acinetobacterpittii
CDH42271Acinetobacterpittii42F
WP000749244Acinetobacterbaumannii
WP000749228Acinetobacterbaumannii
WP000976532Acinetobacterbaumannii
WP000749229Acinetobacterbaumannii
WP017816706Acinetobacterbaumannii
WP000749223Acinetobacterbaumannii
WP010128040SphingomonasspKC8
XP002843946ArthrodermaotaeCBS113480
EFR02023ArthrodermagypseumCBS118893
XP003172434ArthrodermagypseumCBS118893
CCA90310NovosphingobiumspPP1Y
WP013836563NovosphingobiumspPP1Y
YP004538277NovosphingobiumspPP1Y
EHJ58073NovosphingobiumpentaromativoransUS61
WP007016033Novosphingobiumpentaromativorans
EHJ59706NovosphingobiumpentaromativoransUS61
WP007014196Novosphingobiumpentaromativorans
Cluster_Acid_Phosphatase_Type_VI
WP022684581SphingobiumspYL23
Cluster_Acid_Phosphatase_Type_XI
GAC94183PseudozymahubeiensisSY62
YP891024MycobacteriumsmegmatisstrMC2155
WP003898200Mycobacteriumsmegmatis
WP011731558Mycobacteriumsmegmatis
ABK73762MycobacteriumsmegmatisstrMC2155
ELQ85608MycobacteriumsmegmatisMKD8
Cluster_Acid_Phosphatase_Type_V
Cluster_Acid_Phosphatase_Type_VIII
Cluster_Acid_Phosphatase_Type_IX
Cluster_Acid_Phosphatase_Type_VII
Cluster_Acid_Phosphatase_Type_XI
WP007771467RhizobiumspCF080
WP017992239Rhizobiumleguminosarum
WP008531709RhizobiumspPop5
WP006727035Agrobacteriumalbertimagni
AHF87897RhizobiumleguminosarumbvtrifoliiWSM1689
WP004669754Rhizobiumetli
WP020053003Rhizobiumleguminosarum
WP017957892Rhizobiumleguminosarum
WP012490478Rhizobiumetli
WP007822977RhizobiumspCF142
WP012649862Agrobacteriumtumefaciens
WP007700567RhizobiumspAP16
WP018115880RhizobiumspJGI0001005K05
WP016736561Rhizobiumphaseoli
WP017996578Rhizobiumleguminosarum
AHG49936RhizobiumleguminosarumbvtrifoliiCB782
WP018069870Rhizobiumleguminosarum
WP003554171Rhizobiumleguminosarum
WP018482988Rhizobiumleguminosarum
WP018497036Rhizobiumleguminosarum
WP011654976Rhizobiumleguminosarum
WP017968281Rhizobiumleguminosarum
WP018246362Rhizobiumleguminosarum
WP018448849Rhizobiumgallicum
WP003548705Rhizobiumleguminosarum
WP007606229RhizobiumspPDO1076
WP011645597Hyphomonasneptunium
YP759297HyphomonasneptuniumATCC15444
WP015916266Agrobacteriumvitis
Cluster_Acid_Phosphatase_Type_X
WP018775320Arthrobactersp131MFCol61
WP018778514Arthrobactersp161MFSha21
WP003800167Arthrobacterglobiformis
Cluster_Acid_Phosphatase_Type_XIII
AEV38833PseudovibriospFOBEG1
YP005082854PseudovibriospFOBEG1
WP014286658PseudovibriospFOBEG1
WP008548133PseudovibriospJE062
Cluster_Acid_Phosphatase_Type_V
WP011709106Gramellaforsetii
WP011711295Gramellaforsetii
YP863461GramellaforsetiiKT0803
WP008251533gammaproteobacteriumBDW918
EIF42520gammaproteobacteriumBDW918
GAC96123PseudozymahubeiensisSY62
EST07776PseudozymaspGHG001
Cluster_Acid_Phosphatase_Type_XIV
Cluster_Acid_Phosphatase_Type_IV
WP004531657Burkholderiapseudomallei
WP009971598Burkholderiapseudomallei

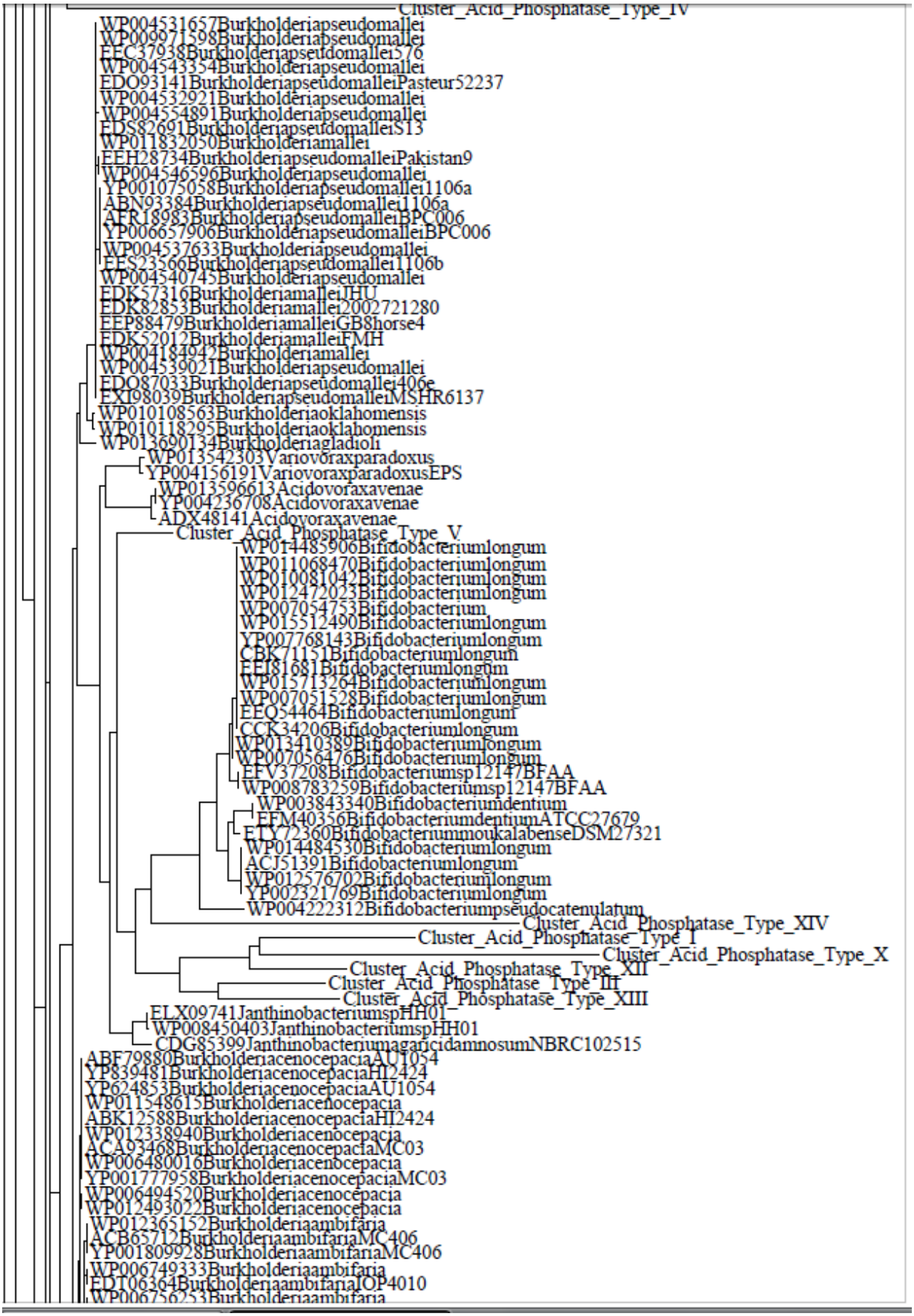
Cluster_Acid_Phosphatase_Type_IV
WP004531657Burkholderiapseudomallei
WP009971598Burkholderiapseudomallei
EEC37938Burkholderiapseudomallei576
WP004543354Burkholderiapseudomallei
EDO93141BurkholderiapseudomalleiPasteur52237
WP004532921Burkholderiapseudomallei
WP004554891Burkholderiapseudomallei
EDS82691BurkholderiapseudomalleiS13
WP011832050Burkholderiamallei
EEH28734BurkholderiapseudomalleiPakistan9
WP004546596Burkholderiapseudomallei
YP001075058Burkholderiapseudomallei1106a
ABN93384Burkholderiapseudomallei1106a
AFR18983BurkholderiapseudomalleiBPC006
YP006657906BurkholderiapseudomalleiBPC006
WP004537633Burkholderiapseudomallei
EES23566Burkholderiapseudomallei1106b
WP004540745Burkholderiapseudomallei
EDK57316BurkholderiamalleiJHU
EDK82853Burkholderiamallei2002721280
EEP88479BurkholderiamalleiGB8horse4
EDK52012BurkholderiamalleiFMH
WP004184942Burkholderiamallei
WP004539021Burkholderiapseudomallei
EDQ87033Burkholderiapseudomallei406e
EXI98039BurkholderiapseudomalleiMSHR6137
WP010108563Burkholderiaoklahomensis
WP010118295Burkholderiaoklahomensis
WP013690134Burkholderiagladioli
WP013542303Variovoraxparadoxus
YP004156191VariovoraxparadoxusEPS
WP013596613Acidovoraxavenae
YP004236708Acidovoraxavenae
ADX48141Acidovoraxavenae
Cluster_Acid_Phosphatase_Type_V
WP014485906Bifidobacteriumlongum
WP011068470Bifidobacteriumlongum
WP010081042Bifidobacteriumlongum
WP012472023Bifidobacteriumlongum
WP007054753Bifidobacterium
WP015512490Bifidobacteriumlongum
YP007768143Bifidobacteriumlongum
CBK71151Bifidobacteriumlongum
EEI81681Bifidobacteriumlongum
WP015713264Bifidobacteriumlongum
WP007051528Bifidobacteriumlongum
EEQ54464Bifidobacteriumlongum
CCK34206Bifidobacteriumlongum
WP013410389Bifidobacteriumlongum
WP007056476Bifidobacteriumlongum
EFV37208Bifidobacteriumsp12147BFAA
WP008783259Bifidobacteriumsp12147BFAA
WP003843340Bifidobacteriumdentium
EFM40356BifidobacteriumdentiumATCC27679
ETX72360BifidobacteriummoukalabenseDSM27321
WP014484530Bifidobacteriumlongum
ACJ51391Bifidobacteriumlongum
WP012576702Bifidobacteriumlongum
YP002321769Bifidobacteriumlongum
WP004222312Bifidobacteriumpseudocatenulatum
Cluster_Acid_Phosphatase_Type_XIV
Cluster_Acid_Phosphatase_Type_I
Cluster_Acid_Phosphatase_Type_X
Cluster_Acid_Phosphatase_Type_XII
Cluster_Acid_Phosphatase_Type_III
Cluster_Acid_Phosphatase_Type_XIII
ELX09741JanthinobacteriumspHH01
WP008450403JanthinobacteriumspHH01
CDG85399JanthinobacteriumagaricidamnosumNBRC102515
ABF79880BurkholderiacenocepaciaAU1054
YP839481BurkholderiacenocepaciaHI2424
YP624853BurkholderiacenocepaciaAU1054
WP011548615Burkholderiacenocepacia
ABK12588BurkholderiacenocepaciaHI2424
WP012338940Burkholderiacenocepacia
ACA93468BurkholderiacenocepaciaMC03
WP006480016Burkholderiacenocepacia
YP001777958BurkholderiacenocepaciaMC03
WP006494520Burkholderiacenocepacia
WP012493022Burkholderiacenocepacia
WP012365152Burkholderiaambifaria
ACB65712BurkholderiaambifariaMC406
YP001809928BurkholderiaambifariaMC406
WP006749333Burkholderiaambifaria
EDT06364BurkholderiaambifariaIOP4010
WP006756253Burkholderiaambifaria

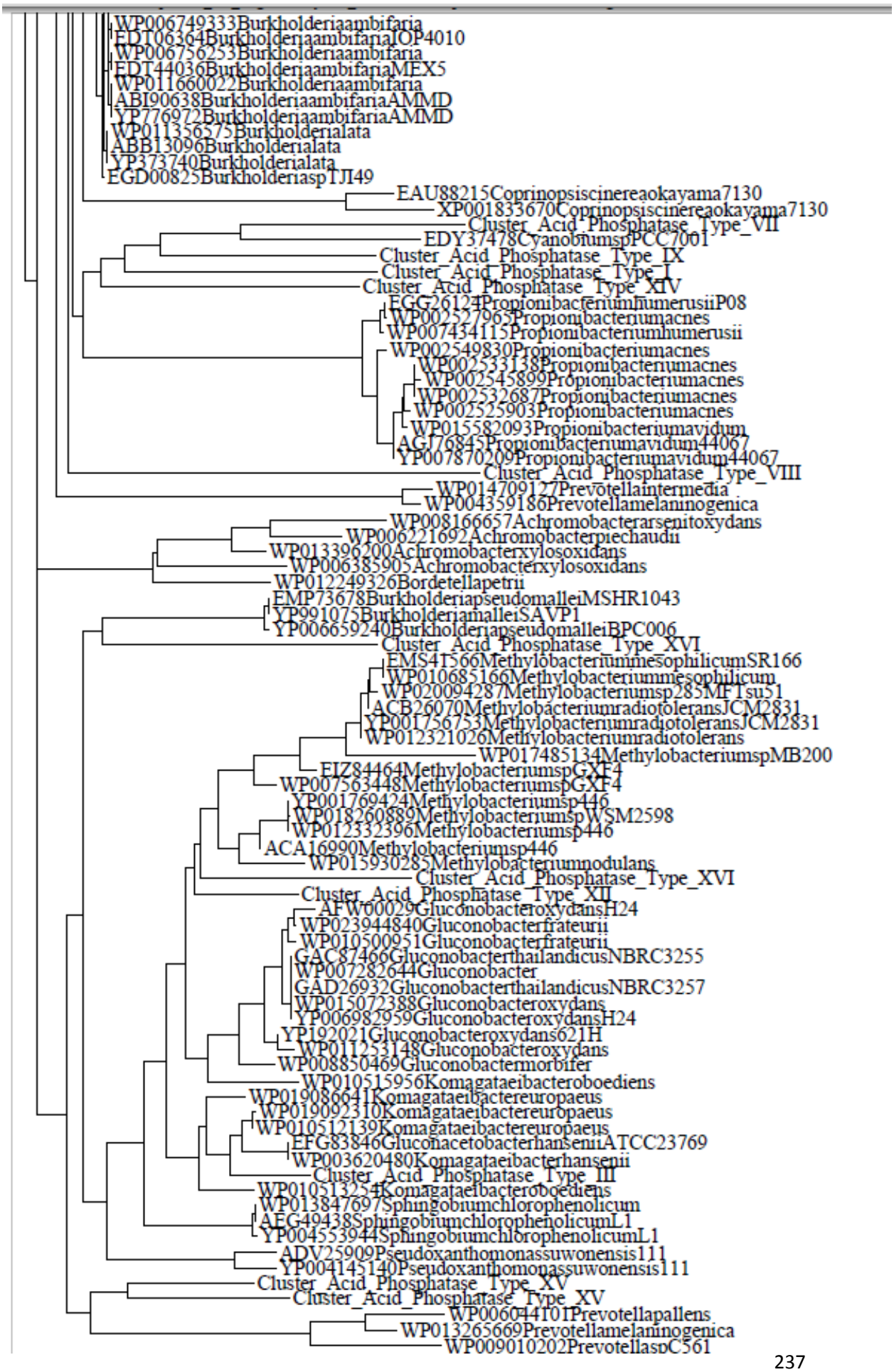
WP006749333Burkholderiaambifaria
EDT06364BurkholderiaambifariaIOP4010
WP006756253Burkholderiaambifaria
EDT44036BurkholderiaambifariaMEX5
WP011660022Burkholderiaambifaria
ABI90638BurkholderiaambifariaAMMD
YP776972BurkholderiaambifariaAMMD
WP011356575Burkholderialata
ABB13096Burkholderialata
YP373740Burkholderialata
EGD00825BurkholderiaspTJI49
EAU88215Coprinopsiscinereaokayama7130
XP001833670Coprinopsiscinereaokayama7130
Cluster_Acid_Phosphatase_Type_VII
EDY37478CyanobiumspPCC7001
Cluster_Acid_Phosphatase_Type_IX
Cluster_Acid_Phosphatase_Type_I
Cluster_Acid_Phosphatase_Type_XIV
EGG26124PropionibacteriumhumerusiiP08
WP002527965Propionibacteriumacnes
WP007434115Propionibacteriumhumerusii
WP002549830Propionibacteriumacnes
WP002533138Propionibacteriumacnes
WP002545899Propionibacteriumacnes
WP002532687Propionibacteriumacnes
WP002525903Propionibacteriumacnes
WP015582093Propionibacteriumavidum
AGJ76845Propionibacteriumavidum44067
YP007870209Propionibacteriumavidum44067
Cluster_Acid_Phosphatase_Type_VIII
WP014709127Prevotellaintermedia
WP004359186Prevotellamelaninogenica
WP008166657Achromobacterarsenitoxydans
WP006221692Achromobacterpiechaudii
WP013396200Achromobacterxylosoxidans
WP006385905Achromobacterxylosoxidans
WP012249326Bordetellapetrii
EMP73678BurkholderiapseudomalleiMSHR1043
YP991075BurkholderiamalleiSAVP1
YP006659240BurkholderiapseudomalleiBPC006
Cluster_Acid_Phosphatase_Type_XVI
EMS41566MethylobacteriummesophilicumSR166
WP010685166Methylobacteriummesophilicum
WP020094287Methylobacteriumsp285MFTsu51
ACB26070MethylobacteriumradiotoleransJCM2831
YP001756753MethylobacteriumradiotoleransJCM2831
WP012321026Methylobacteriumradiotolerans
WP017485134MethylobacteriumspMB200
EIZ84464MethylobacteriumspGXF4
WP007563448MethylobacteriumspGXF4
YP001769424Methylobacteriumsp446
WP018260889MethylobacteriumspWSM2598
WP012332396Methylobacteriumsp446
ACA16990Methylobacteriumsp446
WP015930285Methylobacteriumnodulans
Cluster_Acid_Phosphatase_Type_XVI
Cluster_Acid_Phosphatase_Type_XII
AFW00029GluconobacteroxydansH24
WP023944840Gluconobacterfrateurii
WP010500951Gluconobacterfrateurii
GAC87466GluconobacterthailandicusNBRC3255
WP007282644Gluconobacter
GAD26932GluconobacterthailandicusNBRC3257
WP015072388Gluconobacteroxydans
YP006982959GluconobacteroxydansH24
YP192021Gluconobacteroxydans621H
WP011253148Gluconobacteroxydans
WP008850469Gluconobactermorbifer
WP010515956Komagataeibacteroboediens
WP019086641Komagataeibactereuropaeus
WP019092310Komagataeibactereuropaeus
WP010512139Komagataeibactereuropaeus
EFG83846GluconacetobacterhanseniiATCC23769
WP003620480Komagataeibacterhansenii
Cluster_Acid_Phosphatase_Type_III
WP010513254Komagataeibacteroboediens
WP013847697Sphingobiumchlorophenolicum
AEG49438SphingobiumchlorophenolicumL1
YP004553944SphingobiumchlorophenolicumL1
ADV25909Pseudoxanthomonassuwonensis111
YP004145140Pseudoxanthomonassuwonensis111
Cluster_Acid_Phosphatase_Type_XV
Cluster_Acid_Phosphatase_Type_XV
WP006044101Prevotellapallens
WP013265669Prevotellamelaninogenica
WP009010202PrevotellaspC561

Figure S9a. Phylogenetic tree of cluster VIIIa of the acid phosphatase sequences included in the database.

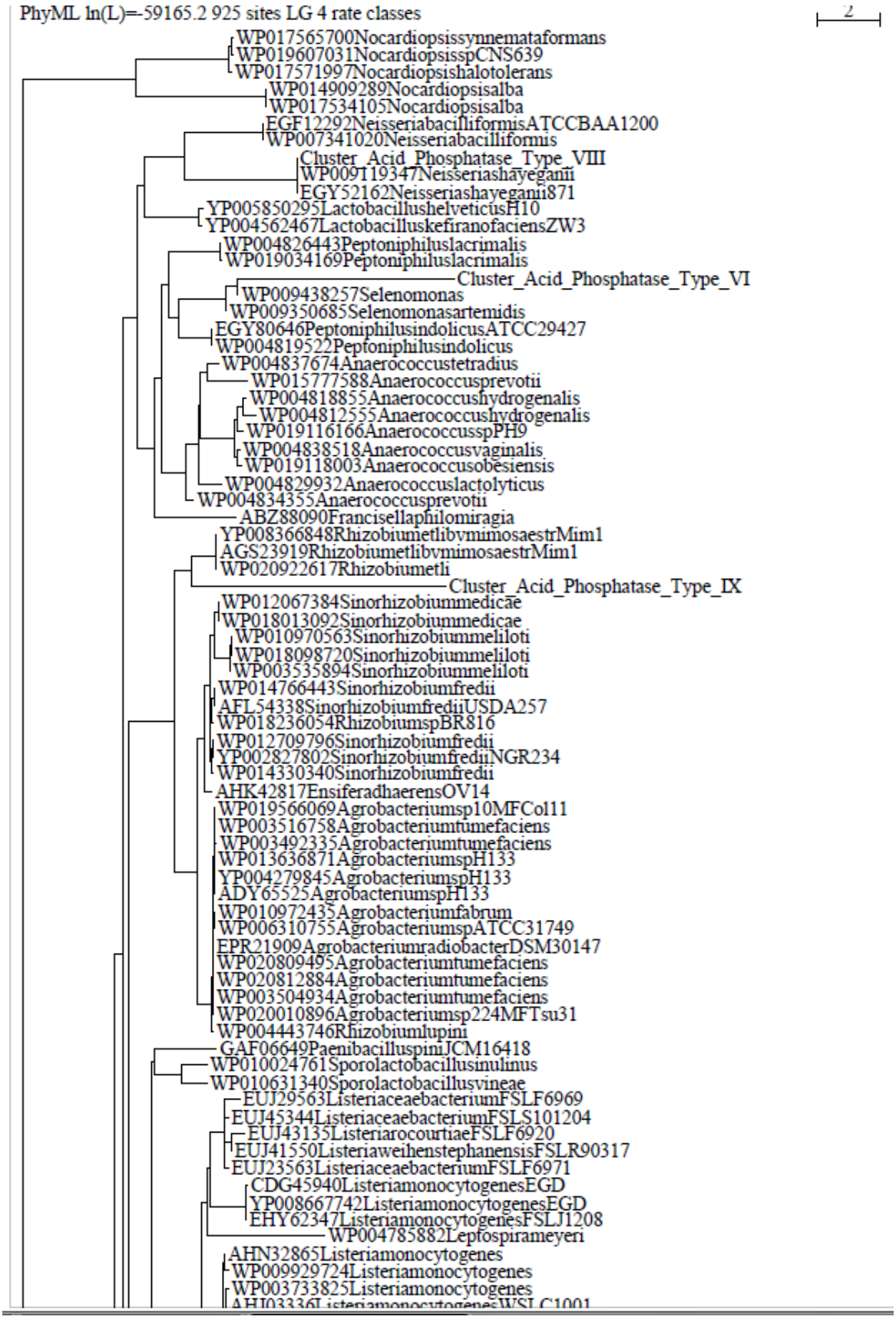

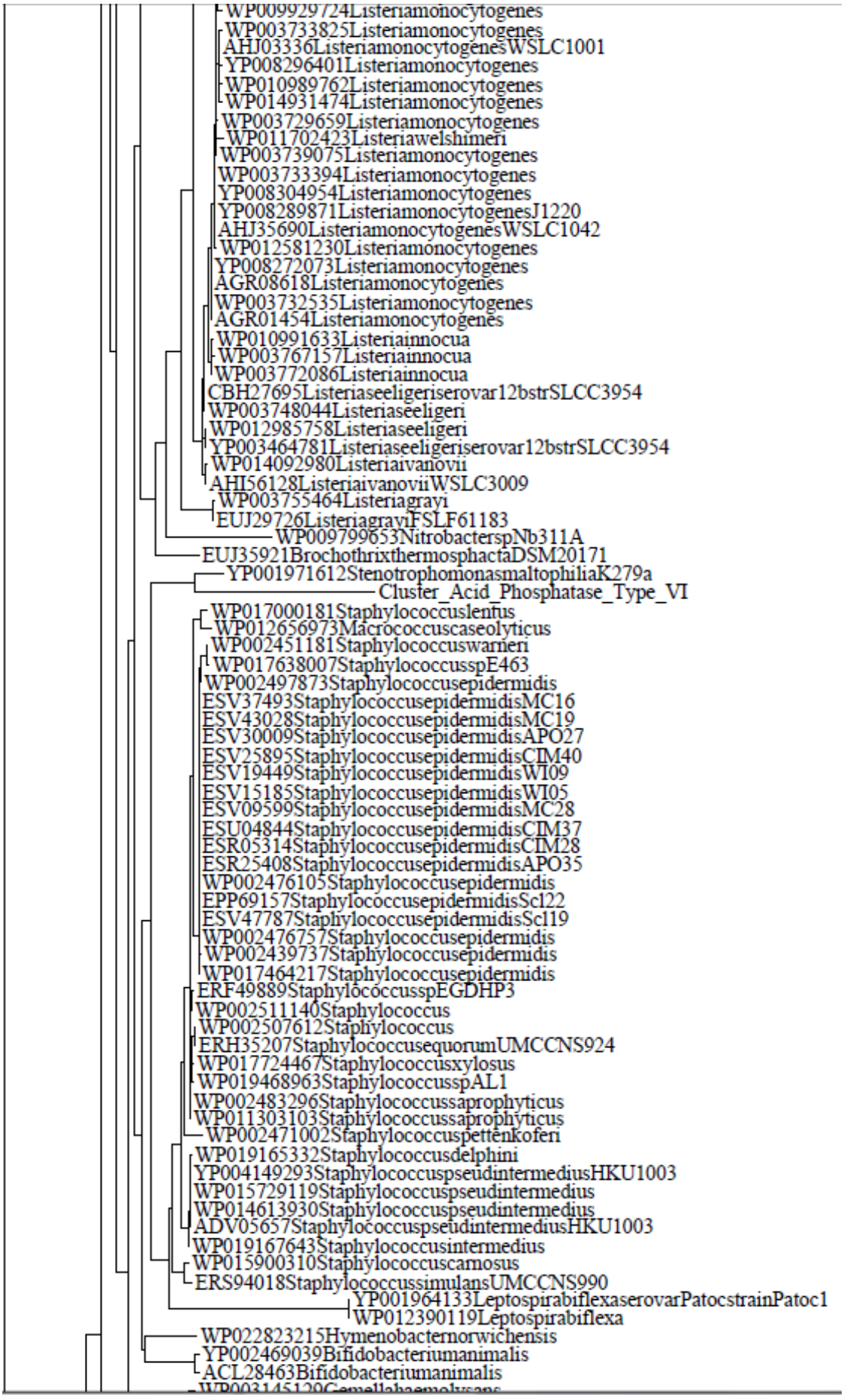
WP009929724Listeriamonocytogenes
WP003733825Listeriamonocytogenes
AHJ03336ListeriamonocytogenesWSLC1001
YP008296401Listeriamonocytogenes
WP010989762Listeriamonocytogenes
WP014931474Listeriamonocytogenes
WP003729659Listeriamonocytogenes
WP011702423Listeriawelshimeri
WP003739075Listeriamonocytogenes
WP003733394Listeriamonocytogenes
YP008304954Listeriamonocytogenes
YP008289871ListeriamonocytogenesJ1220
AHJ35690ListeriamonocytogenesWSLC1042
WP012581230Listeriamonocytogenes
YP008272073Listeriamonocytogenes
AGR08618Listeriamonocytogenes
WP003732535Listeriamonocytogenes
AGR01454Listeriamonocytogenes
WP010991633Listeriainnocua
WP003767157Listeriainnocua
WP003772086Listeriainnocua
CBH27695Listeriaseeligeriserovar12bstrSLCC3954
WP003748044Listeriaseeligeri
WP012985758Listeriaseeligeri
YP003464781Listeriaseeligeriserovar12bstrSLCC3954
WP014092980Listeriaivanovii
AHI56128ListeriaivanoviiWSLC3009
WP003755464Listeriagrayi
EUJ29726ListeriagrayiFSLF61183
WP009799653NitrobacterspNb311A
EUJ35921BrochothrixthermosphactaDSM20171
YP001971612StenotrophomonasmaltophiliaK279a
Cluster_Acid_Phosphatase_Type_VI
WP017000181Staphylococcuslentus
WP012656973Macrococcuscaseolyticus
WP002451181Staphylococcuswarneri
WP017638007StaphylococcusspE463
WP002497873Staphylococcusepidermidis
ESV37493StaphylococcusepidermidisMC16
ESV43028StaphylococcusepidermidisMC19
ESV30009StaphylococcusepidermidisAPO27
ESV25895StaphylococcusepidermidisCIM40
ESV19449StaphylococcusepidermidisWI09
ESV15185StaphylococcusepidermidisWI05
ESV09599StaphylococcusepidermidisMC28
ESU04844StaphylococcusepidermidisCIM37
ESR05314StaphylococcusepidermidisCIM28
ESR25408StaphylococcusepidermidisAPO35
WP002476105Staphylococcusepidermidis
EPP69157StaphylococcusepidermidisScl22
ESV47787StaphylococcusepidermidisScl19
WP002476757Staphylococcusepidermidis
WP002439737Staphylococcusepidermidis
WP017464217Staphylococcusepidermidis
ERF49889StaphylococcusspEGDHP3
WP002511140Staphylococcus
WP002507612Staphylococcus
ERH35207StaphylococcusequorumUMCCNS924
WP017724467Staphylococcusxylosus
WP019468963StaphylococcusspAL1
WP002483296Staphylococcussaprophyticus
WP011303103Staphylococcussaprophyticus
WP002471002Staphylococcuspettenkoferi
WP019165332Staphylococcusdelphini
YP004149293StaphylococcuspseudintermediusHKU1003
WP015729119Staphylococcuspseudintermedius
WP014613930Staphylococcuspseudintermedius
ADV05657StaphylococcuspseudintermediusHKU1003
WP019167643Staphylococcusintermedius
WP015900310Staphylococcuscarnosus
ERS94018StaphylococcussimulansUMCCNS990
YP001964133LeptospirabiflexaserovarPatocstrainPatoc1
WP012390119Leptospirabiflexa
WP022823215Hymenobacternorwichensis
YP002469039Bifidobacteriumanimalis
ACL28463Bifidobacteriumanimalis

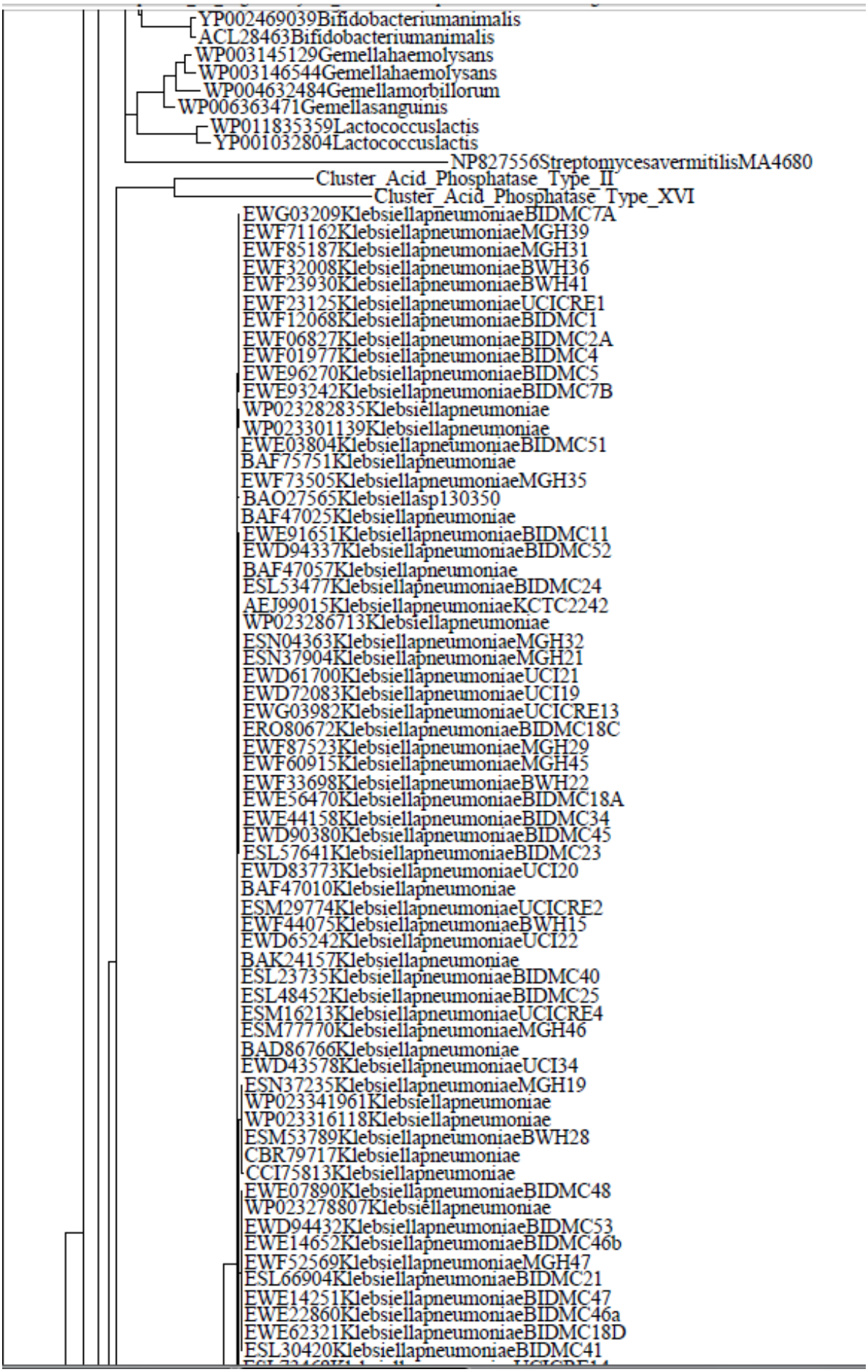
YP002469039Bifidobacteriumanimalis
ACL28463Bifidobacteriumanimalis
WP003145129Gemellahaemolysans
WP003146544Gemellahaemolysans
WP004632484Gemellamorbillorum
WP006363471Gemellasanguinis
WP011835359Lactococcuslactis
YP001032804Lactococcuslactis
NP827556StreptomycesavermitilisMA4680
Cluster_Acid_Phosphatase_Type_II
Cluster_Acid_Phosphatase_Type_XVI
EWG03209KlebsiellapneumoniaeBIDMC7A
EWF71162KlebsiellapneumoniaeMGH39
EWF85187KlebsiellapneumoniaeMGH31
EWF32008KlebsiellapneumoniaeBWH36
EWF23930KlebsiellapneumoniaeBWH41
EWF23125KlebsiellapneumoniaeUCICRE1
EWF12068KlebsiellapneumoniaeBIDMC1
EWF06827KlebsiellapneumoniaeBIDMC2A
EWF01977KlebsiellapneumoniaeBIDMC4
EWE96270KlebsiellapneumoniaeBIDMC5
EWE93242KlebsiellapneumoniaeBIDMC7B
WP023282835Klebsiellapneumoniae
WP023301139Klebsiellapneumoniae
EWE03804KlebsiellapneumoniaeBIDMC51
BAF75751Klebsiellapneumoniae
EWF73505KlebsiellapneumoniaeMGH35
BAO27565Klebsiellasp130350
BAF47025Klebsiellapneumoniae
EWE91651KlebsiellapneumoniaeBIDMC11
EWD94337KlebsiellapneumoniaeBIDMC52
BAF47057Klebsiellapneumoniae
ESL53477KlebsiellapneumoniaeBIDMC24
AEJ99015KlebsiellapneumoniaeKCTC2242
WP023286713Klebsiellapneumoniae
ESN04363KlebsiellapneumoniaeMGH32
ESN37904KlebsiellapneumoniaeMGH21
EWD61700KlebsiellapneumoniaeUCI21
EWD72083KlebsiellapneumoniaeUCI19
EWG03982KlebsiellapneumoniaeUCICRE13
ERO80672KlebsiellapneumoniaeBIDMC18C
EWF87523KlebsiellapneumoniaeMGH29
EWF60915KlebsiellapneumoniaeMGH45
EWF33698KlebsiellapneumoniaeBWH22
EWE56470KlebsiellapneumoniaeBIDMC18A
EWE44158KlebsiellapneumoniaeBIDMC34
EWD90380KlebsiellapneumoniaeBIDMC45
ESL57641KlebsiellapneumoniaeBIDMC23
EWD83773KlebsiellapneumoniaeUCI20
BAF47010Klebsiellapneumoniae
ESM29774KlebsiellapneumoniaeUCICRE2
EWF44075KlebsiellapneumoniaeBWH15
EWD65242KlebsiellapneumoniaeUCI22
BAK24157Klebsiellapneumoniae
ESL23735KlebsiellapneumoniaeBIDMC40
ESL48452KlebsiellapneumoniaeBIDMC25
ESM16213KlebsiellapneumoniaeUCICRE4
ESM77770KlebsiellapneumoniaeMGH46
BAD86766Klebsiellapneumoniae
EWD43578KlebsiellapneumoniaeUCI34
ESN37235KlebsiellapneumoniaeMGH19
WP023341961Klebsiellapneumoniae
WP023316118Klebsiellapneumoniae
ESM53789KlebsiellapneumoniaeBWH28
CBR79717Klebsiellapneumoniae
CCI75813Klebsiellapneumoniae
EWE07890KlebsiellapneumoniaeBIDMC48
WP023278807Klebsiellapneumoniae
EWD94432KlebsiellapneumoniaeBIDMC53
EWE14652KlebsiellapneumoniaeBIDMC46b
EWF52569KlebsiellapneumoniaeMGH47
ESL66904KlebsiellapneumoniaeBIDMC21
EWE14251KlebsiellapneumoniaeBIDMC47
EWE22860KlebsiellapneumoniaeBIDMC46a
EWE62321KlebsiellapneumoniaeBIDMC18D
ESL30420KlebsiellapneumoniaeBIDMC41

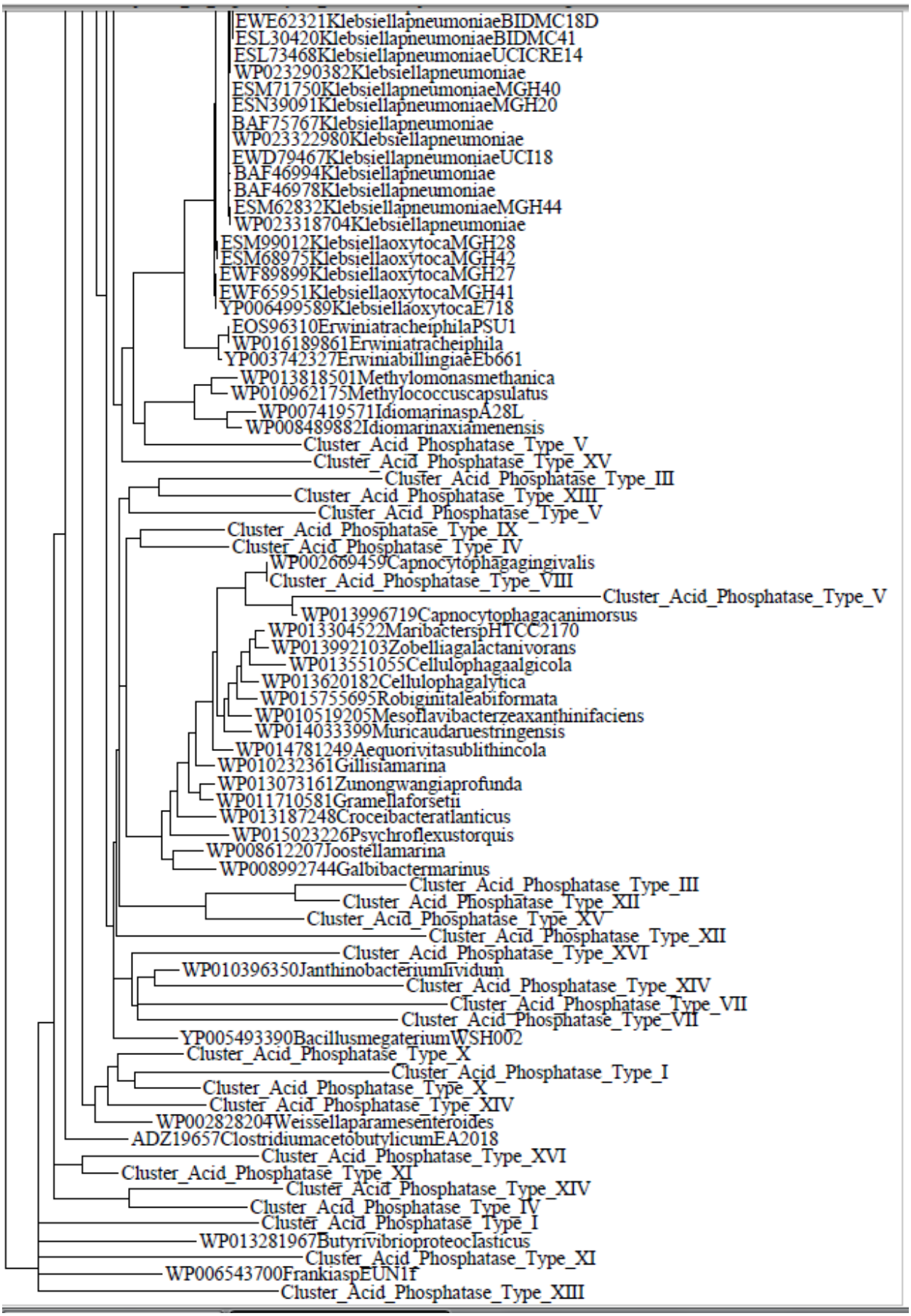
EWE62321KlebsiellapneumoniaeBIDMC18D
ESL30420KlebsiellapneumoniaeBIDMC41
ESL73468KlebsiellapneumoniaeUCICRE14
WP023290382Klebsiellapneumoniae
ESM71750KlebsiellapneumoniaeMGH40
ESN39091KlebsiellapneumoniaeMGH20
BAF75767Klebsiellapneumoniae
WP023322980Klebsiellapneumoniae
EWD79467KlebsiellapneumoniaeUCI18
BAF46994Klebsiellapneumoniae
BAF46978Klebsiellapneumoniae
ESM62832KlebsiellapneumoniaeMGH44
WP023318704Klebsiellapneumoniae
ESM99012KlebsiellaoxytocaMGH28
ESM68975KlebsiellaoxytocaMGH42
EWF89899KlebsiellaoxytocaMGH27
EWF65951KlebsiellaoxytocaMGH41
YP006499589KlebsiellaoxytocaE718
EOS96310ErwiniatracheiphilaPSU1
WP016189861Erwiniatracheiphila
YP003742327ErwiniabillingiaeEb661
WP013818501Methylomonasmethanica
WP010962175Methylococcuscapsulatus
WP007419571IdiomarinaspA28L
WP008489882Idiomarinaxiamenensis
Cluster_Acid_Phosphatase_Type_V
Cluster_Acid_Phosphatase_Type_XV
Cluster_Acid_Phosphatase_Type_III
Cluster_Acid_Phosphatase_Type_XIII
Cluster_Acid_Phosphatase_Type_V
Cluster_Acid_Phosphatase_Type_IX
Cluster_Acid_Phosphatase_Type_IV
WP002669459Capnocytophagagingivalis
Cluster_Acid_Phosphatase_Type_VIII
Cluster_Acid_Phosphatase_Type_V
WP013996719Capnocytophagacanimorsus
WP013304522MaribacterspHTCC2170
WP013992103Zobelliagalactanivorans
WP013551055Cellulophagaalgicola
WP013620182Cellulophagalytica
WP015755695Robiginitalealbiformata
WP010519205Mesoflavibacterzeaxanthinifaciens
WP014033399Muricaudaruestringensis
WP014781249Aequorivitasublithincola
WP010232361Gillisiamarina
WP013073161Zunongwangiaprofunda
WP011710581Gramellaforsetii
WP013187248Croceibacteratlanticus
WP015023226Psychroflexustorquis
WP008612207Joostellamarina
WP008992744Galbibactermarinus
Cluster_Acid_Phosphatase_Type_III
Cluster_Acid_Phosphatase_Type_XII
Cluster_Acid_Phosphatase_Type_XV
Cluster_Acid_Phosphatase_Type_XII
Cluster_Acid_Phosphatase_Type_XVI
WP010396350JanthinobacteriumLividum
Cluster_Acid_Phosphatase_Type_XIV
Cluster_Acid_Phosphatase_Type_VII
Cluster_Acid_Phosphatase_Type_VII
YP005493390BacillusmegateriumWSH002
Cluster_Acid_Phosphatase_Type_X
Cluster_Acid_Phosphatase_Type_I
Cluster_Acid_Phosphatase_Type_X
Cluster_Acid_Phosphatase_Type_XIV
WP002828204Weissellaparamesenteroides
ADZ19657ClostridiumacetobutylicumEA2018
Cluster_Acid_Phosphatase_Type_XVI
Cluster_Acid_Phosphatase_Type_XI
Cluster_Acid_Phosphatase_Type_XIV
Cluster_Acid_Phosphatase_Type_IV
Cluster_Acid_Phosphatase_Type_I
WP013281967Butyrivibrioproteoclasticus
Cluster_Acid_Phosphatase_Type_XI
WP006543700FrankiaspEUN1f
Cluster_Acid_Phosphatase_Type_XIII

Figure S9b. Phylogenetic tree of cluster VIIIb of the acid phosphatase sequences included in the database.

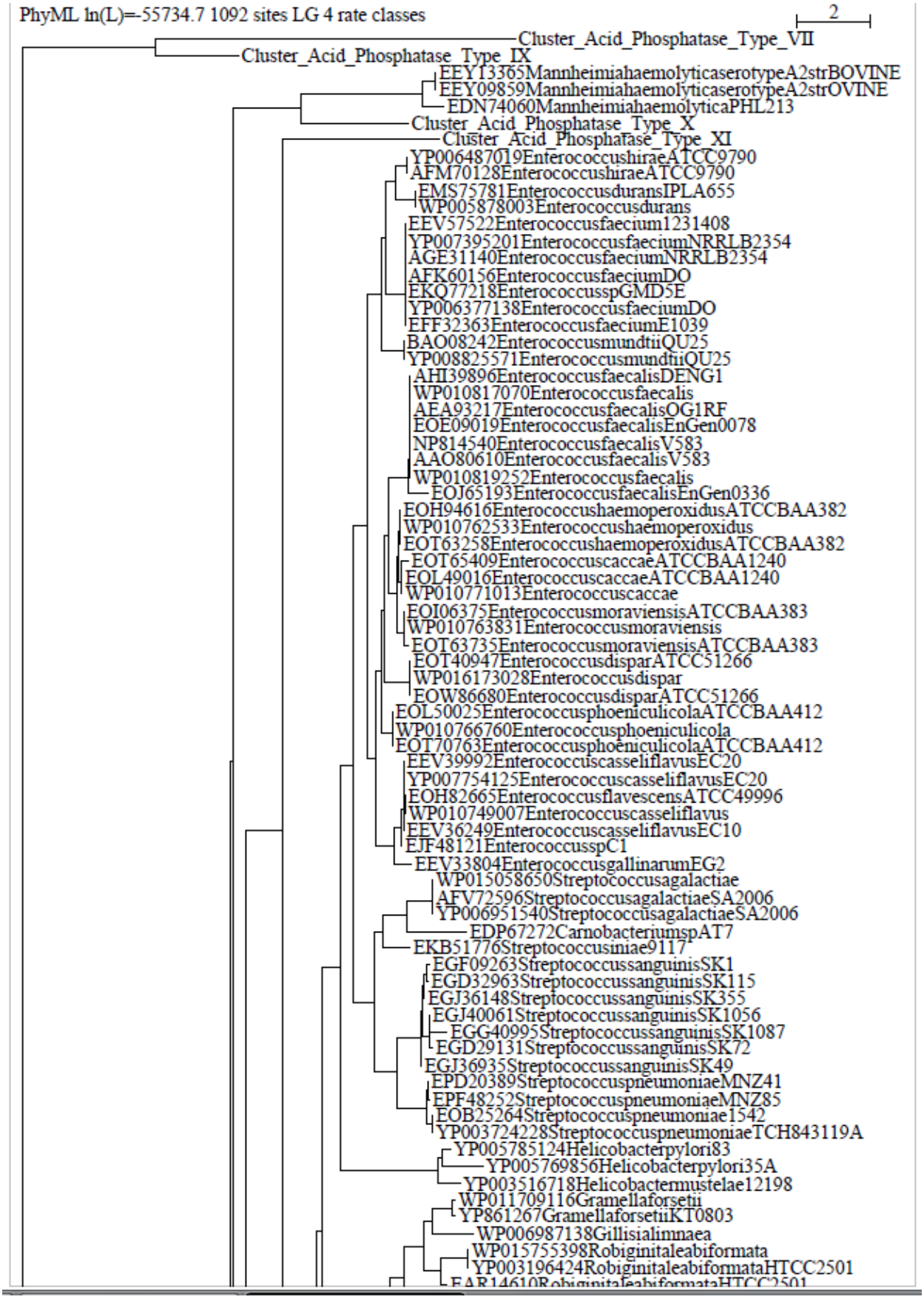

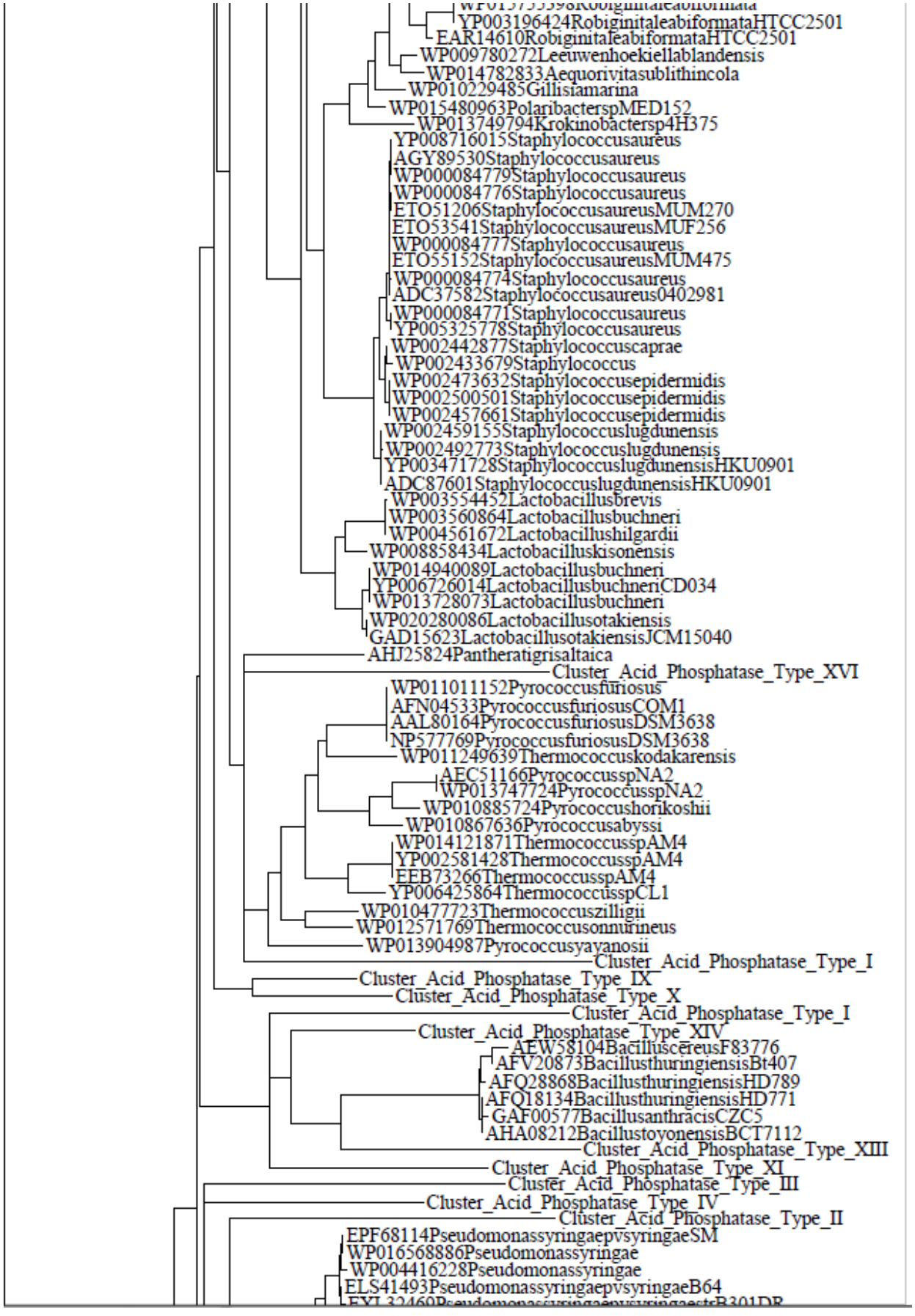
YP003196424RobiginitaleabiformataHTCC2501
EAR14610RobiginitaleabiformataHTCC2501
WP009780272Leeuwenhoekiellablandensis
WP014782833Aequorivitasublithincola
WP010229485Gillisiamarina
WP015480963PolaribacterspMED152
WP013749794Krokinobactersp4H375
YP008716015Staphylococcusaureus
AGY89530Staphylococcusaureus
WP000084779Staphylococcusaureus
WP000084776Staphylococcusaureus
ETO51206StaphylococcusaureusMUM270
ETO53541StaphylococcusaureusMUF256
WP000084777Staphylococcusaureus
ETO55152StaphylococcusaureusMUM475
WP000084774Staphylococcusaureus
ADC37582Staphylococcusaureus0402981
WP000084771Staphylococcusaureus
YP005325778Staphylococcusaureus
WP002442877Staphylococcuscaprae
WP002433679Staphylococcus
WP002473632Staphylococcusepidermidis
WP002500501Staphylococcusepidermidis
WP002457661Staphylococcusepidermidis
WP002459155Staphylococcuslugdunensis
WP002492773Staphylococcuslugdunensis
YP003471728StaphylococcuslugdunensisHKU0901
ADC87601StaphylococcuslugdunensisHKU0901
WP003554452Lactobacillusbrevis
WP003560864Lactobacillusbuchneri
WP004561672Lactobacillushilgardii
WP008858434Lactobacilluskisonensis
WP014940089Lactobacillusbuchneri
YP006726014LactobacillusbuchneriCD034
WP013728073Lactobacillusbuchneri
WP020280086Lactobacillusotakiensis
GAD15623LactobacillusotakiensisJCM15040
AHJ25824Pantheratigrisaltaica
Cluster_Acid_Phosphatase_Type_XVI
WP011011152Pyrococcusfuriosus
AFN04533PyrococcusfuriosusCOM1
AAL80164PyrococcusfuriosusDSM3638
NP577769PyrococcusfuriosusDSM3638
WP011249639Thermococcuskodakarensis
AEC51166PyrococcusspNA2
WP013747724PyrococcusspNA2
WP010885724Pyrococcushorikoshii
WP010867636Pyrococcusabyssi
WP014121871ThermococcusspAM4
YP002581428ThermococcusspAM4
EEB73266ThermococcusspAM4
YP006425864ThermococcusspCL1
WP010477723Thermococcuszilligii
WP012571769Thermococcusonnurineus
WP013904987Pyrococcusyayanosii
Cluster_Acid_Phosphatase_Type_I
Cluster_Acid_Phosphatase_Type_IX
Cluster_Acid_Phosphatase_Type_X
Cluster_Acid_Phosphatase_Type_I
Cluster_Acid_Phosphatase_Type_XIV
AEW58104BacilluscereusF83776
AFV20873BacillusthuringiensisBt407
AFQ28868BacillusthuringiensisHD789
AFQ18134BacillusthuringiensisHD771
GAF00577BacillusanthracisCZC5
AHA08212BacillustoyonensisBCT7112
Cluster_Acid_Phosphatase_Type_XIII
Cluster_Acid_Phosphatase_Type_XI
Cluster_Acid_Phosphatase_Type_III
Cluster_Acid_Phosphatase_Type_IV
Cluster_Acid_Phosphatase_Type_II
EPF68114PseudomonassyringaepvsyringaeSM
WP016568886Pseudomonassyringae
WP004416228Pseudomonassyringae
ELS41493PseudomonassyringaepvsyringaeB64


WP004416228Pseudomonassyringae
ELS41493PseudomonassyringaepvsyringaeB64
EXL32469PseudomonassyringaepvsyringaestrB301DR
EJN36779PseudomonasspGM84
EJN33847PseudomonasspGM80
EJL96015PseudomonasspGM17
EJL99013PseudomonasspGM16
WP015096674PseudomonasspUW4
YP007031382PseudomonasspUW4
AFY21577PseudomonasspUW4
EJM02907PseudomonasspGM102
EJM66665PseudomonasspGM50
EJM16173PseudomonasspGM18
EJN25691PseudomonasspGM79
EJM35916PseudomonasspGM24
EJM29021PseudomonasspGM25
EJM79451PseudomonasspGM60
EJM93684PseudomonasspGM67
EPA94331PseudomonasspG5
WP020799910PseudomonasspG5
EJN30079PseudomonasspGM78
EJM12172PseudomonasspGM21
EJM37103PseudomonasspGM33
EJM58272PseudomonasspGM48
EJM81886PseudomonasspGM74
EJM74527PseudomonasspGM49
EJM74094PseudomonasspGM55
ESW54898PseudomonasfluorescensBBc6R8
WP015278178Pseudomonasstutzeri
AGA87956PseudomonasstutzeriRCH2
YP007241586PseudomonasstutzeriRCH2
YP008210547AcinetobacterbaumanniiBJAB07104
EJN43757AcinetobacterbaumanniiAC12
YP008214291AcinetobacterbaumanniiBJAB0868
ACC58313AcinetobacterbaumanniiACICU
AGQ15452AcinetobacterbaumanniiBJAB07104
AGQ11516AcinetobacterbaumanniiBJAB0868
AGQ07774AcinetobacterbaumanniiBJAB0715
YP008218276AcinetobacterbaumanniiBJAB0715
EKO42251AcinetobacterbaumanniiAC30
YP001847660AcinetobacterbaumanniiACICU
WP009046883Pseudomonaschlororaphis
WP016701630Pseudomonaschlororaphis
ETD35669Pseudomonaschlororaphis
WP023969516Pseudomonaschlororaphis
EJM18215PseudomonasspGM17
WP007920782PseudomonasspGM17
WP009042082Pseudomonaschlororaphis
EJM94603PseudomonasspGM74
WP008047523PseudomonasspGM74
WP015093377PseudomonasspUW4
AFY17839PseudomonasspUW4
YP007027644PseudomonasspUW4
EJM73818PseudomonasspGM55
WP008018814PseudomonasspGM55
WP008149067PseudomonasspGM41
EJN30176PseudomonasspGM78
WP008057369PseudomonasspGM78
EPA97782PseudomonasspG5
WP020796486PseudomonasspG5
AHL32059Pseudomonasbrassicacearum
WP003177779Pseudomonasfluorescens
WP014336457Pseudomonasfluorescens
WP003197580Pseudomonasfluorescens
WP013692197Pseudomonasbrassicacearum
EJM00797PseudomonasspGM102
Cluster_Acid_Phosphatase_Type_XIII
XP001734945EntamoebadispārSAW760
EJM81667PseudomonasspGM60
WP008029852PseudomonasspGM60
EJM93596PseudomonasspGM67
WP008036558PseudomonasspGM67
WP017336428Pseudomonasfluorescens
ERP39941PseudomonasfluorescensNCIMB11764
WP011332366Pseudomonasfluorescens
EJM28716PseudomonasspGM25

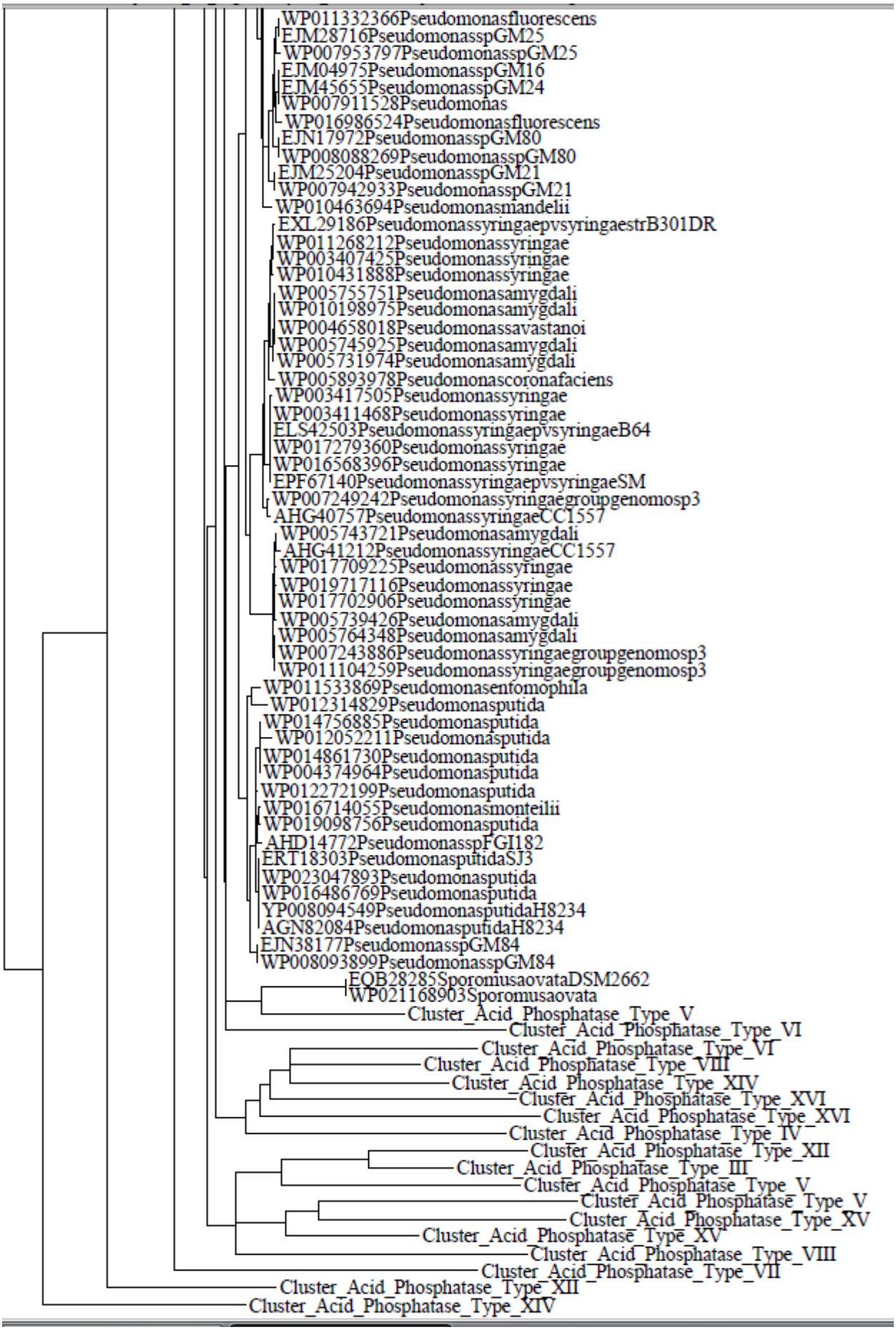
WP011332366Pseudomonasfluorescens
EJM28716PseudomonasspGM25
WP007953797PseudomonasspGM25
EJM04975PseudomonasspGM16
EJM45655PseudomonasspGM24
WP007911528Pseudomonas
WP016986524Pseudomonasfluorescens
EJN17972PseudomonasspGM80
WP008088269PseudomonasspGM80
EJM25204PseudomonasspGM21
WP007942933PseudomonasspGM21
WP010463694Pseudomonasmandelii
EXL29186Pseudomonassyringaepvsyringaestr B301DR
WP011268212Pseudomonassyringae
WP003407425Pseudomonassyringae
WP010431888Pseudomonassyringae
WP005755751Pseudomonasamygdali
WP010198975Pseudomonasamygdali
WP004658018Pseudomonassavastanoi
WP005745925Pseudomonasamygdali
WP005731974Pseudomonasamygdali
WP005893978Pseudomonascoronafaciens
WP003417505Pseudomonassyringae
WP003411468Pseudomonassyringae
ELS42503PseudomonassyringaepvsyringaeB64
WP017279360Pseudomonassyringae
WP016568396Pseudomonassyringae
EPF67140PseudomonassyringaepvsyringaeSM
WP007249242Pseudomonassyringaegroupgenomosp3
AHG40757PseudomonassyringaeCC1557
WP005743721Pseudomonasamygdali
AHG41212PseudomonassyringaeCC1557
WP017709225Pseudomonassyringae
WP019717116Pseudomonassyringae
WP017702906Pseudomonassyringae
WP005739426Pseudomonasamygdali
WP005764348Pseudomonasamygdali
WP007243886Pseudomonassyringaegroupgenomosp3
WP011104259Pseudomonassyringaegroupgenomosp3
WP011533869Pseudomonasentomophila
WP012314829Pseudomonasputida
WP014756885Pseudomonasputida
WP012052211Pseudomonasputida
WP014861730Pseudomonasputida
WP004374964Pseudomonasputida
WP012272199Pseudomonasputida
WP016714055Pseudomonasmonteilii
WP019098756Pseudomonasputida
AHD14772PseudomonasspFGI182
ERT18303PseudomonasputidaSJ3
WP023047893Pseudomonasputida
WP016486769Pseudomonasputida
YP008094549PseudomonasputidaH8234
AGN82084PseudomonasputidaH8234
EJN38177PseudomonasspGM84
WP008093899PseudomonasspGM84
EQB28285SporomusaovataDSM2662
WP021168903Sporomusaovata
Cluster_Acid_Phosphatase_Type_V
Cluster_Acid_Phosphatase_Type_VI
Cluster_Acid_Phosphatase_Type_VI
Cluster_Acid_Phosphatase_Type_VIII
Cluster_Acid_Phosphatase_Type_XIV
Cluster_Acid_Phosphatase_Type_XVI
Cluster_Acid_Phosphatase_Type_XVI
Cluster_Acid_Phosphatase_Type_IV
Cluster_Acid_Phosphatase_Type_XII
Cluster_Acid_Phosphatase_Type_III
Cluster_Acid_Phosphatase_Type_V
Cluster_Acid_Phosphatase_Type_V
Cluster_Acid_Phosphatase_Type_XV
Cluster_Acid_Phosphatase_Type_XV
Cluster_Acid_Phosphatase_Type_VIII
Cluster_Acid_Phosphatase_Type_VII
Cluster_Acid_Phosphatase_Type_XII
Cluster_Acid_Phosphatase_Type_XIV

Figure S10. Phylogenetic tree of cluster IX of the acid phosphatase sequences included in the database.

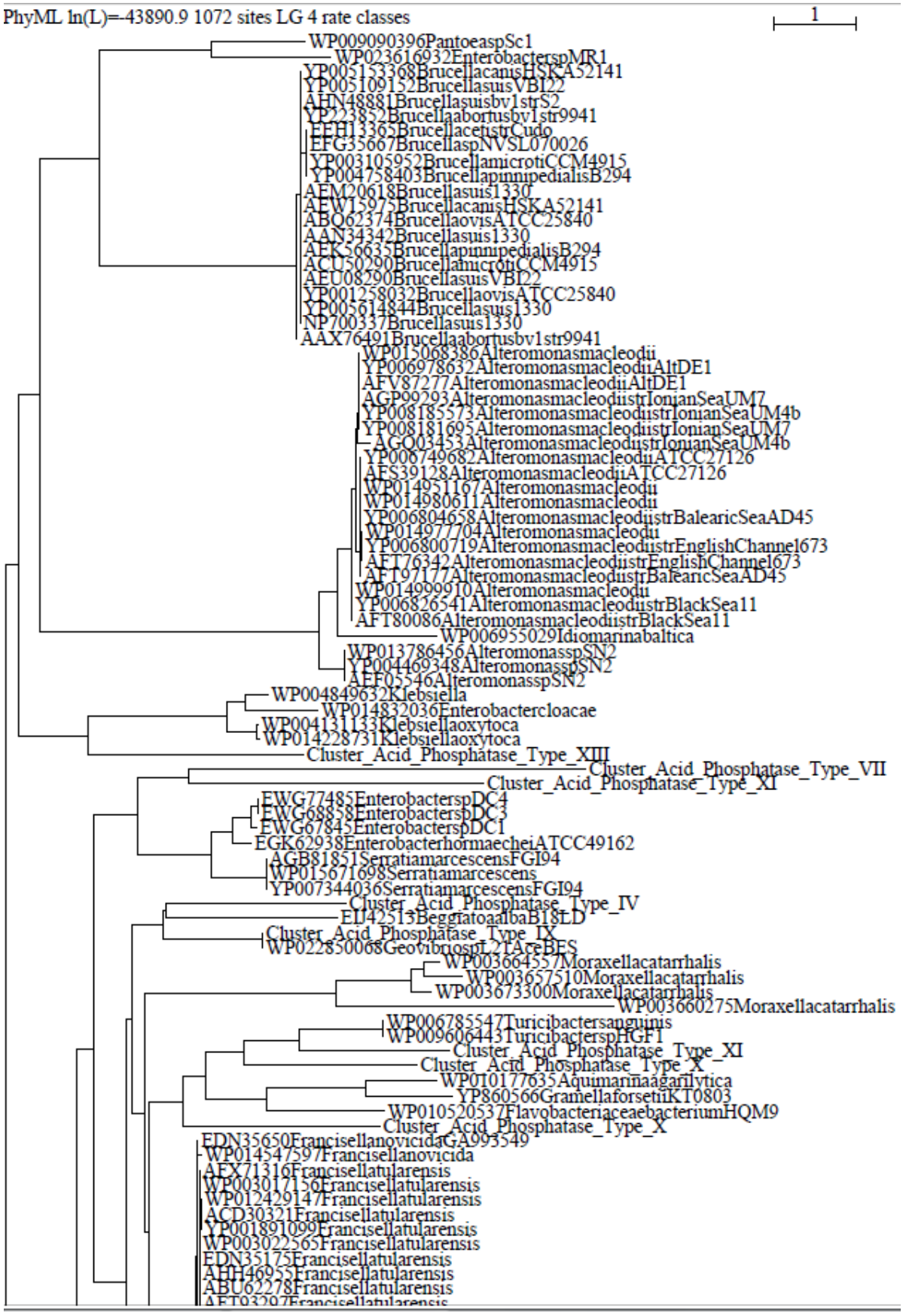

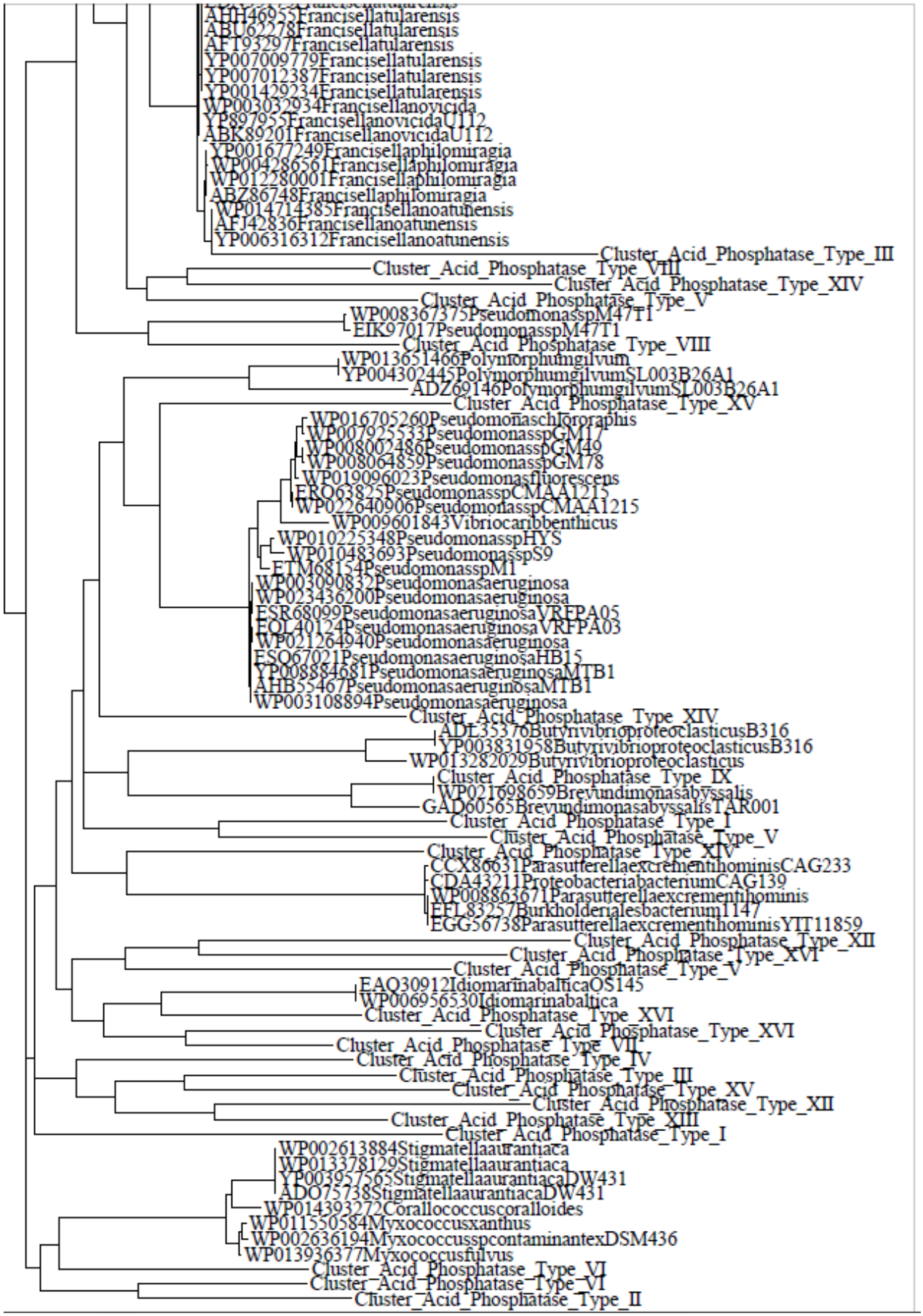
AHH46955Francisellatularensis
ABU62278Francisellatularensis
AFT93297Francisellatularensis
YP007009779Francisellatularensis
YP007012387Francisellatularensis
YP001429234Francisellatularensis
WP003032934Francisellanovicida
YP897955FrancisellanovicidaU112
ABK89201FrancisellanovicidaU112
YP001677249Francisellaphilomiragia
WP004286561Francisellaphilomiragia
WP012280001Francisellaphilomiragia
ABZ86748Francisellaphilomiragia
WP014714385Francisellanoatunensis
AFJ42836Francisellanoatunensis
YP006316312Francisellanoatunensis
Cluster_Acid_Phosphatase_Type_III
Cluster_Acid_Phosphatase_Type_VIII
Cluster_Acid_Phosphatase_Type_XIV
Cluster_Acid_Phosphatase_Type_V
WP008367375PseudomonasspM47T1
EIK97017PseudomonasspM47T1
Cluster_Acid_Phosphatase_Type_VIII
WP013651466Polymorphumgilvum
YP004302445PolymorphumgilvumSL003B26A1
ADZ69146PolymorphumgilvumSL003B26A1
Cluster_Acid_Phosphatase_Type_XV
WP016705260Pseudomonaschlororaphis
WP007925533PseudomonasspGM17
WP008002486PseudomonasspGM49
WP008064859PseudomonasspGM78
WP019096023Pseudomonasfluorescens
ERQ63825PseudomonasspCMAA1215
WP022640906PseudomonasspCMAA1215
WP009601843Vibriocaribbenthicus
WP010225348PseudomonasspHYS
WP010483693PseudomonasspS9
ETM68154PseudomonasspM1
WP003090832Pseudomonasaeruginosa
WP023436200Pseudomonasaeruginosa
ESR68099PseudomonasaeruginosaVRFPA05
EQL40124PseudomonasaeruginosaVRFPA03
WP021264940Pseudomonasaeruginosa
ESQ67021PseudomonasaeruginosaHB15
YP008884681PseudomonasaeruginosaMTB1
AHB55467PseudomonasaeruginosaMTB1
WP003108894Pseudomonasaeruginosa
Cluster_Acid_Phosphatase_Type_XIV
ADL35376ButyrivibrioproteoclasticusB316
YP003831958ButyrivibrioproteoclasticusB316
WP013282029Butyrivibrioproteoclasticus
Cluster_Acid_Phosphatase_Type_IX
WP021698659Brevundimonasabyssalis
GAD60565BrevundimonasabyssalisTAR001
Cluster_Acid_Phosphatase_Type_I
Cluster_Acid_Phosphatase_Type_V
Cluster_Acid_Phosphatase_Type_XIV
CCX86631ParasutterellaexcrementihominisCAG233
CDA43211ProteobacteriabacteriumCAG139
WP008863671Parasutterellaexcrementihominis
EFL83257Burkholderialesbacterium1147
EGG56738ParasutterellaexcrementihominisYIT11859
Cluster_Acid_Phosphatase_Type_XII
Cluster_Acid_Phosphatase_Type_XVI
Cluster_Acid_Phosphatase_Type_V
EAQ30912IdiomarinabalticaOS145
WP006956530Idiomarinabaltica
Cluster_Acid_Phosphatase_Type_XVI
Cluster_Acid_Phosphatase_Type_XVI
Cluster_Acid_Phosphatase_Type_VII
Cluster_Acid_Phosphatase_Type_IV
Cluster_Acid_Phosphatase_Type_III
Cluster_Acid_Phosphatase_Type_XV
Cluster_Acid_Phosphatase_Type_XII
Cluster_Acid_Phosphatase_Type_XIII
Cluster_Acid_Phosphatase_Type_I
WP002613884Stigmatellaaurantiaca
WP013378129Stigmatellaaurantiaca
YP003957565StigmatellaaurantiacaDW431
ADO75738StigmatellaaurantiacaDW431
WP014393272Corallococcuscoralloides
WP011550584Myxococcusxanthus
WP002636194MyxococcusspcontaminantexDSM436
WP013936377Myxococcusfulvus
Cluster_Acid_Phosphatase_Type_VI
Cluster_Acid_Phosphatase_Type_VI
Cluster_Acid_Phosphatase_Type_II

Figure S11a. Phylogenetic tree of cluster Xa of the acid phosphatase sequences included in the database.

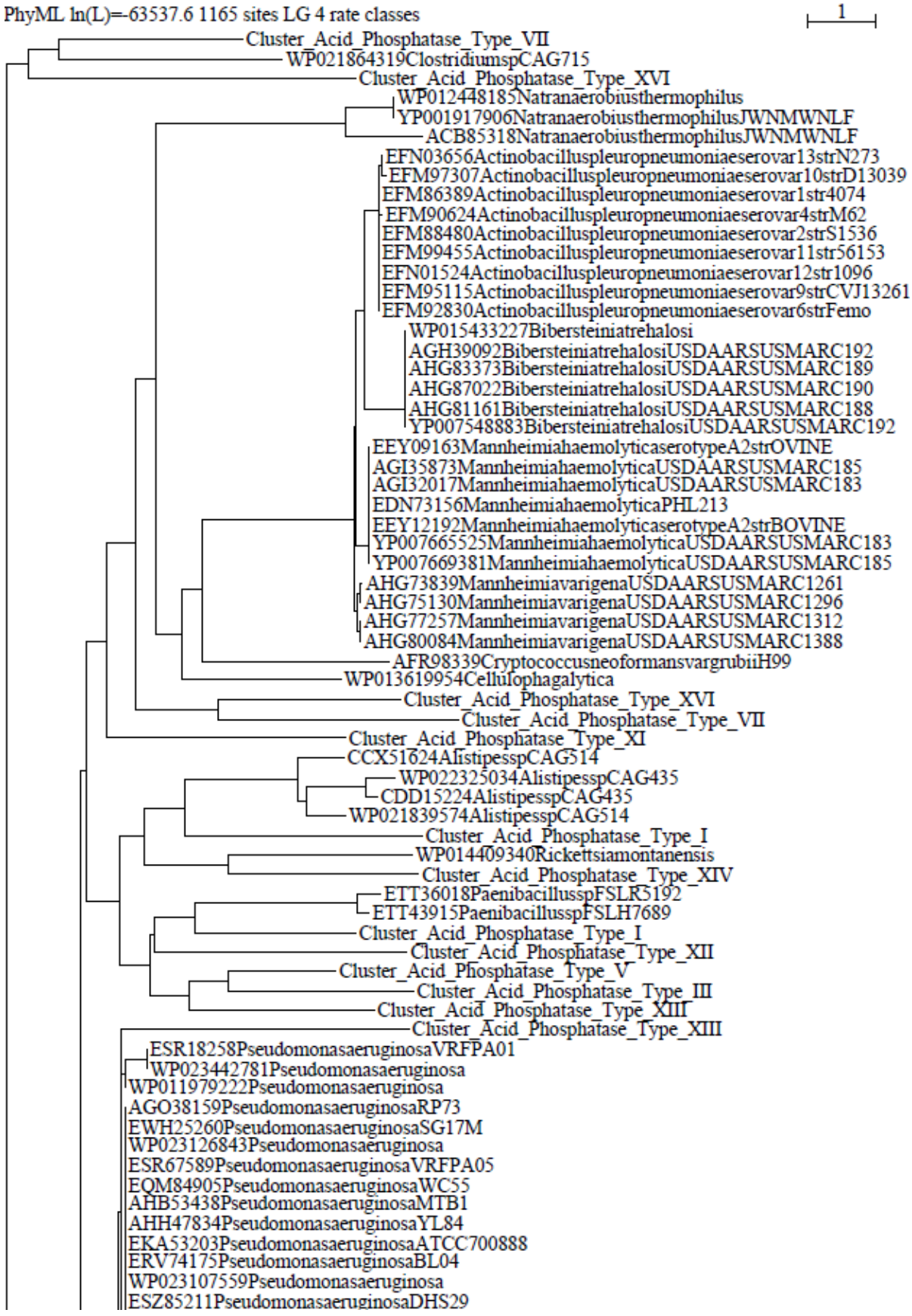

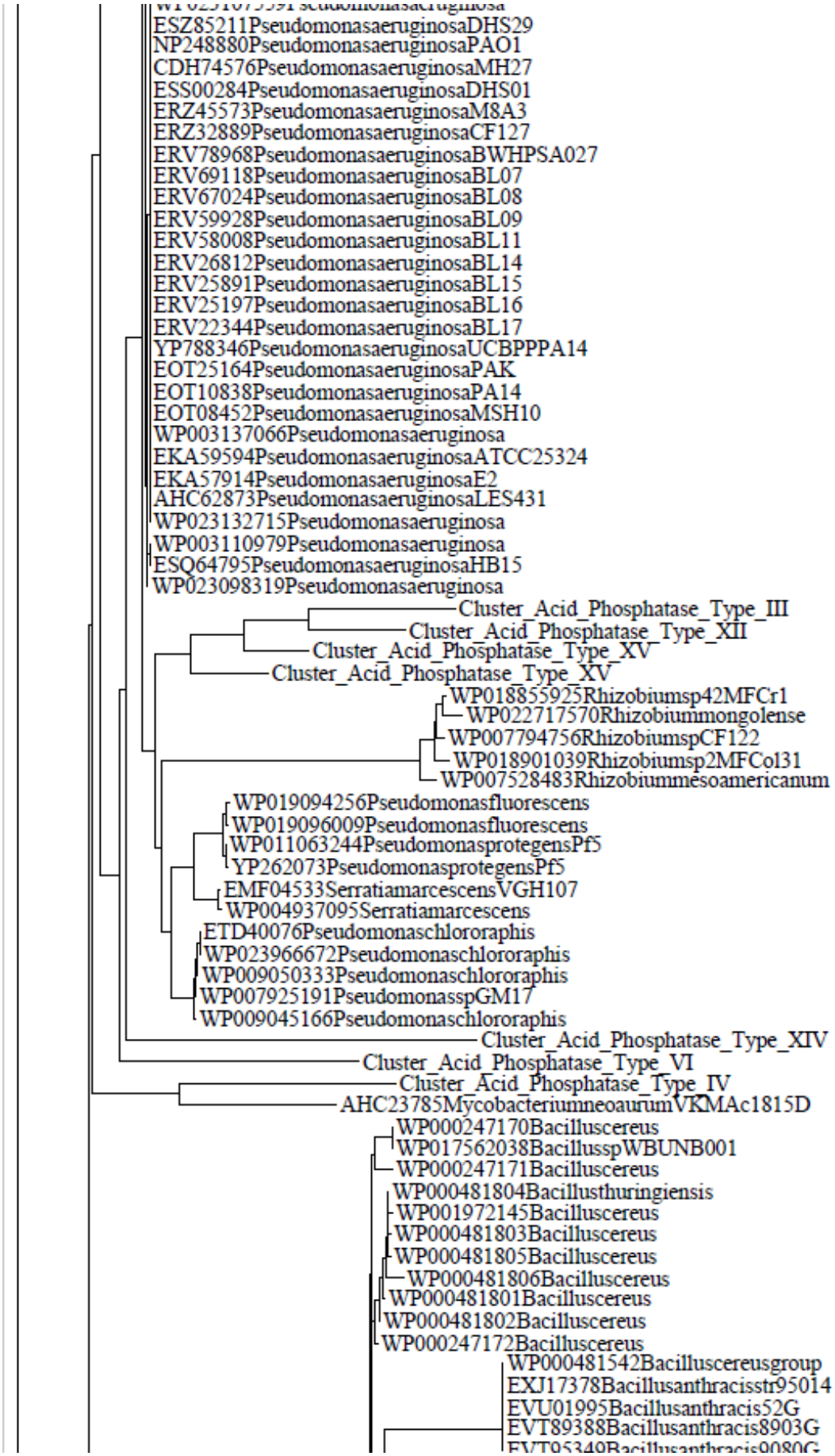
ESZ85211PseudomonasaeruginosaDHS29
NP248880PseudomonasaeruginosaPAO1
CDH74576PseudomonasaeruginosaMH27
ESS00284PseudomonasaeruginosaDHS01
ERZ45573PseudomonasaeruginosaM8A3
ERZ32889PseudomonasaeruginosaCF127
ERV78968PseudomonasaeruginosaBWHPSA027
ERV69118PseudomonasaeruginosaBL07
ERV67024PseudomonasaeruginosaBL08
ERV59928PseudomonasaeruginosaBL09
ERV58008PseudomonasaeruginosaBL11
ERV26812PseudomonasaeruginosaBL14
ERV25891PseudomonasaeruginosaBL15
ERV25197PseudomonasaeruginosaBL16
ERV22344PseudomonasaeruginosaBL17
YP788346PseudomonasaeruginosaUCBPPPA14
EOT25164PseudomonasaeruginosaPAK
EOT10838PseudomonasaeruginosaPA14
EOT08452PseudomonasaeruginosaMSH10
WP003137066Pseudomonasaeruginosa
EKA59594PseudomonasaeruginosaATCC25324
EKA57914PseudomonasaeruginosaE2
AHC62873PseudomonasaeruginosaLES431
WP023132715Pseudomonasaeruginosa
WP003110979Pseudomonasaeruginosa
ESQ64795PseudomonasaeruginosaHB15
WP023098319Pseudomonasaeruginosa
Cluster_Acid_Phosphatase_Type_III
Cluster_Acid_Phosphatase_Type_XII
Cluster_Acid_Phosphatase_Type_XV
Cluster_Acid_Phosphatase_Type_XV
WP018855925Rhizobiumsp42MFCr1
WP022717570Rhizobiummongolense
WP007794756RhizobiumspCF122
WP018901039Rhizobiumsp2MFCol31
WP007528483Rhizobiummesoamericanum
WP019094256Pseudomonasfluorescens
WP019096009Pseudomonasfluorescens
WP011063244PseudomonasprotegensPf5
YP262073PseudomonasprotegensPf5
EMF04533SerratiamarcescensVGH107
WP004937095Serratiamarcescens
ETD40076Pseudomonaschlororaphis
WP023966672Pseudomonaschlororaphis
WP009050333Pseudomonaschlororaphis
WP007925191PseudomonasspGM17
WP009045166Pseudomonaschlororaphis
Cluster_Acid_Phosphatase_Type_XIV
Cluster_Acid_Phosphatase_Type_VI
Cluster_Acid_Phosphatase_Type_IV
AHC23785MycobacteriumneoaurumVKMAc1815D
WP000247170Bacilluscereus
WP017562038BacillusspWBUNB001
WP000247171Bacilluscereus
WP000481804Bacillusthuringiensis
WP001972145Bacilluscereus
WP000481803Bacilluscereus
WP000481805Bacilluscereus
WP000481806Bacilluscereus
WP000481801Bacilluscereus
WP000481802Bacilluscereus
WP000247172Bacilluscereus
WP000481542Bacilluscereusgroup
EXJ17378Bacillusanthracisstr95014
EVU01995Bacillusanthracis52G
EVT89388Bacillusanthracis8903G

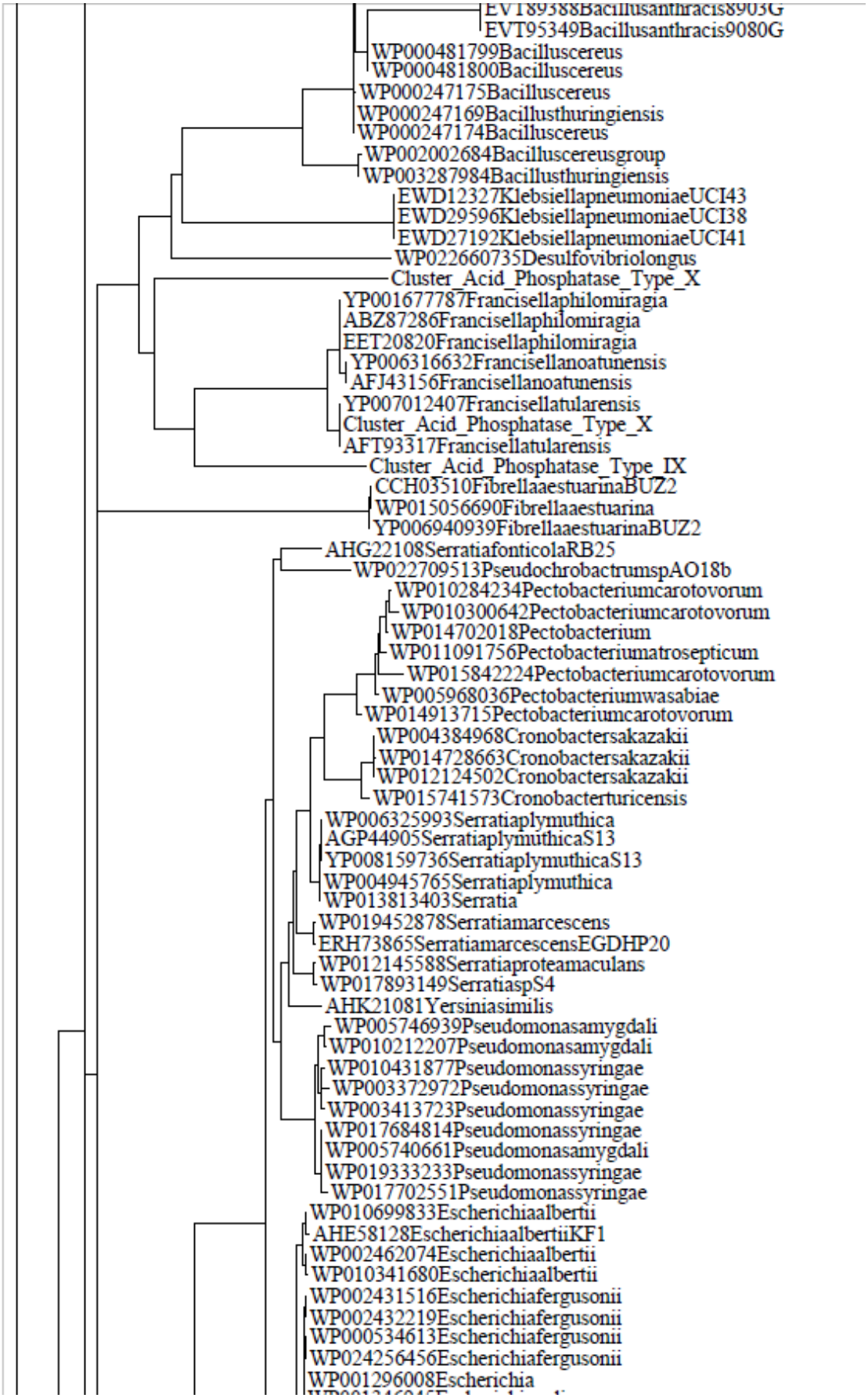
EVT89388Bacillusanthracis8903G
EVT95349Bacillusanthracis9080G
WP000481799Bacilluscereus
WP000481800Bacilluscereus
WP000247175Bacilluscereus
WP000247169Bacillusthuringiensis
WP000247174Bacilluscereus
WP002002684Bacilluscereusgroup
WP003287984Bacillusthuringiensis
EWD12327KlebsiellapneumoniaeUCI43
EWD29596KlebsiellapneumoniaeUCI38
EWD27192KlebsiellapneumoniaeUCI41
WP022660735Desulfovibriolongus
Cluster_Acid_Phosphatase_Type_X
YP001677787Francisellaphilomiragia
ABZ87286Francisellaphilomiragia
EET20820Francisellaphilomiragia
YP006316632Francisellanoatunensis
AFJ43156Francisellanoatunensis
YP007012407Francisellatularensis
Cluster_Acid_Phosphatase_Type_X
AFT93317Francisellatularensis
Cluster_Acid_Phosphatase_Type_IX
CCH03510FibrellaaestuarinaBUZ2
WP015056690Fibrellaaestuarina
YP006940939FibrellaaestuarinaBUZ2
AHG22108SerratiafonticolaRB25
WP022709513PseudochrobactrumspAO18b
WP010284234Pectobacteriumcarotovorum
WP010300642Pectobacteriumcarotovorum
WP014702018Pectobacterium
WP011091756Pectobacteriumatrosepticum
WP015842224Pectobacteriumcarotovorum
WP005968036Pectobacteriumwasabiae
WP014913715Pectobacteriumcarotovorum
WP004384968Cronobactersakazakii
WP014728663Cronobactersakazakii
WP012124502Cronobactersakazakii
WP015741573Cronobacterturicensis
WP006325993Serratiaplymuthica
AGP44905SerratiaplymuthicaS13
YP008159736SerratiaplymuthicaS13
WP004945765Serratiaplymuthica
WP013813403Serratia
WP019452878Serratiamarcescens
ERH73865SerratiamarcescensEGDHP20
WP012145588Serratiaproteamaculans
WP017893149SerratiaspS4
AHK21081Yersiniasimilis
WP005746939Pseudomonasamygdali
WP010212207Pseudomonasamygdali
WP010431877Pseudomonassyringae
WP003372972Pseudomonassyringae
WP003413723Pseudomonassyringae
WP017684814Pseudomonassyringae
WP005740661Pseudomonasamygdali
WP019333233Pseudomonassyringae
WP017702551Pseudomonassyringae
WP010699833Escherichiaalbertii
AHE58128EscherichiaalbertiiKF1
WP002462074Escherichiaalbertii
WP010341680Escherichiaalbertii
WP002431516Escherichiafergusonii
WP002432219Escherichiafergusonii
WP000534613Escherichiafergusonii
WP024256456Escherichiafergusonii
WP001296008Escherichia

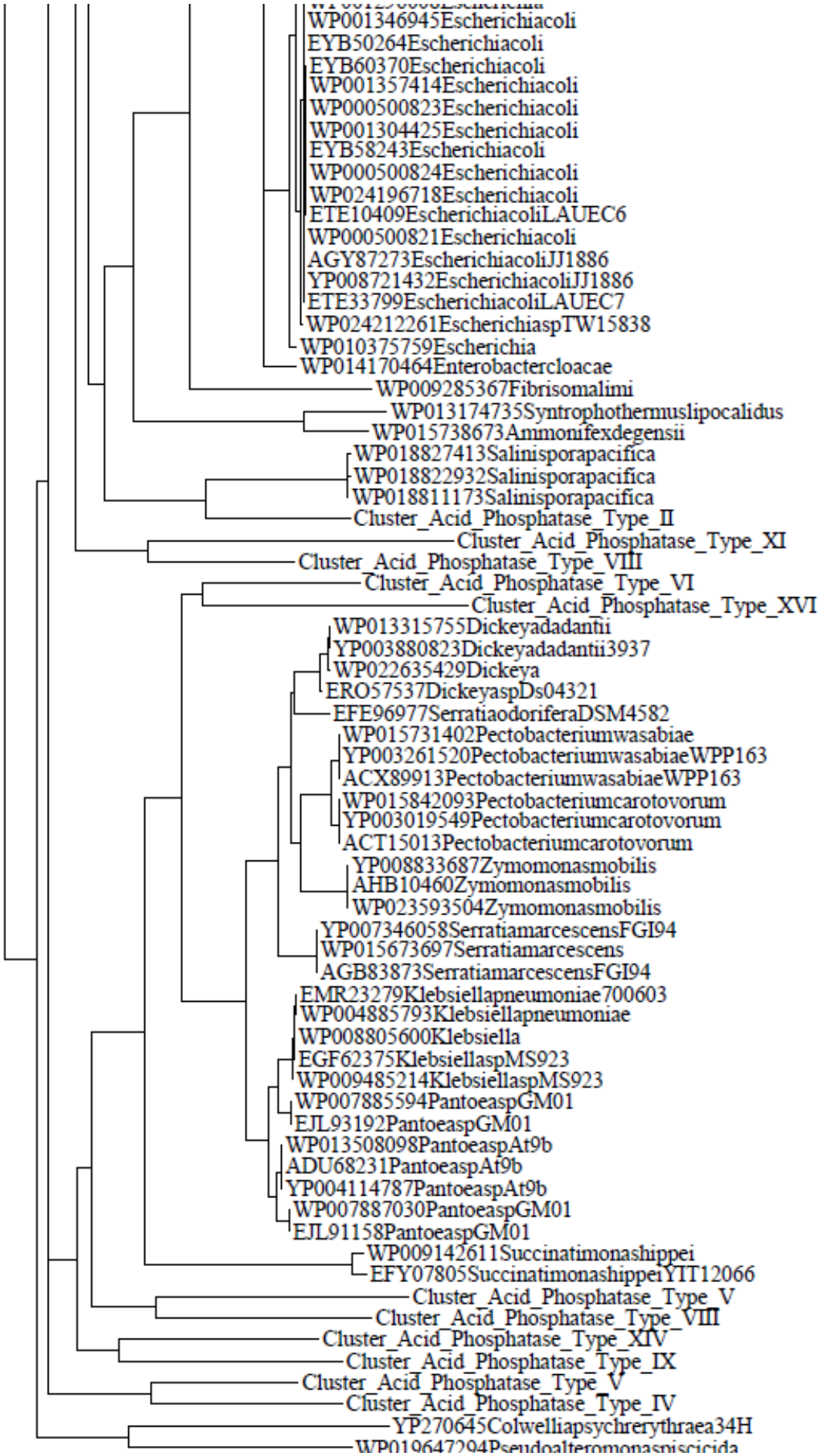
WP001346945Escherichiacoli
EYB50264Escherichiacoli
EYB60370Escherichiacoli
WP001357414Escherichiacoli
WP000500823Escherichiacoli
WP001304425Escherichiacoli
EYB58243Escherichiacoli
WP000500824Escherichiacoli
WP024196718Escherichiacoli
ETE10409EscherichiacoliLAUEC6
WP000500821Escherichiacoli
AGY87273EscherichiacoliJJ1886
YP008721432EscherichiacoliJJ1886
ETE33799EscherichiacoliLAUEC7
WP024212261EscherichiaspTW15838
WP010375759Escherichia
WP014170464Enterobactercloacae
WP009285367Fibrisomalimi
WP013174735Syntrophothermuslipocalidus
WP015738673Ammonifexdegensii
WP018827413Salinisporapacifica
WP018822932Salinisporapacifica
WP018811173Salinisporapacifica
Cluster_Acid_Phosphatase_Type_II
Cluster_Acid_Phosphatase_Type_XI
Cluster_Acid_Phosphatase_Type_VIII
Cluster_Acid_Phosphatase_Type_VI
Cluster_Acid_Phosphatase_Type_XVI
WP013315755Dickeyadadantii
YP003880823Dickeyadadantii3937
WP022635429Dickeya
ERO57537DickeyaspDs04321
EFE96977SerratiaodoriferaDSM4582
WP015731402Pectobacteriumwasabiae
YP003261520PectobacteriumwasabiaeWPP163
ACX89913PectobacteriumwasabiaeWPP163
WP015842093Pectobacteriumcarotovorum
YP003019549Pectobacteriumcarotovorum
ACT15013Pectobacteriumcarotovorum
YP008833687Zymomonasmobilis
AHB10460Zymomonasmobilis
WP023593504Zymomonasmobilis
YP007346058SerratiamarcescensFGI94
WP015673697Serratiamarcescens
AGB83873SerratiamarcescensFGI94
EMR23279Klebsiellapneumoniae700603
WP004885793Klebsiellapneumoniae
WP008805600Klebsiella
EGF62375KlebsiellaspMS923
WP009485214KlebsiellaspMS923
WP007885594PantoeaspGM01
EJL93192PantoeaspGM01
WP013508098PantoeaspAt9b
ADU68231PantoeaspAt9b
YP004114787PantoeaspAt9b
WP007887030PantoeaspGM01
EJL91158PantoeaspGM01
WP009142611Succinatimonashippei
EFY07805SuccinatimonashippeiYIT12066
Cluster_Acid_Phosphatase_Type_V
Cluster_Acid_Phosphatase_Type_VIII
Cluster_Acid_Phosphatase_Type_XIV
Cluster_Acid_Phosphatase_Type_IX
Cluster_Acid_Phosphatase_Type_V
Cluster_Acid_Phosphatase_Type_IV
YP270645Colwelliapsychrerythraea34H

Figure S11b. Phylogenetic tree of cluster Xb of the acid phosphatase sequences included in the database.

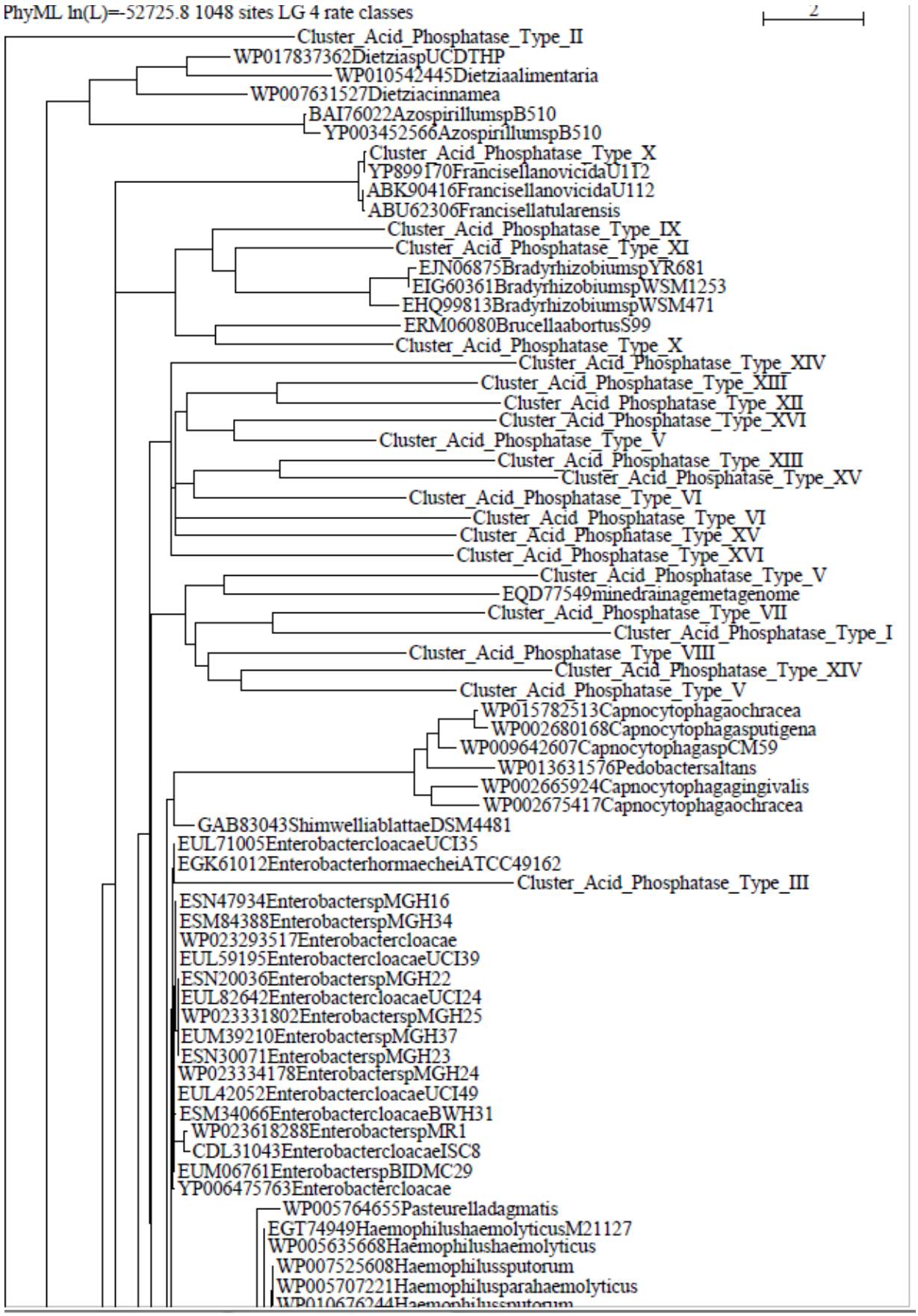

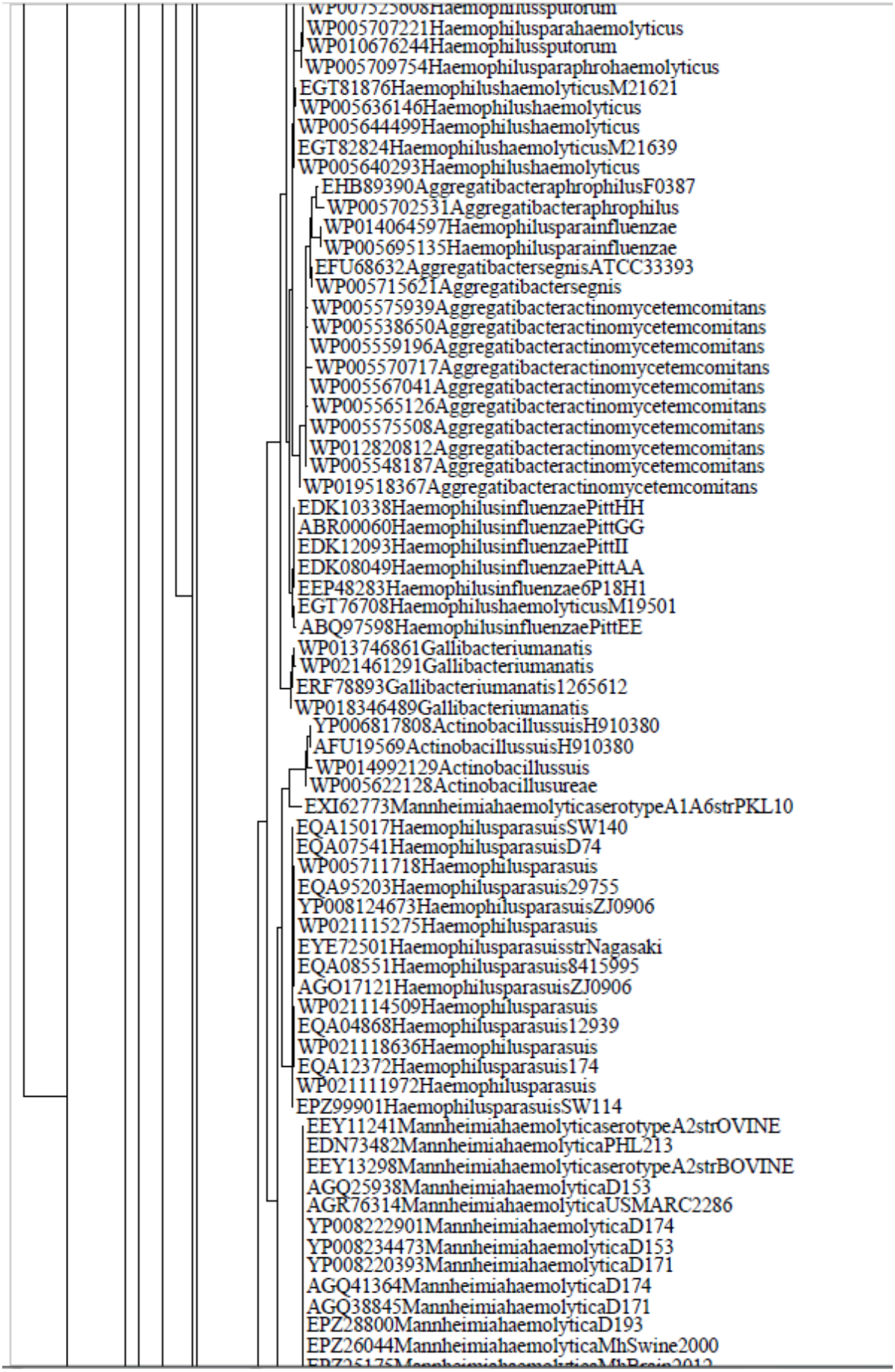
WP005707221HaemophilusparahaemolyticusWP010676244HaemophilusputorumWP005709754HaemophilusparaphrohaemolyticusEGT81876HaemophilushaemolyticusM21621WP005636146HaemophilushaemolyticusWP005644499HaemophilushaemolyticusEGT82824HaemophilushaemolyticusM21639WP005640293HaemophilushaemolyticusEHB89390AggregatibacteraphrophilusF0387WP005702531AggregatibacteraphrophilusWP014064597HaemophilusparainfluenzaeWP005695135HaemophilusparainfluenzaeEFU68632AggregatibactersegnisATCC33393WP005715621AggregatibactersegnisWP005575939AggregatibacteractinomycetemcomitansWP005538650AggregatibacteractinomycetemcomitansWP005559196AggregatibacteractinomycetemcomitansWP005570717AggregatibacteractinomycetemcomitansWP005567041AggregatibacteractinomycetemcomitansWP005565126AggregatibacteractinomycetemcomitansWP005575508AggregatibacteractinomycetemcomitansWP012820812AggregatibacteractinomycetemcomitansWP005548187AggregatibacteractinomycetemcomitansWP019518367AggregatibacteractinomycetemcomitansEDK10338HaemophilusinfluenzaePittHHABR00060HaemophilusinfluenzaePittGGEDK12093HaemophilusinfluenzaePittIIEDK08049HaemophilusinfluenzaePittAAEEP48283Haemophilusinfluenzae6P18H1EGT76708HaemophilushaemolyticusM19501ABQ97598HaemophilusinfluenzaePittEEWP013746861GallibacteriumanatisWP021461291GallibacteriumanatisERF78893Gallibacteriumanatis1265612WP018346489GallibacteriumanatisYP006817808ActinobacillussuisH910380AFU19569ActinobacillussuisH910380WP014992129ActinobacillussuisWP005622128ActinobacillusureaeEXI62773MannheimiahaemolyticaserotypeA1A6strPKL10EQA15017HaemophilusparasuisSW140EQA07541HaemophilusparasuisD74WP005711718HaemophilusparasuisEQA95203Haemophilusparasuis29755YP008124673HaemophilusparasuisZJ0906WP021115275HaemophilusparasuisEYE72501HaemophilusparasuisstrNagasakiEQA08551Haemophilusparasuis8415995AGO17121HaemophilusparasuisZJ0906WP021114509HaemophilusparasuisEQA04868Haemophilusparasuis12939WP021118636HaemophilusparasuisEQA12372Haemophilusparasuis174WP021111972HaemophilusparasuisEPZ99901HaemophilusparasuisSW114EEY11241MannheimiahaemolyticaserotypeA2strOVINEEDN73482MannheimiahaemolyticaPHL213EEY13298MannheimiahaemolyticaserotypeA2strBOVINEAGQ25938MannheimiahaemolyticaD153AGR76314MannheimiahaemolyticaUSMARC2286YP008222901MannheimiahaemolyticaD174YP008234473MannheimiahaemolyticaD153YP008220393MannheimiahaemolyticaD171AGQ41364MannheimiahaemolyticaD174AGQ38845MannheimiahaemolyticaD171EPZ28800MannheimiahaemolyticaD193EPZ26044MannheimiahaemolyticaMhSwine2000

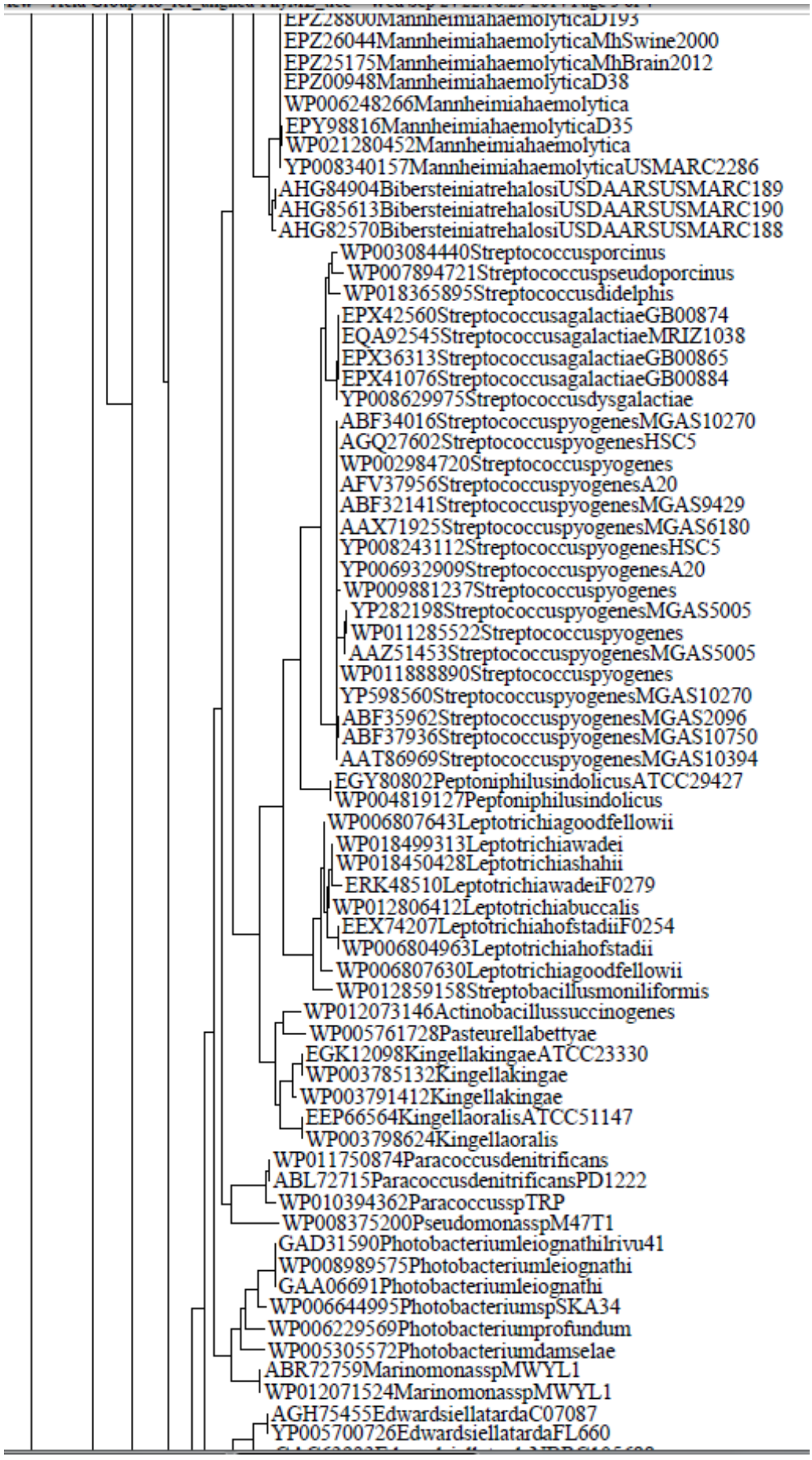
EPZ28800MannheimiahaemolyticaD193
EPZ26044MannheimiahaemolyticaMhSwine2000
EPZ25175MannheimiahaemolyticaMhBrain2012
EPZ00948MannheimiahaemolyticaD38
WP006248266Mannheimiahaemolytica
EPY98816MannheimiahaemolyticaD35
WP021280452Mannheimiahaemolytica
YP008340157MannheimiahaemolyticaUSMARC2286
AHG84904BibersteiniatrehalosiUSDAARSUSMARC189
AHG85613BibersteiniatrehalosiUSDAARSUSMARC190
AHG82570BibersteiniatrehalosiUSDAARSUSMARC188
WP003084440Streptococcusporcinus
WP007894721Streptococcuspseudoporcinus
WP018365895Streptococcusdidelphis
EPX42560StreptococcusagalactiaeGB00874
EQA92545StreptococcusagalactiaeMRIZ1038
EPX36313StreptococcusagalactiaeGB00865
EPX41076StreptococcusagalactiaeGB00884
YP008629975Streptococcusdysgalactiae
ABF34016StreptococcuspyogenesMGAS10270
AGQ27602StreptococcuspyogenesHSC5
WP002984720Streptococcuspyogenes
AFV37956StreptococcuspyogenesA20
ABF32141StreptococcuspyogenesMGAS9429
AAX71925StreptococcuspyogenesMGAS6180
YP008243112StreptococcuspyogenesHSC5
YP006932909StreptococcuspyogenesA20
WP009881237Streptococcuspyogenes
YP282198StreptococcuspyogenesMGAS5005
WP011285522Streptococcuspyogenes
AAZ51453StreptococcuspyogenesMGAS5005
WP011888890Streptococcuspyogenes
YP598560StreptococcuspyogenesMGAS10270
ABF35962StreptococcuspyogenesMGAS2096
ABF37936StreptococcuspyogenesMGAS10750
AAT86969StreptococcuspyogenesMGAS10394
EGY80802PeptoniphilusindolicusATCC29427
WP004819127Peptoniphilusindolicus
WP006807643Leptotrichiagoodfellowii
WP018499313Leptotrichiawadei
WP018450428Leptotrichiashahii
ERK48510LeptotrichiawadeiF0279
WP012806412Leptotrichiabuccalis
EEX74207LeptotrichiahofstadiiF0254
WP006804963Leptotrichiahofstadii
WP006807630Leptotrichiagoodfellowii
WP012859158Streptobacillusmoniliformis
WP012073146Actinobacillussuccinogenes
WP005761728Pasteurellabettyae
EGK12098KingellakingaeATCC23330
WP003785132Kingellakingae
WP003791412Kingellakingae
EEP66564KingellaoralisATCC51147
WP003798624Kingellaoralis
WP011750874Paracoccusdenitrificans
ABL72715ParacoccusdenitrificansPD1222
WP010394362ParacoccusspTRP
WP008375200PseudomonasspM47T1
GAD31590Photobacteriumleiognathilrivu41
WP008989575Photobacteriumleiognathi
GAA06691Photobacteriumleiognathi
WP006644995PhotobacteriumspSKA34
WP006229569Photobacteriumprofundum
WP005305572Photobacteriumdamselae
ABR72759MarinomonasspMWYL1
WP012071524MarinomonasspMWYL1
AGH75455EdwardsiellatardaC07087
YP005700726EdwardsiellatardaFL660


AGH75455EdwardsiellatardaC07087
YP005700726EdwardsiellatardaFL660
GAC63993EdwardsiellatardaNBRC105688
WP024199096Escherichiacoli
EGU39361VibrioscophthalmiLMG19158
WP005593938Vibrioscophthalmi
WP009387822VibriospN418
EGU30327VibriospN418
EDL53603VibrioshiloniiAK1
WP006071542Vibrioshilonii
Cluster_Acid_Phosphatase_Type_XVI
AEG95460EnterobacteraerogenesKCTC2190
EKT65881ProvidenciaalcalifaciensDmel2
EUC96215ProvidenciaalcalifaciensPAL2
EUD03673ProvidenciaalcalifaciensRIMD1656011
EEB47147ProvidenciaalcalifaciensDSM30120
EUD08432ProvidenciaalcalifaciensR901475
EFB73415ProvidenciarustigianiiDSM4541
EKT56911ProvidenciarettgeriDmel1
EFE55613ProvidenciarettgeriDSM1131
EKT62077ProvidenciaburhodogranarieaDSM19968
AFH95250ProvidenciastuartiiMRSN2154
CAA55131Morganellamorganii
EST59519ProteushauseriZMd44
WP023581332Proteushauseri
EEG83832ProteuspenneriATCC35198
AGS59297ProteusmirabilisBB2000
YP008397358ProteusmirabilisBB2000
YP002150495ProteusmirabilisHI4320
EKB01759ProteusmirabilisWGLW6
EKA96464ProteusmirabilisWGLW4
AFE59341RahnellaaquatilisHX2
EWF77405KlebsiellaoxytocaMGH41
EWF92308KlebsiellaoxytocaMGH27
ESN07862KlebsiellaoxytocaMGH28
AHM81919Klebsiellapneumoniae30684NJST2582
AAL59317Klebsiellapneumoniae
EYB74087KlebsiellapneumoniaeKb677
EYB79860KlebsiellapneumoniaeKb140
AHE46870Klebsiellapneumoniae
EOQ56926KlebsiellaspKTE92
ADC60677KlebsiellavariicolaAt22
CDA00527KlebsiellavariicolaCAG634
EUL82190EnterobacteraerogenesUCI28
EUL95955EnterobacteraerogenesUCI15
EUL94052EnterobacteraerogenesUCI16
EHT15002Klebsiellaoxytoca105246
ESS60039EnterobactercloacaeS611
WP023478432Enterobactercloacae
EJI89781KosakoniaradicincitansDSM16656
AHJ75672EnterobactersacchariSP1
CBG90344CitrobacterrodentiumICC168
YP003367081CitrobacterrodentiumICC168
WP001305722Escherichiacoli
EHM51749YokenellaregensburgeiATCC43003
Cluster_Acid_Phosphatase_Type_I
Cluster_Acid_Phosphatase_Type_XI
Cluster_Acid_Phosphatase_Type_XIV
Cluster_Acid_Phosphatase_Type_IV
Cluster_Acid_Phosphatase_Type_VIII
EPS61952Genliseaaurea
Cluster_Acid_Phosphatase_Type_IV
Cluster_Acid_Phosphatase_Type_VII
ADO75544StigmatellaaurantiacaDW431
Cluster_Acid_Phosphatase_Type_III
Cluster_Acid_Phosphatase_Type_XII
YP003957371StigmatellaaurantiacaDW431
Cluster_Acid_Phosphatase_Type_IX

Figure S11c. Phylogenetic tree of cluster Xc of the acid phosphatase sequences included in the database.

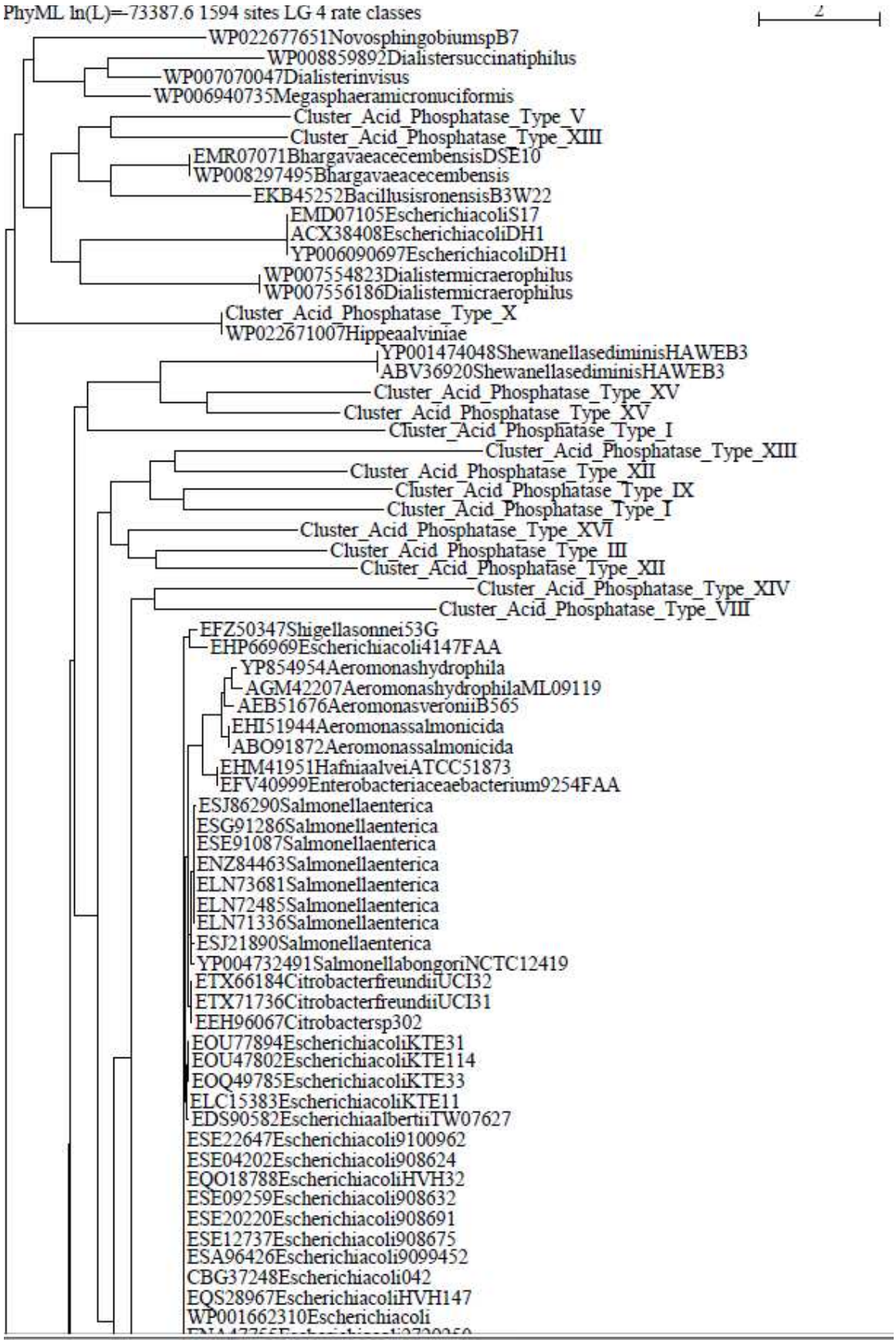

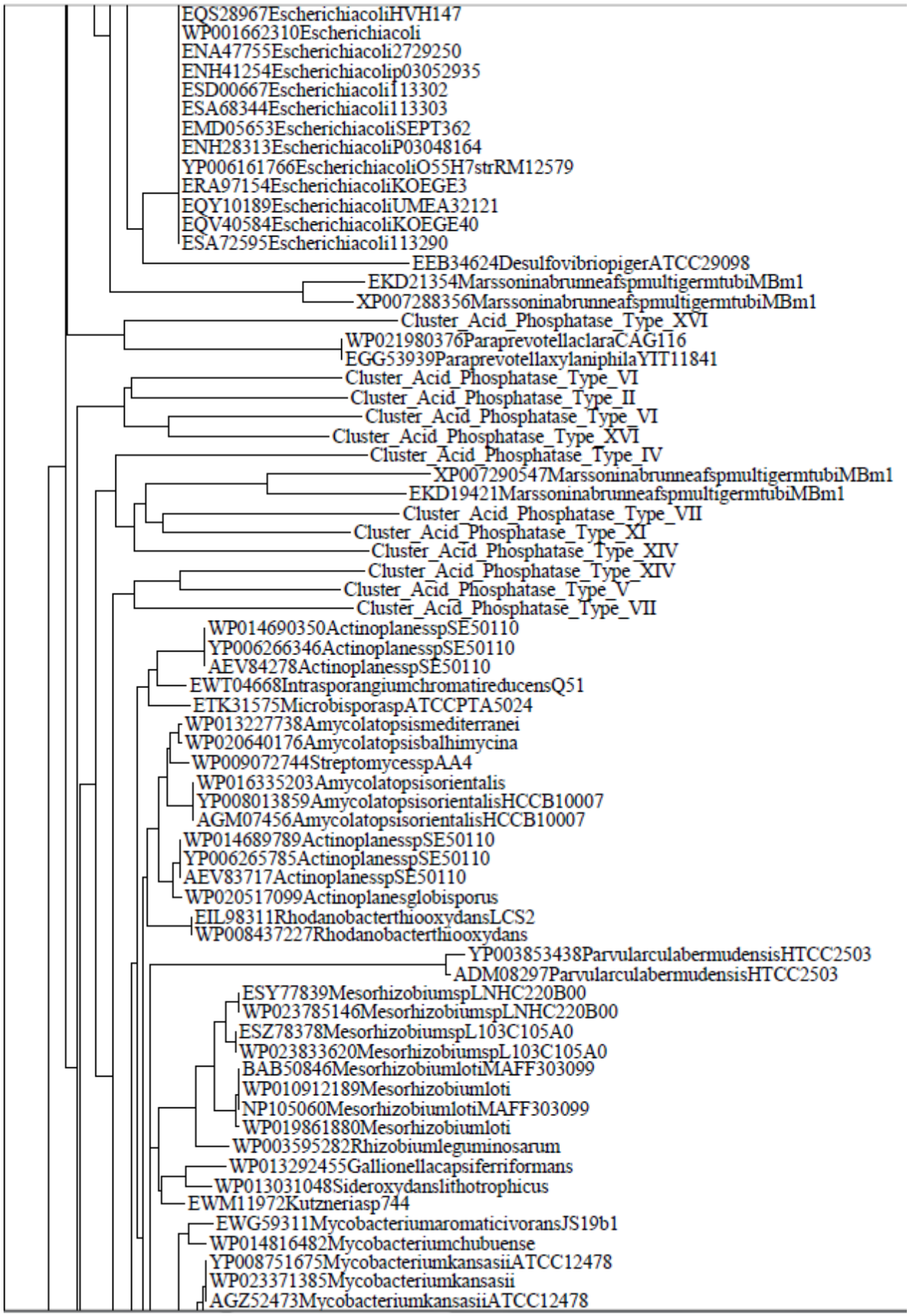
EQS28967EscherichiacoliHVH147
WP001662310Escherichiacoli
ENA47755Escherichiacoli2729250
ENH41254Escherichiacolip03052935
ESD00667Escherichiacoli113302
ESA68344Escherichiacoli113303
EMD05653EscherichiacoliSEPT362
ENH28313EscherichiacoliP03048164
YP006161766EscherichiacoliO55H7strRM12579
ERA97154EscherichiacoliKOEGE3
EQY10189EscherichiacoliUMEA32121
EQV40584EscherichiacoliKOEGE40
ESA72595Escherichiacoli113290
EEB34624DesulfovibriopigerATCC29098
EKD21354MarssoninabrunneafspmultigermtubiMBm1
XP007288356MarssoninabrunneafspmultigermtubiMBm1
Cluster_Acid_Phosphatase_Type_XVI
WP021980376ParaprevotellaclaraCAG116
EGG53939ParaprevotellaxylaniphilaYIT11841
Cluster_Acid_Phosphatase_Type_VI
Cluster_Acid_Phosphatase_Type_II
Cluster_Acid_Phosphatase_Type_VI
Cluster_Acid_Phosphatase_Type_XVI
Cluster_Acid_Phosphatase_Type_IV
XP007290547MarssoninabrunneafspmultigermtubiMBm1
EKD19421MarssoninabrunneafspmultigermtubiMBm1
Cluster_Acid_Phosphatase_Type_VII
Cluster_Acid_Phosphatase_Type_XI
Cluster_Acid_Phosphatase_Type_XIV
Cluster_Acid_Phosphatase_Type_XIV
Cluster_Acid_Phosphatase_Type_V
Cluster_Acid_Phosphatase_Type_VII
WP014690350ActinoplanesspSE50110
YP006266346ActinoplanesspSE50110
AEV84278ActinoplanesspSE50110
EWT04668IntrasporangiumchromatireducensQ51
ETK31575MicrobisporaspATCCPTA5024
WP013227738Amycolatopsismediterranei
WP020640176Amycolatopsisbalhimycina
WP009072744StreptomycesspAA4
WP016335203Amycolatopsisorientalis
YP008013859AmycolatopsisorientalisHCCB10007
AGM07456AmycolatopsisorientalisHCCB10007
WP014689789ActinoplanesspSE50110
YP006265785ActinoplanesspSE50110
AEV83717ActinoplanesspSE50110
WP020517099Actinoplanesglobisporus
EIL98311RhodanobacterthiooxydansLCS2
WP008437227Rhodanobacterthiooxydans
YP003853438ParvularculabermudensisHTCC2503
ADM08297ParvularculabermudensisHTCC2503
ESY77839MesorhizobiumspLNHC220B00
WP023785146MesorhizobiumspLNHC220B00
ESZ78378MesorhizobiumspL103C105A0
WP023833620MesorhizobiumspL103C105A0
BAB50846MesorhizobiumlotiMAFF303099
WP010912189Mesorhizobiumloti
NP105060MesorhizobiumlotiMAFF303099
WP019861880Mesorhizobiumloti
WP003595282Rhizobiumleguminosarum
WP013292455Gallionellacapsiferriformans
WP013031048Sideroxydanslithotrophicus
EWM11972Kutzneriasp744
EWG59311MycobacteriumaromaticivoransJS19b1
WP014816482Mycobacteriumchubuense
YP008751675MycobacteriumkansasiiATCC12478
WP023371385Mycobacteriumkansasii
AGZ52473MycobacteriumkansasiiATCC12478


WP023371385Mycobacteriumkansasii
AGZ52473MycobacteriumkansasiiATCC12478
ETW25879MycobacteriumgastriWayne
WP012393095Mycobacteriummarinum
YP001849529MycobacteriummarinumM
ACC39674MycobacteriummarinumM
AGC61341Mycobacteriumliflandii128FXT
YP007367848Mycobacteriumliflandii128FXT
WP015354799Mycobacteriumliflandii
WP011740611Mycobacteriumulcerans
EID16980MycobacteriumxenopiRIVM700367
WP003919173Mycobacteriumxenopi
WP015630790Mycobacteriumtuberculosis
YP007963182MycobacteriumtuberculosisCASNITR204
AGL28756MycobacteriumtuberculosisCASNITR204
CCJ01115MycobacteriumcanettiiCIPT140070010
YP007959300MycobacteriumtuberculosisstrHaarlemNITR202
WP015628826Mycobacteriumtuberculosis
AGL24871MycobacteriumtuberculosisstrHaarlemNITR202
ETB32727Mycobacteriumavium
WP023864899Mycobacteriumavium
ETB55751Mycobacteriumavium105560
ETB51518Mycobacteriumavium110986
WP023860886Mycobacteriumavium
WP023868119Mycobacteriumavium
WP014383217Mycobacteriumintracellulare
WP007168012Mycobacteriumparascrofulaceum
WP015794842Catenulisporaacidiphila
EWM10147Kutzneriasp744
EWM12357Kutzneriasp744
WP007918648Ktedonobacterracemifer
AHF15991NiabellasoliDSM19437
WP006601907Streptomycesauratus
WP018088530StreptomycesspFxanaC1
WP007268107StreptomycesspC
WP016573628Streptomycesalbulus
EOT02707StreptomycesalbulusCCRC11814
EXU89850StreptomycesalbulusPD1
WP018537696StreptomycesspMspMPM5
WP020122291Streptomycescanus
WP007386002Streptomycessviceus
WP020135559Streptomycessp351MFTsu51
WP014138696Kitasatosporasetae
YP004907355KitasatosporasetaeKM6054
EJJ02900StreptomycesauratusAGR0001
WP006607820Streptomycesauratus
WP014142100Streptomycescattleya
YP004910869StreptomycescattleyaNRRL8057
ETK37368MicrobisporaspATCCPTA5024
EST36587Streptomycesroseochromogenes
WP023544333Streptomycesroseochromogenes
WP011435192FrankiaspCcI3
WP013875372FrankiasymbiontofDatiscaglomerata
WP011604367Frankiaalni
YP713429FrankiaalniACN14a
WP006543515FrankiaspEUN1f
WP007267939StreptomycesspC
WP018556956StreptomycesspBoleA5
WP018530609StreptomycesspHmicA12
WP018523392StreptomycesspKhCrAH244
WP019521208StreptomycesspKhCrAH340
WP010987373Streptomycesavermitilis
NP827148StreptomycesavermitilisMA4680
WP009188259Streptomycesspe14
EFF90682Streptomycesspe14
WP019984617StreptomycesspAmel2xE9
WP010357505Streptomycesacidiscabies

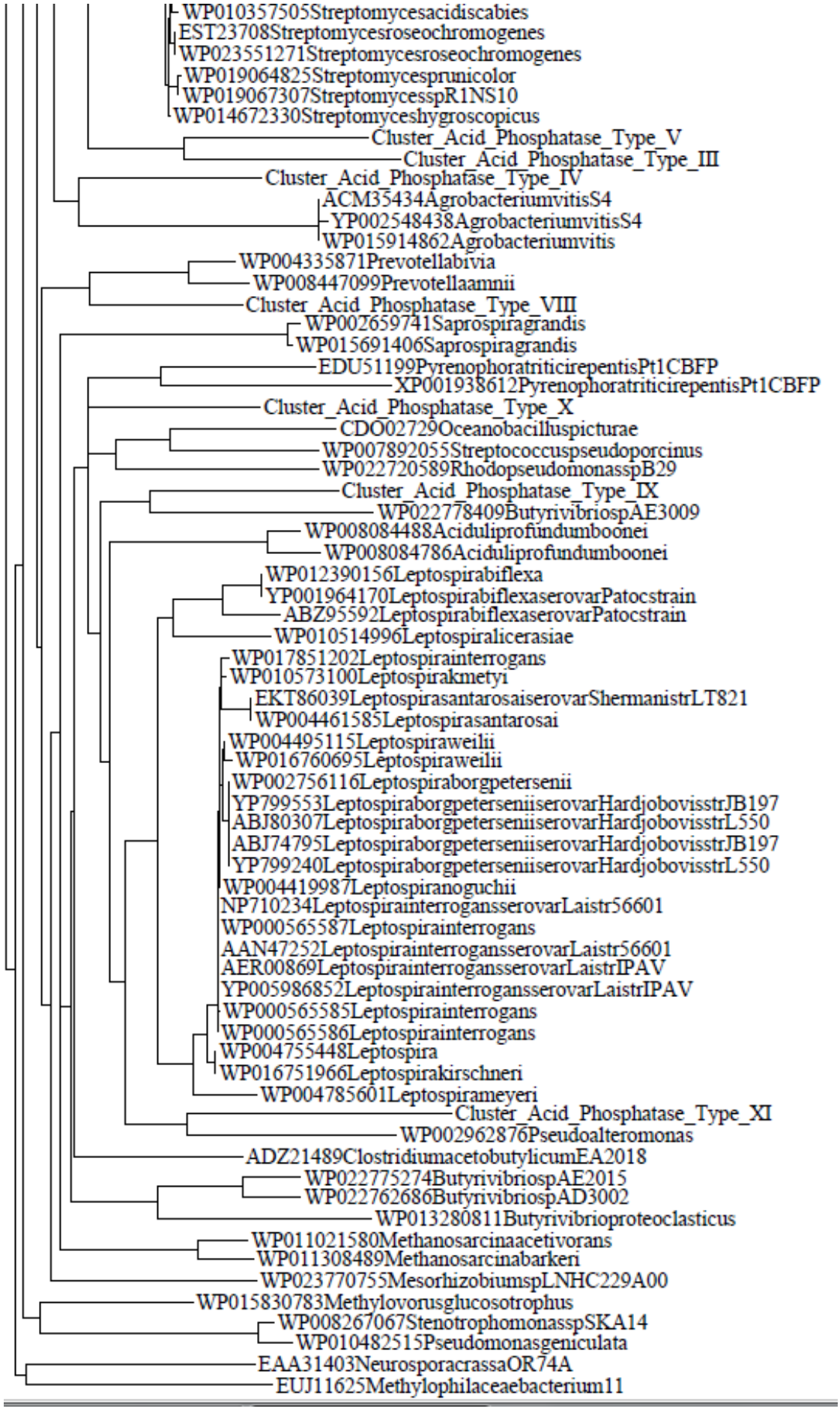
WP010357505Streptomycesacidiscabies
EST23708Streptomycesroseochromogenes
WP023551271Streptomycesroseochromogenes
WP019064825Streptomycesprunicolor
WP019067307StreptomycesspR1NS10
WP014672330Streptomyceshygroscopicus
Cluster_Acid_Phosphatase_Type_V
Cluster_Acid_Phosphatase_Type_III
Cluster_Acid_Phosphatase_Type_IV
ACM35434AgrobacteriumvitisS4
YP002548438AgrobacteriumvitisS4
WP015914862Agrobacteriumvitis
WP004335871Prevotellabivia
WP008447099Prevotellaamnii
Cluster_Acid_Phosphatase_Type_VIII
WP002659741Saprospiragrandis
WP015691406Saprospiragrandis
EDU51199PyrenophoratriticirepentisPt1CBFP
XP001938612PyrenophoratriticirepentisPt1CBFP
Cluster_Acid_Phosphatase_Type_X
CDO02729Oceanobacilluspicturae
WP007892055Streptococcuspseudoporcinus
WP022720589RhodopseudomonasspB29
Cluster_Acid_Phosphatase_Type_IX
WP022778409ButyrivibriospAE3009
WP008084488Aciduliprofundumboonei
WP008084786Aciduliprofundumboonei
WP012390156Leptospirabiflexa
YP001964170LeptospirabiflexaserovarPatocstrain
ABZ95592LeptospirabiflexaserovarPatocstrain
WP010514996Leptospiralicerasiae
WP017851202Leptospirainterrogans
WP010573100Leptospirakmetyi
EKT86039LeptospirasantarosaiserovarShermanistrLT821
WP004461585Leptospirasantarosai
WP004495115Leptospiraweilii
WP016760695Leptospiraweilii
WP002756116LeptospiraborgpetersenII
YP799553LeptospiraborgpetersenIIserovarHardjobovisstrJB197
ABJ80307LeptospiraborgpetersenIIserovarHardjobovisstrL550
ABJ74795LeptospiraborgpetersenIIserovarHardjobovisstrJB197
YP799240LeptospiraborgpetersenIIserovarHardjobovisstrL550
WP004419987Leptospiranoguchii
NP710234LeptospirainterrogansserovarLaistr56601
WP000565587Leptospirainterrogans
AAN47252LeptospirainterrogansserovarLaistr56601
AER00869LeptospirainterrogansserovarLaistrIPAV
YP005986852LeptospirainterrogansserovarLaistrIPAV
WP000565585Leptospirainterrogans
WP000565586Leptospirainterrogans
WP004755448Leptospira
WP016751966Leptospirakirschneri
WP004785601Leptospirameyeri
Cluster_Acid_Phosphatase_Type_XI
WP002962876Pseudoalteromonas
ADZ21489ClostridiumacetobutylicumEA2018
WP022775274ButyrivibriospAE2015
WP022762686ButyrivibriospAD3002
WP013280811Butyrivibrioproteoclasticus
WP011021580Methanosarcinaacetivorans
WP011308489Methanosarcinabarkeri
WP023770755MesorhizobiumspLNHC229A00
WP015830783Methylovorusglucosotrophus
WP008267067StenotrophomonasspSKA14
WP010482515Pseudomonasgeniculata
EAA31403NeurosporacrassaOR74A
EUJ11625Methylophilaceaebacterium11

Figure S12a. Phylogenetic tree of cluster XIa of the acid phosphatase sequences included in the database.

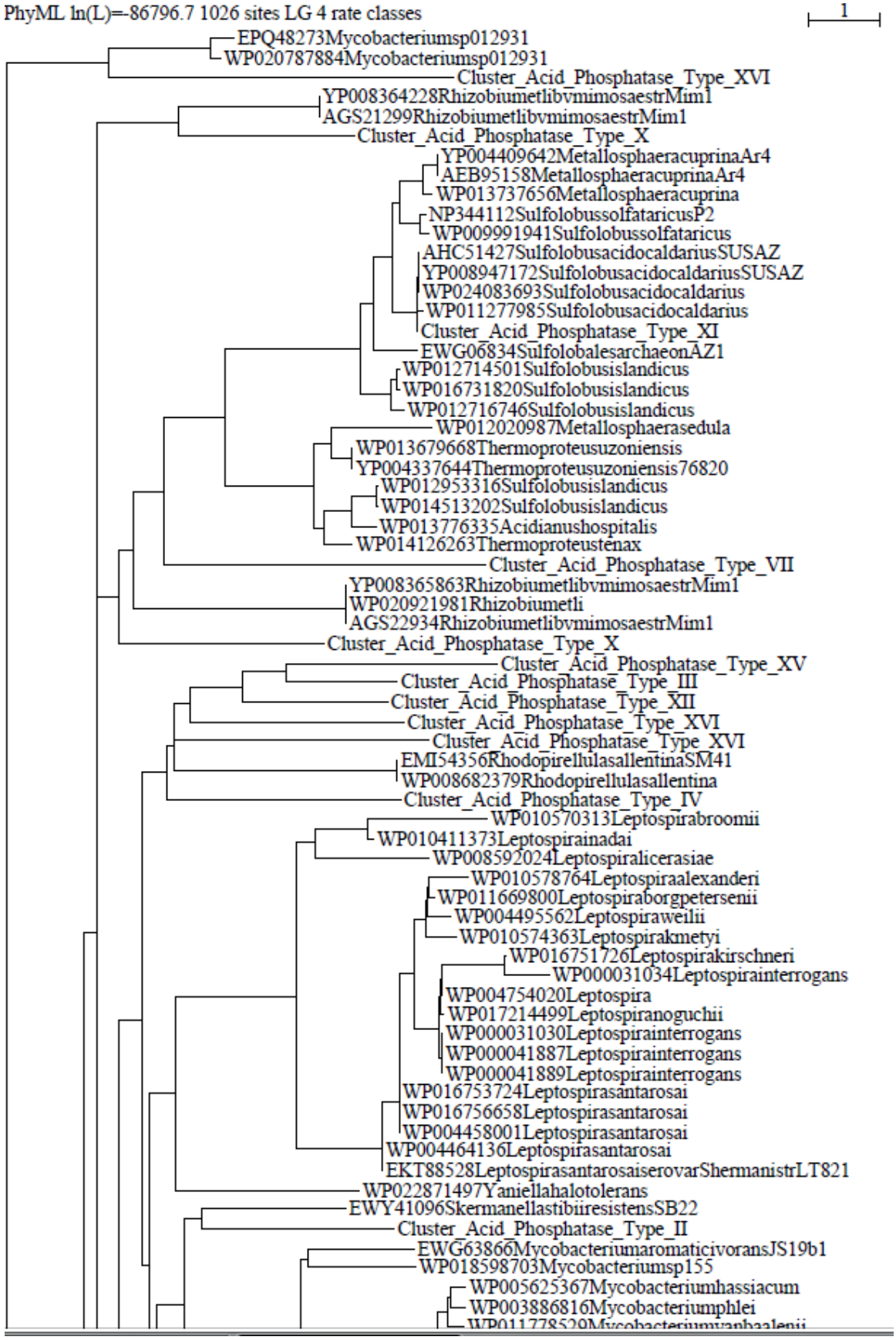

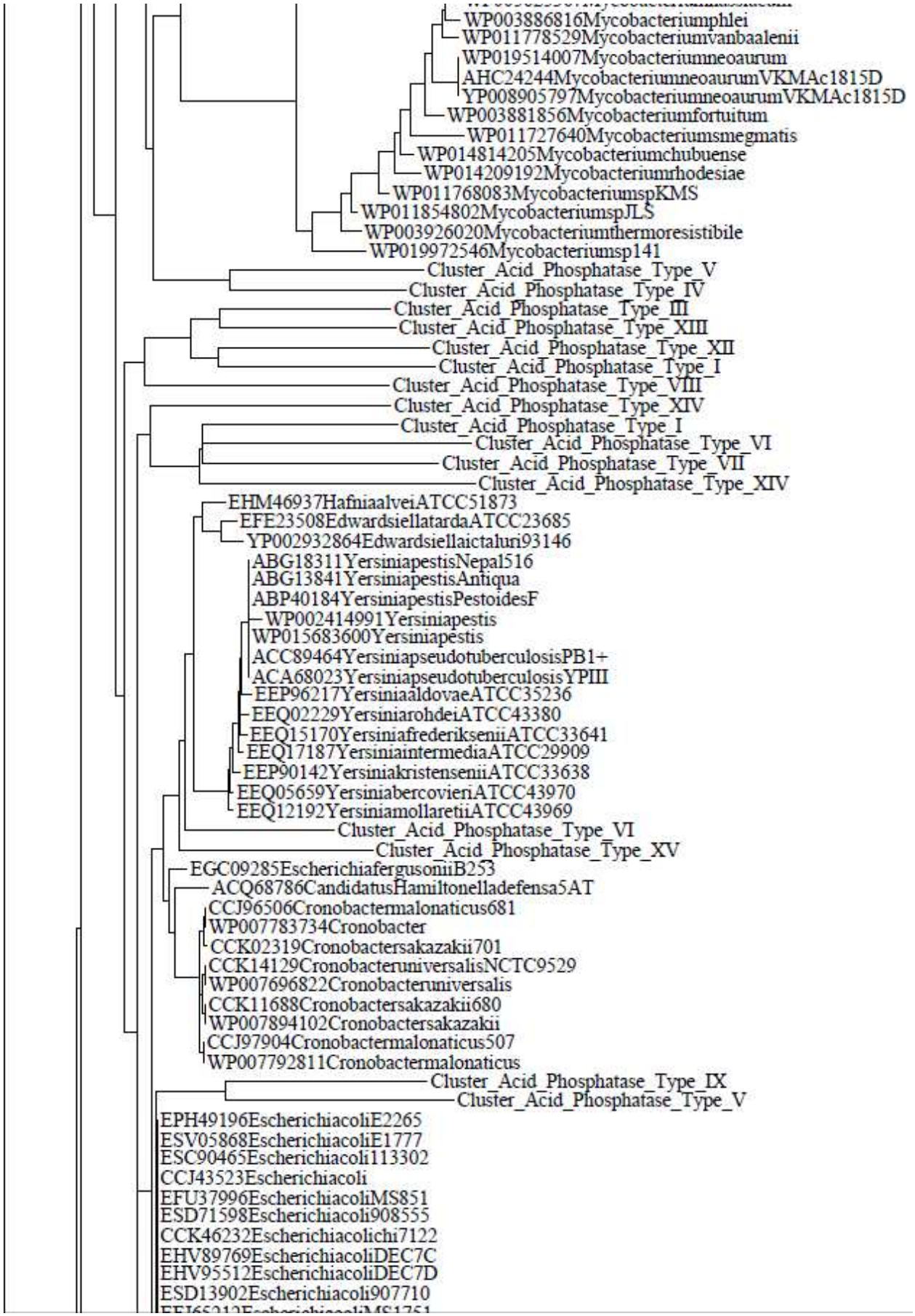
WP003886816Mycobacteriumphlei
WP011778529Mycobacteriumvanbaalenii
WP019514007Mycobacteriumneoaurum
AHC24244MycobacteriumneoaurumVKMAc1815D
YP008905797MycobacteriumneoaurumVKMAc1815D
WP003881856Mycobacteriumfortuitum
WP011727640Mycobacteriumsmegmatis
WP014814205Mycobacteriumchubuense
WP014209192Mycobacteriumrhodesiae
WP011768083MycobacteriumspKMS
WP011854802MycobacteriumspJLS
WP003926020Mycobacteriumthermoresistibile
WP019972546Mycobacteriumsp141
Cluster_Acid_Phosphatase_Type_V
Cluster_Acid_Phosphatase_Type_IV
Cluster_Acid_Phosphatase_Type_III
Cluster_Acid_Phosphatase_Type_XIII
Cluster_Acid_Phosphatase_Type_XII
Cluster_Acid_Phosphatase_Type_I
Cluster_Acid_Phosphatase_Type_VIII
Cluster_Acid_Phosphatase_Type_XIV
Cluster_Acid_Phosphatase_Type_I
Cluster_Acid_Phosphatase_Type_VI
Cluster_Acid_Phosphatase_Type_VII
Cluster_Acid_Phosphatase_Type_XIV
EHM46937HafniaalveiATCC51873
EFE23508EdwardsiellatardaATCC23685
YP002932864Edwardsiellaictaluri93146
ABG18311YersiniapestisNepal516
ABG13841YersiniapestisAntiqua
ABP40184YersiniapestisPestoidesF
WP002414991Yersiniapestis
WP015683600Yersiniapestis
ACC89464YersiniapseudotuberculosisPB1+
ACA68023YersiniapseudotuberculosisYPIII
EEP96217YersiniaaldovaeATCC35236
EEQ02229YersiniarohdeiATCC43380
EEQ15170YersiniafrederiksenniiATCC33641
EEQ17187YersiniaintermediaATCC29909
EEP90142YersiniakristenseniiATCC33638
EEQ05659YersiniabercovieriATCC43970
EEQ12192YersiniamollaretiiATCC43969
Cluster_Acid_Phosphatase_Type_VI
Cluster_Acid_Phosphatase_Type_XV
EGC09285EscherichiafergusoniiB253
ACQ68786CandidatusHamiltonelladefensa5AT
CCJ96506Cronobactermalonaticus681
WP007783734Cronobacter
CCK02319Cronobactersakazakii701
CCK14129CronobacteruniversalisNCTC9529
WP007696822Cronobacteruniversalis
CCK11688Cronobactersakazakii680
WP007894102Cronobactersakazakii
CCJ97904Cronobactermalonaticus507
WP007792811Cronobactermalonaticus
Cluster_Acid_Phosphatase_Type_IX
Cluster_Acid_Phosphatase_Type_V
EPH49196EscherichiacoliE2265
ESV05868EscherichiacoliE1777
ESC90465Escherichiacoli113302
CCJ43523Escherichiacoli
EFU37996EscherichiacoliMS851
ESD71598Escherichiacoli908555
CCK46232Escherichiacolichi7122
EHV89769EscherichiacoliDEC7C
EHV95512EscherichiacoliDEC7D
ESD13902Escherichiacoli907710

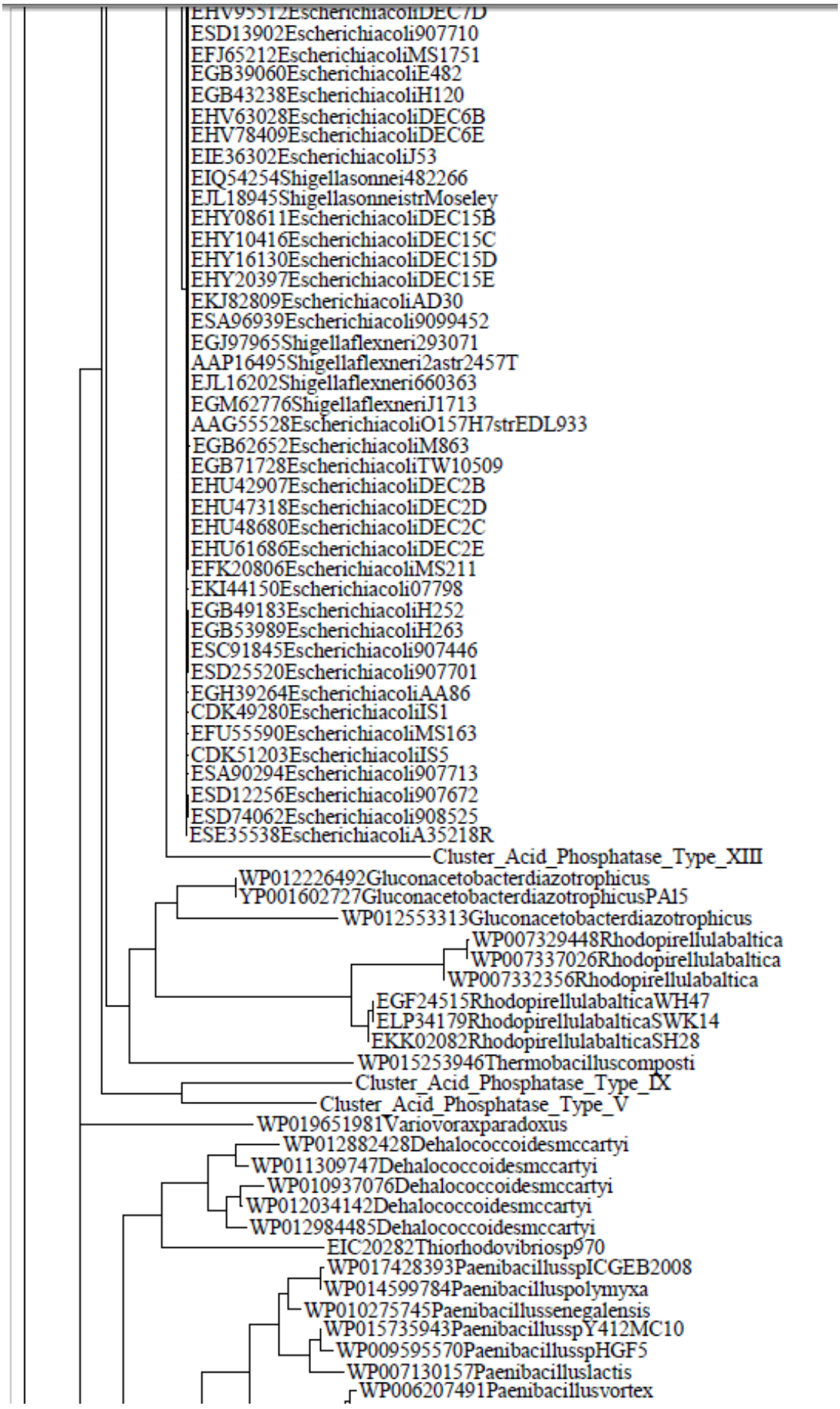
EHV95512EscherichiacoliDEC7D
ESD13902Escherichiacoli907710
EFJ65212EscherichiacoliMS1751
EGB39060EscherichiacoliE482
EGB43238EscherichiacoliH120
EHV63028EscherichiacoliDEC6B
EHV78409EscherichiacoliDEC6E
EIE36302EscherichiacoliJ53
EIQ54254Shigellasonnei482266
EJL18945ShigellasonneistrMoseley
EHY08611EscherichiacoliDEC15B
EHY10416EscherichiacoliDEC15C
EHY16130EscherichiacoliDEC15D
EHY20397EscherichiacoliDEC15E
EKJ82809EscherichiacoliAD30
ESA96939Escherichiacoli9099452
EGJ97965Shigellaflexneri293071
AAP16495Shigellaflexneri2astr2457T
EJL16202Shigellaflexneri660363
EGM62776ShigellaflexneriJ1713
AAG55528EscherichiacoliO157H7strEDL933
EGB62652EscherichiacoliM863
EGB71728EscherichiacoliTW10509
EHU42907EscherichiacoliDEC2B
EHU47318EscherichiacoliDEC2D
EHU48680EscherichiacoliDEC2C
EHU61686EscherichiacoliDEC2E
EFK20806EscherichiacoliMS211
EKI44150Escherichiacoli07798
EGB49183EscherichiacoliH252
EGB53989EscherichiacoliH263
ESC91845Escherichiacoli907446
ESD25520Escherichiacoli907701
EGH39264EscherichiacoliAA86
CDK49280EscherichiacoliIS1
EFU55590EscherichiacoliMS163
CDK51203EscherichiacoliIS5
ESA90294Escherichiacoli907713
ESD12256Escherichiacoli907672
ESD74062Escherichiacoli908525
ESE35538EscherichiacoliA35218R
Cluster_Acid_Phosphatase_Type_XIII
WP012226492Gluconacetobacterdiazotrophicus
YP001602727GluconacetobacterdiazotrophicusPA15
WP012553313Gluconacetobacterdiazotrophicus
WP007329448Rhodopirellulabaltica
WP007337026Rhodopirellulabaltica
WP007332356Rhodopirellulabaltica
EGF24515RhodopirellulabalticaWH47
ELP34179RhodopirellulabalticaSWK14
EKK02082RhodopirellulabalticaSH28
WP015253946Thermobacilluscomposti
Cluster_Acid_Phosphatase_Type_IX
Cluster_Acid_Phosphatase_Type_V
WP019651981Variovoraxparadoxus
WP012882428Dehalococcoidesmccartyi
WP011309747Dehalococcoidesmccartyi
WP010937076Dehalococcoidesmccartyi
WP012034142Dehalococcoidesmccartyi
WP012984485Dehalococcoidesmccartyi
EIC20282Thiorhodovibriosp970
WP017428393PaenibacillusspICGEB2008
WP014599784Paenibacilluspolymyxa
WP010275745Paenibacillussenegalensis
WP015735943PaenibacillusspY412MC10
WP009595570PaenibacillusspHGF5
WP007130157Paenibacilluslactis
WP006207491Paenibacillusvortex

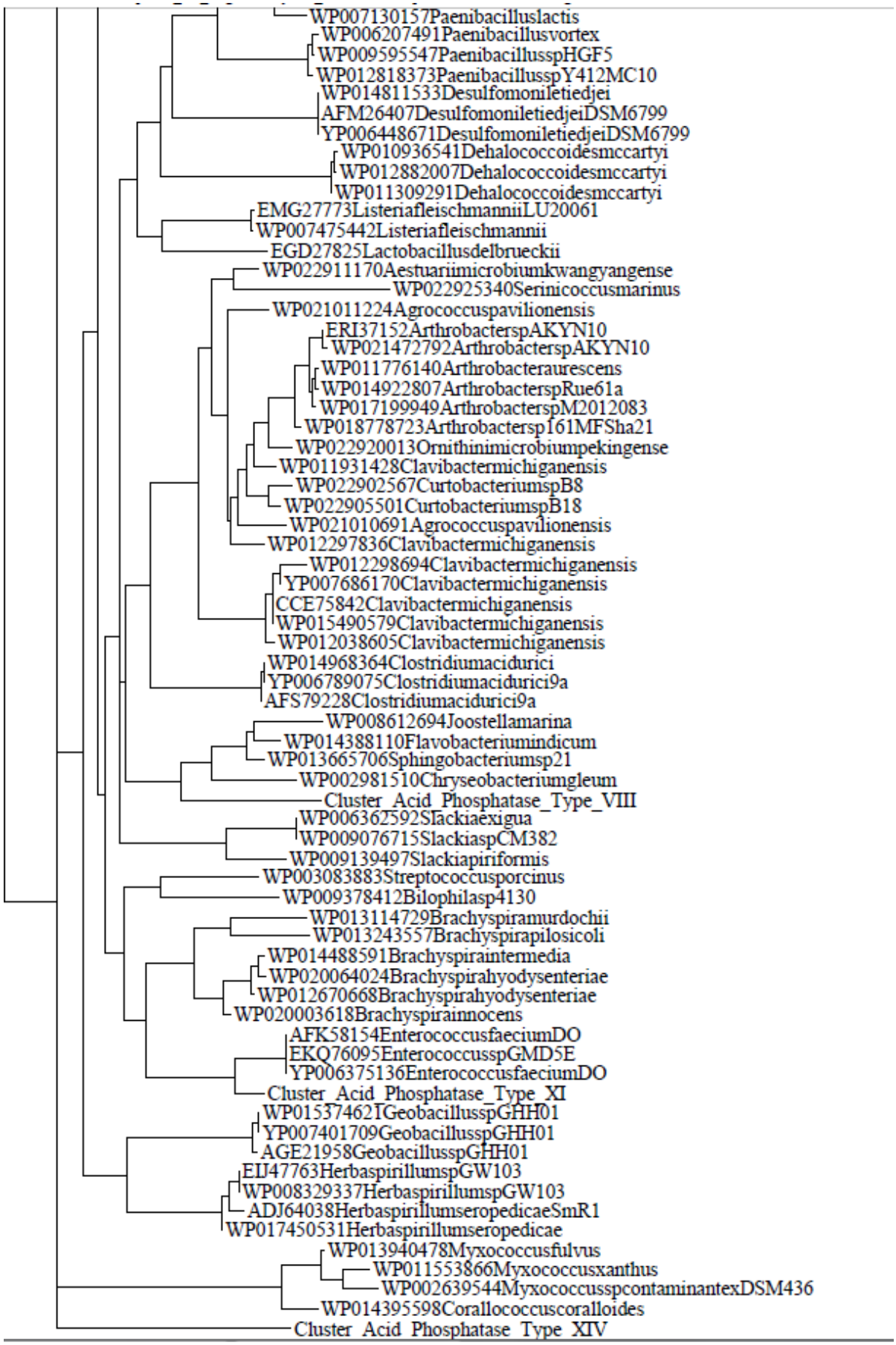
WP007130157Paenibacilluslactis
WP006207491Paenibacillusvortex
WP009595547PaenibacillusspHGF5
WP012818373PaenibacillusspY412MC10
WP014811533Desulfomoniletiedjei
AFM26407DesulfomoniletiedjeiDSM6799
YP006448671DesulfomoniletiedjeiDSM6799
WP010936541Dehalococcoidesmccartyi
WP012882007Dehalococcoidesmccartyi
WP011309291Dehalococcoidesmccartyi
EMG27773ListeriafleischmanniiLU20061
WP007475442Listeriafleischmannii
EGD27825Lactobacillusdelbrueckii
WP022911170Aestuariimicrobiumkwangyangense
WP022925340Serinicoccusmarinus
WP021011224Agrococcuspavilionensis
ERI37152ArthrobacterspAKYN10
WP021472792ArthrobacterspAKYN10
WP011776140Arthrobacteraurescens
WP014922807ArthrobacterspRue61a
WP017199949ArthrobacterspM2012083
WP018778723Arthrobactersp161MFSha21
WP022920013Ornithinimicrobiumpekingense
WP011931428Clavibactermichiganensis
WP022902567CurtobacteriumspB8
WP022905501CurtobacteriumspB18
WP021010691Agrococcuspavilionensis
WP012297836Clavibactermichiganensis
WP012298694Clavibactermichiganensis
YP007686170Clavibactermichiganensis
CCE75842Clavibactermichiganensis
WP015490579Clavibactermichiganensis
WP012038605Clavibactermichiganensis
WP014968364Clostridiumacidurici
YP006789075Clostridiumacidurici9a
AFS79228Clostridiumacidurici9a
WP008612694Joostellamarina
WP014388110Flavobacteriumindicum
WP013665706Sphingobacteriumsp21
WP002981510Chryseobacteriumgleum
Cluster_Acid_Phosphatase_Type_VIII
WP006362592Slackiaexigua
WP009076715SlackiaspCM382
WP009139497Slackiapiriformis
WP003083883Streptococcusporcinus
WP009378412Bilophilasp4130
WP013114729Brachyspiramurdochii
WP013243557Brachyspirapilosicoli
WP014488591Brachyspiraintermedia
WP020064024Brachyspirahyodysenteriae
WP012670668Brachyspirahyodysenteriae
WP020003618Brachyspirainnocens
AFK58154EnterococcusfaeciumDO
EKQ76095EnterococcusspGMD5E
YP006375136EnterococcusfaeciumDO
Cluster_Acid_Phosphatase_Type_XI
WP015374621GeobacillusspGHH01
YP007401709GeobacillusspGHH01
AGE21958GeobacillusspGHH01
EIJ47763HerbaspirillumspGW103
WP008329337HerbaspirillumspGW103
ADJ64038HerbaspirillumseropedicaeSmR1
WP017450531Herbaspirillumseropedicae
WP013940478Myxococcusfulvus
WP011553866Myxococcusxanthus
WP002639544MyxococcusspcontaminantexDSM436
WP014395598Corallococcuscoralloides
Cluster_Acid_Phosphatase_Type_XIV

Figure S12b. Phylogenetic tree of cluster XIb of the acid phosphatase sequences included in the database.

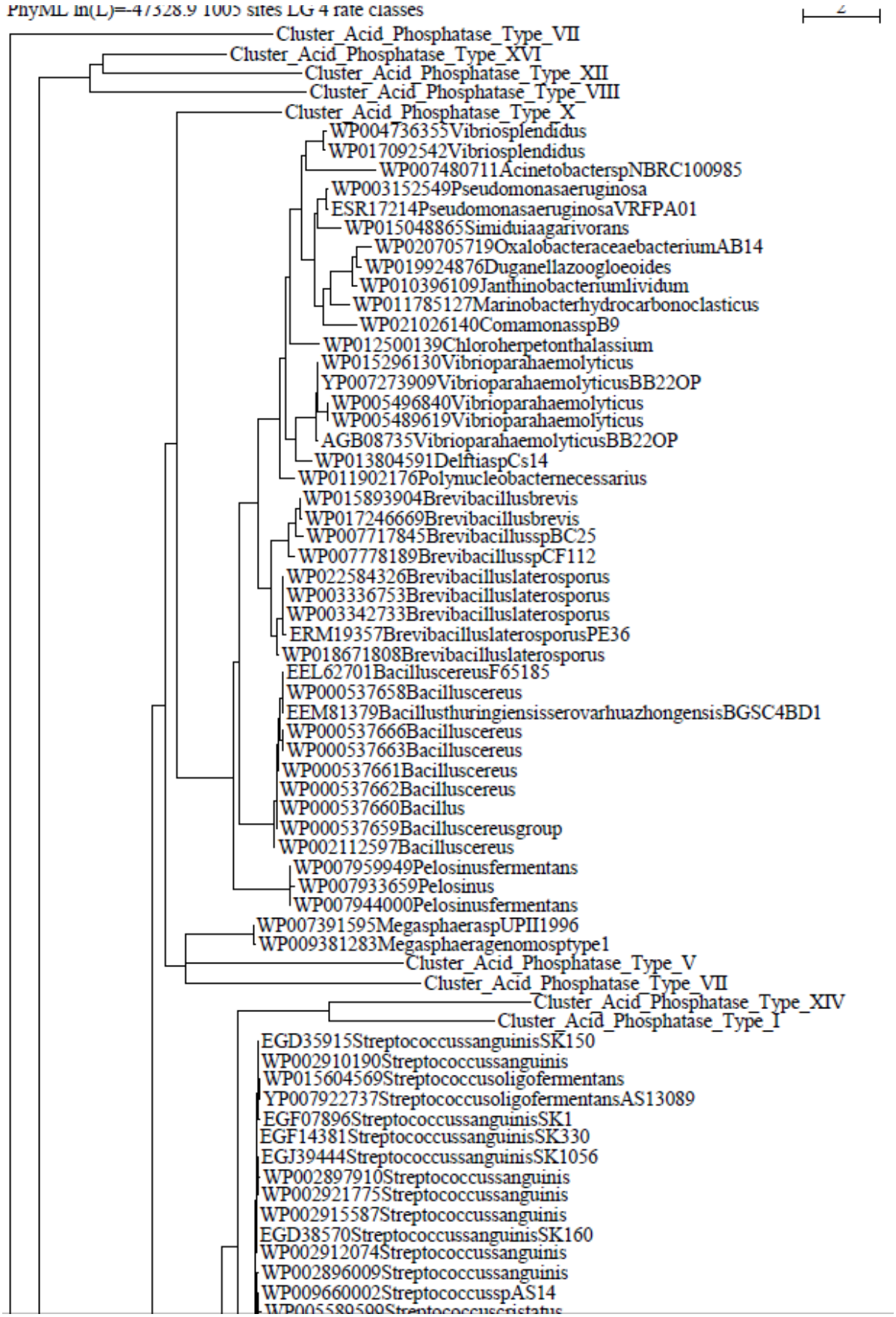


WP009660002StreptococcusspAS14
WP005589599Streptococcuscristatus
AGK70585StreptococcusoligofermentansAS13089
WP002932954Streptococcussanguinis
EGF05002StreptococcussanguinisSK1057
WP004187678Streptococcussanguinis
WP002902700Streptococcussanguinis
WP002900746Streptococcussanguinis
EGJ40857StreptococcussanguinisSK355
WP002919361Streptococcussanguinis
WP002904147Streptococcussanguinis
EGD30360StreptococcussanguinisSK72
YP001034761StreptococcussanguinisSK36
WP012130617Streptococcusgordonii
WP019315791Streptococcusmutans
WP019313958Streptococcusmutans
WP019803746Streptococcusmutans
WP019320663Streptococcusmutans
WP019315223Streptococcusmutans
WP019321592Streptococcusmutans
WP019318779Streptococcusmutans
WP019314344Streptococcusmutans
WP011074563Streptococcusmutans
WP019312531Streptococcusmutans
WP003088016Streptococcusratti
WP009854929Streptococcusgallolyticus
WP013643429Streptococcusgallolyticus
WP014295244Streptococcusmacedonicus
ETW87907StreptococcusthermophilusM17PTZA496
WP012962474Streptococcusgallolyticus
WP003066443Streptococcus
WP015695638Streptococcusinfantarius
WP006531962Streptococcusinfantarius
WP004233219Streptococcusequinus
WP019770710Streptococcussobrinus
WP019777342Streptococcussobrinus
WP019786579Streptococcussobrinus
WP002998509Streptococcus
WP019775697Streptococcussobrinus
WP004226111Streptococcuscriceti
WP014407817Streptococcuspyogenes
WP002988255Streptococcuspyogenes
WP011106606Streptococcuspyogenes
EPX11760StreptococcusagalactiaeLDS623
EPW92583StreptococcusagalactiaeMRIZ1023
EPX12005StreptococcusagalactiaeLDS610
EPX38833StreptococcusagalactiaeGB00867
WP011054969Streptococcuspyogenes
WP002983093Streptococcuspyogenes
YP008243816StreptococcuspyogenesHSC5
AGQ28134StreptococcuspyogenesHSC5
EPT99594StreptococcusagalactiaeBSU108
EPW73988StreptococcusagalactiaeBSU451
WP000446808Streptococcusagalactiae
WP017767232Streptococcusagalactiae
EPV88571StreptococcusagalactiaeFSLS3105
EPX05519StreptococcusagalactiaeMRIZ1217
EPV88455StreptococcusagalactiaeFSLS3251
EPV86208StreptococcusagalactiaeFSLC1487
EPU42032StreptococcusagalactiaeLDS628
EPU41511StreptococcusagalactiaeLDS617
EPU38617StreptococcusagalactiaeMRIZ1216
EPU34541StreptococcusagalactiaeMRIZ1214
EPU33004StreptococcusagalactiaeMRIZ1213
EPT43781StreptococcusagalactiaeFSLS3501
EPT40882StreptococcusagalactiaeFSLS3603
EPT34935StreptococcusagalactiaeFSLS3277

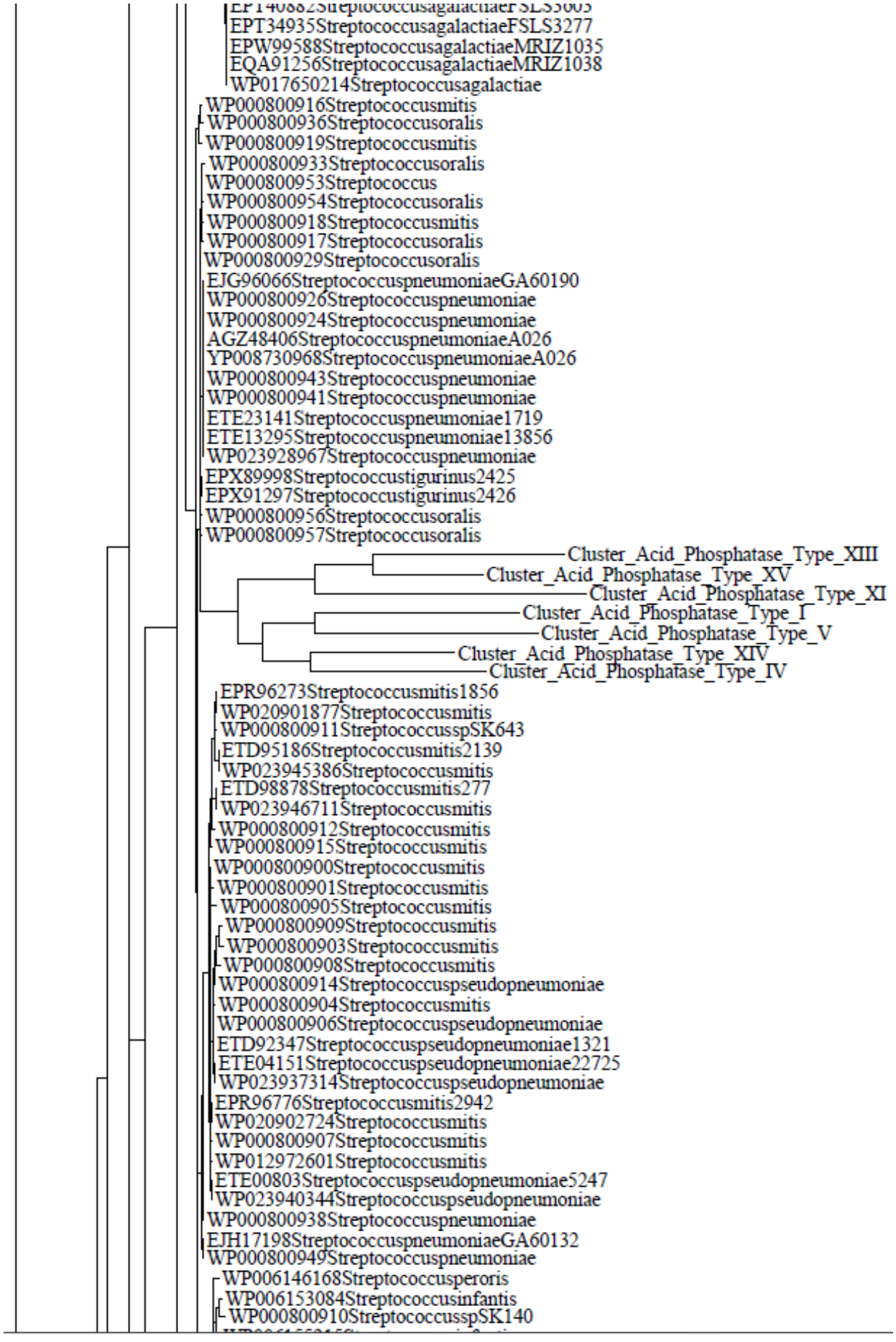
EPT34935StreptococcusagalactiaeFSLS3277
EPW99588StreptococcusagalactiaeMRIZ1035
EQA91256StreptococcusagalactiaeMRIZ1038
WP017650214Streptococcusagalactiae
WP000800916Streptococcusmitis
WP000800936Streptococcusoralis
WP000800919Streptococcusmitis
WP000800933Streptococcusoralis
WP000800953Streptococcus
WP000800954Streptococcusoralis
WP000800918Streptococcusmitis
WP000800917Streptococcusoralis
WP000800929Streptococcusoralis
EJG96066StreptococcuspneumoniaeGA60190
WP000800926Streptococcuspneumoniae
WP000800924Streptococcuspneumoniae
AGZ48406StreptococcuspneumoniaeA026
YP008730968StreptococcuspneumoniaeA026
WP000800943Streptococcuspneumoniae
WP000800941Streptococcuspneumoniae
ETE23141Streptococcuspneumoniae1719
ETE13295Streptococcuspneumoniae13856
WP023928967Streptococcuspneumoniae
EPX89998Streptococcustigurinus2425
EPX91297Streptococcustigurinus2426
WP000800956Streptococcusoralis
WP000800957Streptococcusoralis
Cluster_Acid_Phosphatase_Type_XIII
Cluster_Acid_Phosphatase_Type_XV
Cluster_Acid_Phosphatase_Type_XI
Cluster_Acid_Phosphatase_Type_I
Cluster_Acid_Phosphatase_Type_V
Cluster_Acid_Phosphatase_Type_XIV
Cluster_Acid_Phosphatase_Type_IV
EPR96273Streptococcusmitis1856
WP020901877Streptococcusmitis
WP000800911StreptococcusspSK643
ETD95186Streptococcusmitis2139
WP023945386Streptococcusmitis
ETD98878Streptococcusmitis277
WP023946711Streptococcusmitis
WP000800912Streptococcusmitis
WP000800915Streptococcusmitis
WP000800900Streptococcusmitis
WP000800901Streptococcusmitis
WP000800905Streptococcusmitis
WP000800909Streptococcusmitis
WP000800903Streptococcusmitis
WP000800908Streptococcusmitis
WP000800914Streptococcuspseudopneumoniae
WP000800904Streptococcusmitis
WP000800906Streptococcuspseudopneumoniae
ETD92347Streptococcuspseudopneumoniae1321
ETE04151Streptococcuspseudopneumoniae22725
WP023937314Streptococcuspseudopneumoniae
EPR96776Streptococcusmitis2942
WP020902724Streptococcusmitis
WP000800907Streptococcusmitis
WP012972601Streptococcusmitis
ETE00803Streptococcuspseudopneumoniae5247
WP023940344Streptococcuspseudopneumoniae
WP000800938Streptococcuspneumoniae
EJH17198StreptococcuspneumoniaeGA60132
WP000800949Streptococcuspneumoniae
WP006146168Streptococcusperoris
WP006153084Streptococcusinfantis
WP000800910StreptococcusspSK140

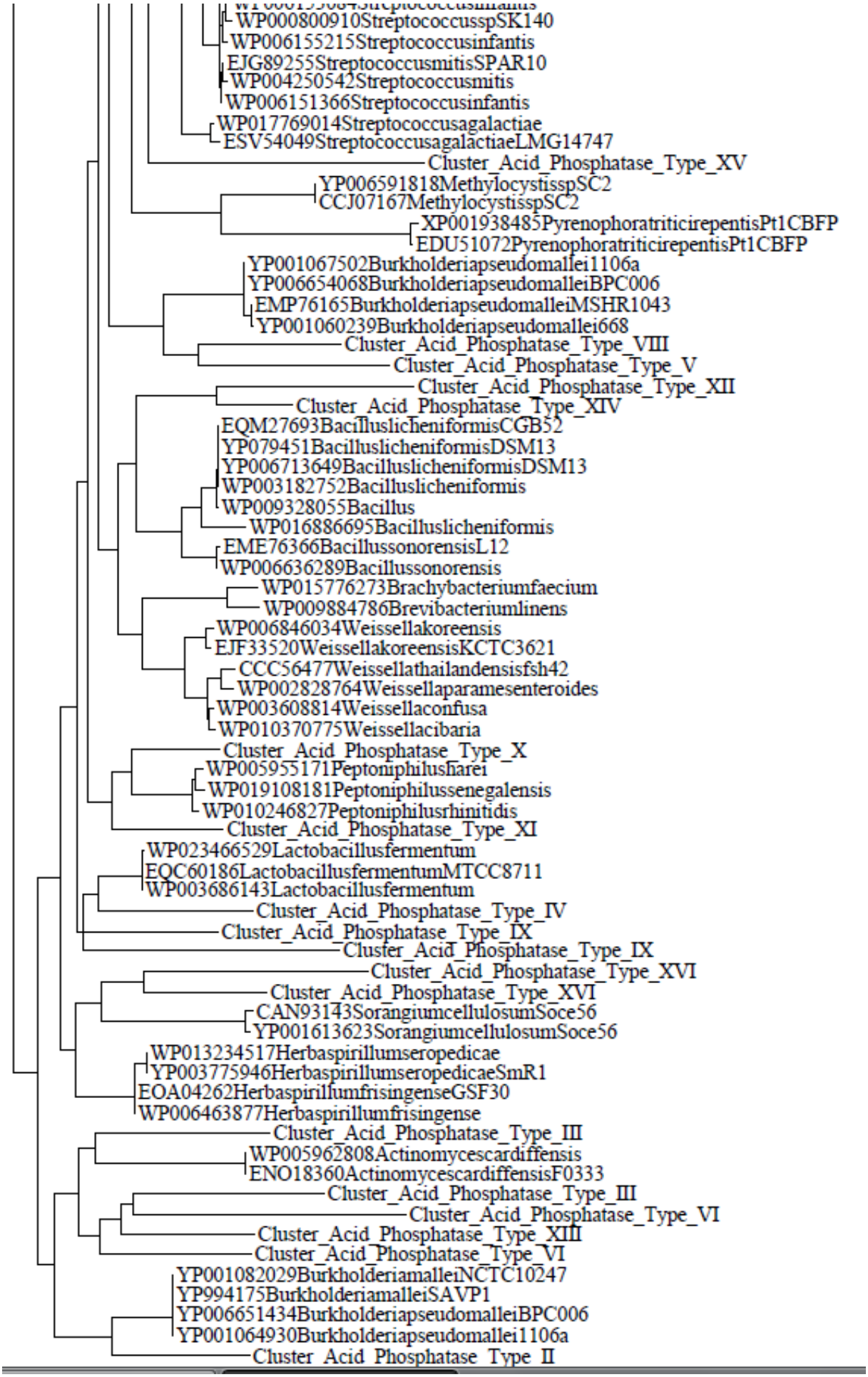
WP000800910StreptococcusspSK140
WP006155215Streptococcusinfantis
EJG89255StreptococcusmitisSPAR10
WP004250542Streptococcusmitis
WP006151366Streptococcusinfantis
WP017769014Streptococcusagalactiae
ESV54049StreptococcusagalactiaeLMG14747
Cluster_Acid_Phosphatase_Type_XV
YP006591818MethylocystisspSC2
CCJ07167MethylocystisspSC2
XP001938485PyrenophoratriticirepentisPt1CBFP
EDU51072PyrenophoratriticirepentisPt1CBFP
YP001067502Burkholderiapseudomallei1106a
YP006654068BurkholderiapseudomalleiBPC006
EMP76165BurkholderiapseudomalleiMSHR1043
YP001060239Burkholderiapseudomallei668
Cluster_Acid_Phosphatase_Type_VIII
Cluster_Acid_Phosphatase_Type_V
Cluster_Acid_Phosphatase_Type_XII
Cluster_Acid_Phosphatase_Type_XIV
EQM27693BacilluslicheniformisCGB52
YP079451BacilluslicheniformisDSM13
YP006713649BacilluslicheniformisDSM13
WP003182752Bacilluslicheniformis
WP009328055Bacillus
WP016886695Bacilluslicheniformis
EME76366BacillussonorensisL12
WP006636289Bacillussonorensis
WP015776273Brachybacteriumfaecium
WP009884786Brevibacteriumlinens
WP006846034Weissellakoreensis
EJF33520WeissellakoreensisKCTC3621
CCC56477Weissellathailandensisfsh42
WP002828764Weissellaparamesenteroides
WP003608814Weissellaconfusa
WP010370775Weissellacibaria
Cluster_Acid_Phosphatase_Type_X
WP005955171Peptoniphilusfarei
WP019108181Peptoniphilussenegalensis
WP010246827Peptoniphilusrhinitidis
Cluster_Acid_Phosphatase_Type_XI
WP023466529Lactobacillusfermentum
EQC60186LactobacillusfermentumMTCC8711
WP003686143Lactobacillusfermentum
Cluster_Acid_Phosphatase_Type_IV
Cluster_Acid_Phosphatase_Type_IX
Cluster_Acid_Phosphatase_Type_IX
Cluster_Acid_Phosphatase_Type_XVI
Cluster_Acid_Phosphatase_Type_XVI
CAN93143SorangiumcellulosumSoce56
YP001613623SorangiumcellulosumSoce56
WP013234517Herbaspirillumseropedicae
YP003775946HerbaspirillumseropedicaeSmR1
EOA04262HerbaspirillumfrisingenseGSF30
WP006463877Herbaspirillumfrisingense
Cluster_Acid_Phosphatase_Type_III
WP005962808Actinomycescardiffensis
ENO18360ActinomycescardiffensisF0333
Cluster_Acid_Phosphatase_Type_III
Cluster_Acid_Phosphatase_Type_VI
Cluster_Acid_Phosphatase_Type_XIII
Cluster_Acid_Phosphatase_Type_VI
YP001082029BurkholderiamalleiNCTC10247
YP994175BurkholderiamalleiSAVP1
YP006651434BurkholderiapseudomalleiBPC006
YP001064930Burkholderiapseudomallei1106a
Cluster_Acid_Phosphatase_Type_II

Figure S13a. Phylogenetic tree of cluster XIIa of the acid phosphatase sequences included in the database.

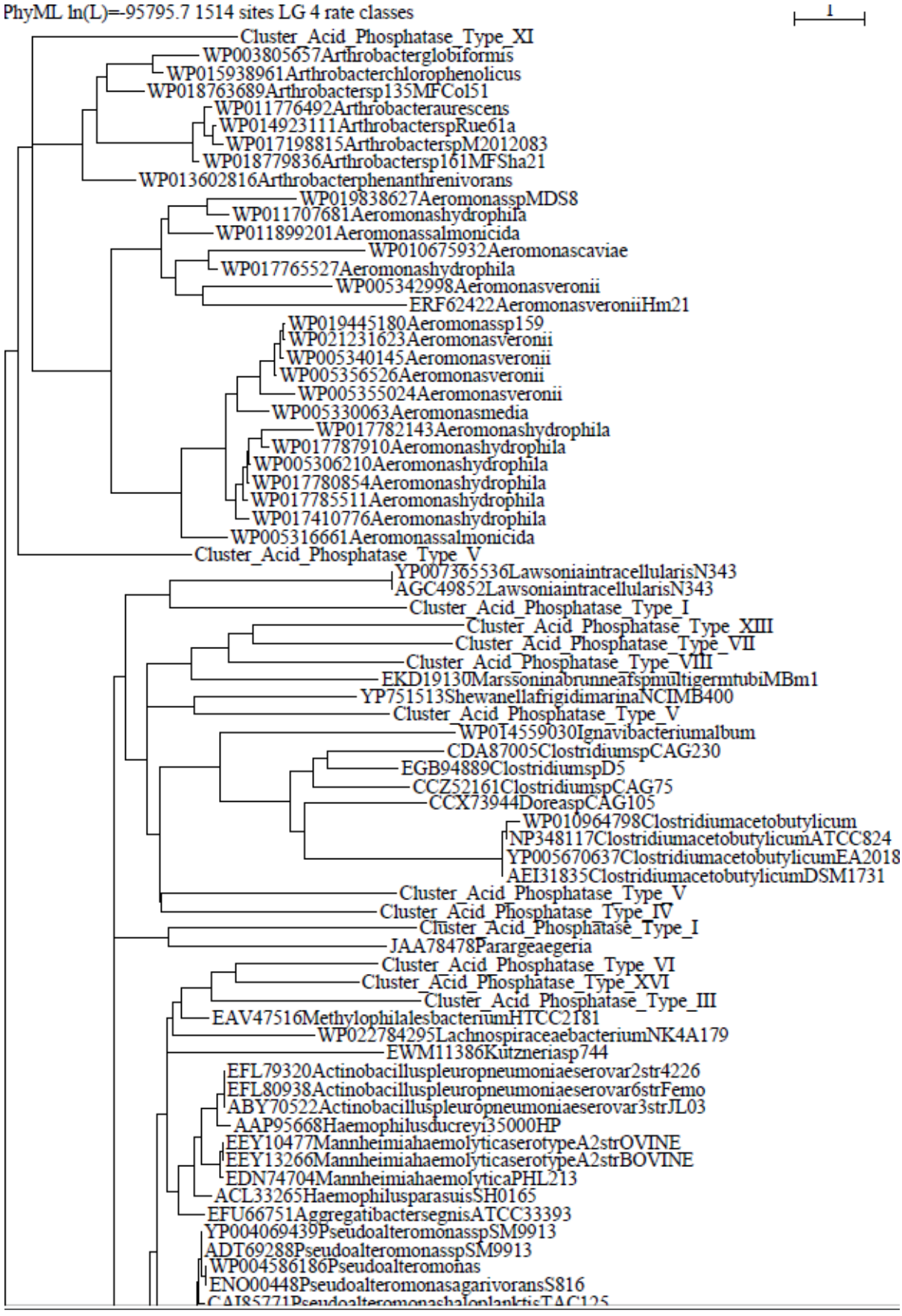

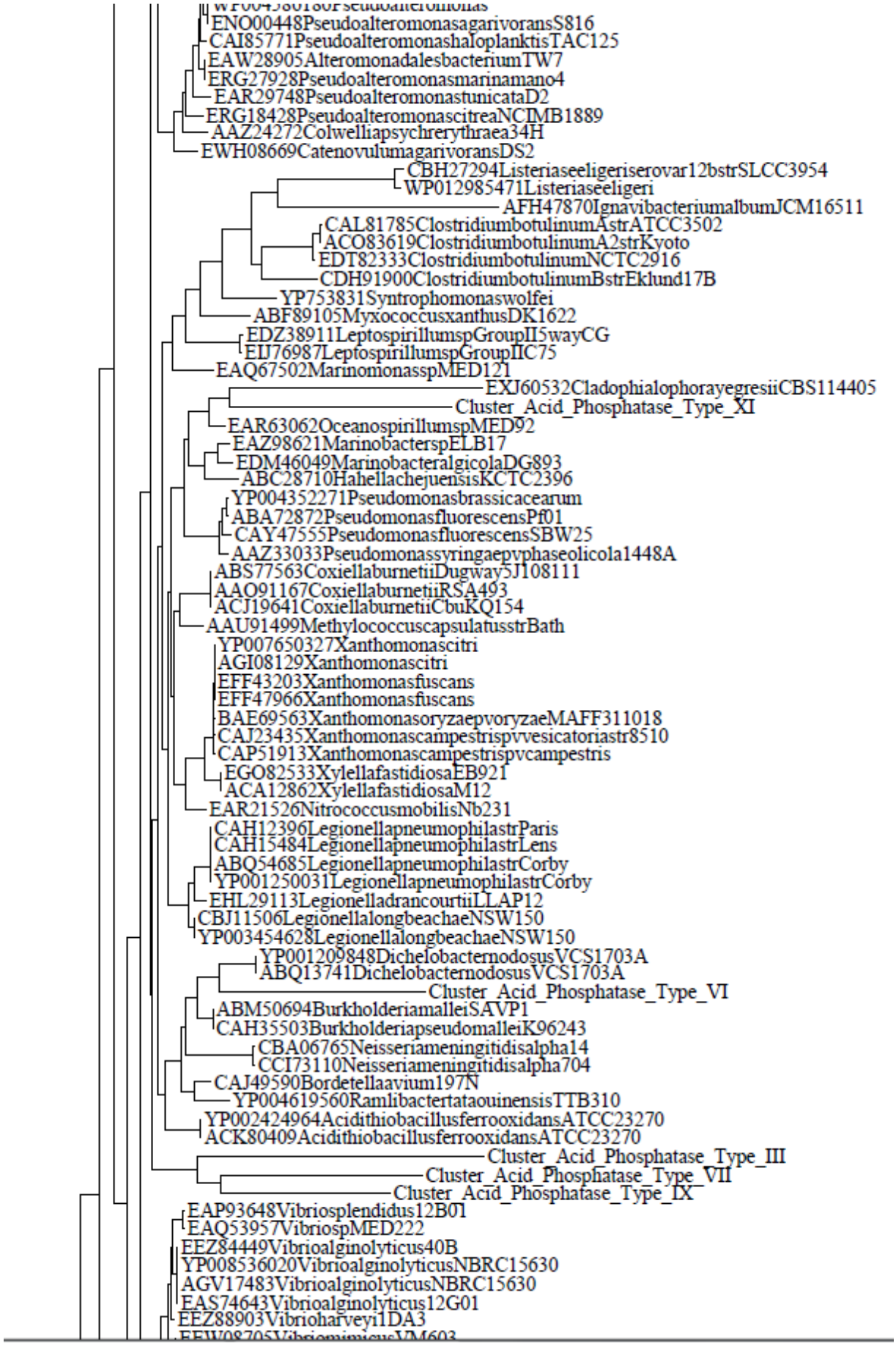
ENO00448PseudoalteromonasagarivoransS816
CAI85771PseudoalteromonashaloplanktisTAC125
EAW28905AlteromonadalesbacteriumTW7
ERG27928Pseudoalteromonasmarinamano4
EAR29748PseudoalteromonastunicataD2
ERG18428PseudoalteromonascitreaNCIMB1889
AAZ24272Colwelliapsychrerythraea34H
EWH08669CatenovulumagarivoransDS2
CBH27294Listeriaseeligeriserovar12bstrSLCC3954
WP012985471Listeriaseeligeri
AFH47870IgnavibacteriumalbumJCM16511
CAL81785ClostridiumbotulinumAstrATCC3502
ACO83619ClostridiumbotulinumA2strKyoto
EDT82333ClostridiumbotulinumNCTC2916
CDH91900ClostridiumbotulinumBstrEklund17B
YP753831Syntrophomonaswolfei
ABF89105MyxococcusxanthusDK1622
EDZ38911LeptospirillumspGroupII5wayCG
EIJ76987LeptospirillumspGroupIIC75
EAQ67502MarinomonasspMED121
EXJ60532CladophialophorayegresiiCBS114405
Cluster_Acid_Phosphatase_Type_XI
EAR63062OceanospirillumspMED92
EAZ98621MarinobacterspELB17
EDM46049MarinobacteralgicolaDG893
ABC28710HahellachejuensisKCTC2396
YP004352271Pseudomonasbrassicacearum
ABA72872PseudomonasfluorescensPf01
CAY47555PseudomonasfluorescensSBW25
AAZ33033Pseudomonassyringaepvphaseolicola1448A
ABS77563CoxiellaburnetiiDugway5J108111
AAQ91167CoxiellaburnetiiRSA493
ACJ19641CoxiellaburnetiiCbuKQ154
AAU91499MethylococcuscapsulatusstrBath
YP007650327Xanthomonascitri
AGI08129Xanthomonascitri
EFF43203Xanthomonasfuscans
EFF47966Xanthomonasfuscans
BAE69563XanthomonasoryzaepvoryzaeMAFF311018
CAJ23435Xanthomonascampestrispvvesicatoriastr8510
CAP51913Xanthomonascampestrispvcampestris
EGO82533XylellafastidiosaEB92I
ACA12862XylellafastidiosaM12
EAR21526NitrococcusmobilisNb231
CAH12396LegionellapneumophilastrParis
CAH15484LegionellapneumophilastrLens
ABQ54685LegionellapneumophilastrCorby
YP001250031LegionellapneumophilastrCorby
EHL29113LegionelladrancourtiiLLAP12
CBJ11506LegionellalongbeachaeNSW150
YP003454628LegionellalongbeachaeNSW150
YP001209848DichelobacternodosusVCS1703A
ABQ13741DichelobacternodosusVCS1703A
Cluster_Acid_Phosphatase_Type_VI
ABM50694BurkholderiamalleiSAVP1
CAH35503Burkholderiapseudomallei K96243
CBA06765Neisseriameningitidisalpha14
CCI73110Neisseriameningitidisalpha704
CAJ49590Bordetellaavium197N
YP004619560RamlibacteriumtataouinensisTTB310
YP002424964AcidithiobacillusferrooxidansATCC23270
ACK80409AcidithiobacillusferrooxidansATCC23270
Cluster_Acid_Phosphatase_Type_III
Cluster_Acid_Phosphatase_Type_VII
Cluster_Acid_Phosphatase_Type_IX
EAP93648Vibriosplendidus12B01
EAQ53957VibriospMED222
EEZ84449Vibrioalginolyticus40B
YP008536020VibrioalginolyticusNBRC15630
AGV17483VibrioalginolyticusNBRC15630
EAS74643Vibrioalginolyticus12G01
EEZ88903Vibrioharveyi1DA3


EAS74643Vibrioalginolyticus12G01
EEZ88903Vibrioharveyi1DA3
EEW08705VibriomimicusVM603
EEW08938VibriomimicusVM573
Cluster_Acid_Phosphatase_Type_XIII
EAR54723PhotobacteriumspSKA34
EAS63829VibrioangustumS14
EAS43458Photobacteriumprofundum3TCK
Cluster_Acid_Phosphatase_Type_XIV
ABK39784Aeromonashydrophila
WP014546149Fibrobactersuccinogenes
YP003249539Fibrobactersuccinogenes
ACX75057Fibrobactersuccinogenes
Cluster_Acid_Phosphatase_Type_XII
AHM77944Klebsiellapneumoniae30684NJST2582
AHM83542Klebsiellapneumoniae30660NJST2581
AEW62879Klebsiellapneumoniae
ABR78507Klebsiellapneumoniae
YP005228481Klebsiellapneumoniae
EPS08431Klebsiellapneumoniae
EPS05700Klebsiellapneumoniae
CAE13011Photorhabdusluminescens
BAH64893Klebsiellapneumoniae
ABE08567EscherichiacoliUTI89
AAN81760EscherichiacoliCFT073
YP006139891EscherichiacoliNA114
AEG37617EscherichiacoliNA114
CCW26170EscherichiacoliO25bH4ST131strEC958
ACT44413EscherichiacoliBL21DE3
ACT40247EscherichiacoliBstrREL606
YP003055184EscherichiacoliBL21DE3
ABJ02178EscherichiacoliAPECO1
ABG70715Escherichiacoli536
YP001597119CoxiellaburnetiiRSA331
EYE85045Salmonellaenterica
EYH73200Salmonellaenterica
WP022562431Salmonellaenterica
YP008645688Salmonellaenterica
CDG08982Salmonellaenterica
CBG25897Salmonellaenterica
CAR34345Salmonellaenterica
CBW19005Salmonellaenterica
CAY75433ErwiniapyrifoliaeDSM12163
YP005803804ErwiniapyrifoliaeDSM12163
CBA19712ErwiniaamylovoraCFBP1430
CBX79609ErwiniaamylovoraATCCBAA2158
CDK17711ErwiniaamylovoraLA636
CDK21080ErwiniaamylovoraLA637
CDK14344ErwiniaamylovoraLA635
YP003530120ErwiniaamylovoraCFBP1430
CCP06143ErwiniaamylovoraMR1
CCP02114ErwiniaamylovoraEa644
CCO98097ErwiniaamylovoraUPN527
CCO92745ErwiniaamylovoraCFBP1232
CCO88988Erwiniaamylovora01SFRBO
CCO85204ErwiniaamylovoraCFBP2585
CCO81401ErwiniaamylovoraEa266
CCO77616ErwiniaamylovoraEa356
EKV55045ErwiniaamylovoraACW56400
CCG86202ErwiniapiriflorinigransCFBP5888
WP023654025Erwiniapiriflorinigrans
WP019091210Komagataeibactereuropaeus
Cluster_Acid_Phosphatase_Type_XII
WP019085349Komagataeibactereuropaeus
WP010510626Komagataeibactereuropaeus
AHI24154GluconacetobacterxylinusE25
WP010516271Komagataeibacteroboediens
BAK84023GluconacetobactermedellinensisNBRC3288
WP014105563Komagataeibactermedellinensis
YP004868393GluconacetobactermedellinensisNBRC3288
EGG78122GluconacetobacterspSXCC1
WP007397476GluconacetobacterspSXCC1
WP003621455Komagataeibacterhansenii

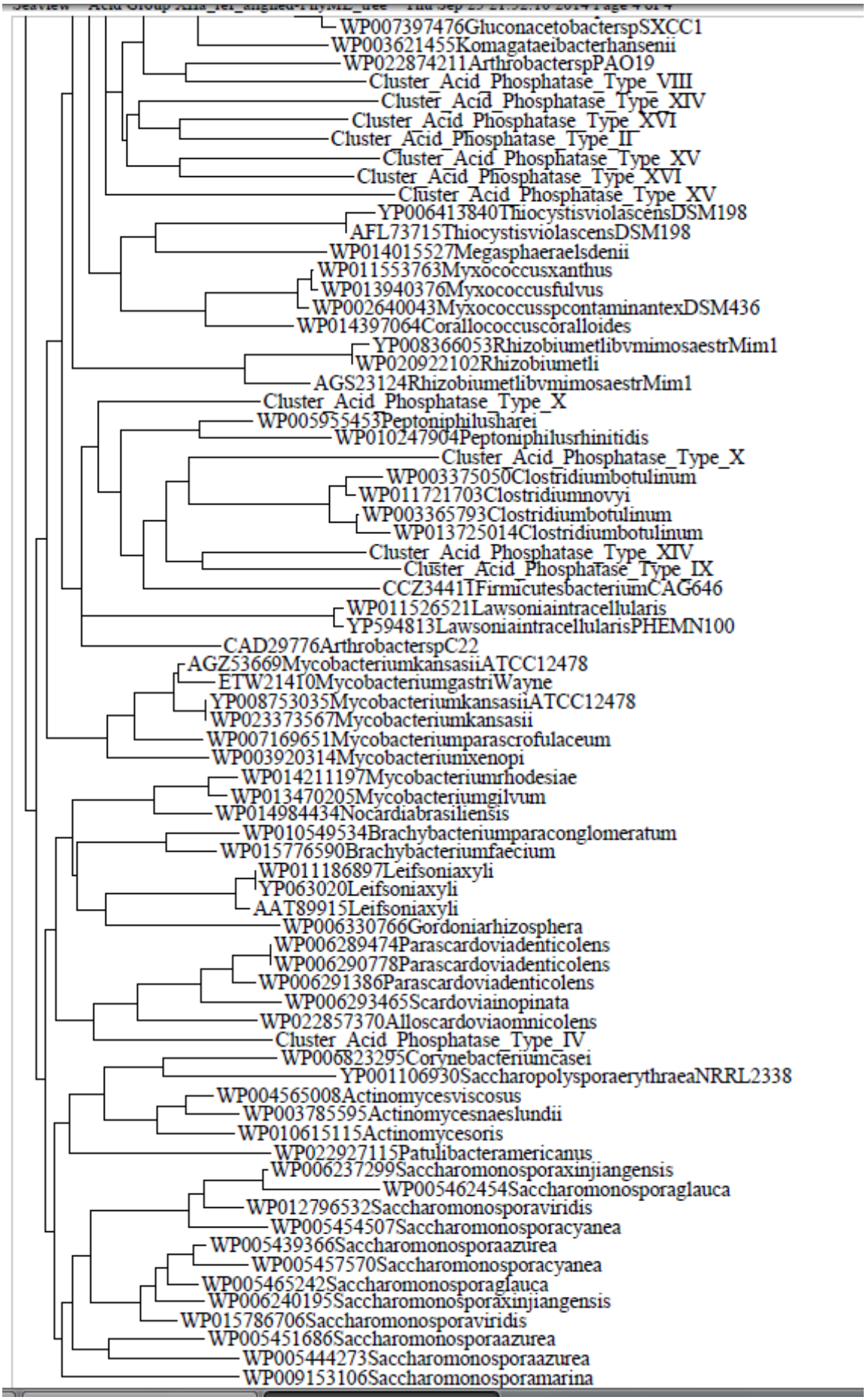
WP007397476GluconacetobacterspSXCC1
WP003621455Komagataeibacterhansenii
WP022874211ArthrobacterspPAO19
Cluster_Acid_Phosphatase_Type_VIII
Cluster_Acid_Phosphatase_Type_XIV
Cluster_Acid_Phosphatase_Type_XVI
Cluster_Acid_Phosphatase_Type_II
Cluster_Acid_Phosphatase_Type_XV
Cluster_Acid_Phosphatase_Type_XVI
Cluster_Acid_Phosphatase_Type_XV
YP006413840ThiocystisviolascensDSM198
AFL73715ThiocystisviolascensDSM198
WP014015527Megasphaeraelsdenii
WP011553763Myxococcusxanthus
WP013940376Myxococcusfulvus
WP002640043MyxococcusspcontaminantexDSM436
WP014397064Corallococcuscoralloides
YP008366053RhizobiumetlibvmimosaestrMim1
WP020922102Rhizobiumetli
AGS23124RhizobiumetlibvmimosaestrMim1
Cluster_Acid_Phosphatase_Type_X
WP005955453Peptoniphilusharei
WP010247904Peptoniphilusrhinitidis
Cluster_Acid_Phosphatase_Type_X
WP003375050Clostridiumbotulinum
WP011721703Clostridiumnovyi
WP003365793Clostridiumbotulinum
WP013725014Clostridiumbotulinum
Cluster_Acid_Phosphatase_Type_XIV
Cluster_Acid_Phosphatase_Type_IX
CCZ34411FirmicutesbacteriumCAG646
WP011526521Lawsoniaintracellularis
YP594813LawsoniaintracellularisPHEMN100
CAD29776ArthrobacterspC22
AGZ53669MycobacteriumkansasiiATCC12478
ETW21410MycobacteriumgastriWayne
YP008753035MycobacteriumkansasiiATCC12478
WP023373567Mycobacteriumkansasii
WP007169651Mycobacteriumparascrofulaceum
WP003920314Mycobacteriumxenopi
WP014211197Mycobacteriumrhodesiae
WP013470205Mycobacteriumgilvum
WP014984434Nocardiabrasiliensis
WP010549534Brachybacteriumparaconglomeratum
WP015776590Brachybacteriumfaecium
WP011186897Leifsoniaxyli
YP063020Leifsoniaxyli
AAT89915Leifsoniaxyli
WP006330766Gordoniarhizosphera
WP006289474Parascardoviadenticolens
WP006290778Parascardoviadenticolens
WP006291386Parascardoviadenticolens
WP006293465Scardoviainopinata
WP022857370Alloscardoviaomnicolens
Cluster_Acid_Phosphatase_Type_IV
WP006823295Corynebacteriumcasei
YP001106930SaccharopolysporaerythraeaNRRL2338
WP004565008Actinomycesviscosus
WP003785595Actinomycesnaeslundii
WP010615115Actinomycesoris
WP022927115Patulibacteramericanus
WP006237299Saccharomonosporaxinjiangensis
WP005462454Saccharomonosporaglauca
WP012796532Saccharomonosporaviridis
WP005454507Saccharomonosporacyanea
WP005439366Saccharomonosporaazurea
WP005457570Saccharomonosporacyanea
WP005465242Saccharomonosporaglauca
WP006240195Saccharomonosporaxinjiangensis
WP015786706Saccharomonosporaviridis
WP005451686Saccharomonosporaazurea
WP005444273Saccharomonosporaazurea
WP009153106Saccharomonosporamarina

Figure S13b. Phylogenetic tree of cluster XIIb of the acid phosphatase sequences included in the database.

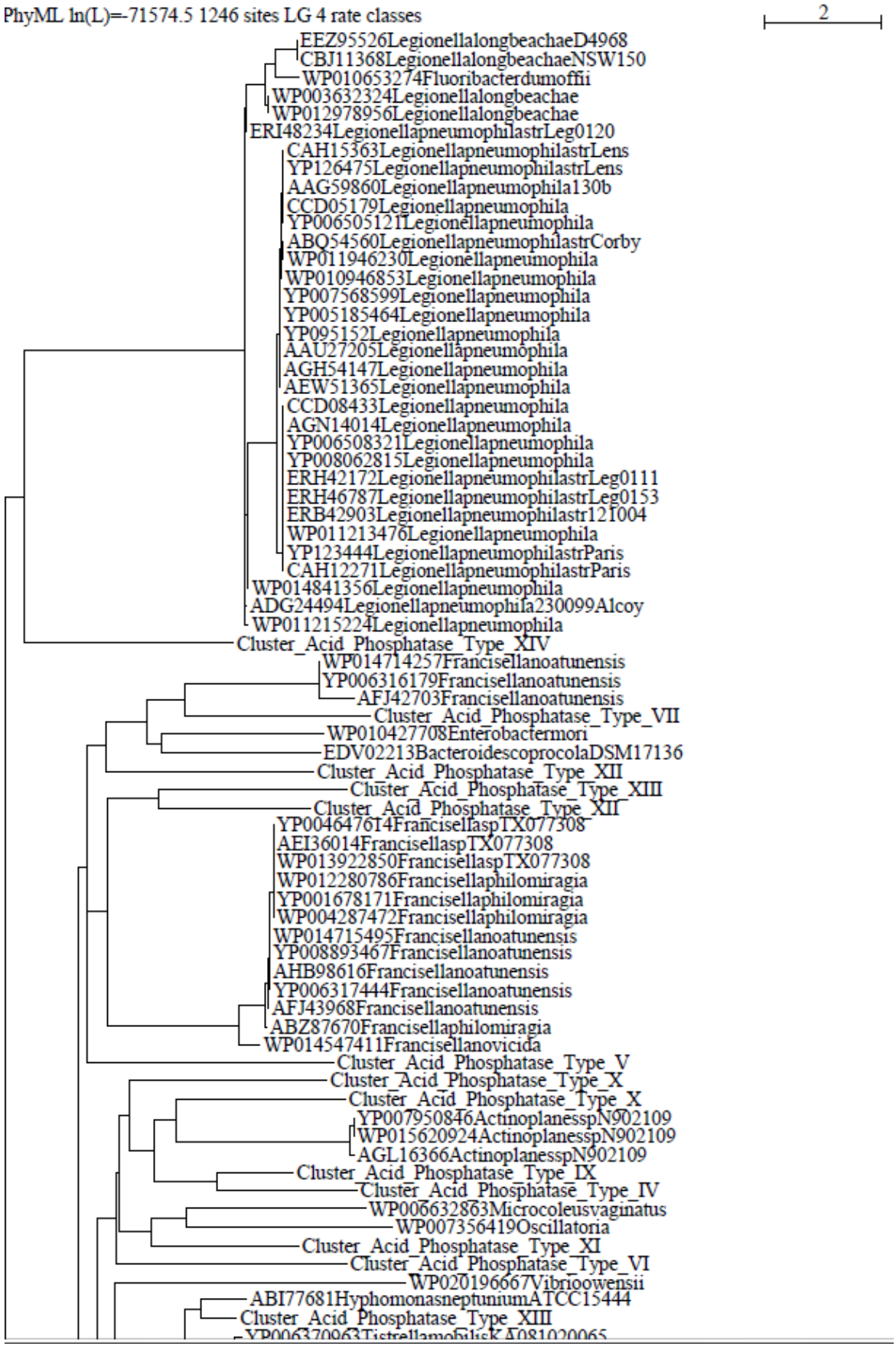

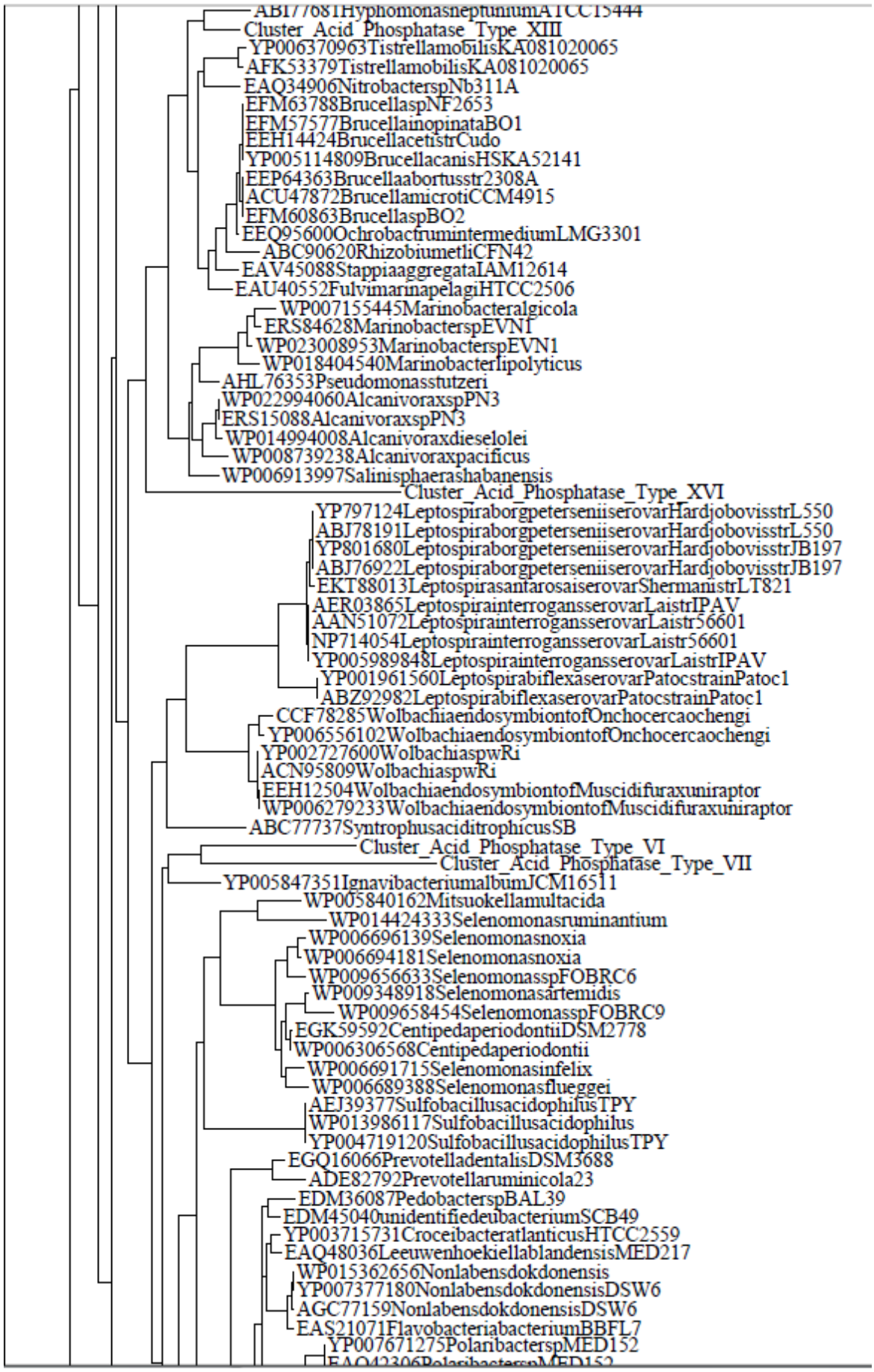
ABI77681HyphomonasneptunumATCC15444
Cluster_Acid_Phosphatase_Type_XIII
YP006370963TistrellamobilisKA081020065
AFK53379TistrellamobilisKA081020065
EAQ34906NitrobacterspNb311A
EFM63788BrucellaspNF2653
EFM57577BrucellainopinataBO1
EEH14424BrucellacetistrCudo
YP005114809BrucellacanisHSKA52141
EEP64363Brucellaabortusstr2308A
ACU47872BrucellamicrotiCCM4915
EFM60863BrucellaspBO2
EEQ95600OchrobactrumintermediumLMG3301
ABC90620RhizobiumetliCFN42
EAV45088StappiaaggregataIAM12614
EAU40552FulvimarinapelagiHTCC2506
WP007155445Marinobacteralgicola
ERS84628MarinobacterspEVN1
WP023008953MarinobacterspEVN1
WP018404540Marinobacterlipolyticus
AHL76353Pseudomonasstutzeri
WP022994060AlcanivoraxspPN3
ERS15088AlcanivoraxspPN3
WP014994008Alcanivoraxdieselolei
WP008739238Alcanivoraxpacificus
WP006913997Salinisphaerashabanensis
Cluster_Acid_Phosphatase_Type_XVI
YP797124LeptospiraborgpetersenniiserovarHardjobovisstrL550
ABJ78191LeptospiraborgpetersenniiserovarHardjobovisstrL550
YP801680LeptospiraborgpetersenniiserovarHardjobovisstrJB197
ABJ76922LeptospiraborgpetersenniiserovarHardjobovisstrJB197
EKT88013LeptospirasantarosaiserovarShermanistrLT821
AER03865LeptospirainterrogansserovarLaistrIPAV
AAN51072LeptospirainterrogansserovarLaistr56601
NP714054LeptospirainterrogansserovarLaistr56601
YP005989848LeptospirainterrogansserovarLaistrIPAV
YP001961560LeptospirabiflexaserovarPatocstrainPatoc1
ABZ92982LeptospirabiflexaserovarPatocstrainPatoc1
CCF78285WolbachiaendosymbiontofOnchocercaochengi
YP006556102WolbachiaendosymbiontofOnchocercaochengi
YP002727600WolbachiaspwRi
ACN95809WolbachiaspwRi
EEH12504WolbachiaendosymbiontofMuscidifuraxuniraptor
WP006279233WolbachiaendosymbiontofMuscidifuraxuniraptor
ABC77737SyntrophusaciditrophicusSB
Cluster_Acid_Phosphatase_Type_VI
Cluster_Acid_Phosphatase_Type_VII
YP005847351IgnavibacteriumalbumJCM16511
WP005840162Mitsuokellamultacida
WP014424333Selenomonasruminantium
WP006696139Selenomonasnoxia
WP006694181Selenomonasnoxia
WP009656633SelenomonasspFOBRC6
WP009348918Selenomonasartemidis
WP009658454SelenomonasspFOBRC9
EGK59592CentipedaperiodontiiDSM2778
WP006306568Centipedaperiodontii
WP006691715Selenomonasinfelix
WP006689388Selenomonasflueggei
AEJ39377SulfobacillusacidophilusTPY
WP013986117Sulfobacillusacidophilus
YP004719120SulfobacillusacidophilusTPY
EGQ16066PrevotelladentalisDSM3688
ADE82792Prevotellaruminicola23
EDM36087PedobacterspBAL39
EDM45040unidentifiedeubacteriumSCB49
YP003715731CroceibacteratlanticusHTCC2559
EAQ48036LeeuwenhoekiellablandensisMED217
WP015362656Nonlabensdokdonensis
YP007377180NonlabensdokdonensisDSW6
AGC77159NonlabensdokdonensisDSW6
EAS21071FlavobacteriabacteriumBBFL7
YP007671275PolaribacterspMED152

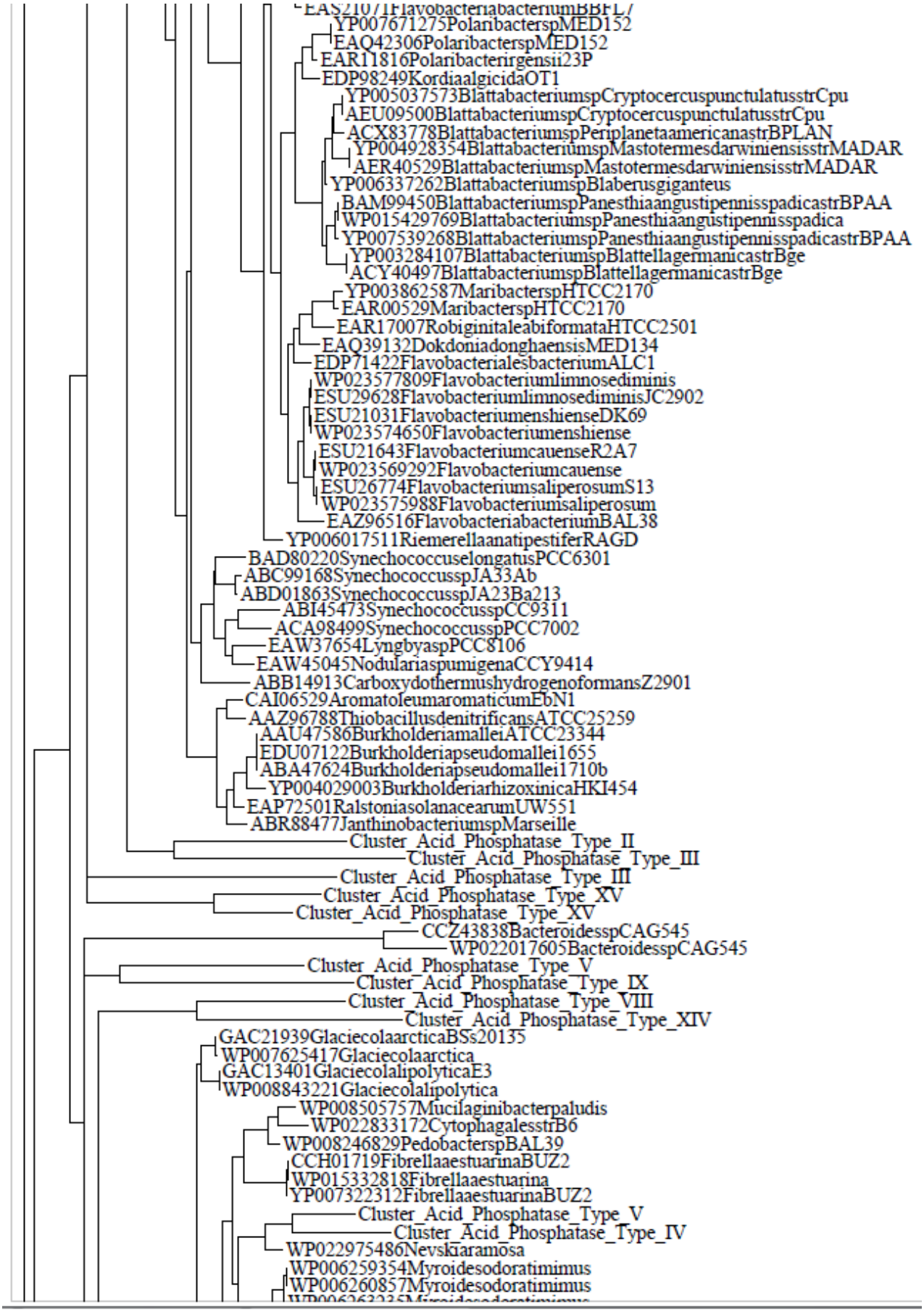
EAS21071FlavobacteriabacteriumBBFL7
YP007671275PolaribacterspMED152
EAQ42306PolaribacterspMED152
EAR11816Polaribacterirgensii23P
EDP98249KordiaalgicidaOT1
YP005037573BlattabacteriumspCryptocercuspunctulatusstrCpu
AEU09500BlattabacteriumspCryptocercuspunctulatusstrCpu
ACX83778BlattabacteriumspPeriplanetaamericanastrBPLAN
YP004928354BlattabacteriumspMastotermesdarwiniensisstrMADAR
AER40529BlattabacteriumspMastotermesdarwiniensisstrMADAR
YP006337262BlattabacteriumspBlaberusgiganteus
BAM99450BlattabacteriumspPanesthiaangustipennisspadicastrBPAA
WP015429769BlattabacteriumspPanesthiaangustipennisspadica
YP007539268BlattabacteriumspPanesthiaangustipennisspadicastrBPAA
YP003284107BlattabacteriumspBlattellagermanicastrBge
ACY40497BlattabacteriumspBlattellagermanicastrBge
YP003862587MaribacterspHTCC2170
EAR00529MaribacterspHTCC2170
EAR17007RobiginitaleabiformataHTCC2501
EAQ39132DokdoniadonghaensisMED134
EDP71422FlavobacterialesbacteriumALC1
WP023577809Flavobacteriumlimnosediminis
ESU29628FlavobacteriumlimnosediminisJC2902
ESU21031FlavobacteriumenshienseDK69
WP023574650Flavobacteriumenshiense
ESU21643FlavobacteriumcauenseR2A7
WP023569292Flavobacteriumcauense
ESU26774FlavobacteriumsaliperosumS13
WP023575988Flavobacteriumsaliperosum
EAZ96516FlavobacteriabacteriumBAL38
YP006017511RiemerellaanatipestiferRAGD
BAD80220SynechococcuselongatusPCC6301
ABC99168SynechococcusspJA33Ab
ABD01863SynechococcusspJA23Ba213
ABI45473SynechococcusspCC9311
ACA98499SynechococcusspPCC7002
EAW37654LyngbyaspPCC8106
EAW45045NodulariaspumigenaCCY9414
ABB14913CarboxydothermushydrogenoformansZ2901
CAI06529AromatoleumaromaticumEbN1
AAZ96788ThiobacillusdenitrificansATCC25259
AAU47586BurkholderiamalleiATCC23344
EDU07122Burkholderiapseudomallei1655
ABA47624Burkholderiapseudomallei1710b
YP004029003BurkholderiarhizoxinicaHKI454
EAP72501RalstoniasolanacearumUW551
ABR88477JanthinobacteriumspMarseille
Cluster_Acid_Phosphatase_Type_II
Cluster_Acid_Phosphatase_Type_III
Cluster_Acid_Phosphatase_Type_III
Cluster_Acid_Phosphatase_Type_XV
Cluster_Acid_Phosphatase_Type_XV
CCZ43838BacteroidesspCAG545
WP022017605BacteroidesspCAG545
Cluster_Acid_Phosphatase_Type_V
Cluster_Acid_Phosphatase_Type_IX
Cluster_Acid_Phosphatase_Type_VIII
Cluster_Acid_Phosphatase_Type_XIV
GAC21939GlaciecolaarcticaBSs20135
WP007625417Glaciecolaarctica
GAC13401GlaciecolalipolyticaE3
WP008843221Glaciecolalipolytica
WP008505757Mucilaginibacterpaludis
WP022833172CytophagalesstrB6
WP008246829PedobacterspBAL39
CCH01719FibrellaaestuarinaBUZ2
WP015332818Fibrellaaestuarina
YP007322312FibrellaaestuarinaBUZ2
Cluster_Acid_Phosphatase_Type_V
Cluster_Acid_Phosphatase_Type_IV
WP022975486Nevskiaramosa
WP006259354Myroidesodoratimimus
WP006260857Myroidesodoratimimus

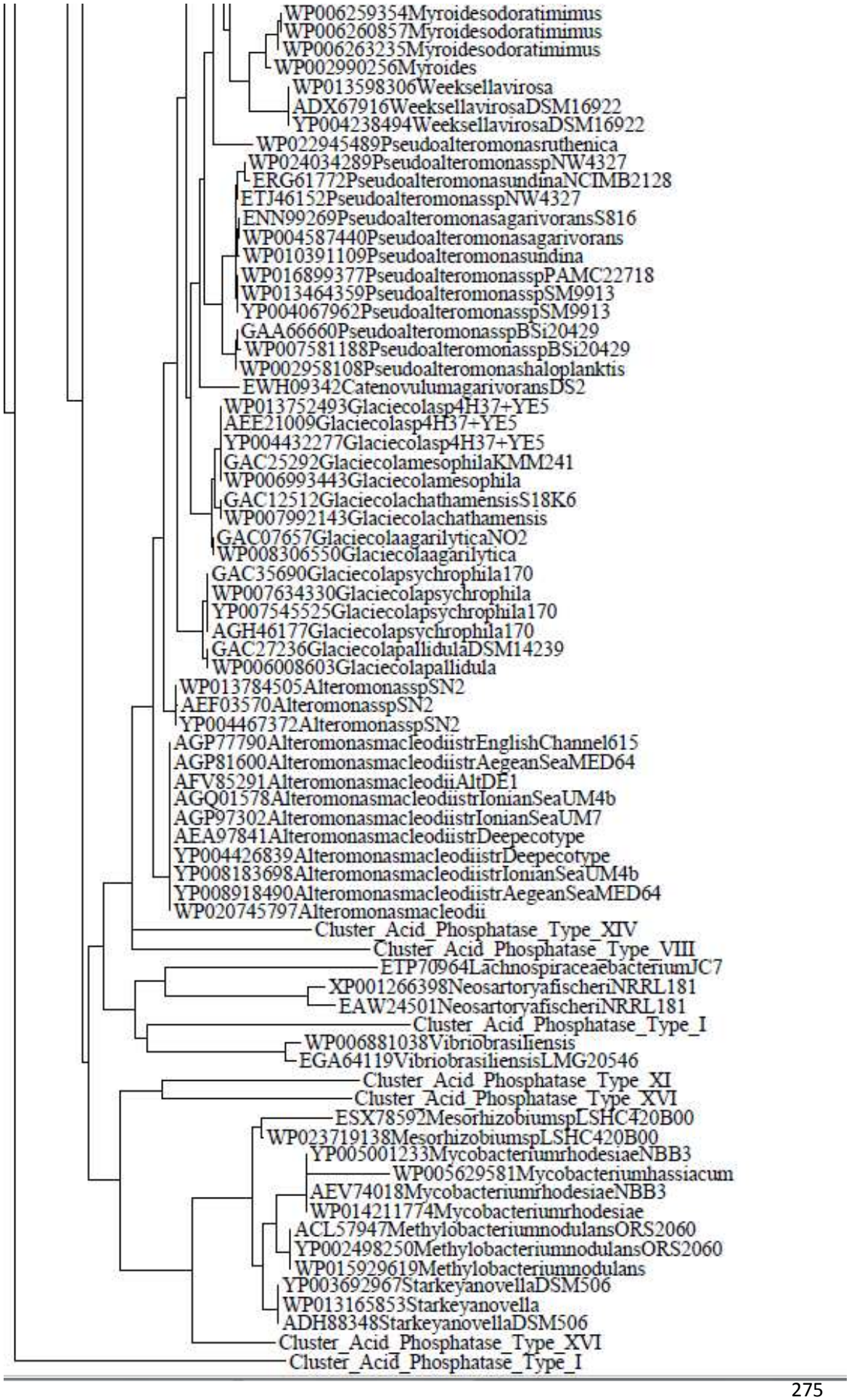
WP006259354Myroidesodoratimimus
WP006260857Myroidesodoratimimus
WP006263235Myroidesodoratimimus
WP002990256Myroides
WP013598306Weeksellavirosa
ADX67916WeeksellavirosaDSM16922
YP004238494WeeksellavirosaDSM16922
WP022945489Pseudoalteromonasruthenica
WP024034289PseudoalteromonasspNW4327
ERG61772PseudoalteromonasundinaNCIMB2128
ETJ46152PseudoalteromonasspNW4327
ENN99269PseudoalteromonasagarivoransS816
WP004587440Pseudoalteromonasagarivorans
WP010391109Pseudoalteromonasundina
WP016899377PseudoalteromonasspPAMC22718
WP013464359PseudoalteromonasspSM9913
YP004067962PseudoalteromonasspSM9913
GAA66660PseudoalteromonasspBSi20429
WP007581188PseudoalteromonasspBSi20429
WP002958108Pseudoalteromonashaloplanktis
EWH09342CatenovulumagarivoransDS2
WP013752493Glaciecolasp4H37+YE5
AEE21009Glaciecolasp4H37+YE5
YP004432277Glaciecolasp4H37+YE5
GAC25292GlaciecolamesophilaKMM241
WP006993443Glaciecolamesophila
GAC12512GlaciecolachathamensisS18K6
WP007992143Glaciecolachathamensis
GAC07657GlaciecolaagarilyticaNO2
WP008306550Glaciecolaagarilytica
GAC35690Glaciecolapsychrophila170
WP007634330Glaciecolapsychrophila
YP007545525Glaciecolapsychrophila170
AGH46177Glaciecolapsychrophila170
GAC27236GlaciecolapallidulaDSM14239
WP006008603Glaciecolapallidula
WP013784505AlteromonasspSN2
AEF03570AlteromonasspSN2
YP004467372AlteromonasspSN2
AGP77790AlteromonasmacleodiistrEnglishChannel615
AGP81600AlteromonasmacleodiistrAegeanSeaMED64
AFV85291AlteromonasmacleodiiAltDE1
AGQ01578AlteromonasmacleodiistrIonianSeaUM4b
AGP97302AlteromonasmacleodiistrIonianSeaUM7
AEA97841AlteromonasmacleodiistrDeepecotype
YP004426839AlteromonasmacleodiistrDeepecotype
YP008183698AlteromonasmacleodiistrIonianSeaUM4b
YP008918490AlteromonasmacleodiistrAegeanSeaMED64
WP020745797Alteromonasmacleodii
Cluster_Acid_Phosphatase_Type_XIV
Cluster_Acid_Phosphatase_Type_VIII
ETP70964LachnospiraceaebacteriumJC7
XP001266398NeosartoryafischeriNRRL181
EAW24501NeosartoryafischeriNRRL181
Cluster_Acid_Phosphatase_Type_I
WP006881038VibriobrasiliensisEGA64119VibriobrasiliensisLMG20546
Cluster_Acid_Phosphatase_Type_XI
Cluster_Acid_Phosphatase_Type_XVI
ESX78592MesorhizobiumspLSHC420B00
WP023719138MesorhizobiumspLSHC420B00
YP005001233MycobacteriumrhodesiaeNBB3
WP005629581Mycobacteriumhassiacum
AEV74018MycobacteriumrhodesiaeNBB3
WP014211774Mycobacteriumrhodesiae
ACL57947MethylobacteriumnodulansORS2060
YP002498250MethylobacteriumnodulansORS2060
WP015929619Methylobacteriumnodulans
YP003692967StarkeyanovellaDSM506
WP013165853Starkeyanovella
ADH88348StarkeyanovellaDSM506
Cluster_Acid_Phosphatase_Type_XVI
Cluster_Acid_Phosphatase_Type_I

Figure S14a. Phylogenetic tree of cluster XIIIa of the acid phosphatase sequences included in the database.

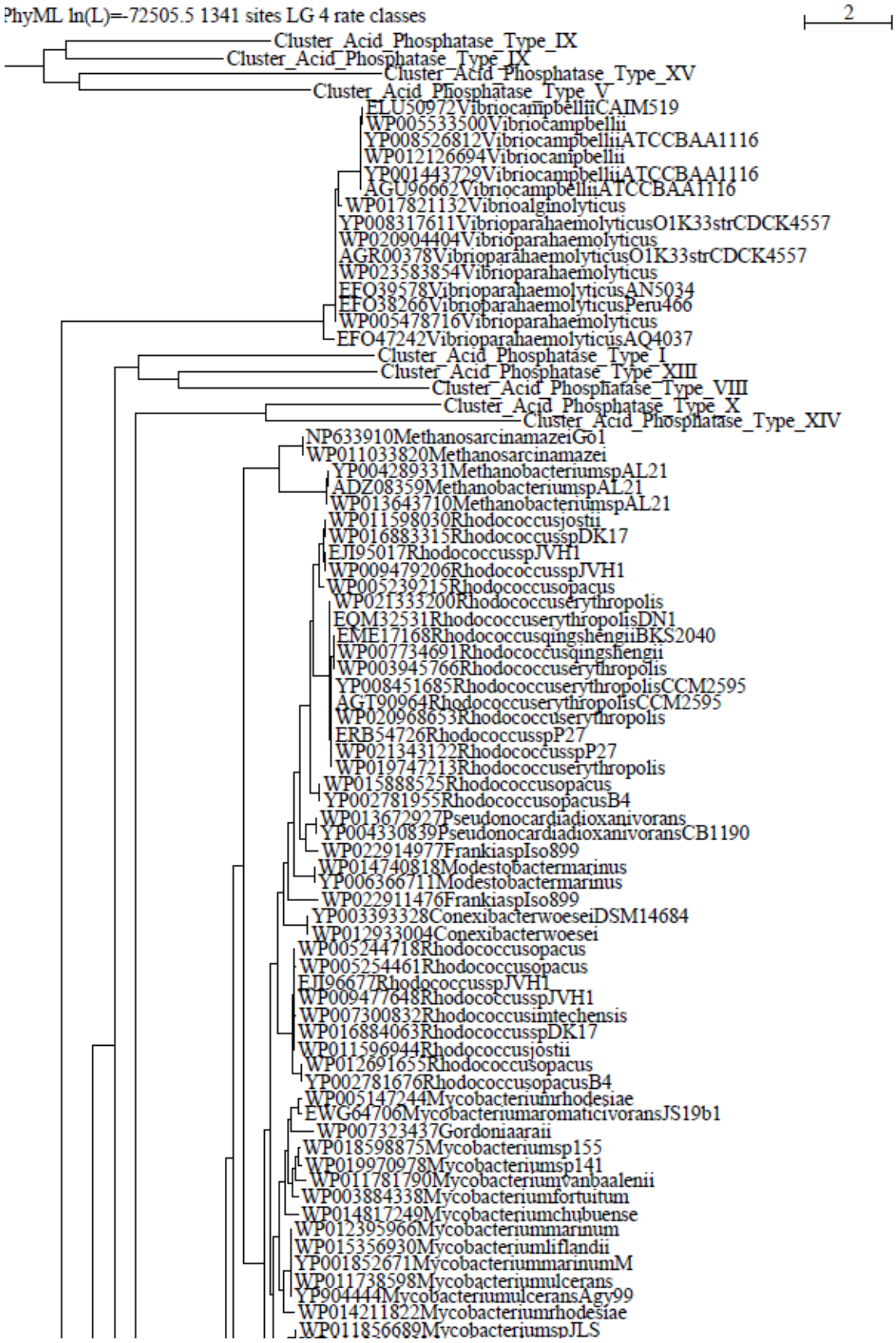

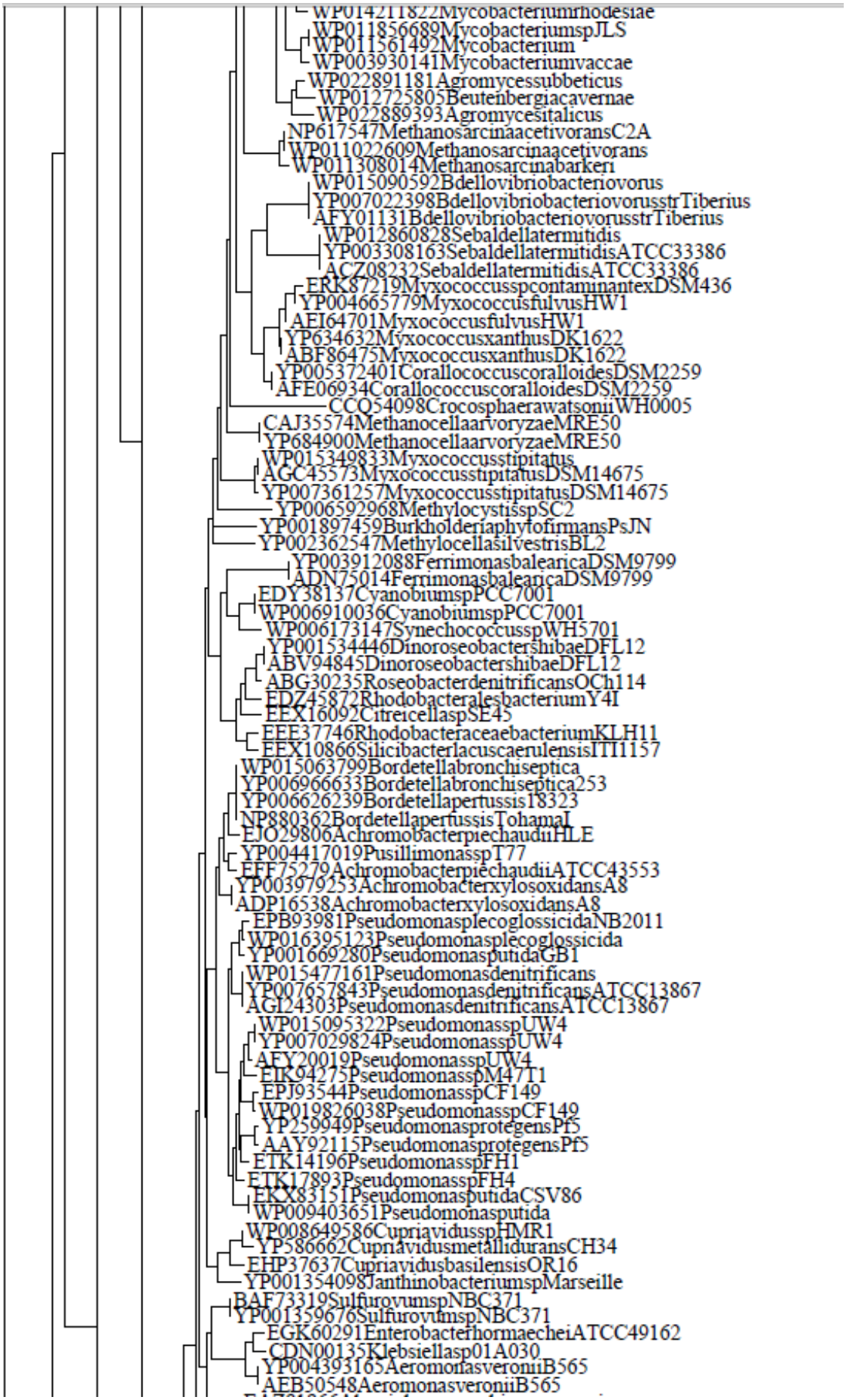
WP014211822MycobacteriumrhodesiaeWP011856689MycobacteriumspJLS
WP011561492Mycobacterium
WP003930141Mycobacteriumvaccae
WP022891181Agromycessubbeticus
WP012725805Beutenbergiacavernae
WP022889393Agromycesitalicus
NP617547MethanosarcinaacetivoransC2A
WP011022609Methanosarcinaacetivorans
WP011308014Methanosarcinabarkeri
WP015090592Bdellovibriobacteriovorus
YP007022398BdellovibriobacteriovorusstrTiberius
AFY01131BdellovibriobacteriovorusstrTiberius
WP012860828Sebaldellatermitidis
YP003308163SebaldellatermitidisATCC33386
ACZ08232SebaldellatermitidisATCC33386
ERK87219MyxococcusspcontaminantexDSM436
YP004665779MyxococcusfulvusHW1
AEI64701MyxococcusfulvusHW1
YP634632MyxococcusxanthusDK1622
ABF86475MyxococcusxanthusDK1622
YP005372401CorallococcuscoralloidesDSM2259
AFE06934CorallococcuscoralloidesDSM2259
CCQ54098CrocosphaerawatsoniiWH0005
CAJ35574MethanocellaarvoryzaeMRE50
YP684900MethanocellaarvoryzaeMRE50
WP015349833Myxococcusstipitatus
AGC45573MyxococcusstipitatusDSM14675
YP007361257MyxococcusstipitatusDSM14675
YP006592968MethylocystisspSC2
YP001897459BurkholderiaphytofirmansPsJN
YP002362547MethylocellasilvestrisBL2
YP003912088FerrimonasbalearicaDSM9799
ADN75014FerrimonasbalearicaDSM9799
EDY38137CyanobiumspPCC7001
WP006910036CyanobiumspPCC7001
WP006173147SynechococcusspWH5701
YP001534446DinoroseobactershibaeDFL12
ABV94845DinoroseobactershibaeDFL12
ABG30235RoseobacterdenitrificansOCh114
EDZ45872RhodobacteralesbacteriumY4I
EEX16092CitreicellaspSE45
EEE37746RhodobacteraceaebacteriumKLH11
EEX10866SilicibacterlacuscaerulensisITI1157
WP015063799Bordetellabronchiseptica
YP006966633Bordetellabronchiseptica253
YP006626239Bordetellapertussis18323
NP880362BordetellapertussisTohamaI
EJO29806AchromobacterpiechaudiiHLE
YP004417019PusillimonasspT77
EFF75279AchromobacterpiechaudiiATCC43553
YP003979253AchromobacterxylosoxidansA8
ADP16538AchromobacterxylosoxidansA8
EPB93981PseudomonasplecoglossicidaNB2011
WP016395123Pseudomonasplecoglossicida
YP001669280PseudomonasputidaGB1
WP015477161Pseudomonasdenitrificans
YP007657843PseudomonasdenitrificansATCC13867
AGI24303PseudomonasdenitrificansATCC13867
WP015095322PseudomonasspUW4
YP007029824PseudomonasspUW4
AFY20019PseudomonasspUW4
EIK94275PseudomonasspM47T1
EPJ93544PseudomonasspCF149
WP019826038PseudomonasspCF149
YP259949PseudomonasprotegensPf5
AAY92115PseudomonasprotegensPf5
ETK14196PseudomonasspFH1
ETK17893PseudomonasspFH4
EKX83151PseudomonasputidaCSV86
WP009403651Pseudomonasputida
WP008649586CupriavidusspHMR1
YP586662CupriavidusmetalliduransCH34
EHP37637CupriavidusbasilensisOR16
YP001354098JanthinobacteriumspMarseille
BAF73319SulfurovumspNBC371
YP001359676SulfurovumspNBC371
EGK60291EnterobacterhormaecheiATCC49162
CDN00135Klebsiellasp01A030
YP004393165AeromonasveroniiB565
AEB50548AeromonasveroniiB565

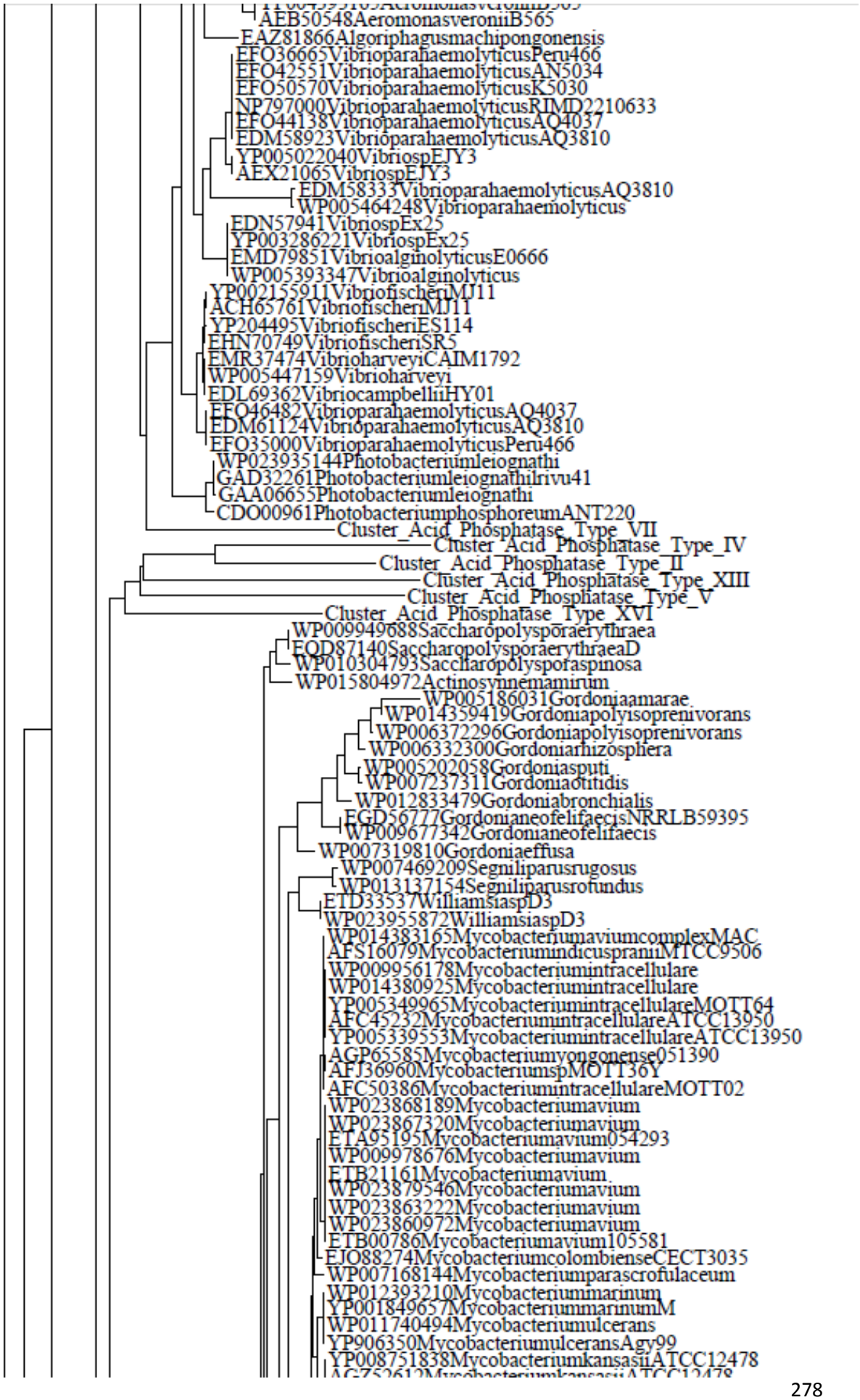
AEB50548AeromonasveroniiB565
EAZ81866Algoriphagusmachipongonensis
EFO36665VibrioparahaemolyticusPeru466
EFO42551VibrioparahaemolyticusAN5034
EFO50570VibrioparahaemolyticusK5030
NP797000VibrioparahaemolyticusRIMD2210633
EFO44138VibrioparahaemolyticusAQ4037
EDM58923VibrioparahaemolyticusAQ3810
YP005022040VibriospEJY3
AEX21065VibriospEJY3
EDM58333VibrioparahaemolyticusAQ3810
WP005464248Vibrioparahaemolyticus
EDN57941VibriospEx25
YP003286221VibriospEx25
EMD79851VibrioalginolyticusE0666
WP005393347Vibrioalginolyticus
YP002155911VibriofischeriMJ11
ACH65761VibriofischeriMJ11
YP204495VibriofischeriES114
EHN70749VibriofischeriSR5
EMR37474VibrioharveyiCAIM1792
WP005447159Vibrioharveyi
EDL69362VibriocampbelliiHY01
EFO46482VibrioparahaemolyticusAQ4037
EDM61124VibrioparahaemolyticusAQ3810
EFO35000VibrioparahaemolyticusPeru466
WP023935144Photobacteriumleiognathi
GAD32261Photobacteriumleiognathilrivu41
GAA06655Photobacteriumleiognathi
CDO00961PhotobacteriumphosphoreumANT220
Cluster_Acid_Phosphatase_Type_VII
Cluster_Acid_Phosphatase_Type_IV
Cluster_Acid_Phosphatase_Type_II
Cluster_Acid_Phosphatase_Type_XIII
Cluster_Acid_Phosphatase_Type_V
Cluster_Acid_Phosphatase_Type_XVI
WP009949688Saccharopolysporaerythraea
EQD87140SaccharopolysporaerythraeaD
WP010304793Saccharopolysporaspinosa
WP015804972Actinosynnemamirum
WP005186031Gordoniaamarae
WP014359419Gordoniapolyisoprenivorans
WP006372296Gordoniapolyisoprenivorans
WP006332300Gordoniarhizosphera
WP005202058Gordoniasputi
WP007237311Gordoniaotitidis
WP012833479Gordoniabronchialis
EGD56777GordonianeofelifaecisNRRLB59395
WP009677342Gordonianeofelifaecis
WP007319810Gordoniaeffusa
WP007469209Segniliparusrugosus
WP013137154Segniliparusrotundus
ETD33537WilliamsiaspD3
WP023955872WilliamsiaspD3
WP014383165MycobacteriumavIumcomplexMAC
AFS16079MycobacteriumindicuspraniiMTCC9506
WP009956178Mycobacteriumintracellulare
WP014380925Mycobacteriumintracellulare
YP005349965MycobacteriumintracellulareMOTT64
AFC45232MycobacteriumintracellulareATCC13950
YP005339553MycobacteriumintracellulareATCC13950
AGP65585Mycobacteriumyongonense051390
AFJ36960MycobacteriumspMOTT36Y
AFC50386MycobacteriumintracellulareMOTT02
WP023868189Mycobacteriumavium
WP023867320Mycobacteriumavium
ETA95195Mycobacteriumavium054293
WP009978676Mycobacteriumavium
ETB21161Mycobacteriumavium
WP023879546Mycobacteriumavium
WP023863222Mycobacteriumavium
WP023860972Mycobacteriumavium
ETB00786Mycobacteriumavium105581
EJO88274MycobacteriumcolombienseCECT3035
WP007168144Mycobacteriumparascrofulaceum
WP012393210Mycobacteriummarinum
YP001849657MycobacteriummarinumM
WP011740494Mycobacteriumulcerans
YP906350MycobacteriumulceransAgy99
YP008751838MycobacteriumkansasiiATCC12478

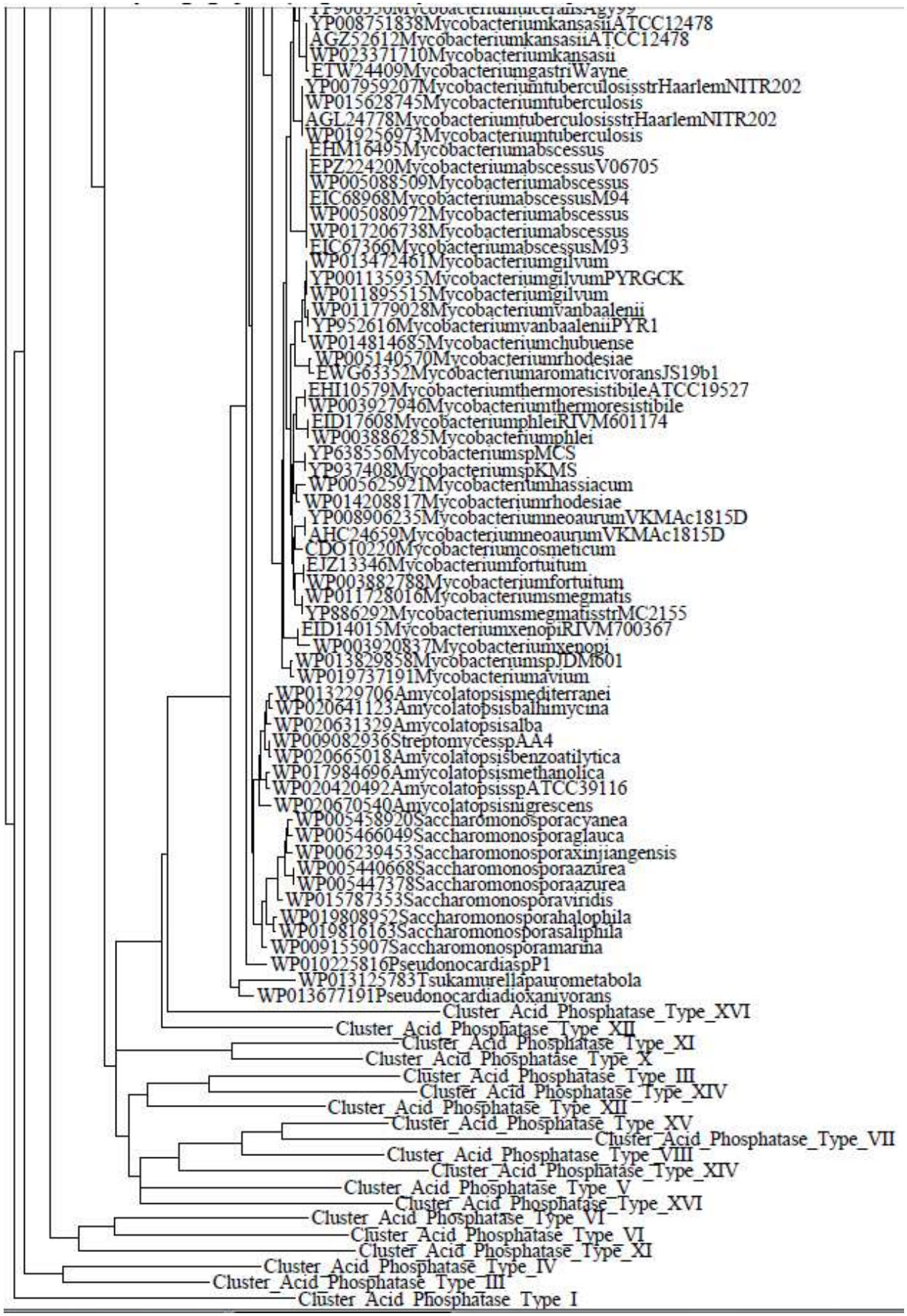
YP008751838MycobacteriumkansasiiATCC12478
AGZ52612MycobacteriumkansasiiATCC12478
WP023371710Mycobacteriumkansasii
ETW24409MycobacteriumgastriWayne
YP007959207MycobacteriumtuberculosisstrHaarlemNITR202
WP015628745Mycobacteriumtuberculosis
AGL24778MycobacteriumtuberculosisstrHaarlemNITR202
WP019256973Mycobacteriumtuberculosis
EHM16495Mycobacteriumabscessus
EPZ22420MycobacteriumabscessusV06705
WP005088509Mycobacteriumabscessus
EIC68968MycobacteriumabscessusM94
WP005080972Mycobacteriumabscessus
WP017206738Mycobacteriumabscessus
EIC67366MycobacteriumabscessusM93
WP013472461Mycobacteriumgilvum
YP001135935MycobacteriumgilvumPYRGCK
WP011895515Mycobacteriumgilvum
WP011779028Mycobacteriumvanbaalenii
YP952616MycobacteriumvanbaaleniiPYR1
WP014814685Mycobacteriumchubuense
WP005140570Mycobacteriumrhodesiae
EWG63352MycobacteriumaromaticivoransJS19b1
EHI10579MycobacteriumthermoresistibileATCC19527
WP003927946Mycobacteriumthermoresistibile
EID17608MycobacteriumphleiRIVM601174
WP003886285Mycobacteriumphlei
YP638556MycobacteriumspMCS
YP937408MycobacteriumspKMS
WP005625921Mycobacteriumhassiacum
WP014208817Mycobacteriumrhodesiae
YP008906235MycobacteriumneoaurumVKMAc1815D
AHC24659MycobacteriumneoaurumVKMAc1815D
CDO10220Mycobacteriumcosmeticum
EJZ13346Mycobacteriumfortuitum
WP003882788Mycobacteriumfortuitum
WP011728016Mycobacteriumsmegmatis
YP886292MycobacteriumsmegmatisstrMC2155
EID14015MycobacteriumxenopiRIVM700367
WP003920837Mycobacteriumxenopi
WP013829858MycobacteriumspJDM601
WP019737191Mycobacteriumavium
WP013229706Amycolatopsismediterranei
WP020641123Amycolatopsisbalhimycina
WP020631329Amycolatopsisalba
WP009082936StreptomycesspAA4
WP020665018Amycolatopsisbenzoatilytica
WP017984696Amycolatopsismethanolica
WP020420492AmycolatopsisspATCC39116
WP020670540Amycolatopsisnigrescens
WP005458920Saccharomonosporacyanea
WP005466049Saccharomonosporaglauca
WP006239453Saccharomonosporaxinjiangensis
WP005440668Saccharomonosporaazurea
WP005447378Saccharomonosporaazurea
WP015787353Saccharomonosporaviridis
WP019808952Saccharomonosporahalophila
WP019816163Saccharomonosporasaliphila
WP009155907Saccharomonosporamarina
WP010225816PseudonocardiaspP1
WP013125783Tsukamurellapaurometabola
WP013677191Pseudonocardiadioxanivorans
Cluster_Acid_Phosphatase_Type_XVI
Cluster_Acid_Phosphatase_Type_XII
Cluster_Acid_Phosphatase_Type_XI
Cluster_Acid_Phosphatase_Type_X
Cluster_Acid_Phosphatase_Type_III
Cluster_Acid_Phosphatase_Type_XIV
Cluster_Acid_Phosphatase_Type_XII
Cluster_Acid_Phosphatase_Type_XV
Cluster_Acid_Phosphatase_Type_VII
Cluster_Acid_Phosphatase_Type_VIII
Cluster_Acid_Phosphatase_Type_XIV
Cluster_Acid_Phosphatase_Type_V
Cluster_Acid_Phosphatase_Type_XVI
Cluster_Acid_Phosphatase_Type_VI
Cluster_Acid_Phosphatase_Type_VI
Cluster_Acid_Phosphatase_Type_XI
Cluster_Acid_Phosphatase_Type_IV
Cluster_Acid_Phosphatase_Type_III
Cluster_Acid_Phosphatase_Type_I

Figure S14b. Phylogenetic tree of cluster XIIIb of the acid phosphatase sequences included in the database.

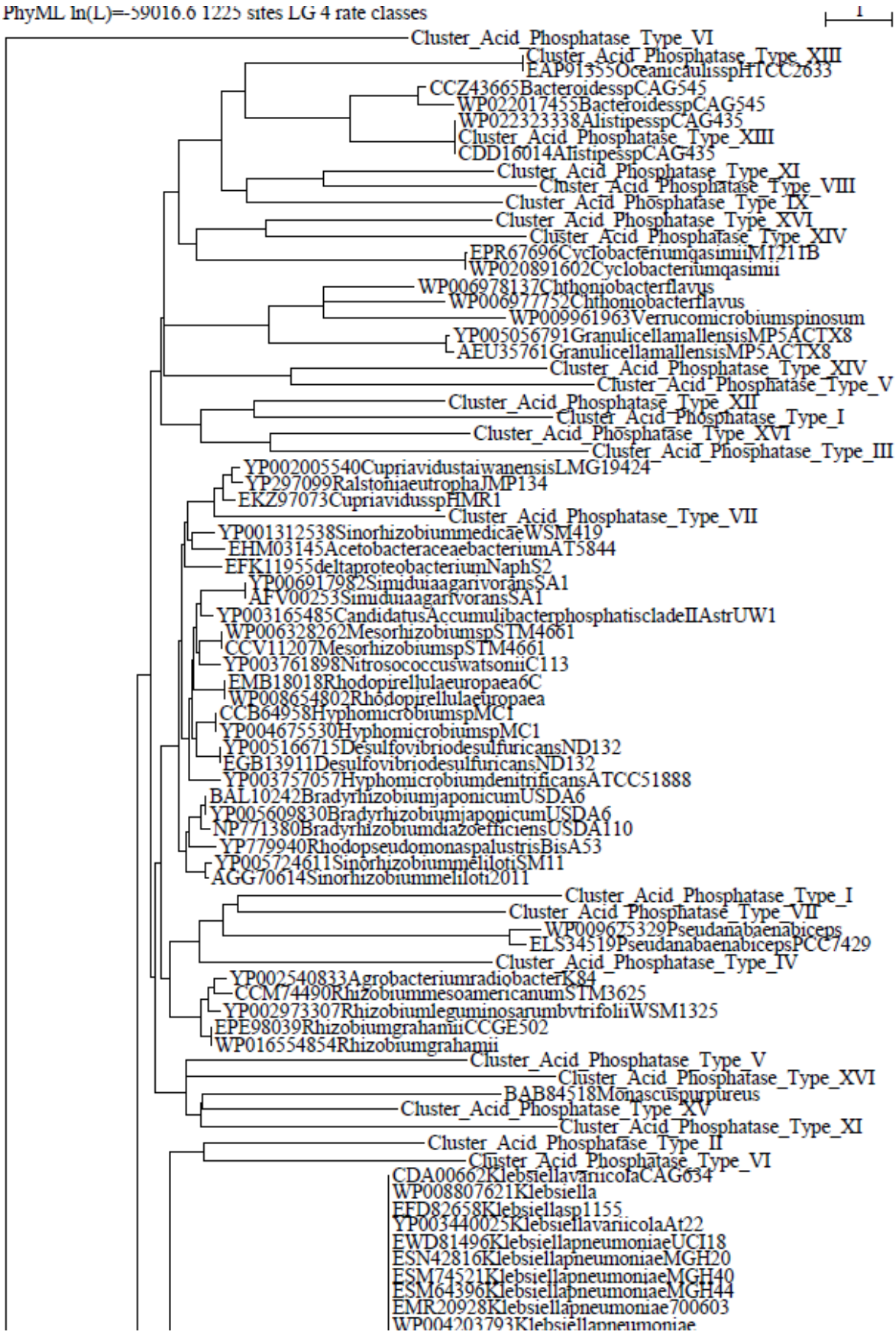


WP004203793KlebsiellapneumoniaeADG46037EnterobacteraerogenesESL89760KlebsiellapneumoniaeUCICRE10ADC58993KlebsiellavariicolaAt22EWF88564KlebsiellaoxytocaMGH27EHS99357Klebsiellaoxytoca105243EHT00241Klebsiellaoxytoca105245CCG29598EnterobacteraerogenesEA1509EWP015366155EnterobacteraerogenesYP007387138EnterobacteraerogenesEA1509EEUM02646EnterobacteraerogenesUCI16YP007873970RaoultellaornithinolyticaB6WP004860829EnterobacteriaceaeAGJ86418RaoultellaornithinolyticaB6ABW37174EnterobacteraerogenesEJF31622EnterobacterspAg1WP016535968CedeceadavisaeEPF18246CedeceadavisaeDSM4568WP008456655EnterobacterspAg1WP006819589YokenellaregensburgeiEHM47381YokenellaregensburgeiATCC43003BAA84942ShimwelliablattaeDSM4481AFJ47775ShimwelliablattaeDSM4481WP002439269ShimwelliablattaeYP006320286ShimwelliablattaeDSM4481ABQ69627RahnellaspFRCY9602ADW76048RahnellaspY9602YP004215175RahnellaspY9602ESS56727EnterobactercloacaeS611WP023481723EnterobactercloacaeWP013366592EnterobacterlignolyticusADO48858EnterobacterlignolyticusSCF1YP003942142EnterobacterlignolyticusSCF1EJI87366KosakoniaradicincitansDSM16656WP007374604KosakoniaradicincitansYP008106739EnterobacterspR4368WP020454018EnterobacterspR4368AGN84478EnterobacterspR4368AHJ74189EnterobactersaccharispSP1EGK36725ShigellaflexneriK227WP000828660ShigelladysenteriaeEGK26050ShigellaflexneriK218EIQ25838ShigellaflexneriK404WP000828661ShigellaWP005119548ShigellaflexneriEKT61734ProvidenciaburhodogranarieaDSM19968WP008912062ProvidenciaburhodogranarieaWP004917790ProvidenciastuartiiCAA46032ProvidenciastuartiiWP014657761ProvidenciastuartiiYP006217674ProvidenciastuartiiMRSN2154AFH94983ProvidenciastuartiiMRSN2154EMP52689MorganellamorganiiSC01WP004239915MorganellamorganiiBAA96744MorganellamorganiiWP004235240MorganellamorganiiCAA45774MorganellamorganiiWP004091793EnterobacteriaceaeEHM43790HafniaalveiATCC51873AHG18582SerratiafonticolaRB25WP009638649SerratiaspM24T3WP017489821gammaproteobacteriumWG36AHN26678GilliamellaapicolaWP018498528LeptotrichiawadeiERK53431LeptotrichiawadeiF0279WP012862605SebaldellatermitidisYP003309954SebaldellatermitidisATCC33386ACZ10023SebaldellatermitidisATCC33386WP013745995GallibacteriumanatisWP006986292CardiobacteriumvalvarumEHM52435CardiobacteriumvalvarumF0432WP006321751SerratiaplymuthicaWP006947705PrevotellamarshiiWP018361719PrevotellananceiensisWP006256268Alloprevotellatannerae WP018968214PrevotellaloescheiiWP021672342PrevotellaspF0091ERJ79240PrevotellaspF0091EFC72908PrevotellamelaninogenicaD18EGN56335PrevotellamultisaccharivoraxDSM17128


EGN56335PrevotellamultisaccharivoraxDSM17128
WP019968950Prevotellamaculosa
WP018967252Prevotellaloescheii
WP004344196Prevotellabuccae
EFU31690PrevotellabuccaeATCC33574
WP007411274PrevotellaspMSX73
WP004341481Prevotellabuccae
EFC76021PrevotellabuccaeD17
YP005013710TannerellaforsythiaATCC43037
AEW20507TannerellaforsythiaATCC43037
WP014224216Tannerellaforsythia
ERI81622BacteroidespyogenesF0041
WP006842883Dysgonomonasmossii
WP013546772Bacteroideshelcogenes
YP004160764BacteroideshelcogenesP36108
YP001297865BacteroidesvulgatusATCC8482
EQR98086BacteroidesvulgatusdnLKV7
WP005840261Bacteroides
CDF18816BacteroidesvulgatusCAG6
ABR38243BacteroidesvulgatusATCC8482
EET15504Bacteroidessp4347FAA
EFV68681Bacteroidessp3140A
WP018110104Bacteroidespropionicifaciens
WP004354343Prevotelladenticola
YP004330094PrevotelladenticolaF0289
EGC85406PrevotelladenticolaCRIS18CA
EEX19825PrevotellaveroralisF0319
WP008823804Prevotellahisticola
WP008448737Prevotellaamnii
BAA33148PrevotellaintermediaATCC25611
WP014708918Prevotellaintermedia
WP021671063PrevotellaspF0091
ERJ80428PrevotellaspF0091
EFC73032PrevotellamelaninogenicaD18
ETT02569PrevotellaspICM33
ADK97283PrevotellamelaninogenicaATCC25845
CDA44899PrevotellaspCAG5226
WP022101085PrevotellaspCAG5226
CCY90382BacteroidesspCAG1076
CDB99587BacteroidesspCAG443
WP021971435BacteroidesspCAG1076
WP022231739BacteroidesspCAG443
ERT59864PrevotellaspBV3P1
WP023057611PrevotellaspBV3P1
WP009161407Prevotellasaccharolytica
EKX96145PrevotellasaccharolyticaF0055
WP018362187Prevotellananceiensis
WP015781957Capnocytophagaochracea
YP003140809CapnocytophagaochraceaDSM7271
ACU92248CapnocytophagaochraceaDSM7271
EFS97038CapnocytophagaochraceaF0287
WP002674231Capnocytophaga
WP002679747Capnocytophagasputigena
EEB65708CapnocytophagasputigenaATCC33612
CDB05862PrevotellaspCAG520
WP022157767PrevotellaspCAG520
WP005880423Oxalobacterformigenes
EEO29723OxalobacterformigenesOXCC13
EHC28557Salmonellaenterica
WP001627552Salmonellaenterica
ERN76633Salmonellaenterica
ERN82050Salmonellaenterica
ESJ13241Salmonellaenterica
WP023249421Salmonellaenterica
WP015589596Salmonellaenterica
CAA45144Salmonellaenterica
AHB96094Salmonellaenterica
EJW37750Salmonellaenterica
ETC67388Salmonellaenterica
AGQ70838Salmonellaenterica
YP008257095Salmonellaenterica
YP005245288Salmonellaenterica
YP005250147Salmonellaenterica
YP005184119Salmonellaenterica
CBW20341Salmonellaenterica
YP005235269Salmonellaenterica
ERF95818Salmonellaenterica
WP021293583Salmonellaenterica
AGQ80217Salmonellaenterica
EJW27631Salmonellaenterica


EJW27631Salmonellaenterica
EJW32755Salmonellaenterica
YP008863706Salmonellaenterica
EHC78778Salmonellaenterica
AHB46794Salmonellaenterica
YP002149231Salmonellaenterica
YP002144678Salmonellaenterica
AAV79878Salmonellaenterica
WP000842405Salmonellaenterica
WP015406173Salmonellaenterica
YP007472191Salmonellaenterica
WP023231119Salmonellaenterica
ESH04992Salmonellaenterica
EHC28827Salmonellaenterica
ELX80486Salmonellaenterica
YP002228885Salmonellaenterica
ESF94209Salmonellaenterica
EPE40906Salmonellaenterica
WP016507462Salmonellaenterica
YP153190Salmonellaenterica
EPE53050Salmonellaenterica
EPE41162Salmonellaenterica
EPE41049Salmonellaenterica
ESO35843Salmonellaenterica
ESO45595Salmonellaenterica
WP000842426Salmonellaenterica
EXX81336Salmonellaenterica
EHC48490Salmonellaenterica
EHC72030Salmonellaenterica
EHC64064Salmonellaenterica
EHN41985Salmonellaenterica
WP000842406Salmonellaenterica
EHC97111Salmonellaenterica
AGF82753Salmonellaenterica
ERN73305Salmonellaenterica
WP000842431Salmonellaenterica
ESJ90344Salmonellaenterica
EJW25499Salmonellaenterica
EIC43575Salmonellaenterica
EIC33417Salmonellaenterica
EYI89703Salmonellaenterica
EIC48593Salmonellaenterica
EYI99388Salmonellaenterica
EIC46295Salmonellaenterica
EIC46109Salmonellaenterica
EYI84081Salmonellaenterica
EJI83050Salmonellaenterica
WP001696828Salmonellaenterica
AHN26080Gilliamellaapicola
EHD14037CommensalibacterintestiniA911
WP008854386Commensalibacterintestini
EUK18321CommensalibacterspMX01
WP005008477Shigellaboydii
EIQ34063Shigellaboydii444474
WP000850661Shigella
EIQ17731ShigellaflexneriK1770
EIQ25288ShigellaflexneriK315
WP000850662Shigellaflexneri
EIQ27894ShigellaflexneriK404
EJL11819ShigellasonneistrMoseley
WP000850660Enterobacteriaceae
WP015704112Enterobacteraerogenes
WP005284678Edwardsiellatarda
EFE23467EdwardsiellatardaATCC23685
WP012848214Edwardsiellatarda
Cluster_Acid_Phosphatase_Type_XV
Cluster_Acid_Phosphatase_Type_XII
Cluster_Acid_Phosphatase_Type_III
GAF18234BacillusspJCM19046
GAF12400BacillusspJCM19045
Cluster_Acid_Phosphatase_Type_XIV
Cluster_Acid_Phosphatase_Type_IV
Cluster_Acid_Phosphatase_Type_X
Cluster_Acid_Phosphatase_Type_X
Cluster_Acid_Phosphatase_Type_V
Cluster_Acid_Phosphatase_Type_VIII
CCC29711SalmonellabongoriNCTC12419
YP004729517SalmonellabongoriNCTC12419
WP015702768Salmonellabongori
Cluster_Acid_Phosphatase_Type_IX
WP007173391Prevotellabergensis

Figure S15a. Phylogenetic tree of cluster XIVa of the acid phosphatase sequences included in the database.

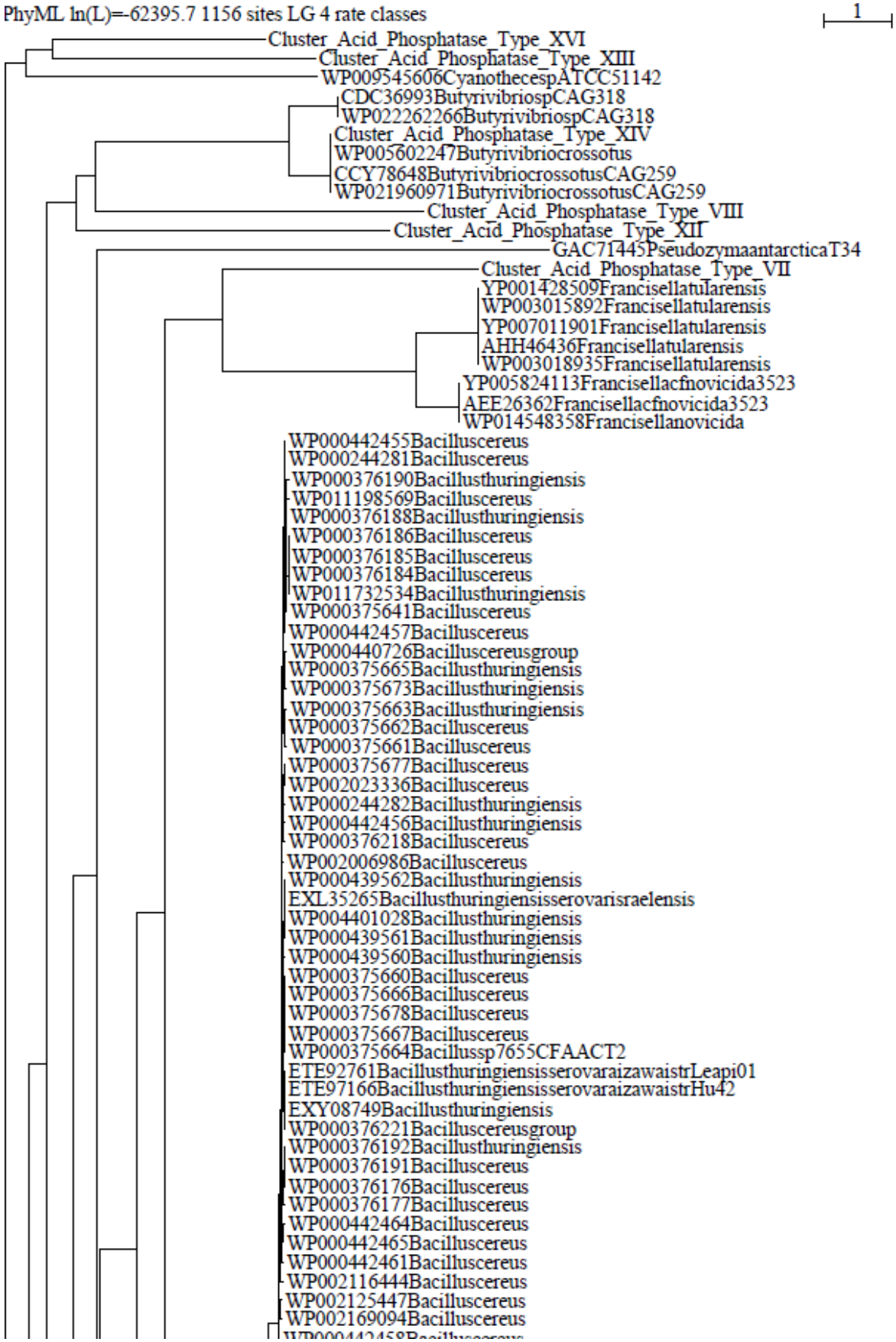

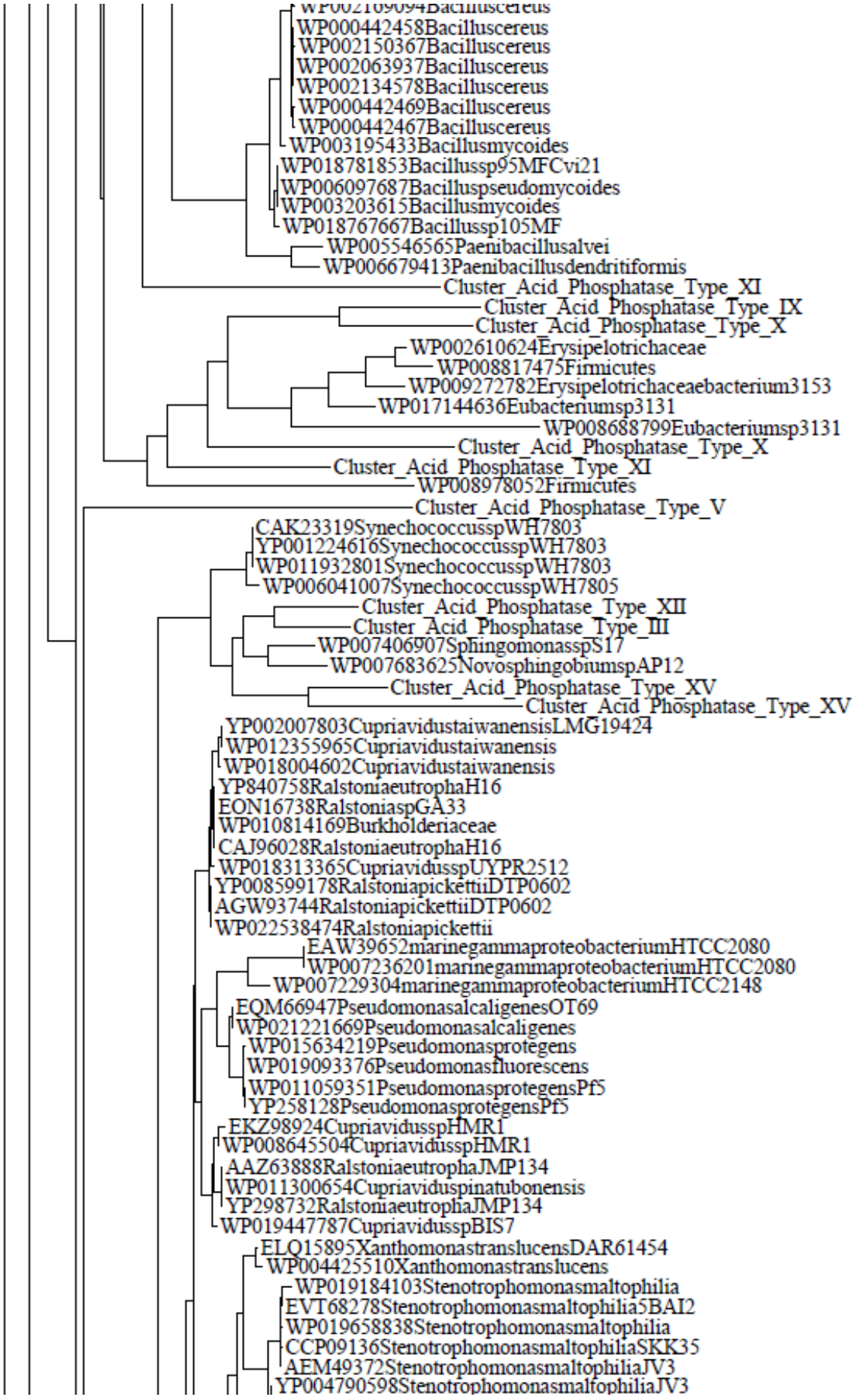
WP000442458Bacilluscereus
WP002150367Bacilluscereus
WP002063937Bacilluscereus
WP002134578Bacilluscereus
WP000442469Bacilluscereus
WP000442467Bacilluscereus
WP003195433Bacillusmycoides
WP018781853Bacillussp95MFCvi21
WP006097687Bacilluspseudomycoides
WP003203615Bacillusmycoides
WP018767667Bacillussp105MF
WP005546565Paenibacillusalvei
WP006679413Paenibacillusdendritiformis
Cluster_Acid_Phosphatase_Type_XI
Cluster_Acid_Phosphatase_Type_IX
Cluster_Acid_Phosphatase_Type_X
WP002610624Erysipelotrichaceae
WP008817475Firmicutes
WP009272782Erysipelotrichaceaebacterium3153
WP017144636Eubacteriumsp3131
WP008688799Eubacteriumsp3131
Cluster_Acid_Phosphatase_Type_X
Cluster_Acid_Phosphatase_Type_XI
WP008978052Firmicutes
Cluster_Acid_Phosphatase_Type_V
CAK23319SynechococcusspWH7803
YP001224616SynechococcusspWH7803
WP011932801SynechococcusspWH7803
WP006041007SynechococcusspWH7805
Cluster_Acid_Phosphatase_Type_XII
Cluster_Acid_Phosphatase_Type_III
WP007406907SphingomonasspS17
WP007683625NovosphingobiumspAP12
Cluster_Acid_Phosphatase_Type_XV
Cluster_Acid_Phosphatase_Type_XV
YP002007803CupriavidustaiwanensisLMG19424
WP012355965Cupriavidustaiwanensis
WP018004602Cupriavidustaiwanensis
YP840758RalstoniaeutrophaH16
EON16738RalstoniaspGA33
WP010814169Burkholderiaceae
CAJ96028RalstoniaeutrophaH16
WP018313365CupriavidusspUYPR2512
YP008599178RalstoniapickettiiDTP0602
AGW93744RalstoniapickettiiDTP0602
WP022538474Ralstoniapickettii
EAW39652marinegammaproteobacteriumHTCC2080
WP007236201marinegammaproteobacteriumHTCC2080
WP007229304marinegammaproteobacteriumHTCC2148
EQM66947PseudomonasalcaligenesOT69
WP021221669Pseudomonasalcaligenes
WP015634219Pseudomonasprotegens
WP019093376Pseudomonasfluorescens
WP011059351PseudomonasprotegensPf5
YP258128PseudomonasprotegensPf5
EKZ98924CupriavidusspHMR1
WP008645504CupriavidusspHMR1
AAZ63888RalstoniaeutrophaJMP134
WP011300654Cupriaviduspinatubonensis
YP298732RalstoniaeutrophaJMP134
WP019447787CupriavidusspBIS7
ELQ15895XanthomonastranslucensDAR61454
WP004425510Xanthomonastranslucens
WP019184103Stenotrophomonasmaltophilia
EVT68278Stenotrophomonasmaltophilia5BAI2
WP019658838Stenotrophomonasmaltophilia
CCP09136StenotrophomonasmaltophiliaSKK35
AEM49372StenotrophomonasmaltophiliaJV3
YP004790598StenotrophomonasmaltophiliaJV3


YP004790598StenotrophomonasmaltophiliaJV3
EQM72864StenotrophomonasmaltophiliaMF89
CCP40087XanthomonastranslucenspvtranslucensDSM18974
WP003476843Xanthomonastranslucens
WP016849419Xanthomonasaxonopodis
YP366213Xanthomonascampestrispvvesicatoriastr8510
WP023905903Xanthomonashortorum
WP011349215Xanthomonaseuvesicatoria
CAJ26213Xanthomonascampestrispvvesicatoriastr8510
WP007971341Xanthomonasfuscans
ETC82516XanthomonashortorumpvcarotaestrM081
WP019184688Stenotrophomonasmaltophilia
WP011189606Desulfotaleapsychrophila
YP066101DesulfotaleapsychrophilaLSv54
WP011189596Desulfotaleapsychrophila
YP066091DesulfotaleapsychrophilaLSv54
WP017364443Methylococcuscapsulatus
YP114641MethylococcuscapsulatusstrBath
WP010961453Methylococcuscapsulatus
AAU91812MethylococcuscapsulatusstrBath
EHP40827CupriavidusbasilensisOR16
WP006160014Cupriavidusbasilensis
WP006855083SynechococcusspWH8016
EHA58634SynechococcusspWH8016
WP009789593SynechococcusspBL107
WP007097261SynechococcusspRS9916
WP010315937SynechococcusspCB0205
ABM77098ProchlorococcusmarinusstrMIT9303
YP001016363ProchlorococcusmarinusstrMIT9303
WP011825023Prochlorococcusmarinus
WP011130936Prochlorococcusmarinus
EKU31071AlcaligenesspHPC1271
WP009455689Alcaligenes
Cluster_Acid_Phosphatase_Type_VII
EKF63883SerratiaplymuthicaA30
YP004506569SerratiaplymuthicaAS9
YP004501617SerratiaspAS12
AEG28968SerratiaspAS13
YP006026032SerratiaspAS13
AEF51260SerratiaspAS12
EKT65058ProvidenciaburhodogranarieaDSM19968
WP008910238Providenciaburhodogranariea
AGQ31890SerratialiquefaciensATCC27592
YP008231122SerratialiquefaciensATCC27592
WP020827644Serratialiquefaciens
WP016979083Pseudomonasfluorescens
ETK22786PseudomonasspFH1
AHC32793PseudomonasspTKP
WP010567864Pseudomonasextremaustralis
WP009041741Pseudomonaschlororaphis
EJL00686Pseudomonaschlororaphis
WP007922577PseudomonasspGM17
YP007997630PseudomonasprotegensCHA0
WP015633797Pseudomonasprotegens
AGL82126PseudomonasprotegensCHA0
YP257466PseudomonasprotegensPf5
WP011058698Pseudomonas
YP008929803PseudomonasspTKP
WP024072723PseudomonasspTKP
WP009046503Pseudomonaschlororaphis
WP016702594Pseudomonaschlororaphis
WP019408369Pseudomonaspsychrophila
WP005014353Bordetellaholmesii
EMD76046BordetellaholmesiiH558
EWM45128Bordetellaholmesii70147
EWM41237Bordetellaholmesii35009
EMD74823BordetellaholmesiiF627
EXF88441Bordetellaholmesii30539
EXX94442Bordetellaholmesii1058

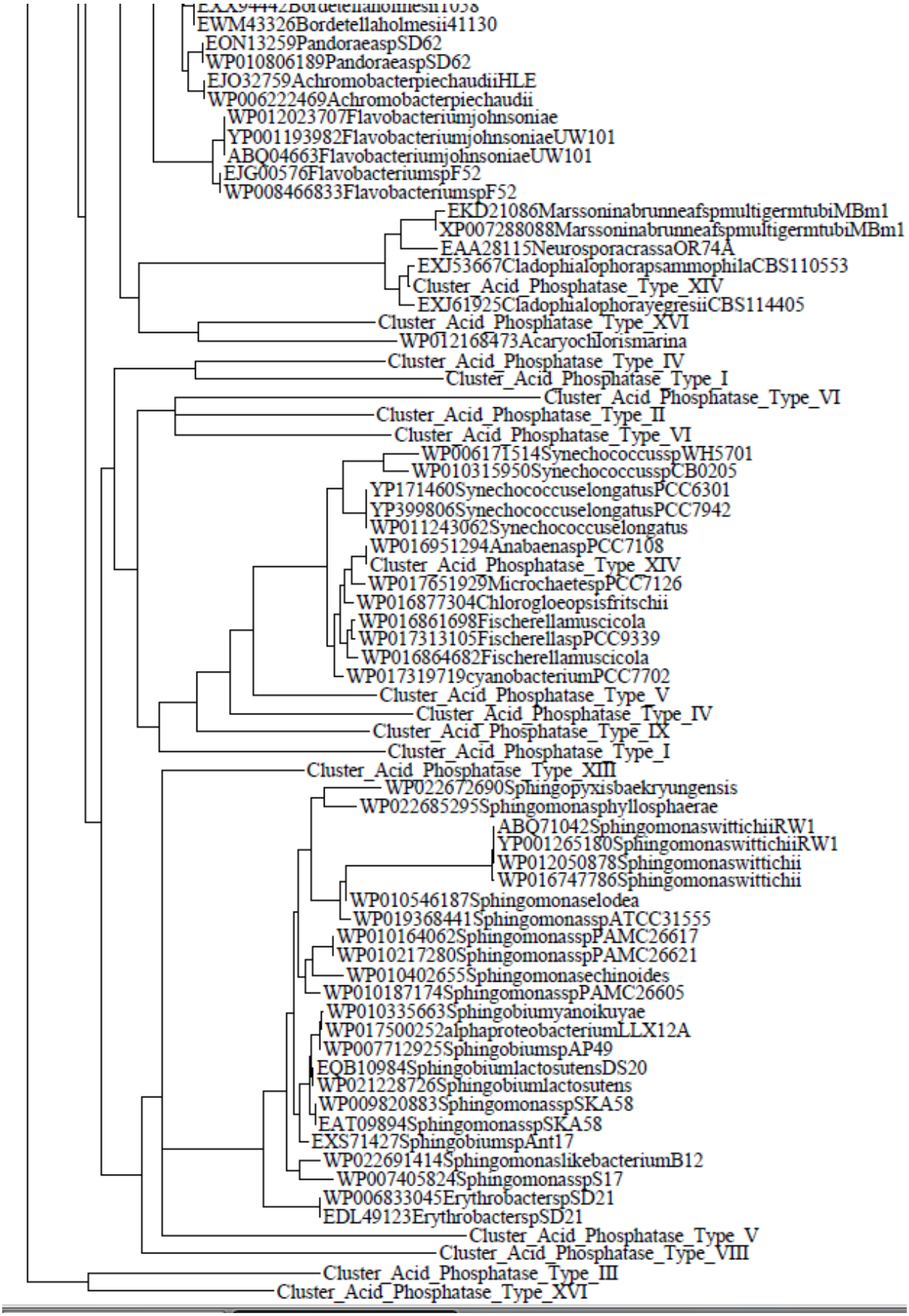
EWM43326Bordetellaholmesii41130
EON13259PandoraeaspSD62
WP010806189PandoraeaspSD62
EJO32759AchromobacterpiechaudiiHLE
WP006222469Achromobacterpiechaudii
WP012023707Flavobacteriumjohnsoniae
YP001193982FlavobacteriumjohnsoniaeUW101
ABQ04663FlavobacteriumjohnsoniaeUW101
EJG00576FlavobacteriumspF52
WP008466833FlavobacteriumspF52
EKD21086MarssoninabrunneafspmultigermtubiMBm1
XP007288088MarssoninabrunneafspmultigermtubiMBm1
EAA28115NeurosporacrassaOR74A
EXJ53667CladophialophorapsammophilaCBS110553
Cluster_Acid_Phosphatase_Type_XIV
EXJ61925CladophialophorayegresiiCBS114405
Cluster_Acid_Phosphatase_Type_XVI
WP012168473Acaryochlorismarina
Cluster_Acid_Phosphatase_Type_IV
Cluster_Acid_Phosphatase_Type_I
Cluster_Acid_Phosphatase_Type_VI
Cluster_Acid_Phosphatase_Type_II
Cluster_Acid_Phosphatase_Type_VI
WP006171514SynechococcusspWH5701
WP010315950SynechococcusspCB0205
YP171460SynechococcuselongatusPCC6301
YP399806SynechococcuselongatusPCC7942
WP011243062Synechococcuselongatus
WP016951294AnabaenaspPCC7108
Cluster_Acid_Phosphatase_Type_XIV
WP017651929MicrochaetespPCC7126
WP016877304Chlorogloeopsisfritschii
WP016861698Fischerellamuscicola
WP017313105FischerellaspPCC9339
WP016864682Fischerellamuscicola
WP017319719cyanobacteriumPCC7702
Cluster_Acid_Phosphatase_Type_V
Cluster_Acid_Phosphatase_Type_IV
Cluster_Acid_Phosphatase_Type_IX
Cluster_Acid_Phosphatase_Type_I
Cluster_Acid_Phosphatase_Type_XIII
WP022672690Sphingopyxisbaekryungensis
WP022685295Sphingomonasphyllosphaerae
ABQ71042SphingomonaswittichiiRW1
YP001265180SphingomonaswittichiiRW1
WP012050878Sphingomonaswittichii
WP016747786Sphingomonaswittichii
WP010546187Sphingomonaselodea
WP019368441SphingomonasspATCC31555
WP010164062SphingomonasspPAMC26617
WP010217280SphingomonasspPAMC26621
WP010402655Sphingomonasechinoides
WP010187174SphingomonasspPAMC26605
WP010335663Sphingobiumyanoikuyae
WP017500252alphaproteobacteriumLLX12A
WP007712925SphingobiumspAP49
EQB10984SphingobiumlactosutensDS20
WP021228726Sphingobiumlactosutens
WP009820883SphingomonasspSKA58
EAT09894SphingomonasspSKA58
EXS71427SphingobiumspAnt17
WP022691414SphingomonaslikebacteriumB12
WP007405824SphingomonasspS17
WP006833045ErythrobacterspSD21
EDL49123ErythrobacterspSD21
Cluster_Acid_Phosphatase_Type_V
Cluster_Acid_Phosphatase_Type_VIII
Cluster_Acid_Phosphatase_Type_III
Cluster_Acid_Phosphatase_Type_XVI

Figure S15b. Phylogenetic tree of cluster XIVb of the acid phosphatase sequences included in the database.

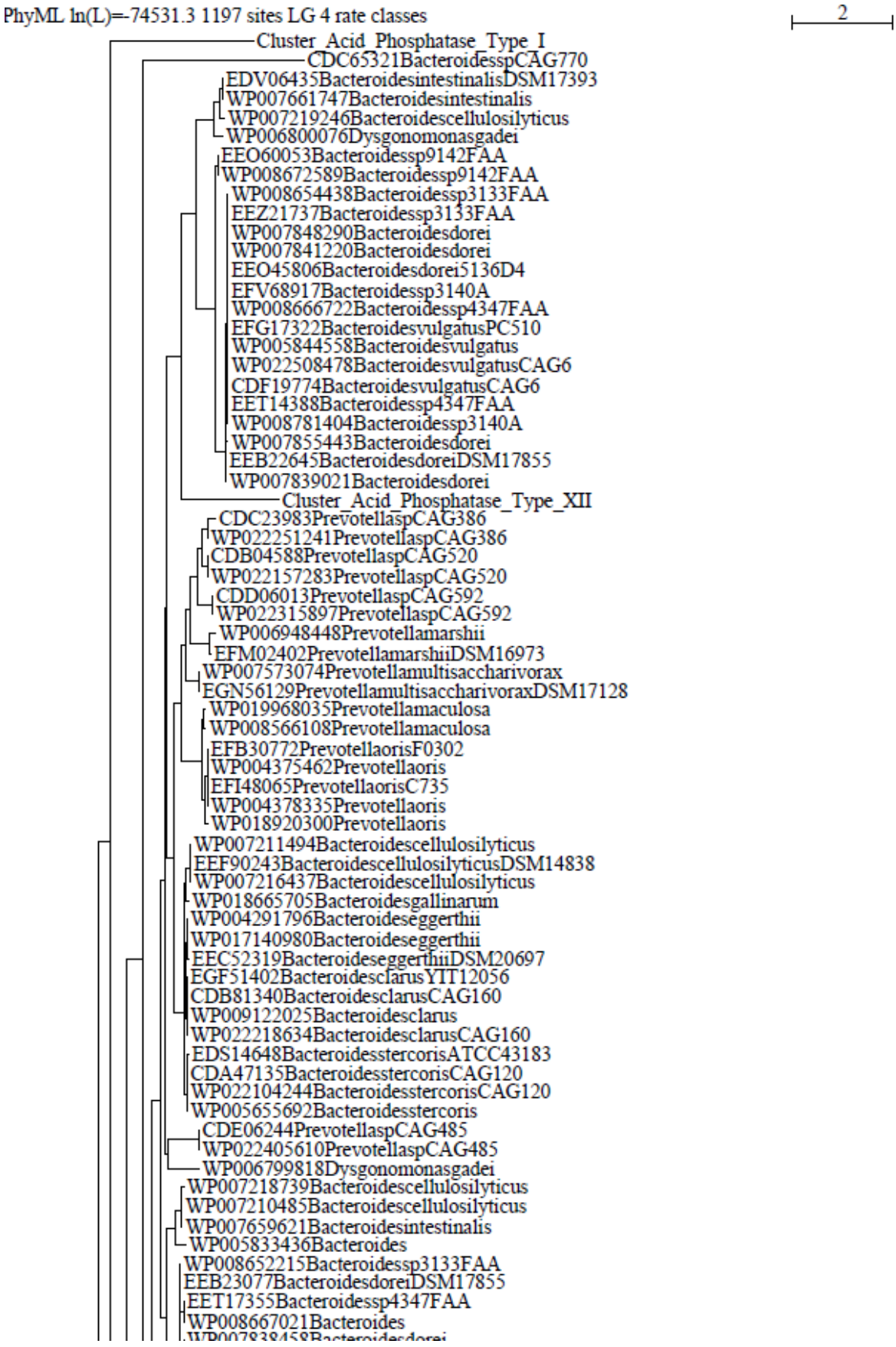

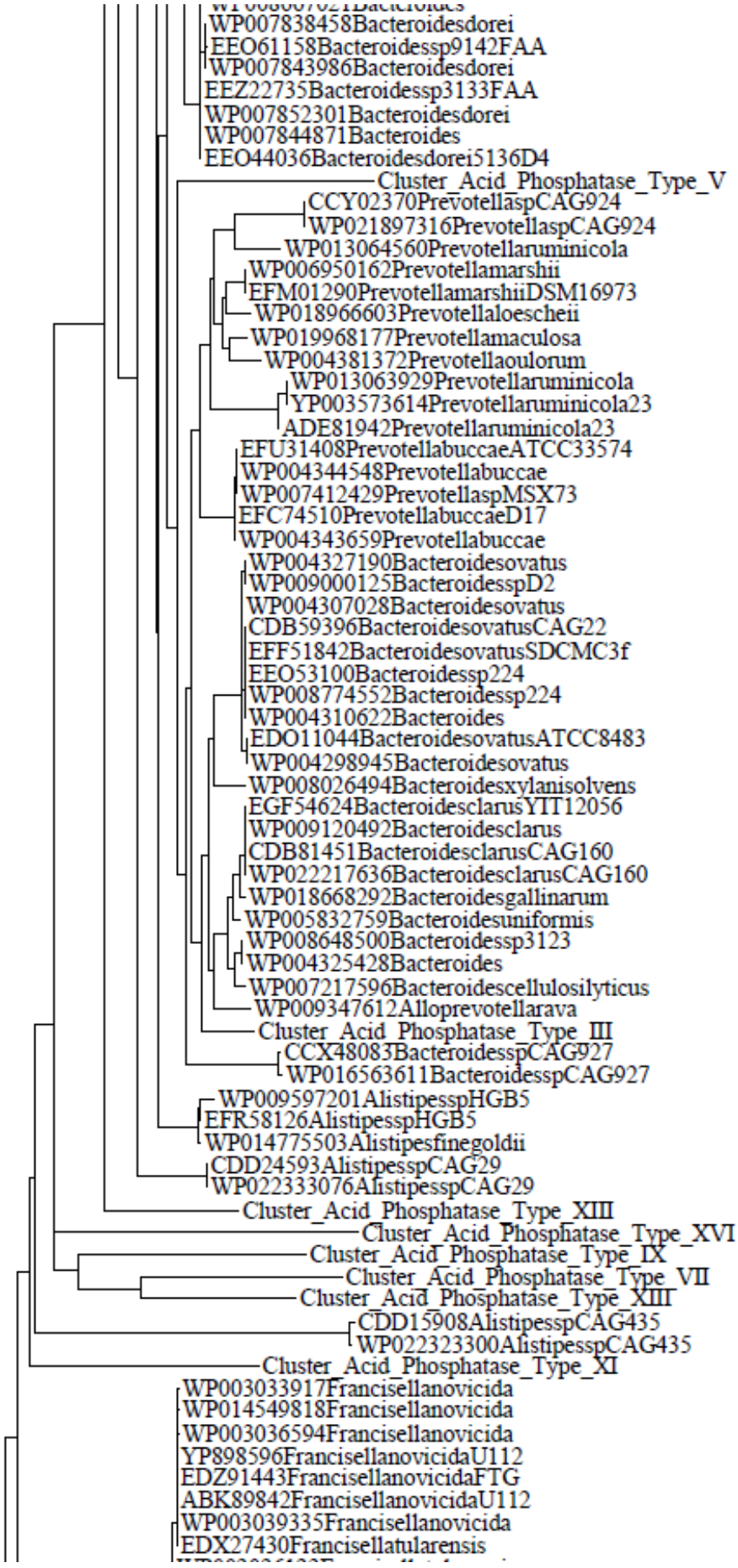
WP007838458Bacteroidesdorei
EEO61158Bacteroidessp9142FAA
WP007843986Bacteroidesdorei
EEZ22735Bacteroidessp3133FAA
WP007852301Bacteroidesdorei
WP007844871Bacteroides
EEO44036Bacteroidesdorei5136D4
Cluster_Acid_Phosphatase_Type_V
CCY02370PrevotellaspCAG924
WP021897316PrevotellaspCAG924
WP013064560Prevotellaruminicola
WP006950162Prevotellamarshii
EFM01290PrevotellamarshiiDSM16973
WP018966603Prevotellaloescheii
WP019968177Prevotellamaculosa
WP004381372Prevotellaoulorum
WP013063929Prevotellaruminicola
YP003573614Prevotellaruminicola23
ADE81942Prevotellaruminicola23
EFU31408PrevotellabuccaeATCC33574
WP004344548Prevotellabuccae
WP007412429PrevotellaspMSX73
EFC74510PrevotellabuccaeD17
WP004343659Prevotellabuccae
WP004327190Bacteroidesovatus
WP009000125BacteroidesspD2
WP004307028Bacteroidesovatus
CDB59396BacteroidesovatusCAG22
EFF51842BacteroidesovatusSDCMC3f
EEO53100Bacteroidessp224
WP008774552Bacteroidessp224
WP004310622Bacteroides
EDO11044BacteroidesovatusATCC8483
WP004298945Bacteroidesovatus
WP008026494Bacteroidesxylanisolvens
EGF54624BacteroidesclarusYIT12056
WP009120492Bacteroidesclarus
CDB81451BacteroidesclarusCAG160
WP022217636BacteroidesclarusCAG160
WP018668292Bacteroidesgallinarum
WP005832759Bacteroidesuniformis
WP008648500Bacteroidessp3123
WP004325428Bacteroides
WP007217596Bacteroidescellulosilyticus
WP009347612Alloprevotellarava
Cluster_Acid_Phosphatase_Type_III
CCX48083BacteroidesspCAG927
WP016563611BacteroidesspCAG927
WP009597201AlistipesspHGB5
EFR58126AlistipesspHGB5
WP014775503Alistipesfinegoldii
CDD24593AlistipesspCAG29
WP022333076AlistipesspCAG29
Cluster_Acid_Phosphatase_Type_XIII
Cluster_Acid_Phosphatase_Type_XVI
Cluster_Acid_Phosphatase_Type_IX
Cluster_Acid_Phosphatase_Type_VII
Cluster_Acid_Phosphatase_Type_XIII
CDD15908AlistipesspCAG435
WP022323300AlistipesspCAG435
Cluster_Acid_Phosphatase_Type_XI
WP003033917Francisellanovicida
WP014549818Francisellanovicida
WP003036594Francisellanovicida
YP898596FrancisellanovicidaU112
EDZ91443FrancisellanovicidaFTG
ABK89842FrancisellanovicidaU112
WP003039335Francisellanovicida
EDX27430Francisellatularensis

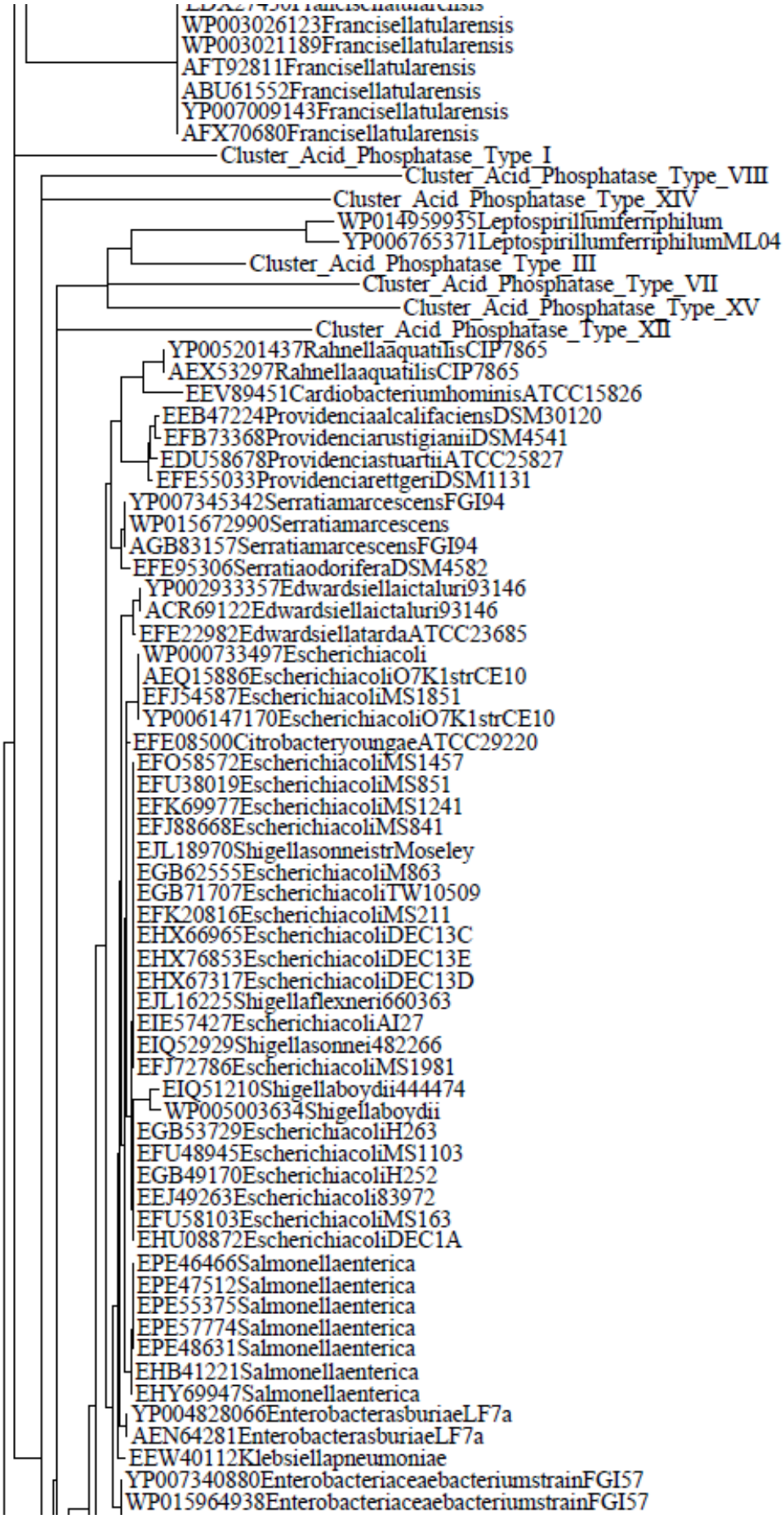
WP003026123Francisellatularensis
WP003021189Francisellatularensis
AFT92811Francisellatularensis
ABU61552Francisellatularensis
YP007009143Francisellatularensis
AFX70680Francisellatularensis
Cluster_Acid_Phosphatase_Type_I
Cluster_Acid_Phosphatase_Type_VIII
Cluster_Acid_Phosphatase_Type_XIV
WP014959935LeptospirillumferriphilumYP006765371LeptospirillumferriphilumML04
Cluster_Acid_Phosphatase_Type_III
Cluster_Acid_Phosphatase_Type_VII
Cluster_Acid_Phosphatase_Type_XV
Cluster_Acid_Phosphatase_Type_XII
YP005201437RahnellaaquatilisCIP7865
AEX53297RahnellaaquatilisCIP7865
EEV89451CardiobacteriumhominisATCC15826
EEB47224ProvidenciaalcalifaciensDSM30120
EFB73368ProvidenciarustigianiiDSM4541
EDU58678ProvidenciastuartiiATCC25827
EFE55033ProvidenciarettgeriDSM1131
YP007345342SerratiamarcescensFGI94
WP015672990Serratiamarcescens
AGB83157SerratiamarcescensFGI94
EFE95306SerratiaodoriferaDSM4582
YP002933357Edwardsiellaictaluri93146
ACR69122Edwardsiellaictaluri93146
EFE22982EdwardsiellatardaATCC23685
WP000733497Escherichiacoli
AEQ15886EscherichiacoliO7K1strCE10
EFJ54587EscherichiacoliMS1851
YP006147170EscherichiacoliO7K1strCE10
EFE08500CitrobacteryoungaeATCC29220
EFO58572EscherichiacoliMS1457
EFU38019EscherichiacoliMS851
EFK69977EscherichiacoliMS1241
EFJ88668EscherichiacoliMS841
EJL18970ShigellasonneistrMoseley
EGB62555EscherichiacoliM863
EGB71707EscherichiacoliTW10509
EFK20816EscherichiacoliMS211
EHX66965EscherichiacoliDEC13C
EHX76853EscherichiacoliDEC13E
EHX67317EscherichiacoliDEC13D
EJL16225Shigellaflexneri660363
EIE57427EscherichiacoliAI27
EIQ52929Shigellasonnei482266
EFJ72786EscherichiacoliMS1981
EIQ51210Shigellaboydii444474
WP005003634Shigellaboydii
EGB53729EscherichiacoliH263
EFU48945EscherichiacoliMS1103
EGB49170EscherichiacoliH252
EEJ49263Escherichiacoli83972
EFU58103EscherichiacoliMS163
EHU08872EscherichiacoliDEC1A
EPE46466Salmonellaenterica
EPE47512Salmonellaenterica
EPE55375Salmonellaenterica
EPE57774Salmonellaenterica
EPE48631Salmonellaenterica
EHB41221Salmonellaenterica
EHY69947Salmonellaenterica
YP004828066EnterobacterasburiaeLF7a
AEN64281EnterobacterasburiaeLF7a
EEW40112Klebsiellapneumoniae
YP007340880EnterobacteriaceaebacteriumstrainFGI57
WP015964938EnterobacteriaceaebacteriumstrainFGI57

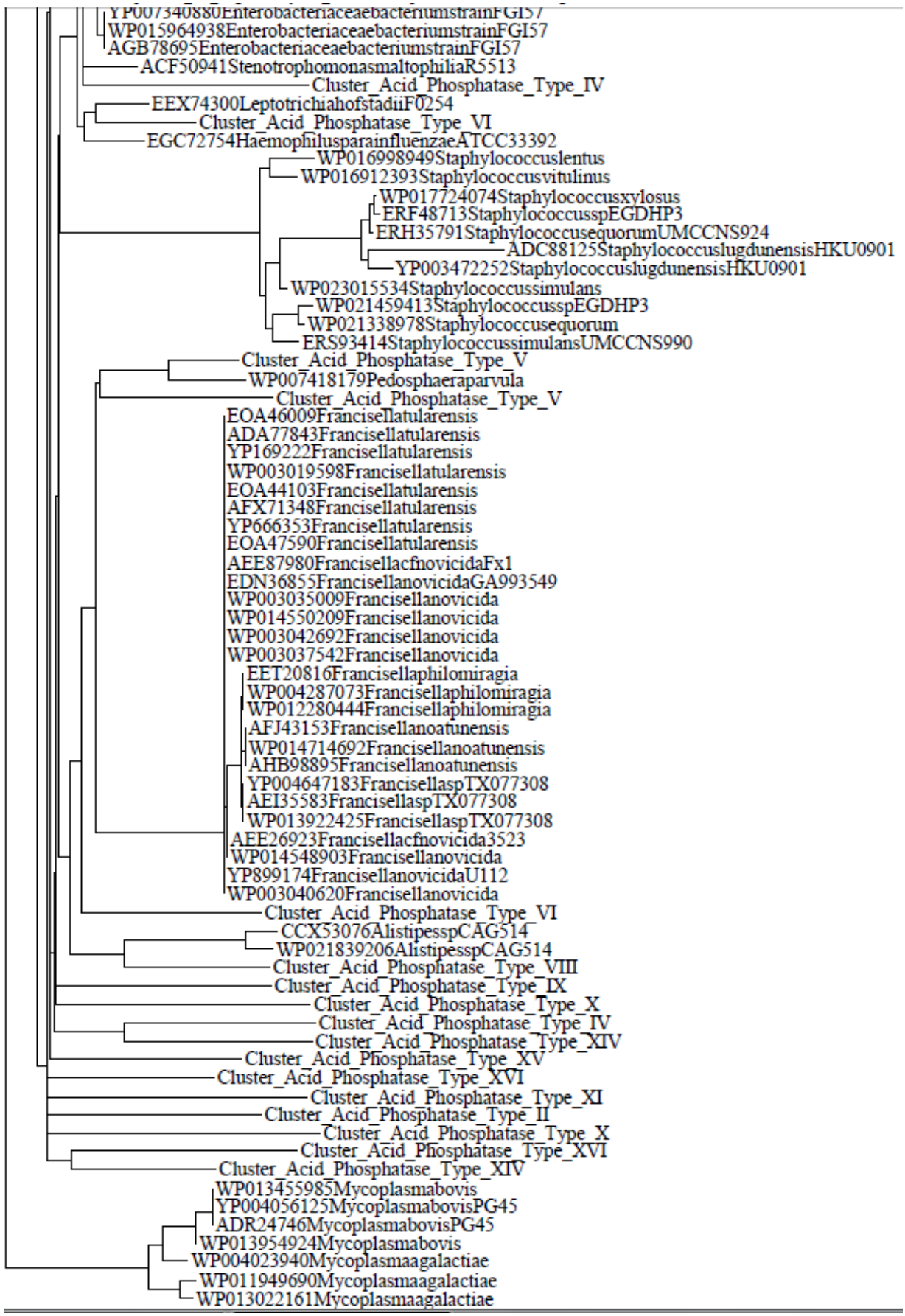
YP007340880EnterobacteriaceaebacteriumstrainFGI57
WP015964938EnterobacteriaceaebacteriumstrainFGI57
AGB78695EnterobacteriaceaebacteriumstrainFGI57
ACF50941StenotrophomonasmaltophiliaR5513
Cluster_Acid_Phosphatase_Type_IV
EEX74300LeptotrichiahofstadiiF0254
Cluster_Acid_Phosphatase_Type_VI
EGC72754HaemophilusparainfluenzaeATCC33392
WP016998949Staphylococcuslentus
WP016912393Staphylococcusvitulinus
WP017724074Staphylococcusxylosus
ERF48713StaphylococcusspEGDHP3
ERH35791StaphylococcusequorumUMCCNS924
ADC88125StaphylococcuslugdunensisHKU0901
YP003472252StaphylococcuslugdunensisHKU0901
WP023015534Staphylococcussimulans
WP021459413StaphylococcusspEGDHP3
WP021338978Staphylococcusequorum
ERS93414StaphylococcussimulansUMCCNS990
Cluster_Acid_Phosphatase_Type_V
WP007418179Pedosphaeraparvula
Cluster_Acid_Phosphatase_Type_V
EOA46009Francisellatularensis
ADA77843Francisellatularensis
YP169222Francisellatularensis
WP003019598Francisellatularensis
EOA44103Francisellatularensis
AFX71348Francisellatularensis
YP666353Francisellatularensis
EOA47590Francisellatularensis
AEE87980FrancisellacfnovicidaFx1
EDN36855FrancisellanovicidaGA993549
WP003035009Francisellanovicida
WP014550209Francisellanovicida
WP003042692Francisellanovicida
WP003037542Francisellanovicida
EET20816Francisellaphilomiragia
WP004287073Francisellaphilomiragia
WP012280444Francisellaphilomiragia
AFJ43153Francisellanoatunensis
WP014714692Francisellanoatunensis
AHB98895Francisellanoatunensis
YP004647183FrancisellaspTX077308
AEI35583FrancisellaspTX077308
WP013922425FrancisellaspTX077308
AEE26923Francisellacfnovicida3523
WP014548903Francisellanovicida
YP899174FrancisellanovicidaU112
WP003040620Francisellanovicida
Cluster_Acid_Phosphatase_Type_VI
CCX53076AlistipesspCAG514
WP021839206AlistipesspCAG514
Cluster_Acid_Phosphatase_Type_VIII
Cluster_Acid_Phosphatase_Type_IX
Cluster_Acid_Phosphatase_Type_X
Cluster_Acid_Phosphatase_Type_IV
Cluster_Acid_Phosphatase_Type_XIV
Cluster_Acid_Phosphatase_Type_XV
Cluster_Acid_Phosphatase_Type_XVI
Cluster_Acid_Phosphatase_Type_XI
Cluster_Acid_Phosphatase_Type_II
Cluster_Acid_Phosphatase_Type_X
Cluster_Acid_Phosphatase_Type_XVI
Cluster_Acid_Phosphatase_Type_XIV
WP013455985Mycoplasmabovis
YP004056125MycoplasmabovisPG45
ADR24746MycoplasmabovisPG45
WP013954924Mycoplasmabovis
WP004023940Mycoplasmaagalactiae
WP011949690Mycoplasmaagalactiae
WP013022161Mycoplasmaagalactiae

Figure S16a. Phylogenetic tree of cluster XVa of the acid phosphatase sequences included in the database.

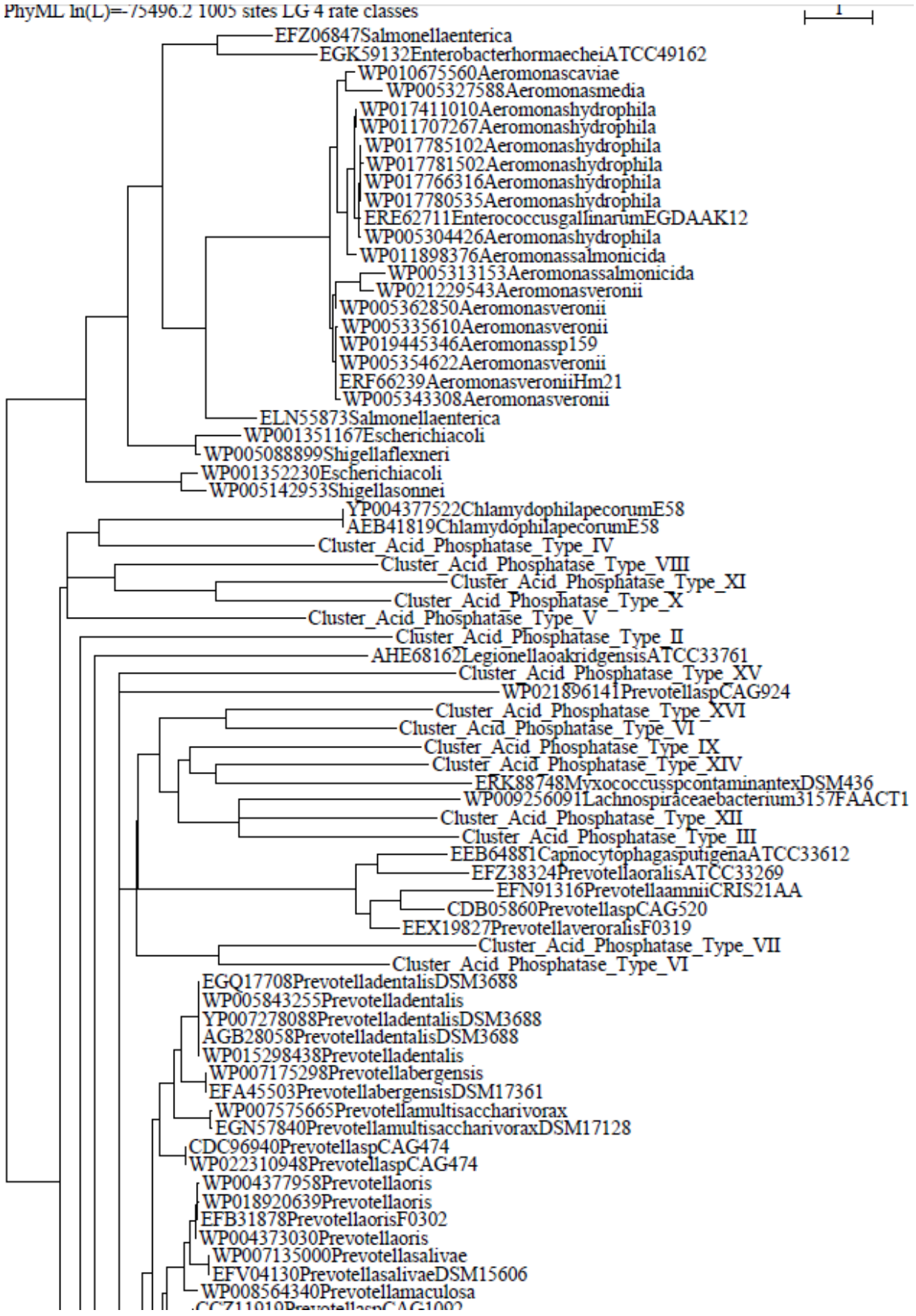


CCZ11919PrevotellaspCAG1092
WP021990751PrevotellaspCAG1092
WP004369143Prevotellaoralis
EFZ38078PrevotellaoralisATCC33269
EKX96958PrevotellasaccharolyticaF0055
WP009161151Prevotellasaccharolytica
WP006848491Prevotellacopri
EFB34717PrevotellacopriDSM18205
WP004347830Prevotellabuccalis
EFA92935PrevotellabuccalisATCC35310
WP008125247Prevotellatimonensis
EFA96946PrevotellatimonensisCRIS5CB1
WP021964384PrevotellaspCAG1185
CCY80685PrevotellaspCAG1185
CCX69937PrevotellaspCAG255
WP021854488PrevotellaspCAG255
WP004351688Prevotelladenticola
AEA20381PrevotelladenticolaF0289
WP013671610Prevotelladenticola
YP004329404PrevotelladenticolaF0289
EGC87405PrevotelladenticolaCRIS18CA
WP007366895Prevotellamultiformis
EGC19250PrevotellamultiformisDSM16608
ERJ76999PrevotellaspF0091
WP021671491PrevotellaspF0091
WP004366998Prevotellanigrescens
WP006044067Prevotellapallens
WP013264558Prevotellamelaninogenica
YP003814082PrevotellamelaninogenicaATCC25845
ADK96026PrevotellamelaninogenicaATCC25845
WP004360020Prevotellamelaninogenica
EFC73196PrevotellamelaninogenicaD18
WP009011556PrevotellaspC561
EEX19246PrevotellaveroralisF0319
WP004382502Prevotellaveroralis
WP018910661Prevotellaveroralis
WP008822804Prevotellahisticola
EFB93474PrevotellabiviaJCVIHMP010
EIM32443PrevotellabiviaDSM20514
WP004336727Prevotellabivia
WP018362403Prevotellananceiensis
WP004344587Prevotellabuccae
EFU31283PrevotellabuccaeATCC33574
WP007412434PrevotellaspMSX73
WP004342063Prevotellabuccae
EFC75710PrevotellabuccaeD17
Cluster_Acid_Phosphatase_Type_X
Cluster_Acid_Phosphatase_Type_XIV
Cluster_Acid_Phosphatase_Type_IX
Cluster_Acid_Phosphatase_Type_V
Cluster_Acid_Phosphatase_Type_XII
Cluster_Acid_Phosphatase_Type_I
CDA96600BacteroidesspCAG709
WP022147840BacteroidesspCAG709
CDC65108BacteroidesspCAG770
WP022284890BacteroidesspCAG770
CCX52980AlistipesspCAG514
WP021839110AlistipesspCAG514
CDD19547AlistipesspCAG435
WP022324758AlistipesspCAG435
Cluster_Acid_Phosphatase_Type_XIII
Cluster_Acid_Phosphatase_Type_VII
EAA27615NeurosporacrassaOR74A
CCY91192BacteroidesspCAG1076
WP021970048BacteroidesspCAG1076
CDB97491BacteroidesspCAG443
WP022233291BacteroidesspCAG443
WP007567142Bacteroidescoprocola
EDV01064BacteroidescoprocolaDSM17136
CDA70915BacteroidescoprocolaCAG162

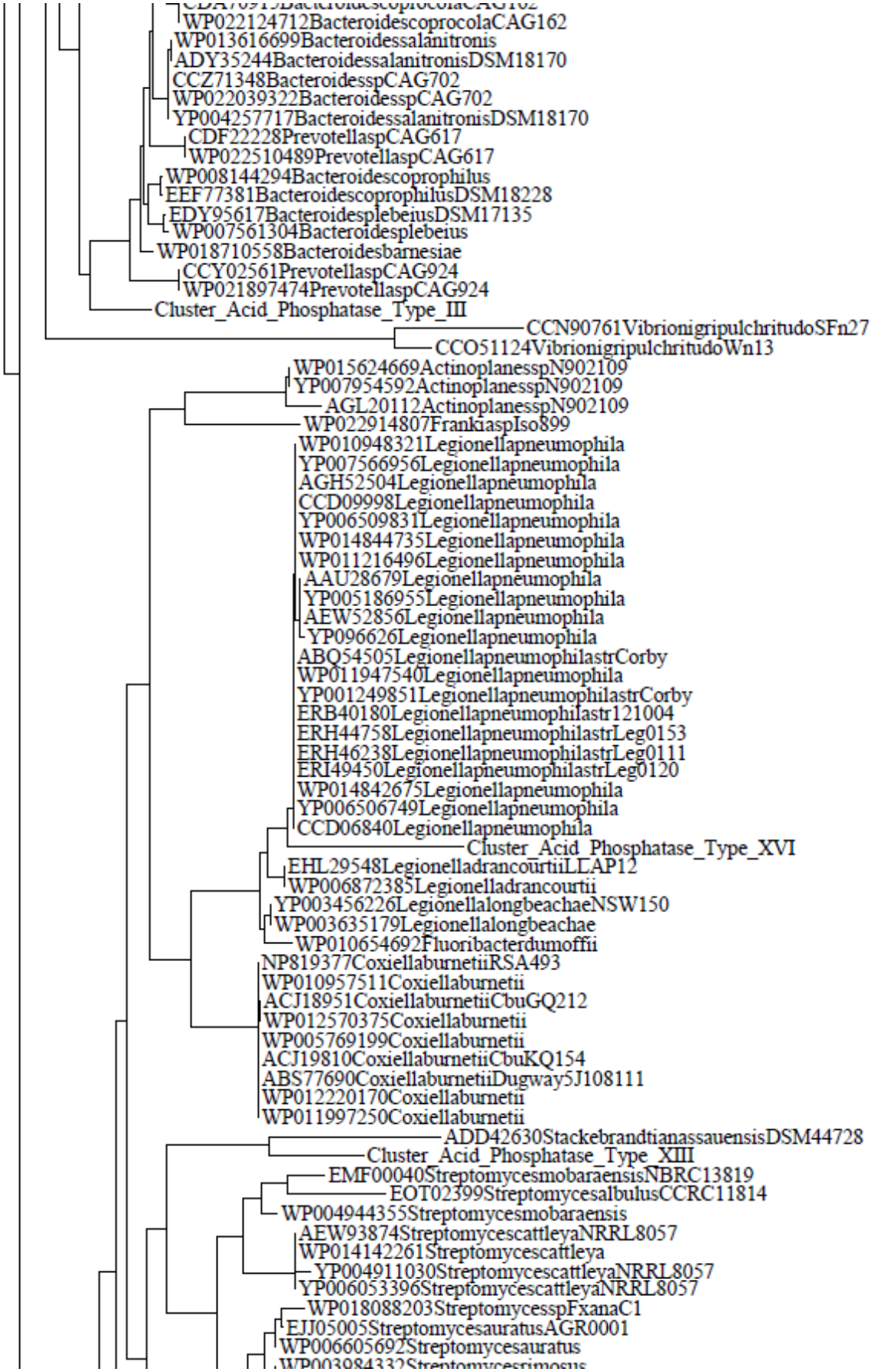
WP022124712BacteroidescoprocolaCAG162
WP013616699Bacteroidessalanitronis
ADY35244BacteroidessalanitronisDSM18170
CCZ71348BacteroidesspCAG702
WP022039322BacteroidesspCAG702
YP004257717BacteroidessalanitronisDSM18170
CDF22228PrevotellaspCAG617
WP022510489PrevotellaspCAG617
WP008144294Bacteroidescoprophilus
EEF77381BacteroidescoprophilusDSM18228
EDY95617BacteroidesplebeiusDSM17135
WP007561304Bacteroidesplebeius
WP018710558Bacteroidesbarnesiae
CCY02561PrevotellaspCAG924
WP021897474PrevotellaspCAG924
Cluster_Acid_Phosphatase_Type_III
CCN90761VibrionigripulchritudoSFn27
CCO51124VibrionigripulchritudoWn13
WP015624669ActinoplanesspN902109
YP007954592ActinoplanesspN902109
AGL20112ActinoplanesspN902109
WP022914807FrankiaspIso899
WP010948321Legionellapneumophila
YP007566956Legionellapneumophila
AGH52504Legionellapneumophila
CCD09998Legionellapneumophila
YP006509831Legionellapneumophila
WP014844735Legionellapneumophila
WP011216496Legionellapneumophila
AAU28679Legionellapneumophila
YP005186955Legionellapneumophila
AEW52856Legionellapneumophila
YP096626Legionellapneumophila
ABQ54505LegionellapneumophilastrCorby
WP011947540Legionellapneumophila
YP001249851LegionellapneumophilastrCorby
ERB40180Legionellapneumophilastr121004
ERH44758LegionellapneumophilastrLeg0153
ERH46238LegionellapneumophilastrLeg0111
ERI49450LegionellapneumophilastrLeg0120
WP014842675Legionellapneumophila
YP006506749Legionellapneumophila
CCD06840Legionellapneumophila
Cluster_Acid_Phosphatase_Type_XVI
EHL29548LegionelladrancourtiiLLAP12
WP006872385Legionelladrancourtii
YP003456226LegionellalongbeachaeNSW150
WP003635179Legionellalongbeachae
WP010654692Fluoribacterdumoffii
NP819377CoxiellaburnetiiRSA493
WP010957511Coxiellaburnetii
ACJ18951CoxiellaburnetiiCbuGQ212
WP012570375Coxiellaburnetii
WP005769199Coxiellaburnetii
ACJ19810CoxiellaburnetiiCbuKQ154
ABS77690CoxiellaburnetiiDugway5J108111
WP012220170Coxiellaburnetii
WP011997250Coxiellaburnetii
ADD42630StackebrandtianassauensisDSM44728
Cluster_Acid_Phosphatase_Type_XIII
EMF00040StreptomycesmobaraensisNBRC13819
EOT02399StreptomycesalbulusCCRC11814
WP004944355Streptomycesmobaraensis
AEW93874StreptomycescattleyaNRRL8057
WP014142261Streptomycescattleya
YP004911030StreptomycescattleyaNRRL8057
YP006053396StreptomycescattleyaNRRL8057
WP018088203StreptomycesspFxanaC1
EJJ05005StreptomycesauratusAGR0001
WP006605692Streptomycesauratus

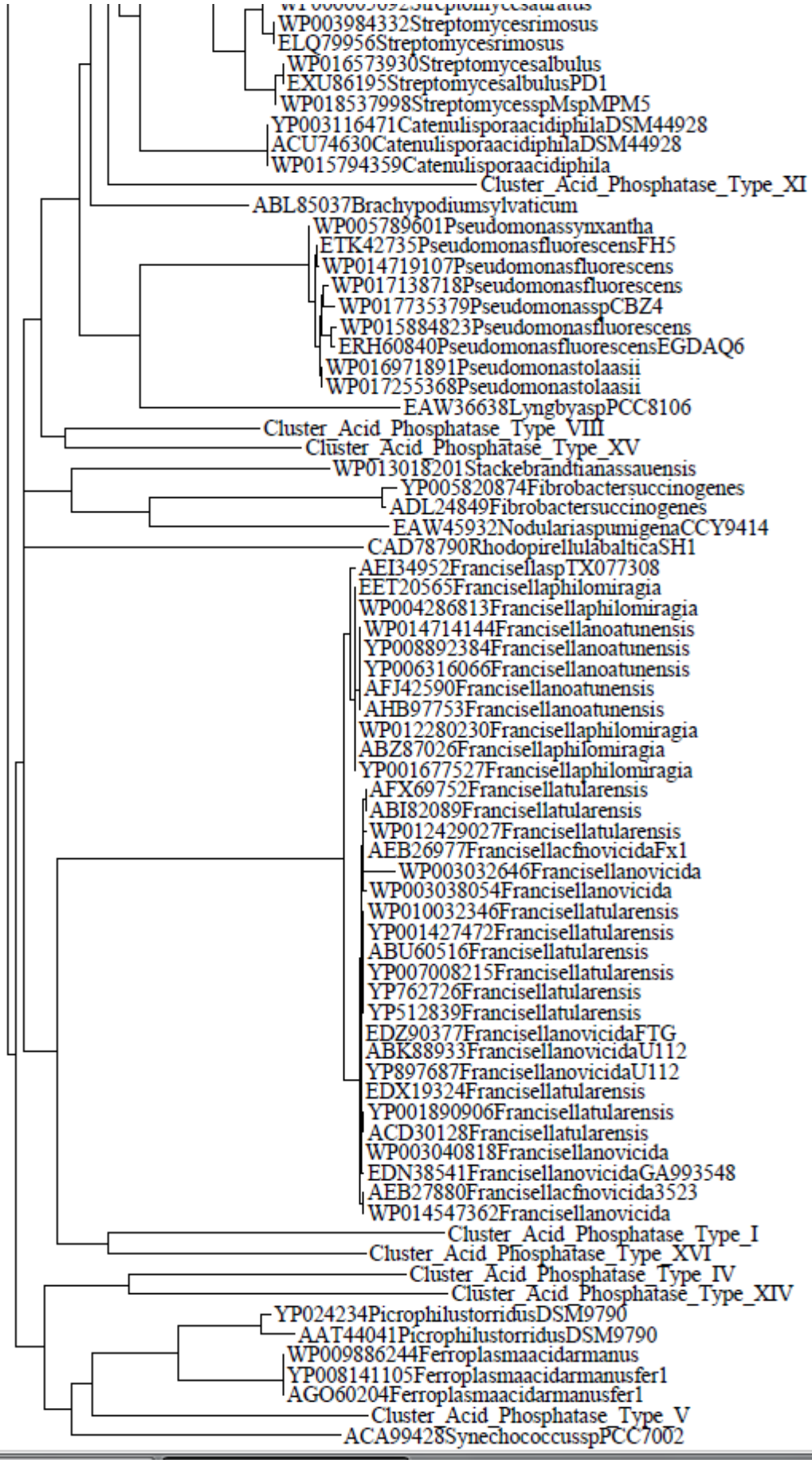
WP003984332Streptomycesrimosus
ELQ79956Streptomycesrimosus
WP016573930Streptomycesalbulus
EXU86195StreptomycesalbulusPD1
WP018537998StreptomycesspMspMPM5
YP003116471CatenulisporaacidiphilaDSM44928
ACU74630CatenulisporaacidiphilaDSM44928
WP015794359Catenulisporaacidiphila
Cluster_Acid_Phosphatase_Type_XI
ABL85037Brachypodiumsylvaticum
WP005789601Pseudomonassynxantha
ETK42735PseudomonasfluorescensFH5
WP014719107Pseudomonasfluorescens
WP017138718Pseudomonasfluorescens
WP017735379PseudomonasspCBZ4
WP015884823Pseudomonasfluorescens
ERH60840PseudomonasfluorescensEGDAQ6
WP016971891Pseudomonastolaasii
WP017255368Pseudomonastolaasii
EAW36638LyngbyaspPCC8106
Cluster_Acid_Phosphatase_Type_VIII
Cluster_Acid_Phosphatase_Type_XV
WP013018201Stackebrandtianassauensis
YP005820874Fibrobactersuccinogenes
ADL24849Fibrobactersuccinogenes
EAW45932NodulariaspumigenaCCY9414
CAD78790RhodopirellulabalticaSH1
AEI34952FrancisellaspTX077308
EET20565Francisellaphilomiragia
WP004286813Francisellaphilomiragia
WP014714144Francisellanoatunensis
YP008892384Francisellanoatunensis
YP006316066Francisellanoatunensis
AFJ42590Francisellanoatunensis
AHB97753Francisellanoatunensis
WP012280230Francisellaphilomiragia
ABZ87026Francisellaphilomiragia
YP001677527Francisellaphilomiragia
AFX69752Francisellatularensis
ABI82089Francisellatularensis
WP012429027Francisellatularensis
AEB26977FrancisellacfnovicidaFx1
WP003032646Francisellanovicida
WP003038054Francisellanovicida
WP010032346Francisellatularensis
YP001427472Francisellatularensis
ABU60516Francisellatularensis
YP007008215Francisellatularensis
YP762726Francisellatularensis
YP512839Francisellatularensis
EDZ90377FrancisellanovicidaFTG
ABK88933FrancisellanovicidaU112
YP897687FrancisellanovicidaU112
EDX19324Francisellatularensis
YP001890906Francisellatularensis
ACD30128Francisellatularensis
WP003040818Francisellanovicida
EDN38541FrancisellanovicidaGA993548
AEB27880Francisellacfnovicida3523
WP014547362Francisellanovicida
Cluster_Acid_Phosphatase_Type_I
Cluster_Acid_Phosphatase_Type_XVI
Cluster_Acid_Phosphatase_Type_IV
Cluster_Acid_Phosphatase_Type_XIV
YP024234PicrophilustorridusDSM9790
AAT44041PicrophilustorridusDSM9790
WP009886244Ferroplasmaacidarmanus
YP008141105Ferroplasmaacidarmanusfer1
AGO60204Ferroplasmaacidarmanusfer1
Cluster_Acid_Phosphatase_Type_V
ACA99428SynechococcusspPCC7002

Figure S16b. Phylogenetic tree of cluster XVb of the acid phosphatase sequences included in the database.

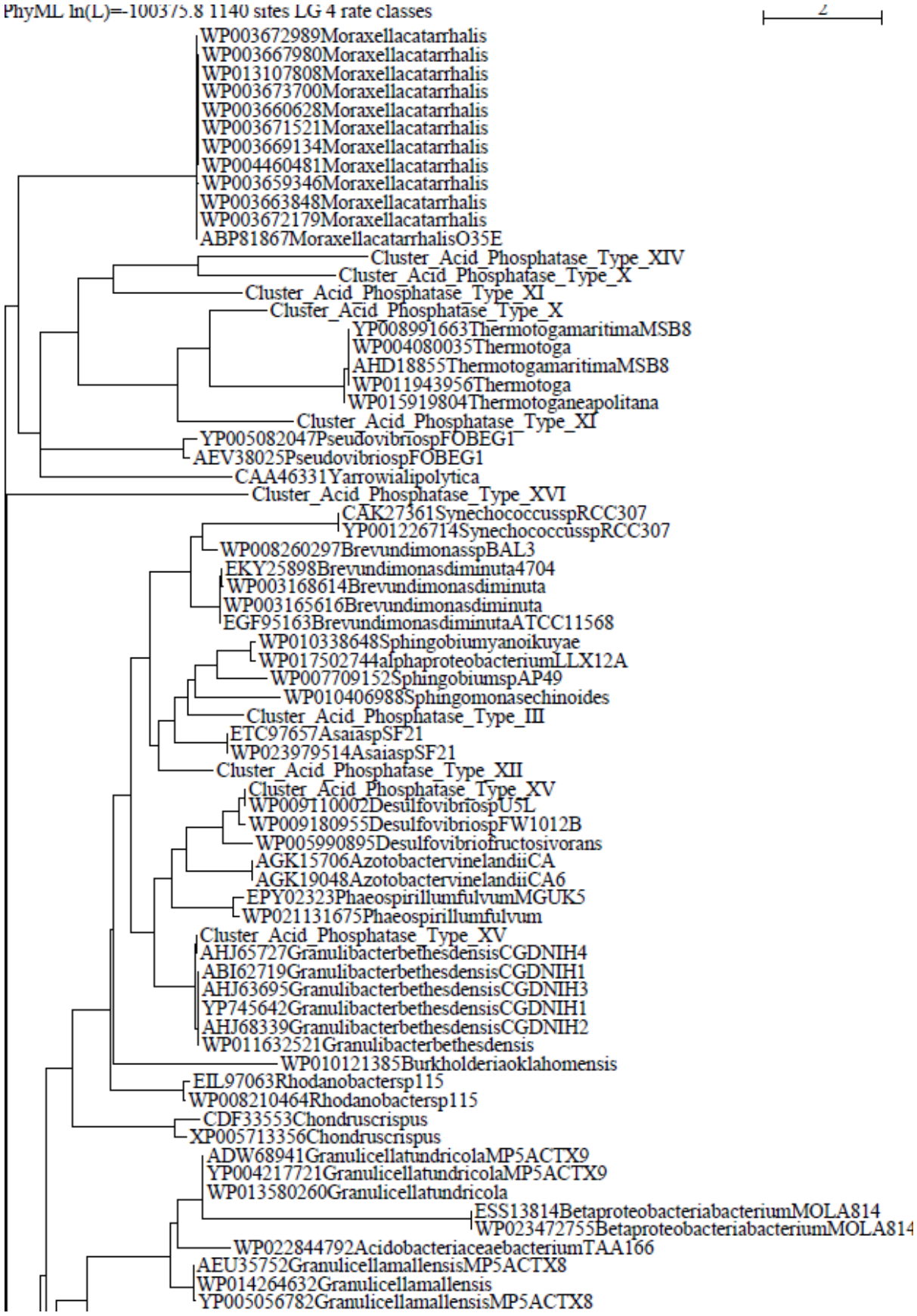

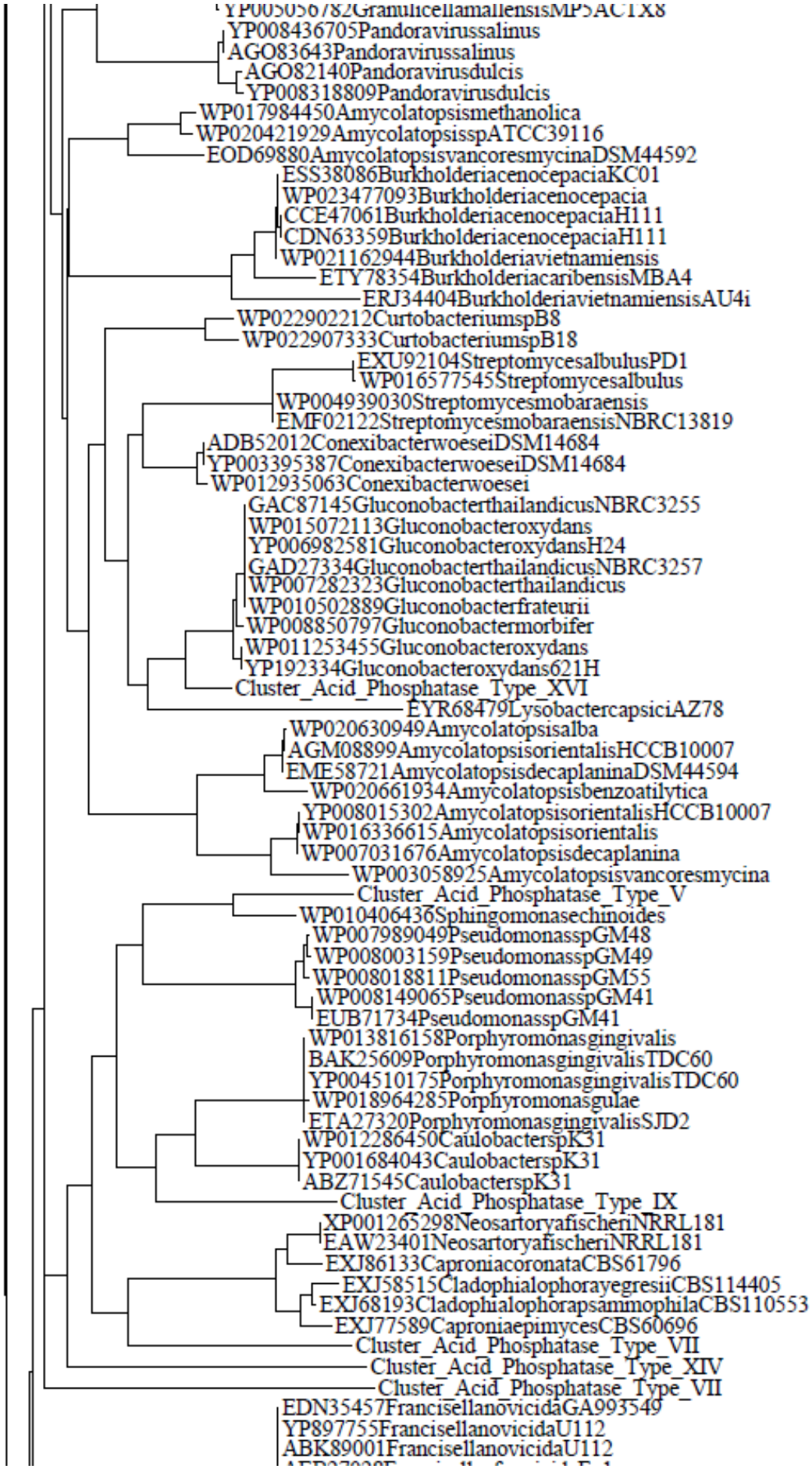
YP008436705Pandoravirussalinus
AGO83643Pandoravirussalinus
AGO82140Pandoravirusdulcis
YP008318809Pandoravirusdulcis
WP017984450Amycolatopsismethanolica
WP020421929AmycolatopsisspATCC39116
EOD69880AmycolatopsisvancoresmycinaDSM44592
ESS38086BurkholderiacenocepaciaKC01
WP023477093Burkholderiacenocepacia
CCE47061BurkholderiacenocepaciaH111
CDN63359BurkholderiacenocepaciaH111
WP021162944Burkholderiavietnamiensis
ETY78354BurkholderiacaribensisMBA4
ERJ34404BurkholderiavietnamiensisAU4i
WP022902212CurtobacteriumspB8
WP022907333CurtobacteriumspB18
EXU92104StreptomycesalbulusPD1
WP016577545Streptomycesalbulus
WP004939030Streptomycesmobaraensis
EMF02122StreptomycesmobaraensisNBRC13819
ADB52012ConexibacterwoeseiDSM14684
YP003395387ConexibacterwoeseiDSM14684
WP012935063Conexibacterwoesei
GAC87145GluconobacterthailandicusNBRC3255
WP015072113Gluconobacteroxydans
YP006982581GluconobacteroxydansH24
GAD27334GluconobacterthailandicusNBRC3257
WP007282323Gluconobacterthailandicus
WP010502889Gluconobacterfrateurii
WP008850797Gluconobactermorbifer
WP011253455Gluconobacteroxydans
YP192334Gluconobacteroxydans621H
Cluster_Acid_Phosphatase_Type_XVI
EYR68479LysobactercapsiciAZ78
WP020630949Amycolatopsisalba
AGM08899AmycolatopsisorientalisHCCB10007
EME58721AmycolatopsisdecaplaninaDSM44594
WP020661934Amycolatopsisbenzoatilytica
YP008015302AmycolatopsisorientalisHCCB10007
WP016336615Amycolatopsisorientalis
WP007031676Amycolatopsisdecaplanina
WP003058925Amycolatopsisvancoresmycina
Cluster_Acid_Phosphatase_Type_V
WP010406436Sphingomonasechinoides
WP007989049PseudomonasspGM48
WP008003159PseudomonasspGM49
WP008018811PseudomonasspGM55
WP008149065PseudomonasspGM41
EUB71734PseudomonasspGM41
WP013816158Porphyromonasgingivalis
BAK25609PorphyromonasgingivalisTDC60
YP004510175PorphyromonasgingivalisTDC60
WP018964285Porphyromonasgulae
ETA27320PorphyromonasgingivalisSJD2
WP012286450CaulobacterspK31
YP001684043CaulobacterspK31
ABZ71545CaulobacterspK31
Cluster_Acid_Phosphatase_Type_IX
XP001265298NeosartoryafischeriNRRL181
EAW23401NeosartoryafischeriNRRL181
EXJ86133CaproniacoronataCBS61796
EXJ58515CladophialophorayegresiiCBS114405
EXJ68193CladophialophorapsammophilaCBS110553
EXJ77589CapronіaepimycesCBS60696
Cluster_Acid_Phosphatase_Type_VII
Cluster_Acid_Phosphatase_Type_XIV
Cluster_Acid_Phosphatase_Type_VII
EDN35457FrancisellanovicidaGA993549
YP897755FrancisellanovicidaU112
ABK89001FrancisellanovicidaU112

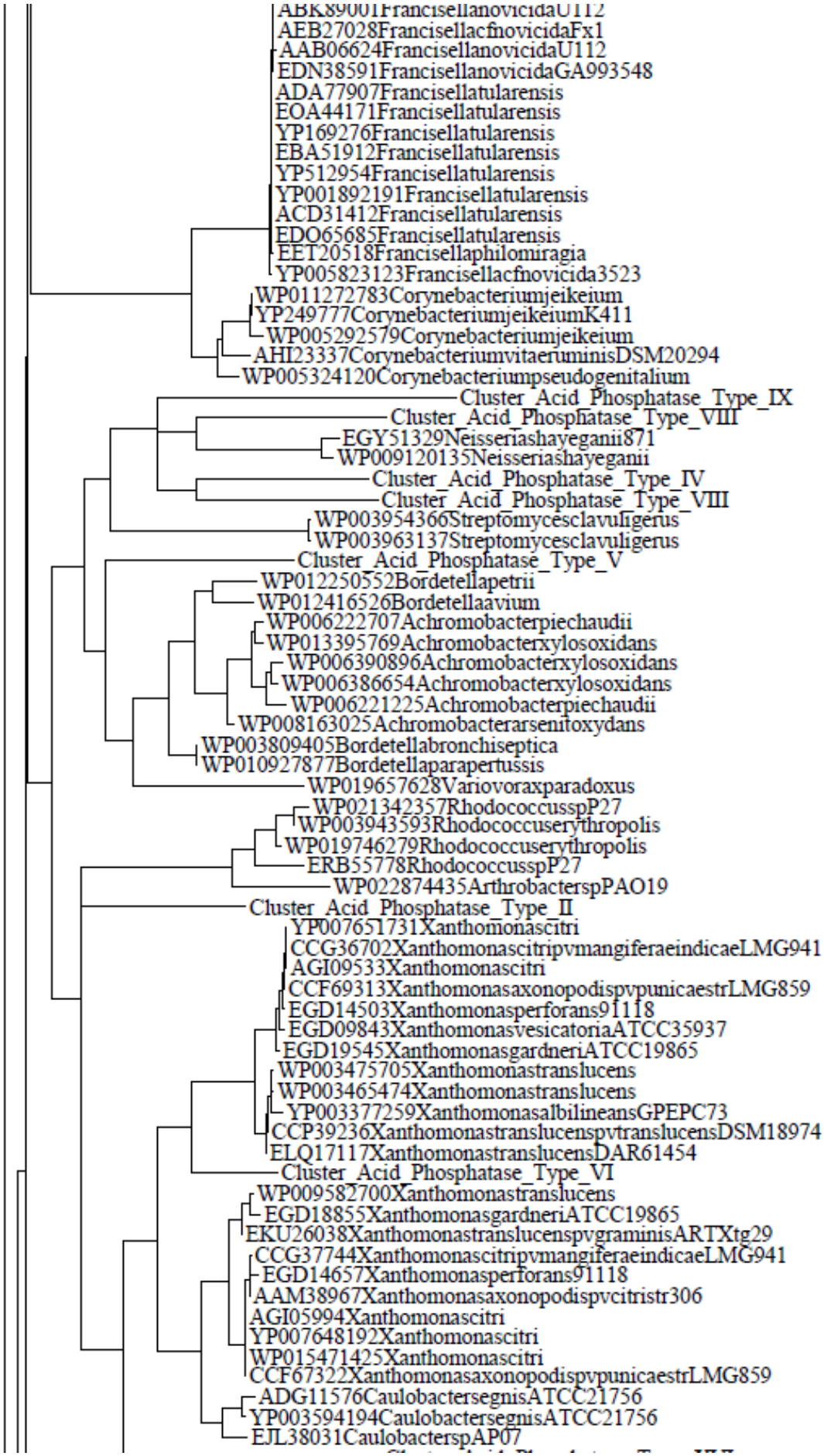
ABK89001FrancisellanovicidaU112
AEB27028FrancisellacfnovicidaFx1
AAB06624FrancisellanovicidaU112
EDN38591FrancisellanovicidaGA993548
ADA77907Francisellatularensis
EOA44171Francisellatularensis
YP169276Francisellatularensis
EBA51912Francisellatularensis
YP512954Francisellatularensis
YP001892191Francisellatularensis
ACD31412Francisellatularensis
EDO65685Francisellatularensis
EET20518Francisellaphilomiragia
YP005823123Francisellacfnovicida3523
WP011272783Corynebacteriumjeikeium
YP249777CorynebacteriumjeikeiumK411
WP005292579Corynebacteriumjeikeium
AHI23337CorynebacteriumvitaeruminisDSM20294
WP005324120Corynebacteriumpseudogenitalium
Cluster_Acid_Phosphatase_Type_IX
Cluster_Acid_Phosphatase_Type_VIII
EGY51329Neisseriashayeganii871
WP009120135Neisseriashayeganii
Cluster_Acid_Phosphatase_Type_IV
Cluster_Acid_Phosphatase_Type_VIII
WP003954366Streptomycesclavuligerus
WP003963137Streptomycesclavuligerus
Cluster_Acid_Phosphatase_Type_V
WP012250552Bordetellapetrii
WP012416526Bordetellaavium
WP006222707Achromobacterpiechaudii
WP013395769Achromobacterxylosoxidans
WP006390896Achromobacterxylosoxidans
WP006386654Achromobacterxylosoxidans
WP006221225Achromobacterpiechaudii
WP008163025Achromobacterarsenitoxydans
WP003809405Bordetellabronchiseptica
WP010927877Bordetellaparapertussis
WP019657628Variovoraxparadoxus
WP021342357RhodococcusspP27
WP003943593Rhodococcuserythropolis
WP019746279Rhodococcuserythropolis
ERB55778RhodococcusspP27
WP022874435ArthrobacterspPAO19
Cluster_Acid_Phosphatase_Type_II
YP007651731Xanthomonascitri
CCG36702XanthomonascitripvmangiferaeindicaeLMG941
AGI09533Xanthomonascitri
CCF69313XanthomonasaxonopodispvpunicaestrLMG859
EGD14503Xanthomonasperforans91118
EGD09843XanthomonasvesicatoriaATCC35937
EGD19545XanthomonasgardneriATCC19865
WP003475705Xanthomonastranslucens
WP003465474Xanthomonastranslucens
YP003377259XanthomonasalbilineansGPEPC73
CCP39236XanthomonastranslucenspvtranslucensDSM18974
ELQ17117XanthomonastranslucensDAR61454
Cluster_Acid_Phosphatase_Type_VI
WP009582700Xanthomonastranslucens
EGD18855XanthomonasgardneriATCC19865
EKU26038XanthomonastranslucenspvgraminisARTXtg29
CCG37744XanthomonascitripvmangiferaeindicaeLMG941
EGD14657Xanthomonasperforans91118
AAM38967Xanthomonasaxonopodispvcitristr306
AGI05994Xanthomonascitri
YP007648192Xanthomonascitri
WP015471425Xanthomonascitri
CCF67322XanthomonasaxonopodispvpunicaestrLMG859
ADG11576CaulobactersegnisATCC21756
YP003594194CaulobactersegnisATCC21756
EJL38031CaulobacterspAP07

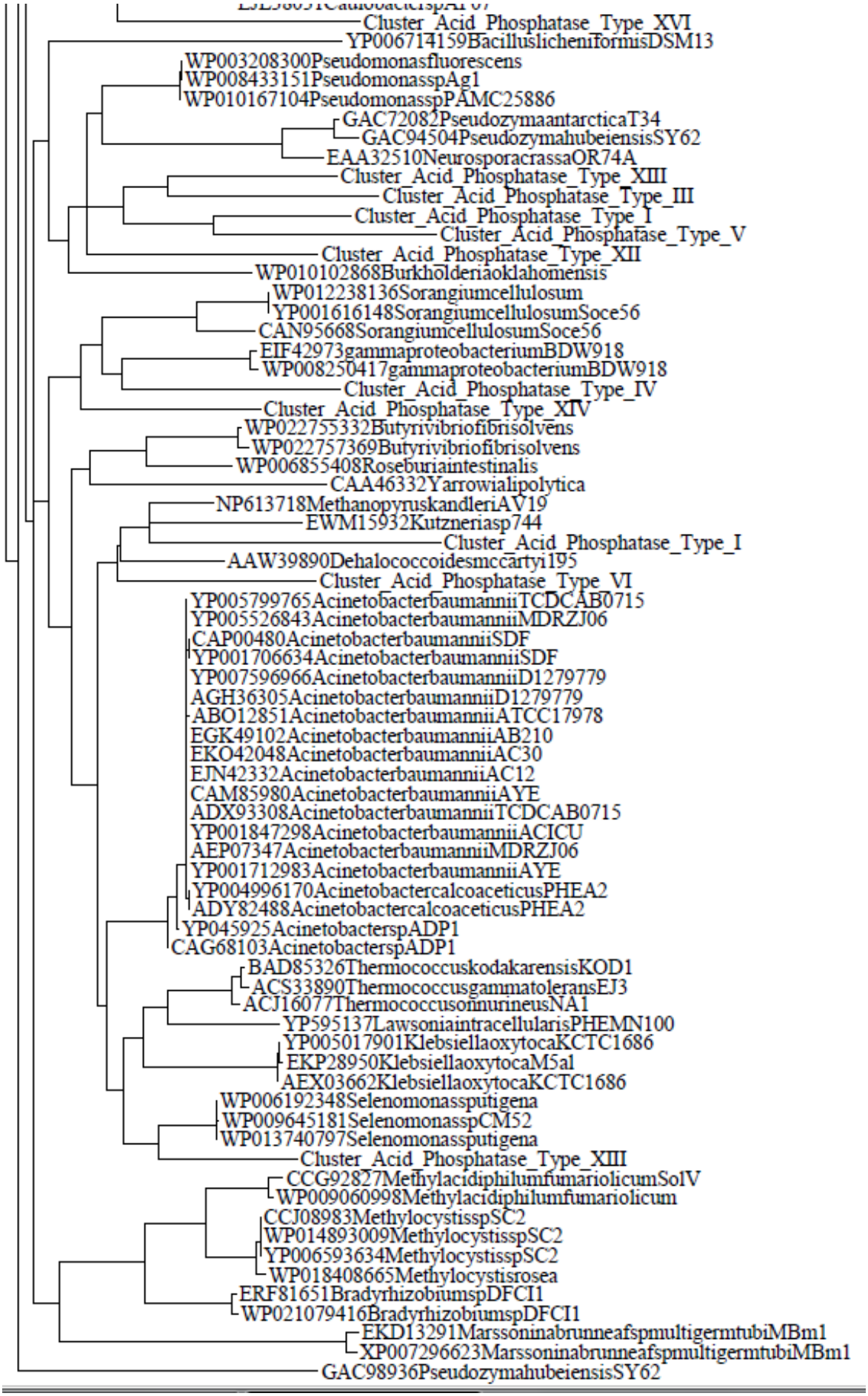
Cluster_Acid_Phosphatase_Type_XVI
YP006714159BacilluslicheniformisDSM13
WP003208300Pseudomonasfluorescens
WP008433151PseudomonasspAg1
WP010167104PseudomonasspPAMC25886
GAC72082PseudozymaantarcticaT34
GAC94504PseudozymahubeiensisSY62
EAA32510NeurosporacrassaOR74A
Cluster_Acid_Phosphatase_Type_XIII
Cluster_Acid_Phosphatase_Type_III
Cluster_Acid_Phosphatase_Type_I
Cluster_Acid_Phosphatase_Type_V
Cluster_Acid_Phosphatase_Type_XII
WP010102868Burkholderiaoklahomensis
WP012238136Sorangiumcellulosum
YP001616148SorangiumcellulosumSoce56
CAN95668SorangiumcellulosumSoce56
EIF42973gammaproteobacteriumBDW918
WP008250417gammaproteobacteriumBDW918
Cluster_Acid_Phosphatase_Type_IV
Cluster_Acid_Phosphatase_Type_XIV
WP022755332Butyrivibriofibrisolvens
WP022757369Butyrivibriofibrisolvens
WP006855408Roseburiaintestinalis
CAA46332Yarrowialipolytica
NP613718MethanopyruskandleriAV19
EWM15932Kutzneriasp744
Cluster_Acid_Phosphatase_Type_I
AAW39890Dehalococcoidesmccartyi195
Cluster_Acid_Phosphatase_Type_VI
YP005799765AcinetobacterbaumanniiTCDCAB0715
YP005526843AcinetobacterbaumanniiMDRZJ06
CAP00480AcinetobacterbaumanniiSDF
YP001706634AcinetobacterbaumanniiSDF
YP007596966AcinetobacterbaumanniiD1279779
AGH36305AcinetobacterbaumanniiD1279779
ABO12851AcinetobacterbaumanniiATCC17978
EGK49102AcinetobacterbaumanniiAB210
EKO42048AcinetobacterbaumanniiAC30
EJN42332AcinetobacterbaumanniiAC12
CAM85980AcinetobacterbaumanniiAYE
ADX93308AcinetobacterbaumanniiTCDCAB0715
YP001847298AcinetobacterbaumanniiACICU
AEP07347AcinetobacterbaumanniiMDRZJ06
YP001712983AcinetobacterbaumanniiAYE
YP004996170AcinetobactercalcoaceticusPHEA2
ADY82488AcinetobactercalcoaceticusPHEA2
YP045925AcinetobacterspADP1
CAG68103AcinetobacterspADP1
BAD85326ThermococcuskodakarensisKOD1
ACS33890ThermococcusgammatoleransEJ3
ACJ16077ThermococcusonnurineusNA1
YP595137LawsoniaintracellularisPHEMN100
YP005017901KlebsiellaoxytocaKCTC1686
EKP28950KlebsiellaoxytocaM5al
AEX03662KlebsiellaoxytocaKCTC1686
WP006192348Selenomonasputigena
WP009645181SelenomonasspCM52
WP013740797Selenomonasputigena
Cluster_Acid_Phosphatase_Type_XIII
CCG92827MethylacidiphilumfumariolicumSolV
WP009060998Methylacidiphilumfumariolicum
CCJ08983MethylocystisspSC2
WP014893009MethylocystisspSC2
YP006593634MethylocystisspSC2
WP018408665Methylocystisrosea
ERF81651BradyrhizobiumspDFCI1
WP021079416BradyrhizobiumspDFCI1
EKD13291MarssoninabrunneafspmultigermtubiMBm1
XP007296623MarssoninabrunneafspmultigermtubiMBm1
GAC98936PseudozymahubeiensisSY62

Figure S17a. Phylogenetic tree of cluster XVIa of the acid phosphatase sequences included in the database.

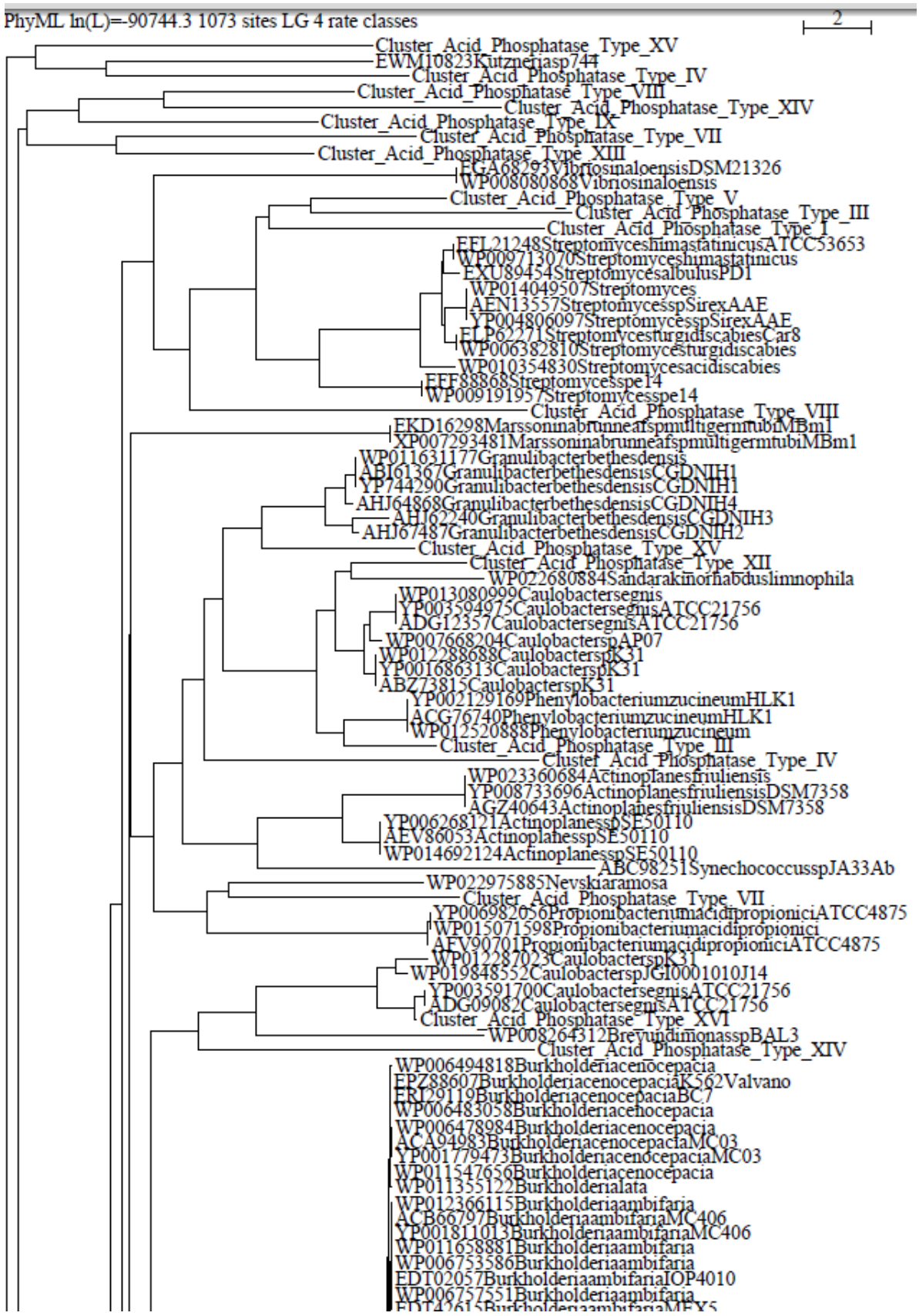


EDT42615Burkholderiaambifariamex5
WP014724845BurkholderiaspKJ006
AFJ88574BurkholderiaspKJ006
YP006335305BurkholderiaspKJ006
WP011882278Burkholderiavietnamiensis
WP014899312Burkholderiacepacia
YP006618238BurkholderiacepaciaGG4
AFQ50544BurkholderiacepaciaGG4
WP006765987Burkholderiadolosa
ETP62591BurkholderiadolosaPC543
EEE03148BurkholderiamultivoransCGD1
WP006396998Burkholderiamultivorans
WP012467933Burkholderiamultivorans
YP001584153BurkholderiamultivoransATCC17616
WP012216955Burkholderiamultivorans
ABX17861BurkholderiamultivoransATCC17616
EJO58976BurkholderiamultivoransATCCBAA247
WP006410212Burkholderiamultivorans
WP006403486Burkholderiamultivorans
EEE09403BurkholderiamultivoransCGD2
WP006408464Burkholderiamultivorans
EEE15321BurkholderiamultivoransCGD2M
EJO58798BurkholderiamultivoransCF2
WP006413945Burkholderiamultivorans
WP010089477Burkholderiaubonensis
WP017329414Burkholderiapyrrocinia
WP015602153Burkholderiathailandensis
AGK49094BurkholderiathailandensisMSMB121
YP007916765BurkholderiathailandensisMSMB121
EIP89235BurkholderiathailandensisMSMB43
WP006023844Burkholderiathailandensis
WP004541829Burkholderiapseudomallei
AGR71222BurkholderiapseudomalleiMSHR305
YP008744123BurkholderiapseudomalleiNCTC13179
AGZ27255BurkholderiapseudomalleiNCTC13179
YP008342193BurkholderiapseudomalleiMSHR305
AHK66726BurkholderiapseudomalleiMSHR520
EBA47231Burkholderiapseudomallei305
ABN83174Burkholderiapseudomallei668
YP001060878Burkholderiapseudomallei668
WP010107102Burkholderiaoklahomensis
WP011852328Burkholderiapseudomallei
WP011205295Burkholderiapseudomallei
YP109929BurkholderiapseudomalleiK96243
CAH37346BurkholderiapseudomalleiK96243
AAF77194Burkholderiamallei
WP009906604Burkholderiathailandensis
AHI63931BurkholderiathailandensisH0587
ABC37172BurkholderiathailandensisE264
AHI73001Burkholderiathailandensis2002721723
YP443696BurkholderiathailandensisE264
WP009910134Burkholderiathailandensis
AHI77418BurkholderiathailandensisE444
AAF66062Burkholderiathailandensis
YP002910064BurkholderiaglumaeBGR1
WP012734261Burkholderiaglumae
ACR27360BurkholderiaglumaeBGR1
AEA58873BurkholderiagladioliBSR3
WP013696253Burkholderiagladioli
YP006793740BurkholderiaphenoliruptrixBR3459a
AFT88757BurkholderiaphenoliruptrixBR3459a
WP014972626Burkholderiaphenoliruptrix
WP013591230BurkholderiaspCCGE1001
ADX58126BurkholderiaspCCGE1001
WP006047385Burkholderiagraminis
EDT12261BurkholderiagramininsC4D1M
WP013341969BurkholderiaspCCGE1003
ADN60436BurkholderiaspCCGE1003
YP003909727BurkholderiaspCCGE1003
WP020068679Burkholderiabryophila
YP004231186BurkholderiaspCCGE1001
YP001861483BurkholderiaphymatumSTM815
WP012404601Burkholderiaphymatum
EIM97302BurkholderiaterraeBS001
WP007587577Burkholderiaterrae
WP007749760BurkholderiaspBT03
EUC18944BurkholderiaspBT03
ETY81932BurkholderiacaribensisMBA4
ACC74437BurkholderiaphymatumSTM815
WP013092795BurkholderiaspCCGE1002
ADG19000BurkholderiaspCCGE1002
YP003608511BurkholderiaspCCGE1002
WP018438364BurkholderiaspJPY251

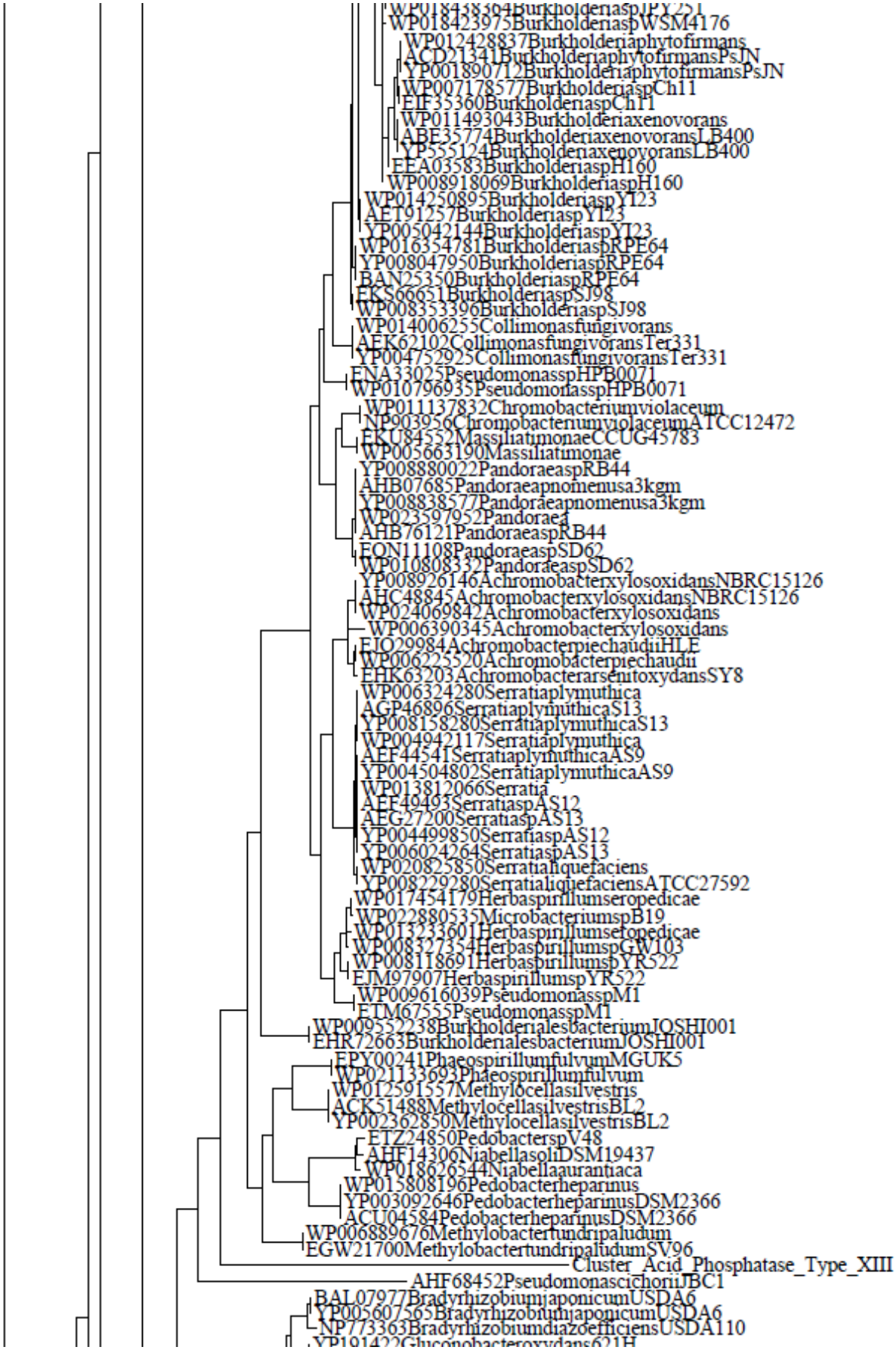
WP018423975BurkholderiaspWSM4176
WP012428837Burkholderiaphytofirmans
ACD21341BurkholderiaphytofirmansPsJN
YP001890712BurkholderiaphytofirmansPsJN
WP007178577BurkholderiaspCh11
EIF35360BurkholderiaspCh11
WP011493043Burkholderiaxenovorans
ABE35774BurkholderiaxenovoransLB400
YP555124BurkholderiaxenovoransLB400
EEA03583BurkholderiaspH160
WP008918069BurkholderiaspH160
WP014250895BurkholderiaspYI23
AET91257BurkholderiaspYI23
YP005042144BurkholderiaspYI23
WP016354781BurkholderiaspRPE64
YP008047950BurkholderiaspRPE64
BAN25350BurkholderiaspRPE64
EKS06651BurkholderiaspSJ98
WP008353396BurkholderiaspSJ98
WP014006255Collimonasfungivorans
AEK62102CollimonasfungivoransTer331
YP004752925CollimonasfungivoransTer331
ENA33025PseudomonasspHPB0071
WP010796935PseudomonasspHPB0071
WP011137832Chromobacteriumviolaceum
NP903956ChromobacteriumviolaceumATCC12472
EKU84552MassiliatimonaeCCUG45783
WP005663190Massiliatimonae
YP008880022PandoraeaspRB44
AHB07685Pandoraeapnomenusa3kgm
YP008838577Pandoraeapnomenusa3kgm
WP023597952Pandoraea
AHB76121PandoraeaspRB44
EON11108PandoraeaspSD62
WP010808332PandoraeaspSD62
YP008926146AchromobacterxylosoxidansNBRC15126
AHC48845AchromobacterxylosoxidansNBRC15126
WP024069842Achromobacterxylosoxidans
WP006390345Achromobacterxylosoxidans
EJO29984AchromobacterpiechaudiiHLE
WP006225520Achromobacterpiechaudii
EHK63203AchromobacterarsenitoxydansSY8
WP006324280Serratiaplymuthica
AGP46896SerratiaplymuthicaS13
YP008158280SerratiaplymuthicaS13
WP004942117Serratiaplymuthica
AEF44541SerratiaplymuthicaAS9
YP004504802SerratiaplymuthicaAS9
WP013812066Serratia
AEF49493SerratiaspAS12
AEG27200SerratiaspAS13
YP004499850SerratiaspAS12
YP006024264SerratiaspAS13
WP020825850Serratialiquefaciens
YP008229280SerratialiquefaciensATCC27592
WP017454179Herbaspirillumseropedicae
WP022880535MicrobacteriumspB19
WP015233601Herbaspirillumsetopedicae
WP008327354HerbaspirillumspGW103
WP008118691HerbaspirillumspYR522
EJM97907HerbaspirillumspYR522
WP009616039PseudomonasspM1
ETM67555PseudomonasspM1
WP009552238BurkholderialesbacteriumJOSHI001
EHR72663BurkholderialesbacteriumJOSHI001
EPY00241PhaeospirillumfulvumMGUK5
WP021133693Phaeospirillumfulvum
WP012591557Methylocellasilvestris
ACK51488MethylocellasilvestrisBL2
YP002362850MethylocellasilvestrisBL2
ETZ24850PedobacterspV48
AHF14306NiabellasoliDSM19437
WP018626544Niabellaaurantiaca
WP015808196Pedobacterheparinus
YP003092646PedobacterheparinusDSM2366
ACU04584PedobacterheparinusDSM2366
WP006889676Methylobacterfundripaludum
EGW21700MethylobacterfundripaludumSV96
Cluster_Acid_Phosphatase_Type_XIII
AHF68452PseudomonascichoriiJBC1
BAL07977BradyrhizobiumjaponicumUSDA6
YP005607565BradyrhizobiumjaponicumUSDA6
NP773363BradyrhizobiumdiazoefficiensUSDA110

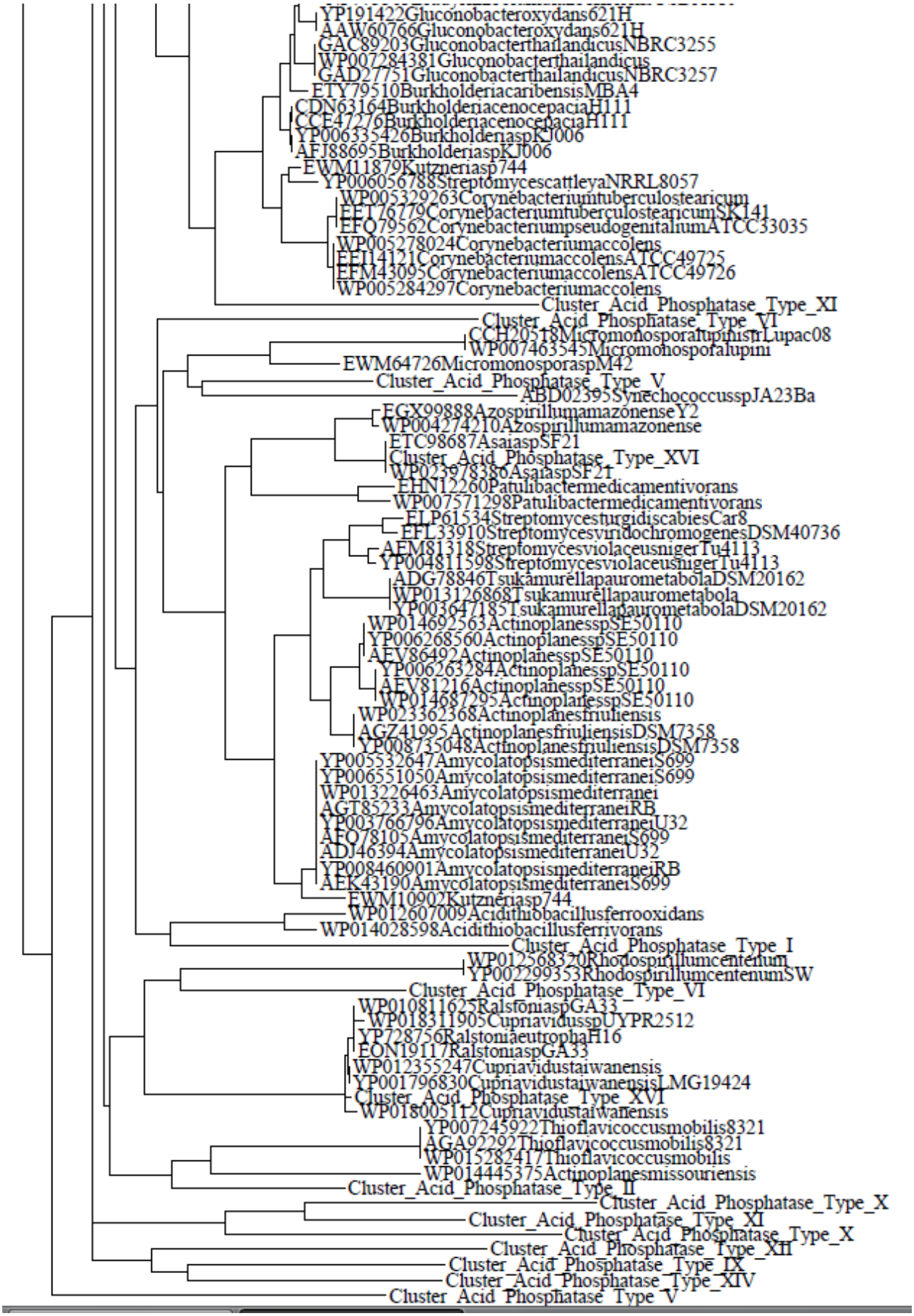
YP191422Gluconobacteroxydans621H
AAW60766Gluconobacteroxydans621H
GAC89203GluconobacterthailandicusNBRC3255
WP007284381Gluconobacterthailandicus
GAD27751GluconobacterthailandicusNBRC3257
ETY79510BurkholderiacaribensisMBA4
CDN63164BurkholderiacenocepaciaH111
CCE47276BurkholderiacenocepaciaH111
YP006335426BurkholderiaspKJ006
AFJ88695BurkholderiaspKJ006
EWM11879Kutzneriasp744
YP006056788StreptomycescattleyaNRRL8057
WP005329263CorynebacteriumtuberculostearicumSK141
EFT76779CorynebacteriumtuberculostearicumSK141
EFQ79562CorynebacteriumpseudogenitaliumATCC33035
WP005278024Corynebacteriumaccolens
EEI14121CorynebacteriumaccolensATCC49725
EFM43095CorynebacteriumaccolensATCC49726
WP005284297Corynebacteriumaccolens
Cluster_Acid_Phosphatase_Type_XI
Cluster_Acid_Phosphatase_Type_VI
CCH20518MicromonosporalupinistrLupac08
WP007463545Micromonosporalupini
EWM64726MicromonosporaspM42
Cluster_Acid_Phosphatase_Type_V
ABD02395SynechococcusspJA23Ba
EGX99888AzospirillumamazonenseY2
WP004274210Azospirillumamazonense
ETC98687AsaiaspSF21
Cluster_Acid_Phosphatase_Type_XVI
WP023978386AsaiaspSF21
EHN12260Patulibactermedicamentivorans
WP007571298Patulibactermedicamentivorans
ELP61534StreptomycesturgidiscabiesCar8
EFL33910StreptomycesviridochromogenesDSM40736
AFM81318StreptomycesviolaceusnigerTu4113
YP004811598StreptomycesviolaceusnigerTu4113
ADG78846TsukamurellapaurometabolaDSM20162
WP013126868Tsukamurellapaurometabola
YP003647185TsukamurellapaurometabolaDSM20162
WP014692563ActinoplanesspSE50110
YP006268560ActinoplanesspSE50110
AEV86492ActinoplanesspSE50110
YP006263284ActinoplanesspSE50110
AEV81216ActinoplanesspSE50110
WP014687295ActinoplanesspSE50110
WP023362368Actinoplanesfriuliensis
AGZ41995ActinoplanesfriuliensisDSM7358
YP008735048ActinoplanesfriuliensisDSM7358
YP005532647AmycolatopsismediterraneiS699
YP006551050AmycolatopsismediterraneiS699
WP013226463Amycolatopsismediterranei
AGT85233AmycolatopsismediterraneiRB
YP003766796AmycolatopsismediterraneiU32
AFO78105AmycolatopsismediterraneiS699
ADJ46394AmycolatopsismediterraneiU32
YP008460901AmycolatopsismediterraneiRB
AEK43190AmycolatopsismediterraneiS699
EWM10902Kutzneriasp744
WP012607009Acidithiobacillusferrooxidans
WP014028598Acidithiobacillusferrivorans
Cluster_Acid_Phosphatase_Type_I
WP012568320Rhodospirillumcentenum
YP002299353RhodospirillumcentenumSW
Cluster_Acid_Phosphatase_Type_VI
WP010811625RalstoniaspGA33
WP018311905CupriavidusspUYPR2512
YP728756RalstoniaeutrophaH16
EON19117RalstoniaspGA33
WP012355247Cupriavidustaiwanensis
YP001796830CupriavidustaiwanensisLMG19424
Cluster_Acid_Phosphatase_Type_XVI
WP018005112Cupriavidustaiwanensis
YP007245922Thioflavicoccusmobilis8321
AGA92292Thioflavicoccusmobilis8321
WP015282417Thioflavicoccusmobilis
WP014445375Actinoplanesmissouriensis
Cluster_Acid_Phosphatase_Type_II
Cluster_Acid_Phosphatase_Type_X
Cluster_Acid_Phosphatase_Type_XI
Cluster_Acid_Phosphatase_Type_X
Cluster_Acid_Phosphatase_Type_XII
Cluster_Acid_Phosphatase_Type_IX
Cluster_Acid_Phosphatase_Type_XIV
Cluster_Acid_Phosphatase_Type_V

Figure S17b. Phylogenetic tree of cluster XVIb of the acid phosphatase sequences included in the database.

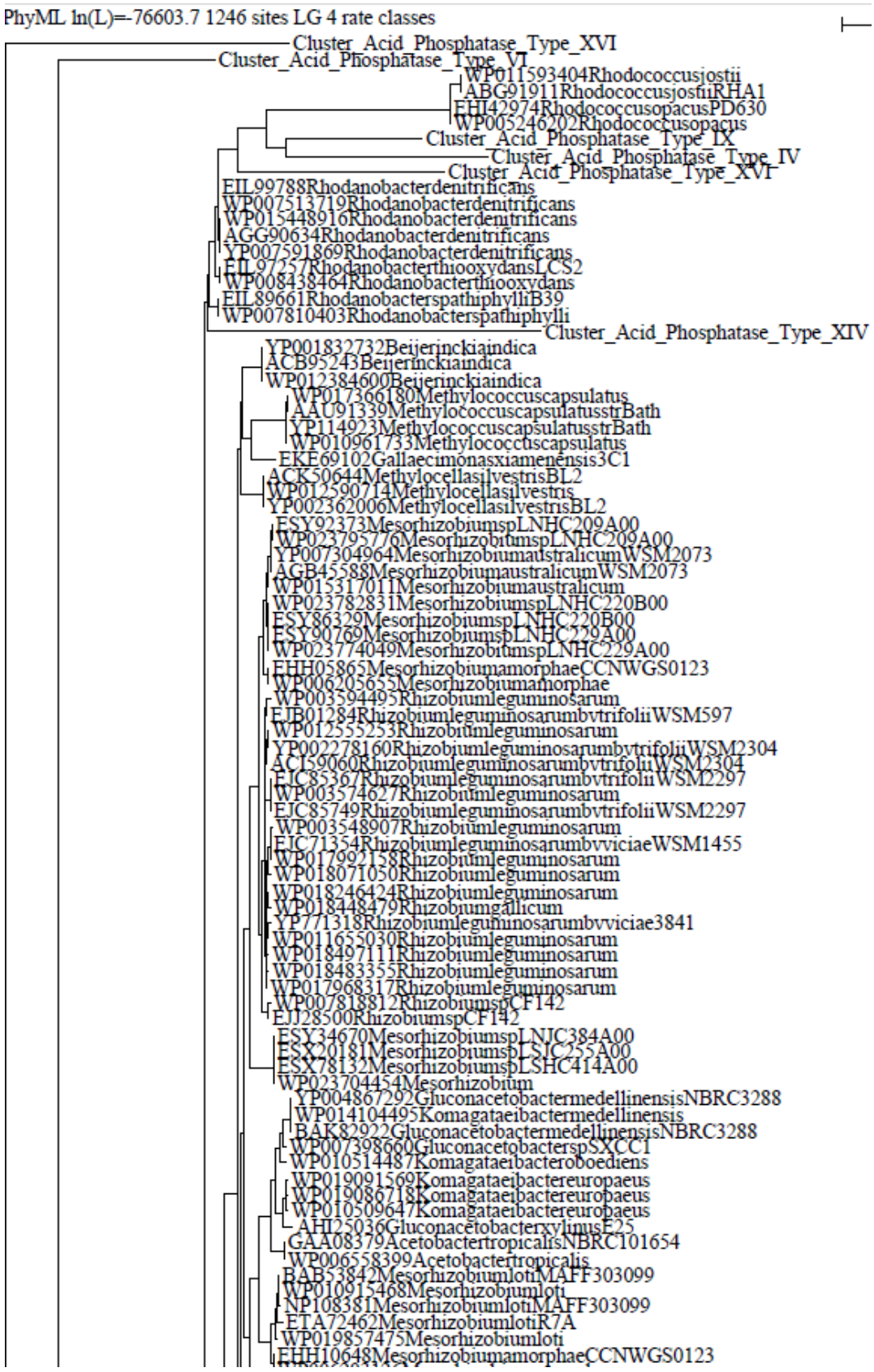

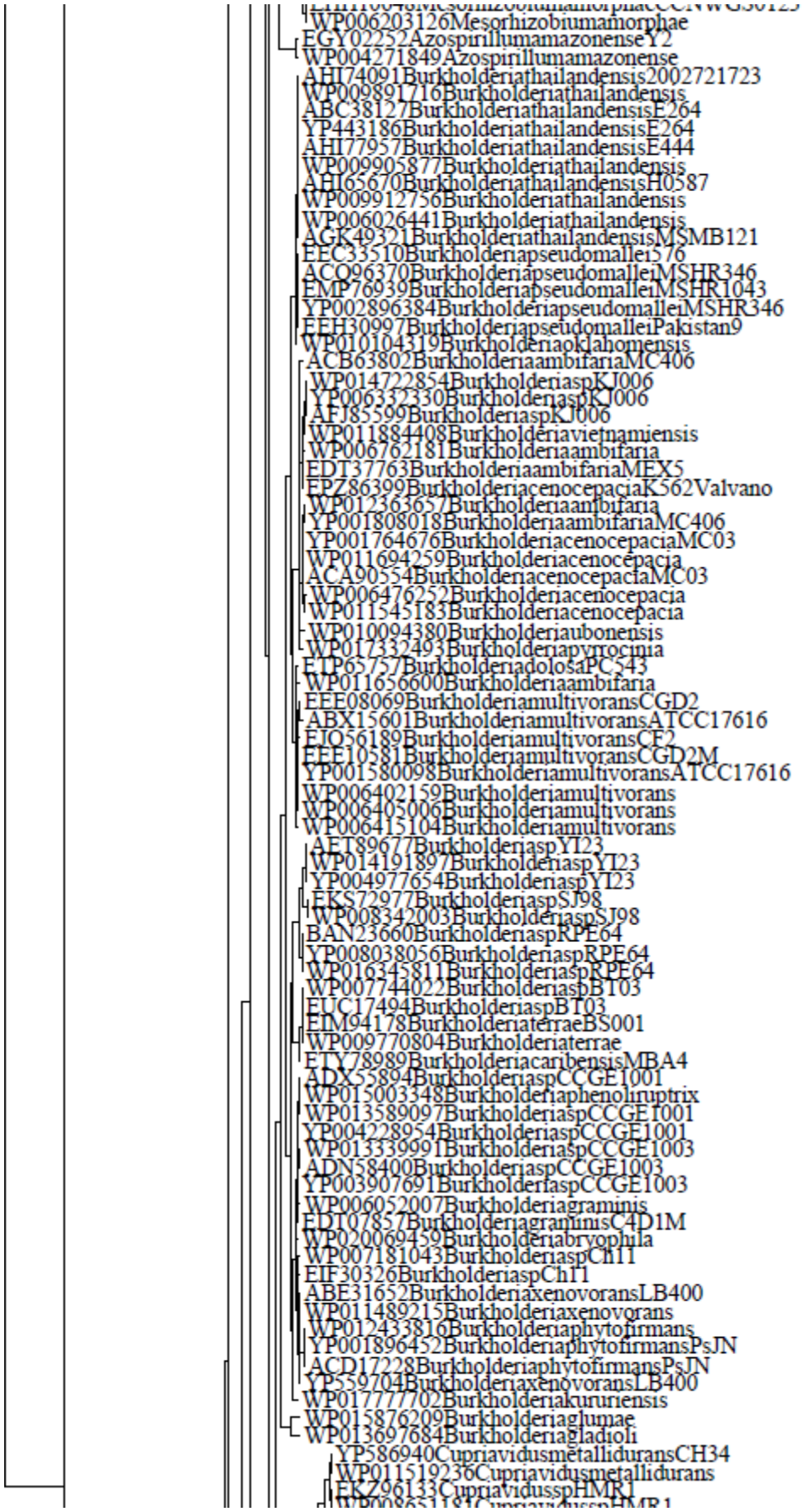
WP006203126Mesorhizobiumamorphae
EGY02252AzospirillumamazonenseY2
WP004271849Azospirillumamazonense
AHI74091Burkholderiathailandensis2002721723
WP009891716Burkholderiathailandensis
ABC38127BurkholderiathailandensisE264
YP443186BurkholderiathailandensisE264
AHI77957BurkholderiathailandensisE444
WP009905877Burkholderiathailandensis
AHI65670BurkholderiathailandensisH0587
WP009912756Burkholderiathailandensis
WP006026441Burkholderiathailandensis
AGK49321BurkholderiathailandensisMSMB121
EEC33510Burkholderiapseudomallei576
ACQ96370BurkholderiapseudomalleiMSHR346
EMP76939BurkholderiapseudomalleiMSHR1043
YP002896384BurkholderiapseudomalleiMSHR346
EEH30997BurkholderiapseudomalleiPakistan9
WP010104319Burkholderiaoklahomensis
ACB63802BurkholderiaambifariaMC406
WP014722854BurkholderiaspKJ006
YP006332330BurkholderiaspKJ006
AFJ85599BurkholderiaspKJ006
WP011884408Burkholderiavietnamiensis
WP006762181Burkholderiaambifaria
EDT37763BurkholderiaambifariaMEX5
EPZ86399BurkholderiacenocepaciaK562Valvano
WP012363657Burkholderiaambifaria
YP001808018BurkholderiaambifariaMC406
YP001764676BurkholderiacenocepaciaMC03
WP011694259Burkholderiacenocepacia
ACA90554BurkholderiacenocepaciaMC03
WP006476252Burkholderiacenocepacia
WP011545183Burkholderiacenocepacia
WP010094380Burkholderiaubonensis
WP017332493Burkholderiapyrrocinia
ETP65757BurkholderiadolosaPC543
WP011656600Burkholderiaambifaria
EEE08069BurkholderiamultivoransCGD2
ABX15601BurkholderiamultivoransATCC17616
EIO56189BurkholderiamultivoransCF2
EEE10581BurkholderiamultivoransCGD2M
YP001580098BurkholderiamultivoransATCC17616
WP006402159Burkholderiamultivorans
WP006405006Burkholderiamultivorans
WP006415104Burkholderiamultivorans
AET89677BurkholderiaspYT23
WP014191897BurkholderiaspYT23
YP004977654BurkholderiaspYT23
EKS72977BurkholderiaspSJ98
WP008342003BurkholderiaspSJ98
BAN23660BurkholderiaspRPE64
YP008038056BurkholderiaspRPE64
WP016345811BurkholderiaspRPE64
WP007744022BurkholderiaspBT03
EUC17494BurkholderiaspBT03
EIM94178BurkholderiaterraeBS001
WP009770804Burkholderiaterrae
ETY78989BurkholderiacaribensisMBA4
ADX55894BurkholderiaspCCGE1001
WP015003348Burkholderiaphenoliruptrix
WP013589097BurkholderiaspCCGE1001
YP004228954BurkholderiaspCCGE1001
WP013339991BurkholderiaspCCGE1003
ADN58400BurkholderiaspCCGE1003
YP003907691BurkholderiaspCCGE1003
WP006052007Burkholderiagraminis
ED107857BurkholderiagraminisC4D1M
WP020069459Burkholderiabryophila
WP007181043BurkholderiaspCh11
EIF30326BurkholderiaspCh11
ABE31652BurkholderiaxenovoransLB400
WP011489215Burkholderiaxenovorans
WP012433816Burkholderiaphytofirmans
YP001896452BurkholderiaphytofirmansPsJN
ACD17228BurkholderiaphytofirmansPsJN
YP559704BurkholderiaxenovoransLB400
WP017777702Burkholderiakururiensis
WP015876209Burkholderiaglumae
WP013697684Burkholderiagladioli
YP586940CupriavidusmetalliduransCH34
WP011519236Cupriavidusmetallidurans
EKZ96133CupriavidusspHMR1


WP019450075CupriavidusspBIS7
WP006159394Cupriavidusbasilensis
WP020201024CupriavidusspWS
YP006032017RalstoniasolanacearumPo82
WP014619097Ralstoniasolanacearum
AEG71481RalstoniasolanacearumPo82
EUJ12622RalstoniasolanacearumP673
WP013210244Ralstoniasolanacearum
EFP68144Ralstoniasp5747FAA
WP009276960Ralstoniasp5747FAA
WP009240603Ralstoniasp5256FAA
EPX99700RalstoniaspAU1208
WP021192637RalstoniaspAU1208
WP011137072Chromobacteriumviolaceum
AAQ61187ChromobacteriumviolaceumATCC12472
NP903195ChromobacteriumviolaceumATCC12472
WP021479044Pseudogulbenkianiaferrooxidans
ERD99525Pseudogulbenkianiaferrooxidans
AEK59983CollimonasfungivoransTer331
WP014004138Collimonasfungivorans
CDG83673JanthinobacteriumagaricidamnosumNBRC102515
WP007884247HerbaspirillumspCF444
EJL81188HerbaspirillumspCF444
WP009549392BurkholderialesbacteriumJOSHI001
EHR70247BurkholderialesbacteriumJOSHI001
WP019701162Acidovoraxavenae
ADX46821Acidovoraxavenae
WP013595313Acidovoraxavenae
YP004235388Acidovoraxavenae
WP022980890IdeonellaspB5081
WP022980891IdeonellaspB5081
CDG82200JanthinobacteriumagaricidamnosumNBRC102515
WP010396729Janthinobacteriumlividum
WP019920196Duganellazoogloeoides
ELX09523JanthinobacteriumspHH01
WP008449981JanthinobacteriumspHH01
WP020702335OxalobacteraceaebacteriumAB14
WP020653718Massilianiastensis
WP017876491JanthinobacteriumspCG3
WP009050864Pseudomonaschlororaphis
EJK99898Pseudomonaschlororaphis
ETD40642Pseudomonaschlororaphis
WP023967487Pseudomonaschlororaphis
WP009045630Pseudomonaschlororaphis
EXF95584PseudomonasfluorescensHK44
WP019693696Pseudomonasfluorescens
WP007939735PseudomonasspGM18
EJM14378PseudomonasspGM18
WP019582403Pseudomonasmandelii
WP018929541Pseudomonas
WP019651136Pseudomonassp45MFCol31
WP007961532PseudomonasspGM30
EUB85466PseudomonasspGM30
WP008079583PseudomonasspGM80
EJN33624PseudomonasspGM80
ERH55324PseudomonasfluorescensEGDAQ6
WP010213389Pseudomonas
WP017478604PseudomonasspPAMC26793
EJL07537Pseudomonaschlororaphis
WP009042027Pseudomonaschlororaphis
WP016703809Pseudomonaschlororaphis
WP009046824Pseudomonaschlororaphis
WP023970345Pseudomonaschlororaphis
WP010445374Pseudomonasfuscovaginae
WP017904387Pseudomonasfuscovaginae
WP017130600Pseudomonasagarici
YP262308PseudomonasprotegensPf5
AAY94450PseudomonasprotegensPf5
WP011063473PseudomonasprotegensPf5
EIK59256PseudomonasfluorescensSS101
WP003188293Pseudomonasfluorescens
AFJ56674PseudomonasfluorescensA506
YP006322203PseudomonasfluorescensA506
WP014716789Pseudomonasfluorescens
ETK42545PseudomonasfluorescensFH5
EIK67235PseudomonassynxanthaBG33R
WP005784523Pseudomonassynxantha
WP017134529Pseudomonasfluorescens
WP017737122PseudomonasspCBZ4
WP016974926Pseudomonasfluorescens
AHC33316PseudomonasspTKP
WP017844504Pseudomonasveronii
WP017253767Pseudomonastolaasii

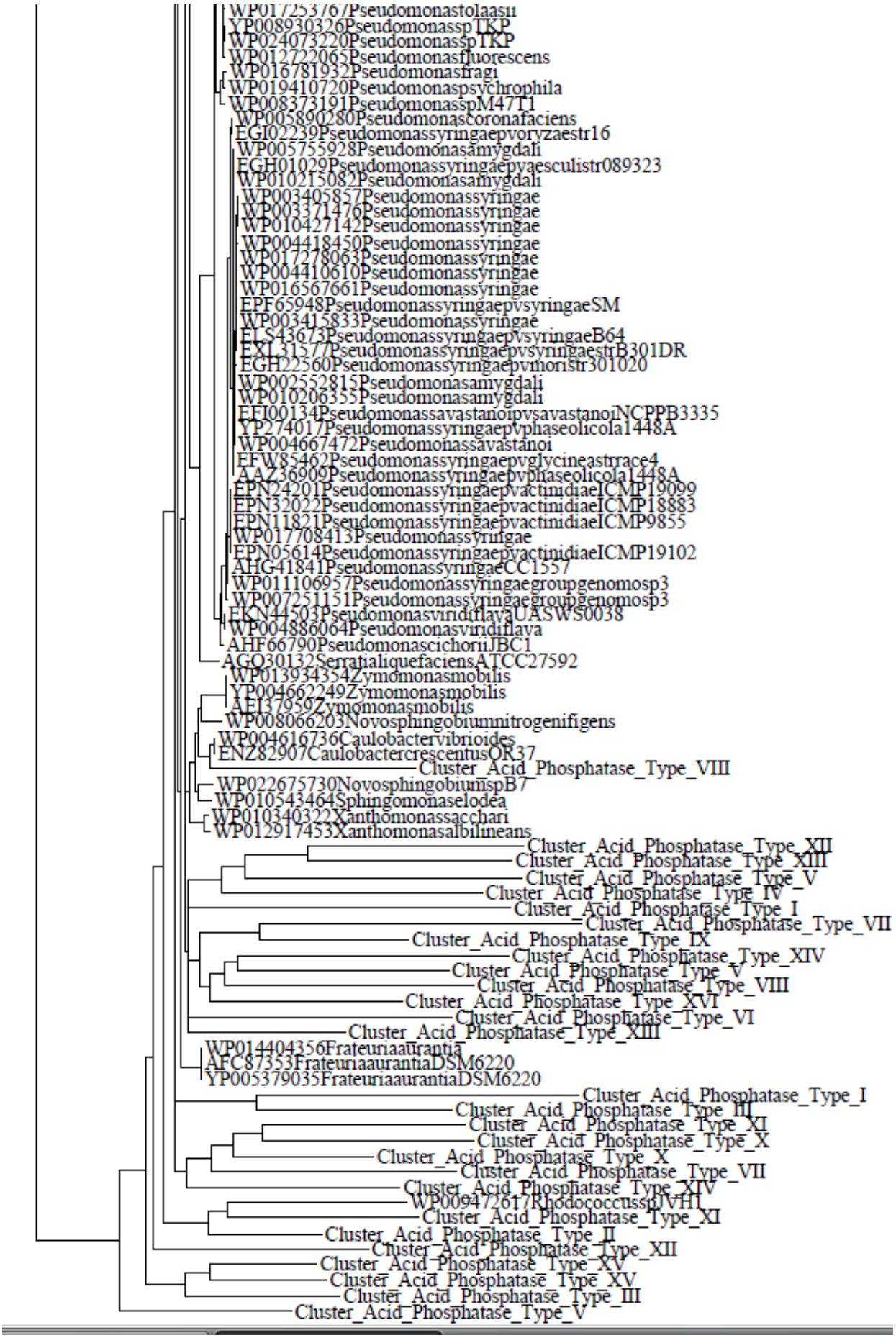
WP017253767Pseudomonastolaasii
YP008930326PseudomonasspTKP
WP024073220PseudomonasspTKP
WP012722065Pseudomonasfluorescens
WP016781932Pseudomonasfragi
WP019410720Pseudomonaspsychrophila
WP008373191PseudomonasspM47T1
WP005890280Pseudomonascoronafaciens
EGI02239Pseudomonassyringaepvoryzaestr16
WP005755928Pseudomonasamygdali
EGH01029Pseudomonassyringaepvaesculistr089323
WP010215082Pseudomonasamygdali
WP003405857Pseudomonassyringae
WP003371476Pseudomonassyringae
WP010427142Pseudomonassyringae
WP004418450Pseudomonassyringae
WP017278063Pseudomonassyringae
WP004410610Pseudomonassyringae
WP016567661Pseudomonassyringae
EPF65948PseudomonassyringaepvsyringaeSM
WP003415833Pseudomonassyringae
ELS43673PseudomonassyringaepvsyringaeB64
EXL31577PseudomonassyringaepvsyringaestrB301DR
EGH22560Pseudomonassyringaepvmoristr301020
WP002552815Pseudomonasamygdali
WP010206355Pseudomonasamygdali
EFI00134PseudomonassavastanoipvsavastanoiNCPPB3335
YP274017Pseudomonassyringaepvphaseolicola1448A
WP004667472Pseudomonassavastanoi
EFW85462Pseudomonassyringaepvglycineastrace4
AAZ36909Pseudomonassyringaepvphaseolicola1448A
EPN24201PseudomonassyringaepvactinidiaeICMP19099
EPN32022PseudomonassyringaepvactinidiaeICMP18883
EPN11821PseudomonassyringaepvactinidiaeICMP9855
WP017708413Pseudomonassyringae
EPN05614PseudomonassyringaepvactinidiaeICMP19102
AHG41841PseudomonassyringaeCC1557
WP011106957Pseudomonassyringaegroupgenomosp3
WP007251151Pseudomonassyringaegroupgenomosp3
EKN44503Pseudomonasviridiflava3UASWS0038
WP004886064Pseudomonasviridiflava
AHF66790PseudomonascichoriiJBC1
AGO30132SerratialiquefaciensATCC27592
WP013934354Zymomonasmobilis
YP004662249Zymomonasmobilis
AEI37959Zymomonasmobilis
WP008066203Novosphingobiumnitrogenifigens
WP004616736Caulobactervibrioides
ENZ82907CaulobactercrescentusOR37
Cluster_Acid_Phosphatase_Type_VIII
WP022675730NovosphingobiumspB7
WP010543464Sphingomonaselodea
WP010340322Xanthomonassacchari
WP012917453Xanthomonasalbilineans
Cluster_Acid_Phosphatase_Type_XII
Cluster_Acid_Phosphatase_Type_XIII
Cluster_Acid_Phosphatase_Type_V
Cluster_Acid_Phosphatase_Type_IV
Cluster_Acid_Phosphatase_Type_I
Cluster_Acid_Phosphatase_Type_VII
Cluster_Acid_Phosphatase_Type_IX
Cluster_Acid_Phosphatase_Type_XIV
Cluster_Acid_Phosphatase_Type_V
Cluster_Acid_Phosphatase_Type_VIII
Cluster_Acid_Phosphatase_Type_XVI
Cluster_Acid_Phosphatase_Type_VI
Cluster_Acid_Phosphatase_Type_XIII
WP014404356Frateuriaaurantia
AFC87353FrateuriaaurantiaDSM6220
YP005379035FrateuriaaurantiaDSM6220
Cluster_Acid_Phosphatase_Type_I
Cluster_Acid_Phosphatase_Type_III
Cluster_Acid_Phosphatase_Type_XI
Cluster_Acid_Phosphatase_Type_X
Cluster_Acid_Phosphatase_Type_VII
Cluster_Acid_Phosphatase_Type_XIV
WP009472617RhodococcusspJVH1
Cluster_Acid_Phosphatase_Type_XI
Cluster_Acid_Phosphatase_Type_II
Cluster_Acid_Phosphatase_Type_XII
Cluster_Acid_Phosphatase_Type_XV
Cluster_Acid_Phosphatase_Type_XV
Cluster_Acid_Phosphatase_Type_III
Cluster_Acid_Phosphatase_Type_V

REFERENCES

Abdelouas, A., Lu, Y., Lutze, W., Nuttall, H. E. (1998). Reduction of U(VI) to U(IV) by indigenous bacteria in contaminated ground water. J Cont Hydrol, 35(1): 217-233

Aguilar-Uscanga, B. and Francois, J. M. (2003). A study of the yeast cell wall composition and structure in response to growth conditions and mode of cultivation. Letters in applied microbiology, 37(3): 268-274

Alimova, A., Katz, A., Steiner, N., Rudolph, E., Wei, H., Jeffrey, C., Steiner, J.C., Gottlieb, P. (2009). Bacteria-clay interaction: structural changes in smectite induced during biofilm formation. Clays Clay Min, 57: 205–212

Alonso, E.E., Springman, S.M., Ng, C.W.W. (2008). Monitoring Large-Scale Tests for Nuclear Waste Disposal. Geotech Geol Eng 26: 817–826

Amayri, S., Reich, T., Arnold, T., Geipel, G., Bernhard, G. (2005). Spectroscopic characterization of alkaline earth uranyl carbonates. J Solid State Chem 178: 567–577

Andersson, C.A. and Bro, R. (2000). The N-way Toolbox for MATLAB. Chemometrics and Intelligent Laboratory Systems 52:1–4

Ankudinov, A.L., Ravel, B., Rehr, J., Conradson, S. (1998). Real-space multiplescattering calculation and interpretation of X-ray absorption near-edge spectra. Phys Rev B, 58: 7565–7575

Armand, G., Leveau, F., Nussbaum, C., de La Vaissiere, R., Noiret, A., Jaeggi, D., Landrein, P., Righini, C. (2014). Geometry and Properties of the Excavation-Induced Fractures at the Meuse/Haute-Marne URL. Rock Mechanics and Rock Engineering, 47(1): 21-41. DOI: 10.1007/s00603-012-0339-6

Astudillo Pastor, J. (2001). El almacenamiento geológico profundo de los residuos radiactivos de alta actividad. Principios básicos y tecnología. ENRESA S.A. ISBN:84-931224-4-0

Bai, J., Li, Z., Fan, F., Wu, X., Tian, W., Yin, X, Zhao, L., Fan, F., Tian, L., Wang, Y., Qin, Z., Guo, J. (2014). Biosorption of uranium by immobilized cells of *Rhodotorula glutinis*. J Radioanal Nuclear Chem, 299(3): 1517-1524

Bai, J., Wu, X., Fan, F., Tian, W., Yin, X., Zhao, L., Fan, F., Li, Z., Tian, L., Qin, Z., Guo, J. (2012). Biosorption of uranium by magnetically modified *Rhodotorula glutinis*. Enzyme Microb Technol, 51(6): 382-387

Banfield, J.P., Barker, W.W., Welch, S.A., Taunton, A. (1999). Biological impact on mineral dissolution: application of the lichen model to understanding mineral weathering in the rhizophere. Proc Natl Acad Sci USA, 96: 3404–3411

Barkleit, A., Moll, H., Bernhard, G. (2008). Interaction of uranium(VI) with lipopolysaccharide. Dalton T, 21: 2879–2886

Barkleit, A., Moll, H., Bernhard, G. (2009). Complexation of uranium(VI) with peptidoglycan. Dalton T, 27: 5379–5385

Barkleit, A., Foerstendorf, H., Li, B., Rossberg, A., Moll, H., Bernhard, G. (2011). Coordination of uranium(VI) with functional groups of bacterial lipopolysaccharide studied by EXAFS and FT-IR spectroscopy. Dalton T, 40(38): 9868-9876

Beal, E.J., House, C.H, Orphan, V.J. (2009). Manganese- and Iron- dependent marine methane oxidation. Science, 325: 184-187

Beazley, M.J., Martinez, R.J., Sobecky, P.A., Webb, S.M., Taillefert, M. (2009). Nonreductive biomineralization of uranium (VI) phosphate via microbial phosphatase activity in anaerobic conditions. Geomicrobiol J, 26 (7): 431–441

Beller, H., (2005). Anaerobic, nitrate-dependent oxidation of U(IV) oxide minerals by the chemolithoautotrophic bacterium *Thiobacillus denitrificans.* App Environ Microbiol, 71: 2170-2174

Benzerara, K., Miot, J., Morin, G., Ona-Nguema, G., Skouri-Panet, F., Férard, C., Ferard, C. (2011). Significance mechanisms and environmental implications of microbial biomineralization. C R Geosci, 343: 160–167

Bernhard, G., Geipel, G., Reich, T., Brendler, V., Amayri, S., Nitsche, H. (2001). Uranyl(VI) carbonate complex formation: Validation of the $Ca_2UO_2(CO_3)_3(aq)$ species. Radiochim Acta, 89: 511–518

Bishop, M.E., Dong, H., Kukkadapu, R.K., Liu, C.X., Edelman, R.E. (2011). Bioreduction of Fe-bearing clay minerals and their reactivity toward pertechnetate (Tc-99). Geochim Cosmochim Acta, 75: 5229–5246

Bohorquez, L.C., Delgado-Serrano, L., López, G., Osorio-Forero, C., Klepac-Ceraj, V., Kolter, R., Junca, H., Baena, S., Zambrano, M.M. (2012). In-depth Characterization via Complementing Culture-Independent Approaches of the Microbial Community in an Acidic Hot Spring of the Colombian Andes. Microb Ecol, 63: 103–115. DOI 10.1007/s00248-011-9943-3

Boivin-Jahns, V., Ruimy, R., Bianchi, A., Daumas, S., Christen, R. (1996). Bacterial Diversity in a Deep-Subsurface Clay Environment. Appl Environ Microbiol, 62(9): 3405–3412

Bonhoure, I., Meca, S., Marti, V., de Pablo, J., Cortina, J.L. (2007). A new timeresolved laser-induced fluorescence spectrometry (TRLFS) data acquisition procedure applied to the uranyl-phosphate system. Radiochim Acta, 95: 165–172

Borremans, B., Hobman, J.L., Provoost, A., Brown, N.L., van Der Lelie, D. (2001). Cloning and functional analysis of the pbr lead resistance determinant of *Ralstonia metallidurans* CH34. J Bacteriol, 183: 5651–5658

Brandl, H., Bosshard, R., Wegmann, M. (1999). Computer-munching microbes: Metal leaching from electronic scrap by bacteria and fungi. Process Metall, 9B: 569–576

Brendler, V., Geipel, G., Bernhard, G., Nitsche, H. (1996). Complexation in the system $UO_2^{2+}/PO_4^{3-}/OH^-$(aq): Investigations at very low ionic strengths. Radiochim Acta, 74: 75–80

Breuker, A., Koweker, G., Blazejak, A. and Schippers, A. (2011). The deep biosphere in terrestrial sediments in the Chesapeake Bay area, Virginia, USA. Front Microbiol, 2: 156

Brookshaw, D.R., Pattrick, R.A.D., Lloyd, J.R. and Vaughan, D.J. (2012). Microbial effects on mineral–radionuclide interactions and radionuclide solid-phase capture processes. Mineral Mag, 76(3): 777-806

Brown, D.A., Kamineni, D.C., Sawicki, J.A., Beveridge, T.J., 1994. Minerals associated with biofilms occurring on exposed rock in a granitic underground research laboratory. Appl Environ Microbiol, 60: 3182–3191

Burns, P.C. (1999). The crystal chemistry of uranium. Reviews in Mineral Geochem, 38: 22-90

Caballero, E. (1985). Quimismo del proceso de bentonitización en la región volcánica de Cabo de Gata (Almería). Doctoral Thesis, University of Granada, Spain

Caballero, E., Reyes, E., Linares, J., Huertas, F. (1985a). Hydrothermal solutions related to bentonite genesis, Cabo de Gata region, Almería, SE Spain. Mineral Petrog Acta, 29-A: 187 y 196

Caballero, E., Reyes, E., Yusta, A., Huertas, F., Linares, J. (1985b). Las bentonitas de la zona del Cabo de Gata, Almería. Geoquímica y mineralogía. Acta Geol Hisp, 20: 267-287

Caballero, E., Jimenez De Cisneros, C., Huertas, F.J., Huertas, F., Pozzuoli, A., Linares, J. (2005). Bentonites from Cabo de Gata, Almeria, Spain: a mineralogical and geochemical overview. Clay Miner, 40: 463-480

Cama, J., Ganor, J., Ayora, C., Lasaga, A. (2000). Smectite dissolution kinetics at 80ºC and pH 8.8. Geochim Cosmochim Acta, 15: 2701-2717

Camarinha-Silva, A., Jáuregui, R., Chaves-Moreno, D., Oxley, A.P.A., Schaumburg, F., Becker, K., Wos-Oxley, M.L., Pieper, D.H. (2014). Comparing the anterior nare bacterial community of two discrete human populations using Illumina amplicon sequencing. Environ Microbiol. DOI: 10.1111/1462-2920.12362

Cardenas, E. and Tiedje, J.M. (2008). New tools for discovering and characterizing microbial diversity. Current Opinion Biotechnol, 19: 544–549

Cavero, J.P. (2011). Anatomía de la historia. Licencia Creative Commons 3.0

Cheung, K. H. and Gu, J. D. (2007). Mechanism of hexavalent chromium detoxification by microorganisms and bioremediation application potential: a review. Int Biodet Biodeg, 59(1): 8-15

Cho, D. H., Chu, K. H. and Kim, E. Y. (2011). Lead uptake and potentiometric titration studies with live and dried cells of *Rhodotorula glutinis*. World J Microbiol Biotechnol, 27(8): 1911-1917

Chung, F. H. (1974a). Quantitative interpretation of X-ray diffraction patterns of mixtures. I. Matrix-flushing method for quantitative multicomponent analysis. Journal J Appl Cryst, 7(6): 519-525

Chung, F.H. (1974b). Quantitative interpretation of X-ray diffraction patterns, II. Adiabatic principle of X-ray diffraction analysis of mixtures. J Appl Cryst, 7: 526–531

Chung, F.H. (1975). Quantitative interpretation of X-ray diffraction patterns of mixtures. III. Simultaneous determination of a set of reference intensities. Journal of Appl Cryst, 8(1): 17-19

Clarke, W.L. (1996). The safe disposal of nuclear waste. Sci Technol Rev, 3: 7-17.

Cormenzana, J.L., García-Gutiérrez, M., Missana, T., Alonso, U. (2008). Modelling large-scale laboratory HTO and strontium diffusion experiments in Mont Terri and Bure clay rocks. Phys Chem Earth, DOI: 10.1016/j.pce.2008.05.006

Cuevas, J., Villar, M.V., Fernandez, A.M., Gomez, P., Martin, P.L. (1997). Pore waters extracted from compacted bentonite subjected to simultaneous heating and hydration. Appl Geochem, 12: 473-481

De Craen, M., Van Geet, M., Honty, M., Weetjens, E., Sillen, X. (2008). Extend of oxidation in Boom Clay as a result of excavation and ventilation of the HADES URF: experimental and modeling assessments. Phys Chem Earth, 33: 350-362

De Jongh, W. K. (1973). X-ray fluorescence analysis applying theoretical matrix corrections. Stainless steel. X-Ray Spectrom, 2:151–158. DOI: 10.1002/xrs.1300020404

de Silóniz, M.I., Payo, E.M., Callejo, M.A., Marquina, D., Peinado, J.M. (2002). Environmental adaptation factors of two yeasts isolated from the leachate of a uranium mineral heap. FEMS Microbiol Lett, 210(2): 233-237

Degnan, P.H. and Ochman, H. (2012). Illumina-based analysis of microbial community diversity. ISMEJ, 6: 183–194

Delgado, A. (1993). Estudio isotopico de los procesos diageneticos e hidrotermales relacionados con la genesis de bentonitas (Cabo de Gata, Almeria). Doctoral Thesis, University of Granada, Spain

Denecke, M.A., Reich, T., Bubner, M., Pompe, S., Heise, K.H., Nitsche, H., Allen, P.G., Bucher, J.J., Edelstein, N.M., Shuh, D. K. (1998). Determination of structural parameters of uranyl ions complexed with organic acids using EXAFS. J Alloys Comp, 271: 123-127

Deniau, I., Devol-Brown, I., Derenne, S., Behar, F., Largeau, C. (2008). Comparison of the bulk geochemical features and thermal reactivity of kerogens from Mol (Boom Clay), Bure (Callovo–Oxfordian argillite) and Tournemire (Toarcian shales) underground research laboratories. Sci Total Environ, 389: 475–485

Dong, H., Jaisi, D.P., Kim, J., Zhang, G. (2009). Microbe-cly-mineral interactions. Am Mineral, 94: 1505-1519

Ekendal, S., O´ Neill, A.H., Thomson, E., Pedersen, K. (2003). Characterisation of yeasts from deep igneous rock aquifers of the Fennoscandian Shield. Microbiol Ecol, 64: 416–428

Eliet, V., Bidoglio, G., Omenetto, N., Parma, L., Grenthe, I. (1995). Characterization of hydroxide complexes of uranium(VI) by time-resolved fluorescence spectroscopy. J Chem Soc Faraday T, 91: 2275–2285

El-Naggar, M.Y., Wanger, G., Leung, K.M., Yuzvinsky, T.D., Southam, G., Yang, J., Lau, W.M., Nealsonm K.H., Gorby, Y.A. (2010). Electrical transport along bacterial nanowires from *Shewanella oneidensis* MR-1. Proc Natl Acad Sci USA, 107: 18127-18131

Feixas Rodríguez, C. (2007). Geología del entorno árido almeriense. Guía didáctica de campo. Consejería de Medio Ambiente de la Junta de Andalucía, 2003-2007. ISBN: 84-933537-0-1

Fernández Soler, J.M. (2007). Geología del entorno árido almeriense. Guía didáctica de campo. Consejería de Medio Ambiente de la Junta de Andalucía, 2003-2007. ISBN: 84-933537-0-1

Fernandez-Sanfrancisco, O. (2011). Mecanismos de tolerancia de bacterias naturales de bentonita frente a radionucléidos y lantánidos. Master thesis, University of Granada, Spain

Finch, R. and Murakami, T. (1999). Systematics and paragenesis of uranium minerals. Rev Mineral, 38: 91-180

Finneran, K.T., Housewright, M.E., Lovley, D.R. (2002). Multiple influences of nitrate on uranium solubility during bioremediation of uranium-contaminated subsurface sediments. Environ Microbiol, 4: 510-516

Fredrickson, J.K., Zachara, J.M., Balkwill, D.L., Kennedy, D., Li, S.M.W., Kostandarithes, H.M., Daly, M.J., Romine, M.F., Brockman, F.J., (2004). Geomicrobialogy of high level nuclear waste-contaminated vadose sediments at the Hanford site, Washignton State. Appl Environ Microbiol, 70: 4230–4241

Fukunaga, S., Jintoku, T., Iwata, Y., Nakayama, M., Tsuji, T., Sakaya, N., Mogi, K.I., Ito, M. (2005). Investigation of microorganisms in bentonite deposits. Geomicrobiol J, 22: 361–370

Gadd, G.M. (2000). Bioremedial potential of microbial mechanisms of metal mobilization and immobilization. Current Opinion Biotechnol, 11: 271- 279

Gadd, G.M. (2009). Biosorption: critical review of scientific rationale, environmental importance and significance for pollution treatment. J Chem Technol Biotechnol, 84: 13–28

Garcia-Romero, E. (2012). Bentonitas del sureste de la Península Ibérica. Workshop Guia de Campo. Sociedad española de arcillas. ISBN: 978-84-695-3858-6

Gates, W.P., Wilkinson, H.T., Stucki, J.W. (1993). Swelling properties of microbially reduced ferruginous smectite. Clays Clay Min, 41: 360–364

Geipel, G., Bernhard, G., Rutsch, M., Brendler, V., Nitsche, H. (2000). Spectroscopic properties of uranium(VI) minerals studied by time-resolved laser-induced fluorescence spectroscopy (TRLFS). Radiochim Acta, 88: 757–762

Glass, J.B. and Orphan, V.J. (2012). Trace metal requirements for microbial enzymes involved in the production and consumption of methane and nitrous oxide. Front Microbiol, 3: 61.

Griffiths, H.B. and Greenwood, A.D. (1972). The concentric bodies of licheniozed fungi. Arch Mikrobiol, 87, 285–302

Gustafsson, J.P., Dassman, E., Backstrom, M. (2009). Towards a consistent geochemical model for prediction of uranium (VI) removal from groundwater by ferrihydrite. Appl Geochem, 24(3): 454–462

Hall, T.A. (1999). BioEdit: a user-friendly biological sequence alignment editor and analysis program for Windows 95/98/NT. Nucl. Acid Ser, 41: 95–98

Hamady, M., Walker, J.J., Harris, J.K., Gold, N.J., and Knight, R. (2008). Error-correcting barcoded primers for pyrosequencing hundreds of samples in multiplex. Nature Meth, 5: 235–237

Hedin, A. (1999) Swedish nuclear fuel and waste management company. Report: TR-99-06

Hedrich, S., Schlömann, M., Johnson, M.D. (2011). The iron-oxidizing proteobacteria. Microbiol, 157: 1551–1564

Huang, Y., Zhang, J., Zhu, L. (2013). Evaluation of the application potential of bentonites in phenanthrene bioremediation by characterizing the biofilm community. Bioresour Technol, 134, 17–23

Hudson, E., Allen, A.P.G., Terminello, L.J. (1996). Polarized X-ray absorption spectroscopy of the uranyl ion: Comparison of experiment and theory. Phys Rev B, 54: 156–165

Huertas, F., Fuentes-Cantillana, J.L., Jullien, F., Rivas, P., Linares, J., Fariña, P., Ghoreychi, M., Jocker, N., Kickmaier, W., Martinez, M.A., Samper, J., Alonso, E., Elorza, F.J. (2000). Full-scale engineered barriers experiment for a deep

geological repository for high level radioactive waste in crystalline host rock (FEBEX project), European Commission, EUR 19147

IAEA, (2003). Scientific and Technical Basis for the Geological Disposal of Radioactive Wastes. TRS No 413, IAEA, Vienna

Imlay, J.A. (2003). Pathways of oxidative damage. Annu Rev Microbiol, 57: 395–418

Irazusta, V., Estévez, C., Amoroso, M.J., de Figueroa, L.I. (2012). Proteomic study of the yeast *Rhodotorula mucilaginosa* RCL-11 under copper stress. BioMetals, 25(3): 517-527

Irazusta, V., Nieto-Peñalver, C. G., Cabral, M. E., Amoroso, M. J., de Figueroa, L. I. (2013). Relationship among carotenoid production, copper bioremediation and oxidative stress in *Rhodotorula mucilaginosa* RCL-11. Proc Biochem, 48(5): 803-809

Itavaara, M., Nyyssonen, M., Kapanen, A., Nousiainen, A., Ahonen, L., Kukkonen, I. (2011). Characterization of bacterial diversity to a depth of 1500 m in the Outokumpu deep borehole, Fennoscandian Shield. FEMS Microbiol Ecol, 77: 295–309

Jaisi, D.P., Dong, H., Liu, C. (2007). Influence of biogenic Fe(II) on the extent of microbial reduction of Fe(III) in clay mineral nontronite, illite, and chlorite. Geochem Cosmochim Acta, 71: 1145-1158

Jaisi, D.P., Dong, H., Morton, JP. (2008). Partitioning of Fe(II) in reduced nontronite (NAu-2) to reactive sites: reactivity in terms of Tc (VII) reduction. Clays Clay Minerals, 56: 175-189

Janssen, P.J., Van Houdt, R., Moors, H., Monsieurs, P., Morin, N., Michaux, A., Benotmane, M.A., Leys, N., Vallaeys, T., Lapidus, A., Monchy, S., Médigue, C., Taghavi, S., McCorkle, S., Dunn, J., van der Lelie, D., Mergeay, M. (2010). The complete genome sequence of *Cupriavidus metallidurans* strain CH34, a master survivalist in harsh and anthropogenic environments. PLoS ONE 5(5): e10433. doi:10.1371/journal.pone.0010433

Jiang, B., Wang, Q., Zhao, Y., Li, L., Hu, X. (2013). Biosorption mechanism of Zn^{2+} and Cd^{2+} by a *Rhodotorula mucilaginosa*. J Pure App Microbiol, 7(3): 1963-1969

Joeng, B.C., Hawes, C., Bonthrone, K.M., Macaskie, L.E. (1997). Localization of enzymatically enhanced heavy metal accumulation *Citrobacter* sp. And metal accumulation in vitro by liposomes containing entrapped enzyme. Microbiol, 43: 2497–2507

Johnson, L., Marschall, P., Zuidema, P., Gribi, P. (2004). Effects of post-disposal gas generation in a repository for spent fuel, high-level waste and long-lived intermediate level waste sited in opalinus clay. National Cooperative for the Disposal of Radioactive Waste (NAGRA), Wettingen (Switzerland). Nagra Technical Report NTB 04-06

Jroundi, F., Merroun, M.L., Arias, J.M., Rossberg, A., Selenska-Pobell, S., González-Muñoz, M.T. (2007). Spectroscopic and microscopic characterization of uranium biomineralization in *Myxococcus xanthus*. Geomicrobiol J, 24(5): 441-449

Kalin, M., Wheeler, W.N., Meinrath, G. (2004). The removal of uranium from mining waste water using algal/microbial biomass. J Environ Radioactiv, 78(2): 151-177

Kalinowski, B.E., Johnsson, A., Arlinger J., Pedersen, K., Ödegaard-Jensen, A., Edberg, F. (2006). Microbial mobilization of uranium from shale mine waste. Geomicrobiol J, 23:157-164

Kavamura, V.N. and Esposito, E. (2010). Biotechnological strategies applied to the decontamination of soils polluted with heavy metals. Biotechnol Adv, 28: 61–69. DOI: 10.1016/j.biotechadv.2009.09.002

Keasling, J.D. and Hupf, G.A. (1996). Genetic manipulation of polyphosphate metabolism affects cadmium tolerance in Escherichia coli. Appl Environ Microbiol, 62(2): 743-746

Knittel, K. and Boetius, A. (2009) Anaerobic oxidation of methane: progress with an unknown process. Ann Rev Microbiol, 63: 311-334

Koban, A., Geipel, G., Rossberg, A., Bernhard, G. (2004). Uranium(VI) complexes with sugar phosphates in aqueous solution. Radiochim Acta, 92: 903–908

Koning, A. J., Lum, P. Y., Williams, J.M., Wright, R. (1993). $DiOC_6$ staining reveals organelle structure and dynamics in living yeast cells. Cell Motil Cytoskel, 25(2): 111-128

Landais, P. and Aranyossy, J.F. (2011). Clays in natural and engineered barriers for radioactive waste confinement. Phys Chem Earth, 36: 1437. DOI:10.1016/j.pce.2011.11.002

Landolt, D., Davenport, A., Payer, J., Shoesmith, D. (2009). A review of materials and corrosion issues regarding canisters for disposal of spent fuel and high-level waste in Opalinus Clay. Swiss Federal Institute of Technology (EPFL), Lausanne (Switzerland). Technical Report 02-05, Nagra

Lane, D.J. (1991). 16S/23S rRNA sequencing. In: Nucleic acid techniques in bacterial systematics. Stackebrandt, E., and Goodfellow, M., eds., John Wiley and Sons, New York, NY, pp. 115-175

Lawrence, J.R., Chenier, M.R., Roy, R., Beaumier, D., Fortin, N., Swehorne, G.D.W., Neu, T.R., Greer, C.W. (2004). Microscale and molecular assessment of impacts of nickel, nutrients and oxygen level on structure and function of river biofilm communities. Appl Environ Microbiol, 70: 4326–4339

Lear, P.R. and Stucki, J.W. (1989). Effects of iron oxidation state on the specific surface area of nontronite. Clays Clay Minerals, 37: 547-552

Leone, G., Reyes, E., Cortecci, G., Pochini, A., Linares, J. (1983). Genesis of bentonites from Cabo de Gata, Almería, Spain: A stable isotope study. Clay Minerals, 18: 227-238

Li, D., Li, Z., Yu, J., Cao, N., Liu, R., Yang, M. (2010). Characterization of bacterial community structure in a drinking water distribution system during an occurrence of red water. Appl Environ Microbiol, 76: 7171–80

Li, Z., Yuan, H., Hu, X. (2008). Cadmium-resistance in growing *Rhodotorula* sp. Y11. Bioresource Technol, 99(5): 1339-1344

Libkind, D., Gadanho, M., van Broock, M., Sampaio, J.P. (2008). Studies on the heterogeneity of the carotenogenic yeast *Rhodotorula mucilaginosa* from Patagonia, Argentina. J Basic Microbiol, 48: 93–98

Lima, A., Romero, E., Piña, Y., Gens, A., Li, X. (2012). Water retention properties of two deep Belgian clay formations. In Unsaturated Soils: Research and Applications (pp. 179-184). Springer Berlin Heidelberg

Linares, J., Huertas, F., Lachica, M., Reyes, E. (1973). Geochemistry of trace elements during the genesis of coloured bentonites. In: Serratosa JM (ed) Proceedings of the International Clay Conference 1972. CSIC, Madrid pp 351-360

Linares, J. (1985). The process of bentonite formation in Cabo de Gata, Almería, Spain. Mineral Petrogr Acta, 29-A: 17-33

Linares, J., Caballero, E., Reyes, E. and Huertas, F. (1987). Trace elements mobility in bentonite formation. Pp. 230-250 in: The Practical Applications of Trace Elements and Isotopes to Enviromental Biogeochemistry and Mineral Resources Evaluation (R.W. Hurst, T.E. Davis & S.S. Augustithis, editors). Theophrastus Publications, Athens

Linares, J., Barahona, E., Huertas, F., Caballero, E., Cuadros, J., Huertas, J., Jiménez de Cisneros, C., Linares, C., Rodriguez, J., Martín-Vivaldi, M.T., Civantos, M.J. (1996). Alteración hidrotermal de las bentonitas de Almería. Monografía, (ENRESA Ed.) Madrid, 151p

Liu, M., Dong, F., Yan, X., Zeng, W., Hou, L., Pang, X. (2010). Biosorption of uranium by *Saccharomyces cerevisiae* and surface interactions under culture conditions. Bioresource Technol, 101(22): 8573-8580

Lloyd, J.R. and Macaskie, L. (2000). Bioremediation of radionuclide-containing wastewaters. In: Lovely, D.R. (Ed.), Enivironmental Microbe-Metal Interactions. ASM Press, Washington, D.C., pp. 277–327

Lloyd, J.R. and Macaskie, L.E., (2002). Biochemical basis of microbe-radionuclide interactions. In: Keith-Roach, M., Livens, F. (Eds.), Interactions of Microorganisms with Radionuclides. Elsevier Sciences, Oxford, UK, pp. 313-342

Lloyd, J.R. and Renshaw, J.C. (2005). Bioremediation of radioactive waste: radionuclide–microbe interactions in laboratory and field-scale studies. Current Op Biotechnol, 16: 254–260

Lopez-Fernandez, M., Fernandez-Sanfrancisco, O., Moreno-Garcia, A., Martin-Sanchez, I., Sanchez-Castro, I., Merroun, M.L. (2014a). Microbial communities in bentonite formations and their interactions with uranium. Appl Geochem 49: 77-86. DOI: http://dx.doi.org/10.1016/j.apgeochem.2014.06.022

Lopez-Fernandez, M., Sánchez-Castro, I., Sandoval, R., Dietmar Pieper, D., Boon, N., Vílchez-Vargas, R., Cherkouk, A., Merroun, M.L. (2014b). Bacterial diversity in bentonites, engineered barrier for deep geological disposal of radioactive wastes. In preparation

Lovley, R.D., Phillips, E.J.P. (1992). Reduction of uranium by *Desulfovibrio desulfuricans*. Appl Environ Microbiol, 58: 850-856

Lovely, D.R., Widman, P.K., Woodward, J.C., Phillips, E.J.P. (1999). Reduction of uranium by cytochrome-c3 of *Desulfovibrio vulgaricus*. Appl Environ Microbiol, 59: 3572–3576

Lu, X., Zhou, X.J., Wang, T.S. (2013). Mechanism of uranium(VI) uptake by *Saccharomyces cerevisiae* under environmentally relevant conditions: Batch, HRTEM, and FTIR studies. J Hazard Mat, 262: 297-303

Lütke, L. (2013). Interaction of selected Actinides (U, Cm) with Bacteria relevant to Nuclear Waste Disposal. Doctoral Thesis TU Dresden, Germany

Lütke, L., Moll, H., Bachvarova, V., Selenska-Pobell, S., Bernhard, G. (2013). The U(VI) speciation influenced by a novel *Paenibacillus* isolate from Mont Terri Opalinus clay. Dalton T, 42(19): 6979-6988

Lushchak, L. and Gospodaryov, D. (2005). Catalases protect cellular proteins form oxidative modification in *Saccharomyces cerevisiae*. Cell Biol Int, 29: 187–192

Macaskie, L.E., Bonthrone, K.M., Yong, P., Goddard, D.T. (2000). Enzymically mediated bioprecipitation of uranium by a *Citrobacter* sp.: a concerted role for

exocellular lipopolysaccharide and associated phosphatase in biomineral formation. Microbiol, 146: 1855–1867

Majumder, A., Bhattacharyya, K., Bhattacharyya, S., Kole, S.C. (2013). Arsenic-tolerant, arsenite-oxidising bacterial strains in the contaminated soils of West Bengal, India. Sci Total Environ, 463: 1006–1014

Makarov, E.S. and Ivanov, V.I. (1960). The crystal structure of meta-autunite, Ca(UO2)2(PO4)2.6H2O. Doklady Akademi Nauk SSSR 132: 673–676

Marcos, N. (2004). Results of the Studies on Bentonite Samples from Serrata de Nijar, Almeria, Spain. Working Report 2004-24, Helsinki University of Technology

Martínez, J.A., Jiménez de Cisneros, C., Caballero, E. (2007). Natural acid sulphate alteration in bentonites (Cabo de Gata, Almeria, SE Spain). Clay Min, 42 (1): 89– 107

Martinez, R.J., Wang, Y., Raimondo, M.A., Coombs, J.M., Barkay, T., Sobecky, P.A. (2006). Horizontal gene transfer of PIB-type ATPases among bacteria isolated from radionuclide- and metal-contaminated subsurface soils. Appl. Environ. Microbiol, 72, 3111–3118

Martinez, R.J., Wu, C.H., Beazley, M.J., Andersen, G.L., Conrad, M.E., Hazen, T.C., Taillefert, M., Sobecky, P.A. (2014). Microbial community responses to organophosphate substrate additions in contaminated subsurface sediments. PloS ONE, 9(6), e100383

Martín-Platero, A.M., Valdivia, E., Maqueda, M., Martínez-Bueno, M. (2007). Fast, convenient and economical method for isolating genomic DNA from lactic-acid bacteria using a modification of the ‘‘protein salting-out’’ procedure. Anal. Biochem, 366: 102–104

Mauclaire, L., McKenzie, J.A., Schwyn, B., Bossart, P. (2007). Detection and cultivation of indigenous microorganisms in Mesozoic claystone core samples from the Opalinus Clay Formation (Mont Terri Rock Laboratory). Phys Chem Earth, Parts A/B/C 32: 232–240

Maurice, P., Vierkorn, M.A., Hersman, L.E., Fulghum, J.E., Ferryman, A. (2001). Enhancement of kaolinite dissolution by an aerobic *Pseudomonas mendocina* bacterium. Geomicrobiol J, 18 (1), 21–35

McMahon, P.B., Chapelle, F.H., Falls, F.W., Bradley, P.M. (1992). Role of microbial processes in linking sandstone diagenesis with organic-rich clays. J Sedimen Petrol, 62: 1-10

Meleshyn, A. (2011). Microbial processes relevant for long-term performance of radioactive waste repositories in clays. GRS-291 Report. http://www.grs.de/publication/GRS-291

Merroun, M.L., Hennig, C., Rossberg, A., Geipel, G., Reich, T., Selenska-Pobell, S. (2002). Molecular and atomic analysis of the uranium complexes formed by three eco-types of *Acidithiobacillus ferrooxidans*. Biochem. Soc. Transact. 30, 669–672

Merroun, M.L., Geipel, G., Nicolai, R., Heise, K.H., Selenska-Pobell, S. (2003a). Complexation of uranium(VI) by three eco-types of *Acidithiobacillus ferrooxidans* studied using time-resolved laser-induced fluorescence spectroscopy and infrared spectroscopy. Biometals, 16(2): 331-339

Merroun, M., Hening, C., Rossberg, A., Reich, T., Selenska-Pobell, S. (2003b). Characterization of U(VI)-*Acidithiobacillus ferrooxidans* complexes using EXAFS, transmission electron microscopy, and energy-dispersive X-ray analysis. Radiochim Acta, 91: 583-591

Merroun, M.L., Raff, J., Rossberg, A., Hennig, C., Reich, T., Selenska-Pobell, S. (2005). Complexation of uranium by cells and S-layer sheets of *Bacillus sphaericus* JG-A12. Appl Environ Microbiol, 71: 5532-5543

Merroun, M., Nedelkova, M., Rossberg, A., Hennig, C., Selenska-Pobell, S. (2006). Interaction mechanisms of bacterial strains isolated from extreme habitats with uranium. Radiochim Acta, 94 (9-11): 723-729

Merroun, M.L. and Selenska-Pobell, S. (2008). Bacterial interactions with uranium: An environmental perspective. J Contam Hydrol, 102: 285-295

Merroun, M.L., Nedelkova, M., Ojeda, J.J., Reitz, T., López-Fernández, M., Arias, J.M., Romero-González, M., Selenska-Pobell, S. (2011). Bio-precipitation of uranium by two bacterial isolates recovered from extreme environments as estimated by potentiometric titration, TEM and X-ray absorption spectroscopic analyses. J Hazard Mat, 197:1-10

Meyer, M. and Kircher, M. (2010). Illumina sequencing library preparation for highly multiplexed target capture and sequencing. Cold Spring Harb Protoc, 6: pdb.prot5448

Mijnendonckx, K., Provoost, A., Ott, C.M., Venkateswaran, K., Mahillon, J., Leys, N., Van Houdt, R. (2013). Characterization of the survival ability of *Cupriavidus metallidurans* and *Ralstonia pickettii* from space-related environments. Microb Ecol, 65(2): 347-60

Miller, J.H. (1972). Experiments in Molecular Genetics. Cold Spring Harbor Laboratory, Cold Spring Harbor, New York, pp. 352–355

Mingorance, M.D., Barahona, E., Fernandez-Galvez, J. (2007). Guidelines for improving organic carbon recovery by the wet oxidation method. Chemosph, 68: 409–413

Moll, H., Stumpf, T., Merroun, M., Rossberg, A., Selenska-Pobell, S., Bernhard, G. (2004). Time-resolved laser fluorescence spectroscopy study on the interaction of curium(III) with *Desulfovibrio äspöensis* DSM 10631T. Environ Science Technol, 38(5): 1455-1459

Moll, H., Glorius, M., Bernhard, G. (2008). Curium(III) Complexation with Desferrioxamine B (DFO) Investigated Using Fluorescence Spectroscopy. Bull Chem Soc Jpn, 81(7): 857–862

Moll, H., Lütke, L., Barkleit, A., Bernhard, G. (2013a). Curium (III) speciation studies with cells of a groundwater strain of *Pseudomonas fluorescens.*Geomicrobiol J, 30(4): 337-346

Moll, H., Lütke, L., Bachvarova, R.S., Geissler, A., Krawczyk-Bärsch, E., Selenska-Pobell, S. (2013b). Microbial diversity in Opalinus Clay and interaction of

dominant microbial strains with actinides.Wissenschaftlich-Technische Berchte, HZDR-036. ISSN 2191-8708

Moll, H., Lütke, L., Bachvarova, V., Cherkouk, A., Selenska-Pobell, S., Bernhard, G. (2014). Interactions of the Mont Terri Opalinus Clay isolate *Sporomusa* sp. MT-2.99 with curium(III) and europium(III). Geomicrobiol J, DOI: 10.1080/01490451.2014.889975

Mondani, L., Benzerara, K., Carriere, M., Christen, R., Mamindy-Pajany, Y., Février, L., Marmier, N., Achouak, W., Nardoux, P., Berthomieu, C., Chapon, V. (2011). Influence of Uranium on Bacterial Communities: A Comparison of Natural Uranium-Rich Soils with Controls. PLoS ONE 6(10): e25771. DOI:10.1371/journal.pone.0025771

Morcillo, F., González-Muñoz, M.T., Reitz, T., Romero-González, M.E., Arias, J.M., Merroun, M.L. (2014). Biosorption and Biomineralization of U(VI) by the Marine Bacterium *Idiomarina loihiensis* MAH1: Effect of Background Electrolyte and pH. PLoS ONE 9(3): e91305. DOI:10.1371/journal.pone.0091305

Moreno-Garcia, A. (2012). Las poblaciones bacterianas de bentonita y sus mecanismos de tolerancia al uranio Master thesis, University of Granada, Spain

Motamedi, M., Karland, O., Pedersen, K. (1996). Survival of sulfate reducing bacteria at different water activities in compacted bentonite. FEMS Microbiol Lett, 141(1): 83–87

Moulin, C., Laszak, I., Moulin, V., Tondre, C. (1998). Time-resolved laser-induced fluorescence as a unique tool for low-level uranium speciation. Appl Spectrosc, 52: 528–535

Münzinger, M., Taraz, K., Budzikiewicz, H., Drechsel, H., Heymann, P., Winkelmann, G., Meyer, J.M. (1999). S, S-rhizoferrin (enantio-rhizoferrin) – a siderophore of *Ralstonia* (*Pseudomonas*) *pickettii* DSM 6297 – the optical antipode of R, R-rhizoferrin isolated from fungi. BioMetals, 12: 189–193

Nadeau, P.H., Peacor, D.R., Yan, J., Hillier, S. (2002). I-S precipitation in pore space as the cause of geopressuring in Mesozoic mudsotnes, Egersund Basin, Norwegian continental shelf. American Mineralogist, 87: 1580-1589

Nagra, (2002). Project Opalinus Clay – Safety Report: Demonstration of Disposal feasibility for spent fuel, vitrified high-level waste and long-lived intermediate level waste (Entsorgungsnachweis). Nagra Technical Report NTB 02-05; Nagra: Switzerland

Nazina, T.M., Lukyanova, E.A., Zakharova, E.V., Konstantinova, L.I., Kalmykov, S.N., Poltaraus, A.B., Zubkov, A.A. (2010). Microorganisms in a Disposal Site for Liquid Radioactive Wastes and Their Influence on Radionuclides. Geomicrobiol J, 27(5): 473-486. DOI: 10.1080/01490451003719044

NEA/CE, (2003). Engineered Barrier Systems and the Safety of Deep Geological Repositories. State-of-the-art Report, NEA/CE, 2003, ISBN: 92-64-18498-8

Nedelkova, M., Merroun, M.L., Rossberg, A., Hennig, C., Selenska-Pobell, S. (2007). *Microbacterium* isolates from the vicinity of a radioactive waste depository and their interactions with uranium. FEMS Microbiol Ecol, 59: 694–705

Newsome, L., Morris, K., Lloyd, J.R. (2014). The biogeochemistry and bioremediation of uranium and other priority radionuclides. Chem Geol, 363: 164–184

Nilgiriwala, K.S., Alahari, A., Rao, A.S., Apte, S.K. (2008). Cloning and overexpression of alkaline phosphatase PhoK from *Sphingomonas* sp. Strain BSAR-1 for bioprecipitation of uranium form alkaline solutions. Appl Environ Microbiol, 74(17): 5516-5523

Nyman, J.L., Marsh, T.L., Ginder-Vogel, M.A., Gentile, M., Fendorf, S., Criddle, C. (2006). Heterogeneous response to biostimulation for U(VI) reduction in replicated sediment microcosms. Biodegrad, 17: 303-16

Ohnuki, T., Ozaki, T., Yoshida, T., Sakamoto, F., Kozai, N., Wakai, E., Francis, A.J.,Lefuji, H. (2005a). Mechanisms of uranium mineralization by the yeast *Saccharomyces cerevisia*e. Geochim Cosmochim Acta, 69(22): 5307-5316

Ohnuki, T., Yoshida, T., Ozaki, T., Samadfam, M., Kozai, N., Yubuta, K., Mitsugashira, T., Kasama, T., Francis, A.J. (2005b). Interactions of uranium with bacteria and kaolinite clay. Chem Geol, 220: 237–243

Ojovan, M. I. and Lee, W.E. (2005). An introduction to nuclear waste immobilisation. Elsevier Science Publishers B.V., Amsterdam

ONDRAF/NIRAS, (2001). Safety Assessment and Feasibility Interim Report 2 (SAFIR 2), NIROND 2001-06 E, ONDRAF/NIRAS, Brussels, Belgium

Onyenwoke, R.U., Brill, J.A., Farahi, K., Wiegel, J. (2004). Sporulation genes in members of the low G+C Gram-type-positive phylogenetic branch (*Firmicutes*). Arch Microbiol, 182: 182–192

Ortiz, L., Volckaert, G., Mallants, D. (2002). Gas generation and migration in Boom Clay, a potential host rock formation for nuclear waste storage. Eng Geol, 64: 287-296

Pace, N.R. (1997). A molecular view of microbial diversity and the biosphere. Science, 276: 734–740

PANalytical (2008). X'Pert HighScore Plus, version 2.2. PANalytical B.V.

Park, D. M. and Jiao, Y. (2014). Modulation of medium pH by Caulobacter crescentus facilitates recovery from uranium-induced growth arrest. Appl Env Microbiol, 80(18): 5680-5688

Pedersen, K. (1999). Subterranean microorganisms and radioactive waste disposal in Sweden. Eng Geol, 52: 163–176

Pedersen, K. (2002a). Microbial processes in the disposal of high level radioactive waste 500 m underground in Fennoscandian shield rocks. In: Keith-Roach MJ, Livens FR (ed) Interactions of microorganisms with radionuclides. Elsevier Science Ltd, Amsterdam, 279-311

Pedersen, K. (2002b). Interaction of Microorganisms with Radionuclides, Elsevier Science Ltd

Pedersen, K. (2013). Metabolic activity of subterranean microbial communities in deep granitic groundwater supplemented with methane and H_2. The ISME J, 7: 839–849

Pentrakova, L., Su, K., Pentrak, M., Stucki, J.W. (2013). A review of microbial redox interactions with structural Fe in clay minerals. Clay Miner, 48: 543–560

Piotrowska-Seget, Z., Cycon, M., Kozdroj, J. (2005). Metal-tolerant bacteria occurring in heavily polluted soil and mine spoil. Appl Soil Ecol, 28: 237–246

Poulain, S., Sergeant, C., Simonoff, M., Le Marrec, C., Altmann, S. (2008). Microbial investigations of Opalinus Clay, an argillaceous formation as a potential host rock under evaluation for a radioactive waste repository. Geomicrobiol J, 25: 240–249

Preveral, S., Gayet, L., Moldes, C., Hoffmann, J., Mounicou, S., Gruet, A., Forestier, C. (2009). A common highly conserved cadmium detoxification mechanism from bacteria to humans heavy metal tolerance conferred by the ATP-binding cassette (ABC) transporter SpHMT1 requires glutathione but not metal-chelating phytochelatin peptides. J Biol Chem, 284(8): 4936-4943

Pruesse, E., Peplies, J., Glöckner, F.O. (2012). SINA: accurate high-throughput multiple sequence alignment of ribosomal RNA genes. Bioinformatics, 28: 1823-1829

Ramirez, S., Cuevas, J., Vigil, R., Leguey, S. (2002). Hydrothermal alteration of `La Serrata' bentonite (Almeria, Spain) by alkaline solutions. Appl Clay Sci, 21: 257-269

Ravel, B. and Newville, J.M. (2005). Synchrotron Radiat 12: 537 – 541

Reasoner, D.J. and Geldreich, E. (1985). A new medium for the enumeration and subculture of bacteria from potable water. Appl Environ Microbiol, 49: 1–7

Reitz, T., Merroun, M.L., Rossberg, A., Steudtner, R., Selenska-Pobell, S. (2011). Bioaccumulation of U(VI) by *Sulfolobus acidocaldarius* at moderate acidic conditions. Radiochim Acta, 99: 1–11

Reitz, T., Rossberg, A., Barkleit, A., Selenska-Pobell, S., Merroun, M.L. (2014). Decrease of U (VI) Immobilization Capability of the Facultative Anaerobic

Strain *Paenibacillus* sp. JG-TB8 under Anoxic Conditions Due to Strongly Reduced Phosphatase Activity. PloS one, 9(8), e102447

Reyes, E., Caballero, E., Huertas, F. and Linares, J. (1987). Bentonite deposits from Cabo de Gata region, Almería, Spain. Field Book Guide, Euroclay-87, Excursion A, 9-32

Reyes, E., Huertas, F. and Linares, J. (1979). Mineralogía y geoquímica de las bentonitas de la zona norte de Cabo de Gata (Almería). V. Area de los Trancos. Estudios Geológicos, 35: 363-370

Rossbach, S., Wilson, T., Kukuk, M., Carty, H. (2000). Elevated zinc induces siderophore biosynthesis genes and zntA-like gene in *Pseudomonas fluorescens*. FEMS Microbiol Lett, 191: 61–70

Said, W.A. and Lewis, D.L. (1991). Quantitative Assessment of the Effects of Metals on Microbial Degradation of Organic Chemicals. App Environ Microbiol, 57(5): 1498-1503

Savage, D. and Chapman, N.A. (1982). Hydrothermal behaviour of simulated waste glass- and waste-rock interaction under repository conditions. Chem Geol, 36: 59–86

Schaefer, M.V., Gorski, C.A., Scherer, M.M. (2011). Spectroscopic evidence for interfatial Fe(II)-Fe(III) electron transfer in a clay mineral. Environ Science Technol, 45: 540-545

Schippers, A., Neretin, L.N., Kallmeyer, J., Ferdelman, T.G., Cragg, B.A., Parkes, R.J., Jørgensen, B.B. (2005). Prokaryotic cells of the deep subseafloor biosphere identified as living bacteria. Nature, 433: 861-864

Schoch, C.L., Seifert, K.A., Huhndorf, S., Robert, V., Spouge, J.L., Levesque, C.A., Chen, W., Fungal Barcoding Consortium (2012). Nuclear ribosomal internal transcribed spacer (ITS) region as a universal DNA barcode marker for fungi. Proc Natl Acad Sci USA, 109: 6241–6246

Selenska-Pobell, S., Kampf, G., Flemming, K., Radeva, G., Satchanska, G. (2001). Bacterial diversity in soil samples from two uranium waste piles as determined

by rep-APD, RISA and 16S rDNA retrieval. Antonie van Leeuwenhoek, 79: 149–161

Service, R.F. (1997). Microbiologists explore life's rich, hidden kingdoms. Science, 275: 1740–1742

Shelobolina, E.S., Vrionis H.A., Findlay, R.H., Lovley, D.R. (2008). *Geobacter uraniireducens* sp. nov., isolated from subsurface sediment undergoing uranium bioremediation. Int J Sys Evol Microbiol, 58: 1075-1078

Shelobolina, E., Konishi, H., Xu, H., Benzine, J., Xiong, M.Y., Wu, T., Blöthe, M., Roden, E. (2012). Isolation of phyllosilicate–iron redox cycling microorganisms from an illite–smectite rich hydromorphic soil. Front Microbiol, 3: 134–143

Singh, G., Şengör, S.S., Bhalla, A., Kumar, S., De, J., Stewart, B., Spycher, N., Ginn, T.M., Peyton, B.M., Sani, R.K. (2014). Reoxidation of Biogenic Reduced Uranium: A Challenge Toward Bioremediation. Crit Rev Env Sci Tec, 44: 391-415

Sitaud, B., Solari, P.L., Schlutig, S., Llorens, I., Hermange, H. (2012). J Nucl Mater, 425: 238 –243

SKAB, (2011). Long-term safety for the final repository for spent nuclear fuel at Forsmark. Main report of the SR-Site Project. Technical Report TR-11-01, Svensk Kärnbränslehantering AB

Smart, N.R. (2009). Corrosion Behavior of Carbon Steel Radioactive Waste Packages: A Summary Review of Swedish and U.K. Research. Corrosion, 65(3): 195-212. DOI: http://dx.doi.org/10.5006/1.3319128

Solari, P.L., Schlutig, S., Hermange, H., Sitaud, B. (2009). J Phys Conf Ser, 190: 012042

Stroes-Gascoyne, S. and West, J.M. (1997). Microbial studies in the Canadian nuclear fuel waste management program. FEMS Microbiol Rev, 20(3-4): 573-590

Stroes-Gascoyne, S. and Sargent, F.P. (1998). The Canadian approach to microbial studies in nuclear waste management and disposal. J Contam Hydrol, 35: 175–190

Stroes-Gascoyne, S., Hamon, C.J., Dixon, D.A., Martino, J.B. (2007a). Microbial analysis of samples from the tunnel sealing experiment at AECL's Underground Research Laboratory. Phys Chem Earth, 32: 219–231

Stroes-Gascoyne, S., Schippers, A., Schwyn, B., Poulain, S., Sergeant, C., Simonoff, M., Le Marrec, C., Altmann, S., Nagaoka, T., Mauclaire, L., McKenzie, J., Daumas, S., Vinsot, A., Beaucaire, C., Matray, J.M. (2007b). Microbial community analysis of Opalinus Clay drill core samples from the Mont Terri Underground Research Laboratory, Switzerland. Geomicrobiol J, 24: 1–17

Stroes-Gascoyne, S. (2010). Microbial occurrence in bentonite-based buffer, backfill and sealing materials from large-scale experiments at AECL's Underground Research Laboratory. Appl Clay Sci, 47(1–2): 36–42

Stroes-Gascoyne, S., Sergeant, C., Schippers, A., Hamon, C.J., Nèble, S., Vesvres, M.H., Barsotti, V., Poulain, S., Le Marrec, C. (2011). Biogeochemical processes in a clay formation in situ experiment: Part D – Microbial analyses – synthesis of results. Appl Geochem, 26: 980–989

Stucki, J.W. and Getty, P.J. (1986). Microbial reduction of iron in nontronite. P. 279 in: Agronomy Abstracts, 1986 annual meetings of the Soil Science Society of America

Stucki, J.W. and Lear, P.R. (1989). Variable oxidation states of iron in the crystal structure of smectite clay minerals. ACS Symposium Series, 415, 330-358

Stucki, J.W., Lee, K., Zhang, L.Z. and Larson R.A. (2002). Effects of iron oxidation state on the surface and structural properties of smectites. Pure App Chem, 74: 2145-2158

Sun, H., Shi, B., Bai, Y., Wang, D. (2014). Bacterial community of biofilms developed under different water supply conditions in a distribution system. Science Total Environ, 472: 99-107

Suzuki, Y. and Banfield, J.F. (2004). Resistance to and accumulation of, uranium by bacteria from a uranium-contaminate site. Geomicrobiol J 21: 113–121

Swanner, E.D., Bekker, A., Pecoits, E., Konhauser, K.O., Cates, N.L., Mojzsis, S.J. (2013). Geochemistry of pyrite from diamictites of the Boolgeeda Iron Formation, Western Australia with implications for the GOE and Paleoproterozoic ice ages. Chem Geol, 362: 131-142

Swanner, E.D., Nell, R.M., Templeton, A.S. (2011). *Ralstonia* species mediate Fe-oxidation in circum neutral, metal-rich subsurface fluids of Henderson mine, CO. Chem Geol, 284: 339–350

Tamura, K., Dudley, J., Nei, M., Kumar, S. (2007). MEGA4: Molecular Evolutionary Genetics Analysis (MEGA) software version 4.0. Mol Biol Evol, 24: 1596-1599

Thury, M. and Bossart, P. (1999). The Mont Terri rock laboratory, a new international research project in a Mesozoic shale formation, in Switzerland. Eng Geol, 52(3): 347-359

Turner, S., Pryer, K.M., Miao, V.P.W., Palmer, J.D. (1999). Investigating deep phylogenetic relationships among cyanobacteria and plastids by small subunit rRNA sequence analysis. J Euk Microbiol, 46: 327–338

Urios, L., Marsal, F., Pellegrini, D., Magot, M. (2012). Microbial diversity of the 180 million-year-old Toarcian argillite from Tournemire, France. Appl Geochem, 27: 1442–1450. DOI:10.1016/j.apgeochem.2011.09.022

Urios, L., Marsal, F., Pellegrini, D., Magot, M. (2013). Microbial Diversity at Iron-Clay Interfaces after 10 Years of Interaction Inside a Deep Argillite Geological Formation (Tournemire, France). Geomicrobiol J, 30(5): 442-453

Utturkar, S.M., Bollmann, A., Brzoska, R.M., Klingeman, D.M., Epstein, S.E., Palumbo, A.V., Brown, S.D. (2013). Draft genome sequence for *Ralstonia* sp. strain OR214, a bacterium with potential for bioremediation.Genome announcements, 1(3), e00321-13. doi:10.1128/genomeA.00321-13

Van Geet, M., Maes, N., Dierckx, A. (2003). Characteristics of the Boom Clay organic matter, a review. Geological Survey of Belgium, Professional paper 2003/1, N. 298: 1-23

Villar, M.V., Fernández-Soler, J.M., Delgado-Huertas, A., Reyes, E., Linares, J., Jiménez de Cisneros, C., Huertas, F.J., Caballero, E., Leguey, S., Cuevas, J., Garralón, A., Fernández, A.M., Pelayo, M., Martín, P.L., Pérez Del Villar, L., Astudillo, J. (2006). The study of Spanish clays for their use as sealing materials in nuclear waste repositories: 20 years of progress. J Iber Geol, 32: 15–36

Villegas, L.B., Amoroso, M.J., de Figueroa, L.I. (2005). Copper tolerant yeasts isolated from polluted area of Argentina. J Basic Microbiol, 45(5): 381–391

Villegas, L.B., Amoroso, M.J., de Figueroa, L.I. (2009). Responses of *Candida fukuyamaensis* RCL-3 and *Rhodotorula mucilaginosa* RCL-11 to copper stress. J Basic Microbiol, 49(4): 395-403

Villegas, L.B., Amoroso, M.J., Lucía, I.C.D.F. (2011). Interaction of copper or chromium with yeasts: Potential application on polluted environmental clean up (Book Chapter). Bioremediation: Biotechnology, Engineering and Environmental Management, 177-206

Von Canstein, H., Ogawa, J., Shimizu, S., Lloyd, J.R. (2008). Secretion of flavins by *Shewanella* species and their role in extracellular electron transfer. App Environ Microbiol, 74: 615-623

Vorhies, J.S. and Gaines, R.R. (2009). Microbial dissolution of clay minerals as a source of iron and silica in marine sediments. Nat Geoscience, 2: 221-225

Walkley, A. and Black, I.A. (1934). An examination of Degtjareff method for determining soil organic matter and a proposed modification of the chromic acid titration method. Soil Sci, 37: 29–37

Wang, J. and Chen, C. (2006). Biosorption of heavy metals by *Saccharomyces cerevisiae*: a review. Biotechnol Adv, 24: 427–451

Wang, J. and Chen, C. (2009). Biosorbents for heavy metals removal and their future. Biotechnol Adv, 27(2): 195–226. DOI: 10.1016/j.biotechadv.2008.11.002

Wang, Y., Frutschi, M., Suvorova, E., Phrommavanh, V., Descostes, M., Osman, A.A., Geipel, G., Bernier-Latmani, R. (2013). Mobile uranium(IV)-bearing colloids in a mining-impacted wetland. Nat Communs, 4:2942

Weber, K.A., Achenbach, L.A., Coates, J.D. (2006). Microorganisms pumping iron: anaerobic microbial iron oxidation and reduction. Nat Rev Microbiol, 4: 752-764

Wersin, P., Leupin, O.X., Mettler, S., Gaucher, E., Mäder, U., De Cannière, P., Vinsot, A., Gabler, H.E., Kunimaro, T., Kiho, K., Eichinger, L. (2011). Biogeochemical processes in a clay formation *in situ*experiment: part A – overview, experimental design and water data of an experiment in the Opalinus Clay at the Mont Terri Underground Research Laboratory, Switzerland. Appl Geochem 26(6): 931-953

West, J.M., Mckinley, I.G., Chapman, N.A. (1982). Microbes in deep geological systems and their possible influence on radioactive waste disposal. Rad Waste Manag Nuc Fuel Cycle 3: 1-15

West, J.M., McKinley, I.G., Stroes-Gascoyne, S. (2002). Microbial effects on waste repository materials. Interactions of Microorganisms with Radionuclides. Elsevier Science Ltd, 255-277

Whitman, W.B., Coleman, D.C., Wiebe, W.J. (1998). Procaryotes: the unseen majority. Proceedings of the National Academy of Sciences of the United States of America 95: 6578-6583

Wouters, K., Moors, H., Boven, P., Leys, N. (2013). Evidence and characteristics of a diverse and metabolically active microbial community in deep subsurface clay borehole water. FEMS Microbiol Ecol 86: 458–473. DOI: 10.1111/1574-6941.12171

Xie, G., Bruce, D.C., Challacombe, J.F., Chertkov, O., Detter, J.C., Gilna, P., Han, C.S., Lucas, S., Misra, M., Myers, G.L., Richardson, P., Tapia, R., Thayer, N., Thompson, L.S., Brettin, T.S., Henrissat, B., Wilson, D.B., McBride, M.J. (2007). Genome sequence of the cellulolytic gliding bacterium *Cytophaga hutchinsonii*. Appl Environ Microbiol, 73(11): 3536-46

Zhang, G., Senko, M.J., Kelly, D.S., Tan, H., Kemner, M.K., Burgos, D.W. (2009). Microbial reduction of iron(III)-rich nontronite and uranium(VI). Geochim Cosmochim Acta, 73(12): 3523-3538

Zhang, C., Dodge, C.J., Malhotra, S.V., Francis, A.J. (2013). Bioreduction and precipitation of uranium in ionic liquid aqueous solution by *Clostridium* sp. Bioresource technology, 136: 752-756

Zuloaga, P. and Astudillo, J. (2012). The Spanish Radioactive Waste Management and the associated research ensuring its development from sound technical and scientific basis. MRS Proc, 1475:imrc11-1475-nw35-il03. DOI:10.1557/opl.2012.552

CONCLUSIONES

De acuerdo con los resultados presentados, las principales conclusiones de esta Tesis Doctoral son:

1. Este es el primer estudio que describe la diversidad microbiana en formaciones de bentonita del Parque Natural de Cabo de Gata (Almería, España) usadas como material de referencia para las barreras artificiales bentoníticas en el concepto del almacenamiento geológico profundo de residuos radiactivos.

2. El estudio de la diversidad bacteriana de las bentonitas del Parque Natural de Cabo de Gata (Almería) realizado mediante métodos moleculares reveló una alta diversidad, principalmente representada por los *phyla* bacterianos *Proteobacteria*, *Bacteroidetes* y *Actinobacteria*.

3. Se aisló un elevado número de cepas microbianas de las muestras de bentonita. La comunidad microbiana aislada estaba dominada por los *phyla* bacterianos *Proteobacteria*, *Firmicutes* y *Actinobacteria*. Además, de la muestra BII-2 se aisló una levadura pigmentada, *Rhodotorula mucilaginosa* BII-R8.

4. Estudios de citometría de flujo demostraron la capacidad de tolerar altas concentraciones de uranio de las células de *R. mucilaginosa* BII-R8. La viabilidad celular de la levadura aislada BII-R8 depende de la concentración de uranio y el tiempo de contacto. El uranio(VI) provoca una detención temporal del crecimiento de más de 24 h en *R. mucilaginosa* BII-R8.

5. Los análisis de TRLFS y XAS indicaron que las células de *R. mucilaginosa* BII-R8 coordinan el U(VI) a través de grupos fosfato orgánicos que presentan una estructura similar a la de la meta-autunita (un mineral de fosfato de uranilo). Se localizaron acúmulos de uranio en la pared celular y a nivel intracelular, en las membranas de los orgánulos.

6. En el caso del curio(III) los análisis realizados mediante TRLFS demostraron que para las células de la levadura *R. mucilaginosa* BII-R8 la bioadsorción del curio(III) es un proceso reversible en el que dos especies de curio(III) fueron identificadas. La especie 1 del complejo Cm(III)-*R. mucilaginosa* BII-R8 se caracteriza por tener una banda de emisión máxima a 599 ± 1 nm y un tiempo medio de vida de luminicencia de 215 ± 36 µs. La especie 2 de Cm(III)-*R. mucilaginosa* BII-R8 mostró una emisión máxima a 602.0 ± 0.5 nm y un tiempo medio de vida de luminiscencia mas corto, de 124 ± 15 µs.

7. El estudio de la estructura de la comunidad bacteriana de los microcosmos, en condiciones aerobias, de las bentonitas españolas reveló diferencias en la diversidad bacteriana debidas al tratamiento con nitrato de uranilo. Especialmente, a través del enriquecimiento de *Pseudomonas* y *Bacillus*, géneros descritos previamente por su papel en la biomineralización de uranio.

8. Se elaboró una base de datos de los genes catabólicos de la fosfatasa ácida, implicada en la biomineralización de uranio, que posibilitará el uso de la información taxonómica de un ecosistema estudiado para entender mejor su potencial catabólico.

9. La comunidad microbiana detectada en las formaciones de bentonita podría afectar a la seguridad del almacenamiento geológico profundo de residuos radiactivos y podría ser usada en la bio-remediación de lugares contaminados con radionucleidos.

CONCLUSIONS

According to the presented results, the main conclusions of this Doctoral Thesis are:

1. This is the first study describing the microbial diversity of bentonite formations in Cabo de Gata National Park (Almeria, Spain) used as reference material for artificial bentonite barriers in the concept of the deep geological repository of radioactive wastes.

2. The study of the bacterial diversity of the bentonite formations of Cabo de Gata National Park (Almeria), by molecular methods revealed a high diversity, mainly represented by bacterial phyla *Proteobacteria*, *Bacteroidetes* and *Actinobacteria*.

3. A high number of microbial strains were isolated from the bentonite samples. The isolated microbial community was dominated by bacterial phyla *Proteobacteria*, *Firmicutes* and *Actinobacteria*. In addition, a pigmented yeast strain *Rhodotorula mucilaginosa* BII-R8 was isolated from sample BII-2.

4. Flow cytometry studies demonstrated the ability of the cells of *R. mucilaginosa* BII-R8 to tolerate high uranium concentrations. The cell viability of the BII-R8 yeast strain is affected by uranium concentration and time contact. U(VI) caused a temporary growth arrest, larger thant 24 h, in *R. mucilaginosa* BII-R8.

5. TRLFS and XAS analyses indicated that *R. mucilaginosa* BII-R8 cells coordinate U(VI) through organic phosphate groups with a similar structure to that of meta-autunite (an uranyl-phosphate mineral phase). The uranium accumulates were localized at the cell wall and intracellularly, at the level of concentric organelle membranes.

6. In the case of Cm(III), TRLFS analysis demonstrated that for the yeast cells of R. mucilaginosa BII-R8, the biosorption of Cm(III) is a reversible and pH dependent process, where two Cm(III) yeast species were detected. Cm(III)-*R. mucilaginosa* BII-R8 specie 1 is characterized by an emission maximum at 599 ± 1 nm and an average luminescence lifetime of 215 ± 36 µs. Whereas Cm(III)-*R. mucilaginosa* BII-R8 specie

2 shows a more red shifted emission maximum at 602.0 ± 0.5 nm and a shorter average luminescence lifetime of 124 ± 15 µs

7. The study of the bacterial community structure of the Spanish bentonites aerobic microcosms revealed a shift in the bacterial diversity induced by the uranyl nitrate treatment. Especially through the enrichment of *Pseudomonas* and *Bacillus*, genera previously described for being involved in the uranium immobilization.

8. A database of acid phosphatase catabolic genes was created to allow the possibility to use the taxonomic information of a studied ecosystem to get better understandings of its catabolic potential.

9. The microbial community detected in the bentonite formations might affect the safety concept of the deep geological repository of radioactive wastes, and could be used in the bioremediation of radionuclide contaminated sites.